

UPHILL CATALYSIS: GENERATION OF HIGHER  
ENERGETIC GEOMETRICAL ISOMERS OF  
(CYCLO)ALKENES USING VISIBLE LIGHT  
PHOTOCATALYSIS AND THEIR UTILIZATION IN  
CHEMICAL SYNTHESSES

By

KAMALJEET SINGH

Master of Science in Applied Chemistry (Pharmaceuticals)  
Guru Nanak Dev University  
Amritsar, Punjab, India  
May 2009

Bachelor of Science in Non-Medical Science  
Punjabi University  
Patiala, Punjab, India  
April 2007

Submitted to the Faculty of the  
Graduate College of the  
Oklahoma State University  
in partial fulfillment of  
the requirements for  
the Degree of  
DOCTOR OF PHILOSOPHY  
July 2018

UPHILL CATALYSIS: GENERATION OF HIGHER  
ENERGETIC GEOMETRICAL ISOMERS OF  
(CYCLO)ALKENES USING VISIBGLE LIGHT  
PHOTOCATALYSIS AND THEIR UTILIZATION IN  
CHEMICAL SYNTHESSES

Dissertation Approved:

Dr. Jimmie. D. Weaver

---

Dissertation Adviser

Dr. Ronald J. Rahaim, Jr.

---

Dr. Christopher J. Fennell

---

Dr. Richard A. Bunce

---

Dr. Junpeng Deng

---

## ACKNOWLEDGEMENTS

I would like to express my sincere gratitude to my advisor Dr. Jimmie D. Weaver for the continuous support of my Ph.D. study and related research, for his patience, motivation, and immense knowledge. I fully enjoyed working in a research environment that stimulates original thinking and initiative, which he created. Dr. Weaver's skillful guidance and innovative ideas are highly appreciated.

I would also like to acknowledge valuable inputs and helpful suggestions from my committee members: Dr. Richard Bunce, Dr. Ronald Rahaim, Dr. Christopher Fennell, and Dr. Junpeng Deng.

I am also thankful to Dr. Reza Latifi for all his help in X-ray crystallography.

I must also thank all my lab mates Amandeep, Sameera, Kip, Mo, Sonal, Majula, Winston, Jon, Ryne, and Anu. It was a great pleasure working with them and sharing ideas. I learnt a lot from these people.

This acknowledgement would not be complete without mentioning my loving wife Amandeep and my son Pavnoor. It is my privilege to thank my wife for her continuous support throughout my graduate school period. Without her support and faith, I would not have made through the graduate school.

Last, but not the least, I would like to thank my father Gurbachan Singh, my mother Balbir Kaur, my brother Harpreet Singh, and my sister Devinder Kaur for their love and support throughout these years. Their encouragement led me to pursue this career and I will forever be indebted for their sacrifices in supporting me.

Name: KAMALJEET SINGH

Date of Degree: JULY, 2018

Title of Study: UPHILL CATALYSIS: GENERATION OF HIGHER ENERGETIC GEOMETRICAL ISOMERS OF (CYCLO)ALKENES USING VISIBLE LIGHT PHOTOCATALYSIS AND THEIR UTILIZATION IN CHEMICAL SYNTHESSES

Major Field: CHEMISTRY

Abstract: We have performed a systematic study of utilizing excited state surfaces to promote endergonic reactions. As such, catalysis of potential endergonic reactions has not been considered since thermal catalysis cannot promote these reactions. However, this limitation can be overcome by utilizing excited state surfaces, from which all reaction directions are essentially exergonic. As a result, excitation can pump reactions in endergonic directions. In an approach to develop such reactions, we developed isomerization of *trans*-styrenoids to their higher energy geometrical *cis*-isomer using visible light and Ir(ppy)<sub>3</sub> as a photocatalyst. This is a rare example of uphill catalysis which is endergonic by 2-7 kcal/mol of energy. We postulated that an energy transfer, from the photo-excited catalyst, was a key step in the operative mechanism. While synthetically useful, this only captured a small fraction of the potential energy of the excited state. In order to utilize a greater portion of the potential energy provided by the photocatalyst, we designed a series of *trans*-cycloalkenes. We envisioned that upon excitation, these cycloalkenes would undergo isomerization and, because of the small ring size, significant distortion from the ideal geometry, resulting in highly strained *trans*-cycloalkenes. The strain associated with the *trans*-cycloalkene raises its ground state energy and simultaneously activates it towards reactions with other functional groups. In contrast, the *cis*-cycloalkenes are completely unreactive in the absence of light and photocatalyst. Thus, we can use light as a stimulus to “turn on” the reactivity. We have utilized this general strategy to develop a novel bioconjugation strategy with azides, facilitate a rare thermal [2+2] cycloaddition with other alkenes, and facilitate an intramolecular hydroalkoxylation of an alkene to form complex, and previously inaccessible, oxabicycles.

## TABLE OF CONTENTS

Chapter	Page
I. INTRODUCTION.....	1
1.1 Historical background.....	1
1.2 Discussion of photocatalyst .....	13
1.21 Quenching by electron transfer mechanism.....	13
1.22 Quenching by energy transfer mechanism.....	14
1.3 References.....	17
II. VISIBLE LIGHT MEDIATED UPHILL CATALYSIS FOR THE SYNTHESIS OF Z- ALKENES .....	19
2.1 Optimization studies .....	19
2.2 Substrate scope of the isomerization reaction.....	21
2.3 Mechanistic studies .....	23
2.4 Utilization of photocatalytic isomerization strategy .....	26
2.5 Summary .....	27
2.6 Experimental procedures .....	27
2.7 References.....	55
III. VISIBLE LIGHT INDUCED RAPID AND SELECTIVE LIGATION WITH STRAIN LOADABLE ALKENES .....	105
3.1 Results and discussion .....	108
3.2. Single-crystal X-ray crystallography .....	126
3.3. Determination of the regiochemistry and relative stereochemistry of the minor isomer.....	127
3.4. Investigation of the plausible reactive species in the reaction (triplet biradical versus strained <i>trans</i> -intermediate).....	129
3.5 Summary .....	130

3.6 Experimental section.....	131
3.7 Insulin ligation experiment .....	150
3.8 References.....	155
Chapter	Page
IV. A RARE THERMAL [2+2] CYCLOADDITION OF ARYL CYCLOHEPTENES .....	186
4.1 Optimization of reaction conditions.....	188
4.2 Stereochemical assessment of diastereomers.....	190
4.3 Computational studies.....	192
4.4 Substrate scope of [ $\pi 2_s + \pi 2_a$ ] cycloaddition.....	193
4.5 Mechanistic investigation of reactive intermediate .....	197
4.6 Summary .....	199
4.7 Experimental procedures .....	199
4.8 [ $\pi 2_s + \pi 2_a$ ] cycloaddition of other substrates.....	219
4.9 References.....	220
V. GENERATION AND UTILIZATION OF <i>TRANS</i> -ARYLCYCLOHEXENES IN SYNTHESIS .....	262
5.1 Optimization studies .....	263
5.2 Substrate scope.....	264
5.3 Computational studies.....	266
5.4 Mechanistic investigation .....	272
5.5 Summary .....	276
5.6 Experimental procedures .....	277
5.7 References.....	286
APPENDIX.....	319

## LIST OF SCHEMES

Scheme	Page
1. Synthesis of <i>Z</i> -alkenyl halides .....	5
2. Partial hydrogenation of alkynes .....	5
3. Synthesis of <i>Z</i> -alkenyl bromides via hydroboration-bromination-elimination.....	6
4. <i>Z</i> -selective ROCM of oxabicycles with styrene .....	6
5. Proposed model for <i>Z</i> selectivity in the ROCM .....	7
6. Triplet sensitized photoisomerization of $\beta$ -ionol .....	9
7. Photocatalytic C–F alkenylation and isomerization.....	10
8. Optimization of reaction conditions.....	20
9. Substrate scope.....	22
10. Stereochemical probe for mechanistic studies.....	26
11. Photochemical <i>E/Z</i> isomerization of non-oxidizable styrene derivatives.....	26
12. Cycloaddition strategies.....	106
13. Cycloaddition of tetrazine with <i>trans</i> -cyclooctene .....	107
14. Initial investigation .....	109
15. Substrate scope of the strain induced [3+2] cycloaddition reaction .....	115
16. Reaction performed in presence of BSA .....	117
17. Attempted cycloaddition of tetrazine with PC8.....	118
18. Conjugation of a tripeptide .....	121
19. Attempt to make bioconjugation conditions more water compatible. ....	126
20. Trapping of <i>t</i> -PC8 with benzyl azide .....	130
21. Proposed mechanism of intramolecular hydroalkoxylation .....	276

## LIST OF TABLES

Table	Page
1. Summary of various substrates with their yields .....	29
2. Summary of substrates with their yield in final step.....	31
3. Stability studies of triazoline products.....	119
4. Reaction outcome in presence of various fluorophores .....	120
5. Optimization of reaction conditions.....	133
6. Reaction outcome in presence of thiols .....	152
7. Stability studies of Traizoline <b>3b</b> .....	154
8. Optimization of [ $\pi 2_s + \pi 2_a$ ] cycloaddition reaction conditions .....	189
9. Substrate scope of [ $\pi 2_s + \pi 2_a$ ] cycloaddition.....	195
10. Substrates producing undesired products/ no product .....	219
11. Optimization of reaction conditions.....	264
12. Scope of the photocatalytic cyclization. ....	265
13. Summary of various substrates <b>A</b> with their yields .....	277
14. Summary of various substrates <b>B</b> with their yields .....	278
15. Summary of various substrates <b>C</b> with their yields. ....	279

## LIST OF FIGURES

Figure	Page
1. Photoredox properties of <i>fac</i> -Ir(ppy) <sub>3</sub> .....	14
2. Singlet-singlet Förster energy transfer.....	15
3. Triplet-triplet Dexter energy transfer.....	16
4. A Stern-Volmer photoquenching plot of <b>1s</b> and <b>2s</b> . ....	24
5. Potential explanation for the isomerization of the alkene.....	24
6. Energy transfer mechanism.....	25
7. Ir(ppy) <sub>3</sub> emission quenching by <b>2s</b> ( <i>Z</i> )-4-(3-(2-(( <i>tert</i> - butyldimethylsilyl)oxy)phenyl)allyl)morpholine. ....	53
8. Ir(ppy) <sub>3</sub> emission quenching by <b>1s</b> ( <i>E</i> )-4-(3-(2-(( <i>tert</i> - butyldimethylsilyl)oxy)phenyl)allyl)morpholine. ....	54
9. Energy landscapes.....	111
10. Demonstration of biotin conjugation to insulin. ....	123
10a. Insulin stability experiment.....	124
11. X-ray crystal structure of major regioisomer <b>3</b> .....	127
12. HSQC data for <b>3a</b> .....	129
13. Minimized energy structure for minor regioisomer <b>3aa</b> or <b>3ab</b> and diastereomer <b>3ac</b> .....	130
14. First order graph between ln([Azide]/[Azide] <sub>0</sub> ) and time.....	150
15. X-ray crystal structure of <b>d-4a</b> .....	190
16. Rationale for the relative stereochemistry of the major observed diastereomer, <b>A1</b> , during [ $\pi 2_s + \pi 2_a$ ] cycloaddition. ....	191
17. The energies of the various diastereomers reported are relative to the phenyl cycloheptene as calculated using B3LYP/6-31 G(d).....	193
18. Conformational analyses.....	267
19. Potential diastereomers that leads to ring closure.....	269
20. Deuterium incorporation with <b>1a</b> and computational identification of axial and equatorial protons of product <b>5a</b> . ....	271
21. Titration of <b>1f</b> with formic acid. ....	273
22. Presumptive transition state geometry identified by HF/3-21G. Proton transfer pathways indicated by dashed lines. ....	274

## CHAPTER I

### INTRODUCTION

#### **1.1 Historical background**

The ability to synthesize molecules is of paramount importance in the modern world. As the scope of organic synthesis continues to grow, our need to study it increases accordingly. The inspection of the nature of chemical reactions reveals that generally only exergonic reactions are developed. Obviously, this is because reactions move in the direction that leads to products which are lower in energy. Importantly, since the principle of microscopic reversibility dictates that any reaction catalysis achieved in one reaction direction will also necessarily facilitate the backward reaction direction, thermal catalysis cannot circumvent this restriction. As such, the catalysis of potential endergonic reactions are generally not considered since thermal catalysis cannot promote these reactions. However, this limitation can be overcome by utilizing excited state surfaces, from which all reaction directions are essentially exergonic. In this context, light has played a pivotal role in not only promoting formally endergonic processes by providing energy, but also generating the electronically excited states from which chemical reactions can take place, that are forbidden in the ground state. The field of photochemistry has allowed the generation and utilization of electronically excited species to promote novel modes of reactivity, which are simply not possible in the ground state. There are some elegant examples in which nature utilizes the photochemical energy to bring about intriguing transformations.<sup>1</sup> For instance, the photochemical formation of Vitamin D,<sup>2</sup> in which the first step of the reaction is initiated by the absorption of a

photon which results in the electrocyclic ring opening of 7-dehydrocholesterol to form previtamin D<sub>3</sub>. Another important photochemical reaction that takes place in the human body is the *cis-trans* photoisomerization of 11-*cis*-retinal chromophore, bound within rhodopsin protein, which is the most important step in vision.<sup>3-4</sup>

Another very important phenomenon is photosynthesis. In photosynthesis nature converts solar energy into stored energy. Plants accomplish photosynthesis with just a couple of photochemical reactions, and store the energy in the form ATP (adenosine triphosphate) and NADPH (reduced nicotinamide adenine dinucleotide phosphate), as well as proton gradients which are used to sustain life.<sup>5</sup> These two compounds can then serve as the energy currency for the subsequent dark reactions, by either undergoing hydrolysis or oxidation respectively. It is one of the very few examples of systems in which energy stored during the endergonic reactions is utilized for further chemical synthesis. In a most elegant fashion, these molecules effectively allow the energy to be stored and then used at a later point in time, and ultimately allow the energy generation (i.e. photon absorption) to be decoupled from the usage step. The ramifications are extraordinary. Nature can effectively develop the catalytic machinery to hydrolyze units of ATP or oxidize units of NADPH until the desired thermal reaction becomes exergonic. On average the hydrolysis of ATP provides ~8 kcal/mol, though the exact amount varies with the conditions. Furthermore, Nature has learned to recycle the energy currency such that energy is not wasted on the currency's construction. Importantly, no synthetic analogs to photosynthesis currently exist. A synthetic equivalent to photosynthesis could allow the potential of the excited state surface to drive reactions in endergonic directions, expanding greatly the possibilities of synthesis.

Most of the photochemical reactions developed utilize UV irradiations to either excite organic molecules directly or in a sensitized manner to higher energy levels. This limitation stems from the fact that most organic molecules do not absorb in the visible region, and instead require higher energetic (short wavelength) UV irradiation to excite those molecules. This limits the

functional group compatibility, and often leads to low selectivity of photochemical reactions. Moreover, UV light requires specialized glassware to carry out reactions, which is expensive and typically requires special cooling apparatus as it gives off substantial heat during UV irradiation. Special space is often dedicated to carrying out these reactions in order to protect people from being exposed to these irradiations. These reasons have effectively limited the application and utilization of photochemistry in synthesis.

Photocatalysis has emerged as a powerful tool in overcoming these limitations posed by direct irradiation using UV light sources. In photocatalysis, a photocatalyst absorbs a visible light photon which then activates the organic molecules by electron or energy transfer processes.<sup>6-9</sup> The intermediate formed as a result of excitation behaves very differently from the corresponding ground state molecule. This difference in the reactivities between the ground state and the excited state brings about the elegant transformations that are simply not possible in the ground state. Photoredox catalysis have the ability to perform redox neutral reactions. This methodology is in sharp contrast to the traditional approaches which requires stoichiometric oxidants and reductants (generally not compatible with each other), since it can generate the oxidant and reductant at disparate times during the reaction.

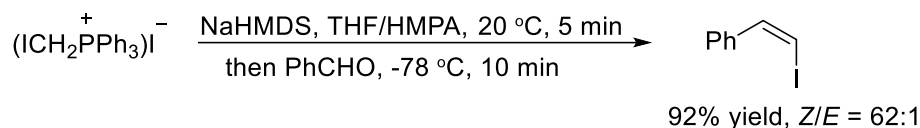
Much of the work in this thesis focuses on energy transfer, in which a molecule is promoted to its higher energy excited state. However, the excited state surfaces are typically relatively flat and quickly relax back to ground state. While this means that the energetics of almost all reactions are now more favorable, this provides limited modes of control over reactivity. One alternative approach to performing bond making and breaking directly on the excited state molecule would be to rely on the transfer of energy from the excited state molecule to the ground state molecule, in which properties of the ground state molecules might play a greater role in the relative rates of processes. The central idea of this research work was to develop strategies to utilize photochemical energy for the development of synthetic methodologies. The primary strategy explored in this thesis

is the *cis-to-trans* isomerization of acyclic alkenes. Since the *cis* isomers of acyclic alkenes are higher in energy compared to their *trans* isomers, thermal catalysis cannot directly isomerize the *trans* alkenes to *cis*-alkenes. On the other hand, photocatalysis can excite the molecules to higher energy states from where all other reactions are downhill in nature. This approach would enable us to drive the reactions in an endergonic direction by performing *trans* to *cis* isomerization of acyclic alkenes. Similarly, when the reaction is applied to a cyclic alkene, due to the inability of the cyclic alkene to accommodate the ideal alkene geometry, a highly strained *trans*-cycloalkene would be formed. The strain associated with *trans*-cycloalkenes could then be utilized to facilitate ground state synthesis. Collectively, this would allow the harvesting of visible light energy to generally drive synthesis.

Alkenes are ubiquitous in nature and are also found in biologically relevant motifs.<sup>10-13</sup> These oftentimes serve as building blocks for a variety of chemical transformations such as enantioselective hydrogenation,<sup>14-15</sup> hydrohalogenation,<sup>16-17</sup> hydroboration,<sup>18-20</sup> epoxidation,<sup>21-22</sup> and ozonolysis<sup>23-24</sup> of alkenes. The acyclic alkenes can exist in two different stereoisomeric forms namely the *E*- or *Z*-isomer. Generally, the *E*-isomer of acyclic alkenes are thermodynamically more favorable than the *Z*-isomer. For instance, *trans*-but-2-ene is approximately 1.2 kcal/mol stable than its *cis* isomer.<sup>25</sup> In this case, the difference in energy is due to the increased interactions between the methyl groups present on the same side of the *cis* isomer. These stereoisomers of alkenes have different physical properties, and can have different outcomes during stereoselective reactions which depend on the geometric isomer employed in the reaction. Therefore, synthetic access to either isomer is a crucial component of alkene synthesis. Generally speaking, only a handful of methodologies is available to access *Z*-alkenes selectively in comparison to *E*-alkenes.

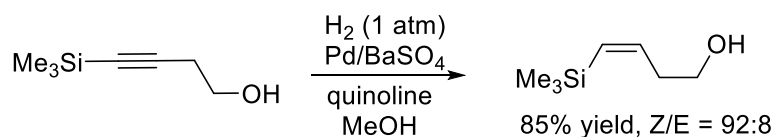
Wittig olefination is one of the classical examples utilized for the selective synthesis of *Z*-alkenes.<sup>26</sup> In this reaction, a phosphorus ylide reacts with the carbonyl compound to yield the desired *Z*-alkene in good to excellent selectivities along with the stoichiometric generation of

phosphine oxide as the side product. For example, the Wittig reaction was utilized by Stork in the preparation of *Z*-alkenyl halides<sup>27</sup> (Scheme 1). In the first step, sodium hexamethyldisilazane (NaHMDS) deprotonates the iodoalkyl phosphonium salt to generate the ylide which reacts with the aldehyde to produce the *Z*-alkenyl halide in good to excellent stereoselectivity (Scheme 1).



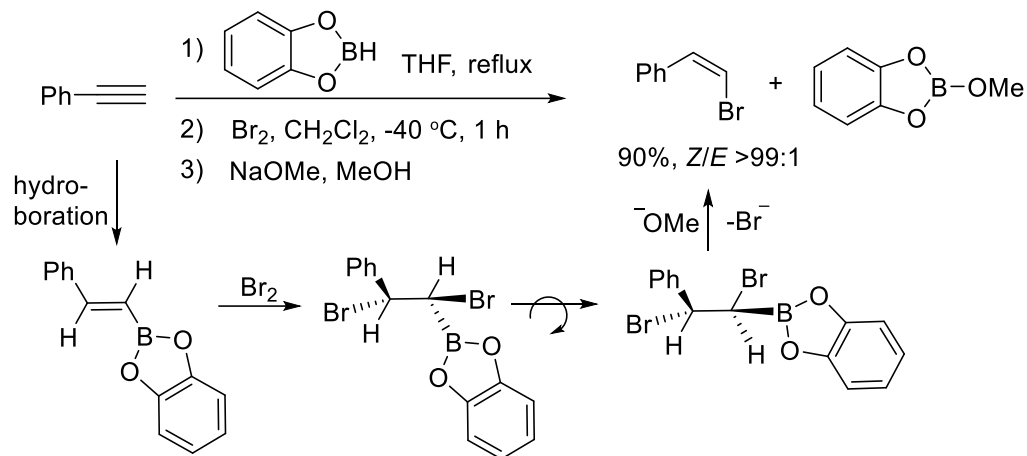
Scheme 1. Synthesis of *Z*-alkenyl halides

Another strategy that is widely used for the synthesis of disubstituted *Z*-alkenes is the partial hydrogenation of alkynes using Lindlar's catalyst.<sup>28</sup> The Pd catalyst used in the Lindlar's reduction is deposited on CaCO<sub>3</sub> and is poisoned with lead acetate or lead oxide and quinoline. The poison (quinolone, pyridine, ethylenediamine) reversibly adsorbs onto the catalyst and competes with the adsorption of product alkene, which avoids the over reduction of desired product alkenes to alkanes.<sup>29</sup> This procedure was utilized by Overman in the synthesis of *Z*-buten-1-ol<sup>30</sup> (Scheme 2).



Scheme 2. Partial hydrogenation of alkynes

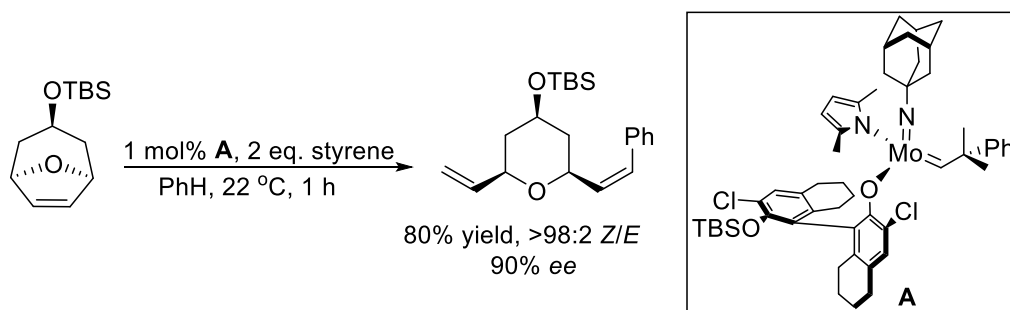
In 1973, the Brown group reported a multistep methodology to convert alkynes into alkenyl bromides with high *Z*-selectivity.<sup>31</sup> This procedure involves the *syn*-hydroboration of the alkynes to yield substituted alkenes. This is followed by the *trans*-bromination of the corresponding alkenes and the base induced *trans*-elimination of the boron and bromine results in the desired alkenyl bromides in high selectivities (Scheme 3).



Scheme 3. Synthesis of *Z*-alkenyl bromides via hydroboration-bromination-elimination

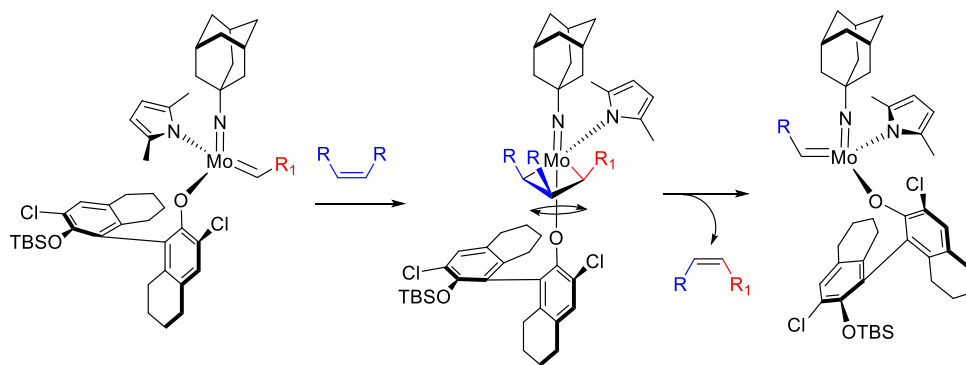
Another more recently developed methodology that has been utilized for the stereoselective synthesis of *Z*-alkenes is cross metathesis. Alkene metathesis reaction has been widely used in total synthesis due to the mildness and the ubiquity of alkenes as starting materials.<sup>32</sup> The key challenge in alkene metathesis is controlling the geometry of alkenes, and care must be taken to prevent the kinetically formed *Z*-alkene from undergoing a secondary isomerization reaction with the catalyst to produce the more stable *E*-alkene. Various iterations of catalysts have been designed, since the first report of preparation and characterization of an active metathesis catalyst<sup>33</sup> in 1980, and high levels of *Z*-selectivity for certain alkenes can be achieved.<sup>34-35</sup>

In 2009, a first example of highly selective ring opening cross-metathesis (ROCM) was reported by Schrock and Hoveyda. The ROCM reaction of oxabicycles with styrene produces the trisubstituted tetrahydropyran product in high *Z*-selectivity and enantioselectivity. (Scheme 4)<sup>36</sup>



#### Scheme 4. Z-selective ROCM of oxabicycles with styrene

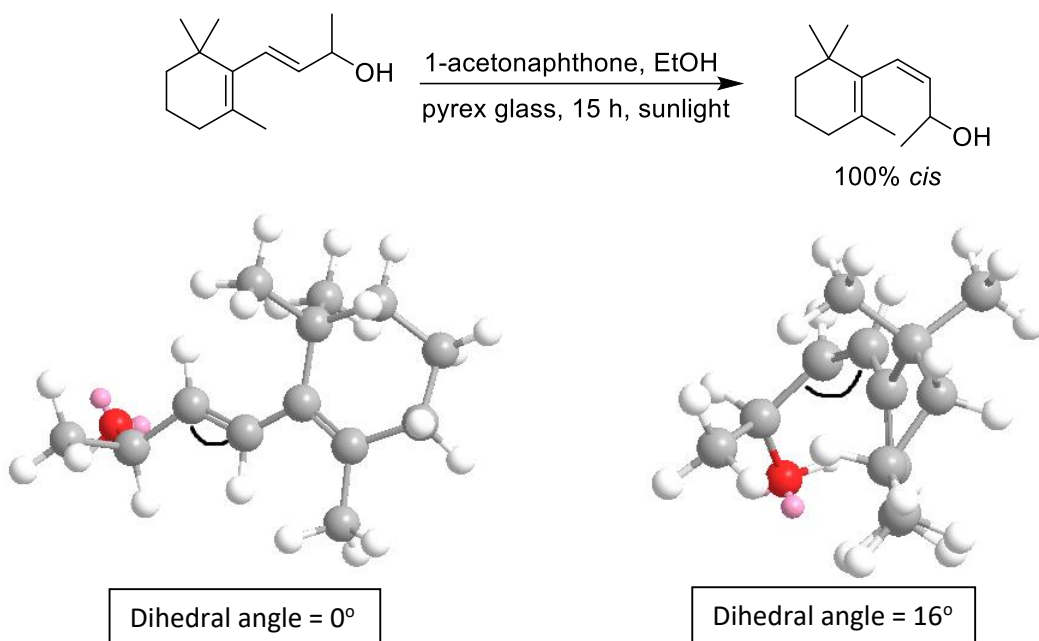
The size difference between the small imido ligand (adamantyl) and the large aryloxide ligand was considered pivotal for the Z-selectivity. It is worth mentioning that when a smaller adamantyl imido ligand was replaced with a bulky 2,6-diisopropylphenyl imido group, no product was observed. This could be due to the fact that a large arylimido group, together with the bulky aryloxide ligand, makes the Mo complex too sterically crowded to allow the formation of *syn* or *anti* alkylidene and subsequent metathesis to take place. The bulky but freely rotating Mo-O bond in combination with the small imido ligand favors the approach of the incoming alkene to form *cis*-metallacyclobutane. Such approach, after cycloreversion, produces the Z-alkenes in high selectivity (Scheme 5)



#### Scheme 5. Proposed model for Z selectivity in the ROCM

All of the methodologies discussed above utilize the ground state reactivities of various reagents to achieve the Z-alkenes. On the other hand, excited state surface has also been utilized to isomerize *E*-alkenes to Z-alkenes. The direct irradiation of alkenes with a light source of longer wavelength (>310 nm) allows to enrich the reaction mixture of stilbene and its derivative with *cis*-isomer. The reactions occurring from the singlet excited states under direct irradiation is accompanied by other side reactions taking place due to the symmetry allowed reactions. For instance, the isomerization of stilbene is accompanied by slow and irreversible formation of

dihydrophenanthrene.<sup>37</sup> One way to circumvent this limitation is sensitization. The advantage of the reaction occurring from a triplet state is that symmetry allowed reactions are not feasible from the triplet state and hence avoid side reactions that takes place from the singlet excited state. The photochemical isomerization of alkenes (dienes, polyenes, stilbenes) has been achieved via direct irradiation of UV light or in the presence of triplet sensitizers.<sup>38-41</sup> The various planar triplet sensitizers that have been employed in these photochemical isomerization of alkenes generally are benzene, benzophenone, Michler's ketone, benzil, 9-fluorenone, benzanthrone, and others with varying triplet energies. The selective triplet sensitization of one of the isomers can lead to the enrichment of the other stereoisomer. For instance, the *trans* isomer of  $\beta$ -ionol isomerizes completely (100%) to its *cis* isomer in the presence of 1-acetonaphthone ( $E_T = 57$  kcal/mol) (Scheme 6).<sup>42</sup> This is due to the presence of methyl groups close to the double bond which makes the *cis* isomer extremely congested and forces it to exist in a twisted conformation. The dihedral angle (calculated using Chem 3D software) for the *trans* isomer was found to be  $0^\circ$  and suggests that the double bond is planar with the cyclohexene ring. On the other hand, the dihedral angle for the *cis* isomer was found to be  $16^\circ$  out of plane (as shown in Scheme 6). As a result, the triplet energy of the *cis* isomer is raised ( $E_T = 72$  kcal/mol)<sup>43</sup> allowing the sensitizer to selectively excite the *trans* isomer resulting in build up of the *cis* alkene.

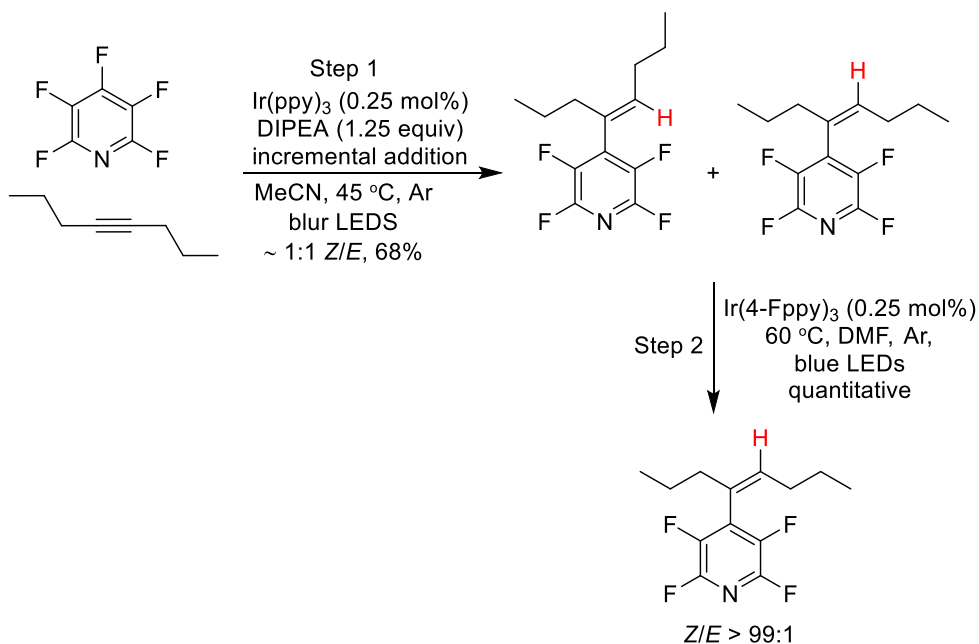


Scheme 6. Triplet sensitized photoisomerization of  $\beta$ -ionol

Not only has selective sensitization of one isomer been utilized to achieve selectivity but the sterics associated with the sensitizer's molecular structure have also been evaluated. The sterically hindered sensitizer has shown biasedness for the triplet energy transfer towards the *trans* alkenes. In 1966, Hammond evaluated the effect of steric hindrance to energy transfer.<sup>44</sup> It was found that the rate, and hence the photostationary state ratio of the alkenes, of triplet energy transfer to the *trans* and *cis* stilbene was different when structurally different sensitizers with similar triplet energy were employed. For instance, benzophenone gave a mixture of stilbene in the ratio of 1.45 *cis/trans* whereas when more sterically demanding 2,4,6-triisopropylbenzophenone was used as the sensitizer, the *cis/trans* ratio increased to 1.92 indicating sensitivity to sterics and more specifically a less efficient energy transfer to *cis*-stilbene compared to its *trans* isomer.

In 2016, our group demonstrated the photocatalytic C–F alkenylation of perfluoroarenes with alkynes.<sup>45</sup> In this reaction, the fragmentation of the C–F bond is initiated by the addition of an electron to the perfluoroarene. This leads to a perfluoroaryl radical which undergoes addition to the alkyne and subsequent hydrogen atom abstraction by the incipient vinyl radical to preferentially

give the *trans* alkene (Scheme 7, step 1). The photocatalyst then undergoes an energy transfer process as compared to electron transfer process from the excited state to isomerize the *E*-alkene and enrich the reaction mixture with thermodynamically less favorable *Z*-alkene (Scheme 7, step 2). The exact selectivity depends primarily on the substituent of the alkyne, with larger groups giving higher selectivity. With the judicious choice of photocatalyst, both the electron and energy transfer process are controlled and selective access to either isomers of alkene can be achieved.<sup>46</sup> Our observation is somewhat different than Hammond's in that we also observe a difference between the rates of electron transfer and energy transfer, rather than just a substrate selectivity.



Scheme 7. Photocatalytic C–F alkenylation and isomerization

The bulk of this research work deals with the isomerization of alkenes using visible light and a transition metal based photocatalyst iridium phenylpyridine, Ir(ppy)<sub>3</sub>, or its analogs. This study started with the development of a mild methodology to isomerize acyclic *E*-styrenoids to the corresponding *Z*-isomers.<sup>47</sup> Here we show that, by exciting the photocatalyst to its excited triplet state, the photocatalyst undergoes an energy transfer process which results in the excitation of the ground state *E*-alkene to its triplet excited state. The excited triplet biradical can undergo rotation

about the former double bond. As it approaches a 90° rotation about the former double bond, it is believed to approach a conical intersection, where it undergoes intersystem crossing very near the transition state for rotation about the double bond. From this transition state it can further relax to give the *E*- or *Z*-alkene. Typically, the photostationary state favors the *Z*-alkenes. The Stern-Volmer quenching studies provide evidence into the operative mechanism and will be discussed in Chapter II.

We envisioned that if the same isomerization strategy was applied to the cyclic alkenes, we might be able to capture some of the photochemical energy by isomerization of the cyclic *cis*-alkenes to cyclic *trans*-alkenes. The *trans*-cycloalkenes would be strained because of the necessary deformation associated with the achieving the *trans*-geometry within a small ring. We expected that the relative lifetime of the strained species to be longer than the excited state species, and that this strain could be harnessed in controllable thermal transformations.<sup>48</sup> With judicious choice and computational screening, we synthesized a cycloheptene ring fused with a benzene ring, such that the double bond in the cycloheptene ring is in conjugation with the benzene ring. Upon exposure to visible light and a photocatalyst, this alkene underwent isomerization to transiently generate a very strained benzofused *trans*-cycloheptene which was captured with various aliphatic azides to give a [3+2] cycloaddition reaction and generate triazoline products (Chapter III). The concept of harvesting visible light energy was further applied to develop a rare thermal [2+2] cycloaddition reaction of phenylcycloheptene to produce cyclobutanes in a diastereoselective fashion. Computational analysis of the reaction reveals that this cycloaddition reaction is net endergonic in nature, highlighting the ability of photocatalysis to facilitate contra-thermodynamic catalysis (Chapter IV).

Another important chemical transformation that was developed on the same principle of harvesting visible light energy was the synthesis of cyclic bridged ethers from phenylcyclohexenols in presence of a mild acid. The generation of *trans*-cyclohexene in the presence of a photocatalyst

and visible light enables the hydro alkoxylation of the trans-cycloalkene by an internal hydroxyl group to generate cyclic bridged ethers. Computational studies and kinetic experiments help unravel the mechanism of the etherification of phenylcyclohexenols (Chapter V).

Many researchers have capitalized on strain energy to promote synthesis and bring about novel reactions. In 2011, Danishefsky *et al* showed that highly strained cyclobutenone reacts rapidly with cyclopentadiene to give [4+2] Diels-Alder cycloadducts at room temperature, whereas cyclopentenone results in greatly diminished activity even at elevated temperatures.<sup>49-51</sup> Strained alkenes also exhibit high reactivity as compared to their strain-free analogs.<sup>52-54</sup> Fox and coworkers have utilized preformed *trans*-cyclooctenes, which undergo click reaction with tetrazines resulting in [4+2] Diels-Alder cycloadduct.<sup>55</sup> In a parallel context, Garg and co-workers have shown that the highly strained molecules need not to be isolated, particularly cycloarynes, were generated from the reaction of corresponding *ortho*-silyl triflate and cesium fluoride *in situ*, which were trapped by various trapping agents such as furan, *N*-Boc pyrrole, 2-pyrone, 1,3-dimethyl-2-imidazolidinone, imidazole, azides, ylides, nitrones, and others to give the respective cycloaddition products formed as result of release of strain from the cycloaryne intermediates. This strategy has enabled the synthesis of complex and medicinally relevant organic molecules, such as (-)-tubingensin B, (-)-teleocicin A-2, and (-)-*N*-Methylwelwitindolinone B isothiocyanate.<sup>56-58</sup> Light energy is utilized by nature to drive important processes such as photosynthesis. Light induced chemical reactions are initiated by the absorption of light, which generates highly reactive species that undergo chemical changes. This includes light induced Diels-Alder cycloaddition reaction,<sup>59</sup> photoinduced cycloaddition of tetrazoles and alkenes,<sup>60</sup> photoinduced thiol-ene/-yne reactions,<sup>61</sup> strain induced cycloaddition reaction between photochemically produced cyclooctynes and azides.<sup>62</sup> Light induced chemical reactions have the advantage over conventional thermal reactions in that these reactions provide the potential for spatial and temporal control since photons can be delivered to a specific area as needed.<sup>63</sup>

Another class of strained molecules that has been utilized is the *trans*-cycloalkenes, which are strained because of the deformation of the ideal olefin geometry, the strain energy is inversely proportional to the ring size. While *trans*-cyclooctenes are sufficiently stable to be isolated,<sup>64</sup> *trans*-cycloheptene,<sup>65</sup> and *trans*-cyclohexenes<sup>66</sup> have only been observed at low temperatures via direct UV-photolysis. The smaller cyclic *trans*-alkenes have not been utilized for the purpose of chemical synthesis, but rather most studies have focused on proving their mere existence as real intermediates.

## 1.2 Discussion of photocatalyst

The transition metal complex that was mostly used in this study was the *fac*-tris[2-phenylpyridinato-*C*<sup>2</sup>,*N*]iridium(III), Ir(ppy)<sub>3</sub>, along with its analogs. This photocatalyst shows a maximum absorption at 375 nm with its absorbance extending into the visible region ranging from 320 to 480 nm.<sup>67</sup> This absorption band is due to both the spin allowed and the spin forbidden metal to ligand charge transfer (MLCT). Upon absorption of a photon in the visible region, an electron present in the t<sub>2g</sub> orbital of the metal gets excited to the π\* (also called LUMO) of the ligand. The resulting species has very unique properties as the metal center is oxidized and simultaneously the ligand is reduced. The MLCT singlet excited state rapidly converts itself to a longer-lived lower energy triplet excited state via intersystem crossing (ISC). The longer lifetime of the triplet excited state is due to the fact that its decay to the singlet ground state is spin forbidden.<sup>68</sup> The excited state of Ir(ppy)<sub>3</sub> has a relatively long lifetime (τ = 1.9 μs) and the triplet state energy of Ir(ppy)<sub>3</sub> is 56 kcal/mol above its ground state.<sup>69</sup> The excited photocatalyst has remarkable properties of both being oxidant and reductant (Fig. 1). From the excited state, the photocatalyst can be quenched either by electron transfer mechanism (oxidatively or reductively)<sup>70</sup> or by energy transfer pathway.<sup>47</sup>

### 1.21 Quenching by electron transfer mechanism

In the oxidative quenching cycle (Figure 1, upper half), the  $^*Ir(ppy)_3^{3+}$  serves the role of a reductant ( $E_{1/2}^{(IV)/(III)*} = -1.73$  V vs SCE)<sup>71</sup> and donates an electron to the electron acceptor (**A**). Examples of oxidative quenchers include aryl iodides ( $E_{1/2}^{red} = -1.67$  V vs SCE).<sup>72</sup> This redox event leads to the formation of radical anion of **A** and the oxidized photocatalyst  $Ir(ppy)_3^{4+}$ . This oxidized photocatalyst is a potent oxidant ( $E_{1/2}^{(IV)/(III)} = 0.77$  V vs SCE) and can accept an electron from a donor (**D**), generating radical cation of **D** and simultaneously returning the catalyst to the ground state completing the photocatalytic cycle.

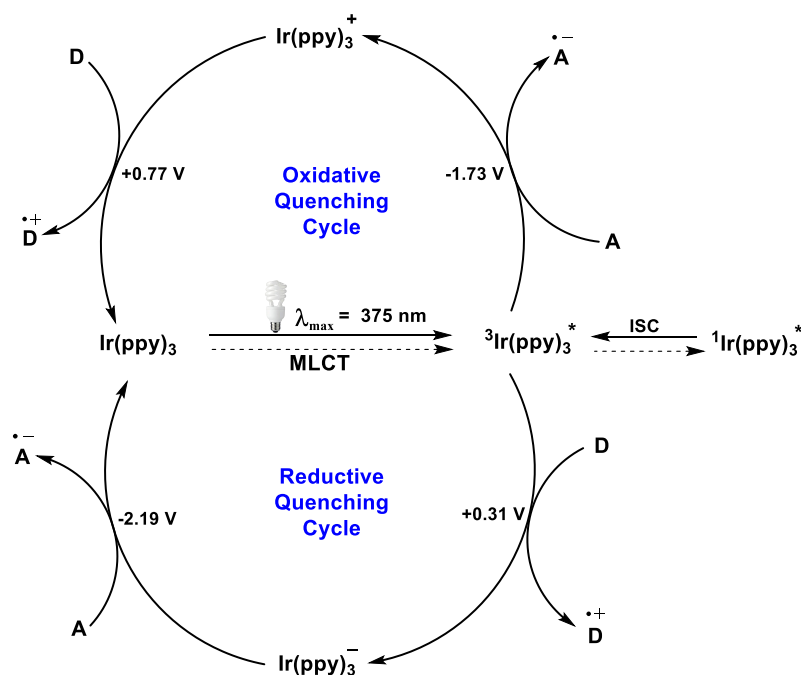


Figure 1 Photoredox properties of *fac*-Ir(ppy)<sub>3</sub>

In the reductive quenching pathway (Figure 1, lower half), the  $^*Ir(ppy)_3^{3+}$  behaves as an oxidant ( $E_{1/2}^{(III)*/(II)} = 0.31$  V vs SCE)<sup>70</sup> and accepts an electron from a donor (**D**) species  $Ir(ppy)_3^{2+}$  and generating radical cation of **D**. This intermediate Ir(II) is one of the most potent reductants known ( $E_{1/2}^{(III)/(II)} = -2.19$  V vs SCE) and can donate an electron to an acceptor molecule (**A**), generating radical anion of **A** and ground state Ir(III) species and closing the photocatalytic cycle.

## 1.22 Quenching by energy transfer mechanism

The excited photocatalyst can also be quenched back to its ground state by a different type of mechanism apart from the two discussed in section 1.21. This mechanism is operated by energy transfer between the excited state photocatalyst (**PC**) and a ground state molecule (**M**). This energy transfer mechanism can take place by two different types of interactions; either by dipole-dipole interactions (also known as Förster energy transfer)<sup>73</sup> or by electron exchange (orbital overlap) mechanism (also known as Dexter energy transfer).<sup>74</sup>

On absorption of a photon of light, the donor molecule **PC** goes to its excited singlet state  $^1\text{PC}^*$  (Figure 2). The excited donor molecule then transfers its energy to the ground state acceptor molecule **M**. As a result, the excited donor molecule  $\text{PC}^*$  returns back to its ground state simultaneously exciting the acceptor molecule to its singlet excited state  $^1\text{M}^*$ . In Förster energy transfer mechanism, the interactions with which the energy transfer takes place are dipole-dipole in nature. The electrons do not change molecules or orbitals but instead two transitions take place simultaneously. Since no electrons are exchanged between the molecules, the Förster energy transfer mechanism does not require any physical contact between donor and acceptor molecules to take place. It has been found that the rate of energy transfer in such type of mechanism is inversely proportional to the sixth power of the distance between the interacting molecules.<sup>75</sup> This dipole-dipole energy transfer is spin forbidden and occurs only in singlet-singlet energy transfer.<sup>76</sup> This stems from the fact that the transitions that conserve the multiplicity are associated with the large transition dipoles.<sup>77</sup>

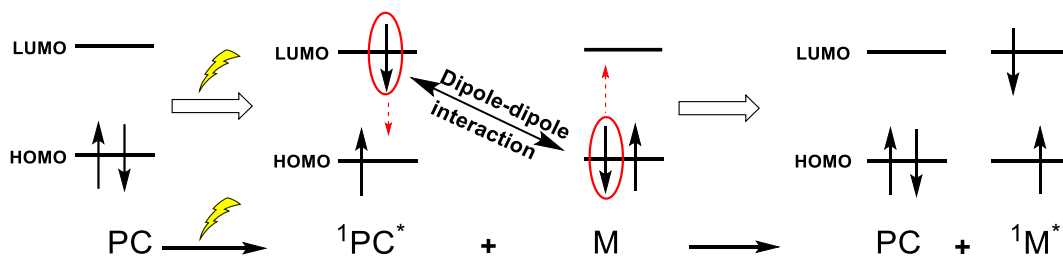


Figure 2 Singlet-singlet Förster energy transfer

The other type of energy transfer mechanism is called Dexter energy pathway, which results from the collision between the molecules. On absorption of photon of light, the donor molecule **PC** goes to its excited singlet state  $^1\text{PC}^*$  (Figure 3). After ISC, the molecule goes to the lower energy longer lived triplet excited state  $^3\text{PC}^*$ . From the triplet excited state, the electron in the former LUMO of donor molecule is transferred to the LUMO of the acceptor molecule. Simultaneously, one of the electrons present in the HOMO of the acceptor molecule transfers to the former HOMO of the donor molecule. As a result, the acceptor molecule is now in its triplet excited state ( $^3\text{M}^*$ ) returning the excited donor back to its ground state. The Dexter energy transfer mechanism differs from the Förster energy transfer mechanism in several key manners. In the Dexter energy transfer, the orbital overlap is crucial. This is evidenced by the fact that the rate of energy transfer falls off exponentially when the orbitals of  $^3\text{PC}^*$  and **M** cannot obtain an intimate overlap<sup>76</sup>. It is worth noting that this is a concerted two electron transfer process requiring a good overlap between the former HOMO of  $^3\text{PC}^*$  and the HOMO of **M**, as well as the former LUMO of  $^3\text{PC}^*$  and the LUMO of **M**, which is a greater degree of orbital overlap restriction than most chemical reactions.

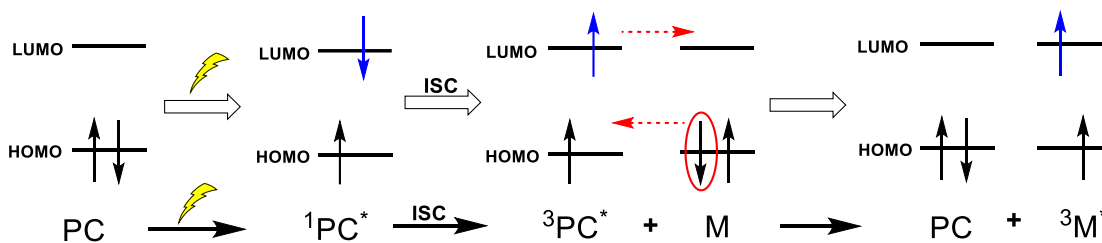


Figure 3 Triplet-triplet Dexter energy transfer

## References

1. Hoff, W. D.; van Stokkum, I. H.; van Ramesdonk, H. J.; van Brederode, M. E.; Brouwer, A. M.; Fitch, J. C.; Meyer, T. E.; van Grondelle, R.; Hellingwerf, K. J., *Biophys. J.* **1994**, *67*, 1691.
2. Anderson, N. A.; Shiang, J. J.; Sension, R. J., *J. Phy. Chem. A* **1999**, *103*, 10730.
3. Wald, G., *Nature* **1968**, *219*, 800.
4. Johnson, P. J. M.; Halpin, A.; Morizumi, T.; Prokhorenko, V. I.; Ernst, O. P.; Miller, R. J. D., *Nat. Chem.* **2015**, *7*, 980.
5. van Grondelle, R.; Dekker, J. P.; Gillbro, T.; Sundstrom, V., *Biochimica et Biophysica Acta* **1994**, *1187*, 1.
6. Prier, C. K.; Rankic, D. A.; MacMillan, D. W. C., *Chem. Rev.* **2013**, *113*, 5322.
7. Koike, T.; Akita, M., *Synlett* **2013**, *24*, 2492.
8. Hari, D. P.; Konig, B., *Chem. Commun.* **2014**, *50*, 6688.
9. Nicewicz, D. A.; Nguyen, T. M., *ACS Catal.* **2014**, *4*, 355.
10. Levenson, A. S.; Jordan, V. C., *Eur. J. Cancer* **1999**, *35*, 1628.
11. McKinley, N. F.; O'Shea, D. F., *J. Org. Chem.* **2006**, *71*, 9552.
12. Molander, G. A.; St. Jean, D. J., *J. Org. Chem.* **2002**, *67*, 3861.
13. Williams, R. B.; Norris, A.; Slebodnick, C.; Merola, J.; Miller, J. S.; Andriantsiferana, R.; Rasamison, V. E.; Kingston, D. G. I., *J. Nat. Prod.* **2005**, *68*, 1371.
14. Troutman, M. V.; Appella, D. H.; Buchwald, S. L., *J. Am. Chem. Soc.* **1999**, *121*, 4916.
15. Smidt, S. P.; Zimmermann, N.; Studer, M.; Pfaltz, A., *Chem. Eur. J.* **2004**, *10*, 4685.
16. Castellanos, A.; Fletcher, S. P., *Chem. Eur. J.* **2011**, *17*, 5766.
17. Hennecke, U., *Chem. Asian J* **2012**, *7*, 456.
18. Brown, H. C.; Jadhav, P. K.; Bhat, K. S., *J. Am. Chem. Soc.* **1988**, *110*, 1535.
19. Yamamoto, Y.; Fujikawa, R.; Umemoto, T.; Miyaura, N., *Tetrahedron* **2004**, *60*, 10695.
20. Greenhalgh, M. D.; Thomas, S. P., *Chem. Commun.* **2013**, *49*, 11230.
21. Katsuki, T.; Sharpless, K. B., *J. Am. Chem. Soc.* **1980**, *102*, 5974.
22. McGarrigle, E. M.; Gilheany, D. G., *Chem Rev.* **2005**, *105*, 1563.
23. Horie, O.; Moortgat, G. K., *Acc. Chem. Res.* **1998**, *31*, 387.
24. Willand-Charnley, R.; Fisher, T. J.; Johnson, B. M.; Dussault, P. H., *Org. Lett.* **2012**, *14*, 2242.
25. Matta, F. C.; Sadjadi, S. A.; Braden, D. A.; Frenking, G., *J. Comput. Chem.* **2016**, *37*, 143.
26. Bergelson, L. D.; Shemyakin, M. M., *Tetrahedron* **1963**, *19*, 149.
27. Stork, G.; Zhao, K., *Tetrahedron Lett.* **1989**, *30*, 2173.
28. Lindlar, H., *Helv. Chim. Acta* **1952**, *35*, 446.
29. Gruttadauria, M.; Noto, R.; Deganello, G.; Liotta, L. F., *Tetrahedron Lett.* **1999**, *40*, 2857.
30. Flann, C.; Malone, T. C.; Overman, L. E., *J. Am. Chem. Soc.* **1987**, *109*, 6097.
31. Brown, H. C.; Hamaoka, T.; Ravindran, N., *J. Am. Chem. Soc.* **1973**, *95*, 6456.
32. Nicolaou, K. C.; Bulger, P. G.; Sarlah, D., *Angew. Chem. Int. Ed.* **2005**, *44*, 4490.
33. Schrock, R.; Rocklage, S.; Wengrovius, J.; Rupprecht, G.; Fellmann, J., *J. Mol. Catal.* **1980**, *8*, 73.
34. Schrock, R. R.; Murdzek, J. S.; Bazan, G. C.; Robbins, J.; DiMare, M.; O'Regan, M., *J. Am. Chem. Soc.* **1990**, *112*, 3875.
35. Sanford, M. S.; Love, J. A.; Grubbs, R. H., *J. Am. Chem. Soc.* **2001**, *123*, 6543.
36. Ibrahim, I.; Yu, M.; Schrock, R. R.; Hoveyda, A. H., *J. Am. Chem. Soc.* **2009**, *131*, 3844.
37. A. Gilbert, Handbook of Organic Photochemistry and Photobiology, ed. W. M. Horspool and P.-S. Song, 1st edn, CRC Press, 1995, 291.
38. Hammond, G. S.; Saltiel, J.; Lamola, A. A.; Turro, N. J.; Bradshaw, J. S.; Cowan, D. O.; Counsell, R. C.; Vogt, V.; Dalton, C., *J. Am. Chem. Soc.* **1964**, *86*, 3197.

39. Snyder, J. J.; Tise, F. P.; Davis, R. D.; Kropp, P. J., *J. Org. Chem.* **1981**, *46*, 3609.
40. Arai, T.; Tokumaru, K., *Chem. Rev.* **1993**, *93*, 23.
41. Zhao, Y.-P.; Yang, L.-Y.; Liu, R. S. H., *Green Chem.* **2009**, *11*, 837.
42. Zhao, Y.-P.; Campbell, R. O.; Liu, R. S. H., *Green Chem.* **2008**, *10*, 1038.
43. Ramamurthy, V.; Liu, R. S. H., *J. Am. Chem. Soc.* **1976**, *98*, 2935.
44. Herkstroeter, W. G.; Jones, L. B.; Hammond, G. S., *J. Am. Chem. Soc.* **1966**, *88*, 4777.
45. Singh, A.; Fennell, C. J.; Weaver, J. D., *Chem. Sci.* **2016**, *7*, 6796.
46. Senaweera, S. M.; Singh, A.; Weaver, J. D., *J. Am. Chem. Soc.* **2014**, *136*, 3002.
47. Singh, K.; Staig, S. J.; Weaver, J. D., *J. Am. Chem. Soc.* **2014**, *136*, 5275.
48. Singh, K.; Fennell, C. J.; Coutsias, E. A.; Latifi, R.; Hartson, S.; Weaver, J. D., *Chem* **2018**, *4*, 124.
49. Li, X.; Danishefsky, S. J., *J. Am. Chem. Soc.* **2010**, *132*, 11004.
50. Paton, R. S.; Kim, S.; Ross, A. G.; Danishefsky, S. J.; Houk, K. N., *Angew. Chem.* **2011**, *123*, 10550.
51. Ross, A. G.; Li, X.; Danishefsky, S. J., *J. Am. Chem. Soc.* **2012**, *134*, 16080.
52. Wilson, M. R.; Taylor, R. E., *Angew. Chem. Int. Ed.* **2013**, *52*, 4078.
53. Kallepu, S.; Gollapelli, K. K.; Nanubolu, J. B.; Chegondi, R., *Chem. Commun.* **2015**, *51*, 16840.
54. Walczak, M. A. A.; Krainz, T.; Wipf, P., *Acc. Chem. Res.* **2015**, *48*, 1149.
55. Blackman, M. L.; Royzen, M.; Fox, J. M., *J. Am. Chem. Soc.* **2008**, *130*, 13518.
56. Medina, J. M.; McMahon, T. C.; Jiménez-Osés, G.; Houk, K. N.; Garg, N. K., *J. Am. Chem. Soc.* **2014**, *136*, 14706.
57. Shah, T. K.; Medina, J. M.; Garg, N. K., *J. Am. Chem. Soc.* **2016**, *138*, 4948.
58. Medina, J. M.; Ko, J. H.; Maynard, H. D.; Garg, N. K., *Macromolecules* **2017**, *50*, 580.
59. Arumugam, S.; Popik, V. V., *J. Am. Chem. Soc.* **2011**, *133*, 5573.
60. Wang, Y.; Song, W.; Hu, W. J.; Lin, Q., *Angew. Chem. Int. Ed.* **2009**, *48*, 5330.
61. Hoyle, C. E.; Lowe, A. B.; Bowman, C. N., *Chem. Soc. Rev.* **2010**, *39*, 1355.
62. Poloukhine, A. A.; Mbua, N. E.; Wolfert, M. A.; Boons, G.-J.; Popik, V. V., *J. Am. Chem. Soc.* **2009**, *131*, 15769.
63. Orski, S. V.; Poloukhine, A. A.; Arumugam, S.; Mao, L.; Popik, V. V.; Locklin, J., *J. Am. Chem. Soc.* **2010**, *132*, 11024.
64. Cope, A. C.; Pike, R. A.; Spencer, C. F., *J. Am. Chem. Soc.* **1953**, *75*, 3212.
65. Inoue, Y.; Ueoka, T.; Kuroda, T.; Hakushi, T., *J. Chem. Soc., Perkin Trans. 2* **1983**, 983.
66. Bonneau, R.; Jousot-Dubien, J.; Salem, L.; Yarwood, A. J., *J. Am. Chem. Soc.* **1976**, *98*, 4329.
67. Singh, A.; Teegardin, K.; Kelly, M.; Prasad, K. S.; Krishnan, S.; Weaver, J. D., *J. Organomet. Chem.* **2015**, *776*, 51.
68. Kalyanasundaram, K., *Coord. Chem. Rev.* **1982**, *46*, 159.
69. Hofbeck, T.; Yersin, H., *Inorg. Chem.* **2010**, *49*, 9290.
70. McNally, A.; Prier, C. K.; MacMillan, D. W. C., *Science* **2011**, *334*, 1114.
71. Tucker, J. W.; Stephenson, C. R. J., *J. Org. Chem.* **2012**, *77*, 1617.
72. Nguyen, J. D.; D'Amato, E. M.; Narayanam, J. M. R.; Stephenson, C. R. J., *Nat. Chem.* **2012**, *4*, 854.
73. Speiser, S., *J. Photochem.* **1983**, *22*, 195.
74. Speiser, S., *Chem. Rev.* **1996**, *96*, 1953.
75. Stryer, L.; Haugland, R. P., *Proc. Natl. Acad. Sci. USA* **1967**, *58*, 719.
76. Dexter, D. L., *J. Chem. Phys.* **1953**, *21*, 836.
77. Förster, T., *Ann. Physik.* **1948**, *437*, 55.

## CHAPTER II

### VISIBLE LIGHT MEDIATED UPHILL CATALYSIS FOR THE SYNTHESIS OF *Z*-ALKENES

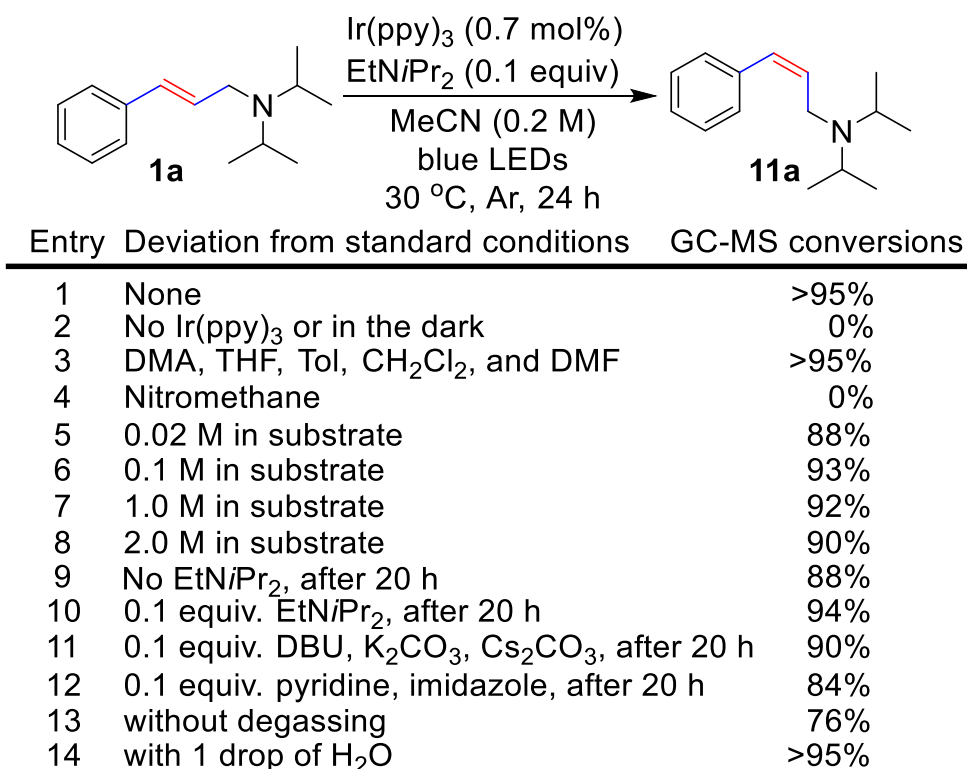
With the aim of developing endergonic reactions, we sought to develop a methodology for isomerization of *trans*-styrenoids to their respective *cis* isomers. Since no amount of thermal catalysis operating on ground state surface can drive the isomerization reaction in an endergonic direction, we decided to utilize the excited state surfaces from where all the subsequent reactions are downhill in nature. Photocatalysis has the ability to “pump” or circumvent the normal thermodynamic constraints of a reaction. In other words, the more energetic product can actually be favored as a result of the catalysis. From a synthetic perspective, such a process could take advantage of the many existing methods<sup>1-3</sup> to synthesize the *E*-alkenes for the synthesis of *Z*-alkenes which could give it a distinct advantage.

Allylamines are an important class of biologically active molecules, and in contrast to the *E*-isomer, accessing the *Z*-isomers is particularly challenging. Most commonly, partial hydrogenation-over a poisoned catalyst, of protected propargylamines is employed. This requires starting from the alkyne as well as a protection and deprotection step.<sup>4</sup> Thus, there is a real need for methods that can efficiently deliver *Z*-allylamines in fewer steps which utilize more accessible starting materials and consequently seemed like a good place to start our investigation.

#### **2.1 Optimization studies**

Our initial efforts focused on cinnamyl derived amines (Scheme 8). The reaction parameters were investigated utilizing **1a**. Fortuitously, our initial conditions gave, within the

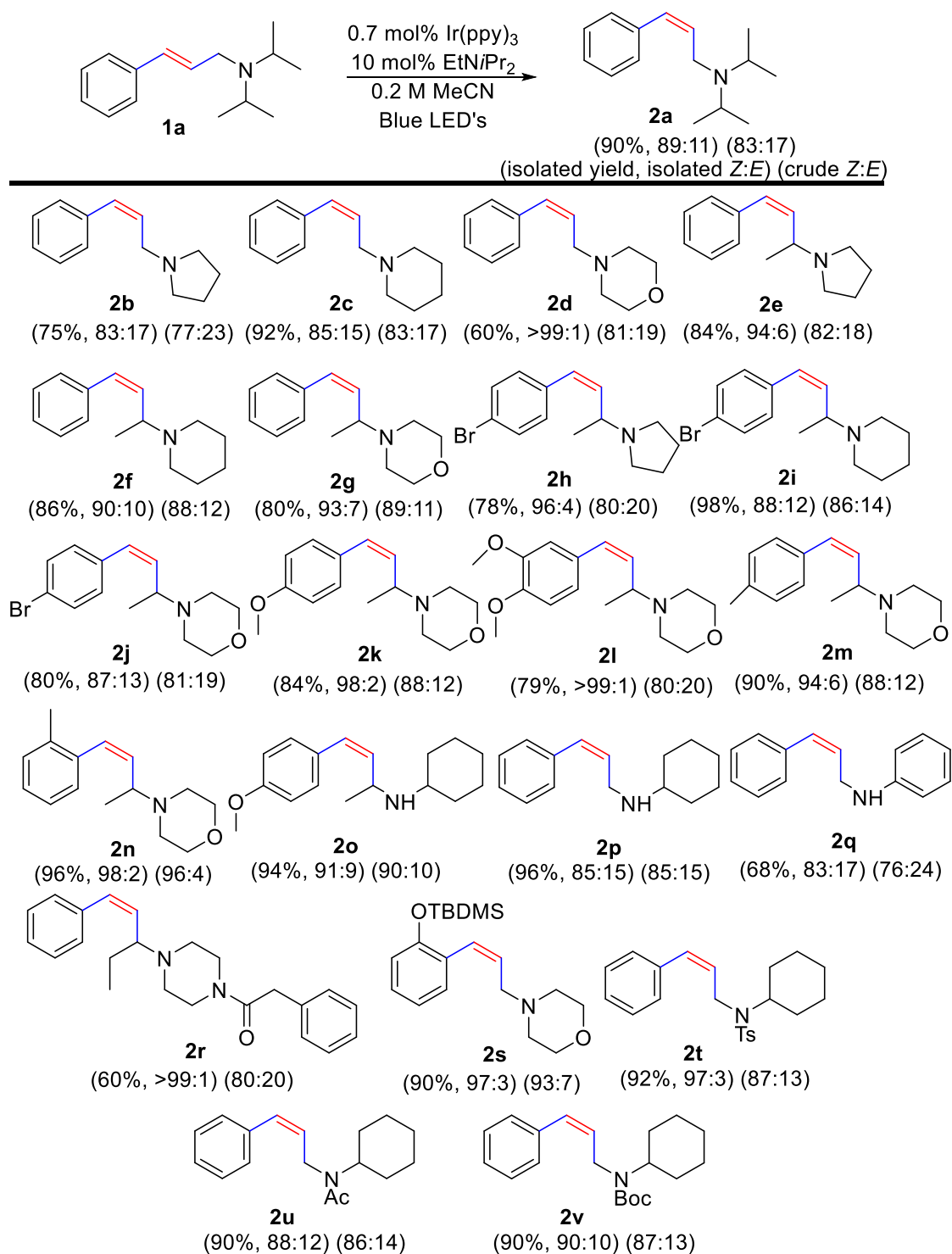
detection limits,<sup>5</sup> almost exclusively the Z-isomer (**11a**). Controls showed that both the photocatalyst *fac*-tris[2-phenylpyridinato-C<sup>2</sup>,N] iridium (III), [Ir(ppy)<sub>3</sub>] and light were essential (entry 2). Remarkably, the isomerization worked well in a number of solvents (entry 3) with the exception of nitromethane (entry 4) which may be due to quenching of the excited photocatalyst by solvent.<sup>6</sup> Interestingly, the reaction works well over a range of concentrations (entries 5-8). The effect of the external base was probed both by removing it (entry 9) and by substituting it (entry 10-12). While the effect is subtle, *i*Pr<sub>2</sub>NEt does seem to promote the reaction and is easily removed *in vacuo* after reaction completion. Other bases were less effective. The presence of air prevents the isomerization from occurring but otherwise is not detrimental (entry 13). Conveniently, the reaction did not display moisture sensitivity (entry 14) adding to the operational simplicity of the method.



Scheme 8. Optimization of reaction conditions

## 2.2 Substrate scope of the isomerization reaction

Having established reaction conditions, we next sought to evaluate the scope of the reaction (Scheme 9). The reaction works well for a number of other methylene carbinamines (**2b**, **2c**, **2d**), as well as substrates with a methine carbinamine (**2e**, **2f**, **2g**). Reaction with aryl bromides (**2h**, **2i**, **2j**) highlight the orthogonality of this chemistry to other late transition metal chemistry (i.e. Pd-catalyzed cross-couplings). Substitution is well tolerated at the 4-position (**2k**, **2m**), the 3-position (**2l**), and the 2-position (**2n**). Furthermore, the reaction tolerates secondary aliphatic amines (**2o**, **2p**) and aromatic amines (**27q**). The reaction tolerates amides (**2r**) giving better than 99:1 (*Z:E*) after chromatography. Additionally, acid labile silyl ether (**2s**), which would be difficult to retain during a partial hydrogenation under acidic conditions, is a particularly good substrate. Finally, several common *N*-protecting groups were evaluated. Tosyl (**2t**), *N*-acyl (**2u**) and even acid sensitive *N*-Boc protected amines (**2v**) worked well. It is noteworthy, that the reactions are remarkably clean with essentially no other chemistry occurring under these conditions and in most cases the lower isolated yields are simply the result of the partial resolution of the alkenes by chromatography.



Scheme 9. Substrate scope. Crude and isolated *Z/E* ratios are calculated from  $^1\text{H}$  NMR

### 2.3 Mechanistic studies

Having explored the scope, we next began to consider the mechanism. Given the uphill nature of the reaction in the ground state as well as the need for the photocatalyst and light, we believed it was unlikely that the reaction could be proceeding by a purely thermal process. Rather, the reaction must be driven by light. Given that substrates do not absorb light in the visible region as well as the need for the photocatalyst, a direct photochemical isomerization is unlikely. Instead, the selectivity of the reaction must result primarily from a difference in rates of photoquenching event of the photocatalyst by the *E*- and *Z*-isomers. With *E* and *Z* isomers in hand, we were able to investigate this question by performing photoquenching studies with both isomers. In this study, the Ir(ppy)<sub>3</sub> is excited by absorption of photons at the appropriate wavelength (370 nm) to facilitate a metal ligand charge transfer-excited state which emits at 520 nm. Quenching of the excited photocatalyst can be observed by monitoring the disappearance of the emissive wavelength (520 nm). From the slope of the line generated by plotting of I<sup>0</sup>/I (I = emission intensity) vs. concentration of the quencher we can glean information regarding the rate of the quenching event. The slope of the lines in this Stern-Volmer plot is proportional to the rate of the quenching event.<sup>7</sup> Indeed, we found that **1s** (>99:1, *E*:*Z*) quenches the emission of the excited catalyst with a slope of 0.0915 while **2s** (3:97, *E*:*Z*) quenches the excited state of the catalyst with a slope of 0.012. These results suggest that the *E*-isomer quenches the photoexcited state with a relative rate 8-fold greater than that of the *Z*-isomer,<sup>8</sup> confirming our suspicions and suggesting that the geometrical isomers quench the photocatalyst at significantly different rates (Figure 4).

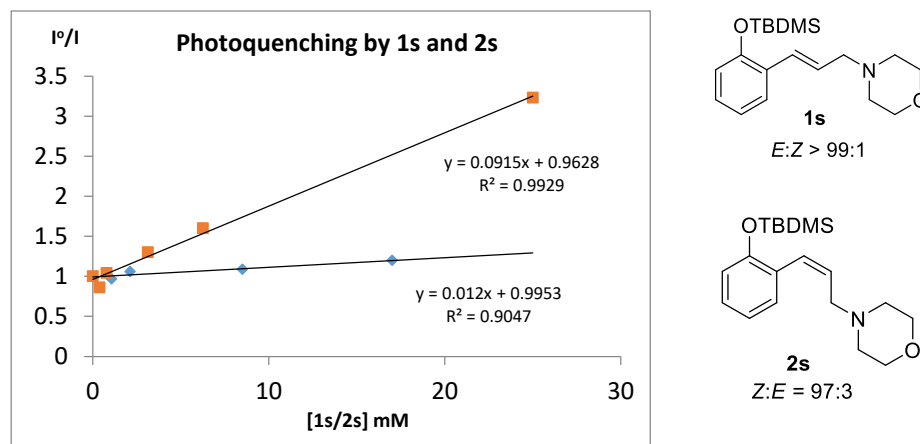


Figure 4. A Stern-Volmer photoquenching plot of **1s** and **2s**

Having established that the difference in the rate of quenching of the photoexcited catalyst by the two isomers is responsible for the buildup of the *Z*-isomer, we wanted to understand the nature of the quenching event. Two conceivable mechanisms that lead to photoquenching of  $\text{Ir}(\text{ppy})_3^*$  catalyst are outlined below. In the first scenario (Figure 5), reductive quenching by electron transfer from the amine to the excited photocatalyst<sup>9</sup> to give radical cation **1w**. Upon amine oxidation, the  $\alpha$ -C-H becomes significantly more acidic<sup>10</sup> and could be reversibly deprotonated by an exogenous base to give allylic radical **1wa**. Radical **1wb** is expected to have a diminished barrier towards *cis*-*trans* isomerization<sup>11</sup> and would lead to **2wb**. This species would undergo protonation and back electron transfer to afford **2w**, which is slower to quench the excited photocatalyst than **1w**, resulting in buildup of **2w**.

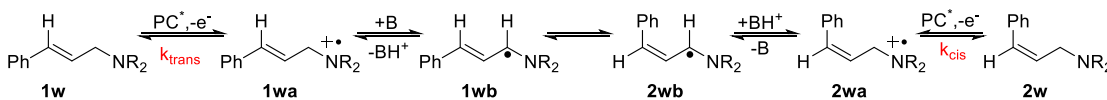


Figure 5. Potential explanation for the isomerization of the alkene

We next considered an energy transfer mechanism in which energy transfer from the photoexcited catalyst leads to a biradical intermediate (**1ww**, Figure 6), which is expected to rapidly lead to intermediate **I** which has the critical geometry in which a 90° rotation about the C-C has occurred. Intermediate **I** can undergo intersystem crossing to give either *E*-**1w** or *Z*-**1w**. A buildup

of **Z-1w** would result from a greater  $k_{tt}$  value.<sup>12</sup> Interestingly, in contrast to what we observe, Yoon has reported a related triplet sensitized [2+2] of related cinnamyl ethers in which he observed rapid isomerization of both *E* and *Z* isomers. Irrespective of starting from either geometrical isomer of the cinnamyl derivative (*E* or *Z*), the reaction produced the same product. One intriguing potential explanation is the difference in emissive energy of the different photocatalysts used.<sup>13</sup> Specifically, the catalyst used by Yoon has a greater emissive energy (470 nm, 61 kcal/mol) than the Ir(ppy)<sub>3</sub> catalyst (520 nm in MeCN, 55 kcal/mol). This implies that using a catalyst of higher energy, it is possible to excite both of the stereoisomers of alkenes to excited states generating the corresponding triplet biradicals.

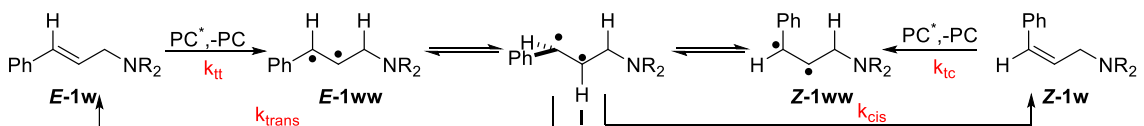
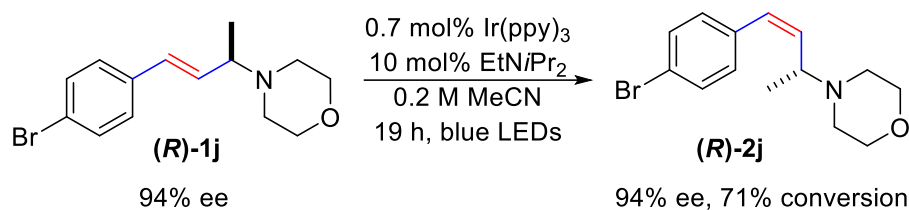


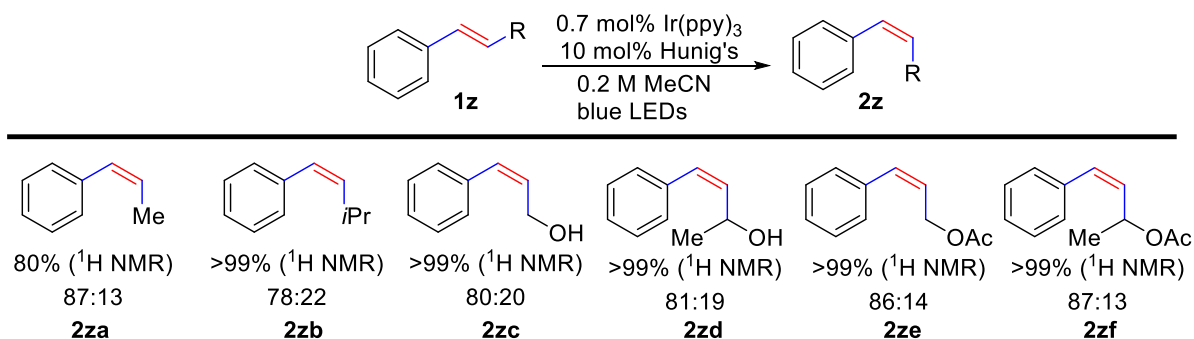
Figure 6. Energy transfer mechanism

Given that for the radicals **1wb** and **2wb** (Fig 5), inversion of  $sp^3$  hybridized carbon should be rapid,<sup>14</sup> we expected that if the reductive quenching mechanism were operative, any stereochemical information at the carbinamine stereocenter would be lost. Thus, we synthesized a chiral, nonracemic alkene (**R**)-**1j** and subjected it to the reaction conditions (Scheme 10). Upon photocatalytic *E*, *Z*-isomerization, no racemization was detected, suggesting that the reductive quenching mechanism is not operating and direct energy transfer as the operative mechanism. Moreover, the rate of the energy transfer was found to be slower (only 71% conversion observed after 19 h of irradiation) as compared to when racemic substrate was used (81% conv. after 16 h), indicating a matched and mismatched substrate catalyst pair (recall the photocatalyst is chiral and racemic), and highlighting the dependency of the energy transfer on the orbital overlap.



Scheme 10. Stereochemical probe for mechanistic studies

If direct energy transfer mechanism is operative, then it would be reasonable to assume that the amine may not be a necessary structural component (Scheme 11). Thus, we subjected simple *trans*-styrenes (**1z**) to the reaction conditions. Indeed, the substrates underwent isomerization to **2z** in good (*Z:E*) ratios and high yields, further supporting the direct energy transfer mechanism and suggesting a much broader scope for this reaction should be possible.



Scheme 11. Photochemical *E/Z* isomerization of non-oxidizable styrene derivatives

## 2.4 Utilization of photocatalytic isomerization strategy

The isomerization strategy developed here has been utilized by various researchers highlighting the usefulness of this methodology. For instance, Rueping utilized the visible light mediated isomerization conditions to synthesize *Z*-stilbenes in high yields with good to high *Z*-selectivities.<sup>15</sup> The reaction was performed in an ionic liquid phase where the olefin was easily separated using an apolar solvent phase. The recovered catalyst was reused and no loss in activity of the catalyst was observed until eight cycles. Further applicability of the methodology was

demonstrated by scaling up the reaction to a 1.8 g scale. Similarly, Reiser also designed a new polyisobutylene tagged Ir photocatalyst.<sup>16</sup> This catalyst was utilized for the isomerization of *E*-styrenyl acetates to their corresponding *Z*-isomers. The catalyst demonstrated excellent activity in batch and flow reactions and could be reused without a significant decrease in activity. Gilmour also demonstrated the catalytic *E-Z* isomerization of cinnamic esters utilizing riboflavin as a sensitizer.<sup>17</sup> In the case of cinnamic acids, the isomerized *Z*-cinnamic acid, under oxygen atmosphere, cyclizes intramolecularly to furnish coumarins in high yields. In a similar context, Li reported the isomerization of cinnamates using Ir(ppy)<sub>3</sub> and visible light.<sup>18</sup> Further, *ortho*-(*E*)-hydroxycinnamates underwent isomerization to generate its *Z*-isomer, and subsequently lactonized to produce the coumarin derivatives.

## 2.5 Summary

In conclusion, we have demonstrated a novel approach to access thermodynamically less stable alkenes directly from the more stable and easily synthesized *E*-alkenes in synthetically useful ratios and yields. Importantly, the starting alkenes are readily available and the photocatalyst is both highly efficient and commercially available. The reaction is remarkably clean and allows for the incorporation of a number of functional groups and maintains the stereochemistry of adjacent stereocenters within the substrates. Our preliminary mechanistic experiments indicate that the reaction proceeds by selective triplet sensitization of the *E*-alkene, suggesting that the reaction should be general to the styrenyl motif. This reaction serves as a rare example of uphill catalysis, which arguably is an underutilized strategy in the catalysis field and the reaction provides useful insight into this process. Recently, this methodology has attracted attention of various researchers to access *Z*-alkenes selectively and utilize it in further synthesis.

## 2.6 Experimental procedures

All reagents were obtained from commercial suppliers (Aldrich, VWR, TCI chemicals, Oakwood chemicals, Alfa Aesar) and used without further purification unless otherwise noted. Acetonitrile ( $\text{CH}_3\text{CN}$ ) was dried using molecular sieves. Photocatalyst *fac*-tris(2-phenyl pyridinato- $\text{C}^2$ , *N*)iridium(III)  $\text{Ir}(\text{ppy})_3$ , 99% (purity),  $\text{Ir}(\text{ppy})_3$  was obtained from Sigma Aldrich. Amano lipase PS from *Burkholderia cepacia* was purchased from Sigma Aldrich. Cinnamyl alcohol was purchased from Alfa Aesar. Reactions were monitored by thin layer chromatography (TLC), obtained from Sorbent Technologies (Silica XHL TLC Plates, w/UV254, glass backed, 250  $\mu\text{m}$ , 20 x 20 cm), and were visualized with ultraviolet light, potassium permanganate stain or GC-MS (QP 2010S, Shimadzu equipped with auto sampler).

Photocatalytic reactions were set up in a light bath which is described below. Strips of blue LEDs (18 LEDs/ft) were purchased from Solid Apollo and were wrapped around on the walls of glass crystallization dish and secured with masking tape and then wrapped with aluminum foil. A lid which rested on the top was fashioned from cardboard and holes were made such that reaction tubes (12 x 75 mm cultural borosilicate tube) were held firmly in the cardboard lid which was placed on the top of the bath. Water was added to the bath such that the tubes were submerged in the water which was maintained at 30  $^\circ\text{C}$  with the aid of a sand bath connected to a thermostat. Flash chromatography was carried out with Merck 60  $\text{\AA}$ , 230-400 mesh silica gel. NMR spectra were obtained on a 400 MHz Bruker Avance III spectrometer or a 400 MHz Unity Inova spectrometer unless noted.  $^1\text{H}$  and  $^{13}\text{C}$  NMR chemical shifts are reported in ppm relative to the residual protio solvent peak ( $^1\text{H}$ ,  $^{13}\text{C}$ ). High resolution mass spectra (HRMS) analysis were performed on a LTQ-Orbitrap XL by Thermo Scientific Ltd. Enantiomeric excess was determined using a Daicel Chiralpak AD-H column on HPLC instrument by Shimadzu, equipped with LC-20AD pump, SIL-20A autosampler and SPD-20AV UV detector. Quenching studies were performed on a Varian Carey Eclipse fluorescence spectrophotometer. Optical rotation was measured on an Autopol V by Rudolph Research Analytical.

## Synthesis of methine carbinamines

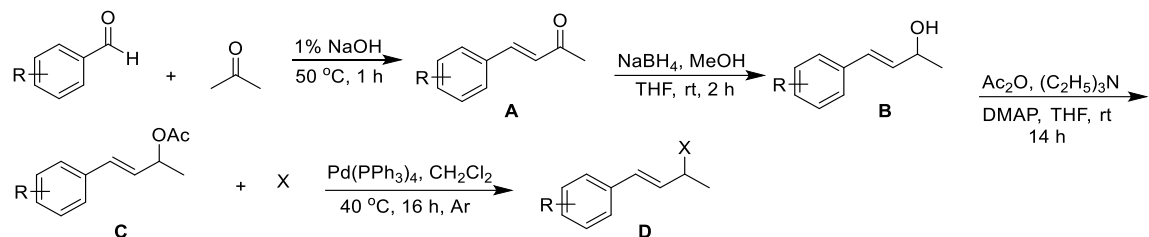


**Table 1: Summary of various substrates with their yields**

S.No.	R	X	% yield (after four steps)
1.	H	Pyrrolidine	16
2.	H	Piperidine	55
3.	H	Morpholine	66
4.	2-methyl	Morpholine	46
5.	4-methyl	Morpholine	14
6.	4-bromo	Pyrrolidine	54
7.	4-bromo	Piperidine	60
8.	4-bromo	Morpholine	54
9.	4-methoxy	Morpholine	67
10.	4-methoxy	Cyclohexylamine	21
11.	3,4-dimethoxy	Morpholine	34

### General procedure A for the synthesis of enones

To an oven-dried round-bottomed flask equipped with magnetic stir bar was added the aromatic aldehyde (1.0 equiv.), acetone (20 equiv.), water (10 equiv.) and 1% sodium hydroxide solution (10 equiv.). The reaction mixture was heated at 50 °C for 1-2 hours. The reaction was monitored by TLC. After the complete consumption of the starting aldehyde, the reaction mixture

was neutralized with 1N HCl and extracted with ethyl acetate (EtOAc) (2 x 30 mL). The organic layer was separated and dried over MgSO<sub>4</sub>. The solvent was evaporated to yield the  $\alpha,\beta$ -unsaturated carbonyl compound **A** which was used without any further purification.

#### **General procedure B for the synthesis of $\alpha,\beta$ unsaturated alcohols**

To an oven-dried round-bottomed flask equipped with a magnetic stir bar was added the  $\alpha,\beta$ -unsaturated carbonyl compound (1.0 equiv.) and a 1:3 mixture of tetrahydrofuran (THF) and methanol (MeOH), (0.65 M) and then the mixture was cooled to 0 °C. Sodium borohydride (NaBH<sub>4</sub>), (2.0 equiv.) was added portion-wise and the reaction mixture was allowed to warm to room temperature and stirred for 2 hours. The reaction was monitored by TLC. After the complete consumption of the starting material, the reaction mixture was quenched with saturated NH<sub>4</sub>Cl and the solvent volume was reduced under vacuum. The residue left behind was extracted with ethyl acetate (EtOAc) (3 x 30 mL). The organic layer was separated and dried over MgSO<sub>4</sub>. The solvent was evaporated to yield the allylic alcohol **B**, which was used without further purification.

#### **General procedure C for the acylation of $\alpha,\beta$ unsaturated alcohols**

To an oven-dried round-bottomed flask equipped with a magnetic stir bar was added the allylic alcohol **B** (1.0 equiv.), THF (1.35 M), acetic anhydride (1.2 equiv.), 4-(dimethylamino)pyridine (DMAP), (0.005 equiv.), and triethylamine (1.8 equiv.). The reaction mixture was stirred at 0 °C for 1 hour and then warmed to room temperature and stirred for 14 hours. The reaction was monitored by TLC. After the complete consumption of the starting material, the solvent was removed under vacuum. The residual oil was diluted with EtOAc. The organic layer was then washed with water and brine and then dried over MgSO<sub>4</sub> to obtain the desired allylic acetate **C**, which was used without further purification.

#### **General procedure D for the synthesis of *trans* allylic amines**

To an oven-dried round-bottomed flask equipped with a magnetic stir bar was added the allylic acetate **C** (1.0 equiv.), dichloromethane ( $\text{CH}_2\text{Cl}_2$ ), (0.53 M), tetrakis(triphenylphosphine)palladium(0),  $\text{Pd}(\text{PPh}_3)_4$ , (0.03 equiv.) and amine X (1.2 equiv.) under an Argon atmosphere. The reaction mixture was then heated to 40 °C for 16 hours. The reaction was monitored by TLC. After the complete consumption of the starting material the reaction mixture was quenched with  $\text{NH}_4\text{OH}$ . The organic layer was then separated, dried over  $\text{MgSO}_4$  and concentrated to obtain the crude product that was purified by normal phase chromatography. Normal phase chromatography was performed with Teledyne ISCO automated chromatography system using  $\text{CH}_2\text{Cl}_2$  in MeOH gradients over 0-70 column volumes or 40% EtOAc in hexanes (containing 1% triethylamine) over 0-40 column volumes using flow rates from 18 mL/min to 35 mL/min on a Rediseq column of 4 g, 12 g, or 24 g with product detection at 254 and 288 nm.

#### Synthesis of methylene carbinamines

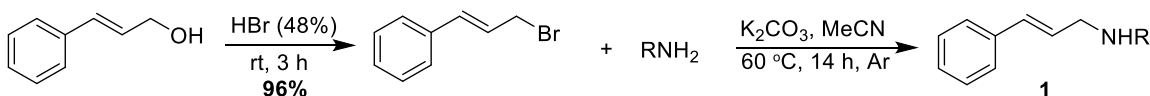


**Table 2: Summary of substrates with their yield in final step**

S. No.	$\text{RNH}_2$	% yield ( <b>1</b> )
1	Pyrrolidine	68
2	Piperidine	73
3	Morpholine	78
4	Diisopropylamine	45
5	Cyclohexylamine	67
6	Aniline	94

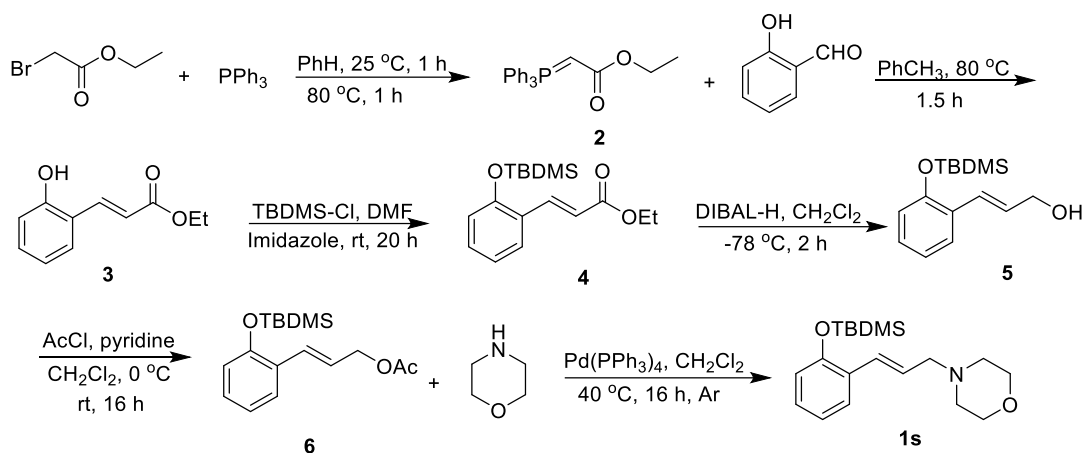
#### Synthesis of cinnamyl bromide

Cinnamyl bromide was synthesized by a procedure adapted from that reported by Cromwell. To an oven-dried round-bottomed flask equipped with a magnetic stir bar was added cinnamyl alcohol (6.0 g, 0.045 mol) and hydrogen bromide (48%) (100 mL) at 0 °C and the reaction mixture was warmed to room temperature and stirred for 3 hours. The reaction was monitored by TLC. After the complete consumption of the starting material the reaction mixture was quenched by saturated sodium bicarbonate and extracted with EtOAc (2 x 50 mL). The organic layer was separated, dried over MgSO<sub>4</sub> and the solvent was removed under reduced pressure to obtain a brown solid (8.5 g, 96%) which was used without further purification.

#### **General procedure E for the synthesis of *trans*-allylic amines**

To an oven-dried round-bottomed flask equipped with a magnetic stir bar was added cinnamyl bromide (1.0 equiv.), MeCN (1.0 M), anhydrous K<sub>2</sub>CO<sub>3</sub> (1.2 equiv.) and amine Y (4.0 equiv.) and the reaction mixture was heated at 60 °C for 14 hours under Ar. The reaction was monitored by TLC. After the complete consumption of the starting material, the solvent was removed under vacuum. The residue left behind was washed with sodium bicarbonate and extracted with CH<sub>2</sub>Cl<sub>2</sub>. The organic layer was separated, dried over MgSO<sub>4</sub> and the solvent was removed under reduced pressure to obtain the crude product that was purified using normal phase chromatography. Normal phase chromatography was performed with a Teledyne ISCO automated chromatography system using MeOH: CH<sub>2</sub>Cl<sub>2</sub> gradients over 0-40 column volumes using flow rates from 18 mL/min to 35 mL/min on a Rediseq column of 4 g, 12 g, or 24 g with product detection at 254 and 288 nm.

#### **Synthesis of (*E*)-4-(3-(2-((*tert*-butyldimethylsilyl)oxy)phenyl)allyl)morpholine (1s)**



### Synthesis of Wittig reagent (**2**)

To an oven-dried round-bottomed flask equipped with a magnetic stir bar was added ethyl 2-bromoacetate (1.0 g, 5.99 mmol), benzene (6.3 mL), and triphenylphosphine (1.75 g, 6.67 mmol) and the reaction mixture was heated at  $25^\circ\text{C}$  for 1 hour and then heated at  $80^\circ\text{C}$  for another 1 h. The precipitates formed were filtered, washed with ether (3 x 50 mL) and then dried. The white compound was then dissolved in a minimum volume of water. To the solution was then added 5% NaOH solution (20 mL) and the mixture was vigorously shaken. The precipitates formed were then filtered and washed with water (2 x 50 mL) and dried to obtain white ylide **2** (1.7 g, 82%).

### Synthesis of ethyl (E)-3-(2-hydroxyphenyl)acrylate (**3**)

To an oven-dried round-bottomed flask equipped with a magnetic stir bar was added 4-hydroxy benzaldehyde (0.5 g, 4.1 mmol), toluene (7.3 mL), Wittig reagent **2** (1.71 g, 4.90 mmol) and the reaction mixture was stirred at  $80^\circ\text{C}$  for 90 min. The solvent was removed under reduced pressure. The residue was then purified by normal phase chromatography using 15% EtOAc in hexanes gradients over 0-40 column volumes to obtain colorless oil **3** (0.78 g, 99%).

### Synthesis of ethyl (E)-3-(2-((*tert*-butyldimethylsilyl)oxy)phenyl)acrylate (**4**)

To an oven dried-round-bottomed flask equipped with a magnetic stir bar was added **3** (0.78 g, 4.06 mmol) in DMF (7 mL). To this was added a solution of imidazole (0.69 g, 10.15 mmol) and *tert*-butyldimethylsilyl chloride (0.67 g, 4.46 mmol) in DMF (3 mL). After stirring at 25 °C for 20 h, water was added and the mixture was extracted with EtOAc (2 x 40 mL). The organic layer was separated washed with 1 M NaOH (2 x 20 mL) and water (4 x 20 mL) and then dried over MgSO<sub>4</sub>. The solvent was evaporated under reduced pressure and the residue was purified by normal phase chromatography using 20% EtOAc in hexanes gradients over 0-30 column volumes to obtain **4** as oil (1.1 g, 88%).

#### **Synthesis of (*E*)-3-(2-((*tert*-butyldimethylsilyl)oxy)phenyl)prop-2-en-1-ol (**5**)**

A solution of ester **4** (1.1 g, 3.59 mmol) in CH<sub>2</sub>Cl<sub>2</sub> (22.4 mL) was cooled to -78 °C and DIBAL-H 1 M in hexanes (4.4 mL, 24.7 mmol). After stirring for 2 h at -78 °C, the reaction mixture was warmed to rt and stirred for 3 h. The reaction was quenched with methanol (3 mL) and saturated sodium potassium tartrate solution (30 mL) was added and stirred at rt for 1 h. The mixture was then acidified by 1 N HCl (2 mL). The solution was extracted with CH<sub>2</sub>Cl<sub>2</sub> (3 x 30 mL). The organic layer was separated and dried over MgSO<sub>4</sub>. Evaporation of the solvent resulted in a colorless oil **5** (0.9 g, 95%) which was used without further purification.

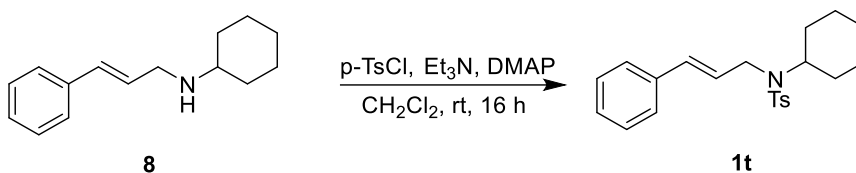
#### **Synthesis of (*E*)-3-(2-((*tert*-butyldimethylsilyl)oxy)phenyl)allyl acetate (**6**)**

To an oven-dried round-bottomed flask equipped with a magnetic stir bar was added alcohol **5** (0.9 g, 3.40 mmol), pyridine (1.10 mL, 13.6 mmol) and CH<sub>2</sub>Cl<sub>2</sub> (14.8 mL). The solution was cooled to 0 °C and acetyl chloride (1.07 g, 13.6 mmol) was added slowly. The reaction mixture was then warmed to room temperature and stirred for 18 h. Aqueous saturated copper sulfate solution (10 mL) was added to the reaction mixture and then extracted with CH<sub>2</sub>Cl<sub>2</sub> (2 x 30 mL). The organic layer was separated and dried over MgSO<sub>4</sub>. The solvent was removed under reduced pressure to afford crude acetate **6** (1.0 g, 96%), which was used without further purification.

### Synthesis of (*E*)-4-(3-(2-((*tert*-butyldimethylsilyloxy)phenyl)allyl)morpholine (**1s**)

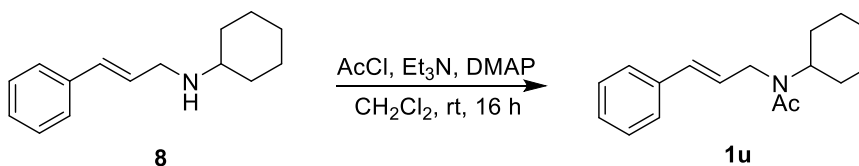
The general procedure D was followed using acetate **6** (0.25 g, 0.82 mmol), morpholine (70 mg, 0.98 mmol), tetrakis(triphenylphosphine)palladium(0), (Pd(PPh<sub>3</sub>)<sub>4</sub>) (30 mg, 0.024 mmol) and CH<sub>2</sub>Cl<sub>2</sub> (1.4 mL) to obtain the title compound **1s** (0.17 g, 53%) as a yellow oil.

### Synthesis of *N*-cinnamyl-*N*-cyclohexyl-4-methylbenzenesulfonamide (**1t**)



To an oven-dried round-bottomed flask equipped with a magnetic stir bar was added amine **8** (0.2 g, 0.93 mmol) [Table 2 (entry 5)], dry CH<sub>2</sub>Cl<sub>2</sub> (10 mL), triethylamine (0.19 mL, 1.40 mmol), 4-(dimethylamino)pyridine (0.6 mg, 0.005 mmol) and the mixture was cooled to 0 °C. *p*-Toluenesulfonyl chloride (0.21g, 1.12 mmol) was then added and the mixture was allowed to warm to rt. After stirring for 16 h, water was added and the mixture and extracted with CH<sub>2</sub>Cl<sub>2</sub> (2 x 20 mL). The organic phase was separated, dried over MgSO<sub>4</sub> and the solvent was removed under reduced pressure to afford **1t** (0.29 g, 84%) as brown oil, which was used without further purification.

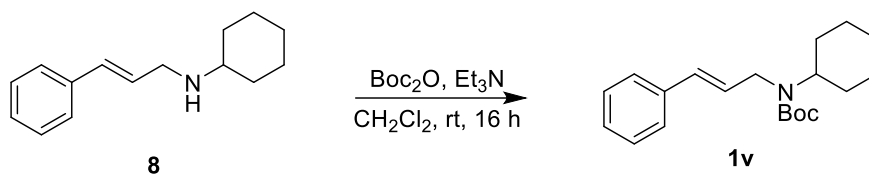
### Synthesis of *N*-cinnamyl-*N*-cyclohexylacetamide (**1u**)



To an oven-dried round-bottomed flask equipped with a magnetic stir bar was added amine **8** (0.2 g, 0.93 mmol) [Table 2 (entry 5)], dry CH<sub>2</sub>Cl<sub>2</sub> (10 mL), triethylamine (0.32 mL, 2.33 mmol), 4-(dimethylamino)pyridine (11.0 mg, 0.09 mmol) and acetyl chloride (0.15 g, 1.86 mmol). After

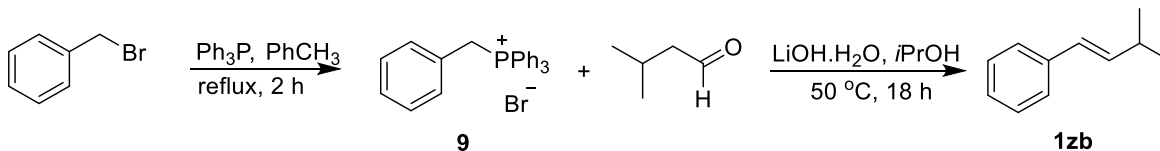
stirring for 16 h, saturated  $\text{NH}_4\text{Cl}$  was added and the mixture was extracted with  $\text{CH}_2\text{Cl}_2$  (2 x 20 mL). The organic phase was washed with saturated  $\text{NaHCO}_3$  (2 x 20 mL), separated, dried over  $\text{MgSO}_4$  and the solvent was removed under reduced pressure to afford **1u** (0.21 g, 88%) as an oil, which was used without further purification.

#### Synthesis of *tert*-butyl cinnamyl(cyclohexyl)carbamate (**1v**)



To an oven-dried round-bottomed flask equipped with magnetic stir bar was added amine **8** (0.13 g, 0.60 mmol) [Table 2 (entry 5)], dry  $\text{CH}_2\text{Cl}_2$  (8 mL), triethylamine (0.13 mL, 0.90 mmol) and Boc-anhydride (0.20 g, 0.90 mmol). After stirring for 16 h, water was added and the mixture was extracted with  $\text{CH}_2\text{Cl}_2$  (2 x 15 mL). The organic phase was washed with brine, separated, dried over  $\text{MgSO}_4$  and solvent was removed under reduced pressure to afford **1v** (0.17 g, 90%) as an oil, which was used without further purification.

#### Synthesis of (*E*)-(3-methylbut-1-en-1-yl)benzene (**1z**)



#### Synthesis of Wittig reagent (**9**)

To an oven-dried round-bottomed flask equipped with a magnetic stir bar was added triphenylphosphine (4.6 g, 17.54 mmol), toluene (15 mL) and benzyl bromide (3.0 g, 17.54 mmol) and the reaction mixture was refluxed for 2 hours. The mixture was cooled to room temperature. The precipitates formed were filtered and washed with diethyl ether (3 x 50 mL) and dried under

reduced pressure on rotavap to afford **9** as a white salt (6.0 g, 79%), which was used without further purification.

### Synthesis of (*E*)-(3-methylbut-1-en-1-yl)benzene (**1zb**)

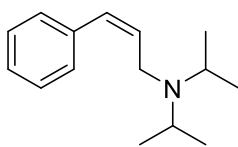
To an oven-dried round-bottomed flask equipped with magnetic stir bar was added **9** (1.3 g, 3.05 mmol), isopropanol (10 mL) and lithium hydroxide monohydrate (0.18 g, 4.16 mmol). The mixture was stirred for 15 min. Then 3-methylbutanal (0.20 g, 2.77 mmol) was added and the reaction mixture was stirred at 50 °C for 18 h. The reaction mixture was quenched with water and extracted with EtOAc (2 x 20 mL). The organic layer was separated, and dried over MgSO<sub>4</sub>. The solvent was removed under reduced pressure. The residue was then purified by normal phase chromatography using hexane gradients over 0-10 column volumes to obtain colorless liquid **1z** (0.22 g, 54%, 71:29 *E:Z*).

### General procedure F for the photocatalytic isomerization of the *trans*-allylic amines to *cis*-allylic amines **2a** – **2v**

A 12 x 75 mm borosilicate test tube fitted with a rubber septum was charged with *fac*-tris(2-phenyl pyridinato-C<sup>2</sup>, *N*) Iridium(III) (Ir(ppy)<sub>3</sub>) (0.007 equiv, X mL of a 1.88 mM stock solution of catalyst in CH<sub>3</sub>CN where X was used to make a 0.20 M solution of the *trans*-allylic amine), *trans*-allylic amine (1 equiv.), Hünig's base (0.1 equiv.) were added and the reaction mixture was degassed via Ar bubbling for 5-10 min and then left under positive Ar pressure by removing the exit needle. The tube was placed in a light bath (description above) and the lower portion of the tube was submerged in the water bath which was maintained at 30 °C. The reaction was monitored by GC-MS. When the *trans*-allylic amine reached the maximum conversion to the *cis*-allylic amine (*i.e.*, the conversion does not change even after prolonged exposure to blue light), the CH<sub>3</sub>CN was removed *via* rotavap. The crude product was purified by normal phase chromatography. Normal phase chromatography was performed with a Teledyne ISCO automated

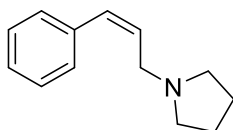
chromatography system using CH<sub>2</sub>Cl<sub>2</sub> in MeOH gradients over 0-40 column volumes or 40% EtOAc in hexanes (containing 1% triethylamine) over 0-40 column volumes with flow rates from 18 mL/min to 35 mL/min on a Redisep column of 4 g, 12 g, or 24 g with product detection at 254 and 288 nm.

**(Z)-N,N-diisopropyl-3-phenylprop-2-en-1-amine (2a)**



The general procedure **F** was followed using (*E*)-*N,N*-diisopropyl-3-phenylprop-2-en-1-amine (50 mg, 0.23 mmol), *N,N*-diisopropylethylamine (4.1 μL, 0.02 mmol) and 1.2 mL (1.6 μmol) of a stock solution of Ir(ppy)<sub>3</sub> in CH<sub>3</sub>CN to afford **2a** in 90% yield (45 mg, 0.21 mmol) as yellow oil with *Z*:*E* ratio of 89:11 (crude *Z*:*E* ratio 83:17). The substrate was purified by flash chromatography using 40% EtOAc in hexanes (containing 1% triethylamine) (0 to 100% of EtOAc) with the product eluting at 30%. <sup>1</sup>H NMR (400 MHz, CDCl<sub>3</sub>) δ 7.36 – 7.27 (m, 2H), 7.24 – 7.14 (m, 3H), 6.38 (d, *J* = 11.9 Hz, 1H), 5.75 (dt, *J* = 12.0, 6.1 Hz, 1H), 3.35 (dd, *J* = 6.1, 2.1 Hz, 2H), 3.01 (hept, *J* = 6.6 Hz, 2H), 0.95 (d, *J* = 6.6 Hz, 12H). <sup>13</sup>C NMR (101 MHz, CDCl<sub>3</sub>) δ 137.65, 135.65, 128.91, 128.25, 128.06, 126.50, 48.83, 43.44, 20.78. Calculated HRMS (ESI) for C<sub>14</sub>H<sub>19</sub>NO [M+H]<sup>+</sup> is 218.1909, found 218.1897.

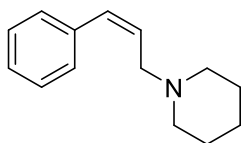
**(Z)-1-(3-phenylallyl)pyrrolidine (2b)**



The general procedure **F** was followed using (*E*)-1-(3-phenylallyl)pyrrolidine (40 mg, 0.21 mmol), *N,N*-diisopropylethylamine (3.5 μL, 0.02 mmol) and 1.1 mL (1.5 μmol) of stock solution of Ir(ppy)<sub>3</sub> in CH<sub>3</sub>CN to afford **2b** in 75% yield (30 mg, 0.16 mmol) as yellow oil with *Z*:*E* ratio of 83:17 (crude *Z*:*E* ratio 77:23). The substrate was purified by flash chromatography using 40% EtOAc in hexane (containing 1% triethylamine) (0 to 100% of EtOAc) with product eluting at 25%. <sup>1</sup>H NMR (400 MHz, CDCl<sub>3</sub>) δ 7.41 – 7.32 (m, 2H), 7.31 – 7.26 (m, 1H), 7.24 – 7.17 (m, 2H), 6.70 (d, *J* = 11.7 Hz, 1H), 5.96 (dt, *J* = 12.0, 6.6 Hz, 1H), 3.68 – 3.60 (m, 2H), 2.89 – 2.78 (m, 4H), 1.97 – 1.85 (m,

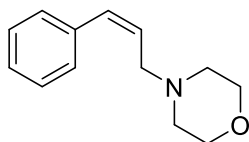
4H).  $^{13}\text{C}$  NMR (101 MHz,  $\text{CDCl}_3$ )  $\delta$  137.37, 130.17, 129.04, 128.21, 126.88, 126.41, 54.25, 54.12, 23.63. Calculated HRMS (ESI) for  $\text{C}_{13}\text{H}_{17}\text{N}$   $[\text{M}+\text{H}]^+$  is 188.1439, found 188.1424.

#### (Z)-1-(3-phenylallyl)piperidine (2c)



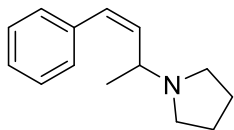
The general procedure **F** was followed using (*E*)-1-(3-phenylallyl)piperidine (50 mg, 0.25 mmol), *N,N*-diisopropylethylamine (4.3  $\mu\text{L}$ , 0.02 mmol) and 1.2 mL (1.8  $\mu\text{mol}$ ) of stock solution of  $\text{Ir}(\text{ppy})_3$  in  $\text{CH}_3\text{CN}$  to afford **2c** in 92% yield (46 mg, 0.20 mmol) as yellow oil with *Z:E* ratio of 85:15 (crude *Z:E* ratio 83:17). The substrate was purified by flash chromatography using  $\text{CH}_2\text{Cl}_2$  in MeOH (0 to 30% of MeOH) with the product eluting at 13%.  $^1\text{H}$  NMR (400 MHz,  $\text{CDCl}_3$ )  $\delta$  7.31 – 7.21 (m, 2H), 7.25 – 7.17 (m, 3H), 6.54 (d,  $J = 11.8$  Hz, 1H), 5.80 (dt,  $J = 12.2, 6.4$  Hz, 1H), 3.25 (dd,  $J = 6.4, 1.9$  Hz, 2H), 2.40 (br s, 4H), 1.65 – 1.51 (apparent p, 4H), 1.47 – 1.32 (m, 2H).  $^{13}\text{C}$  NMR (101 MHz,  $\text{CDCl}_3$ )  $\delta$  137.29, 130.71, 130.39, 128.91, 128.08, 126.73, 57.15, 54.72, 26.06, 24.33. Calculated HRMS (ESI) for  $\text{C}_{14}\text{H}_{19}\text{N}$   $[\text{M}+\text{H}]^+$  is 202.1596, found 202.1580.

#### (Z)-4-(3-phenylallyl)morpholine (2d)



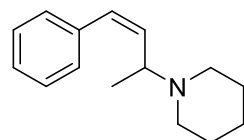
The general procedure **F** was followed using (*E*)-1-(3-phenylallyl)morpholine (45 mg, 0.22 mmol), *N,N*-diisopropylethylamine (3.6  $\mu\text{L}$ , 0.02 mmol) and 1.1 mL (1.5  $\mu\text{mol}$ ) of stock solution of  $\text{Ir}(\text{ppy})_3$  in  $\text{CH}_3\text{CN}$  to afford **2d** in 67% yield (30 mg, 0.15 mmol) as a colorless oil with *Z:E* ratio of >99:1 (crude *Z:E* ratio 81:19). The substrate was purified by flash chromatography using 40% EtOAc in hexanes (containing 1% triethylamine) (0 to 100% of EtOAc) with the product eluting at 40%.  $^1\text{H}$  NMR (400 MHz,  $\text{CDCl}_3$ )  $\delta$  7.30 – 7.22 (m, 2H), 7.21 – 7.13 (m, 3H), 6.52 (d,  $J = 11.8$  Hz, 1H), 5.70 (dt,  $J = 12.0, 6.5$  Hz, 1H), 3.64 (t,  $J = 4.0$  Hz, 4H), 3.19 (dd,  $J = 6.5, 1.9$  Hz, 2H), 2.38 (apparent s, 4H).  $^{13}\text{C}$  NMR (101 MHz,  $\text{CDCl}_3$ )  $\delta$  137.18, 131.88, 129.22, 129.08, 128.36, 127.16, 67.23, 56.83, 53.92. Calculated HRMS (ESI) for  $\text{C}_{13}\text{H}_{17}\text{NO}$   $[\text{M}+\text{H}]^+$  is 204.1388, found 204.1378.

### **(Z)-1-(4-phenylbut-3-en-2-yl)pyrrolidine (2e)**



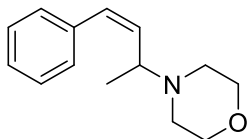
The general procedure **F** was followed using (*E*)-1-(4-phenylbut-3-en-2-yl)pyrrolidine (50 mg, 0.25 mmol), *N,N*-diisopropylethylamine (3.8  $\mu$ L, 0.02 mmol) and 1.2 mL (1.7  $\mu$ mol) of stock solution of Ir(ppy)<sub>3</sub> in CH<sub>3</sub>CN to afford **2e** in 84% yield (42 mg, 0.21 mmol) as yellow oil with a *Z:E* ratio 94:6 (crude *Z:E* ratio 82:18). The substrate was purified by flash chromatography using 40% EtOAc in hexanes (containing 1% triethylamine) (0 to 100% of EtOAc) with the product eluting at 30%. <sup>1</sup>H NMR (400 MHz, CDCl<sub>3</sub>)  $\delta$  7.37 – 7.30 (m, 2H), 7.25 – 7.20 (m, 3H), 6.49 (d, *J* = 11.8 Hz, 1H), 5.75 (dd, *J* = 11.8, 9.8 Hz, 1H), 3.50 – 3.31 (m, 1H), 2.69 – 2.49 (m, 4H), 1.86 – 1.70 (m, 4H), 1.33 (d, *J* = 6.5 Hz, 3H). <sup>13</sup>C NMR (101 MHz, CDCl<sub>3</sub>)  $\delta$  137.49, 136.48, 128.79, 128.57, 128.13, 126.65, 57.06, 52.05, 23.33, 20.63. Calculated HRMS (ESI) for C<sub>14</sub>H<sub>19</sub>N [M+H]<sup>+</sup> is 202.1596, found 202.1584.

### **(Z)-1-(4-phenylbut-3-en-2-yl)piperidine (2f)**



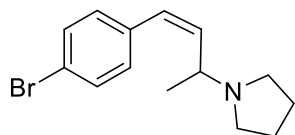
The general procedure **F** was followed using (*E*)-1-(4-phenylbut-3-en-2-yl)piperidine (50 mg, 0.23 mmol), *N,N*-diisopropylethylamine (4.0  $\mu$ L, 0.02 mmol) and 1.2 mL (1.6  $\mu$ mol) of stock solution of Ir(ppy)<sub>3</sub> in CH<sub>3</sub>CN to afford **2f** in 86% yield (43 mg, 0.20 mmol) as yellow oil with a *Z:E* ratio of 90:10 (crude *Z:E* ratio 88:12). The substrate was purified by flash chromatography using CH<sub>2</sub>Cl<sub>2</sub> in MeOH (0 to 30% of MeOH) with the product eluting at 10%. <sup>1</sup>H NMR (400 MHz, CDCl<sub>3</sub>)  $\delta$  7.43 – 7.32 (m, 2H), 7.32 – 7.24 (m, 3H), 6.57 (d, *J* = 11.8 Hz, 1H), 5.75 (dd, *J* = 11.8, 10.0 Hz, 1H), 3.57 – 3.46 (m, 1H), 2.68 – 2.53 (m, 2H), 2.54 – 2.40 (m, 2H), 1.76 – 1.55 (m, 4H), 1.52 – 1.38 (m, 2H), 1.31 (d, *J* = 6.5 Hz, 3H). <sup>13</sup>C NMR (101 MHz, CDCl<sub>3</sub>)  $\delta$  137.47, 130.24, 128.91, 128.40, 126.98, 126.48, 57.65, 51.25, 26.10, 24.61, 18.49. Calculated HRMS (ESI) for C<sub>15</sub>H<sub>21</sub>N [M+H]<sup>+</sup> is 216.1752, found 216.1742.

### **(Z)-4-(4-phenylbut-3-en-2-yl)morpholine (2g)**



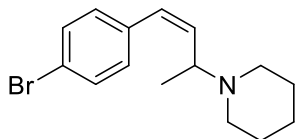
The general procedure **F** was followed using (*E*)-4-(4-phenylbut-3-en-2-yl)morpholine (50 mg, 0.23 mmol), *N,N*-diisopropylethylamine (4.1  $\mu$ L, 0.02 mmol) and 1.2 mL (1.6  $\mu$ mol) of stock solution of Ir(ppy)<sub>3</sub> in CH<sub>3</sub>CN to afford **2g** in 80% yield (40 mg, 0.18 mmol) as yellow oil with a *Z:E* ratio of 93:7 (crude *Z:E* ratio 89:11). The substrate was purified by flash chromatography using 40% EtOAc in hexanes (containing 1% triethylamine) (0 to 100% of EtOAc) with the product eluting at 40%. <sup>1</sup>H NMR (400 MHz, CDCl<sub>3</sub>)  $\delta$  7.40 – 7.32 (m, 2H), 7.30 – 7.24 (m, 3H), 6.58 (d, *J* = 11.8 Hz, 1H), 5.66 (dd, *J* = 11.8, 9.8 Hz, 1H), 3.72 (t, *J* = 4.7 Hz, 4H), 3.50 – 3.36 (m, 1H), 2.61 – 2.52 (m, 2H), 2.52 – 2.43 (m, 2H), 1.26 (d, *J* = 6.5 Hz, 3H). <sup>13</sup>C NMR (101 MHz, CDCl<sub>3</sub>)  $\delta$  135.37, 132.85, 128.4, 126.85, 126.32, 124.95, 65.34, 55.24, 48.80, 16.13. Calculated HRMS (ESI) for C<sub>14</sub>H<sub>19</sub>NO [M+H]<sup>+</sup> is 218.1545, found 218.1533.

#### (*Z*)-1-(4-(4-bromophenyl)but-3-en-2-yl)pyrrolidine (**2h**)



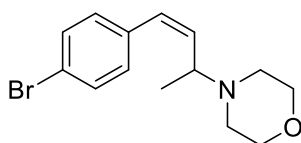
The general procedure **F** was followed using (*E*)-1-(4-(4-bromophenyl)but-3-en-2-yl)pyrrolidine (50 mg, 0.18 mmol), *N,N*-diisopropylethylamine (3.1  $\mu$ L, 0.02 mmol) and 0.9 mL (1.2  $\mu$ mol) of stock solution of Ir(ppy)<sub>3</sub> in CH<sub>3</sub>CN to afford **2h** in 78% yield (39 mg, 0.14 mmol) as a yellow oil with a *Z:E* ratio of 96:4 (crude *Z:E* ratio 80:20). The substrate was purified by flash chromatography using CH<sub>2</sub>Cl<sub>2</sub> in MeOH (0 to 30% of MeOH) with product eluting at 15%. <sup>1</sup>H NMR (400 MHz, CDCl<sub>3</sub>)  $\delta$  7.51 (d, *J* = 8.4 Hz, 2H), 7.01 (d, *J* = 8.3 Hz, 2H), 6.72 (d, *J* = 11.6 Hz, 1H), 6.09 (dd, *J* = 11.5, 10.4 Hz, 1H), 4.02 – 3.89 (m, 1H), 3.11 (br s, 4H), 2.09 – 1.96 (m, 4H), 1.67 (d, *J* = 6.6 Hz, 3H). <sup>13</sup>C NMR (101 MHz, CDCl<sub>3</sub>)  $\delta$  134.08, 133.11, 132.07, 129.85, 128.42, 122.24, 58.55, 51.51, 23.41, 18.42. Calculated HRMS (ESI) for C<sub>14</sub>H<sub>18</sub>BrN [M+H]<sup>+</sup> is 280.0701, found is 280.0688.

#### (*Z*)-1-(4-(4-bromophenyl)but-3-en-2-yl)piperidine (**2i**)



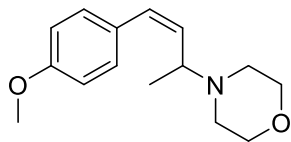
The general procedure **F** was followed using (*E*)-1-(4-(4-bromophenyl)but-3-en-2-yl)piperidine (50 mg, 0.17 mmol), *N,N*-diisopropylethylamine (3.0  $\mu$ L, 0.02 mmol) and 0.9 mL (1.2  $\mu$ mol) of stock solution of Ir(ppy)<sub>3</sub> in CH<sub>3</sub>CN to afford **2i** in 98% yield (48 mg, 0.16 mmol) as a yellow oil with a *Z:E* ratio of 88:12 (crude *Z:E* ratio 86:14). The substrate was purified by flash chromatography using 40% EtOAc in hexanes (containing 1% triethylamine) (0 to 100% of EtOAc) with the product eluting at 35%. <sup>1</sup>H NMR (400 MHz, CDCl<sub>3</sub>)  $\delta$  7.43 (d, *J* = 8.4 Hz, 2H), 7.13 (d, *J* = 8.4 Hz, 2H), 6.41 (d, *J* = 11.8 Hz, 1H), 5.71 (dd, *J* = 11.8, 9.9 Hz, 1H), 3.39 – 3.26 (m, 1H), 2.55 – 2.42 (m, 2H), 2.43 – 2.32 (m, 2H), 1.61 – 1.50 (m, 4H), 1.45 – 1.34 (m, 2H), 1.20 (d, *J* = 6.5 Hz, 3H). <sup>13</sup>C NMR (101 MHz, CDCl<sub>3</sub>)  $\delta$  136.42, 131.24, 130.45, 128.27, 127.75, 120.58, 57.22, 51.06, 26.27, 24.62, 18.07. Calculated HRMS (ESI) for C<sub>15</sub>H<sub>20</sub>BrN [M+H]<sup>+</sup> is 294.0857, found 294.0844.

**(Z)-4-(4-(4-bromophenyl)but-3-en-2-yl)morpholine (2j)**



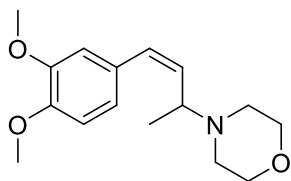
The general procedure **F** was followed using (*E*)-4-(4-(4-bromophenyl)but-3-en-2-yl)morpholine (50 mg, 0.17 mmol), *N,N*-diisopropylethylamine (3.0  $\mu$ L, 0.02 mmol) and 0.9 mL (1.2  $\mu$ mol) of stock solution of Ir(ppy)<sub>3</sub> in CH<sub>3</sub>CN to afford **2j** in 80% yield (40 mg, 0.14 mmol) as a yellow oil with a *Z:E* ratio of 87:13 (crude *Z:E* ratio 81:19). The substrate was purified by flash chromatography using CH<sub>2</sub>Cl<sub>2</sub> in MeOH (0 to 30% of MeOH) with the product eluting at 10%. <sup>1</sup>H NMR (400 MHz, CDCl<sub>3</sub>)  $\delta$  7.45 (d, *J* = 8.3 Hz, 2H), 7.12 (d, *J* = 8.4 Hz, 2H), 6.46 (d, *J* = 11.8 Hz, 1H), 5.66 (dd, *J* = 11.6, 10.0 Hz, 1H), 3.68 (t, *J* = 4.7 Hz, 4H), 3.38 – 3.28 (m, 1H), 2.57 – 2.47 (m, 2H), 2.47 – 2.39 (m, 2H), 1.21 (d, *J* = 6.5 Hz, 3H). <sup>13</sup>C NMR (101 MHz, CDCl<sub>3</sub>)  $\delta$  136.09, 135.54, 131.34, 130.37, 129.16, 120.82, 67.18, 57.07, 50.58, 17.75. Calculated HRMS (ESI) for C<sub>14</sub>H<sub>18</sub>BrNO [M+H]<sup>+</sup> is 296.0650, found 296.0632.

**(Z)-4-(4-(4-methoxyphenyl)but-3-en-2-yl)morpholine (2k)**



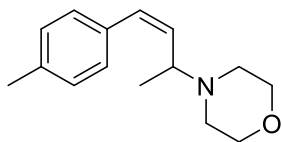
The general procedure **F** was followed using (*E*)-4-(4-(4-methoxyphenyl)but-3-en-2-yl)morpholine (50 mg, 0.20 mmol), *N,N*-diisopropylethylamine (7.4  $\mu$ L, 0.02 mmol) and 1.0 mL (1.4  $\mu$ mol) of stock solution of Ir(ppy)<sub>3</sub> in CH<sub>3</sub>CN to afford **2k** in 84% yield (42 mg, 0.17 mmol) as yellow oil with a *Z:E* ratio of 98:2 (crude *Z:E* ratio 88:12). The substrate was purified by flash chromatography using CH<sub>2</sub>Cl<sub>2</sub> in MeOH (0 to 30% of MeOH) with the product eluting at 13%. <sup>1</sup>H NMR (400 MHz, CDCl<sub>3</sub>)  $\delta$  7.19 (d, *J* = 8.6 Hz, 2H), 6.87 (d, *J* = 8.7 Hz, 2H), 6.47 (d, *J* = 11.8 Hz, 1H), 5.54 (dd, *J* = 11.8, 9.8 Hz, 1H), 3.81 (s, 3H), 3.69 (t, *J* = 4.7 Hz, 4H), 3.47 – 3.36 (m, 1H), 2.58 – 2.50 (m, 2H), 2.50 – 2.41 (m, 2H), 1.23 (d, *J* = 6.5 Hz, 3H). <sup>13</sup>C NMR (101 MHz, CDCl<sub>3</sub>)  $\delta$  158.64, 133.58, 130.20, 129.99, 129.95, 113.81, 67.42, 57.35, 55.45, 50.87, 18.11. Calculated HRMS (ESI) for C<sub>15</sub>H<sub>21</sub>NO<sub>2</sub> [M+H]<sup>+</sup> is 248.1651, found 248.1641.

**(Z)-4-(4-(3,4-dimethoxyphenyl)but-3-en-2-yl)morpholine (2l)**



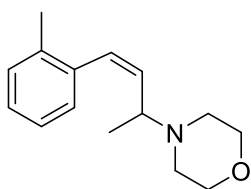
The general procedure **F** was followed using (*E*)-4-(4-(3,4-dimethoxyphenyl)but-3-en-2-yl)morpholine (70 mg, 0.26 mmol), *N,N*-diisopropylethylamine (4.6  $\mu$ L, 0.03 mmol) and 1.4 mL (1.8  $\mu$ mol) of stock solution of Ir(ppy)<sub>3</sub> in CH<sub>3</sub>CN to afford **2l** in 79% yield (55 mg, 0.20 mmol) as a yellow oil with a *Z:E* ratio of >99:1 (crude *Z:E* ratio 80:20). The substrate was purified by flash chromatography using 40% EtOAc in hexanes (containing 1% triethylamine) (0 to 100% of EtOAc) with the product eluting at 50%. <sup>1</sup>H NMR (400 MHz, CDCl<sub>3</sub>)  $\delta$  6.84 (apparent s, 3H), 6.48 (d, *J* = 11.8 Hz, 1H), 5.56 (dd, *J* = 11.8, 9.7 Hz, 1H), 3.89 (s, 3H), 3.88 (s, 3H), 3.70 (t, *J* = 4.7 Hz, 4H), 3.51 – 3.42 (m, 1H), 2.59 – 2.52 (m, 2H), 2.52 – 2.45 (m, 2H), 1.23 (d, *J* = 6.5 Hz, 3H). <sup>13</sup>C NMR (101 MHz, CDCl<sub>3</sub>)  $\delta$  148.51, 147.98, 133.49, 130.09, 130.02, 121.30, 112.13, 110.88, 67.20, 57.16, 55.84, 55.79, 50.49, 17.60. Calculated HRMS (ESI) for C<sub>16</sub>H<sub>23</sub>NO<sub>3</sub> [M+H]<sup>+</sup> is 278.1756, found 278.1745.

**(Z)-4-(4-(p-tolyl)but-3-en-2-yl)morpholine (2m)**



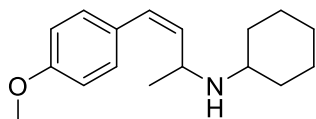
The general procedure **F** was followed using (*E*)-4-(4-(*p*-tolyl)but-3-en-2-yl)morpholine (50 mg, 0.22 mmol), *N,N*-diisopropylethylamine (3.8  $\mu$ L, 0.02 mmol) and 1.1 mL (1.5  $\mu$ mol) of stock solution of Ir(ppy)<sub>3</sub> in CH<sub>3</sub>CN to afford **2m** in 90% yield (45 mg, 0.19 mmol) as a yellow oil with a *Z*:*E* ratio of 94:6 (crude *Z*:*E* ratio 88:12). The substrate was purified by flash chromatography using CH<sub>2</sub>Cl<sub>2</sub> in MeOH (0 to 30% of MeOH) with product eluting at 7%. <sup>1</sup>H NMR (400 MHz, CDCl<sub>3</sub>)  $\delta$  7.14 (apparent s, 4H), 6.51 (d, *J* = 11.8 Hz, 1H), 5.59 (dd, *J* = 11.8, 9.8 Hz, 1H), 3.69 (t, *J* = 4.7 Hz, 4H), 3.46 – 3.37 (m, 1H), 2.57 – 2.49 (m, 2H), 2.49 – 2.42 (m, 2H), 2.35 (s, 3H), 1.23 (d, *J* = 6.5 Hz, 3H). <sup>13</sup>C NMR (101 MHz, CDCl<sub>3</sub>)  $\delta$  136.76, 134.53, 134.28, 130.39, 129.12, 128.88, 67.41, 57.38, 50.90, 21.39, 18.22. Calculated HRMS (ESI) for C<sub>15</sub>H<sub>21</sub>NO [M+H]<sup>+</sup> is 232.1701, found 232.1698.

#### (*Z*)-4-(4-(*o*-tolyl)but-3-en-2-yl)morpholine (**2n**)



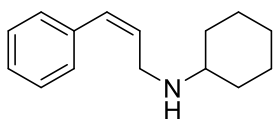
The general procedure **F** was followed using (*E*)-4-(4-(*o*-tolyl)but-3-en-2-yl)morpholine (50 mg, 0.22 mmol), *N,N*-diisopropylethylamine (3.8  $\mu$ L, 0.02 mmol) and 1.1 mL (1.5  $\mu$ mol) of stock solution of Ir(ppy)<sub>3</sub> in CH<sub>3</sub>CN to afford **2n** in 96% yield (48 mg, 0.21 mmol) as a yellow oil with a *Z*:*E* ratio of 98:2 (crude *Z*:*E* ratio 96:4). The substrate was purified by flash chromatography using 40% EtOAc in hexanes (containing 1% triethylamine) (0 to 100% of EtOAc) with the product eluting at 40%. <sup>1</sup>H NMR (400 MHz, CDCl<sub>3</sub>)  $\delta$  7.19 – 7.16 (m, 2H), 7.15 (d, *J* = 4.2 Hz, 1H), 7.12 (d, *J* = 6.3 Hz, 1H), 6.57 (d, *J* = 11.6 Hz, 1H), 5.68 (dd, *J* = 11.6, 9.9 Hz, 1H), 3.69 (t, *J* = 4.7 Hz, 4H), 3.21 – 3.09 (m, 1H), 2.60 – 2.46 (m, 2H), 2.45 – 2.36 (m, 2H), 2.25 (s, 3H), 1.19 (d, *J* = 6.5 Hz, 3H). <sup>13</sup>C NMR (101 MHz, CDCl<sub>3</sub>)  $\delta$  136.38, 136.0, 134.06, 130.0, 129.79, 128.91, 127.14, 125.40, 67.13, 57.28, 50.63, 19.93, 18.39. Calculated HRMS (ESI) for C<sub>15</sub>H<sub>21</sub>NO [M+H]<sup>+</sup> is 232.1701, found 232.1689.

**(Z)-N-(4-(4-methoxyphenyl)but-3-en-2-yl)cyclohexanamine (2o)**



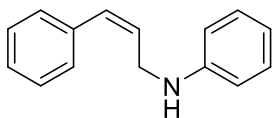
The general procedure **F** was followed using (*E*)-*N*-(4-(4-methoxyphenyl)but-3-en-2-yl)cyclohexanamine (50 mg, 0.18 mmol), *N,N*-diisopropylethylamine (3.1  $\mu$ L, 0.02 mmol) and 1.0 mL (1.2  $\mu$ mol) of stock solution of Ir(ppy)<sub>3</sub> in CH<sub>3</sub>CN to afford **2o** in 78% yield (39 mg, 0.14 mmol) as a yellow oil with a *Z:E* ratio of 91:9 (crude *Z:E* ratio 90:10). The substrate was purified by flash chromatography using CH<sub>2</sub>Cl<sub>2</sub> in MeOH (0 to 30% of MeOH) with the product eluting at 18%. <sup>1</sup>H NMR (400 MHz, CDCl<sub>3</sub>)  $\delta$  7.13 (d, *J* = 8.5 Hz, 2H), 6.86 (d, *J* = 6.6 Hz, 2H), 6.48 (d, *J* = 11.6 Hz, 1H), 5.50 (dd, *J* = 11.5, 9.8 Hz, 1H), 4.10 – 3.98 (m, 1H), 3.80 (s, 3H), 2.58 – 2.47 (m, 1H), 1.89 (br s, 1H), 1.73 – 1.47 (m, 4H), 1.34 (d, *J* = 6.5 Hz, 3H), 1.26 – 1.06 (m, 4H), 1.07 – 0.88 (m, 2H). <sup>13</sup>C NMR (101 MHz, CDCl<sub>3</sub>)  $\delta$  158.66, 130.06, 129.74, 129.58, 127.61, 113.80, 55.34, 54.12, 47.28, 25.86, 25.29, 24.95, 21.28. Calculated HRMS (ESI) for C<sub>17</sub>H<sub>25</sub>NO [M+H]<sup>+</sup> is 188.1439, found 188.1424.

**(Z)-N-(3-phenylallyl)cyclohexanamine**



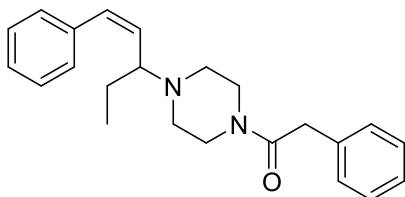
The general procedure **F** was followed using (*E*)-*N*-(3-phenylallyl)cyclohexanamine (50 mg, 0.18 mmol), *N,N*-diisopropylethylamine (3.1  $\mu$ L, 0.02 mmol) and 1.2 mL (1.6  $\mu$ mol) of stock solution of Ir(ppy)<sub>3</sub> in CH<sub>3</sub>CN to afford **2p** in 78% yield (39 mg, 0.14 mmol) as a yellow oil with a *Z:E* ratio of 85:15 (crude *Z:E* ratio 85:15). The substrate was purified by flash chromatography using CH<sub>2</sub>Cl<sub>2</sub> in MeOH (0 to 30% of MeOH) with the product eluting at 15%. <sup>1</sup>H NMR (400 MHz, CDCl<sub>3</sub>)  $\delta$  7.36 – 7.27 (m, 2H), 7.25 – 7.16 (m, 3H), 6.50 (d, *J* = 11.6 Hz, 1H), 5.76 (dt, *J* = 11.9, 6.6 Hz, 1H), 3.56 (dd, *J* = 6.6, 1.7 Hz, 2H), 3.20 (br s, 1H), 2.57 – 2.41 (m, 1H), 1.83 (d, *J* = 11.8 Hz, 2H), 1.74 – 1.63 (m, 2H), 1.26 – 1.02 (m, 6H). <sup>13</sup>C NMR (101 MHz, CDCl<sub>3</sub>)  $\delta$  137.16, 130.94, 128.93, 128.41, 127.15, 126.53, 56.58, 44.58, 33.19, 26.20, 25.22. Calculated HRMS (ESI) for C<sub>15</sub>H<sub>21</sub>N [M+H]<sup>+</sup> is 216.1752, found 216.1745.

### (Z)-N-(3-phenylallyl)aniline (**2q**)



The general procedure **F** was followed using (*E*)-*N*-(3-phenylallyl)aniline (50 mg, 0.18 mmol), *N,N*-diisopropylethylamine (3.1  $\mu$ L, 0.02 mmol) and 1.2 mL (1.7  $\mu$ mol) of stock solution of Ir(ppy)<sub>3</sub> in CH<sub>3</sub>CN to afford **2q** in 68% yield (34 mg, 0.16 mmol) as a yellow oil with a *Z*:*E* ratio of 83:17 (crude *Z*:*E* ratio 76:24). The substrate was purified by flash chromatography using EtOAc in hexanes (0 to 20% of EtOAc) with the product eluting at 5%. <sup>1</sup>H NMR (400 MHz, CDCl<sub>3</sub>)  $\delta$  7.31 – 7.25 (m, 2H), 7.23 – 7.17 (m, 3H), 7.17 – 7.12 (m, 1H), 7.11 – 7.05 (m, 2H), 6.68 – 6.53 (m, 1H), 6.50 (d, *J* = 7.9 Hz, 2H), 5.72 (dt, *J* = 11.8, 6.5 Hz, 1H), 3.94 (d, *J* = 6.5 Hz, 2H), 3.71 (br s, 1H). <sup>13</sup>C NMR (101 MHz, CDCl<sub>3</sub>)  $\delta$  148.09, 136.90, 131.74, 129.91, 129.46, 129.04, 128.58, 127.44, 117.85, 113.27, 42.53. Calculated HRMS (ESI) for C<sub>15</sub>H<sub>15</sub>N [M]<sup>+</sup> is 209.1204, found 209.2663.

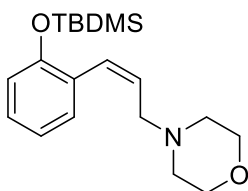
### (Z)-2-phenyl-1-(4-(1-phenylpent-1-en-3-yl)piperazin-1-yl)ethan-1-one (**2r**)



The starting (*E*)-2-phenyl-1-(4-(1-phenylpent-1-en-3-yl)piperazin-1-yl)ethan-1-one was synthesized following the general procedure **A** through **D** with only one modification that 2-butanone (2.8 equiv.) was used instead of acetone. The overall yield is 48% (over four steps). Then general procedure **F** was followed using (*E*)-2-phenyl-1-(4-(1-phenylpent-1-en-3-yl)piperazin-1-yl)ethan-1-one (50 mg, 0.15 mmol), *N,N*-diisopropylethylamine (2.6  $\mu$ L, 0.02 mmol) and 0.8 mL (1.0  $\mu$ mol) of stock solution of Ir(ppy)<sub>3</sub> in CH<sub>3</sub>CN to afford **2r** in 60% yield (30 mg, 0.09 mmol) as a yellow oil with a *Z*:*E* ratio of >99:1 (crude *Z*:*E* ratio 80:20). The substrate was purified by flash chromatography using 40% EtOAc in hexanes (containing 1% triethylamine) (0 to 100% of EtOAc) with product eluting at 45%. <sup>1</sup>H NMR (400 MHz, CDCl<sub>3</sub>)  $\delta$  7.41 – 7.36 (m, 4H), 7.36 – 7.32 (m, 3H), 7.30 – 7.23 (m, 3H), 6.72 (d, *J* = 11.8 Hz, 1H), 5.58 (dd, *J* = 11.7, 1.2 Hz, 1H), 5.15 (s, 2H), 3.59 – 3.44 (m, 4H), 3.44 – 3.32 (m, 1H), 2.57 (appr s, 2H), 2.41 (appr s, 2H), 1.82 – 1.68 (m, 1H), 1.62 – 1.46 (m, 1H), 0.94 (t, *J* = 7.4

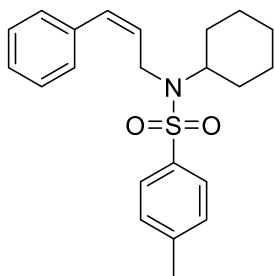
Hz, 3H). <sup>13</sup>C NMR (101 MHz, CDCl<sub>3</sub>) δ 155.10, 137.30, 136.73, 132.32, 131.91, 128.59, 128.41, 128.11, 127.90, 127.81, 126.73, 66.96, 62.16, 49.05, 44.11, 24.82, 10.54

**(Z)-4-(3-(2-((tert-butyldimethylsilyloxy)phenyl)allyl)morpholine (2s)**



The general procedure **F** was followed using (*E*)-4-(3-(2-((*tert*-butyldimethylsilyloxy)phenyl)allyl)morpholine (50 mg, 0.15 mmol), *N,N*-diisopropylethylamine (2.6 μL, 0.02 mmol) and 0.8 mL (1.0 μmol) of stock solution of Ir(ppy)<sub>3</sub> in CH<sub>3</sub>CN to afford **2s** in 90% yield (45 mg, 0.13 mmol) as a yellow oil with a *Z*:*E* ratio of 97:3 (crude *Z*:*E* ratio 93:7). The substrate was purified by flash chromatography using CH<sub>2</sub>Cl<sub>2</sub> in MeOH (0 to 20% of MeOH) with the product eluting at 5%. <sup>1</sup>H NMR (400 MHz, CDCl<sub>3</sub>) δ 7.15 (d, *J* = 7.7 Hz, 2H), 6.92 (td, *J* = 7.2, 0.8 Hz, 1H), 6.81 (dd, *J* = 8.0, 1.2 Hz, 1H), 6.69 (d, *J* = 11.8 Hz, 1H), 5.76 (dt, *J* = 11.9, 6.5 Hz, 1H), 3.71 (t, *J* = 4.8 Hz, 4H), 3.21 (dd, *J* = 6.5, 1.9 Hz, 2H), 2.44 (appr s, 4H), 0.99 (s, 9H), 0.18 (s, 6H). <sup>13</sup>C NMR (101 MHz, CDCl<sub>3</sub>) δ 157.53, 134.57, 132.69, 132.66, 132.50, 132.40, 124.88, 123.47, 71.15, 60.86, 57.79, 29.95, 22.44, 0.00. Calculated HRMS (ESI) for C<sub>19</sub>H<sub>31</sub>NO<sub>2</sub>Si [M+H]<sup>+</sup> is 334.2202, found 334.2191.

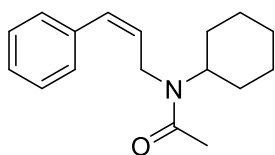
**(Z)-N-cyclohexyl-4-methyl-N-(3-phenylallyl)benzenesulfonamide (2t)**



The general procedure **F** was followed using (*E*)-*N*-cyclohexyl-4-methyl-*N*-(3-phenylallyl)benzenesulfonamide (50 mg, 0.14 mmol), *N,N*-diisopropylethylamine (2.4 μL, 0.01 mmol) and 1.0 mL (0.9 μmol) of stock solution of Ir(ppy)<sub>3</sub> in CH<sub>3</sub>CN to afford **2t** in 92% yield (46 mg, 0.12 mmol) as a white solid with a *Z*:*E* ratio of 97:3 (crude *Z*:*E* ratio 87:13). The substrate was purified by flash chromatography using EtOAc in hexanes (0 to 20% of EtOAc) with product eluting at 10%. <sup>1</sup>H NMR (400 MHz, CDCl<sub>3</sub>) δ 7.70 (d, *J* = 8.1 Hz, 2H), 7.42 – 7.34 (m, 2H), 7.32 – 7.25 (m, 3H), 7.22 (d, *J* = 7.4 Hz, 2H), 6.47 (d, *J* = 11.7 Hz, 1H), 5.74 (dt,

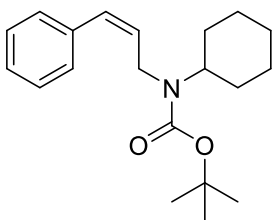
$J = 11.9, 6.0$  Hz, 1H), 4.16 – 4.09 (m, 2H), 3.78 – 3.67 (m, 1H), 2.44 (s, 3H), 1.73 – 1.63 (m, 2H), 1.63 – 1.54 (m, 2H), 1.26 – 1.17 (m, 4H), 0.95 – 0.89 (m, 2H).  $^{13}\text{C}$  NMR (101 MHz,  $\text{CDCl}_3$ )  $\delta$  143.00, 138.95, 136.77, 131.84, 129.81, 129.77, 128.95, 128.51, 127.29, 127.12, 58.16, 41.70, 31.92, 26.22, 25.44, 21.71

**(Z)-N-cyclohexyl-N-(3-phenylallyl)acetamide (2u)**



The general procedure **F** was followed using (*E*)-*N*-cyclohexyl-*N*-(3-phenylallyl)acetamide (50 mg, 0.19 mmol), *N,N*-diisopropylethylamine (3.5  $\mu\text{L}$ , 0.02 mmol) and 1.0 mL (1.4  $\mu\text{mol}$ ) of stock solution of  $\text{Ir}(\text{ppy})_3$  in  $\text{CH}_3\text{CN}$  to afford **2u** in 90% yield (45 mg, 0.17 mmol) as a yellow oil with a *Z:E* ratio of 88:12 (crude *Z:E* ratio 86:14). The substrate was purified by flash chromatography using EtOAc in hexanes (0 to 20% of EtOAc) with the product eluting at 10%. **Rotamer b**  $^1\text{H}$  NMR (400 MHz,  $\text{CDCl}_3$ )  $\delta$  7.37 – 7.27 (m, 2H), 7.24 – 7.14 (m, 3H), 6.43 (dd,  $J = 42.1, 11.7$  Hz, 1H), 5.53 (ddd,  $J = 17.5, 11.7, 5.8$  Hz, 1H), 4.46 – 4.35 (m, 1H), 4.04 (dd,  $J = 5.8, 2.1$  Hz, 2H), 1.86 (s, 3H), 1.81 – 1.59 (m, 6H), 1.30 (m, 4H). **Rotamer a** 7.37 – 7.27 (m, 2H), 7.24 – 7.14 (m, 3H), 6.43 (dd,  $J = 42.1, 11.7$  Hz, 1H), 5.53 (ddd,  $J = 17.5, 11.7, 5.8$  Hz, 1H), 4.16 (dd,  $J = 5.8, 2.1$  Hz, 2H), 3.51 – 3.37 (m, 1H), 2.09 (s, 3H), 1.79 – 1.54 (m, 6H), 1.25 – 1.15 (m, 4H).  $^{13}\text{C}$  NMR (400 MHz,  $\text{CDCl}_3$ )  $\delta$  170.65, 170.08, 137.10, 136.32, 131.73, 130.83, 130.50, 129.08, 128.88, 128.53, 128.35, 127.52, 126.95, 126.36, 58.36, 52.91, 42.41, 39.92, 31.88, 30.90, 26.00, 25.83, 25.62, 25.22, 22.37, 22.06. Calculated HRMS (ESI) for  $\text{C}_{17}\text{H}_{23}\text{NO}$   $[\text{M}+\text{H}]^+$  is 258.1858, found 258.1848.

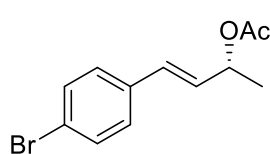
**(tert-butyl (Z)-cyclohexyl(3-phenylallyl)carbamate (2v)**



The general procedure **F** was followed using *tert*-butyl (*E*)-cyclohexyl(3-phenylallyl)carbamate (50 mg, 0.16 mmol), *N,N*-diisopropylethylamine (2.8  $\mu\text{L}$ , 0.02 mmol) and 0.8 mL (1.1  $\mu\text{mol}$ ) of stock solution of  $\text{Ir}(\text{ppy})_3$  in  $\text{CH}_3\text{CN}$  to afford **2v** in 90% yield (45 mg, 0.14 mmol) as a yellow oil

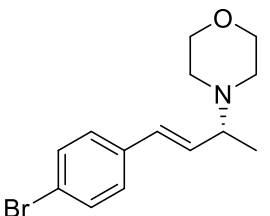
with a *Z:E* ratio of 90:10 (crude *Z:E* ratio 87:13). The substrate was purified by flash chromatography using EtOAc in hexanes (0 to 20% of EtOAc) with the product eluting at 5%. <sup>1</sup>H NMR (400 MHz, CDCl<sub>3</sub>) δ 7.39 – 7.27 (m, 3H), 7.25 – 7.19 (m, 2H), 6.41 (d, *J* = 11.7 Hz, 1H), 5.66 – 5.56 (apparent s, 1H), 4.04 (apparent s, 2H), 3.97 – 3.80 (apparent s, 1H), 1.78 – 1.62 (m, 4H), 1.41 (s, 9H), 1.31 – 1.17 (m, 6H). <sup>13</sup>C NMR (101 MHz, CDCl<sub>3</sub>) δ 155.53, 137.14, 132.67, 128.91, 128.65, 128.33, 126.95, 79.46, 54.98, 41.34, 31.39, 28.60, 26.08, 25.61. Calculated HRMS (ESI) for C<sub>20</sub>H<sub>29</sub>NO<sub>2</sub> [M+H]<sup>+</sup> is 316.2277, found 316.2259.

### Synthesis of enantioenriched *trans*-allylic acetate.



**(*R, E*)-4-(4-bromophenyl)but-3-en-2-yl acetate** : To an oven-dried round-bottomed flask equipped with magnetic stir bar was added allylic alcohol **B** (Scheme 1) (3.0 g, 13.2 mmol), TBME (12 mL), Lipase PS (250 mg) and vinyl acetate (1.8 mL, 19.2 mmol) and the reaction mixture was stirred at room temperature for 18 hours. The suspension was then filtered to remove the Lipase PS. The filtrate was concentrated under reduced pressure and the residue then purified by normal phase chromatography using 40% EtOAc in hexanes gradients (0 to 50% of EtOAc) (product eluting at 15%) to obtain the title compound (1.1 g, 31%, 99% ee) as a colorless oil. The *R* configuration of the product was assumed based on analogy with literature precedent.

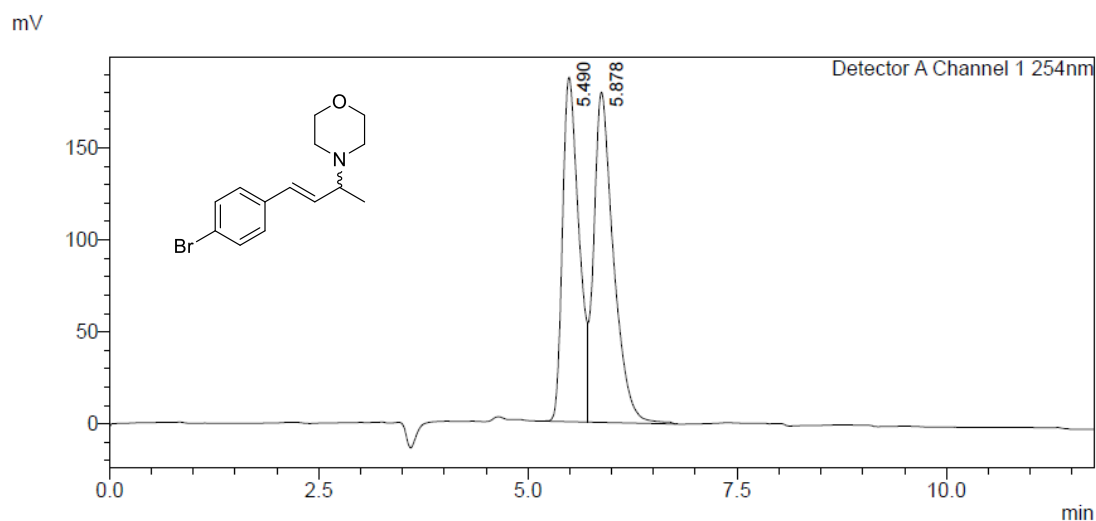
### Synthesis of enantioenriched *trans*-allylic amine (*R*)-1j



**(*R, E*)-4-(4-(4-bromophenyl)but-3-en-2-yl)morpholine** : To an oven-dried round-bottomed flask equipped with magnetic stir bar was added (*R,E*)-4-(4-bromophenyl)but-3-en-2-yl acetate (200 mg, 0.75 mmol, 99% ee), dry toluene (1.5 ml), tetrakis(triphenylphosphine)palladium(0), (Pd(PPh<sub>3</sub>)<sub>4</sub>), (26.0 mg, 0.02 mmol) and morpholine (0.10 ml, 0.90 mmol) and the reaction mixture was stirred at 50 °C for 4 hours under Ar atmosphere. The reaction was monitored by TLC. After

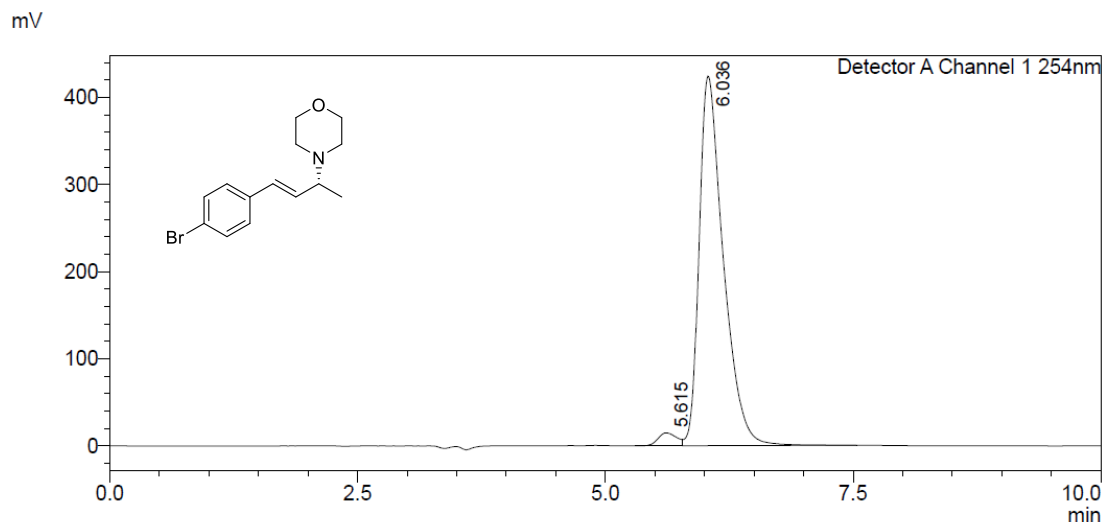
the complete consumption of the starting material, the reaction mixture was quenched with  $\text{NH}_4\text{OH}$ . The organic layer was separated, dried over  $\text{MgSO}_4$  and concentrated to obtain the crude product that was purified by normal phase chromatography using 40% EtOAc in hexanes (containing 1% triethylamine) gradients (0 to 100% of EtOAc), with the product eluting at 40%, to obtain the title compound (150 mg, 0.51 mmol, 94% ee) as a yellow colored oil. We assume that the Tsuji-Trost allylic amination proceeds with double inversion of the stereocenter and hence we ended up with net retention of the configuration of the starting allylic acetate.<sup>12</sup> HPLC analysis (AD-H, 10% ethanol/(0.1% triethylamine in hexanes), 1.0 mL/min, 254 nm) indicated 94% ee:  $t_R$  (major) = 6.0 min.,  $t_R$  (minor) = 5.6 min.  $[\alpha]_D^{20} = +50.35$  (c 2.0,  $\text{CHCl}_3$ ).  $^1\text{H}$  NMR (400 MHz,  $\text{CDCl}_3$ )  $\delta$  7.43 (d,  $J = 8.3$  Hz, 2H), 7.23 (d,  $J = 8.4$  Hz, 2H), 6.40 (d,  $J = 15.9$  Hz, 1H), 6.16 (dd,  $J = 15.9, 8.1$  Hz, 1H), 3.73 (t,  $J = 4.6$  Hz, 4H), 3.07 – 2.96 (m, 1H), 2.60 – 2.50 (m, 4H), 1.25 (d,  $J = 6.5$  Hz, 3H).  $^{13}\text{C}$  NMR (101 MHz,  $\text{CDCl}_3$ )  $\delta$  135.91, 133.09, 131.71, 130.08, 127.85, 121.21, 67.26, 63.02, 50.78, 17.65.

### Racemic 1j



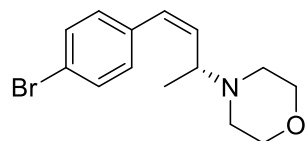
Peak#	Ret. Time	Area	Height	Conc.	Unit	Mark	Name
1	5.490	2557075	187076	46.530			
2	5.878	2938499	179347	53.470		V	
Total		5495574	366423				

**(R)-1j** 94% ee



Peak#	Ret. Time	Area	Height	Conc.	Unit	Mark	Name
1	5.615	192295	14805	2.600			
2	6.036	7203030	424263	97.400		SV	
Total		7395325	439068				

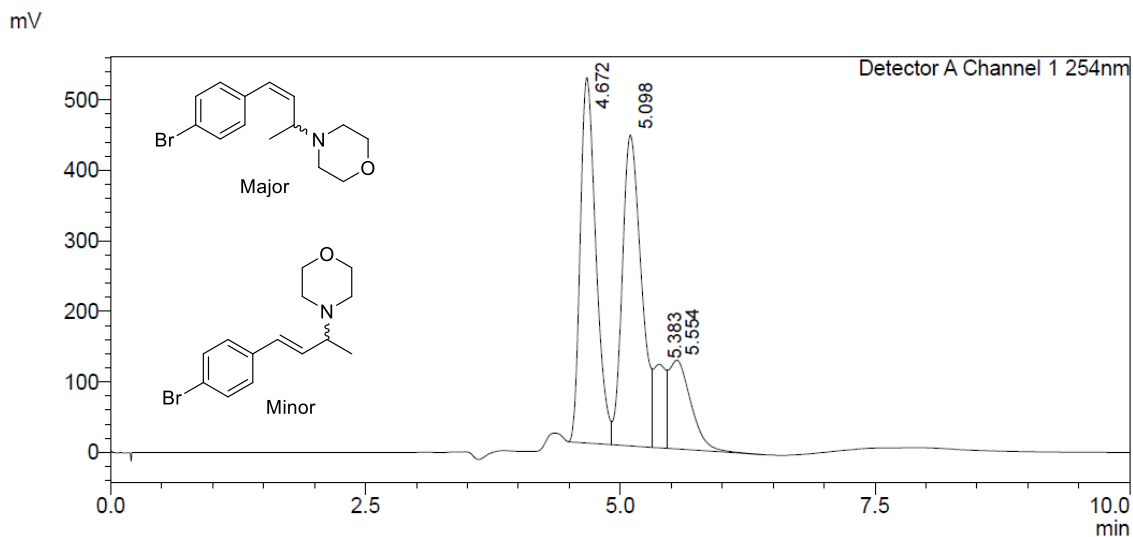
**(R, Z)-4-(4-(4-bromophenyl)but-3-en-2-yl)morpholine (R)-2j**



The general procedure **F** was followed using (*R,E*)-4-(4-(4-bromophenyl)but-3-en-2-yl)morpholine (50 mg, 0.17 mmol, 94% ee), *N,N*-diisopropylethylamine (3.0  $\mu$ L, 0.02 mmol) and 0.90 mL (1.2  $\mu$ mol) of stock solution of Ir(ppy)<sub>3</sub> in CH<sub>3</sub>CN to afford (**R**)-**2j** in 88% yield (44 mg, 0.15 mmol, 94% ee) as a yellow oil with a *Z*:*E* ratio of 79:21 (crude *Z*:*E* ratio 77:23). The substrate was purified by flash chromatography using 40% EtOAc in hexanes (containing 1% triethylamine) (0 to 100% of EtOAc) with the product eluting at 40%. HPLC analysis (AD-H, 10% ethanol/(0.1% triethylamine in hexanes), 1.0 mL/min, 254 nm) indicated 94% ee:  $t_R$  (major) = 5.1 min.,  $t_R$  (minor) = 4.7 min.  $[\alpha]_D^{20} = +29.88$  (c 0.80, CHCl<sub>3</sub>). <sup>1</sup>H NMR (400 MHz, CDCl<sub>3</sub>)  $\delta$  7.48 (d, *J* = 8.4 Hz, 2H), 7.15 (d, *J* = 8.3 Hz, 2H), 6.49 (d, *J* = 11.8 Hz, 1H), 5.69 (dd, *J* = 11.8, 9.8 Hz, 1H), 3.72 (t, *J* = 4.7 Hz, 4H), 3.43 – 3.30 (m, 1H), 2.60 – 2.50 (m, 2H), 2.51 – 2.41 (m, 2H), 1.24 (d, *J* = 6.5 Hz, 3H).

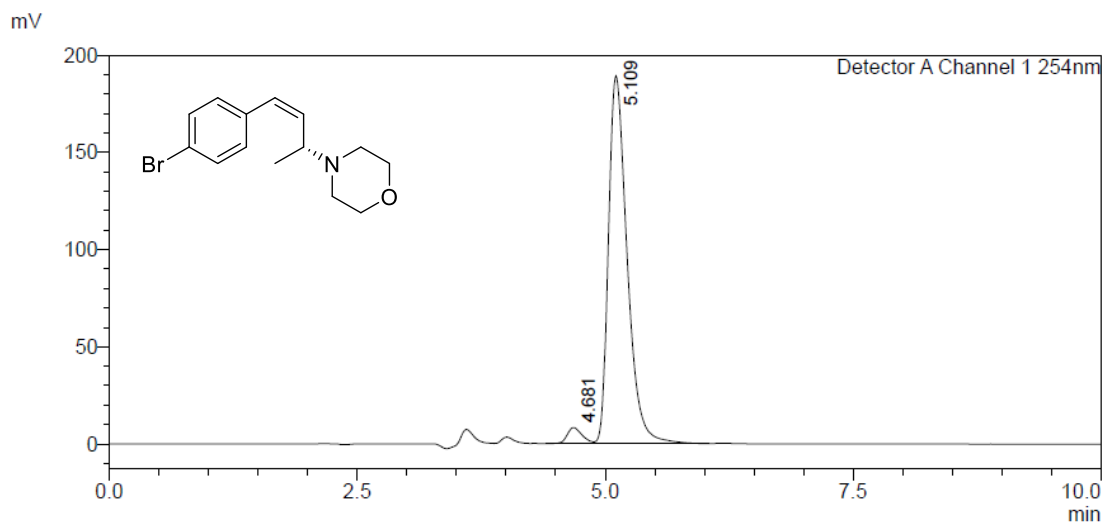
$^{13}\text{C}$  NMR (101 MHz,  $\text{CDCl}_3$ )  $\delta$  136.09, 135.54, 131.34, 130.37, 129.16, 120.82, 67.18, 57.07, 50.58, 17.75. Calculated HRMS (ESI) for  $\text{C}_{14}\text{H}_{18}\text{BrNO}$   $[\text{M}+\text{H}]^+$  is 296.0650, found 296.0632.

**Racemic (*R*)-2j (Major) and (*R*)-1j (Minor)**



Peak#	Ret. Time	Area	Height	Conc.	Unit	Mark	Name
1	4.672	5575177	517858	39.234			
2	5.098	5763604	440669	40.560		V	
3	5.383	974626	118437	6.859		V	
4	5.554	1896562	125790	13.347		V	
Total		14209968	1202754				

**(*R*)-2j 94% ee**



Peak#	Ret. Time	Area	Height	Conc.	Unit	Mark	Name
1	4.681	86463	8203	3.373			
2	5.109	2476666	189098	96.627		V	
Total		2563129	197300				

### Emission Quenching Experiment

Emission intensities were recorded on Varian Carey Eclipse fluorescence spectrophotometer. All solutions of Ir(ppy)<sub>3</sub> in MeCN were excited at 370 nm and the emission intensities were observed at 520 nm. In this experiment, 1.0 μM of Ir(ppy)<sub>3</sub> in MeCN was added to the appropriate amount of the quencher (**1s** or **2s**) in a 1.0 cm quartz cuvette. After degassing each solution with a stream of Ar for 15 minutes, the emission spectra were recorded.

**Figure 7. Ir(ppy)<sub>3</sub> emission quenching by 2s (Z)-4-(3-(2-((tert-butyl)dimethylsilyl)oxy)phenyl)allyl)morpholine**

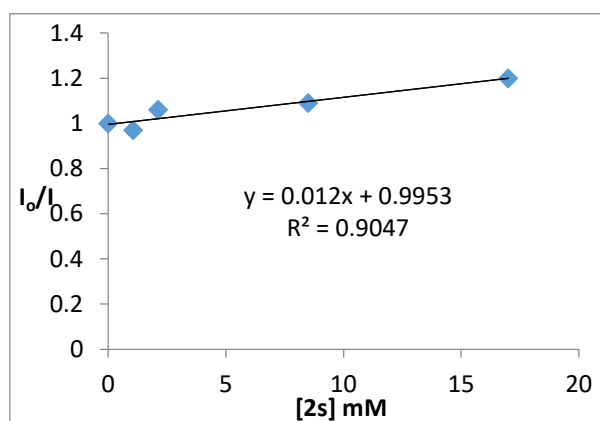
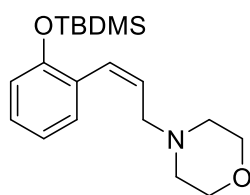
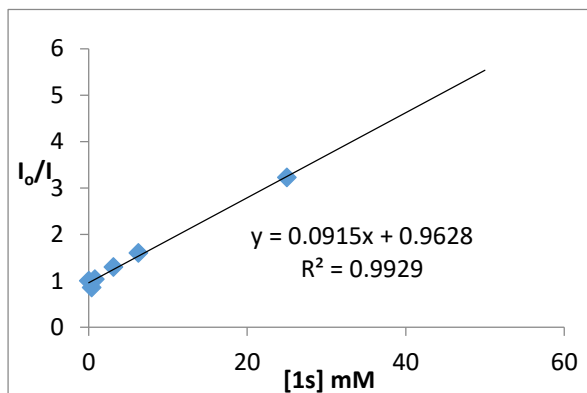
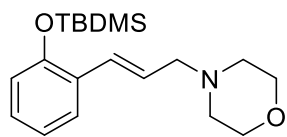


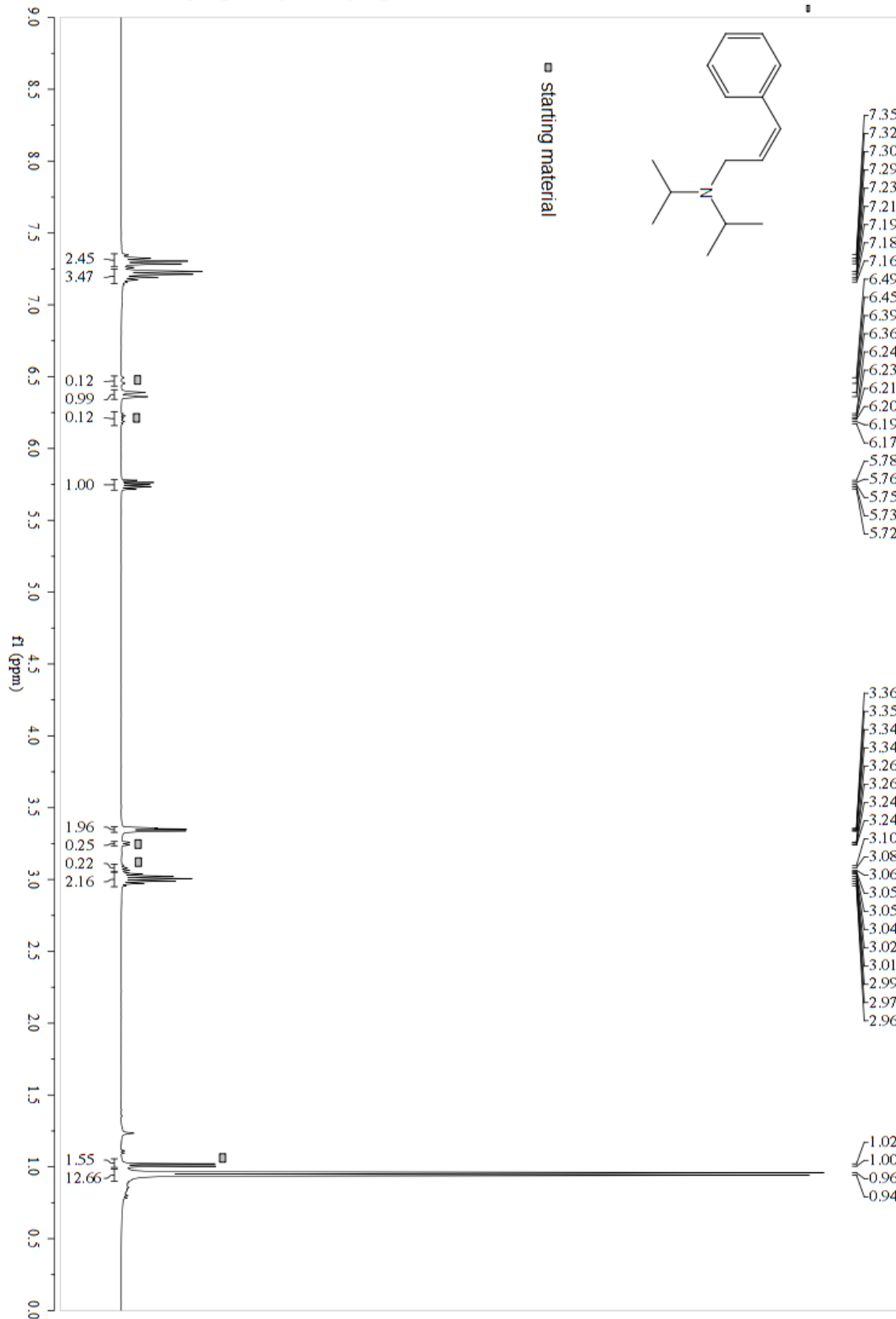
**Figure 8. Ir(ppy)<sub>3</sub> emission quenching by 1s (*E*)-4-(3-(2-((*tert*-butyldimethylsilyl)oxy)phenyl)allyl)morpholine**



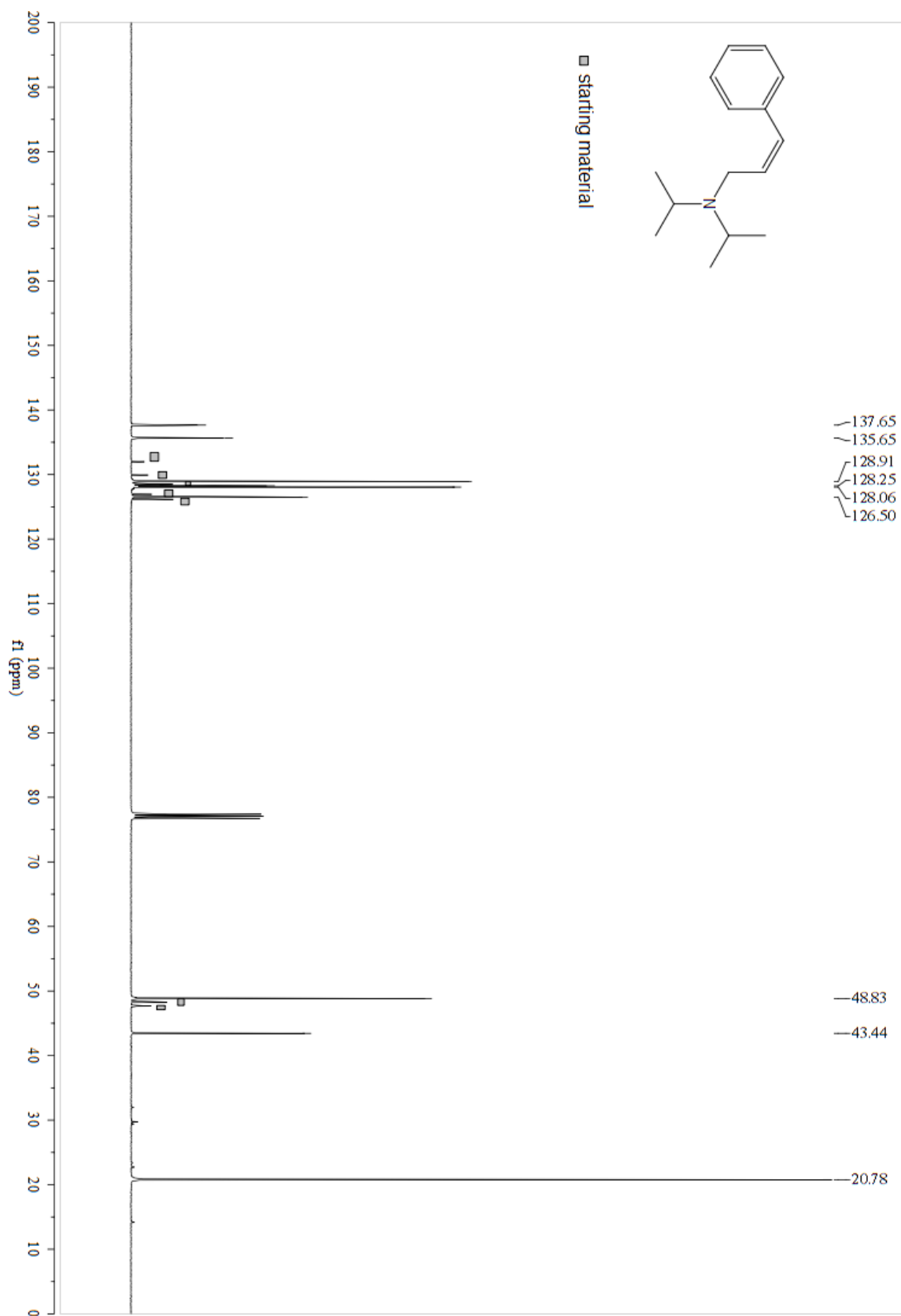
## 2.7 References

1. Ramamurthy, V.; Liu, R. S. H., *J. Am. Chem. Soc.* **1976**, *98*, 2935.
2. Gottumukkala, A. L.; Madduri, A. V. R.; Minnaard, A. J., *ChemCatChem* **2012**, *4*, 462.
3. Chen, C.; Dugan, T. R.; Brennessel, W. W.; Weix, D. J.; Holland, P. L., *J. Am. Chem. Soc.* **2014**, *136*, 945.
4. Tomassy, B.; Zwierzak, A., *Synth. Commun.* **1998**, *28*, 1201.
5. No special measures were taken to increase the sensitivity the GCMS towards our samples or to quantify these results but rather were used to illuminate the relevant trends.
6. Acree, W. E.; Pandey, S.; Tucker, S. A.; Fetzer, J. C., *Polycyclic Aromatic Compounds* **1997**, *12*, 71.
7. Turro, N. J.; Ramamurthy, V.; Scaiano, J. C.; University Science Books: Sausalito, Calif., 2010, p xxxiii, 1084 p
8. Given that the Z-isomer is not geometrically pure, we are hesitant to assume any greater precision
9. Lalevée, J.; Tehfe, M.-A.; Dumur, F.; Gimes, D.; Blanchard, N.; Morlet-Savary, F.; Fouassier, J. P., *ACS Macro Lett.* **2012**, *1*, 286.
10. Freeman, D. B.; Furst, L.; Condie, A. G.; Stephenson, C. R. J., *Org. Lett.* **2012**, *14*, 94.
11. Dibble, T. S.; Sha, Y.; Thornton, W. F.; Zhang, F., *J. Phy. Chem. A* **2012**, *116*, 7603.
12. Hammond, G. S.; Saltiel, J.; Lamola, A. A.; Turro, N. J.; Bradshaw, J. S.; Cowan, D. O.; Counsell, R. C.; Vogt, V.; Dalton, C., *J. Am. Chem. Soc.* **1964**, *86*, 3197.
13. Lu, Z.; Yoon, T. P., *Angew. Chem. Int. Ed.* **2012**, *51*, 10329.
14. Paddon-Row, M. N.; Houk, K. N., *J. Am. Chem. Soc.* **1981**, *103*, 5046.
15. Fabry, D. C.; Ronge, M. A.; Rueping, M., *Chem. Eur. J.* **2015**, *21*, 5350.
16. Rackl, D.; Kreitmeier, P.; Reiser, O., *Green Chem.* **2016**, *18*, 214.
17. Metternich, J. B.; Gilmour, R., *J. Am. Chem. Soc.* **2015**, *137*, 11254.
18. Zhan, K.; Li, Y., *Catalysts* **2017**, *7*, 337.
19. Brenna, E.; Dei Negri, C.; Fuganti, C.; Gatti, F. G.; Serra, S., *Tetrahedron: Asymmetry* **2004**, *15*, 335.

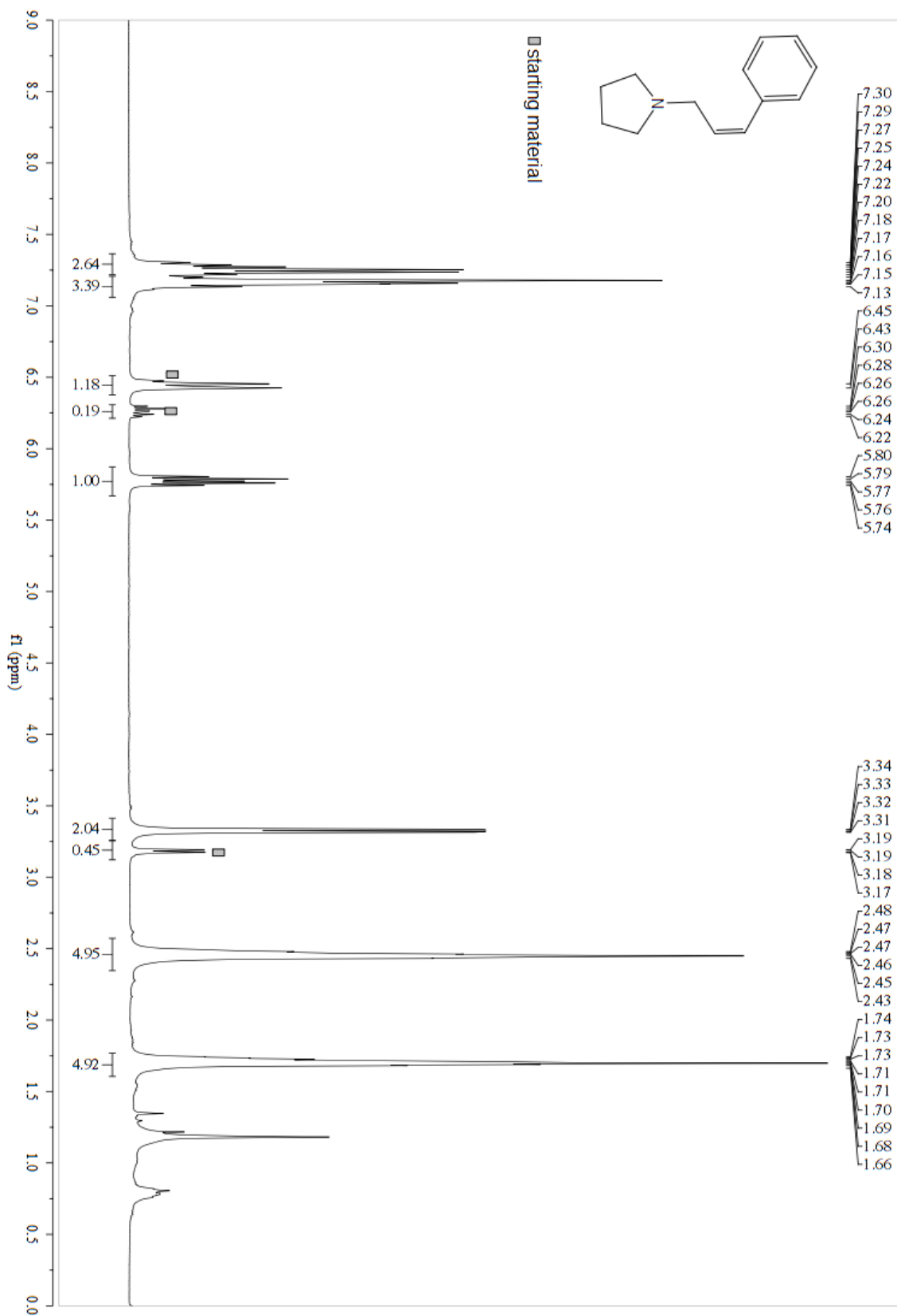
**2a (Z)-N,N-diisopropyl-3-phenylprop-2-en-1-amine**



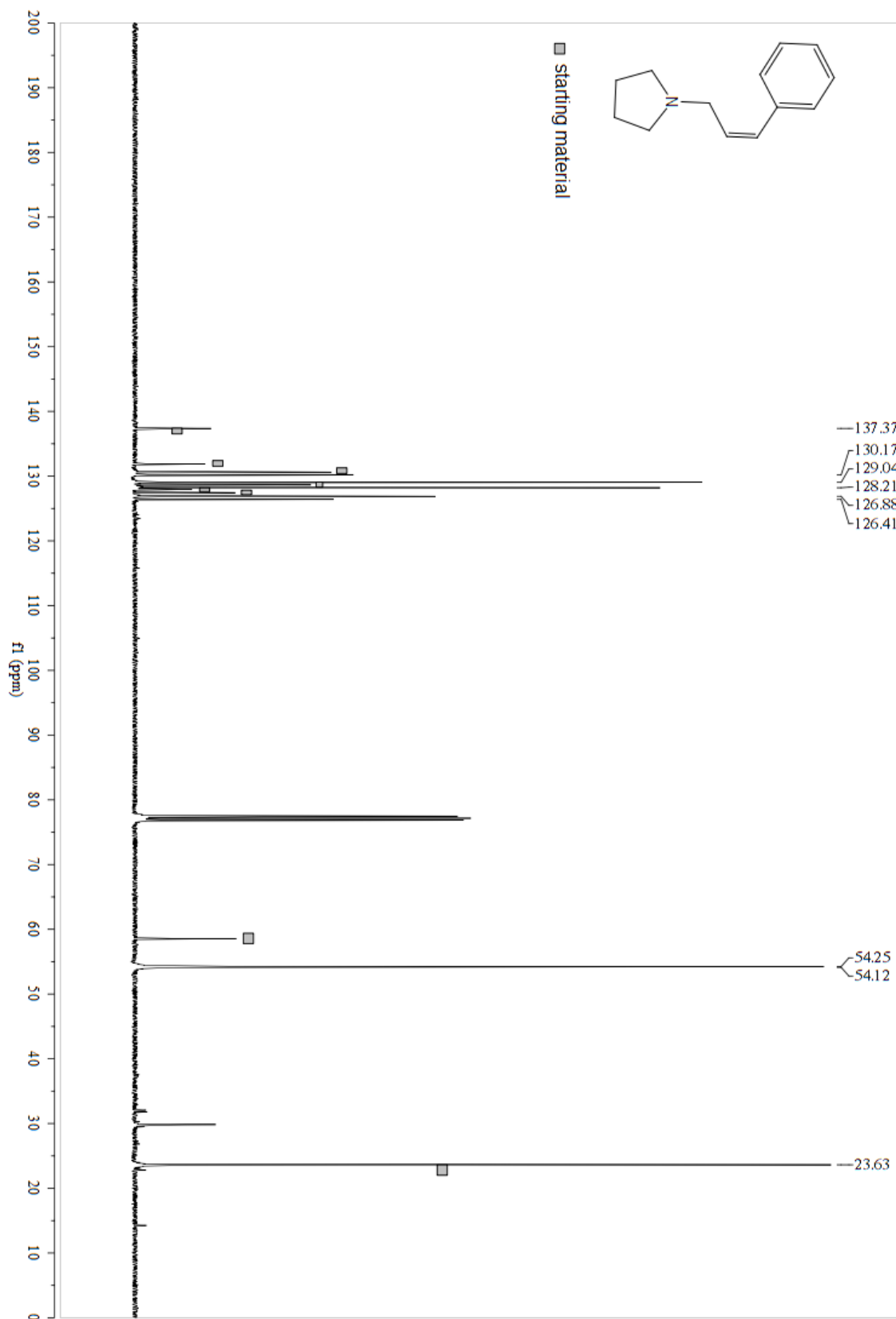
**2a (Z)-N,N-diisopropyl-3-phenylprop-2-en-1-amine**



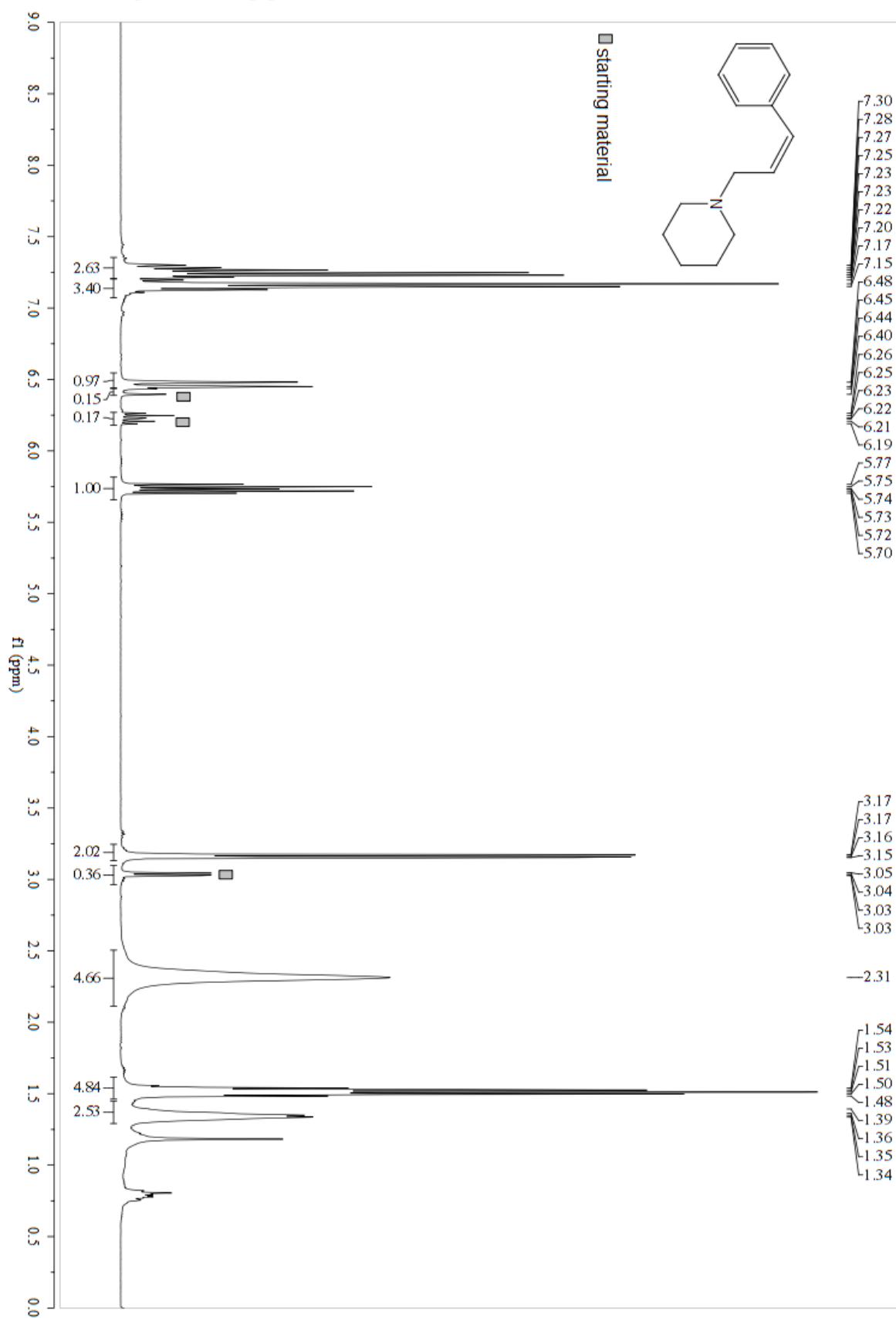
**2b (Z)-1-(3-phenylallyl)pyrrolidine**



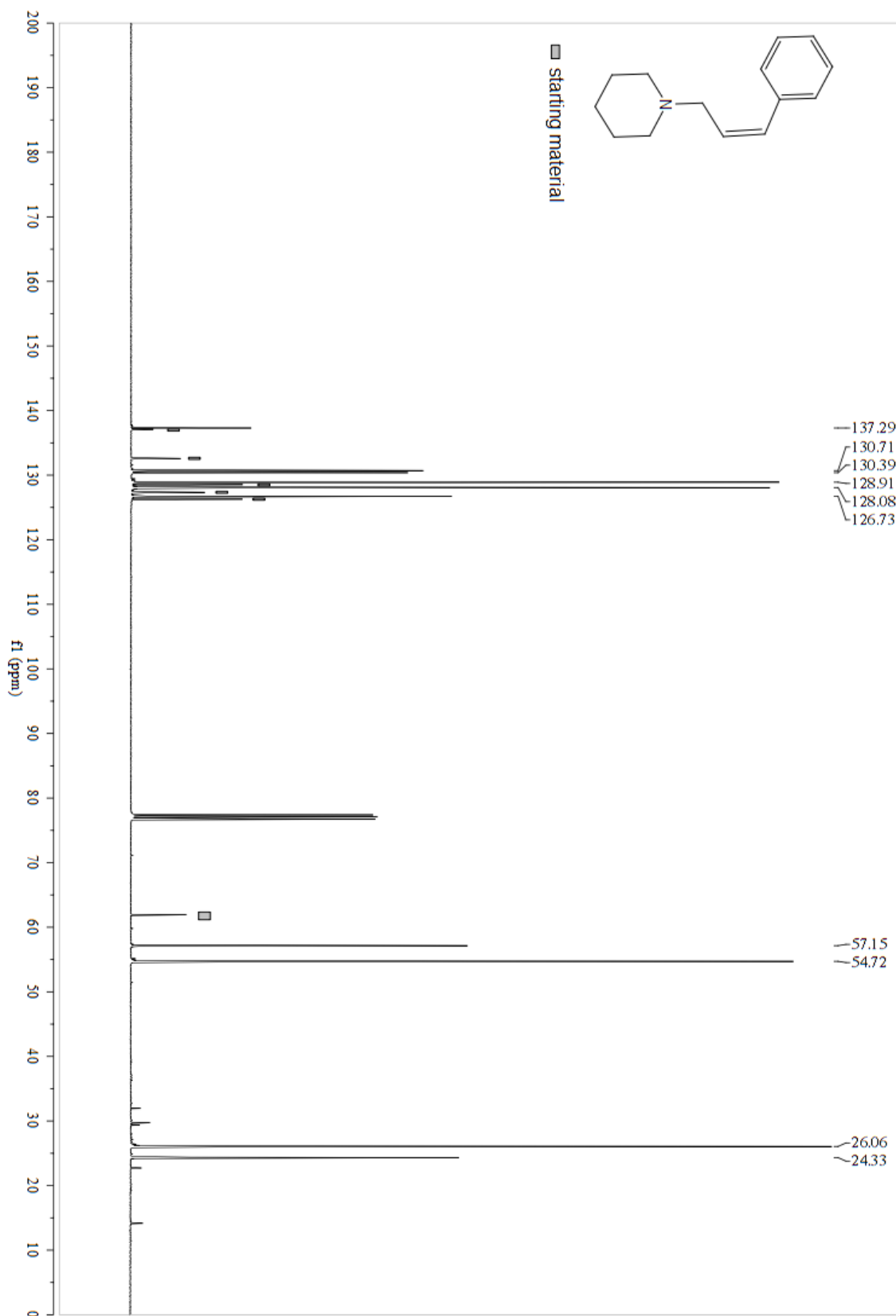
**2b (Z)-1-(3-phenylallyl)pyrrolidine**



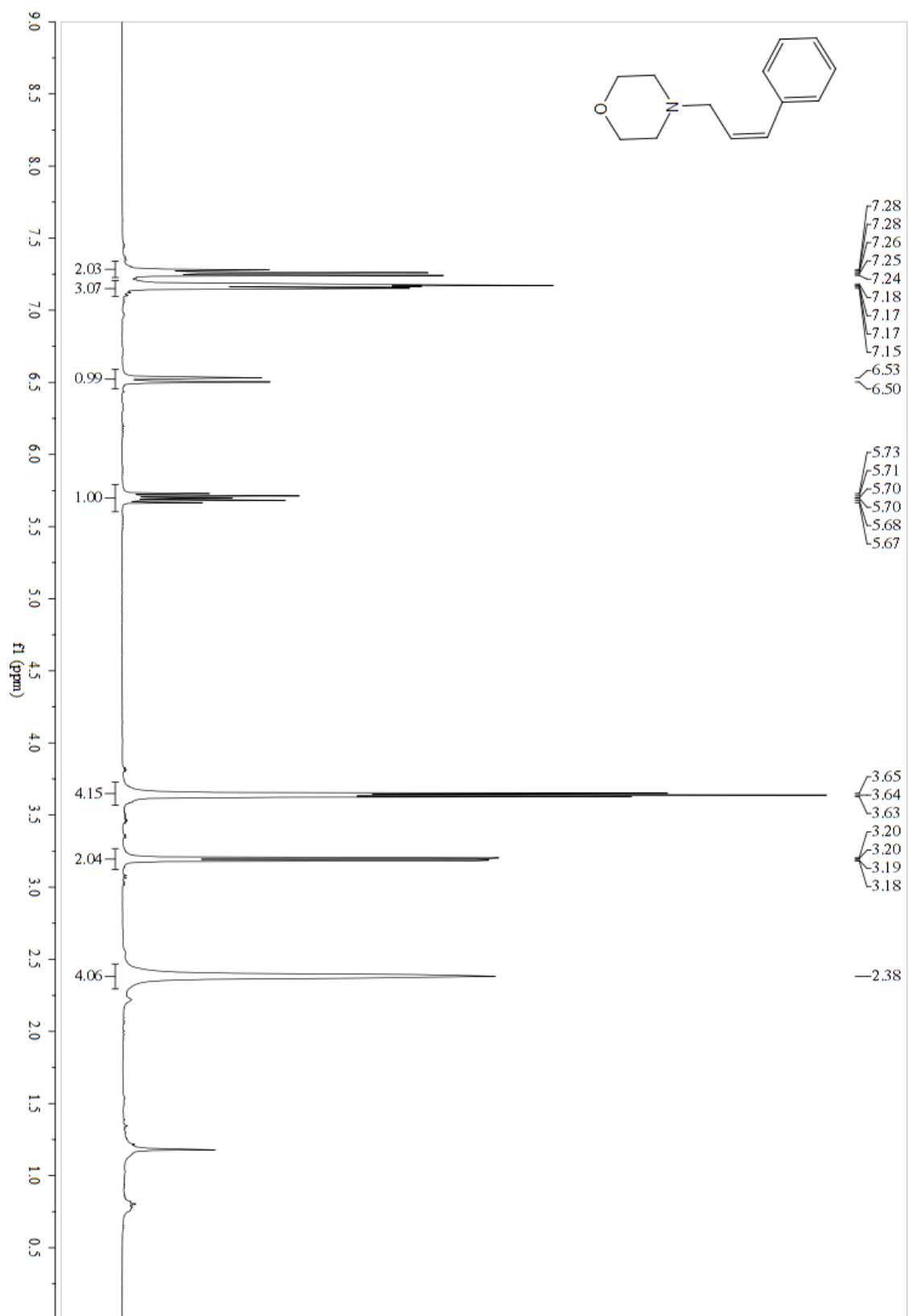
## 2c (Z)-1-(3-phenylallyl)piperidine



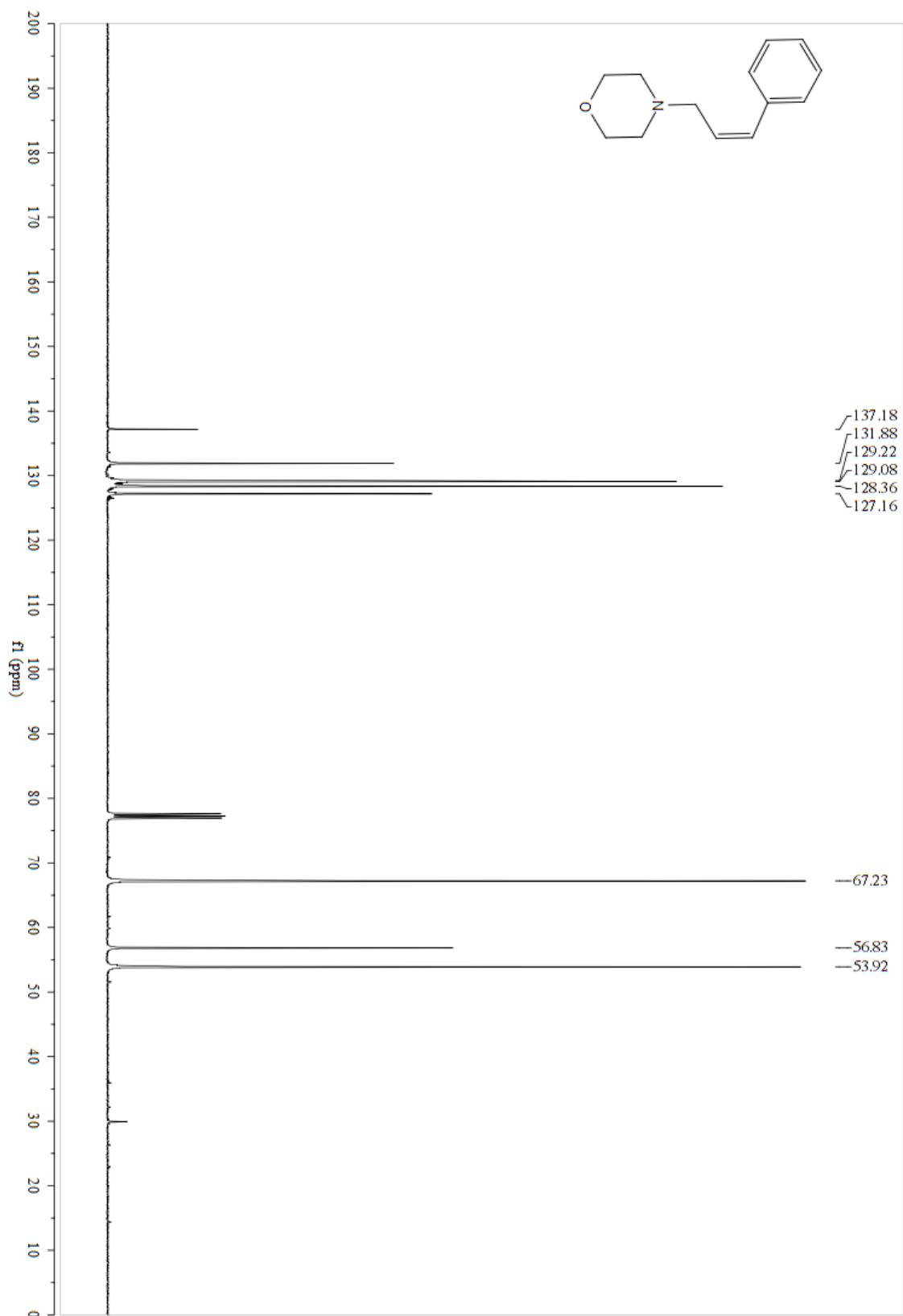
**2c (Z)-1-(3-phenylallyl)piperidine**



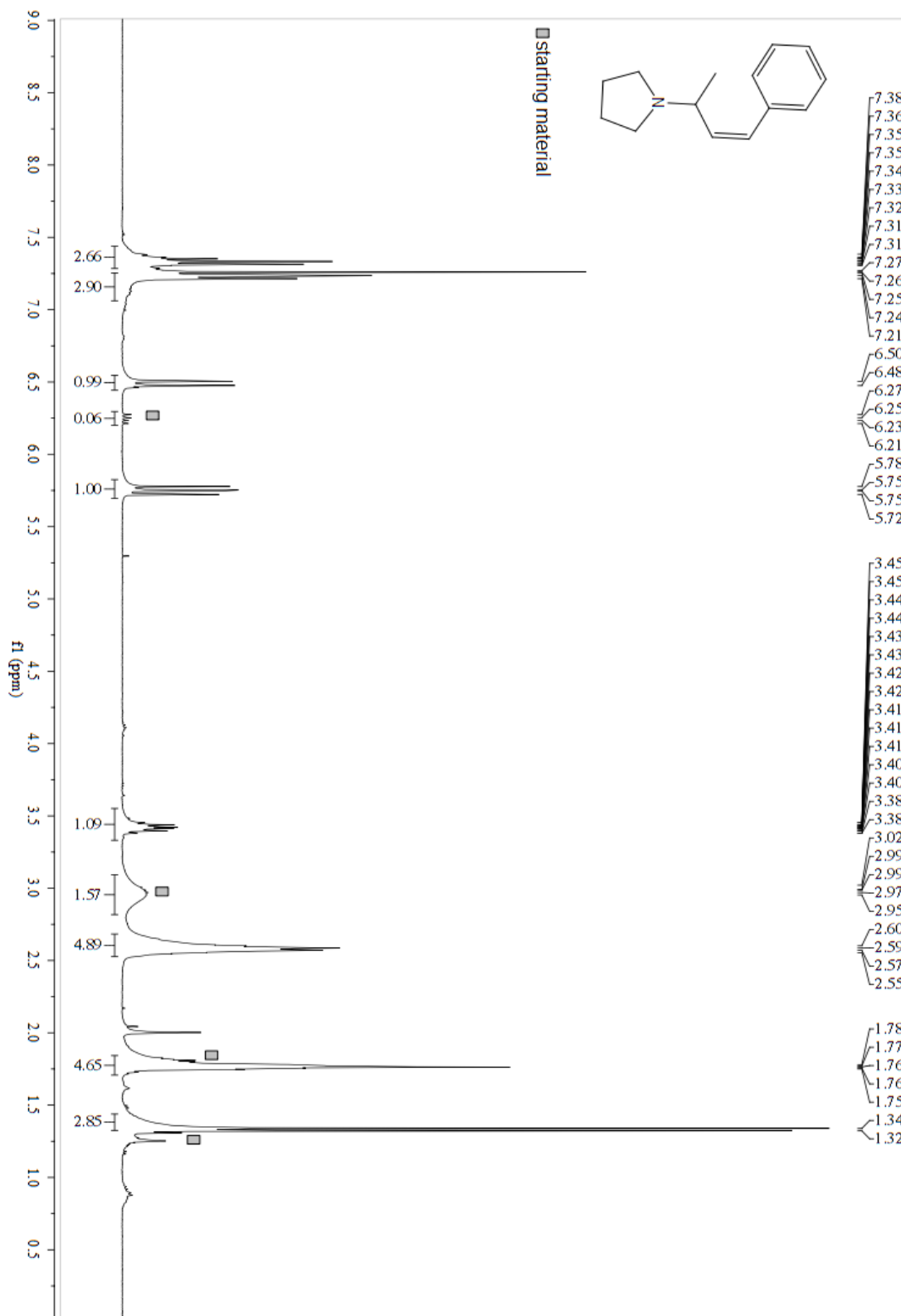
**2d (Z)-4-(3-phenylallyl)morpholine**



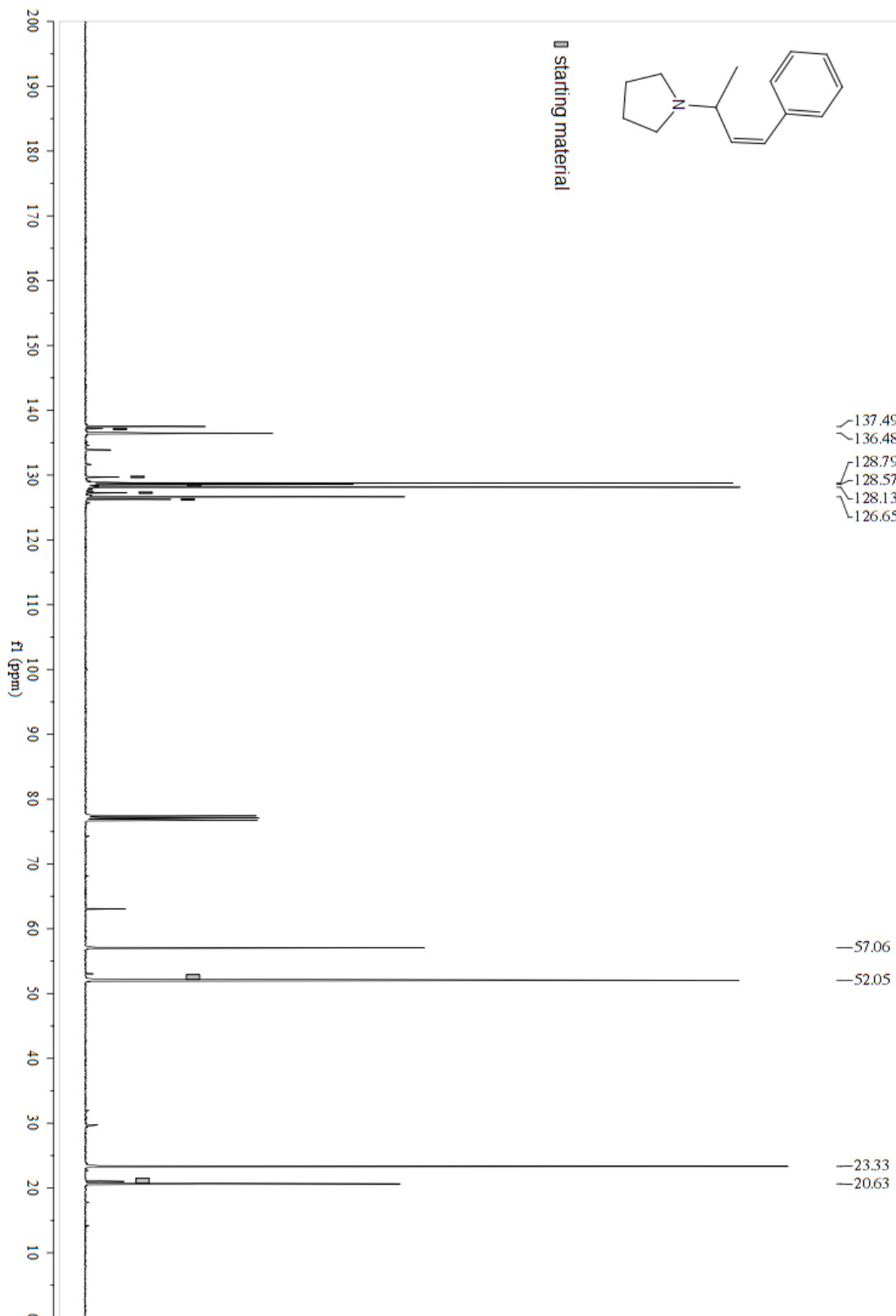
**2d (Z)-4-(3-phenylallyl)morpholine**



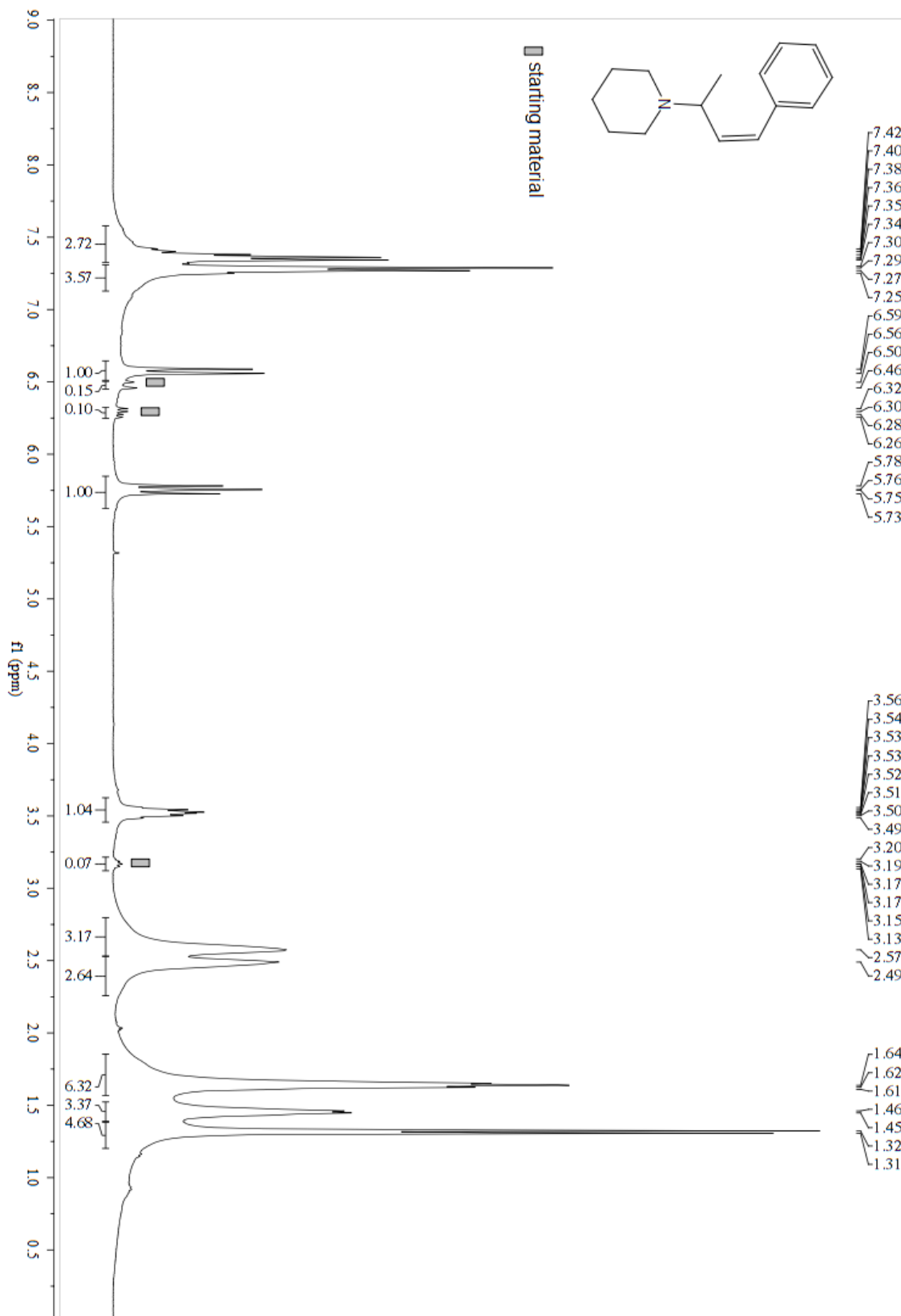
**2e (Z)-1-(4-phenylbut-3-en-2-yl)pyrrolidine**



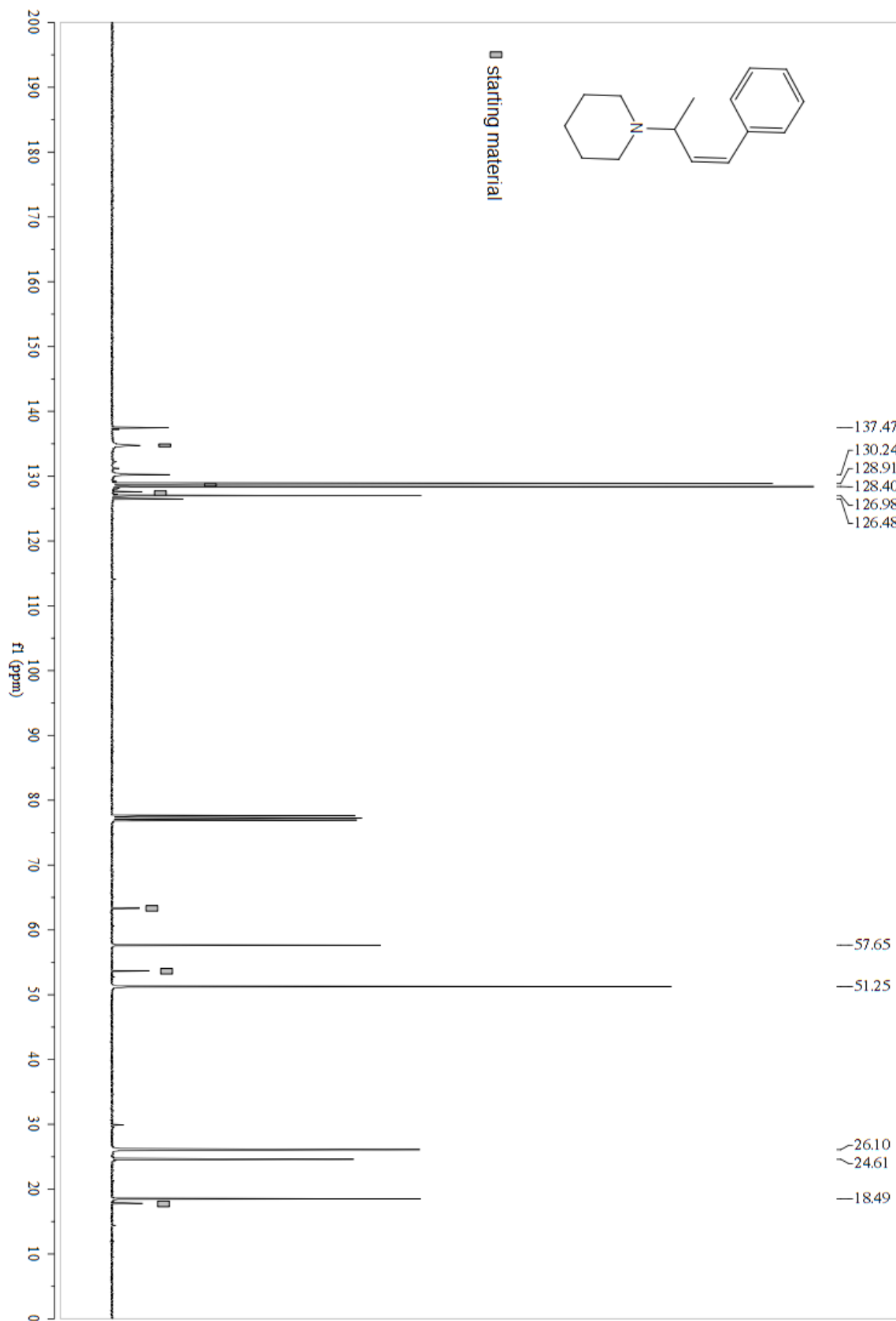
**2e (Z)-1-(4-phenylbut-3-en-2-yl)pyrrolidine**



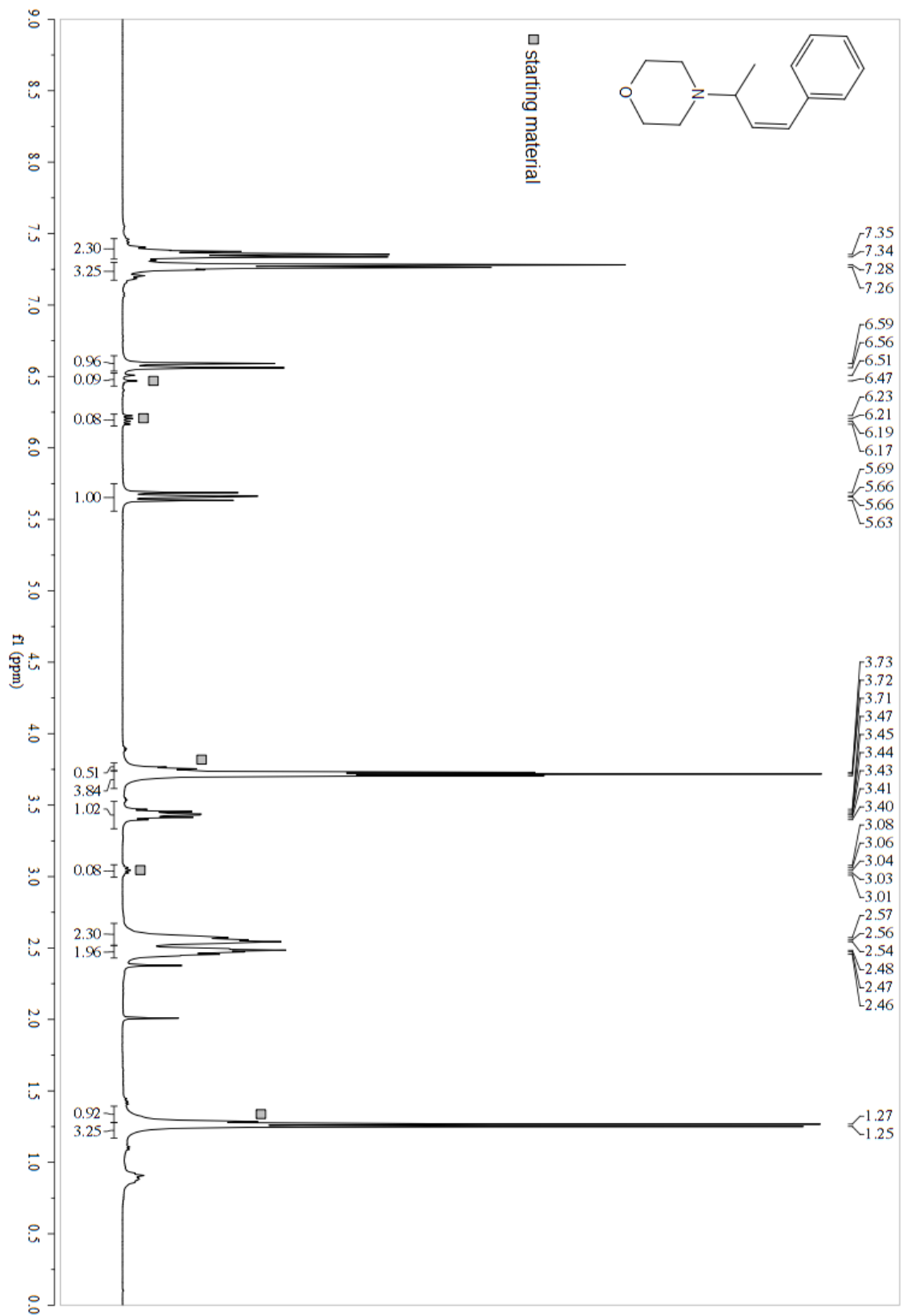
**2f (Z)-1-(4-phenylbut-3-en-2-yl)piperidine**



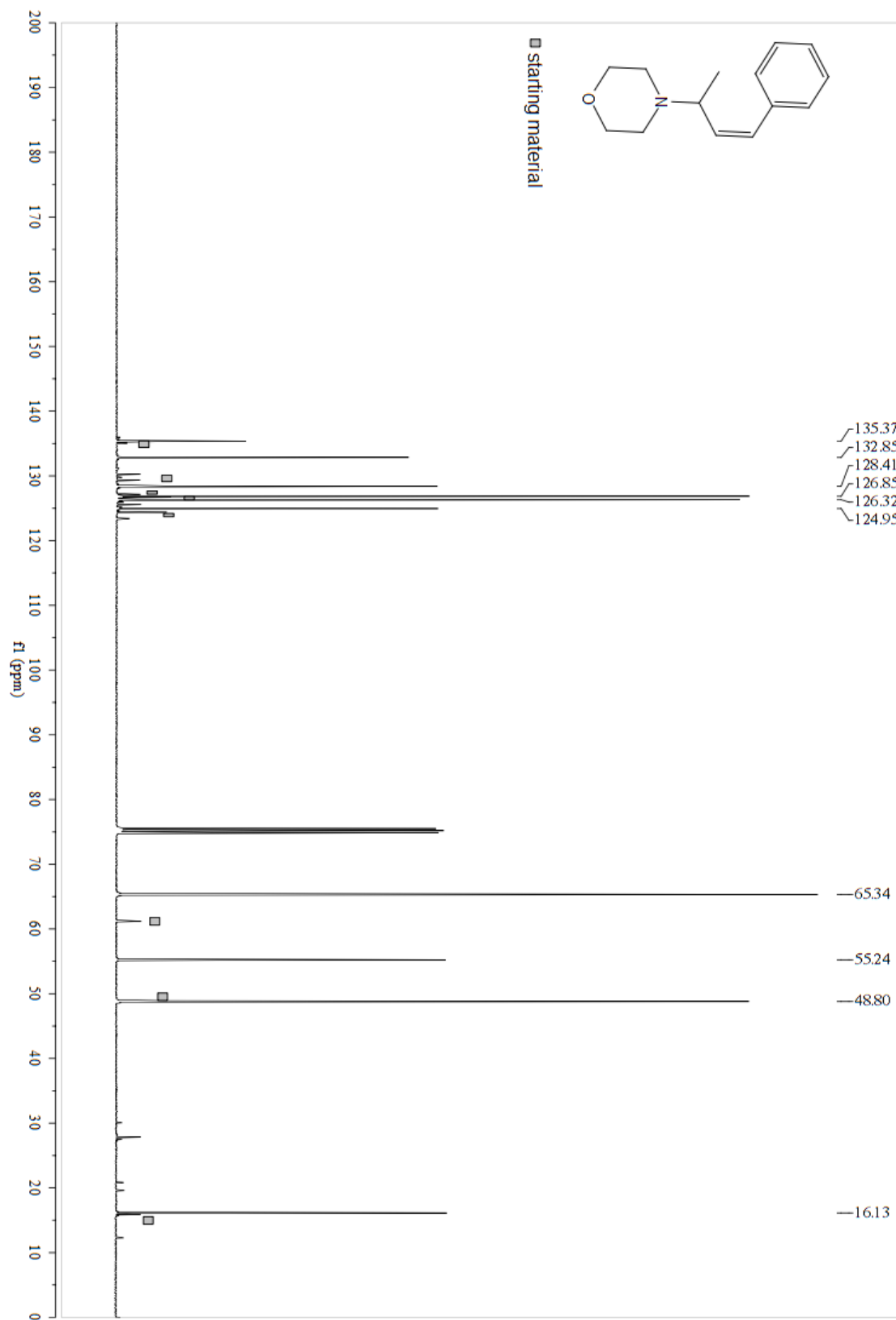
**2f (Z)-1-(4-phenylbut-3-en-2-yl)piperidine**



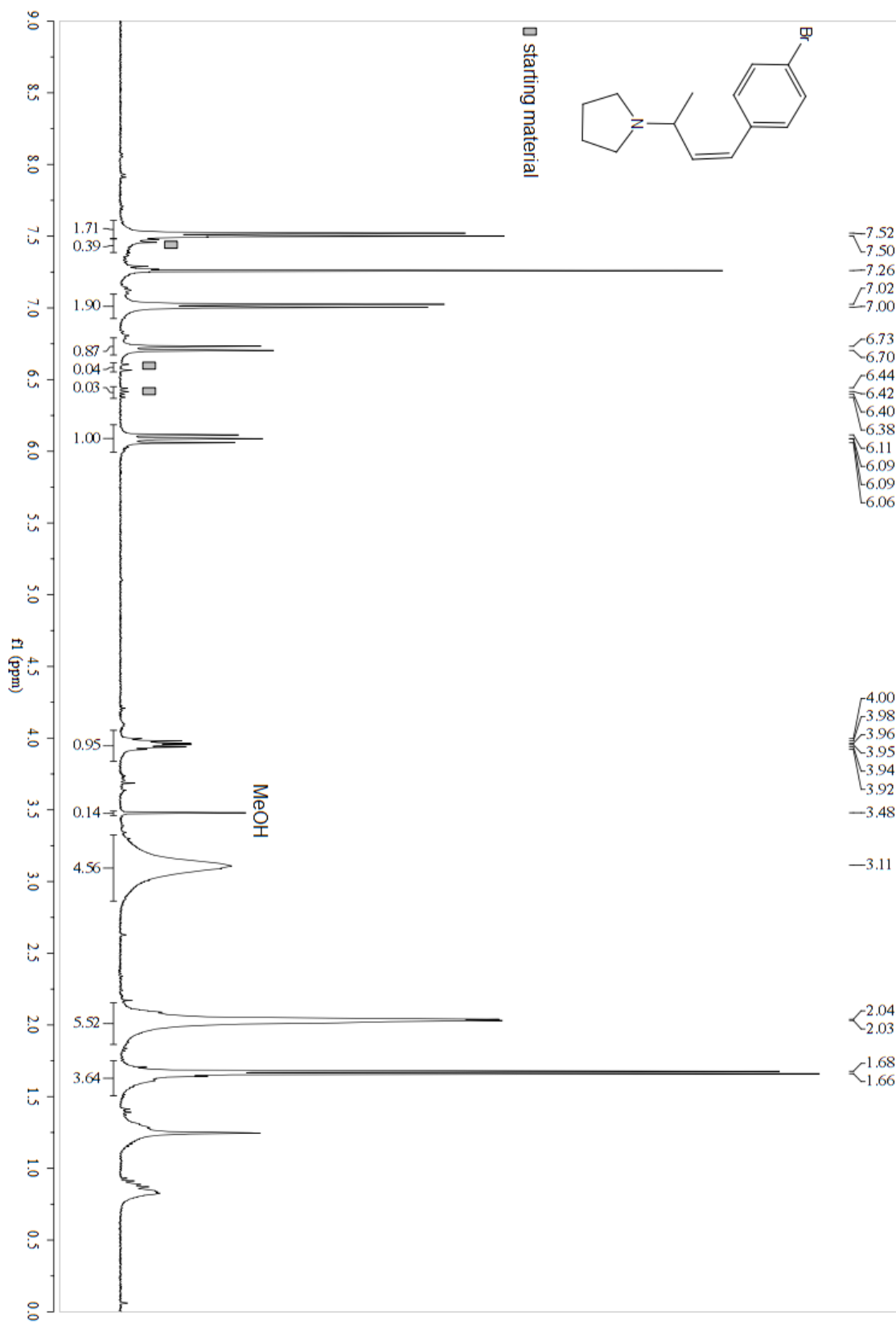
**2g (Z)-4-(4-phenylbut-3-en-2-yl)morpholine**



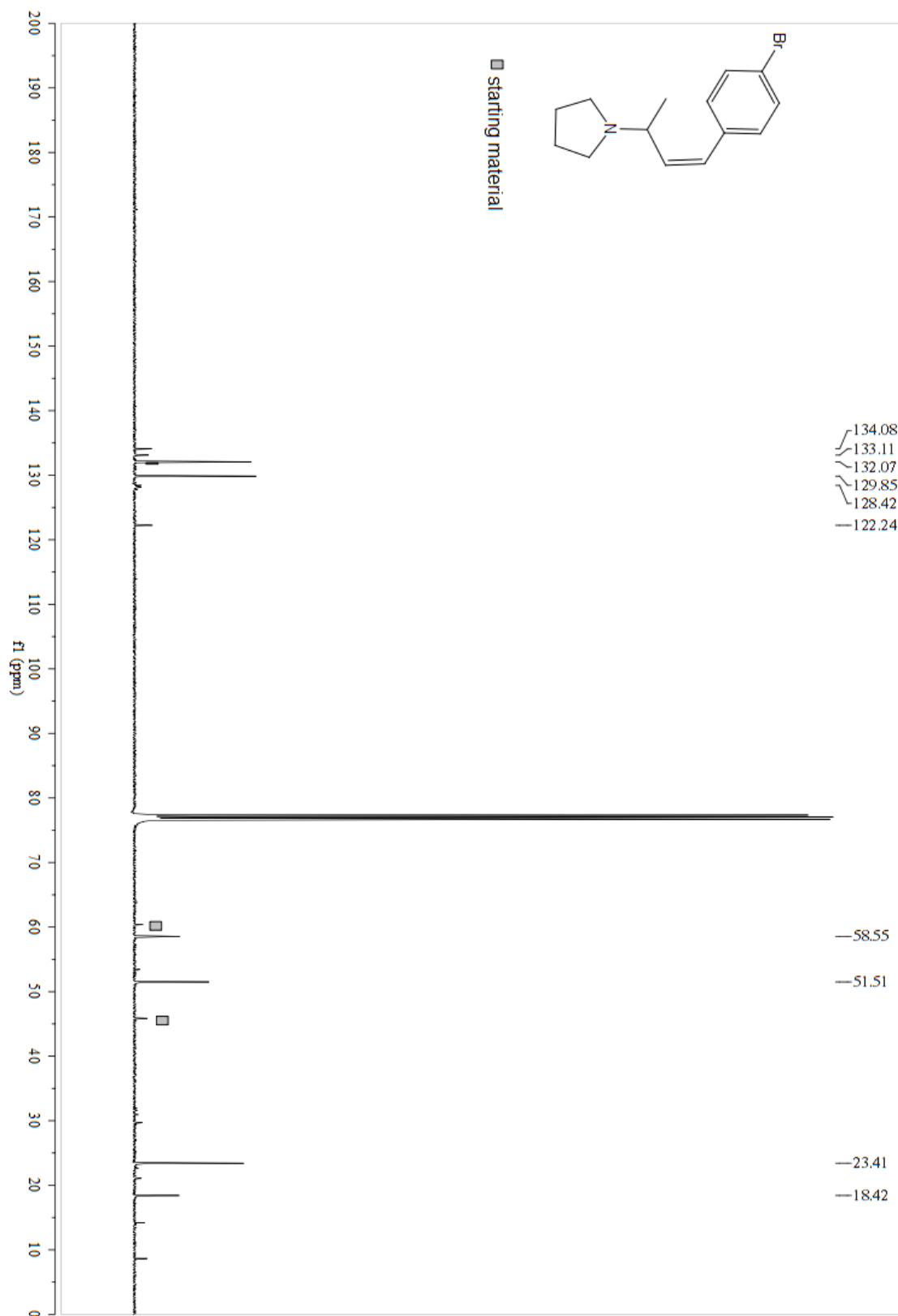
2g (Z)-4-(4-phenylbut-3-en-2-yl)morpholine



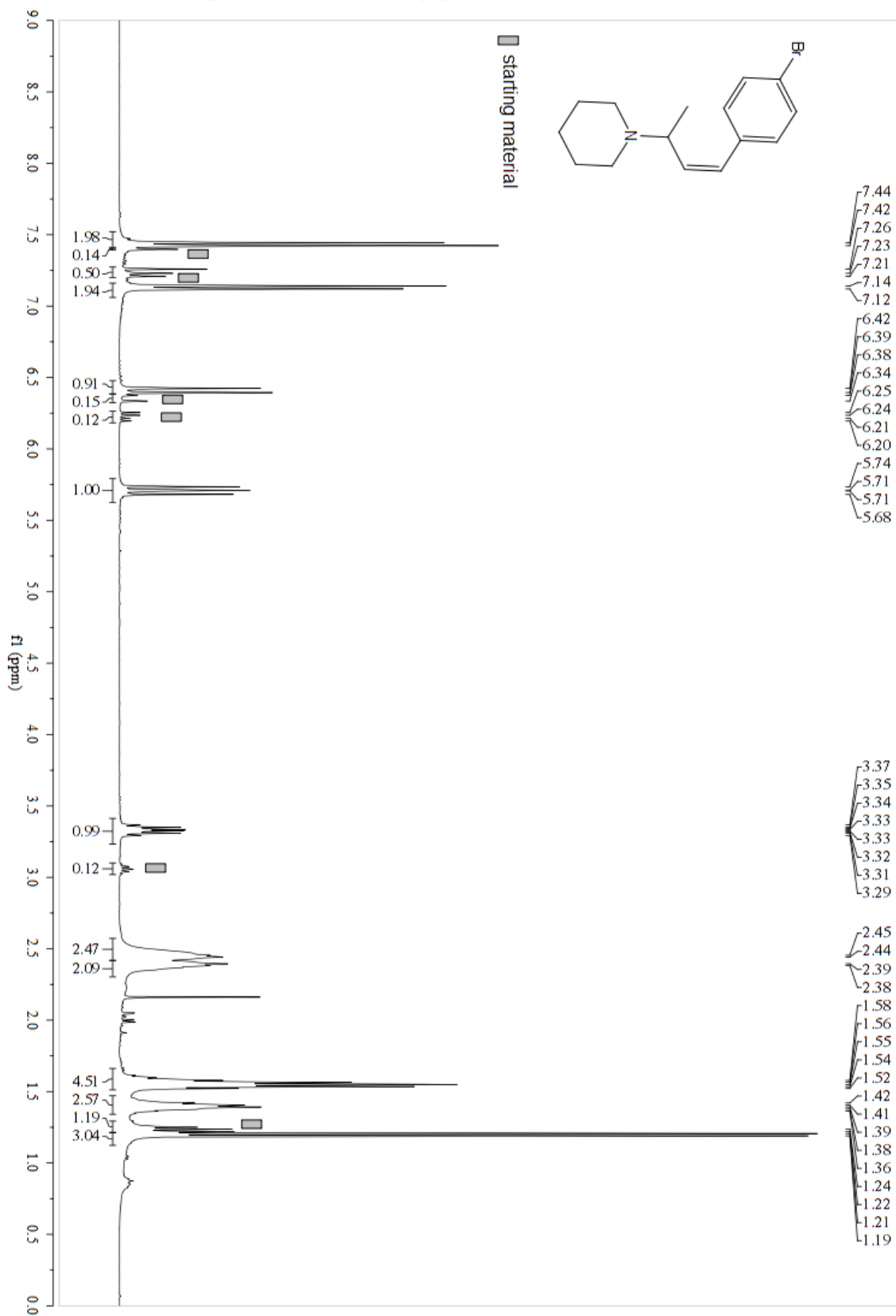
**2h (Z)-1-(4-(4-bromophenyl)but-3-en-2-yl)pyrrolidine**



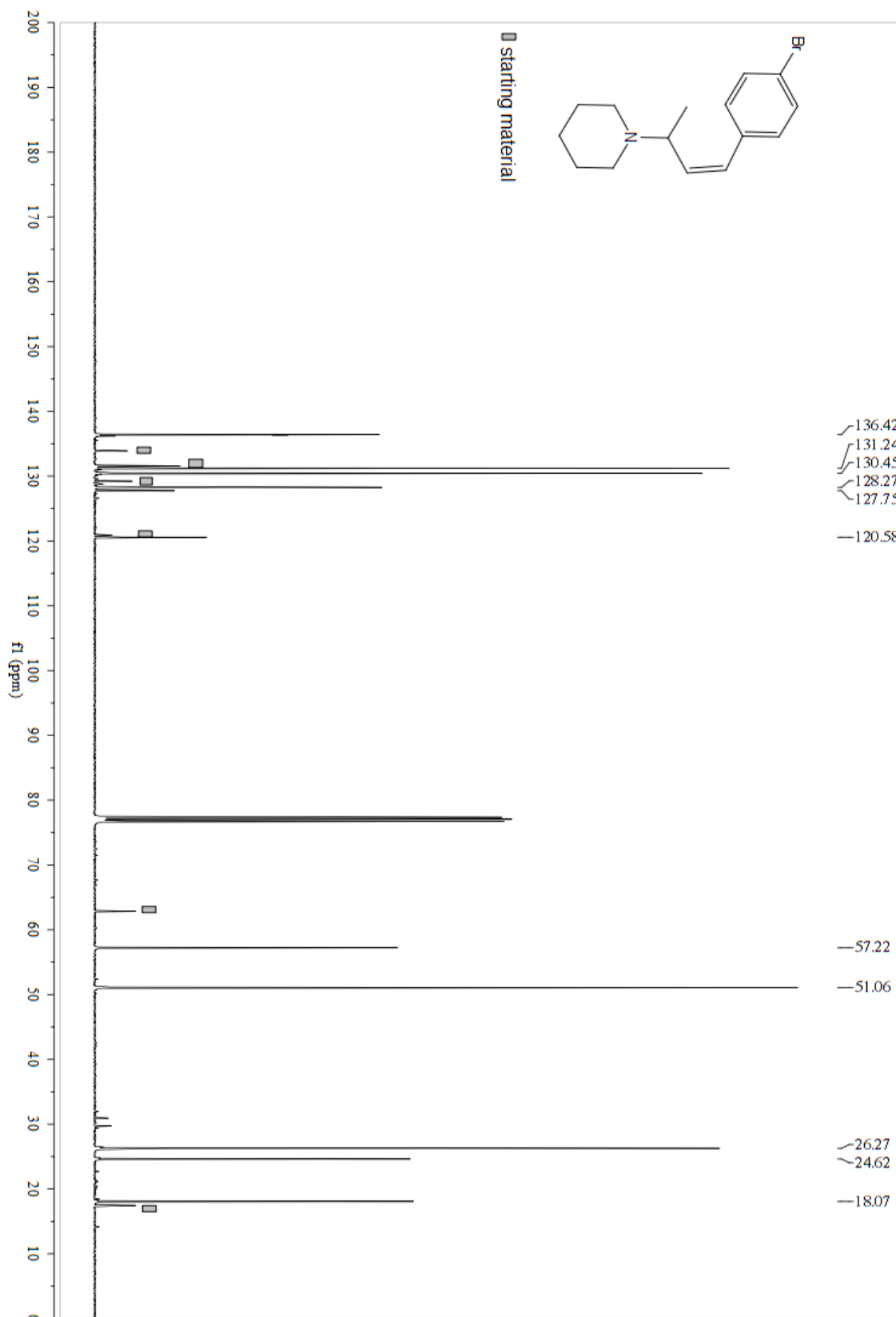
## 2h (Z)-1-(4-(4-bromophenyl)but-3-en-2-yl)pyrrolidine



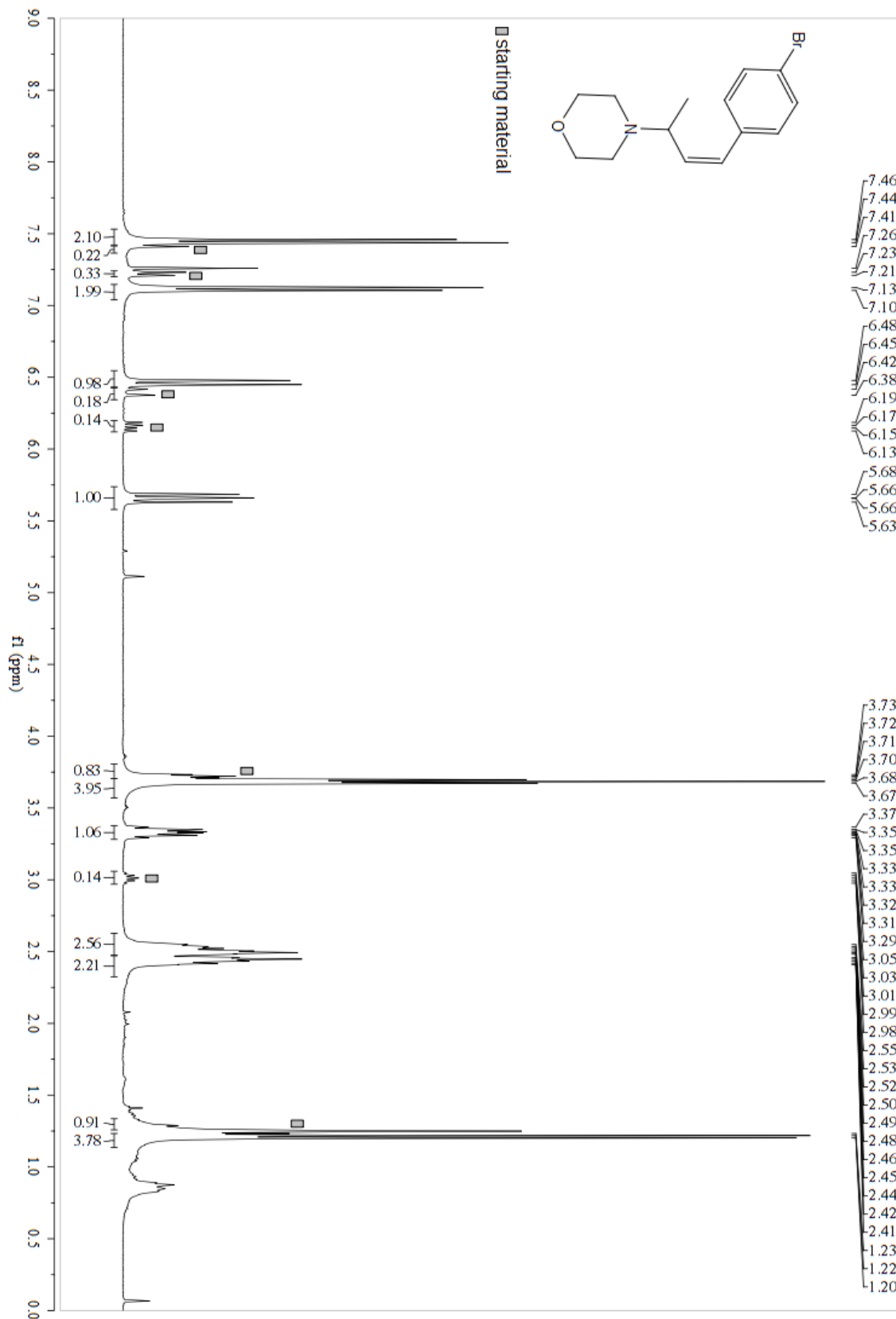
2i (Z)-1-(4-(4-bromophenyl)but-3-en-2-yl)piperidine



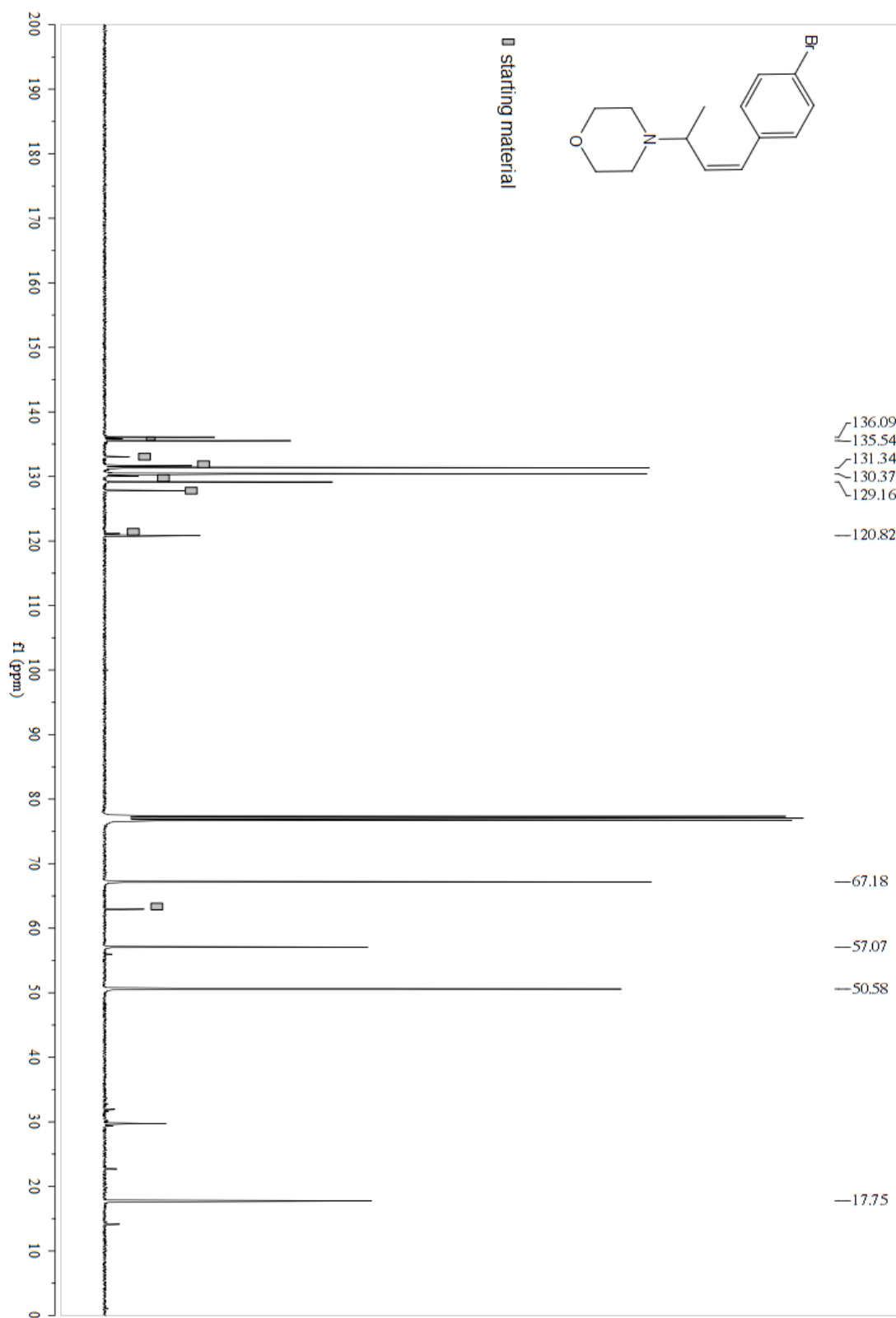
**2i (Z)-1-(4-(4-bromophenyl)but-3-en-2-yl)piperidine**



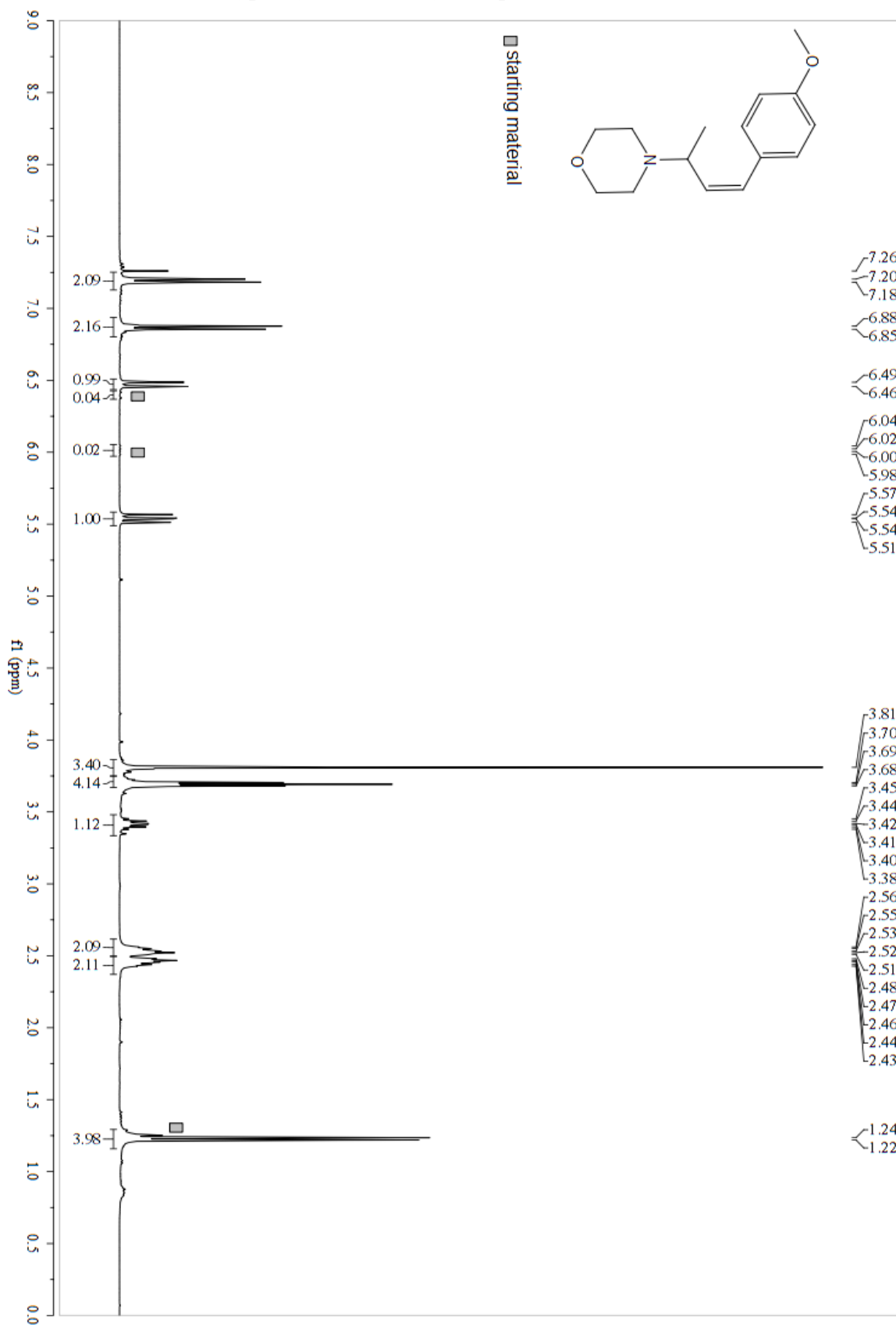
2j (Z)-4-(4-(4-bromophenyl)but-3-en-2-yl)morpholine



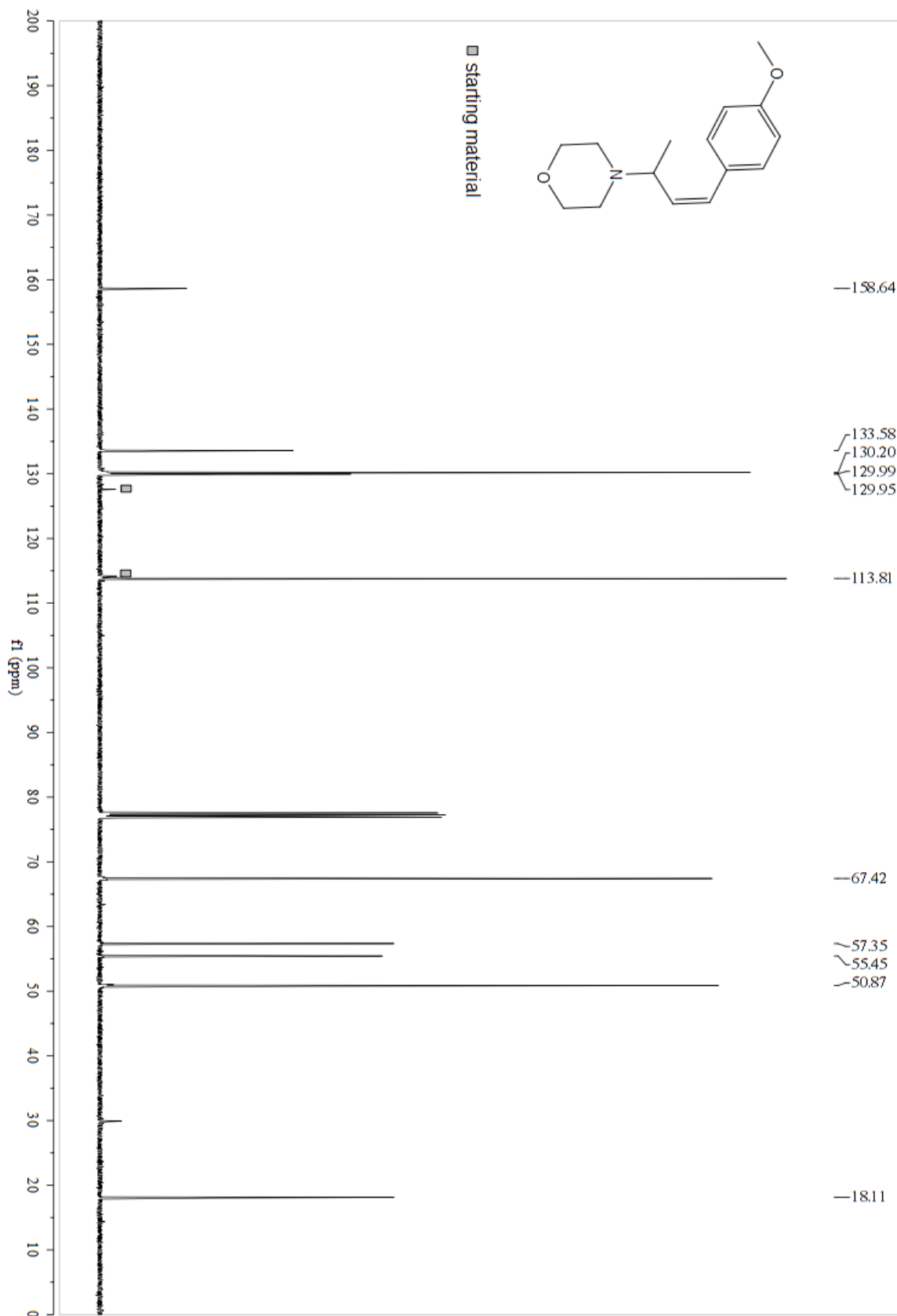
## 2j (Z)-4-(4-(4-bromophenyl)but-3-en-2-yl)morpholine



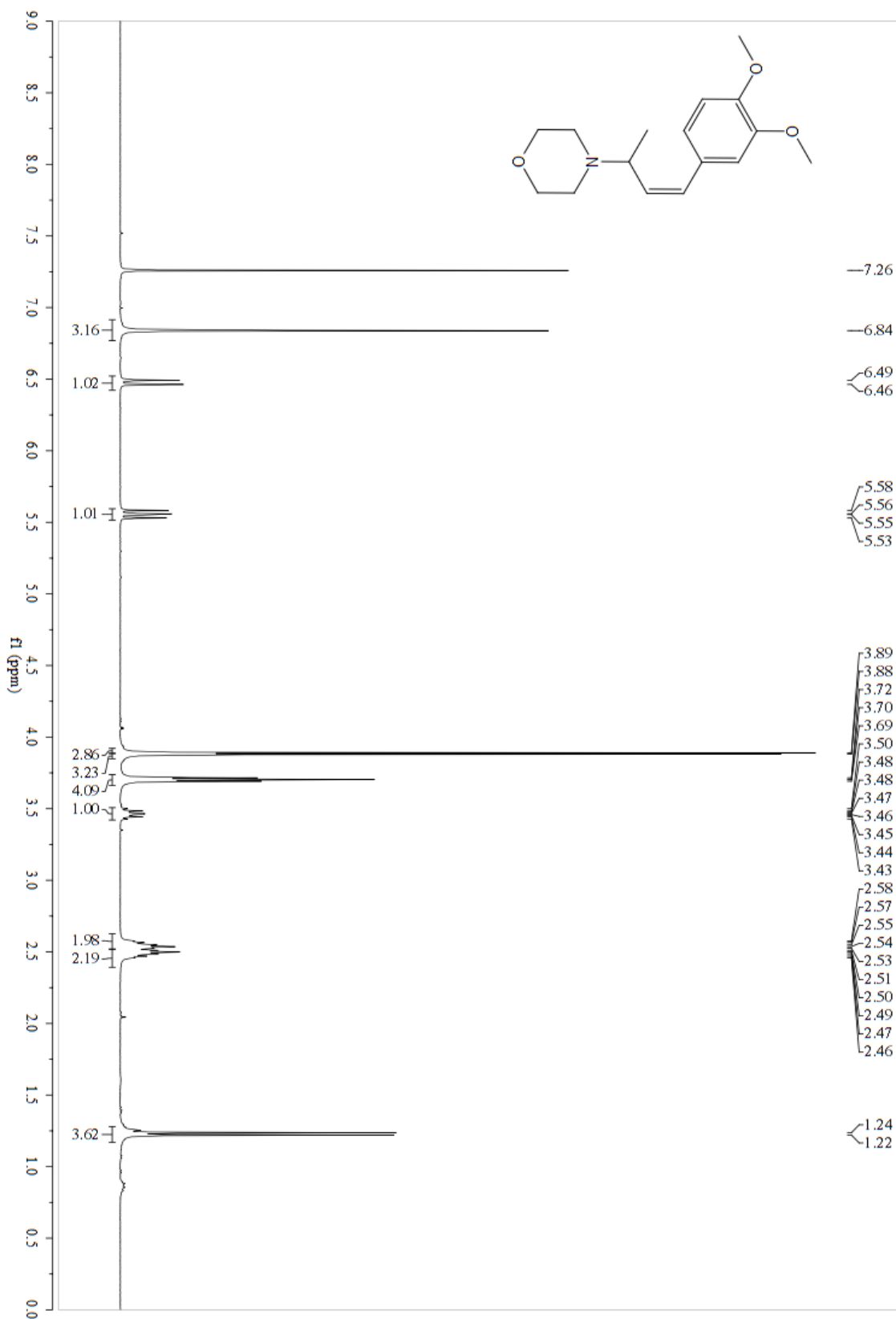
**2k (Z)-4-(4-(4-methoxyphenyl)but-3-en-2-yl)morpholine**



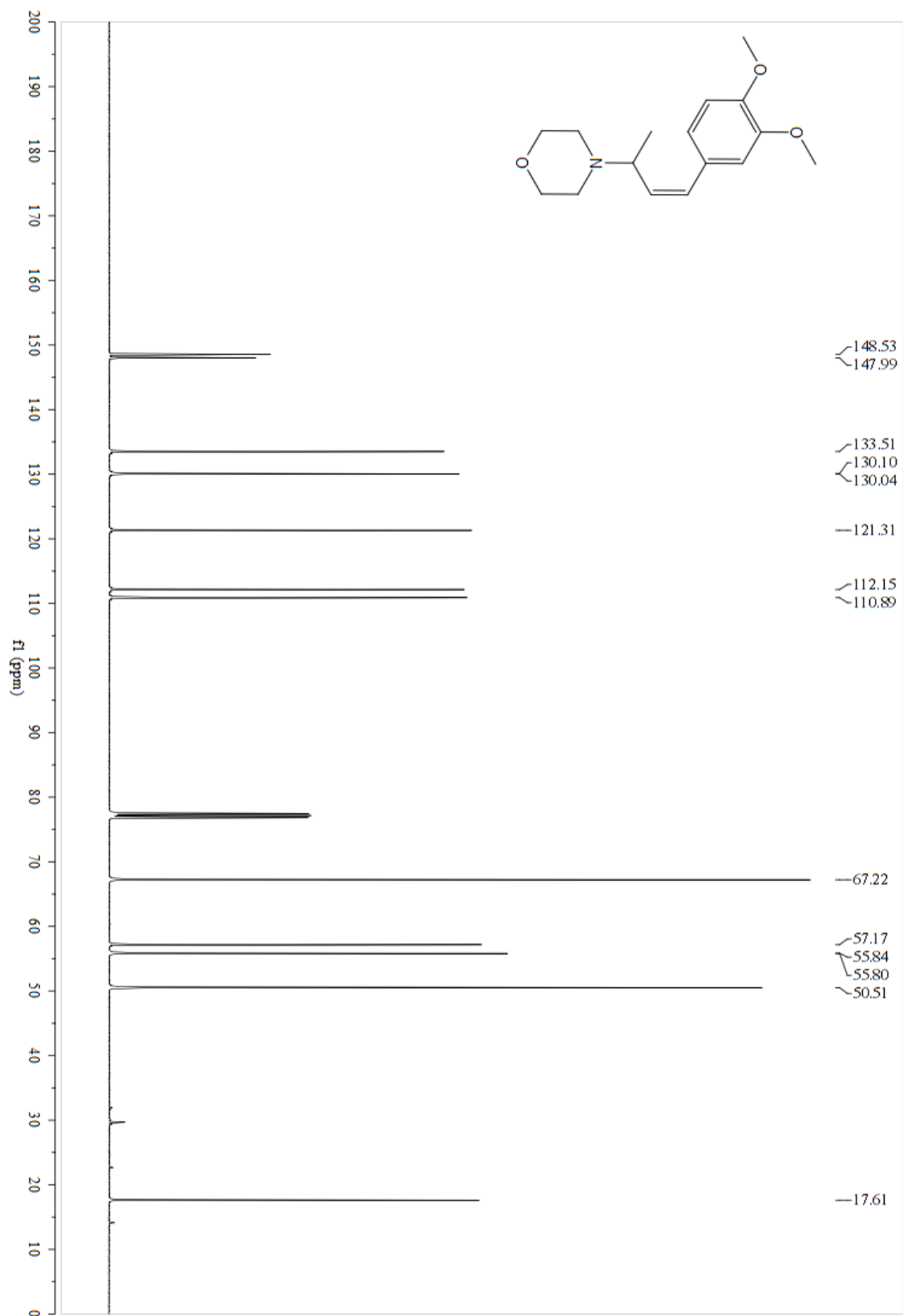
**2k (Z)-4-(4-(4-methoxyphenyl)but-3-en-2-yl)morpholine**



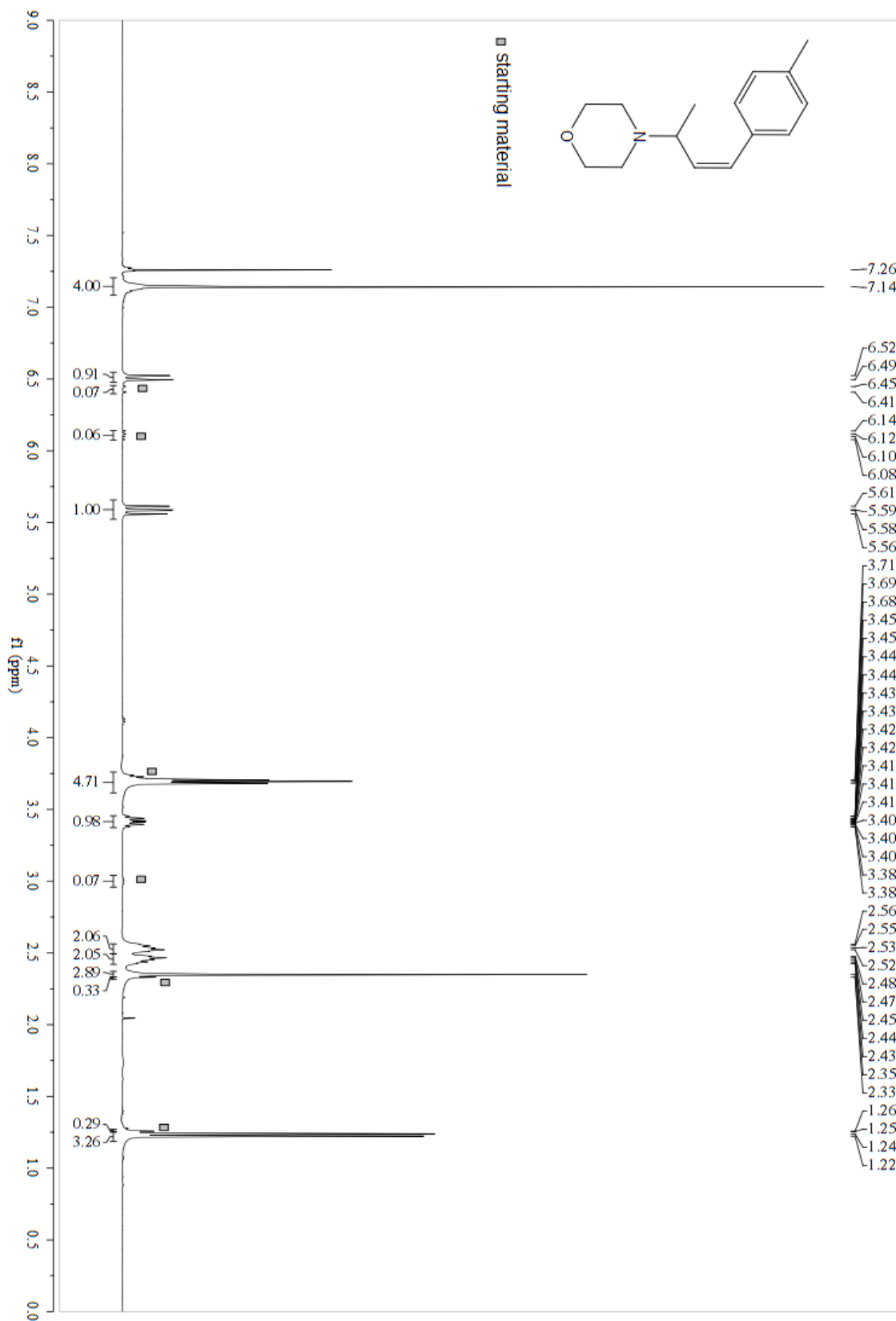
21 (Z)-4-(4-(3,4-dimethoxyphenyl)but-3-en-2-yl)morpholine



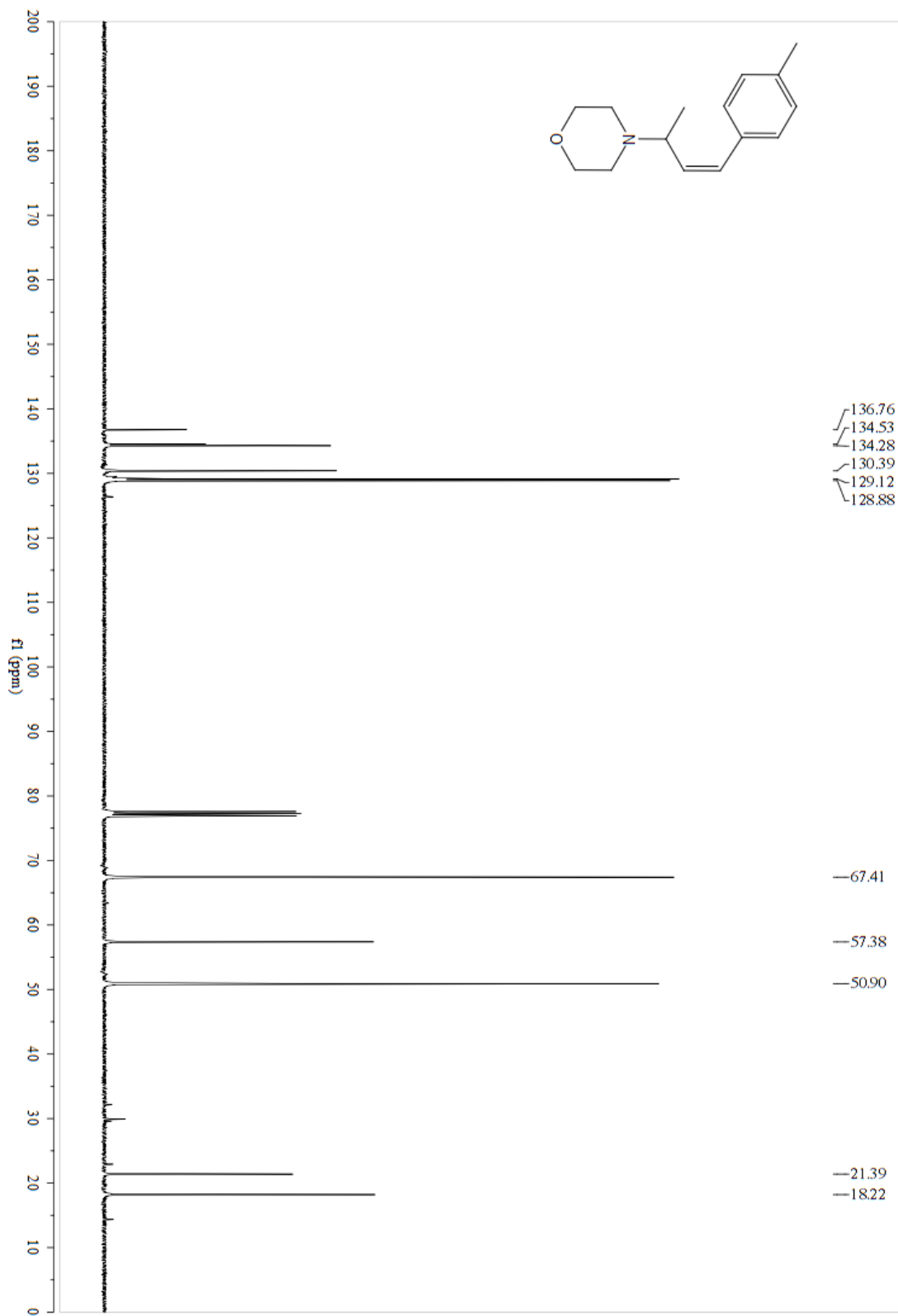
2l (Z)-4-(4-(3,4-dimethoxyphenyl)but-3-en-2-yl)morpholine



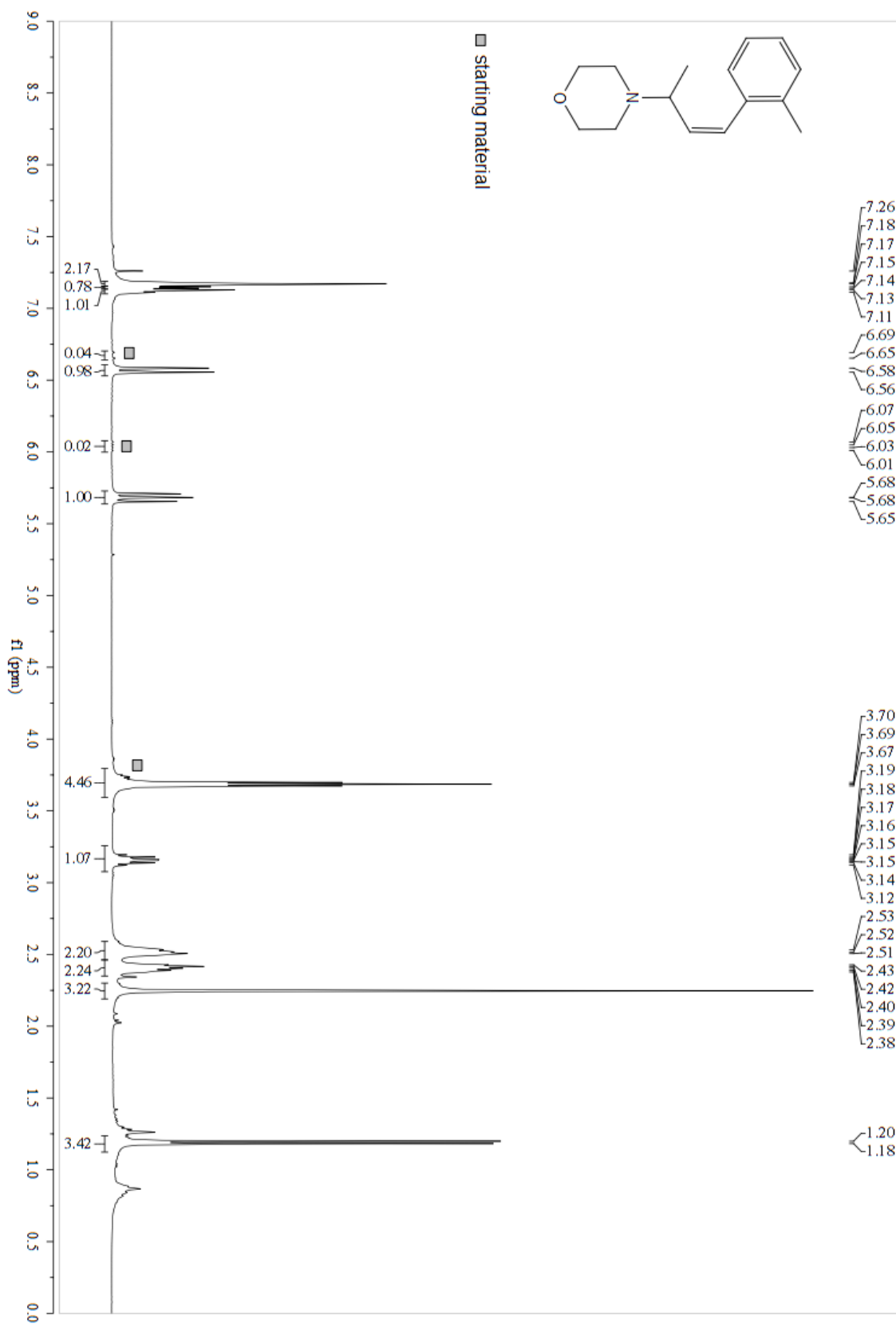
2m (Z)-4-(4-(p-tolyl)but-3-en-2-yl)morpholine



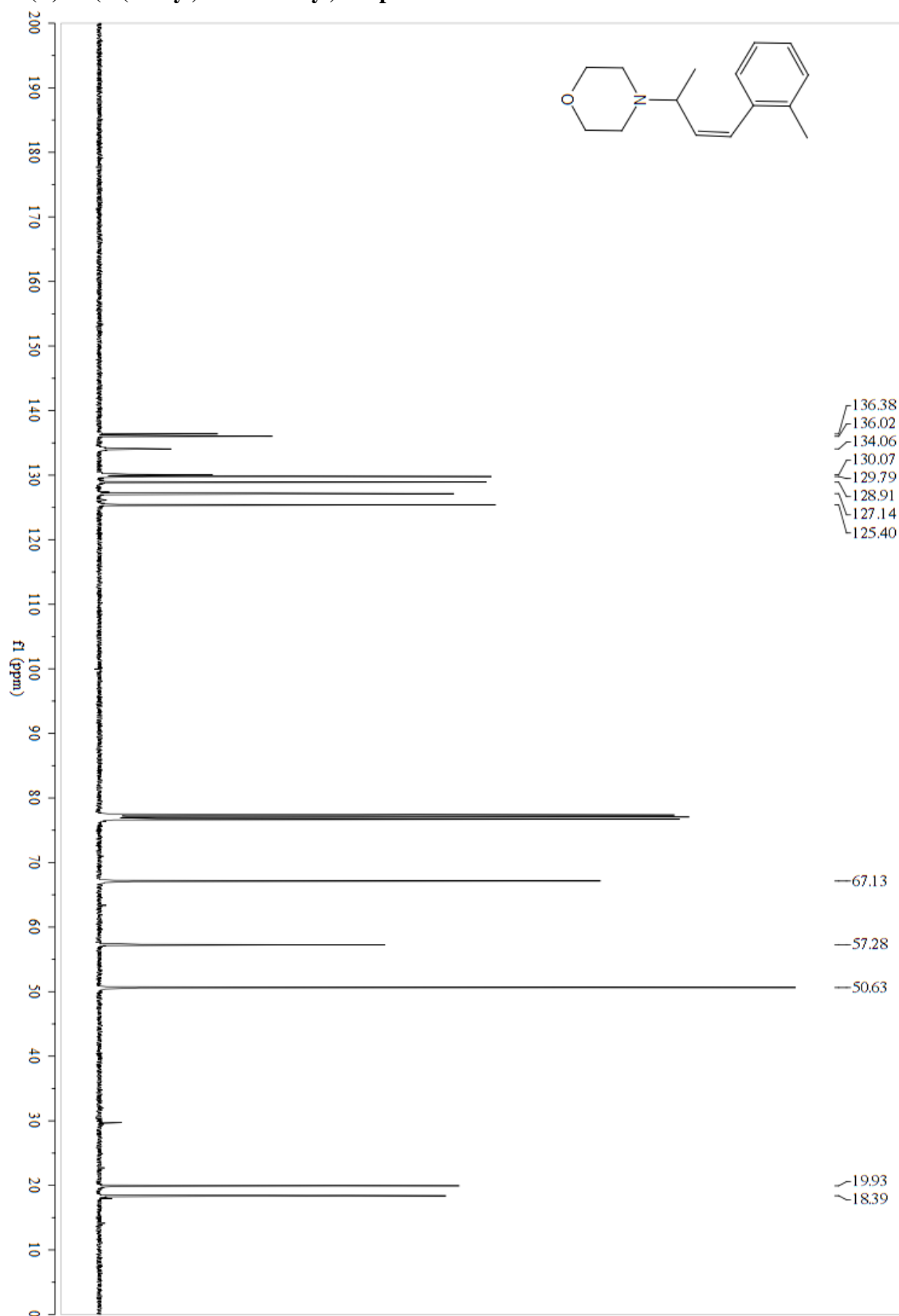
2m (Z)-4-(4-(p-tolyl)but-3-en-2-yl)morpholine



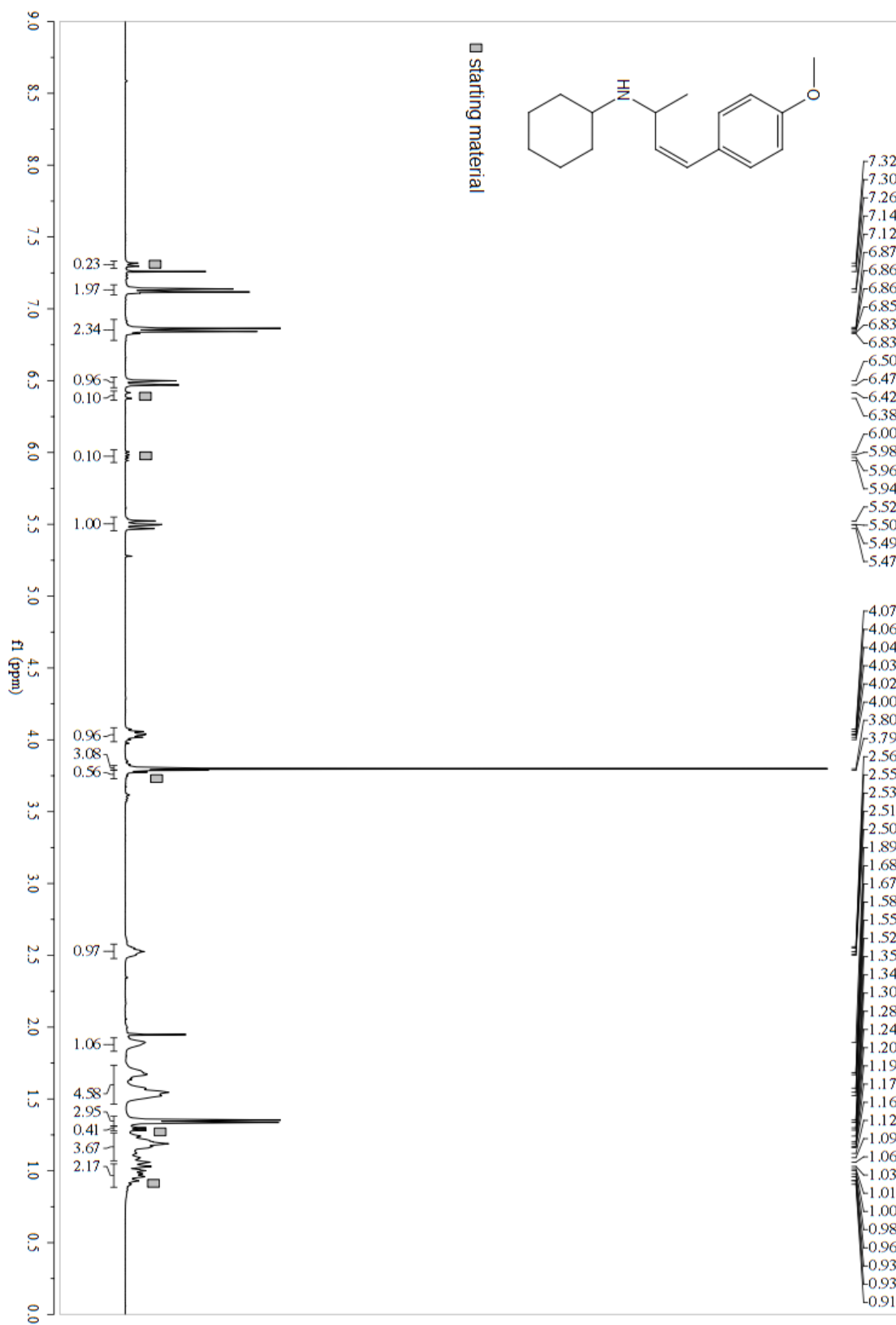
**2n (Z)- 4-(4-(o-tolyl)but-3-en-2-yl)morpholine**



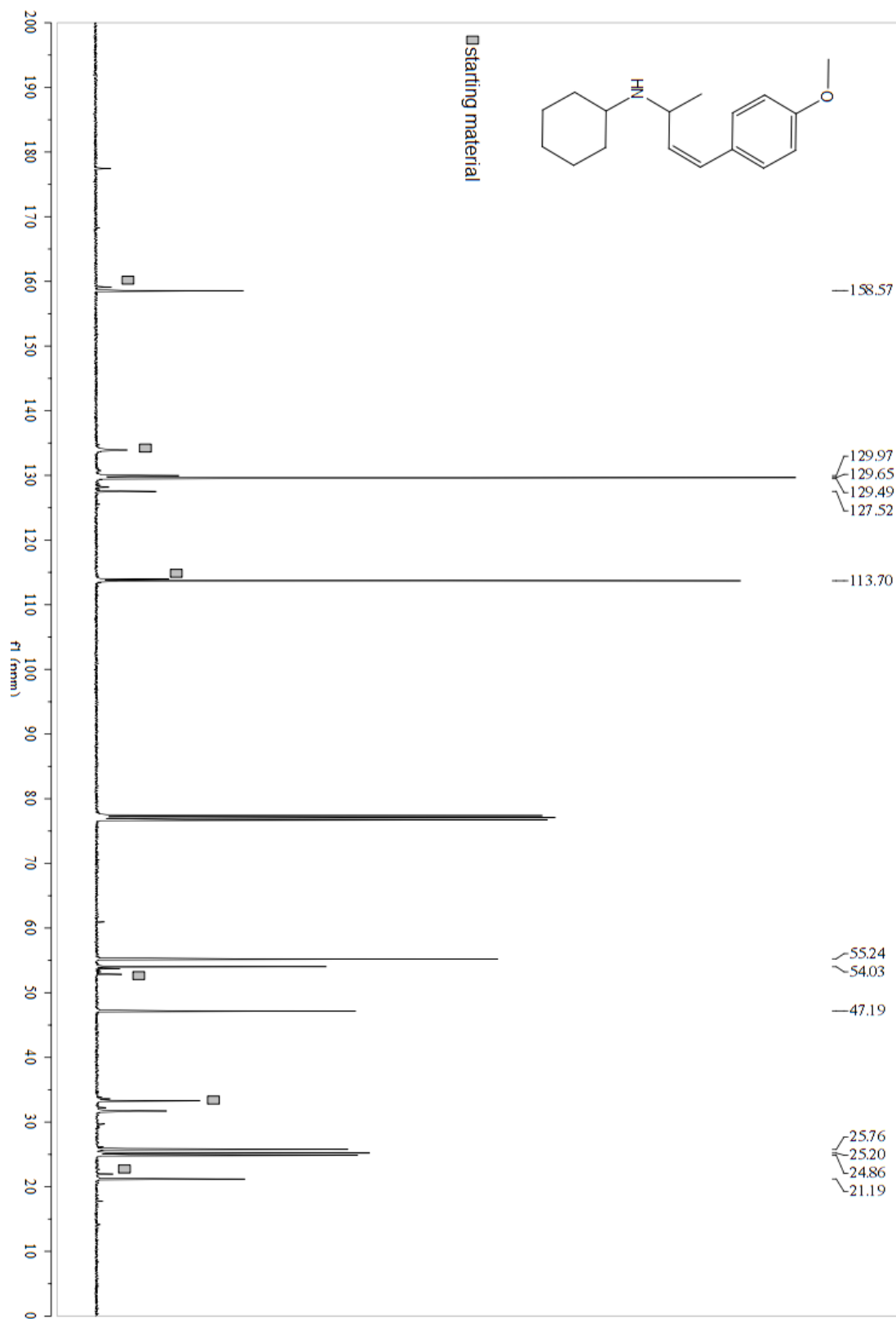
**2n (Z)- 4-(4-(o-tolyl)but-3-en-2-yl)morpholine**



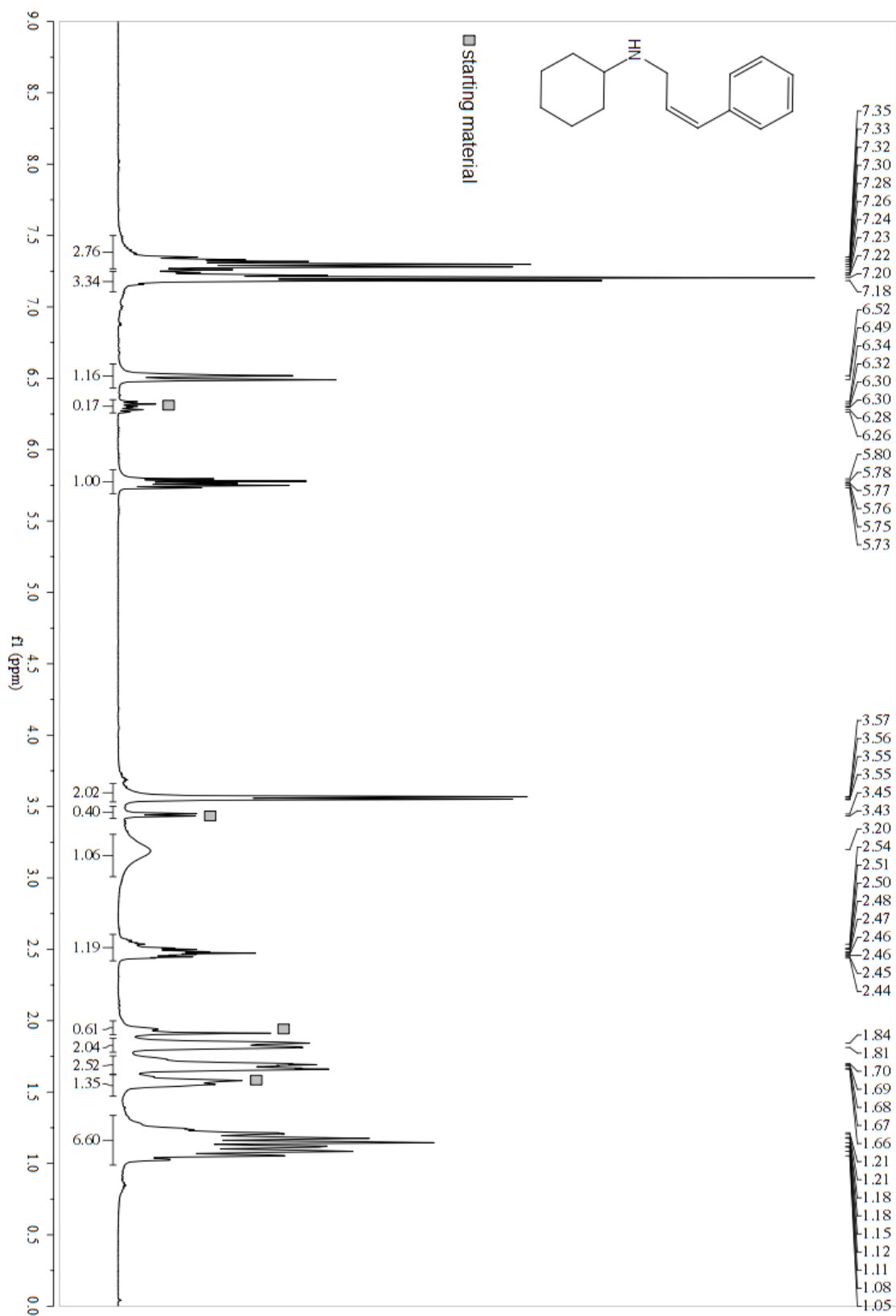
**2o (Z)-N-(4-(4-methoxyphenyl)but-3-en-2-yl)cyclohexanamine**



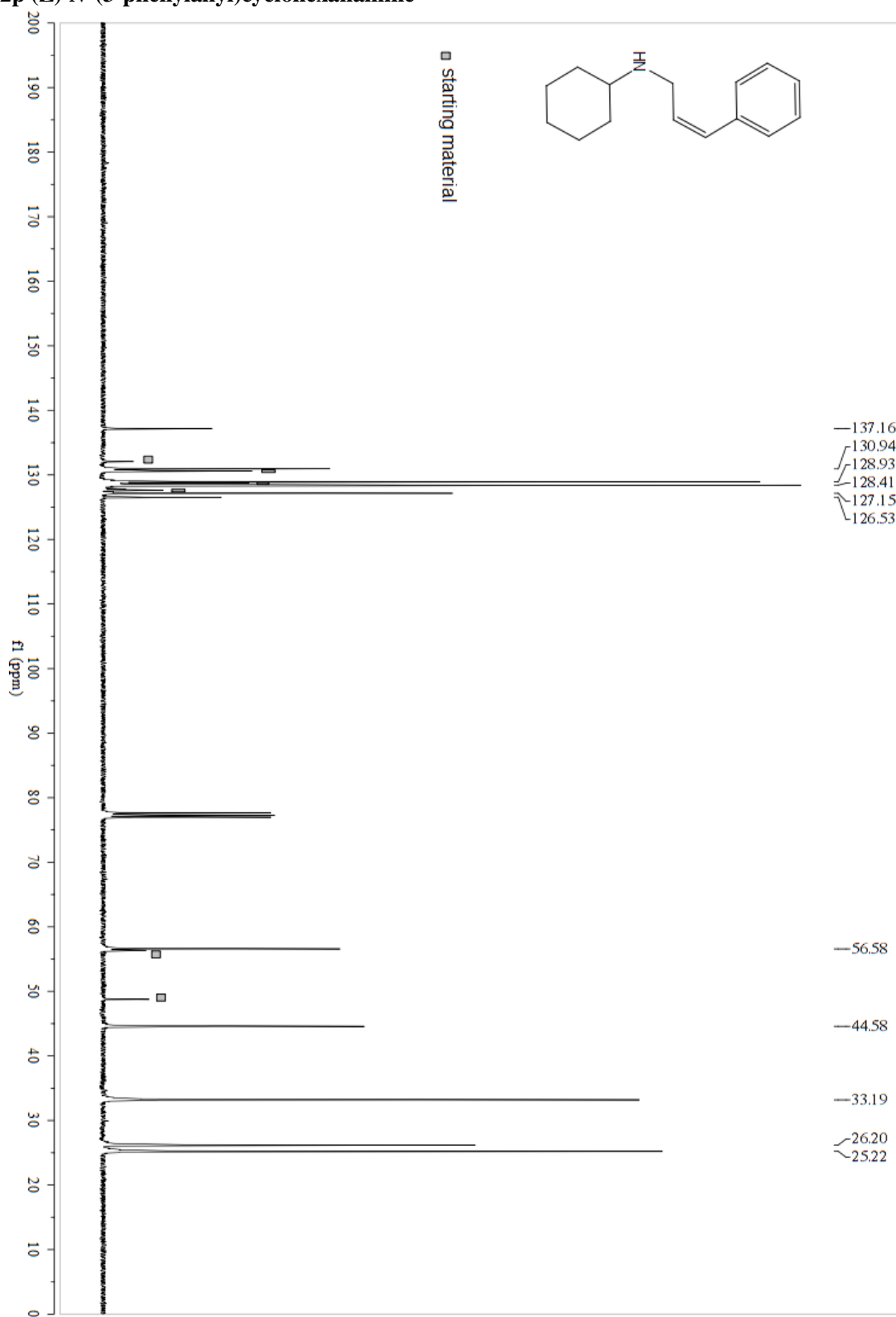
**2o (Z)-N-(4-(4-methoxyphenyl)but-3-en-2-yl)cyclohexanamine**



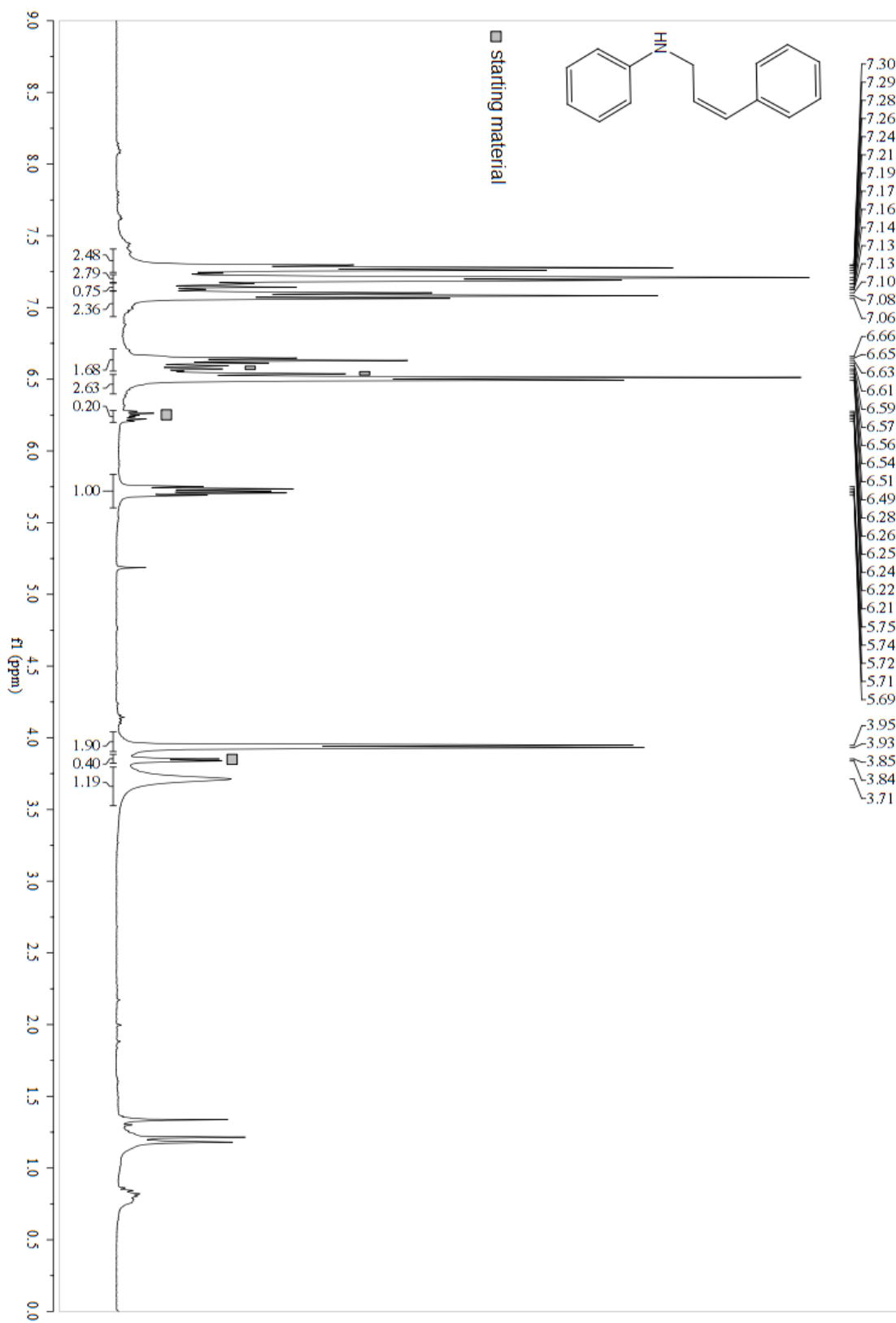
**2p (Z)-N-(3-phenylallyl)cyclohexanamine**



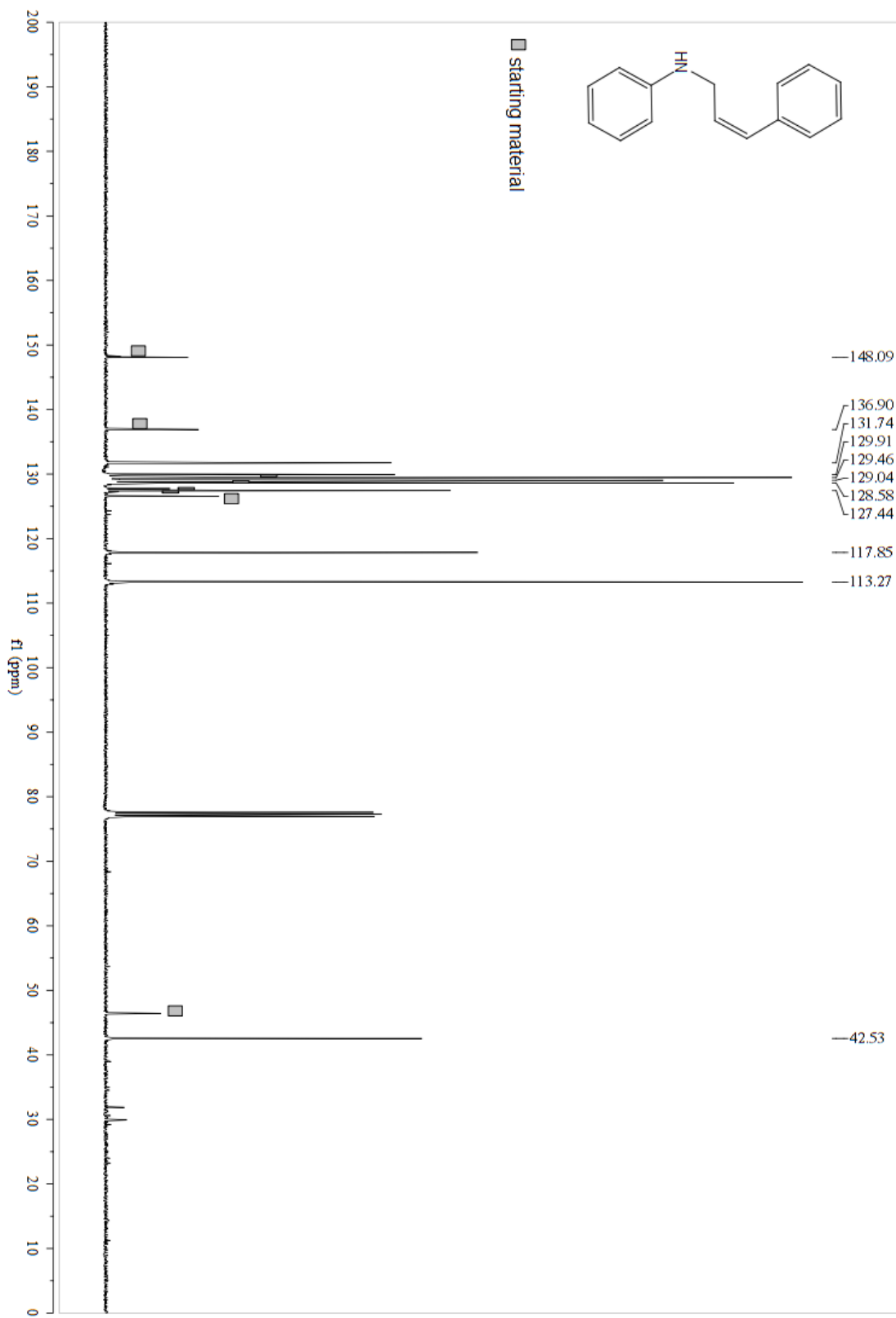
**2p (Z)-N-(3-phenylallyl)cyclohexanamine**



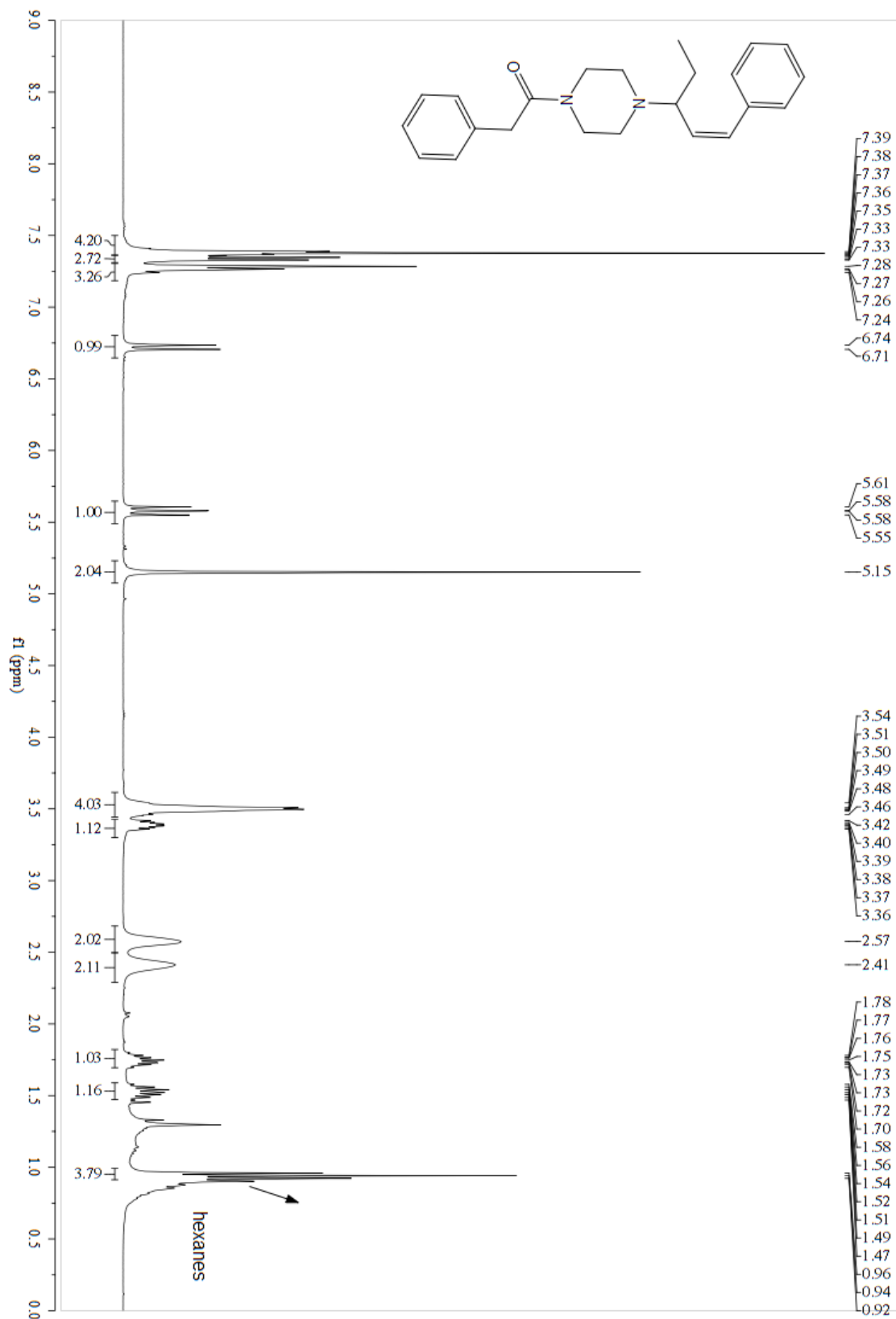
2q (Z)-N-(3-phenylallyl)aniline



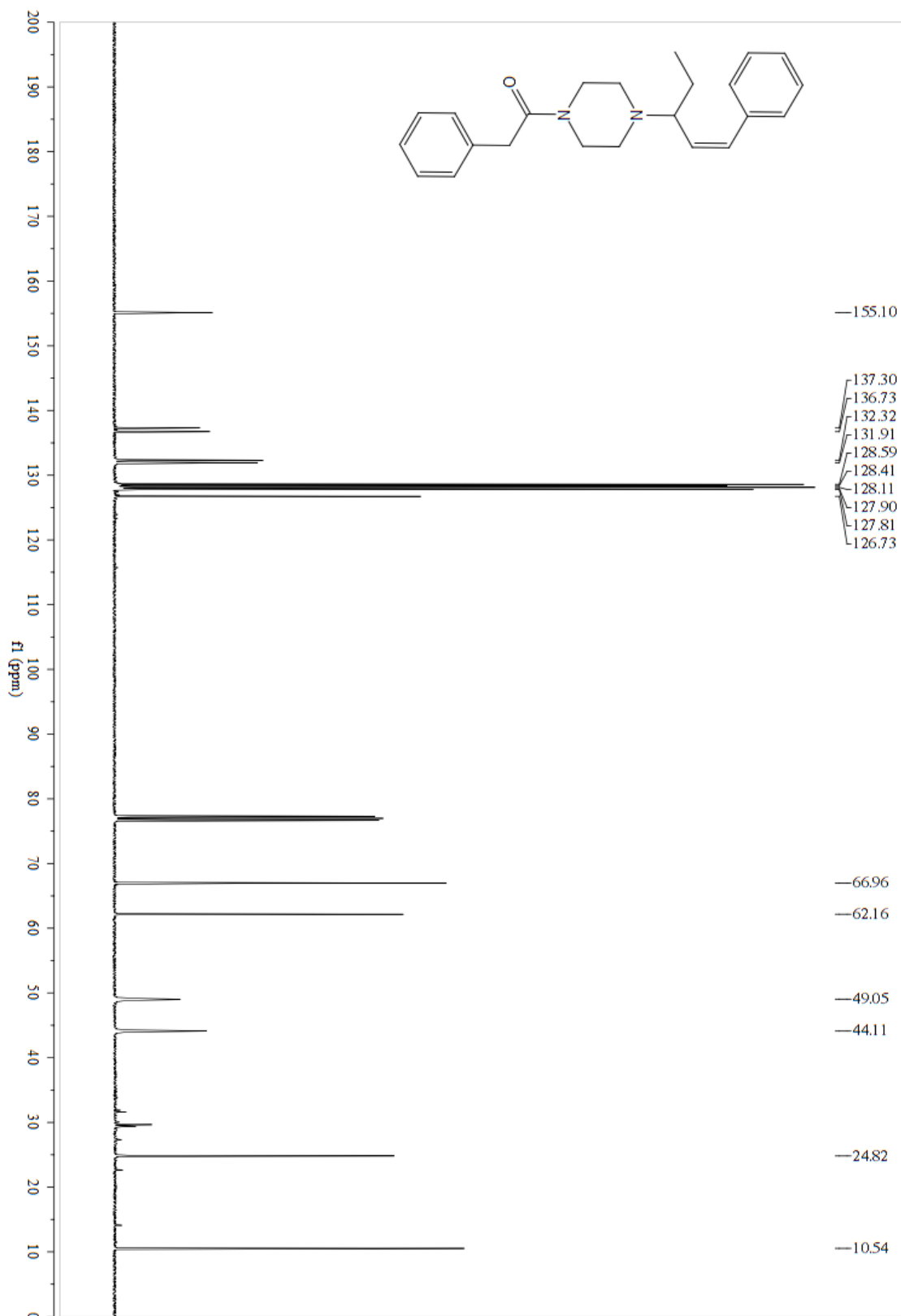
2q (Z)-N-(3-phenylallyl)aniline



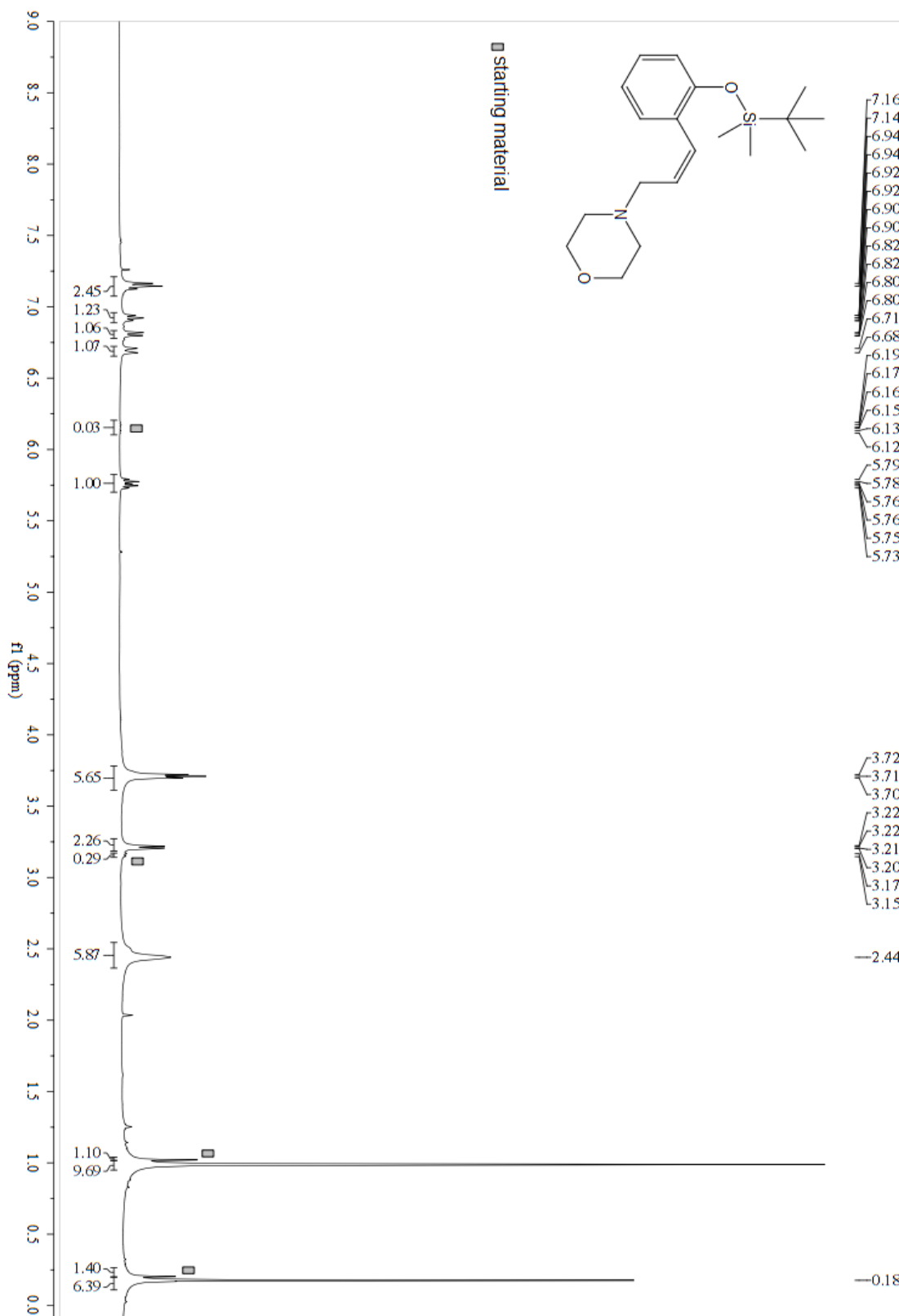
**2r (Z)-2-phenyl-1-(4-(1-phenylpent-1-en-3-yl)piperazin-1-yl)ethan-1-one**



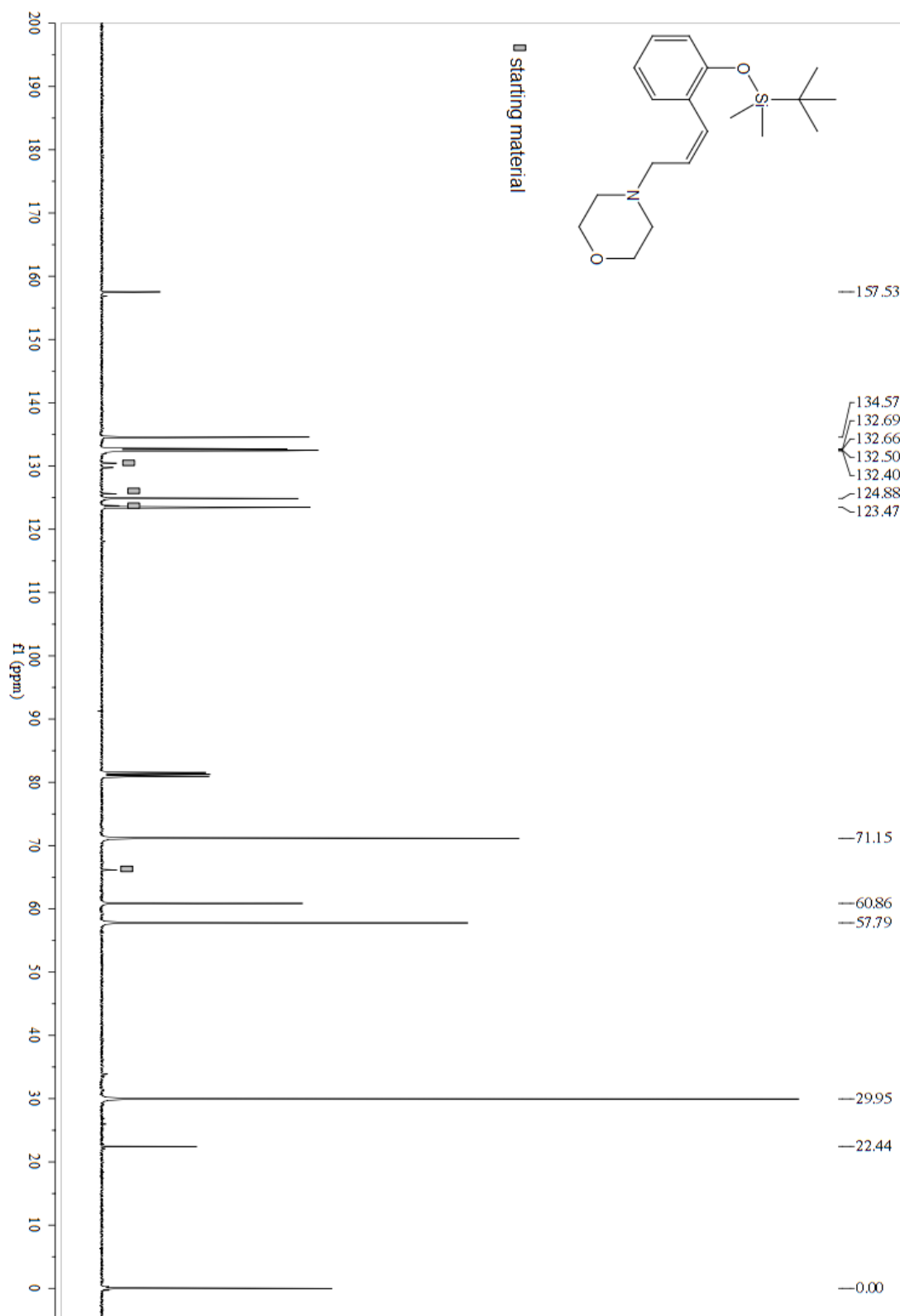
**2r (Z)-2-phenyl-1-(4-(1-phenylpent-1-en-3-yl)piperazin-1-yl)ethan-1-one**



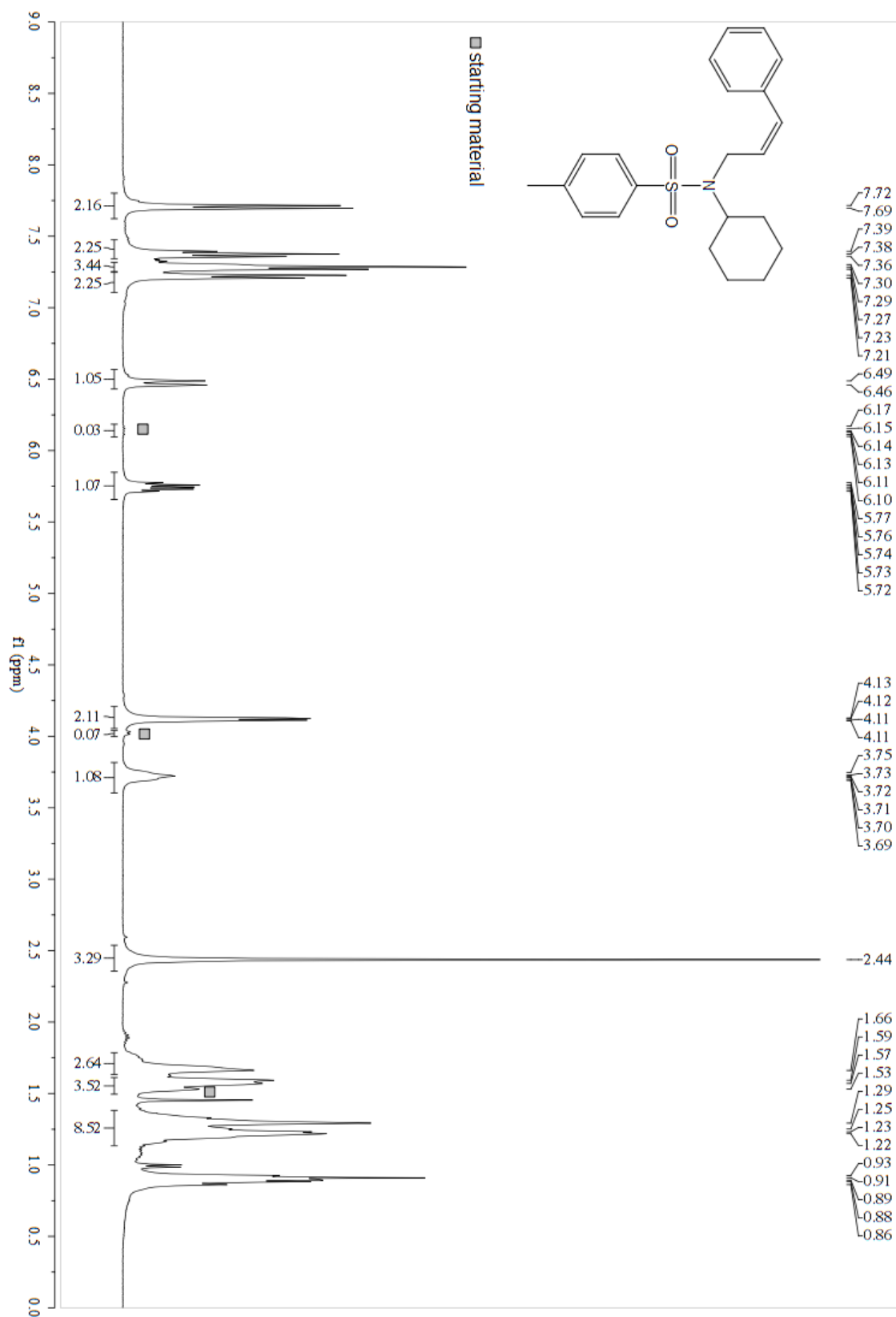
2s (Z)-4-(3-(2-((*tert*-butyldimethylsilyl)oxy)phenyl)allyl)morpholine



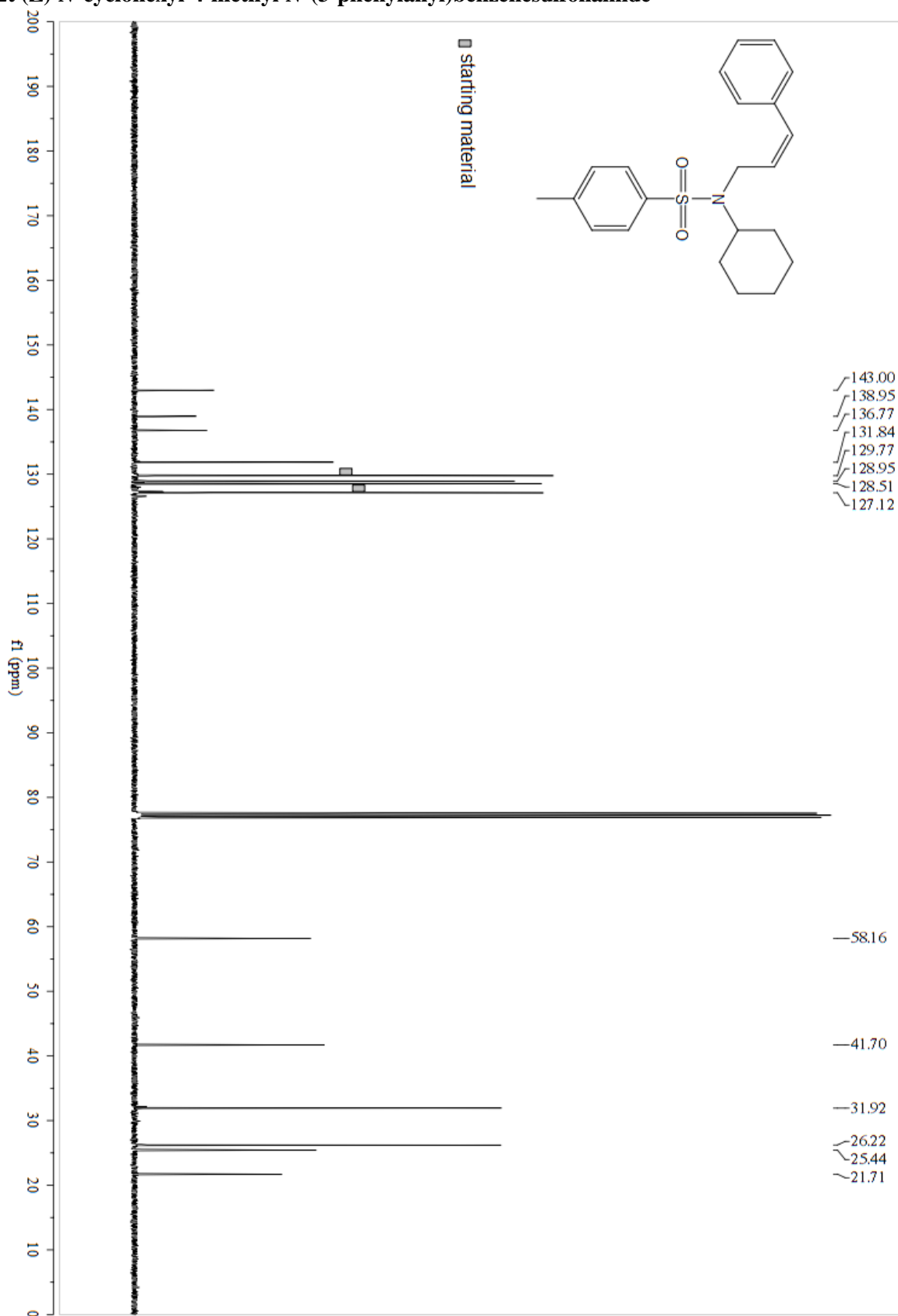
2s (Z)-4-(3-(2-((*tert*-butyldimethylsilyl)oxy)phenyl)allyl)morpholine



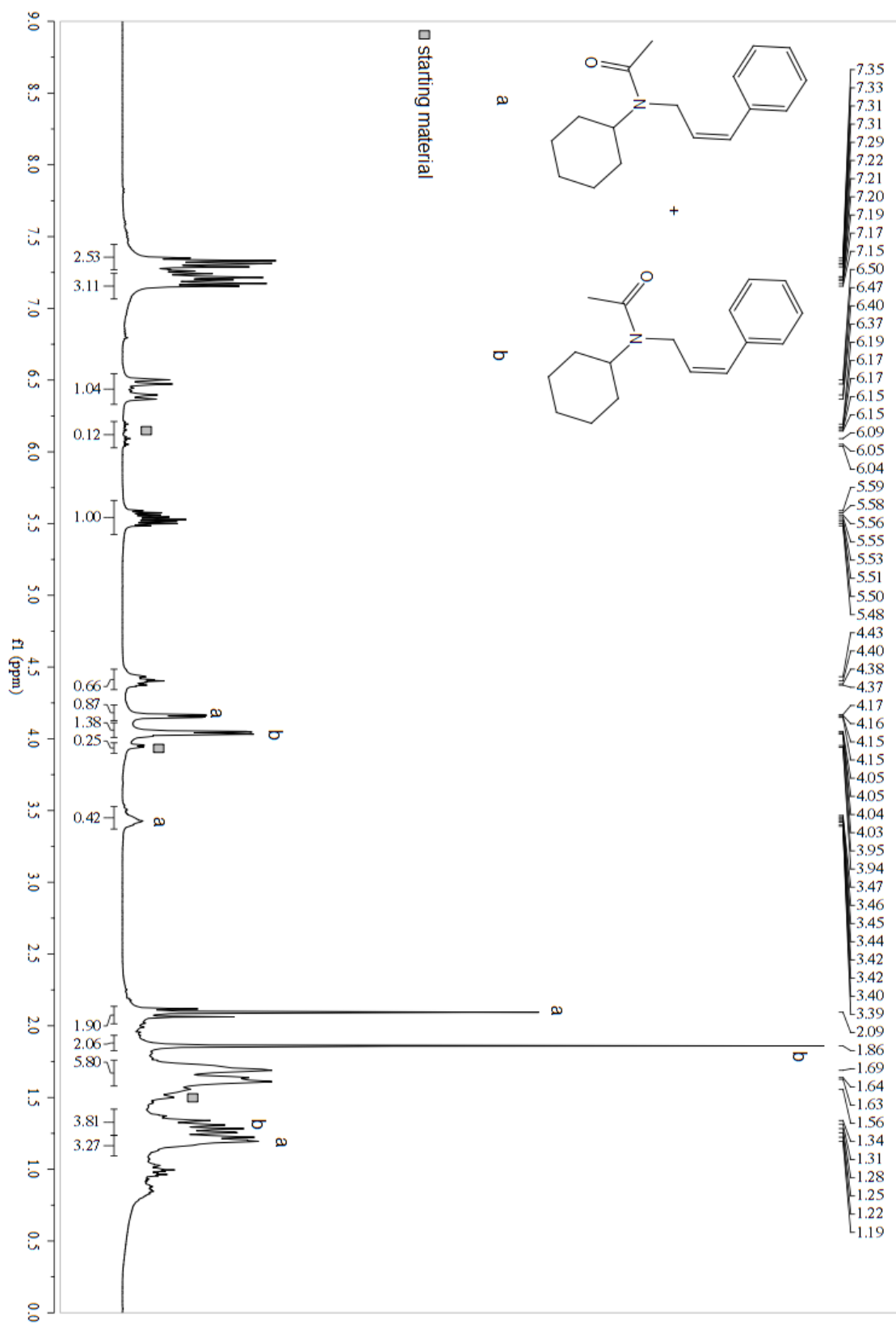
**2t (Z)-N-cyclohexyl-4-methyl-N-(3-phenylallyl)benzenesulfonamide**



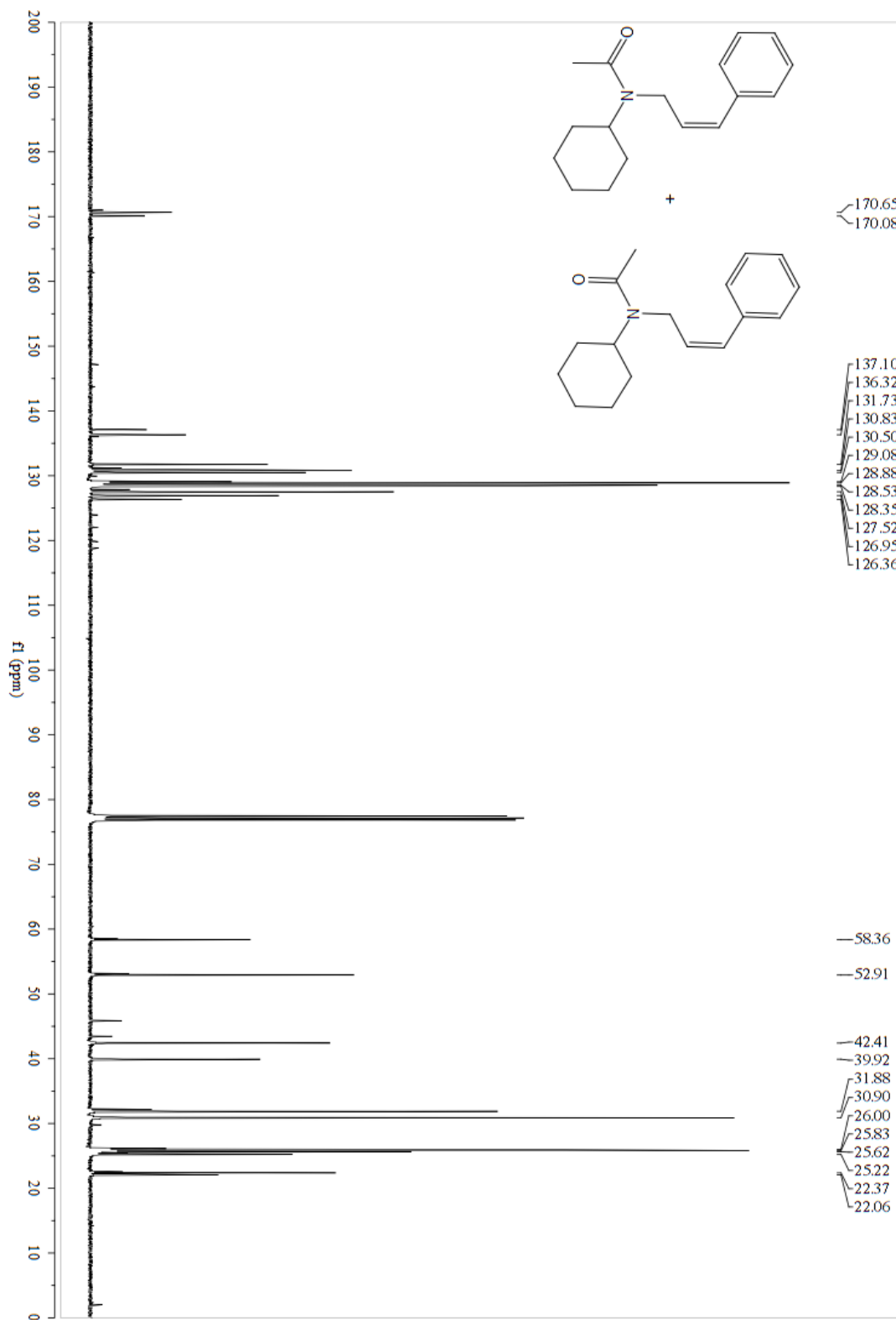
2t (Z)-N-cyclohexyl-4-methyl-N-(3-phenylallyl)benzenesulfonamide



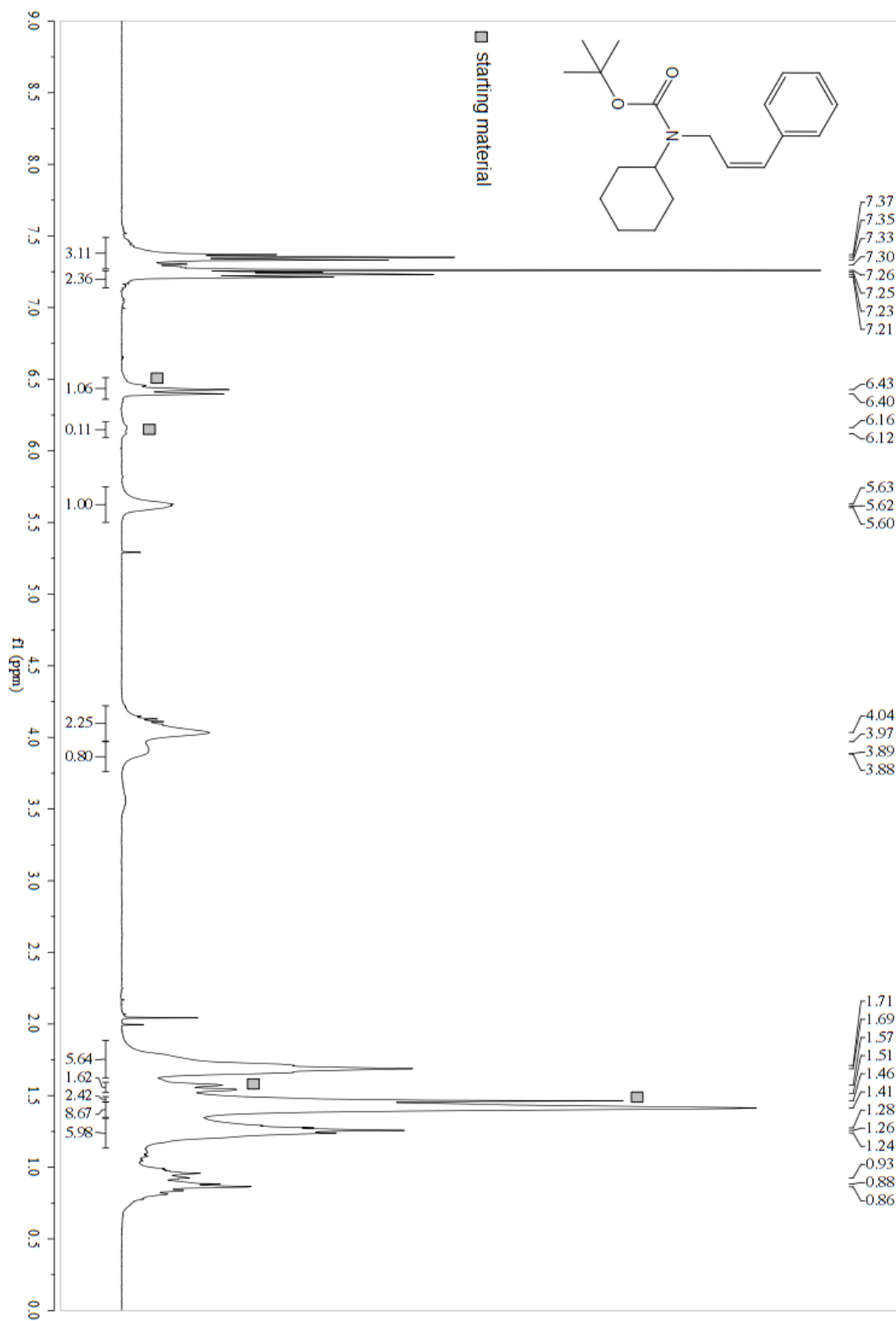
**2u (Z)-N-cyclohexyl-N-(3-phenylallyl)acetamide**



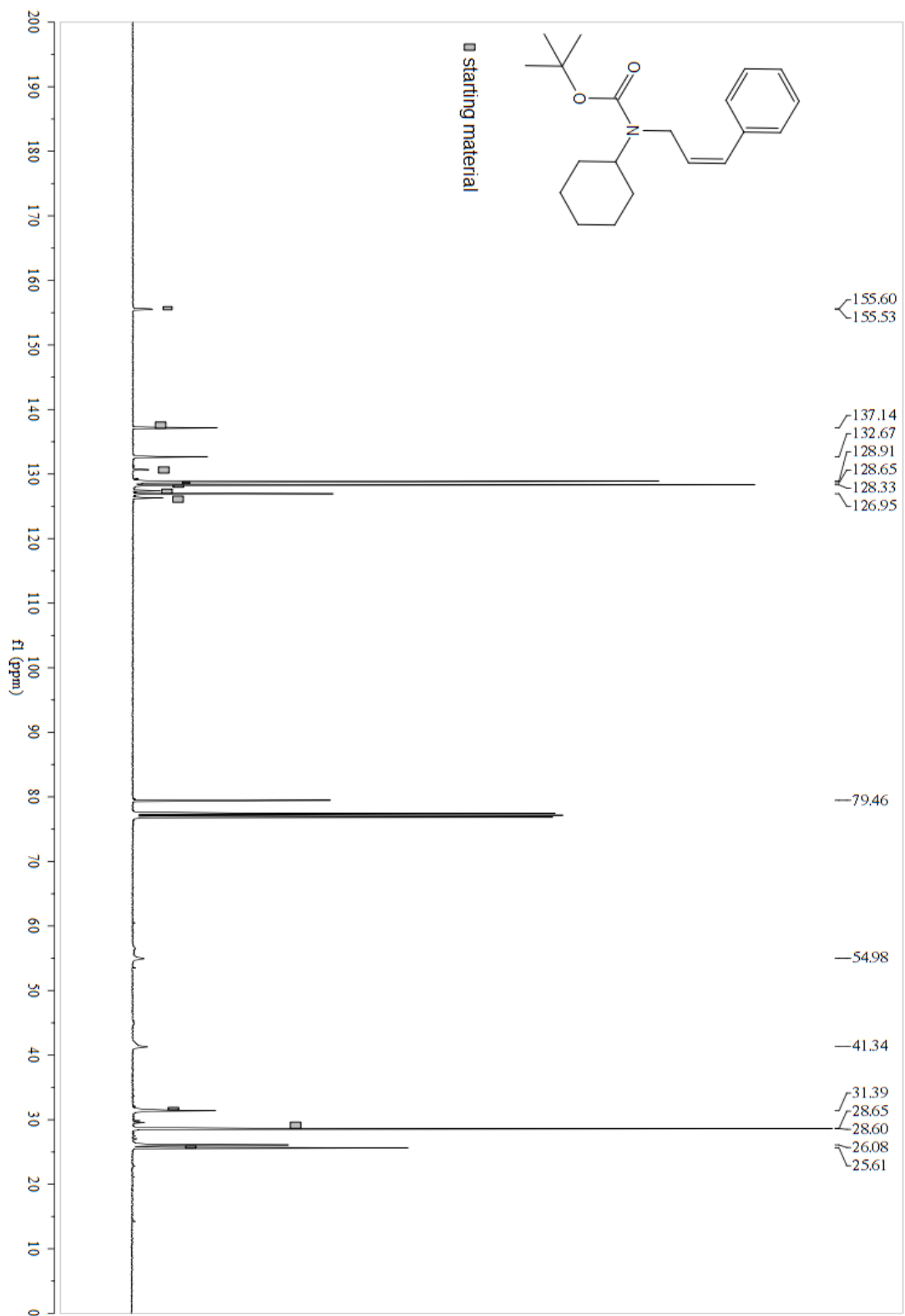
**2u (Z)-N-cyclohexyl-N-(3-phenylallyl)acetamide**



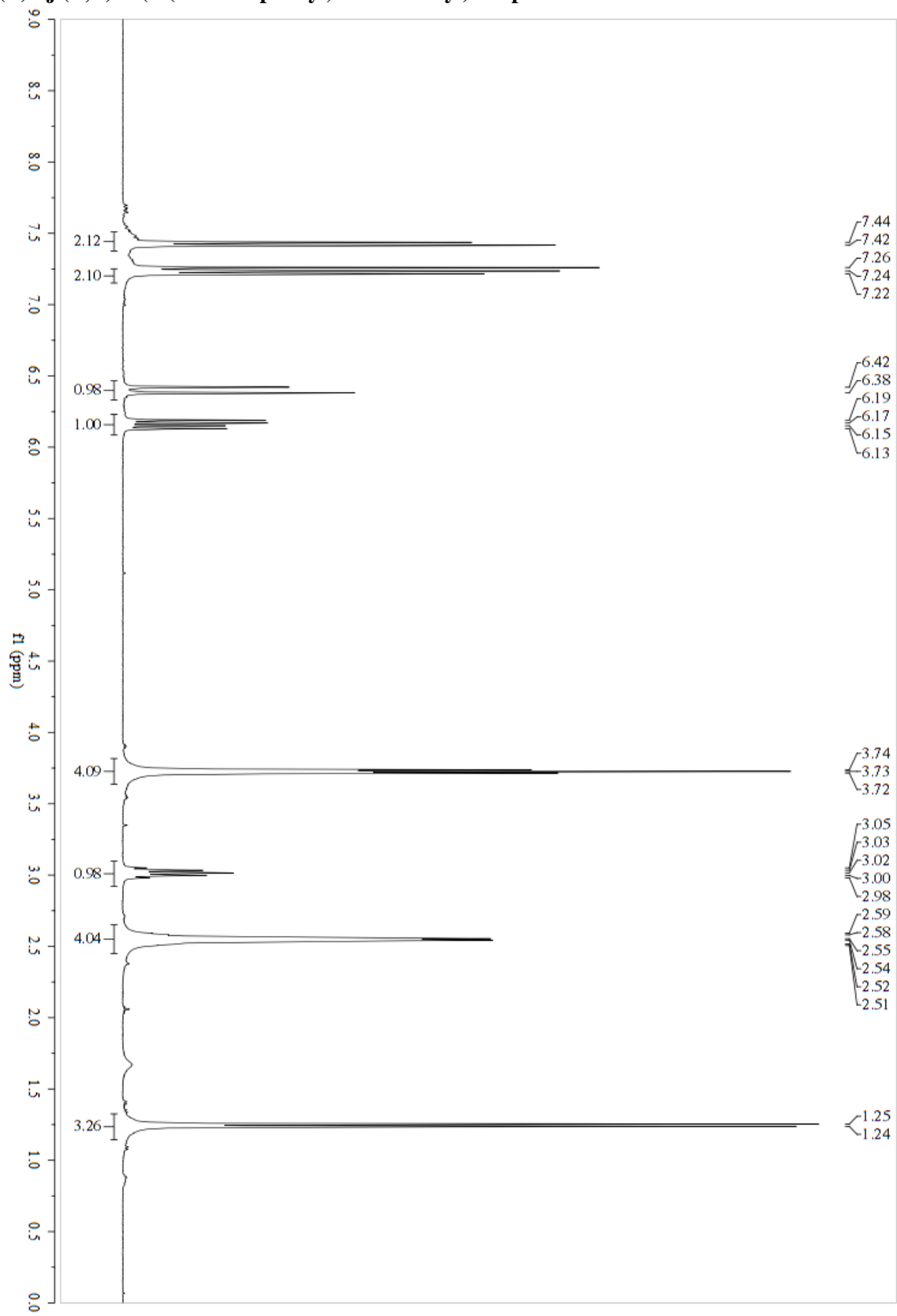
**2v (*tert*-butyl (*Z*)-cyclohexyl(3-phenylallyl)carbamate)**



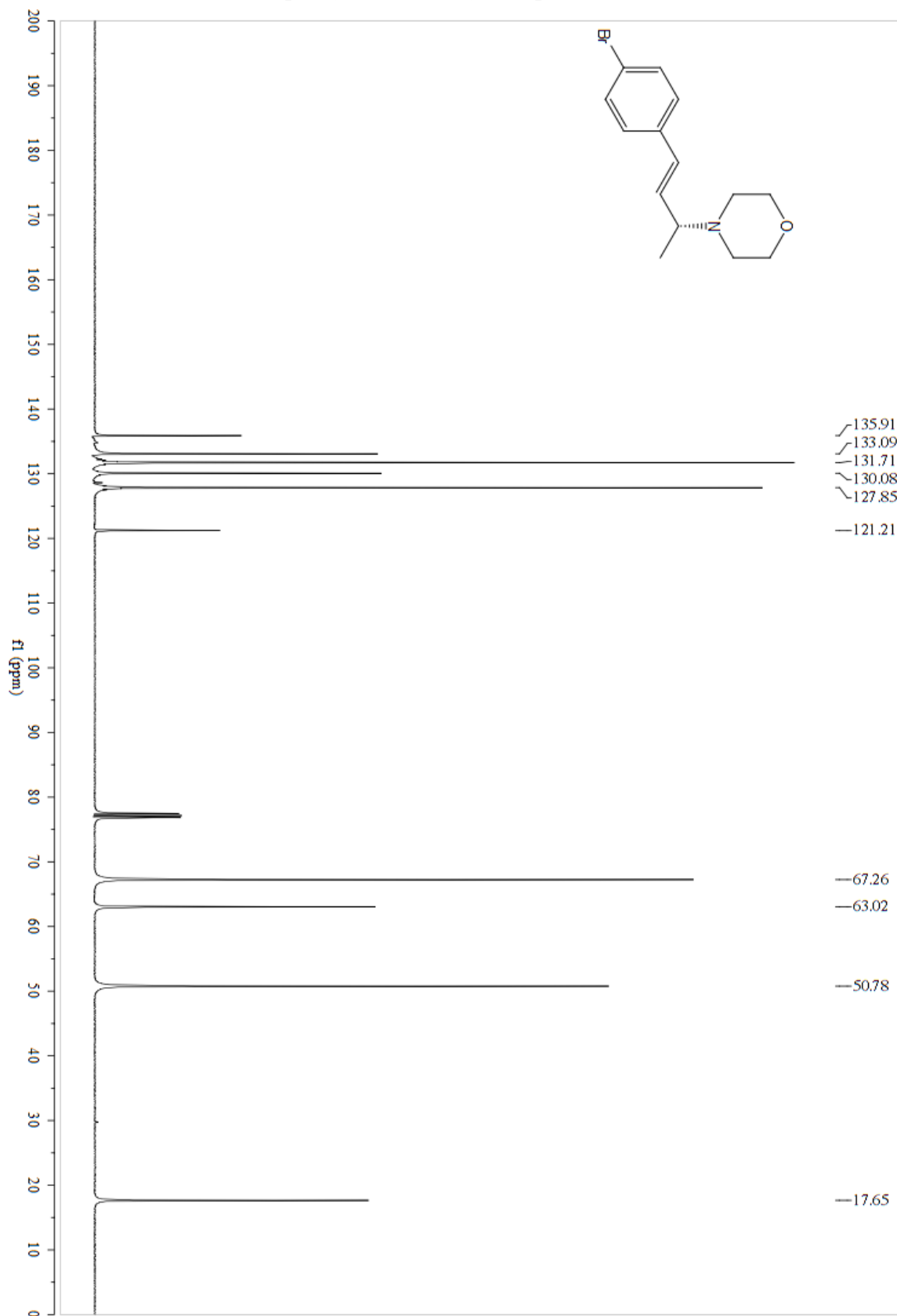
**Z-2v (*tert*-butyl (*Z*)-cyclohexyl(3-phenylallyl)carbamate)**



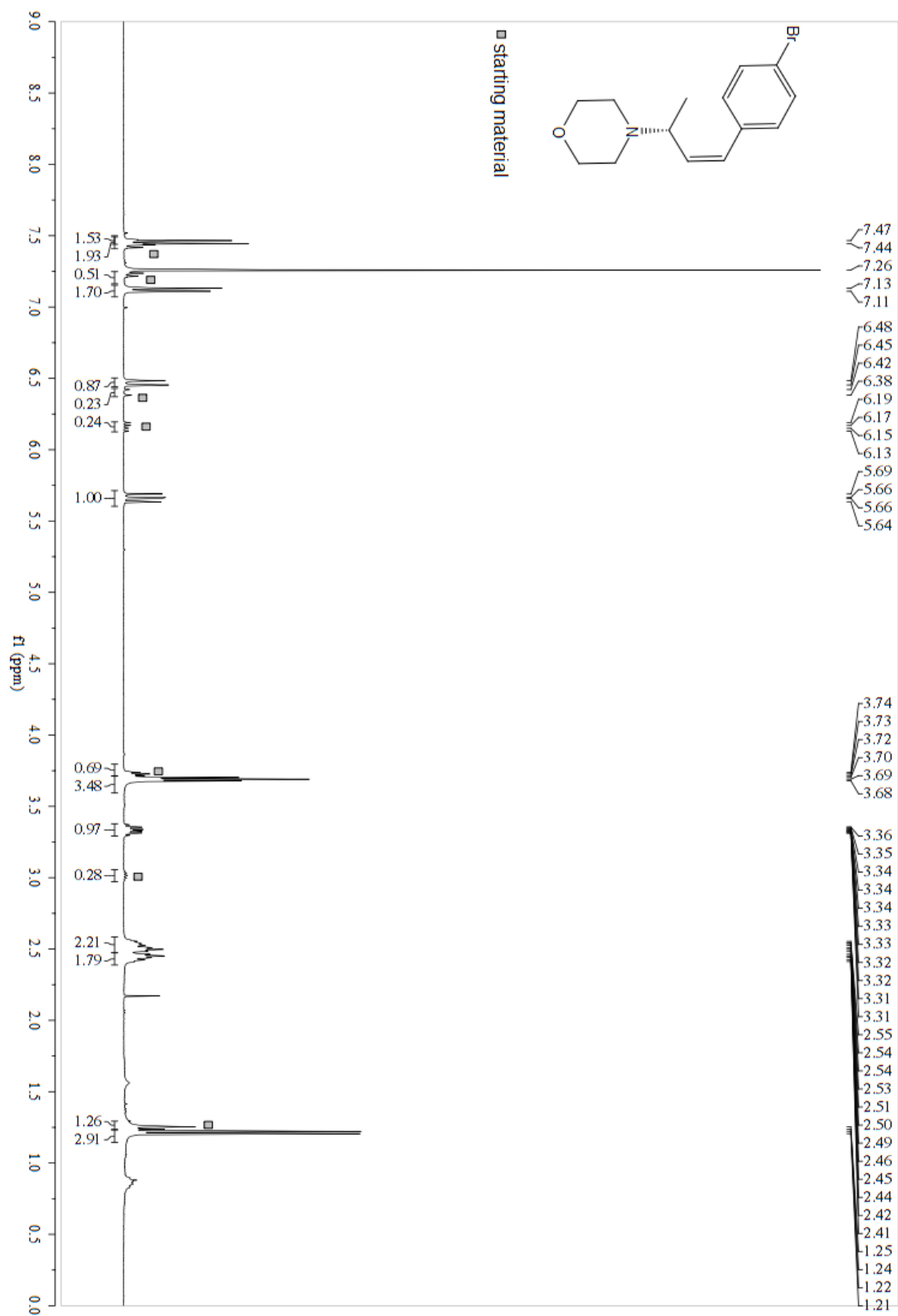
**(R)-1j (R,E)-4-(4-(4-bromophenyl)but-3-en-2-yl)morpholine**



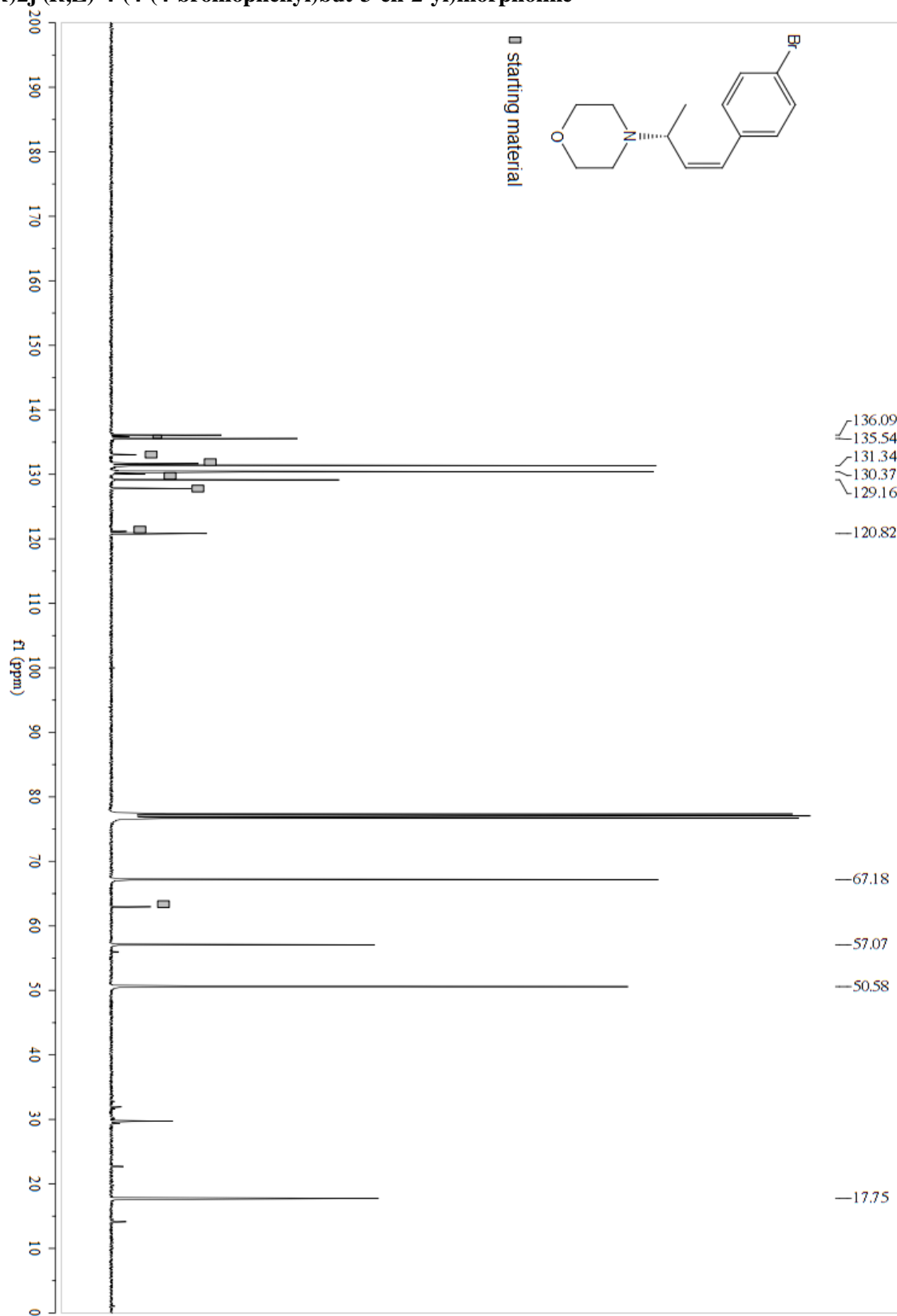
**(R)-1j (R,E)-4-(4-(4-bromophenyl)but-3-en-2-yl)morpholine**



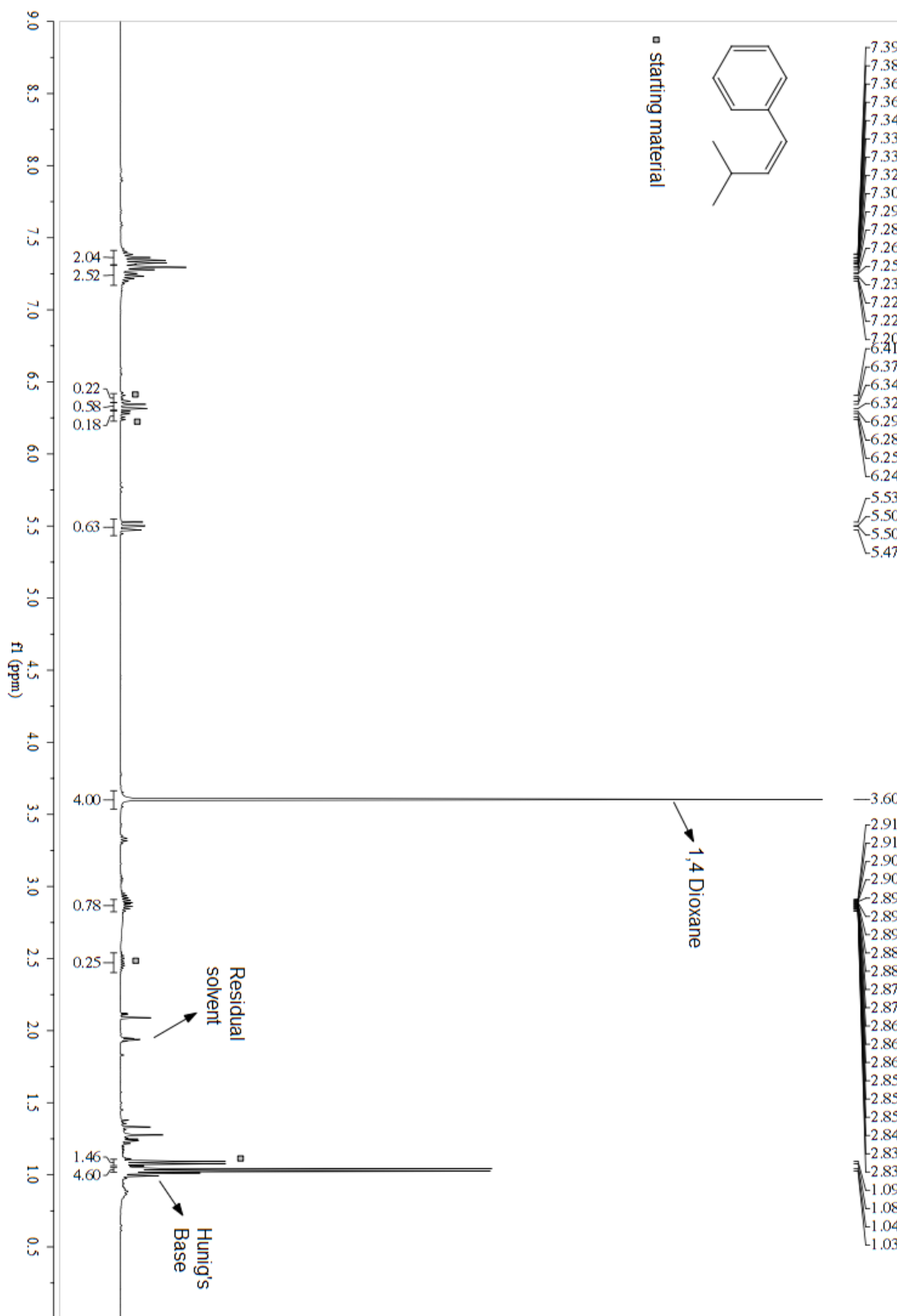
**(R)-2j (R,Z)-4-(4-(4-bromophenyl)but-3-en-2-yl)morpholine**



**(R)2j (R,Z)-4-(4-(4-bromophenyl)but-3-en-2-yl)morpholine**



**2z (Z)-(3-methylbut-1-en-1-yl)benzene**



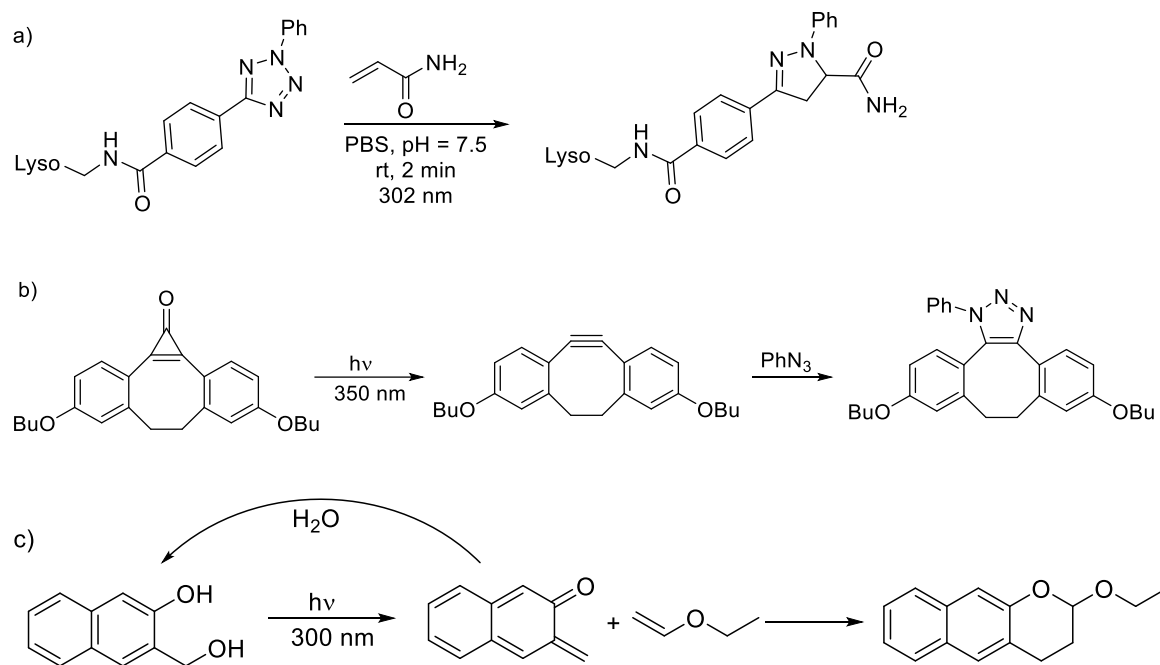
## CHAPTER III

### VISIBLE LIGHT INDUCED RAPID AND SELECTIVE LIGATION WITH STRAIN LOADABLE ALKENES

After successfully developing the methodology for the *E/Z* isomerization of styrenoids, which could drive the reaction in an endergonic direction, we sought to utilize the higher energy products resulting from an endergonic reaction selectively in further useful synthesis. After double bond isomerization of acyclic alkenes, we obtained the *Z*-alkenes as the major products which are typically 3-8 kcal/mol higher in energy than their *E*-isomers. Meanwhile, we were pumping 55-60 kcal/mol of energy into the system from the photocatalyst. Thus, we felt that this was an inefficient utilization of the potential energy of the excited photocatalyst, as most of its energy was wasted, and only 3-8 kcal/mol of energy was harvested. We started contemplating strategies that might allow us to utilize the full potential of the photocatalyst and harvest more of the visible light energy. One straightforward approach to capture more of the energy was to convert it to ring strain. The isomerization of *cis*-cyclic alkenes to the corresponding *trans*-isomer will generate a highly strained endergonic product, which we anticipated would be less prone to undergo subsequent reexcitation because of an induced lack of conjugation. Furthermore, we anticipated that we could harness the increased energy of the *trans*-isomer to drive subsequent strain releasing reactions.

Strain-induced couplings have proven useful in bioconjugation, but often require significant effort to ensure that the reactivity is used productively. The use of external stimuli, such as light, can offer an additional level of control not available in other methods.<sup>1-2</sup> The ability to use

light to toggle chemistry on and off offers the convenience of spatial and temporal control. Several examples of light induced bioconjugation systems have been developed over the last decade, and most commonly, these make use of short wavelength light. This light is typically used to convert an otherwise unreactive molecule to a reactive molecule that undergoes bond formation with a non-natural functional group. In this manner, upon UV irradiation, tetrazoles can extrude  $N_2$  to form highly reactive nitrile imine dipoles,<sup>3-5</sup> which undergo cycloaddition with alkenes (Scheme 12a). This strategy has been used by Lin to label proteins within *E. coli* cells.<sup>6</sup> Additionally, Lin has also shown that reactive nitrile ylides generated from the photolysis of 2H-azirines<sup>7</sup> 302 nm can be used for the PEGylation of a lysozyme.<sup>8</sup> Similarly, cyclopropanones have been used as a photolabile surrogate for strained cycloalkynes,<sup>9</sup> which upon unmasking undergo



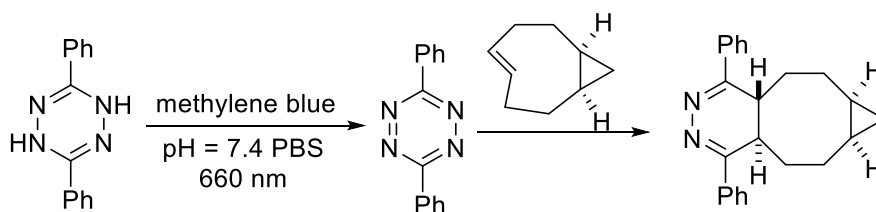
Scheme 12 a) Cycloaddition of tetrazole-containing lysozyme with acrylamide. b) Cycloaddition of photolabile cyclopropanones with azides. c) Cycloaddition of photochemically generated *o*-naphthoquinone methide with vinyl ether

rapid reaction with azides (Scheme 12b). In a similar context, Popik utilized 3-hydroxy-2-naphthalenemethanol derivatives which upon UV irradiation undergo photochemical dehydration

to generate highly reactive *o*-naphthoquinone methides which rapidly react with vinyl ethers to generate benzochroman cycloadducts (Scheme 12c).

However, in all of these examples the light stimulation serves to irreversibly unmask a reactive molecule, and aside from preventing undesired reactions prior to the start of the reaction, little additional control is gained compared to non-stimulated strain induced reactions. In order for the field of light mediated bioconjugation to move forward, we need new strategies that provide enhanced control of reactivity.

The cycloaddition of tetrazines with *trans*-cyclooctenes provides the greatest rate constants to date (from  $2 \times 10^3$  to  $1 \times 10^6$   $\text{M}^{-1}\text{s}^{-1}$ ),<sup>10-11</sup> owing in part to the strained nature of the *trans*-cyclooctene, the most strained isolable alkene known. However, the built in reactivity of both partners can decrease the practicality of this system *via* nontrivial syntheses and handling concerns.<sup>12</sup> Very recently, Fox<sup>13</sup> has shown that visible light and catalytic methylene blue can be used to oxidize dihydrotetrazine, *in situ*, to give the highly reactive tetrazine, which undergoes rapid conjugation, circumventing some of the aforementioned issues (Scheme 13).



Scheme 13. Cycloaddition of tetrazine with *trans*-cyclooctene

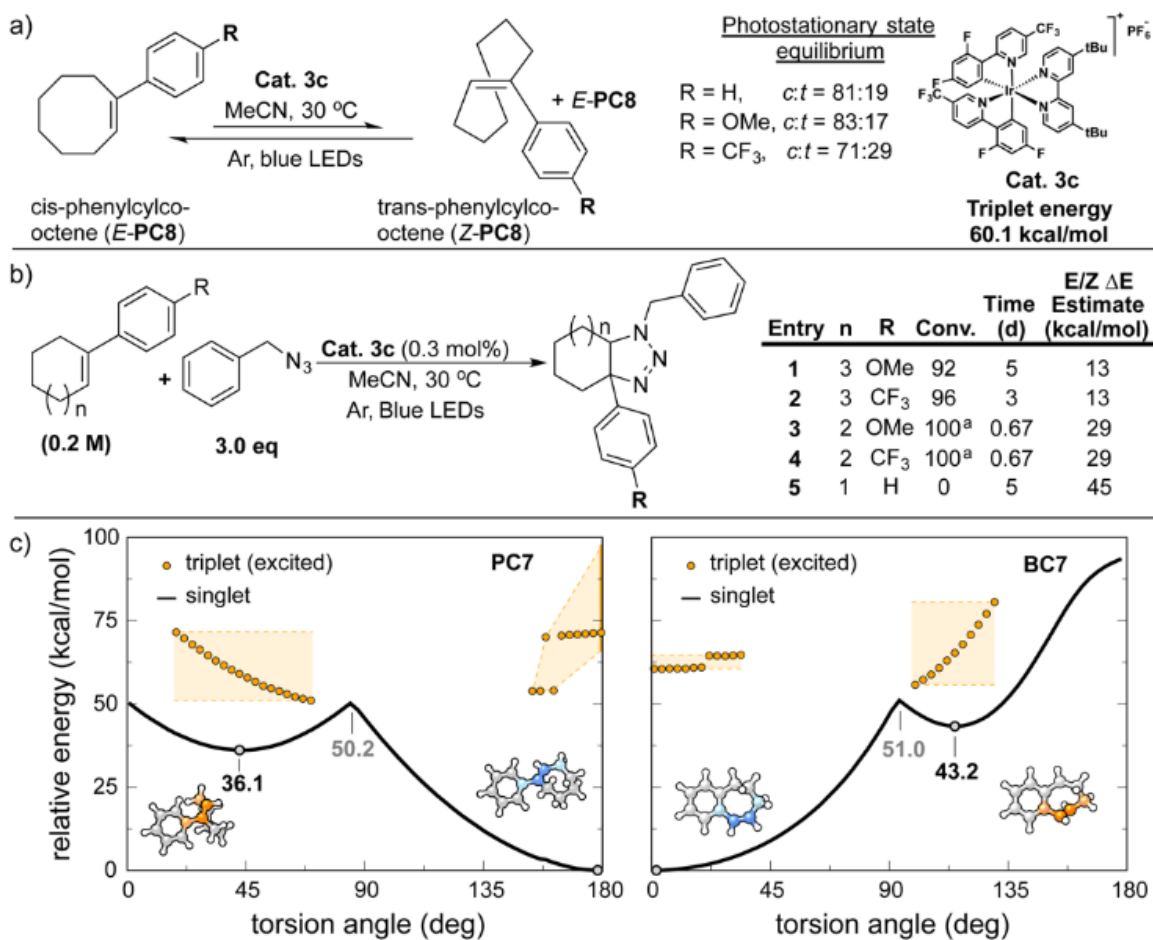
We were curious to see if we could find an alkene, which upon isomerization, would capture some of the photochemical energy in the form of ring strain that could be utilized for bimolecular couplings. The cyclic alkene after isomerization distorts from its ideal geometry and could generate a highly strained *trans*-cycloalkene which could selectively undergo coupling with other reagents or simply revert back to the *cis* isomer thermally. The desired coupling would depend

on the concentration of the reactive *trans*-cycloalkene generated such that very low concentrations of the *trans*-cycloalkene is generated. The release of strain from such a *trans*-cycloalkene would result in desired bimolecular coupling minimizing the formation of side products as the reactive *trans*-cycloalkene will not build up in large concentrations. If successful, we would be able to apply visible light as a trigger that would generate a reactive alkene, potentially capable of undergoing bioconjugation. It was expected that this might circumvent some of the circuitous syntheses of popular strained molecules currently being used for bioorthogonal coupling. Furthermore, unlike other photo-initiated processes which utilize the photochemical energy to irreversibly unmask the reactive group, our system would simply capture photochemical energy which would give rise to a steady, catalytic concentration of a more reactive form of the same molecule, a currently unexplored strategy.

### 3.1 Results and Discussion

At the outset, we considered azides as the coupling partner. They are relatively inert towards biological functional groups, result in minimal perturbation to the system, and are known to undergo reaction with alkenes to form triazolines.<sup>14</sup> It is also known that electron deficient<sup>15</sup> and strained alkenes<sup>16-17</sup> react faster with azides. Bach calculated the energy barrier for the cycloaddition of methyl azide to cyclooctyne and *E*-cyclooctene, and found that addition of methyl azide to cyclooctyne has a lower barrier than *E*-cyclooctene by 3.1 kcal/mol.<sup>18</sup> In addition, Houk performed a theoretical study on the cycloaddition of strained alkenes and azides and concluded that only *trans*-cyclooctene would be sufficiently rapid for use at room temperature, perhaps, somewhat diminishing interest in the alkene azide cycloaddition.<sup>17</sup> However, in this study, only isolable *trans*-cycloalkenes were considered, leaving the possibility for potential discovery of a smaller alkene which would react more rapidly. Early photochemical studies have shown that the *trans*-cycloalkenes could be formed *via* excitation to the excited state using UV light, which suggested that formation could be possible using visible light and a photocatalyst.<sup>19-22</sup>

We initiated our study using (*E*)-1-phenylcyclooct-1-ene (*E*-**PC8**, Scheme 14a). We were pleased to see the isomerized alkene (*Z*)-1-phenylcyclooct-1-ene (*Z*-**PC8**) was formed under these conditions. While the photostationary state equilibrium was disappointing from a synthetic view (19-29%), it was encouraging from an energetic standpoint. Caldwell has estimated the energy difference for the *E*, *Z*-isomers of phenyl cyclooctene at 13.3 kcal/mol,<sup>23</sup> suggesting that we were able to skew the product distribution away from the thermodynamic equilibrium by nearly 10-orders of magnitude using visible light. Since our intention was to generate the reactive alkenes *in situ*, rather than isolating the unstable molecules, we were not dissuaded.



Scheme 14 Initial investigation. a) First effort to capture photochemical energy as ring strain. b) Attempts to chemically capture strained alkenes. c) Calculated torsion angle energy landscapes about the ring alkene bonds in (left) **PC7** and (right) **BC7**. <sup>a</sup>Significant dimerization observed

We next evaluated the ability to form triazolines as a function of alkene ring size (Scheme 14b). It was anticipated that the *trans*-cycloalkene would be continually consumed by the azide, and the photocatalytic system would reestablish the equilibrium. In contrast to their reactivity upon UV-light irradiation,<sup>24</sup> alkyl azides are generally stable to visible light, which is important to avoid competing types of photochemistry. We were pleased to see that 7 and 8 membered *trans*-alkenes (entries 1-4) afforded the desired triazoline product. While the rates of the reaction displayed some electronic dependence in the **PC8** system, in general, it was disappointingly slow (3-5 d). In contrast, despite no observation of *trans*-isomer (<sup>1</sup>H NMR) in the **PC7** series, the reaction required less than 0.67 d to reach completion. This suggested a strong correlation between ring strain and reaction rate and provided evidence that a transient alkene could result in faster coupling than the **PC8** system. Unfortunately, significant dimerization<sup>25</sup> was also observed in the case of the **PC7** system. Meanwhile, cyclohexene, **PC6**, failed to give any conversion even after 5 d of irradiation (entry 5).

In order to better understand the observed reactivity and guide future efforts, we performed a computational evaluation of the energy landscapes showing conversion between the *Z* and *E* forms of **PC6**, **PC7**, and **PC8**. We generated both singlet and triplet excitation landscapes with MP2/cc-pVTZ calculations in order to assess both the strain energy loaded upon isomerization and to gauge how features of the excitation process could influence the reactive behavior of these systems. As expected, *Z*-**PC7** (Scheme 14c and Figure 9a) has over twice the strain energy of *Z*-**PC8** (Figure 9b), supporting the observed difference in reactivity. While **PC6** has a similar excitation energy, the *trans*-isomer, while accessible, is only transiently stable with a reversion barrier to the *cis*-isomer near room temperature thermal energy (Figure 9f). The predicted short-lived nature helps explain the inability of **PC6** to undergo bimolecular reaction to form the triazoline.

Given that a transient amount of the *trans*-cycloheptene gave a substantial rate increase compared to observable amounts of the **PC8** system, we sought to modify these systems to increase

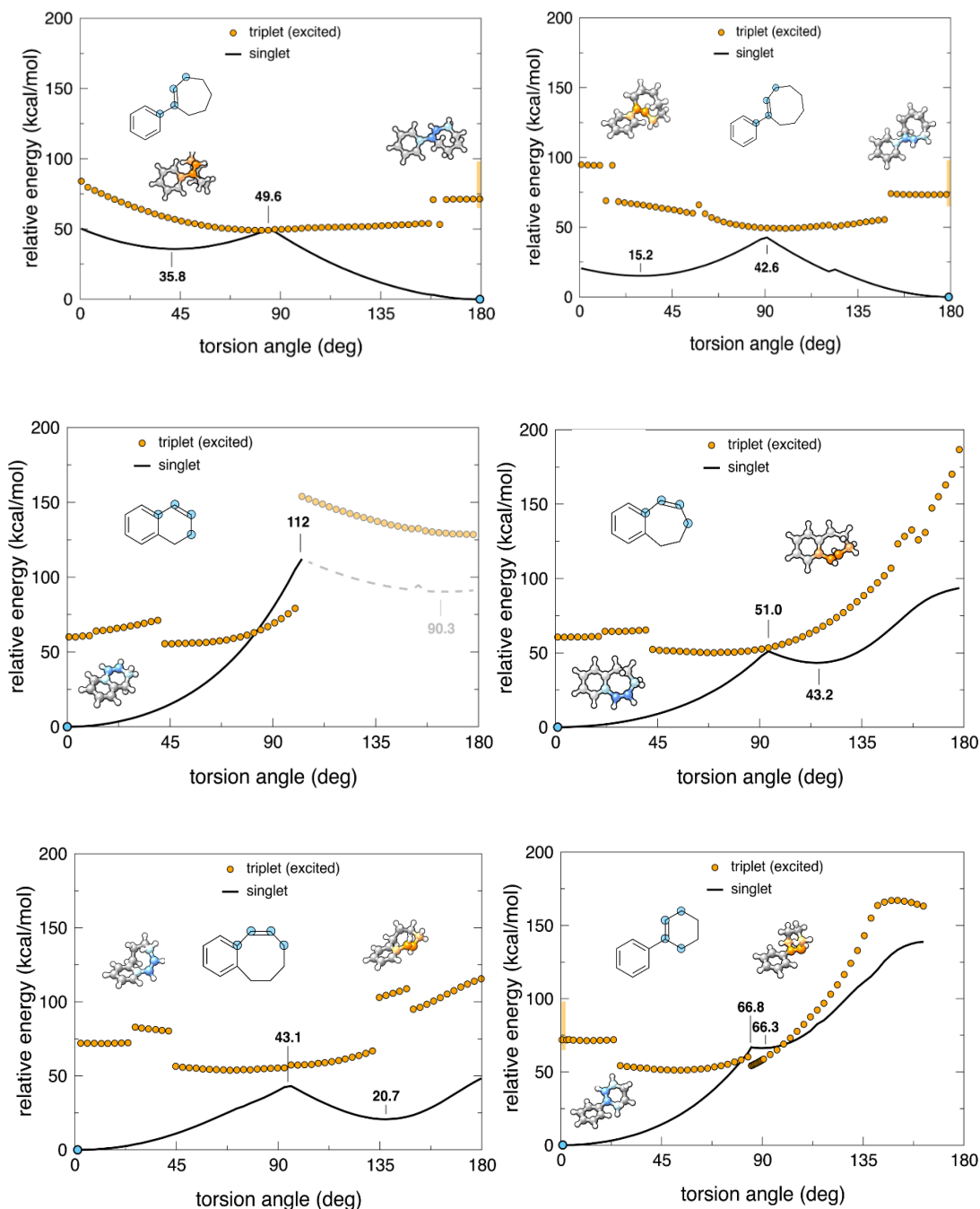
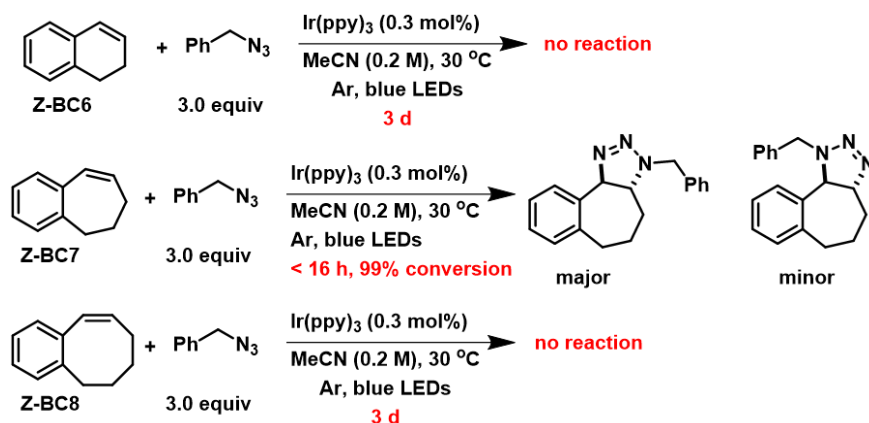


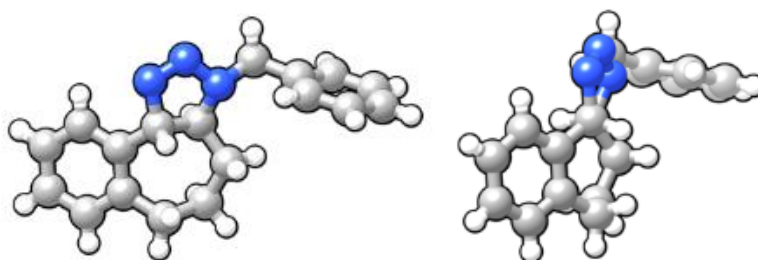
Figure 9. Energy landscapes. Singlet and triplet state energies for a torsion drive about the highlighted double bond for a) 1-phenylcyclohept-1-ene, b) 1-phenylcyclooct-1-ene, c) 1,2-dihydronaphthalene, d) 6,7-dihydro-5H-benzo[7]annulene, e) 5,6,7,8-tetrahydrobenzo[8]annulene, f) 1-phenylcyclohex-1-ene

the concentration of the reactive conformer(s). We envisioned that rigidification of the cycle could potentially result in increased strain energy and increased barriers to interconversion. These changes, along with potentially more efficient energy transfer due to the fusion of the aryl ring which reinforces conjugation with the double bond, might lead to increased concentration of more reactive strained species. Thus, we fused the essential aryl group to the ring system, giving benzocyclohexene, -heptene, and -octene (**Z-BC6**, **Z-BC7**, and **Z-BC8**, Scheme 14d). We performed similar energy landscape calculations on these compounds (Scheme 14c and Figures 9c, 9d, and 9e), and they partly support these expectations. In the case of **BC7**, there is indeed a roughly 7 kcal/mol increase in strain energy relative to **PC7** upon isomerization; however, the interconversion barrier, relative to the low energy isomers, is essentially unchanged. Notably, the forced conjugation in **BC7** lowers the triplet excitation energy from the unstrained conformer compared to the **PC7**. In fact, the excitation of **PC7** occurs over a 30 kcal/mol band due to the thermally accessible ground state conformers. Said differently, because of the ring fusion in **BC7**, the forced conjugation would allow the bulk of the population is excitable, and this is not the case for **PC7**. This will likely result in a more efficient excitation and an increased excited state population when under visible light irradiation. Calculations on **BC6** and **BC8** (Figures 9c, 9e) predict poor reactivity for both. In **BC6**, *trans*-isomer is not geometrically accessible from the triplet, which instead would be expected to undergo ISC and give a “hot” or vibrationally excited *cis*-isomer. In **BC8**, due to atomic crowding in the octene ring, the alkene rotates perpendicular to the benzene and conjugation is severely broken. As a consequence, the excitation energy is closer to an aliphatic alkene and well above the triplet energy of the photocatalyst used. We synthesized and tested the photocatalytic reactivity of these three aryl fused ring systems (Scheme 14d), and the results are fully consistent with the calculations. Of these, **BC7** certainly shows the greatest promise given its predicted higher strain energy and greater potential concentration of reactive species, both supporting an expected increase in the rate of the subsequent bimolecular cycloadditions.



Scheme 14d. Reaction results for **BC6**, **BC7**, and **BC8** triazoline.

Our attempts to trap the transient *E*-**BC7** with benzyl azide were successful. We were pleased to find that the reaction went to completion in less than one day, with only 2 regioisomers as the sole products. Both are single diastereomers with *trans*-ring junctions. An X-ray structure of the major product (Scheme 14e) clearly shows the *trans*-ring fusion of the triazoline, which is most readily explained by a concerted or nearly concerted [3+2] cycloaddition of the azide and *E*-**BC7**. While we have not shown this, we anticipate that the *cis* ring fusion would be thermodynamically more favorable, and would be feasible if a step-wise process were to have occurred. Control reactions indicate the necessity of the photocatalyst and indicate that there is no background reaction with *Z*-**BC7**.

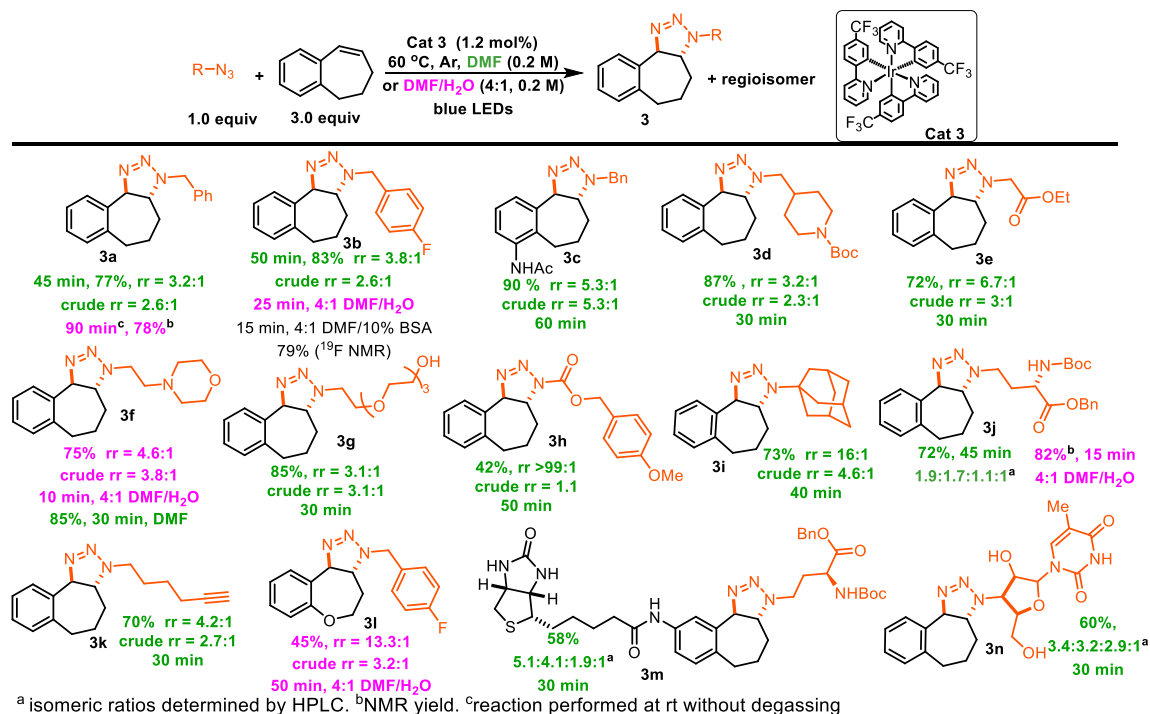


Scheme 14e. Two views of the crystal structure of major product showing *trans* ring fusion.

Despite our initial excitement over these preliminary findings, there were a number of issues that might preclude its utility for bioconjugation purposes that needed to be addressed. These issues included slow kinetics, problematic dimerization of alkene, use of excess azide, strict use of

inert environment, use of pure MeCN, the unknown toxicity of iridium and its potential to cause undesired redox chemistry, and the instability of the triazoline motif. Fortunately, the dimerization of the **BC7** system proved to be much slower than that of the **PC7** system, so slow that it was no longer problematic. We then focused on increasing the rate of the reaction and utilizing the azide as the limiting reagent. Although the reaction works with either alkene or azide as the limiting component, we assumed that the azide was the most valuable component of the reaction mixture. This seemed reasonable given the overwhelming number of examples of incorporation of azides into biomolecules, and functioning under azide limiting conditions would allow this chemistry to function as a drop in solution and require little to no alteration of existing biological systems. Optimization included solvent, photocatalyst structure and loading, alkene loading, photon dependency, substrate concentration, and temperature effects. We found that the use of DMF, commercially available *fac*-tris-Ir(4'-CF<sub>3</sub>-ppy)<sub>3</sub> (**Cat. PC1**) at 1.2 mol%, 60 °C, and 3 equivalents of the alkene partner all led to increases in the rate of the reaction. Under optimal reaction conditions, both the photocatalyst and the alkene fell out of the rate expression, such that no further rate increase was observed by increasing the concentration of these reagents. Using these conditions, a first order rate constant was determined to be  $k = 2.4 \pm 0.9 \times 10^{-3} \text{ s}^{-1}$ , with a half-life of only  $t_{1/2} = 4.8 \text{ min}$ . Furthermore, we expect this is a lower estimate for the rate constant since it was performed using an easily monitored substrate, which is known to react slower than others. In direct competition experiments between the photoconjugation of several azides with **BC7** and Cu-catalyzed azide alkyne cycloaddition (CuAAC), the photoconjugation reaction was found to be up to 100 fold faster. Given that CuAAC has been used for bioconjugation, suggests that the photoconjugation of **BC7** takes place with sufficient rates for bioconjugation applications.

In order to better understand the nature of the reaction, we began to investigate the scope of the reaction using these optimized conditions (Scheme 15). In bioconjugation, the surface of biomolecules may severely limit access to the azide substrate, so we were pleased to see that the reaction works well across a range of sterically hindered azides, even with sterically demanding 1-azidoadamantane (**3i**). Often, the modest isolated yields are a reflection of the separation of the minor regioisomer during purification, not a lack of reactivity. Despite the frequent use of iridium-based photocatalysts in promoting redox reactions,<sup>26-28</sup> the conditions proved to be tolerant of a number of biologically relevant functional groups, such as amino acid derivatives (**3j** and **3m**), amines (**3d**, **3f**, and **4l**), amides (**3c** and **3m**) alcohols (**3g** and **3n**), esters (**3e**), electron rich arenes (**3h**), and purine bases or sugar molecules (**3n**). In addition, it tolerates a number of unnatural functional groups such as aryl-bromides (**3l**) and -fluorides (**3b**), and alkynes (**3k**). This functional group tolerance is likely a result of the mild conditions and the fast quenching of the excited state photocatalyst by the alkene. In other words, excess alkene serves to protect sensitive functional groups by dissipating the photochemical energy in the form of bond motion, much like the



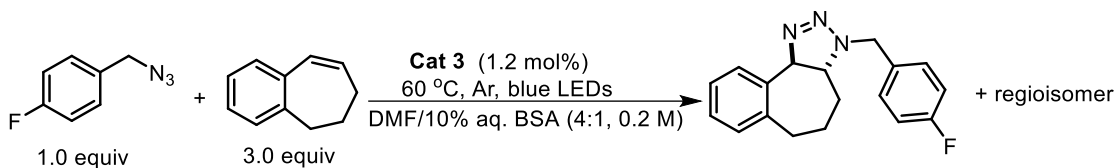
Scheme 15. Substrate scope of strain induced [3+2] cycloaddition reaction.

protective action of cinnamic acid based sunscreens.<sup>29</sup> Smooth intermolecular coupling to give **3k** demonstrates the orthogonal nature of these reaction conditions towards traditional alkyne, azide cycloadditions which would be expected to give the fused triazole product. The doubly orthogonal nature of the reaction makes it even more attractive, since alkynes could be later used for further functionalization via traditional click chemistry.<sup>30</sup>

While the geometry of the ring is a prerequisite to reactivity, initial exploration suggests that the aryl ring (**3c** and **3m**) and the seven-membered ring (**3l**) can both tolerate substitution. In the future, further evaluation will focus on the development of probes, and fine tuning of the reactivity and improvement of physicochemical properties of the molecule. Acetamides (**3c** and **3m**) were found to be well tolerated in the reaction and allowed the facile coupling of a biotin labeled alkene with a protected amino acid derivative (**3m**). This example highlights one significant advantage to this approach when compared to other strain induced couplings: derivatization of the alkene is rapid and trivial, and it provides biochemical tools that are indefinitely stable until subjected to the reaction conditions. In the case of conjugation chemistry, it may be advantageous if the stereochemical environment of the substrate does not affect the rate of conjugation, or it may result in failed couplings. Fortunately, stereocenters on the azide do not hamper the cycloaddition (**3j**, **3m**, and **3n**).

Finally, knowing that we want to use this chemistry on biological systems in which proteins might interfere in undesired ways, we subjected **BC7** and 4-fluorobenzyl azide to normal reaction conditions but instead of pure DMF, a 4:1 DMF:10% aqueous bovine serum albumin (BSA) solution was used (Scheme 16). Gratifyingly, under these conditions 79% (<sup>19</sup>F NMR yield) of the desired product **3b** was formed. Given the possibility of interference or unselective reaction on the protein surface, a high yield of the desired product indicates that the BSA interfered with neither yield nor chemoselectivity (83% yield was obtained under standard conditions). Serendipitously, it also led us to discover that the reaction was further accelerated by the presence of water, given that

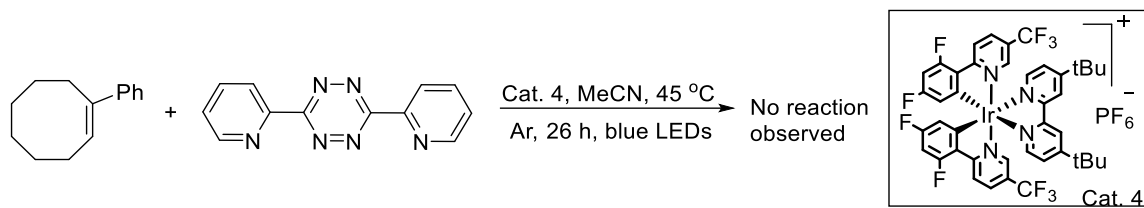
the reaction takes near 50 minutes to complete in dry DMF but less than 15 minutes, which represents an upper limit, in the presence of the BSA solution.



Scheme 16. Reaction performed in presence of BSA

Under these conditions the reaction mixture was homogenous, but at higher water loadings the photocatalyst precipitates, which precludes using this specific set of reaction components in a purely aqueous system. However, we believe the aqueous solubility can be increased via a number of strategies, and this is currently being pursued in our lab. We were pleased to find that this acceleration was a general trend (Scheme 15, conditions B), with most substrates experiencing a roughly three-fold increase in rate, though we have made no attempts to directly quantify this acceleration. The source of this acceleration may be due to a decrease in the transition state volume ( $\Delta V^\ddagger$ ), a case in which the use of water has been shown to lead to an acceleration.<sup>31-32</sup> Alternatively, it is possible that the *trans*-alkene adopts a zwitterionic form to relieve strain and is stabilized by a more polar solvent, leading to a greater concentration of the reactive form.

Tetrazines are known to have enhanced reactivity when compared to azides, and also undergo cycloaddition with strained alkenes. Thus, we briefly explored this possibility. We exposed *E*-PC8 to 3,6-di(pyridin-2-yl)-1,2,4,5-tetrazine in presence of **Cat. 4**, MeCN at 45 °C, no cycloaddition product was observed (Scheme 17). Importantly, no strained *Z*-PC8 was detected (as is the case, in the absence of the tetrazine) and both the reactants were recovered unchanged after 18 hours of the irradiation. One explanation for this is that the fuchsia colored 3,6-diphenyl-1,2,4,5-tetrazine could itself absorb in the visible light region and might be responsible for the observed lack of reactivity.

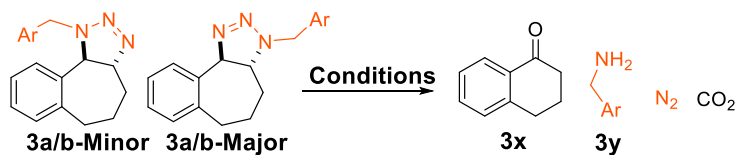
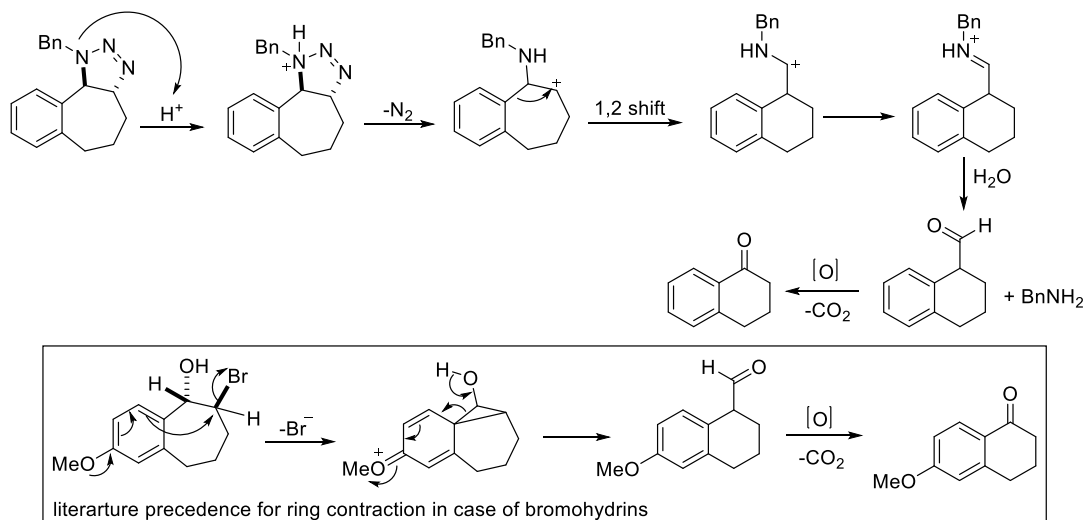


Scheme 17. Attempted cycloaddition of tetrazine with PC8

In contrast to triazoles, triazolines are not aromatic and are quite susceptible to further chemistry. Traditionally, the observed rate of triazoline decomposition was comparable to that of its formation, possibly deterring investigation of its use in conjugation chemistry.<sup>33</sup> However, the use of **BC7** under photocatalytic conditions effectively amplifies the rate of the triazoline formation, such that appreciable decomposition does not occur on the reaction time scale, allowing isolation of the triazoline products. Since the triazolines can be formed and isolated, the inherently greater lability of the triazolines might be a unique asset if decomposition could be intentionally induced.<sup>34</sup> In other words, rapid conjugation could then be followed by controlled release of the amine product. In fact, Gamble has demonstrated that hydrolysis susceptible triazolines formed *via* the 1,3-dipolar cycloaddition of azide with *trans*-cyclooctene is a viable prodrug activation strategy.<sup>35</sup>

To investigate the stability, **3a** was subjected to a number of conditions (Table 3). Extended reaction time (24 h) led to no detectable decomposition (entry 1). However, upon isolation and storage at 4 °C, the major isomer shows no decomposition for up to three years (and counting). The minor regioisomer is notably less stable and decomposes both upon storage (entry 2) and in solution (~7 d) even in the absence of the photocatalyst (entry 3). Decomposition is further accelerated when chromatography on silica is attempted (entry 4). Basic alumina was found to be an appropriate chromatography medium which did not lead to the decomposition of the minor isomer (entry 5). However, upon exposure of the products to acidic environments, we observed rapid decomposition and gas evolution, presumably N<sub>2</sub> and CO<sub>2</sub>. The isolation of alpha-tetralone from decomposed

mixtures was surprising, but has precedent<sup>36</sup> and presumably arises from ring contraction, followed by hydrolysis, oxidation, and an oxidative decarboxylation. Upon brief exposure of the crude reaction mixture containing **3a** to TFA (entry 6) a 38% yield of **3x** was obtained, suggesting this may be a viable release strategy. Further studies aimed at increasing this yield *via* optimization of the alkene structure and conditions are underway. As an aside, it could also provide an alternative route to the Staudinger reaction, which produces hard to separate triphenylphosphine oxide, during the reduction of azides.



Entry	<b>3a/3b</b> Conditions	Result
1)	<b>3a</b> cat-Ir(ppy) <sub>3</sub> , 60 °C, Ar, DMF, blue LEDs	No decomposition, 24 h
2)	<b>3a</b> Isolated compounds, 4 °C, 2 years	<b>3a-Major</b> no decomp. <b>3a-Minor</b> decomp.
3)	<b>3a</b> DMF, exposed to air	<b>3a-Minor</b> decomposes
4)	<b>3a</b> silica chromatography	Some <b>3a-Minor</b> decomposition
5)	<b>3a</b> basic alumina chromatography	No decomposition
6)	<b>3b</b> TFA 5 min	Rapid decomposition, <b>3y</b> 38%

Table 3. Stability studies of triazoline products.

Given the frequent use of dyes as fluorophores for labelling cells in many bioconjugation reactions, the effect of fluorophores on the reaction outcome was evaluated. It was anticipated that the outcome of the reactions could potentially be effected partially, or even completely, by the

presence of dyes due to competitive absorption of photons or possibly undesired quenching of the excited photocatalyst by the dye. Hence, experiments were performed in which various dyes, absorbing at different wavelengths, were added to the reaction mixture. The results are tabulated below (Table 4). The desired triazoline product **3a** was formed, albeit with lower efficiencies compared to the standard conditions absent of any extra dye. Increasing the amount of dye (2,7-dichlorofluorescein) present in the reaction to more than 8X fold that of the photocatalyst, resulted in a 42% (NMR yield) of the desired triazoline product, **3a**, within 6 hours of irradiation. With some effort it should be possible to design a system that selectively excites a photocatalyst even in the presence of another dye, which is supported by the results of Table 4.

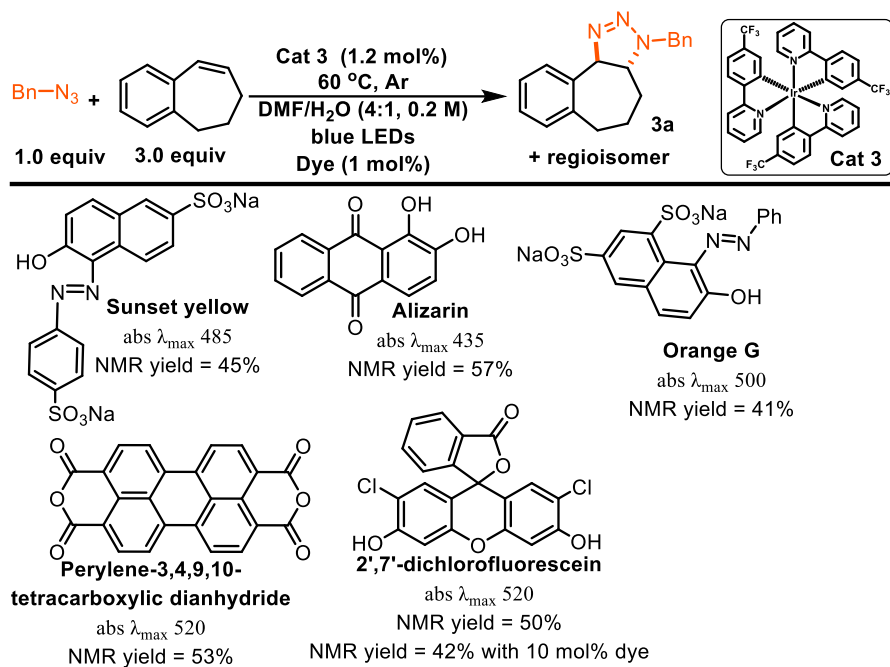
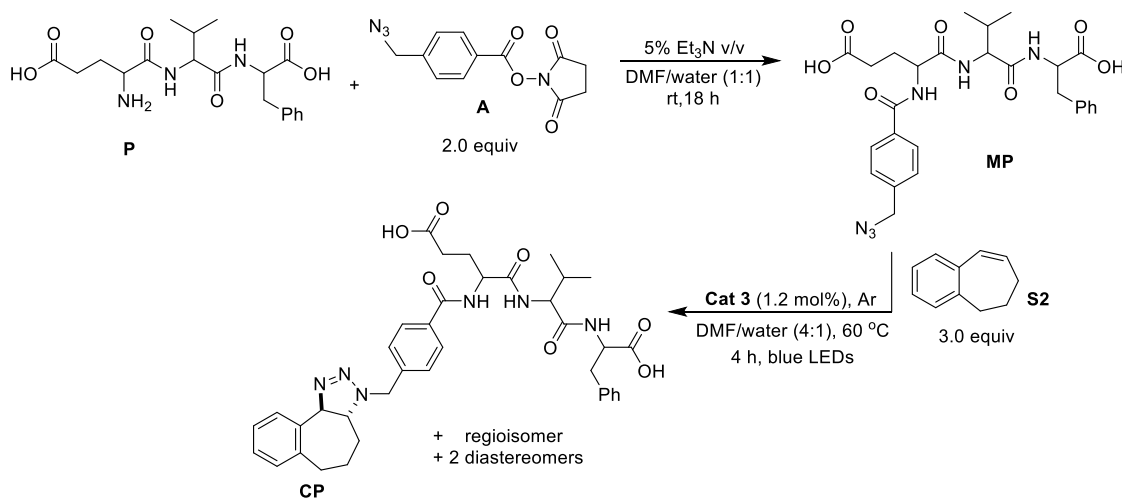


Table 4. Reaction outcome in presence of various fluorophores

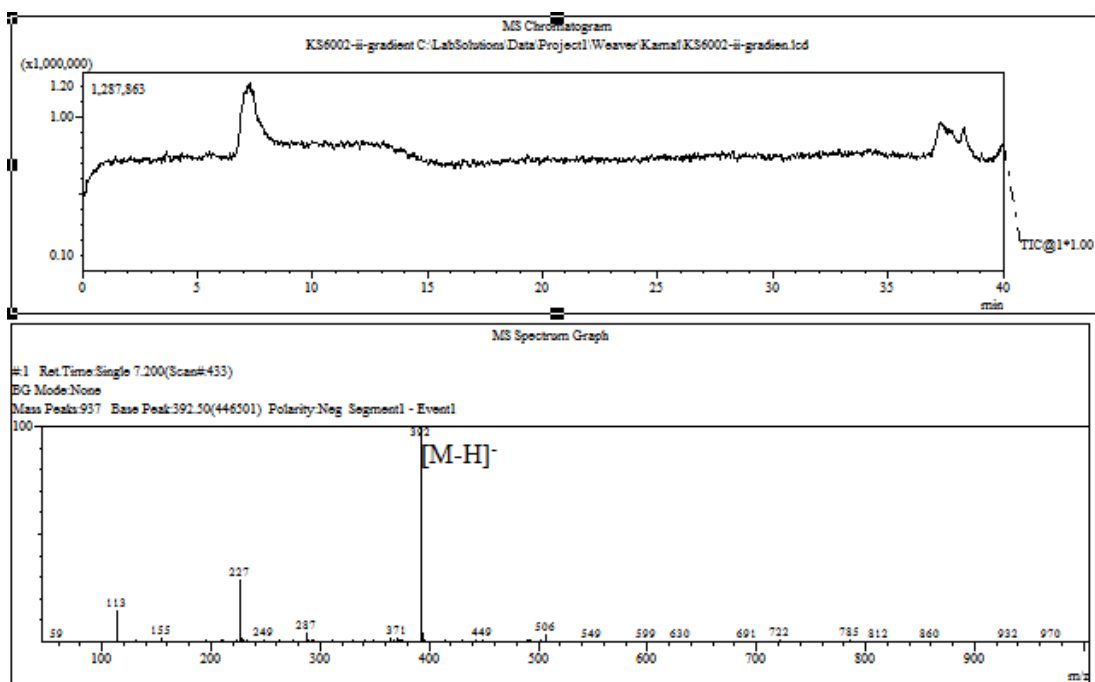
In order to showcase the applicability of this novel photoconjugation approach, the reaction conditions were applied on a small tripeptide (**P**). A commercially available tripeptide was modified with an azide (**MP**) and then conjugated with the **BC7** under standard conditions (Scheme 18). Within 4 hours of the irradiation, complete conversion to the desired conjugated tripeptide (**CP**) mass was observed by LCMS. The masses consistent with all three tripeptide derivatives, **P**,

**MP**, and **CP**, can be observed by LCMS. The observed masses are 392 [M-H]<sup>-</sup> for **P**, 551 [M-H]<sup>-</sup> for **MP**, and 695 [M-H]<sup>-</sup>, 667 [M-N<sub>2</sub>-H]<sup>-</sup>, 685 [M-N<sub>2</sub>+H<sub>2</sub>O-H]<sup>-</sup> for **CP**. The LCMS traces and annotated TICs for **P**, **MP** and **CP** are shown below.

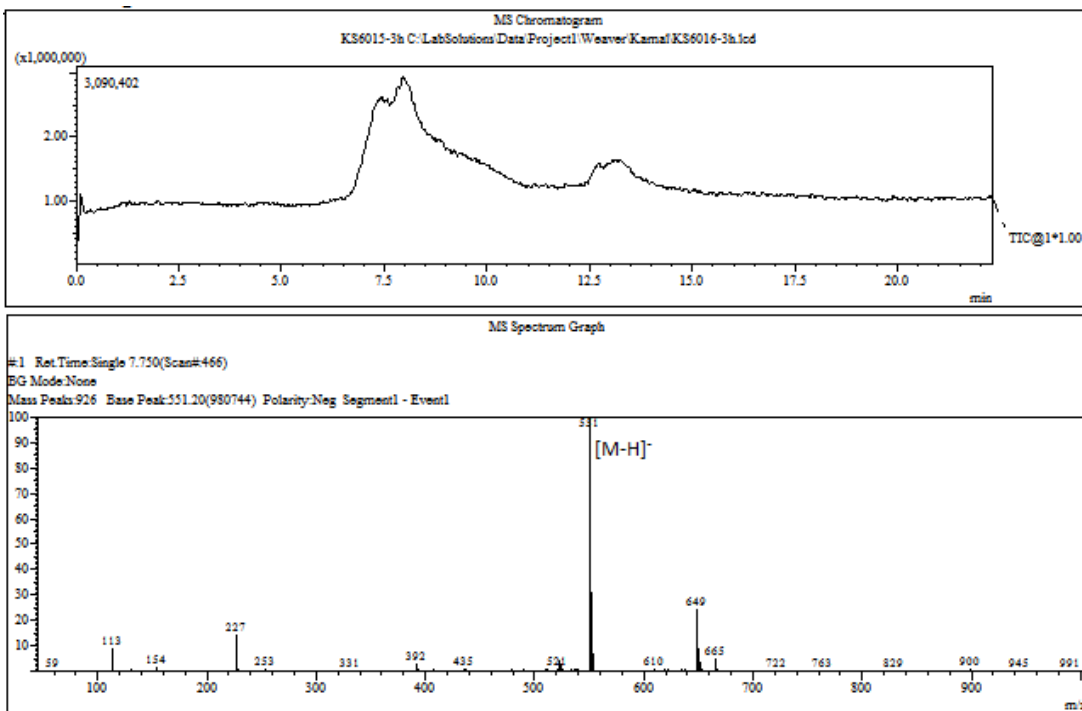


Scheme 18. Conjugation of a tripeptide

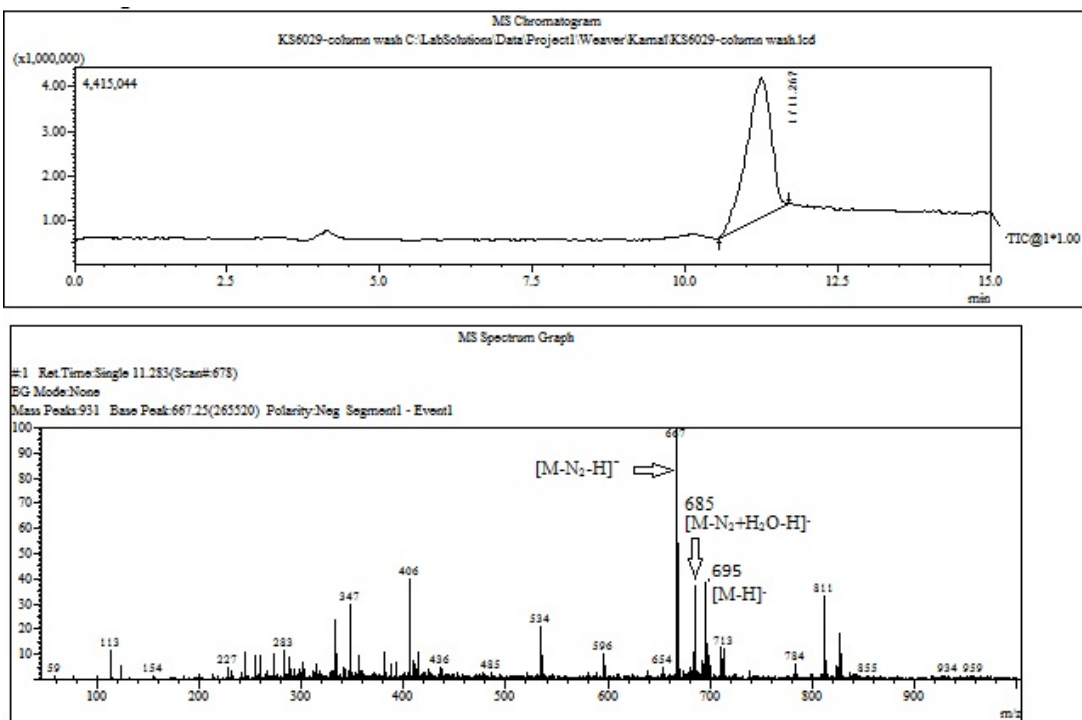
LCMS trace of **P**



LCMS trace of **MP**



LCMS trace of CP



While we had observed that the reaction could take place selectively in the presence of BSA, we also investigated the ability to perform the chemistry directly on a biomolecule. This would demonstrate that the photoconjugation takes place with sufficient rate to be useful even with large molecules which have smaller diffusion constants, and are present at much lower concentrations, typical of proteins. The *N*-termini of insulin (bovine), a peptide hormone which plays a key role in the metabolism of glucose and is made up of two peptide chains connected by disulfide bridges, were unselectively modified with an azide modified benzoylating reagent (**A**, Figure 10). The mixture of un-, mono-, di-, and tri-modified insulin (21.8  $\mu\text{M}$ ) were next subjected to the photoconjugation reaction (**Cat. 3**, 0.1  $\mu\text{g}$ ), with biotin modified benzocycloheptene (**BC7-B**, 1.2 mM), which took place at room temperature, and with no degassing. In less than 15 minutes,

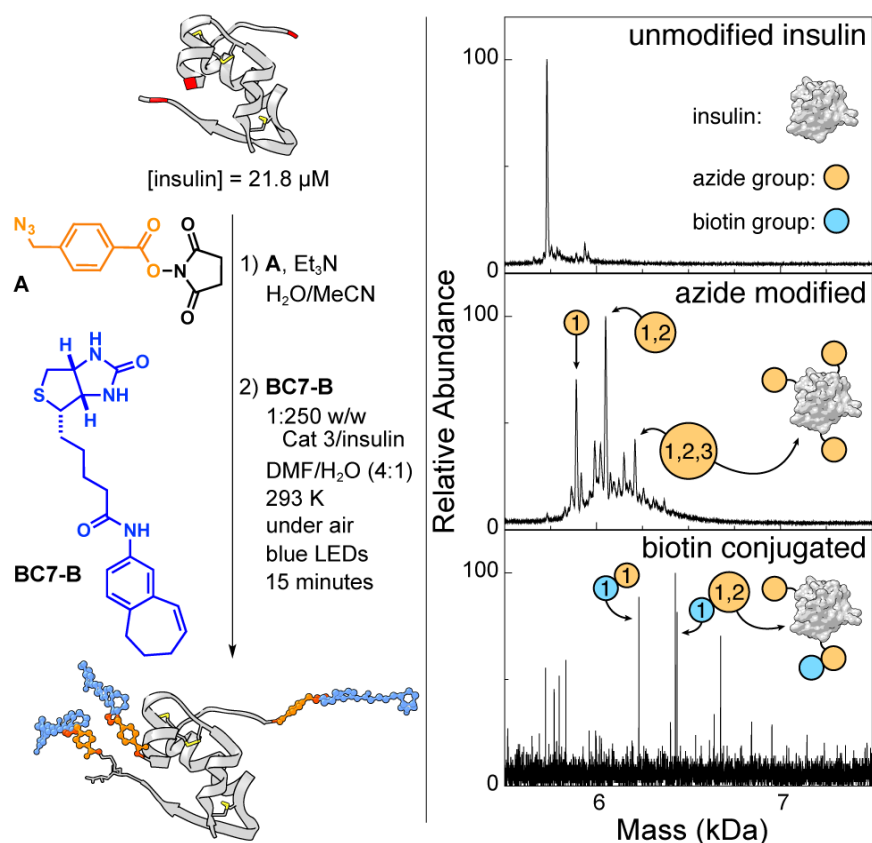


Figure 10. Demonstration of biotin conjugation to insulin using strain-loadable alkene coupling. There are three modifiable sites on the insulin structure highlighted in red: the A and B strand *N*-termini and the lysine residue on the B strand. The MALDI spectra on the right show modification and identification of two variants of the monoconjugated protein.

all of the modified insulin was consumed. New masses consistent with the mono- and di-conjugated product were detected.<sup>37</sup> The conjugation of insulin was further supported by the SDS-PAGE experiment and subsequent silver staining. New bands of slightly higher molecular weight than the unmodified insulin and azide modified insulin were detected.

The alkene behaves as a sunscreen in order to protect the insulin from the photocatalyst in a sense that it dissipates the photochemical energy in the form of bond motion. When the alkene was left out of the irradiated reaction mixture for 12 hours (Figure 10a), the modified insulin was broken into its constituent chains (top spectrum), highlighting the protective nature of the alkene and suggesting that even redox sensitive biomolecules can tolerate the reaction conditions, provided the alkene is present to quench the excited photocatalyst. It is quite possible that the tertiary structure of insulin was lost, due to the solvent.

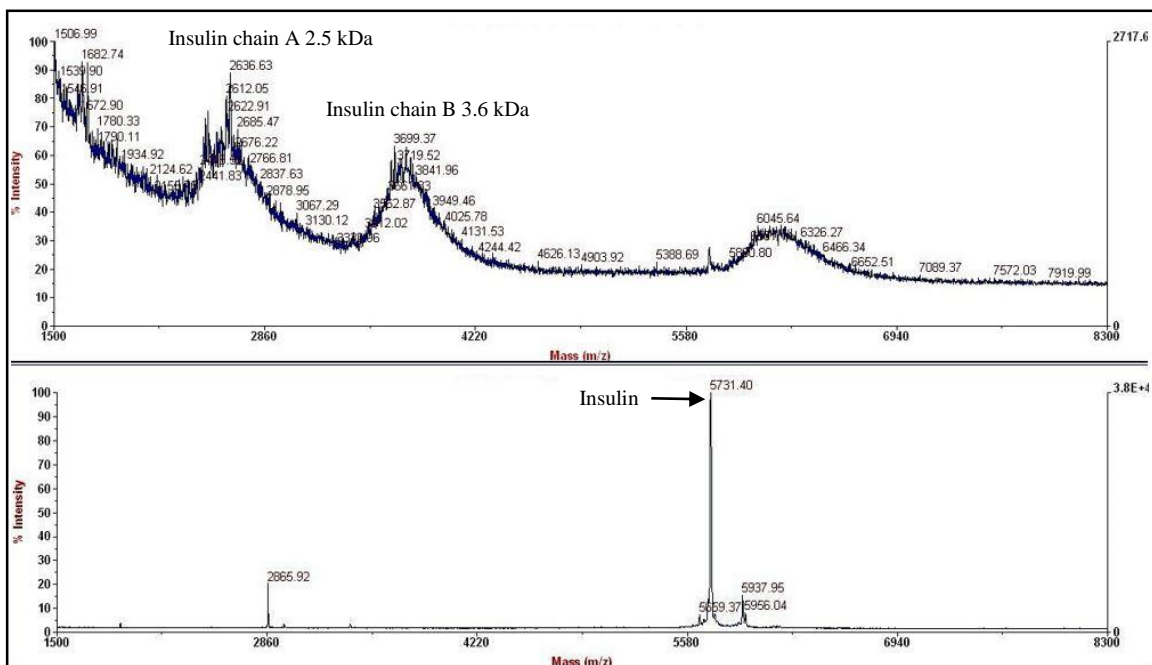


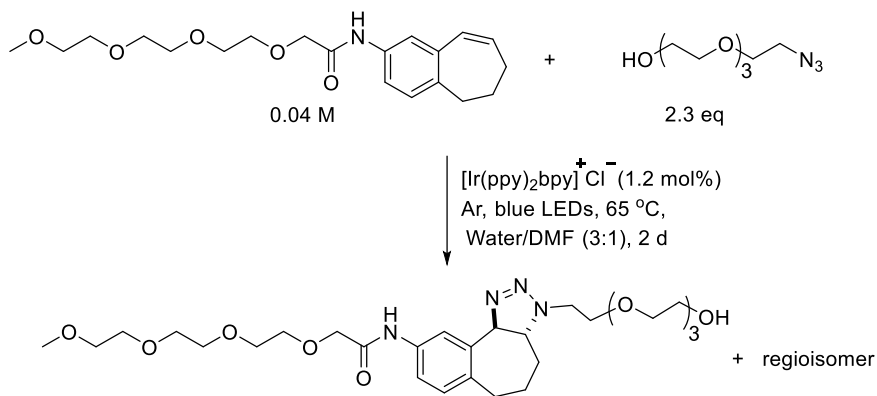
Figure 10a. Insulin stability experiment.

The use of DMF is necessary due to the low solubility of this particular photocatalyst in water, and it is expected that modifications to the structure of the photocatalyst can lead to increased aqueous solubility, which could eliminate this problem. As a side note, it may also lead to

diminished redox potentials, which could make it even more compatible with redox sensitive substrates. Furthermore, the photoconjugation is not necessarily limited to Ir-based photocatalysts. Recently, Gilmour has shown that riboflavin is also an effective photocatalyst for photoisomerization of alkenes, indicating that it might be possible to use the water soluble vitamin with the appropriate modifications to accomplish the photoconjugation.<sup>38</sup> We also attempted the [3+2] cycloaddition reaction utilizing riboflavin as a photocatalyst instead of **Cat. 3**. We did not observe the desired triazoline products and the starting alkene was recovered unreacted after 24 hours of irradiation time. One probable reason could be the lower triplet energy of riboflavin (50 kcal/mol) as compared to the **Cat. 3** (56.4 kcal/mol) which results in inefficient sensitization of alkene.

In an attempt to move towards more biocompatible conditions (*i.e.* mostly aqueous solvent), a reaction was performed with more water soluble catalyst [4-F Ir(ppy)<sub>2</sub>bpy]<sup>+</sup>PF<sub>6</sub><sup>-</sup> (1.0 mg of catalyst is completely miscible in 1.0 mL of 3:2 DMF/water, 1 ppm) as compared to **Cat 3** (1.0 mg of catalyst did not dissolve completely even in 100 mL of 3:2 DMF/water system). However, this catalyst has a lower triplet energy (51.4 kcal/mol vs. 56.4 kcal/mol) which was expected to decrease the overall efficiency of the reaction.<sup>39</sup> Indeed, when a more aqueous rich 3:2 DMF/water solvent system was used, the reaction produced the desired triazoline product **3a**, but required 9 hours of irradiation to reach completion, compared to the <1 h typical of the standard conditions. This result suggests designing a photocatalyst that is both more water soluble and emits at a higher energy, will allow this reaction to take place in water. On this point, the counter ions on the heteroleptic Ir complexes have significant effect on the solubilities of complexes. By changing the counter ion from PF<sub>6</sub><sup>-</sup> to Cl<sup>-</sup>, we were able to further increase the solubility of the catalyst [Ir(ppy)<sub>2</sub>bpy]<sup>+</sup>Cl<sup>-</sup> in water (1.1 mg of catalyst is completely miscible in 0.7 mL of 9:1 water/ DMF, 1.6 ppm). We also designed alkenes and azides so as to increase their solubility in water by attaching ethylene glycol linkers onto them. As a result, we were able to accommodate 3:1

water/DMF ratio without any of the reagents and catalyst precipitating out of the reaction mixture. When this reaction mixture was exposed to blue light, desired product was produced but the reaction took 2 days to reach completion (Scheme 19).



Scheme 19. Attempt to make bioconjugation conditions more water compatible.

As the water content increases in the reaction mixture, the photophysical properties of the catalyst change and a red shifting (i.e. longer wavelengths) of the emission, and lowering of the triplet energy, is observed. As a result, the sensitization of alkene by the photocatalyst becomes inefficient. While the rate decrease is undesirable, this result is promising in the sense that it does indicate that if we could design a catalyst that has appropriate triplet energy for energy transfer as well as greater water solubility, then we should be able to accomplish the reaction in water.

### 3.2. Single-crystal X-ray crystallography

The crystal structure of compound **3a** (major regoisomer) is shown below (Figure 11). For compound **3a**, crystals were grown by slow evaporation of the chloroform solvent. The crystals were then removed from the crystallization vial and immediately coated with non-drying immersion oil for microscopy (Type B, Formula Code: 1248) on a glass slide. A suitable crystal was mounted in oil on a MiTeGen loop and cooled to 100 K in a stream of cold N<sub>2</sub> using Bruker

Kryoflex low temperature device. X-ray diffraction data for all complexes were collected on a Bruker Smart APEX II diffractometer with a CCD detector using combinations of  $\varphi$  and  $\omega$  scans with Mo(K $\alpha$ ) radiation ( $\lambda = 0.71073 \text{ \AA}$ ). Unit cell determination and data collection were done using the APEX2 software package, while data integration employed the Bruker SAINT software package. Multi-scan absorption corrections were done by using SADABS. All structures were solved by direct methods and refined by full-matrix least-squares on  $F^2$  using the SHELXTL suite.

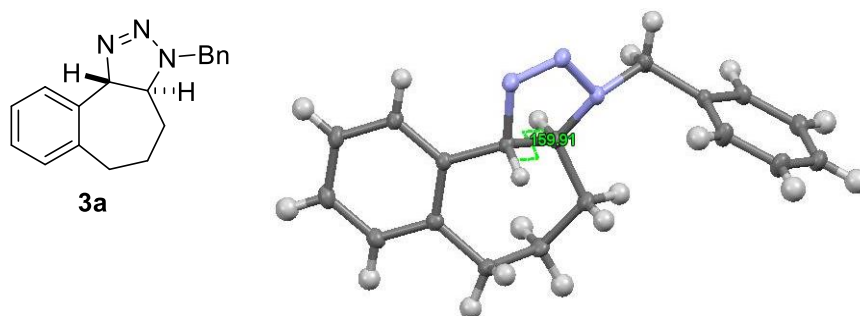
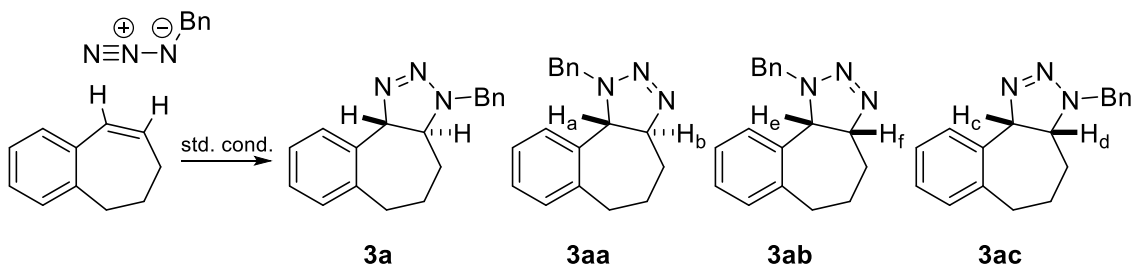


Figure 11. X-ray crystal structure of major regioisomer **3a**.

The non-hydrogen atoms were refined anisotropically and hydrogen atoms were placed geometrically and refined using the riding model. Images were generated by using ORTEP-3. CCDC 1525656 contains the crystallographic data. These data can be obtained free of charge from The Cambridge Crystallographic Data Centre via [www.ccdc.cam.ac.uk/data\\_request/cif](http://www.ccdc.cam.ac.uk/data_request/cif)

### 3.3. Determination of the regiochemistry and relative stereochemistry of the minor isomer



Generally, the photocatalytic cycloaddition produced two isomers as determined by NMR, a major (**3a** or **3ac**) and a minor isomer (**3aa** or **3ab**) whose relative amounts appear to have some dependence on the nature of the azide. The identity of the isomers formed in the reaction, both regio- and diastereomeric, was determined in the following manner. First, the identity of the major

isomer (**3a**), after isolation was determined from the crystal structure, which confirmed both the regioisomeric assignment and the *trans*-ring fusion. However, we were not able to obtain a crystal structure for the minor isomer. Thus, without making any assumptions we considered all the possibilities. This includes regioisomer **3aa** and its *syn* diastereomer **3ab**, and the *syn* diastereomer of **3a** (i.e. **3ac**). The relative configuration (i.e. *syn* vs. *anti*) (**3a** vs **3ac**) was established by the coupling constants of the methine protons ( $H_a$  and  $H_b$ ) on the ring junction in the  $^1\text{H}$  NMR. The protons on the respective carbons were assigned based on HSQC (Figure 12). The coupling constant between  $H_a$  and  $H_b$  was found to be 15.4 Hz suggestive of *trans* geometry between  $H_a$  and  $H_b$  protons.

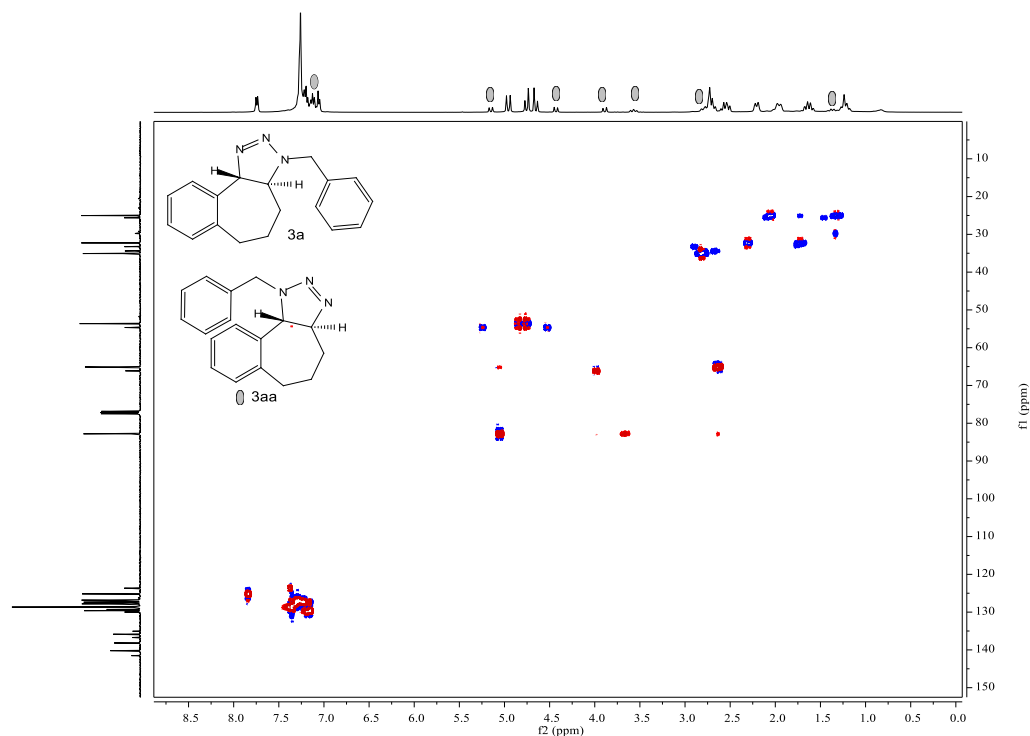


Figure 12. HSQC data for **3a**

In order to better anticipate the expected coupling constants, the geometries of all the potential isomers were calculated (Figure 13). The dihedral angle between  $H_a$  and  $H_b$  (in **3aa**) was found to be  $151.7^\circ$  after energy minimization using simple MM2 calculations. Whereas, when the

structure of regioisomer **3ab** and diastereomer **3ac** were minimized, the dihedral angle between H<sub>c</sub> and H<sub>d</sub> in case of **3ac** was found to be 49.8° and in the case of **3ab**, the dihedral angle between H<sub>e</sub> and H<sub>f</sub> was found to be 34.8°. According to the Karplus curve for ethane derivatives, the magnitude of the coupling constant observed (15.4 Hz) is consistent with a large dihedral angle (i.e. 151.7°) of **3aa**. Furthermore, the small dihedral angles calculated for **3ab** and **3ac** would be expected to give a very small coupling constant. Thus, the large (15.7 Hz) coupling constant observed by <sup>1</sup>H NMR, does not correspond to **3ab** or **3ac**. This corroborates that the minor product observed in the reaction is the *trans*, regioisomer, diastereomer **3aa**. Indicating that the reaction only takes place with the *trans*-**BC7** but that the regiochemistry (i.e. the orientation of the azide) can be unselective.

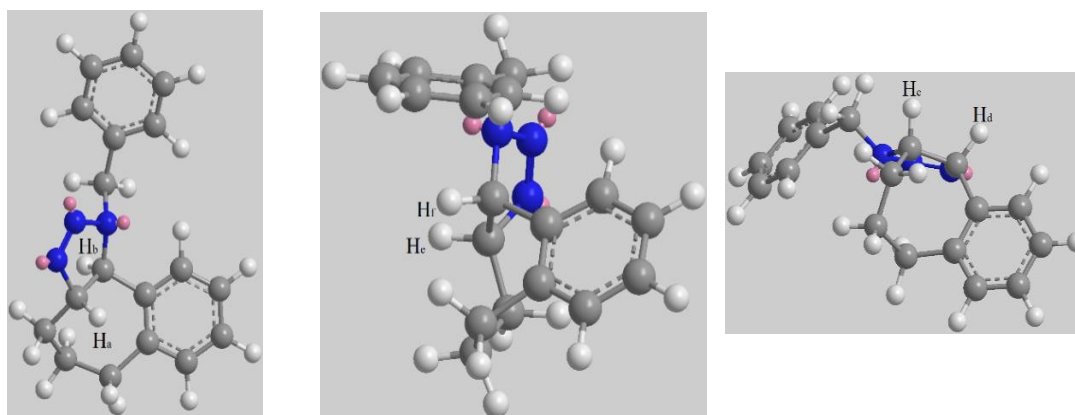


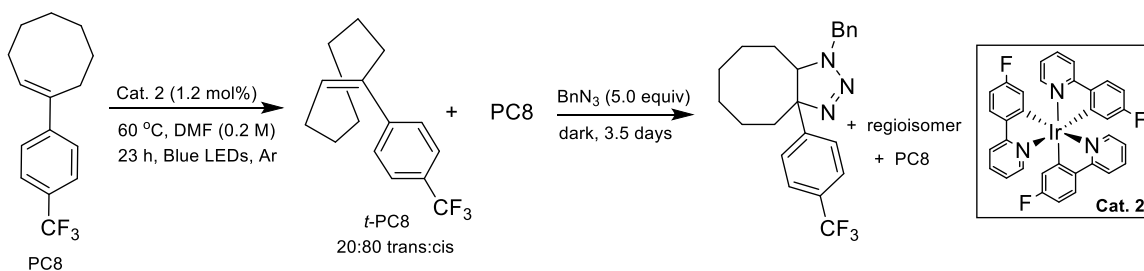
Figure 13. Minimized energy structure for minor regioisomer **3aa** or **3ab** and diastereomer **3ac**.

### 3.4. Investigation of the plausible reactive species in the reaction (triplet biradical versus strained *trans*-intermediate)

Based on the geometry of the products and the lack of reactivity of the relaxed alkene, we believe that the reaction is occurring through a high energy *trans*-singlet (i.e the strained alkene). However, it is not possible to completely rule out that electronically excited species are involved. To probe the nature of the reactive intermediate, an experiment was performed using phenyl cyclooctenes (**PC8**) as the substrate. Since *trans*-phenyl cyclooctene (*t*-**PC8**) can be formed to a

significant extent under the photocatalytic conditions, we opted to use **PC8** as a surrogate for the strained, singlet alkene. Thus, by first forming the strained alkene (*t*-**PC8**), and then turning off the lights, we could ensure the nature of the intermediate before adding the azide. While we still cannot completely rule out the possibility of reaction through a biradical, we have demonstrated the ability of the strained alkene to undergo cycloaddition.

An NMR tube was charged with **PC8** (15.3 mg, 0.06 mmol), **Cat. 2** (0.56 mg, 1.2 mol%), and DMF (0.2 M). The reaction mixture was degassed with Ar for 10 minutes and then the NMR tube was sealed with parafilm. The progress of reaction was monitored over time by <sup>1</sup>HNMR. After 23 hours, it appeared to have reached a photostationary state at 20% of the *t*-**PC8**. Then, after covering the tube with foil, effectively halting the production of excited species and more *t*-**PC8**, benzyl azide (40.0 mg, 0.30 mmol) was added to the NMR tube which was allowed to stand at rt for 3.5 days. The *t*-**PC8** slowly reacted with the benzyl azide to give the desired [3+2] cycloaddition product along with its regioisomer. The *cis*-**PC8** was still seen sitting unchanged in the reaction mixture. This outcome suggests that the ground state *trans*-alkene is a competent reaction partner, though it does not rule out the possibility of participation from other high energy intermediates in the reaction (Scheme 20). The slower reaction rates are not surprising given the significantly reduced amount of strain associated with *t*-**PC8** when compared to *t*-**BC7**.



Scheme 20. Trapping of *t*-**PC8** with benzyl azide

### 3.5 Summary

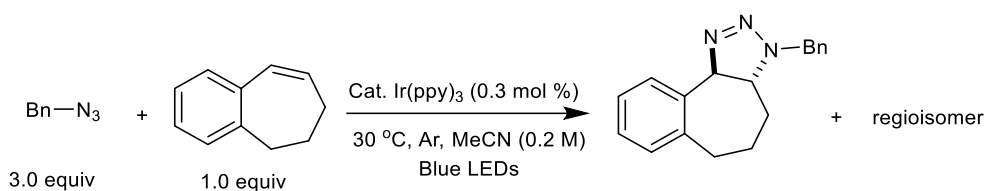
In conclusion, we have taken the idea of energy harvesting from concept to practice, providing conditions that allow kinetically and thermodynamically stable benzofused cycloheptene, *Z-BC7*, to undergo fast and chemoselective cycloaddition with substituted azides upon exposure to visible light. The reaction takes place under mild conditions that can be used to work with biological molecules. The operative mechanism involves energy transfer from a photocatalyst to *Z-BC7* which results in isomerization to an extremely strained and kinetically unstable alkene, *E-BC7*, meaning that no background reaction occurs in the absence of photocatalyst or light, and provides a strategy for temporal control that is simply not available to strain-promoted reactions. The designed relief mechanism of **BC7** is unique among photo-initiated processes. In contrast to others, it provides a steady-state concentration of highly reactive alkene throughout the duration of the reaction. The reaction tolerates a broad range of azides which give triazoline products. A unique aspect of this conjugation strategy is that the products can be conveniently and purposefully decomposed by the addition of weak acid sources, releasing the amine which corresponds to the azide. Finally, we have shown that the conjugation reaction can be performed on modified proteins such as insulin which are reasonably soluble and stable in organic solvents, in short reaction times, at biologically relevant concentrations, and temperatures. From initial synthetic concept to an applied tool ready for further development, this work presents a powerful and flexible strategy for complex chemical transformations via the conversion of photochemical energy to intramolecular ring strain, facilitating transformations even on challenging bimolecular systems.

### 3.6 Experimental Section

All reagents were obtained from commercial suppliers (Aldrich, VWR, TCI chemicals, Oakwood chemicals, Alfa Aesar) and used without further purification unless otherwise noted. *N,N*-dimethylformamide (DMF) was used from a solvent purification system. Some of the azides were purchased from Sigma Aldrich, while other azides were synthesized according to literature

procedures. 1-Benzosuberone was purchased from TCI chemicals and Sigma Aldrich. Biotin was purchased from Oakwood chemicals. 16.5% Mini-PROTEAN Tris-Tricine Gel, 10-well, 50  $\mu$ L, Tricine sample buffer, 10 x Tricine/SDS buffer, Coomassie blue stain and Precision Plus protein standard were purchased from BioRad. The tripeptide was purchased from Sigma Aldrich. Reactions were monitored by thin layer chromatography (TLC) which were obtained from Sorbent Technologies (Silica XHL TLC Plates w/UV254, glass backed 250  $\mu$ m, 20 x 20 cm), and were visualized with ultraviolet light, or potassium permanganate stain. Additionally, reactions were occasionally monitored by  $^1\text{H-NMR}$  (400 MHz Bruker Avance III spectrometer). Flash chromatography was carried out with Acros Organics 60  $\text{\AA}$ , 50-200 micron basic alumina on an automated combiflash R<sub>f</sub> version 2.1.19 equipped with UV and ELS detectors. NMR spectra were obtained on 400 MHz Bruker Avance III spectrometer or 400 MHz Unity Inova spectrometer or 600 MHz Unity Inova spectrometer unless otherwise noted.  $^1\text{H}$  and  $^{13}\text{C}$  NMR chemical shifts are reported in ppm relative to the residual protio solvent peak ( $^1\text{H}$ ,  $^{13}\text{C}$ ). High resolution mass spectra (HRMS) analysis was performed on a LTQ-OrbitrapXL by Thermo Scientific Ltd. or Applied Biosystems Voyager MALDI-TOF.

### 3.61 Optimization Studies

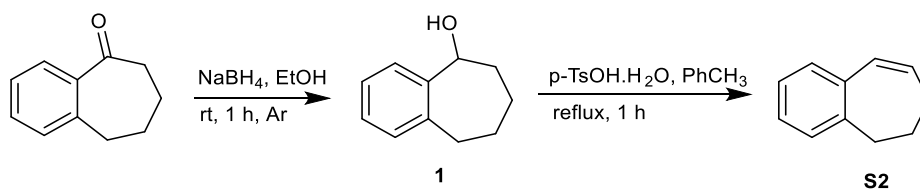


Entry	Modification from original	Completion time <sup>a</sup>
1	None	21 h
2	Azide as limiting and 3.0 equiv of alkene	7 h
3 <sup>b</sup>	DMF as solvent	3 h
4 <sup>b</sup>	1.2 mol% Cat. Ir(ppy) <sub>3</sub>	2 h
5 <sup>b</sup>	Cat. 3 instead of Ir(ppy) <sub>3</sub>	2.5 h
6 <sup>b</sup>	1.2 mol% Cat. 3	2 h
7 <sup>b</sup>	Entry 6 but in air	2.5 h
8 <sup>b</sup>	1.2 mol% Cat. 3 at 60 °C	45 min
9 <sup>b</sup>	Same as entry 8 but with 4:1 DMF/water	25 min
10 <sup>b</sup>	No Ir(ppy) <sub>3</sub>	nr
11 <sup>b</sup>	No blue LEDs	nr

<sup>a</sup>based on <sup>1</sup>H NMR. <sup>b</sup>Azide is limiting and alkene is 3.0 equiv. nr = no reaction

Table 5. Optimization of reaction conditions

### 3.62. Synthesis of 6,7-dihydro-5H-benzo[7]annulene (S2)



To a flame-dried, round-bottomed flask equipped with a magnetic stir bar was added 1-benzosuberone (2.0 g, 12.48 mmol), and EtOH (0.25 M). NaBH<sub>4</sub> (567.7 mg, 14.98 mmol) was then added to the reaction mixture portion-wise under an Ar atmosphere, and the reaction mixture was stirred at room temperature for 1 hour. The reaction mixture was then quenched with 1N HCl (15 mL). The solvent was then removed under reduced pressure. The crude material thus obtained was diluted with CH<sub>2</sub>Cl<sub>2</sub> (50 mL) and washed with water (2 x 10 mL). The organic layer was separated, dried over MgSO<sub>4</sub>, and concentrated to yield a white solid, **1**, (2.0 g, 98%) which was used without further purification.

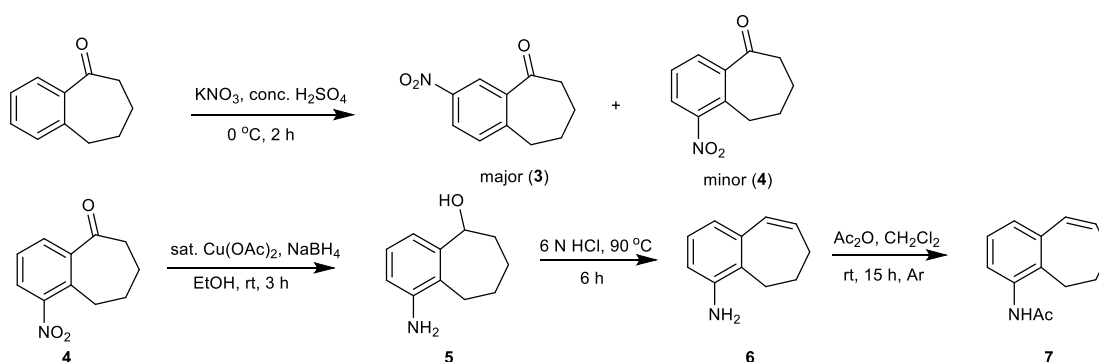
To a flame-dried, round-bottomed flask equipped with a magnetic stir bar, was added alcohol **1** (2.0 g, 12.32 mmol), toluene (30 mL), and *p*-toluenesulfonic acid monohydrate (234.4 mg, 1.24 mmol). The reaction mixture was refluxed for 1 hour. After reaction completion

(monitored by TLC), sat. NaHCO<sub>3</sub> (100 mL) was added, the resulting mixture was extracted with ethyl acetate EtOAc (2 x 100 mL). The combined organic layer was washed with brine (100 mL), dried over MgSO<sub>4</sub>, and concentrated to give a colorless liquid **S2** (1.5 g, 87%), which was used without further purification.

### 3.63. Synthesis of *N*-(6,7-dihydro-5*H*-benzo[7]annulen-4-yl)acetamide (**7**)

#### Nitration of 1-benzosuberone<sup>40</sup>

To a round-bottomed flask equipped, with a magnetic stir bar was added 1-benzosuberone (1.0 g, 6.25 mmol) and conc. H<sub>2</sub>SO<sub>4</sub> (15.5 mL) and the mixture was cooled to 0 °C. To this cooled solution was added a solution of KNO<sub>3</sub> (695.5 mg, 6.88 mmol) in conc. H<sub>2</sub>SO<sub>4</sub> (3.1 mL), dropwise. The reaction mixture was stirred at 0 °C for 2 hours. The mixture was then poured into ice/water (150 mL), and stirred for another 30 min. The aqueous layer was then extracted with EtOAc (250 mL). The organic layer was washed with brine (100 mL), dried over MgSO<sub>4</sub>, and concentrated under reduced pressure. The crude product obtained was then purified by column chromatography on silica gel (EtOAc/hexanes = 5:95) to afford both the isomers [major isomer (**3**) (820 mg, 64%) and minor isomer (**4**) (210 mg, 16%)].



#### Synthesis of alcohol **5**<sup>41</sup>

To a flame-dried, round-bottomed flask equipped with a magnetic stir bar was added **4** (210 mg, 1.02 mmol), and EtOH (11.3 mL). To this solution was added a saturated solution of

copper (II) acetate (4.2 mL), and then NaBH<sub>4</sub> (426.4 mg, 11.26 mmol) was added portion wise. The reaction mixture was stirred at room temperature for 3 hours. Brine (10 mL) was added and ethanol was removed under reduced pressure. The black residue, thus obtained, was diluted with EtOAc (100 mL), washed with brine (50 mL), and sat. NaHCO<sub>3</sub> (50 mL). The organic layer was dried over MgSO<sub>4</sub> and concentrated under vacuum to obtain **5**, as a light brown solid (162.9 mg, 90%), which was used without further purification.

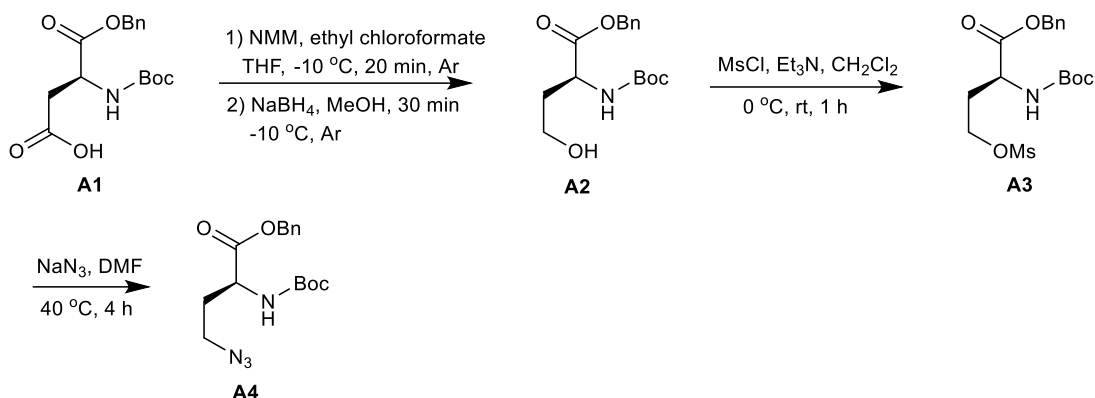
### **Synthesis of alkene 6**

To a round-bottomed flask equipped with a magnetic stir bar was added **5** (120 mg, 0.68 mmol) and 6 N HCl (3.8 mL). The reaction mixture was heated to 90 °C for 6 hours. After cooling, the reaction mixture was neutralized with 1 M NaOH solution, and the aqueous layer was extracted with EtOAc (3 x 30 mL). The combined organic layer was dried over MgSO<sub>4</sub> and concentrated to afford **6** (100 mg, 92%), which was used without further purification.

### **Acylation of alkene 6**

To a flame-dried, round-bottomed flask equipped with a magnetic stir bar was added alkene **6** (100 mg, 0.62 mmol), dry CH<sub>2</sub>Cl<sub>2</sub> (0.1 M), and acetic anhydride (75.5 mg, 0.74 mmol), under an Ar atmosphere. The reaction mixture was stirred at room temperature for 16 hours. Sat. sodium carbonate (10 mL) was added and the layers were separated. The organic layer was dried over MgSO<sub>4</sub> and concentrated under vacuum to deliver **7** (115 mg, 92%), which was used without further purification.

### **3.64. Synthesis of Azidohomoalanine A4<sup>42</sup>**



### Synthesis of alcohol A2

To a flame-dried, three necked, round-bottomed flask equipped with a magnetic stir bar was added **A1** (1.0 g, 3.09 mmol) and tetrahydrofuran (THF) (11.9 mL), under an Ar atmosphere. The solution was cooled to -10 °C and 4-methylmorpholine (312.6 mg, 3.09 mmol) was added and the solution was stirred for 15 min. Ethyl chloroformate (335.3 mg, 3.09 mmol) was then added dropwise over 10 min and the reaction mixture was stirred for an additional 20 min, at the same temperature. Subsequently, under a flow of Ar, NaBH<sub>4</sub> (700 mg, 18.54 mmol) was added in one portion. Then, MeOH (30 mL) was added at a rate such that the temperature of the reaction mixture did not rise above -8 °C. The reaction mixture was stirred at -10 °C for further 30 min. Then 1M HCl (10 mL) was added slowly, and the mixture was allowed to warm to rt. The solvent was removed under reduced pressure. The aqueous solution left behind was extracted with EtOAc (3 x 40 mL). The combined organic layers were dried over MgSO<sub>4</sub>, and concentrated to give the crude product which was purified by column chromatography on silica gel (MeOH/CH<sub>2</sub>Cl<sub>2</sub> = 3:97) to yield the alcohol **A2** (830 mg, 87%)

### Mesylation of alcohol A2

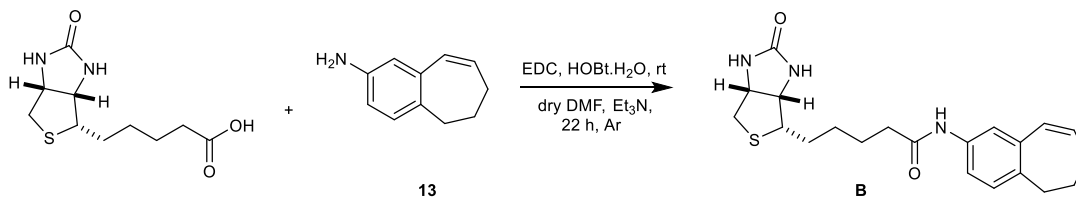
To a flame-dried, round-bottomed flask equipped with a magnetic stir bar was added alcohol **A2** (830 mg, 2.68 mmol), dry CH<sub>2</sub>Cl<sub>2</sub> (20.6 mL), and triethylamine (650.7 mg, 6.43 mmol) under an Ar atmosphere, and the reaction mixture was cooled to 0 °C. Methanesulfonyl chloride

(368.9 mg, 3.22 mmol) was added dropwise to the reaction mixture. The ice bath was removed, and the resulting solution was stirred at room temperature for 1 hour. Sat.  $\text{NH}_4\text{Cl}$  (20 mL) was added and the layers were separated. The organic layer was washed with brine (2 x 30 mL). The combined aqueous layers were extracted with  $\text{CH}_2\text{Cl}_2$  (2 x 30 mL), and the combined organic layers were dried over  $\text{MgSO}_4$ , and concentrated under vacuum to obtain the mesylate **A3** (1.0 g, 96%), which was used without further purification.

### Azidation of A3

To a flame-dried, round-bottomed flask equipped with a magnetic stir bar was added **A3** (1.0 g, 2.58 mmol) and dry DMF (0.3 M) under an Ar atmosphere. To this solution, was added sodium azide (251.6 mg, 3.87 mmol), and the reaction mixture was heated at 40 °C, for 4 hours. Water (5 mL) was added, and the resulting mixture was extracted with EtOAc (2 x 20 mL). The combined organic layers were washed with water (3 x 10 mL), and then brine (10 mL). The organic layer was then dried over  $\text{MgSO}_4$ , and concentrated under vacuum to afford the crude product, which was purified by column chromatography on silica gel (EtOAc/hexanes = 8:92) to yield a colorless oil **A4** (560 mg, 75%).

### 3.65. Synthesis of Biotinylated amide **B**<sup>43</sup>

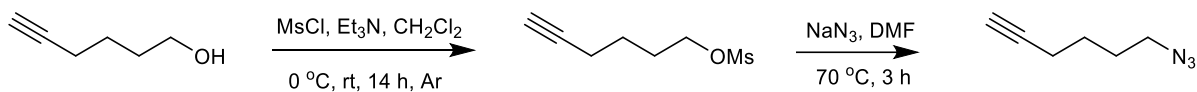


To a flame-dried, round-bottomed flask equipped with a magnetic stir bar was added biotin (831.6 mg, 3.41 mmol), 1-ethyl-3-(3-dimethylaminopropyl)carbodiimide (780 mg, 4.07 mmol), hydroxybenzotriazole monohydrate (627.2 mg, 4.07 mmol), triethylamine (652.7 mg, 6.45 mmol), alkene **13** (550 mg, 3.41 mmol), and dry DMF (0.1 M), under an Ar atmosphere. The reaction mixture was stirred at room temperature for 22 hours. The reaction mixture was poured into water

(50 mL) and the resulting precipitate was collected by filtration. The crude solid was further purified by column chromatography on silica gel (MeOH/CH<sub>2</sub>Cl<sub>2</sub> = 6:94) to afford biotinylated amide **B** (750 mg, 57%).

Alkene **13** was prepared from **3** following similar procedure that was used to synthesize alkene **6** from **4**

### 3.66. Synthesis of 6-azidohex-1-yne<sup>44</sup>



#### Synthesis of hex-5-yn-1-yl methanesulfonate

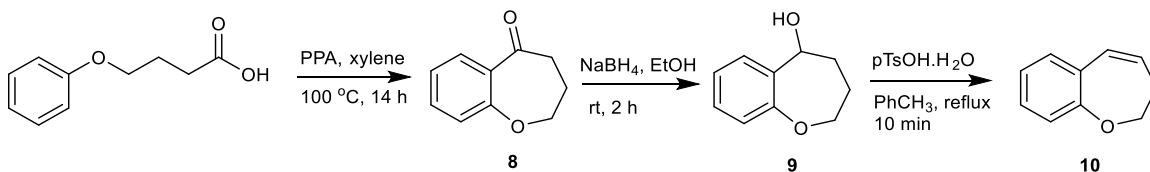
To a flame-dried, round-bottomed flask equipped with a magnetic stir bar was added hex-5-yn-1-ol (500 mg, 5.09 mmol), dry CH<sub>2</sub>Cl<sub>2</sub> (50 mL), and triethylamine (618.3 mg, 6.11 mmol). The reaction mixture was cooled to 0 °C, and methanesulfonyl chloride (641.9 mg, 5.60 mmol) was added dropwise under argon. The reaction mixture was then allowed to warm to room temperature and stirred for 14 hours. The reaction was quenched by slow addition of 0.05 M HCl (20 mL) and the layers were separated. The organic layer was washed with sat. NaHCO<sub>3</sub> (20 mL), dried over MgSO<sub>4</sub>, and concentrated under vacuum to afford a pale yellow liquid (881.2 mg, 98%), which was used further without purification.

#### Synthesis of 6-azidohex-1-yne

To a flame-dried, round-bottomed flask equipped with a magnetic stir bar was added hex-5-yn-1-yl methanesulfonate (881.2 mg, 5.0 mmol), dry DMF (15 mL), and sodium azide (812.9 mg, 12.5 mmol), under an Ar atmosphere. The reaction mixture was then heated to 70 °C for 3 hours. Then, after cooling, water (20 mL) was added, and the reaction mixture was extracted with diethyl ether (3 x 20 mL). The combined organic layers were dried over MgSO<sub>4</sub>, and concentrated

under vacuum to yield a pale yellow liquid (400 mg, 65%), which was used without further purification.

### 3.67. Synthesis of 2,3-dihydrobenzo[b]oxepine<sup>45</sup>



#### Synthesis of ketone **8**

To a stirred solution of polyphosphoric acid (6.06 g) in xylene (15 mL), was added a solution of 4-phenoxybutyric acid (1.81 g, 10.0 mmol) in xylene (10 mL). After stirring for 14 h, the reaction mixture was allowed to cool to room temperature and diluted with cold water. The organic layer was separated, washed with water (20 mL), brine (20 mL), dried over MgSO<sub>4</sub>, and concentrated under reduced pressure. The resulting residue was purified by column chromatography (hexane/ethyl acetate = 95:5) to give **8** (480.0 mg, 30%) as a pale yellow oil.

#### Synthesis of alcohol **9**

To a flame-dried round-bottomed flask equipped with a magnetic stir bar was added **8** (480 mg, 2.96 mmol) and EtOH (9.9 mL). To this solution was added NaBH<sub>4</sub> (168.1 mg, 4.44 mmol) portion-wise. The reaction mixture was stirred at room temperature for 2 hours. The reaction was quenched with sat. NH<sub>4</sub>Cl (20 mL). The solvent was then removed under reduced pressure. The crude material was diluted with CH<sub>2</sub>Cl<sub>2</sub> (50 mL), and washed with water (2 x 10 mL). The organic layer was dried over MgSO<sub>4</sub> and concentrated to afford a crude product that was purified by column chromatography (CH<sub>2</sub>Cl<sub>2</sub>) to give **9** (280 mg, 58%) as an off-white solid.

#### Synthesis of alkene **10**

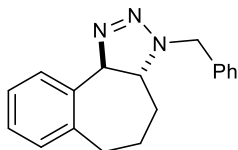
To a flame-dried, round-bottomed flask equipped with a magnetic stir bar was added alcohol **1** (280 mg, 1.71 mmol), toluene (10.0 mL), and *p*-toluenesulfonic acid monohydrate (32.5 mg, 0.17 mmol) and the reaction mixture was refluxed for 10 minutes. When the reaction was complete (by TLC), sat. NaHCO<sub>3</sub> (20 mL) was added, and the resulting mixture was extracted with ethyl acetate (2 x 20 mL). The combined organic layer was washed with brine (10 mL), dried over MgSO<sub>4</sub>, and concentrated to deliver a colorless liquid **10** (230 mg, 93%), which was used further without purification.

### 3.68. General procedure A for the synthesis of triazolines

An NMR tube was charged with a solution of azide (1.0 equiv), alkene **S2** (3.0 equiv), **Cat. 3** (1.2 mol%) in DMF (0.2 M), and a sealed capillary containing deuterated benzene. The tube was capped with a rubber septum and the reaction mixture was degassed with argon bubbling for 10-15 minutes. The tubes were then sealed with parafilm and placed in the light bath. The progress of the reaction was monitored by <sup>1</sup>H NMR. To minimize unintentional reaction, the tube was quickly covered with aluminum foil after removing from the light bath and kept in the dark until being placed in the NMR instrument. After completion of the reaction, the mixture was diluted with EtOAc and washed with water. The organic layer was dried over MgSO<sub>4</sub> and concentrated to obtain the crude product that was purified by normal phase chromatography. Normal phase chromatography was performed with a Teledyne ISCO automated chromatography system using basic alumina as the stationary phase and either EtOAc/hexanes or MeOH/CH<sub>2</sub>Cl<sub>2</sub> as mobile phase unless otherwise noted.

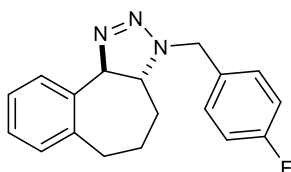
**((3aR,10bR)-3-benzyl-3,3a,4,5,6,10b-hexahydrobenzo[3,4]cyclohepta[1,2-d][1,2,3]triazole)**

**(3a)**



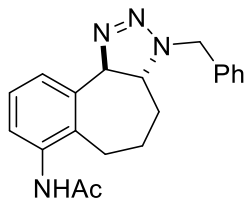
The general procedure **A** was followed using benzyl azide (32 mg, 0.24 mmol), alkene **S2** (104 mg, 0.72 mmol), **Cat. 3** (2.4 mg, 1.2 mol%) and DMF (3.6 mL) to afford **3a** in 77% yield (51 mg, 0.18 mmol) as a colorless oil with rr = 3.2:1 (crude rr = 2.6:1). The substrate was purified by column chromatography on basic alumina (EtOAc/hexanes = 6:94). <sup>1</sup>H NMR (400 MHz, CDCl<sub>3</sub>) δ 7.74 (d, *J* = 7.4 Hz, 1H), 7.27 (appr s, 2H), 7.24 – 7.16 (m, 3H), 7.16 – 7.09 (m, 2H), 7.07 (t, *J* = 7.3 Hz, 1H), 4.96 (d, *J* = 16.3 Hz, 1H), 4.76 (d, *J* = 15.1 Hz, 1H), 4.66 (d, *J* = 15.1 Hz, 1H), 2.85 – 2.62 (m, 2H), 2.62 – 2.46 (m, 1H), 2.20 (d, *J* = 12.8 Hz, 1H), 1.96 (d, *J* = 15.9 Hz, 1H), 1.71 – 1.54 (m, 1H), 1.30 – 1.12 (m, 1H); <sup>13</sup>C NMR (101 MHz, CDCl<sub>3</sub>) δ 140.2, 138.1, 135.8, 129.6, 128.6, 128.5, 127.8, 127.3, 126.8, 125.1, 82.8, 65.1, 53.6, 35.0, 32.2, 25.0; HRMS (*m/z*): [M+H]<sup>+</sup> calcd. for C<sub>18</sub>H<sub>19</sub>N<sub>3</sub>, 278.1652; observed, 278.1647.

**((3aR,10bR)-3-(4-fluorobenzyl)-3,3a,4,5,6,10b-hexahydrobenzo[3,4]cyclohepta[1,2-d][1,2,3]triazole) (3b)**



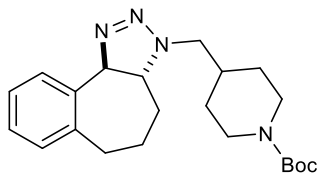
The general procedure **A** was followed using 1-(azidomethyl)-4-fluorobenzene (27.2 mg, 0.18 mmol), alkene **S2** (77.9 mg, 0.54 mmol), **Cat. 3** (1.8 mg, 1.2 mol%) and DMF/water = 4:1 (0.9 mL) to afford **3b** in 83% yield (44.6 mg, 0.15 mmol) as a colorless oil with rr = 3.8:1 (crude rr = 2.6:1). The substrate was purified by column chromatography on basic alumina (EtOAc/hexanes = 2:98). <sup>1</sup>H NMR (400 MHz, CDCl<sub>3</sub>) δ 7.80 (d, *J* = 7.4 Hz, 1H), 7.34 – 7.25 (m, 3H), 7.25 – 7.17 (m, 1H), 7.14 (d, *J* = 7.3 Hz, 1H), 7.06 – 6.94 (m, 2H), 5.04 (d, *J* = 16.2 Hz, 1H), 4.78 (d, *J* = 15.1 Hz, 1H), 4.69 (d, *J* = 15.1 Hz, 1H), 2.90 – 2.73 (m, 2H), 2.59 (ddd, *J* = 14.9, 11.1, 2.9 Hz, 1H), 2.34 – 2.18 (m, 1H), 2.15 – 1.98 (m, 1H), 1.81 – 1.61 (m, 1H), 1.39 – 1.20 (m, 1H); <sup>13</sup>C NMR (101 MHz, CDCl<sub>3</sub>) δ 162.4 (d, *J* = 246.2 Hz), 140.2, 138.1, 131.6 (d, *J* = 3.2 Hz), 130.2 (d, *J* = 8.1 Hz), 129.7, 127.5, 126.9, 125.2, 115.6 (d, *J* = 21.5 Hz), 82.9, 65.2, 52.9, 35.1, 32.3, 25.1; <sup>19</sup>F NMR (376 MHz, CDCl<sub>3</sub>) δ -114.40 – -114.70 (m).

**(*N*-((3*aR*,10*bR*)-3-benzyl-3,3*a*,4,5,6,10*b*-hexahydrobenzo[3,4]cyclohepta[1,2-*d*][1,2,3]triazol-7-yl)acetamide) (3c)**



The general procedure **A** was followed using benzyl azide (26.6 mg, 0.20 mmol), *N*-(6,7-dihydro-5*H*-benzo[7]annulen-4-yl)acetamide (120.8 mg, 0.60 mmol), **Cat. 3** (2.1 mg, 1.2 mol%) and DMF (1.8 mL) to afford **3c** in 90% yield (60.2 mg, 0.18 mmol) as a colorless oil with *rr* = 5.3:1 (crude *rr* = 5.3:1). The substrate was purified by column chromatography on basic alumina (EtOAc/hexanes = 30:70). <sup>1</sup>H NMR (400 MHz, CDCl<sub>3</sub>) δ 7.66 (d, *J* = 6.8 Hz, 1H), 7.28 (s, 5H), 7.22 – 7.07 (m, 2H), 4.98 (d, *J* = 16.3 Hz, 1H), 4.77 (d, *J* = 15.1 Hz, 1H), 4.68 (d, *J* = 15.1 Hz, 1H), 3.05 – 2.89 (m, 1H), 2.68 – 2.49 (m, 1H), 2.45 – 2.29 (m, 1H), 2.17 (s, 3H), 2.00 – 1.87 (m, 1H), 1.76 – 1.62 (m, 1H), 1.39 – 1.25 (m, 1H); <sup>13</sup>C NMR (101 MHz, CDCl<sub>3</sub>) δ 169.3, 139.7, 136.1, 135.8, 134.4, 128.8, 128.6, 127.9, 127.2, 125.9, 124.2, 82.70, 64.9, 53.7, 32.5, 27.7, 24.1, 23.8; HRMS (*m/z*): [M+Na]<sup>+</sup> calcd. for C<sub>20</sub>H<sub>22</sub>N<sub>4</sub>O, 357.1686; observed, 357.1680.

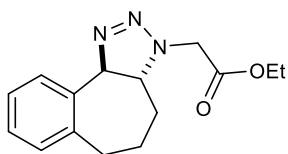
**(*tert*-butyl 4-(((3*aR*,10*bR*)-4,5,6,10*b*-tetrahydrobenzo[3,4]cyclohepta[1,2-*d*][1,2,3]triazol-3(3*aH*)-yl)methyl)piperidine-1-carboxylate) (3d)**



The general procedure **A** was followed using *tert*-butyl 4-(azidomethyl)piperidine-1-carboxylate (57.6 mg, 0.24 mmol), alkene **S2** (103.8 mg, 0.72 mmol), **Cat. 3** (2.4 mg, 1.2 mol%) and DMF (1.2 mL) to afford **3d** in 87% yield (80.0 mg, 0.21 mmol) as a colorless oil with *rr* = 3.2:1 (crude *rr* = 2.3:1). The substrate was purified by column chromatography on basic alumina (EtOAc/hexanes = 4:96). <sup>1</sup>H NMR (400 MHz, CDCl<sub>3</sub>) δ 7.77 (d, *J* = 7.4 Hz, 1H), 7.34 – 6.97 (m, 3H), 4.91 (d, *J* = 16.2 Hz, 1H), 4.11 (appr s, 2H), 3.40 (dd, *J* = 5.4 Hz, 1H), 3.01 – 2.85 (m, 1H), 2.84 – 2.74 (m, 2H), 2.73 – 2.56 (m, 3H), 2.50 – 2.24 (m, 1H), 2.16 – 2.04 (m, 1H), 2.03 – 1.91 (m, 1H), 1.88 – 1.75 (m, 1H), 1.75 – 1.62 (m, 2H), 1.43 (s, 9H), 1.41 – 1.28 (m, 1H), 1.27 – 1.18 (m, 1H), 1.19 – 1.07 (m, 1H); <sup>13</sup>C NMR (101 MHz, CDCl<sub>3</sub>) δ 154.9, 140.2, 138.3, 129.8, 127.5, 126.9, 125.2, 82.4,

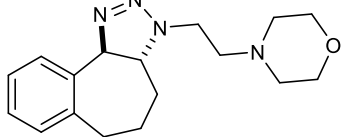
79.5, 67.0, 57.5, 55.12, 43.7, 35.2, 32.7, 30.3, 28.6, 25.2; HRMS (m/z):  $[M+Na]^+$  calcd. for  $C_{22}H_{32}N_4O_2$ , 407.2417; observed, 407.2403.

**(Ethyl 2-((3aR,10bR)-4,5,6,10b-tetrahydrobenzo[3,4]cyclohepta[1,2-d][1,2,3]triazol-3(3aH)-yl)acetate) (3e)**



The general procedure **A** was followed using ethyl 2-azidoacetate (46.2 mg, 0.36 mmol), alkene **S2** (156.0 mg, 1.08 mmol), **Cat. 3** (3.6 mg, 1.2 mol%) and DMF (1.8 mL) to afford **3e** in 72% yield (71.5 mg, 0.26 mmol) as a colorless oil with rr = 6.7:1 (crude rr = 3:1). The substrate was purified by column chromatography on basic alumina (EtOAc/hexanes = 2:98).  $^1H$  NMR (400 MHz,  $CDCl_3$ )  $\delta$  7.80 (d,  $J = 7.5$  Hz, 1H), 7.31 – 7.24 (m, 1H), 7.22 – 7.17 (m, 1H), 7.13 (d,  $J = 7.4$  Hz, 1H), 5.06 (d,  $J = 16.0$  Hz, 1H), 4.40 (d,  $J = 17.8$  Hz, 1H), 4.24 (d,  $J = 17.7$  Hz, 1H), 4.17 (q,  $J = 7.1$  Hz, 2H), 3.03 – 2.92 (m, 1H), 2.85 – 2.76 (m, 2H), 2.41 – 2.30 (m, 1H), 2.15 – 2.04 (m, 1H), 1.77 (qd,  $J = 13.0, 3.6$  Hz, 1H), 1.45 – 1.34 (m, 1H), 1.25 (t,  $J = 7.1$  Hz, 3H);  $^{13}C$  NMR (101 MHz,  $CDCl_3$ )  $\delta$  169.0, 140.1, 137.98, 129.7, 127.5, 127.0, 125.1, 83.6, 65.4, 61.3, 49.8, 35.1, 32.1, 25.1, 14.2. HRMS (m/z):  $[M+H]^+$  calcd. for  $C_{18}H_{19}N_3$ , 274.1550; observed, 274.1545.

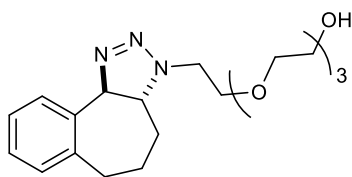
**(4-(2-((3aR,10bR)-4,5,6,10b-tetrahydrobenzo[3,4]cyclohepta[1,2-d][1,2,3]triazol-3(3aH)-yl)ethyl)morpholine) (3f)**



The general procedure **A** was followed using 4-(2-azidoethyl)morpholine (37.6 mg, 0.24 mmol), alkene **S2** (103.8 mg, 0.72 mmol), **Cat. 3** (2.4 mg, 1.2 mol%) and DMF/water = 4:1 (1.2 mL) to afford **3f** in 75% yield (54.1 mg, 0.18 mmol) as a colorless oil with rr = 4.6:1 (crude rr = 3.8:1). The substrate was purified by column chromatography on basic alumina (EtOAc/hexanes = 6:94).  $^1H$  NMR (400 MHz,  $CDCl_3$ )  $\delta$  7.77 (d,  $J = 7.3$  Hz, 1H), 7.25 – 7.20 (m, 1H), 7.20 – 7.14 (m, 1H), 7.11 (d,  $J = 6.9$  Hz, 1H), 4.93 (d,  $J = 16.2$  Hz, 1H), 3.65 (t,  $J = 4.0$  Hz, 4H), 3.59 – 3.42

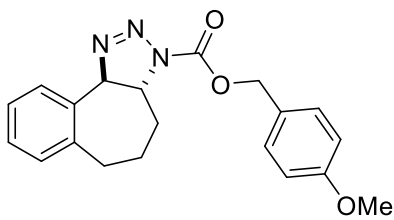
(m, 2H), 3.01 – 2.81 (m, 1H), 2.83 – 2.72 (m, 2H), 2.72 – 2.60 (m, 2H), 2.55 – 2.44 (m, 4H), 2.40 – 2.32 (m, 1H), 2.15 – 1.98 (m, 1H), 1.78 – 1.62 (m, 1H), 1.45 – 1.30 (m, 1H); <sup>13</sup>C NMR (101 MHz, CDCl<sub>3</sub>) δ 140.2, 138.4, 129.7, 127.5, 127.0, 125.2, 82.6, 67.1, 66.3, 56.5, 53.9, 46.3, 35.2, 32.6, 25.3; HRMS (m/z): [M+Na]<sup>+</sup> calcd. for C<sub>17</sub>H<sub>24</sub>N<sub>4</sub>O, 323.1842; observed, 323.1825.

**(2-(2-(2-(2-((3aR,10bR)-4,5,6,10b-tetrahydrobenzo[3,4]cyclohepta[1,2-d][1,2,3]triazol-3(3aH)-yl)ethoxy)ethoxy)ethoxy)ethan-1-ol) (3g)**



The general procedure **A** was followed using 2-(2-(2-(2-azidoethoxy)ethoxy)ethoxy)ethan-1-ol (79.2 mg, 0.36 mmol), alkene **S2** (155.7 mg, 1.08 mmol), **Cat. 3** (3.6 mg, 1.2 mol%) and DMF (1.8 mL) to afford **3g** in 86% yield (112.6 mg, 0.31 mmol) as a colorless oil with rr = 3:1 (crude rr = 3:1). The substrate was purified by column chromatography on basic alumina (EtOAc/hexanes = 1:99). <sup>1</sup>H NMR (400 MHz, CDCl<sub>3</sub>) δ 7.72 (d, *J* = 7.4 Hz, 1H), 7.23 – 7.14 (m, 1H), 7.15 – 7.09 (m, 1H), 7.06 (d, *J* = 7.2 Hz, 1H), 4.88 (d, *J* = 16.4 Hz, 1H), 4.05 – 3.79 (m, 1H), 3.79 – 3.67 (m, 2H), 3.65 – 3.44 (m, 15H), 2.90 – 2.65 (m, 2H), 2.65 – 2.50 (m, 1H), 2.48 – 2.32 (m, 1H), 2.15 – 1.90 (m, 1H), 1.66 (q, *J* = 13.0 Hz, 1H), 1.42 – 1.23 (m, 1H); <sup>13</sup>C NMR (101 MHz, CDCl<sub>3</sub>) δ 140.3, 138.3, 129.7, 127.4, 126.9, 125.2, 82.6, 72.6, 70.7, 70.6, 70.5, 70.4, 69.3, 66.5, 61.8, 48.8, 35.2, 32.3, 25.2; HRMS (m/z): [M+Na]<sup>+</sup> calcd. for C<sub>19</sub>H<sub>29</sub>N<sub>3</sub>O<sub>4</sub>, 386.2050; observed, 386.2035.

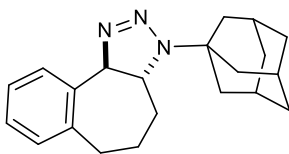
**(4-methoxybenzyl (3aR,10bR)-4,5,6,10b-tetrahydrobenzo[3,4]cyclohepta[1,2-d][1,2,3]triazole-3(3aH)-carboxylate) (3h)**



The general procedure **A** was followed using 4-methoxybenzyl carbonazidate (49.6 mg, 0.24 mmol), alkene **S2** (103.8 mg, 0.72 mmol), **Cat. 3** (2.4 mg, 1.2 mol%) and DMF (1.2 mL) to afford **3h** in 42% yield (35.3 mg, 0.10 mmol) as a colorless oil as a

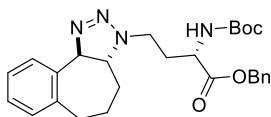
single regioisomer (crude rr = 1.1:1). The substrate was purified by column chromatography on basic alumina (EtOAc/hexanes = 4:96). <sup>1</sup>H NMR (400 MHz, CDCl<sub>3</sub>) δ 7.51 (d, *J* = 6.5 Hz, 1H), 7.35 (d, *J* = 7.7 Hz, 2H), 7.25 – 7.17 (m, 2H), 7.04 (d, *J* = 6.6 Hz, 1H), 6.91 (d, *J* = 7.7 Hz, 2H), 5.13 (s, 1H), 3.82 (s, 2H), 3.68 (d, *J* = 6.2 Hz, 1H), 3.18 – 2.96 (m, 1H), 2.81 (appr s, 1H), 2.71 – 2.49 (m, 1H), 2.25 – 2.09 (m, 1H), 1.95 – 1.77 (m, 1H), 1.62 (appr s, 2H), 1.14 – 0.95 (m, 1H); <sup>13</sup>C NMR (101 MHz, CDCl<sub>3</sub>) δ 163.7, 159.8, 138.1, 134.5, 130.3, 130.1, 128.8, 128.3, 128.2, 127.0, 114.1, 68.1, 55.4, 41.9, 39.4, 30.97, 26.4, 22.1; HRMS (*m/z*): [M+Na-N<sub>2</sub>]<sup>+</sup> calcd. for C<sub>20</sub>H<sub>21</sub>N<sub>3</sub>O<sub>3</sub>, 346.1414; observed, 346.1409.

**((3aR,10bR)-3-((3S,5S,7S)-adamantan-1-yl)-3,3a,4,5,6,10b-hexahydrobenzo[3,4]cyclohepta[1,2-d][1,2,3]triazole) (3i)**



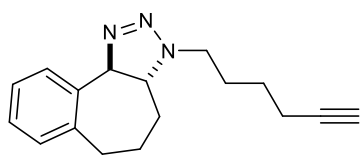
The general procedure **A** was followed using 1-azidoadamantane (42.4 mg, 0.24 mmol), alkene **S2** (103.8 mg, 0.72 mmol), **Cat. 3** (2.4 mg, 1.2 mol%) and DMF (0.36 mL) to afford **3i** in 73% yield (56.2 mg, 0.175 mmol) as a colorless oil with rr 16:1 (crude rr = 4.6:1). The substrate was purified by column chromatography on basic alumina (EtOAc/hexanes = 1:99). <sup>1</sup>H NMR (400 MHz, CDCl<sub>3</sub>) δ 7.59 (d, *J* = 7.4 Hz, 1H), 7.17 (t, *J* = 7.3 Hz, 1H), 7.10 (t, *J* = 7.3 Hz, 1H), 7.05 (d, *J* = 7.1 Hz, 1H), 4.96 (d, *J* = 15.5 Hz, 1H), 3.01 – 2.88 (m, 1H), 2.86 – 2.63 (m, 2H), 2.64 – 2.45 (m, 1H), 2.14 – 2.00 (m, 6H), 1.97 (d, *J* = 15.4 Hz, 1H), 1.77 (d, *J* = 11.5 Hz, 3H), 1.67 – 1.51 (m, 7H), 1.45 – 1.26 (m, 1H); <sup>13</sup>C NMR (101 MHz, CDCl<sub>3</sub>) δ 140.3, 139.3, 129.4, 127.3, 126.8, 125.0, 83.5, 62.4, 58.6, 41.4, 37.0, 36.5, 35.2, 29.7, 25.7; HRMS (*m/z*): [M+H]<sup>+</sup> calcd. for C<sub>31</sub>H<sub>27</sub>N<sub>3</sub>, 322.2278; observed, 322.2273.

**(Benzyl (S)-2-((tert-butoxycarbonyl)amino)-4-((3aR,10bR)-4,5,6,10b-tetrahydrobenzo[3,4]cyclohepta[1,2-d][1,2,3]triazol-3(3aH)-yl)butanoate) (3j)**



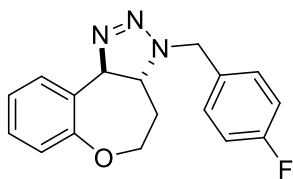
The general procedure **A** was followed using benzyl (S)-4-azido-2-((tert-butoxycarbonyl)amino)butanoate (60.0 mg, 0.18 mmol), alkene **S2** (77.9 mg, 0.54 mmol), **Cat. 3** (1.8 mg, 1.2 mol%) and DMF (0.9 mL) to afford **3j** in 72% yield (62.2 mg, 0.13 mmol) as an off white solid. Crude rr cannot be determined since no diagnostic signals for minor regioisomer could be identified. The substrate was purified by column chromatography on basic alumina (EtOAc/hexanes = 10:90). <sup>1</sup>H NMR (400 MHz, CDCl<sub>3</sub>) δ 7.70 (d, *J* = 7.1 Hz, 1H), 7.39 – 6.93 (m, 8H), 5.43 – 4.97 (m, 3H), 4.97 – 4.70 (m, 1H), 4.61 – 4.19 (m, 1H), 3.45 – 3.09 (m, 2H), 2.91 – 2.58 (m, 2H), 2.56 – 2.39 (m, 1H), 2.38 – 1.86 (m, 3H), 1.74 – 1.53 (m, 2H), 1.36 (s, 9H), 1.33 – 1.21 (m, 1H); <sup>13</sup>C NMR (101 MHz, CDCl<sub>3</sub>) δ 172.2, 155.3, 140.1, 138.0, 135.2, 129.6, 128.6, 128.5, 128.4, 127.4, 126.8, 125.0, 82.6, 80.1, 67.3, 66.7, 51.8, 45.6, 35.1, 32.3, 30.8, 28.3, 25.1; HRMS (m/z): [M+Na]<sup>+</sup> calcd. for C<sub>27</sub>H<sub>34</sub>N<sub>4</sub>O<sub>4</sub>, 501.2472; observed, 501.2457.

**((3aR,10bR)-3-(hex-5-yn-1-yl)-3,3a,4,5,6,10b-hexahydrobenzo[3,4]cyclohepta[1,2-d][1,2,3]triazole) (3k)**



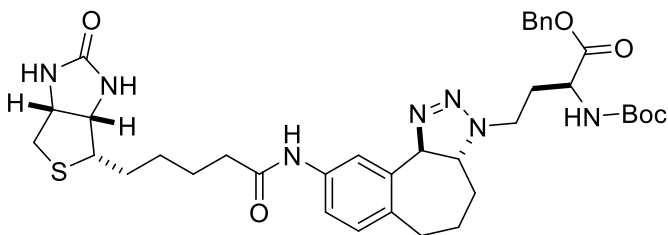
The general procedure **A** was followed using 6-azidohex-1-yne (29.6 mg, 0.24 mmol), alkene **S2** (103.8 mg, 0.72 mmol), **Cat. 3** (2.4 mg, 1.2 mol%) and DMF (1.2 mL) to afford **3k** in 70% yield (45.4 mg, 0.17 mmol) as a colorless oil with rr = 4.2:1 (crude rr = 2.7:1). The substrate was purified by column chromatography on basic alumina (EtOAc/hexanes = 1:99). <sup>1</sup>H NMR (400 MHz, CDCl<sub>3</sub>) δ 7.78 (d, *J* = 7.4 Hz, 1H), 7.25 – 7.20 (m, 1H), 7.21 – 7.14 (m, 1H), 7.12 (d, *J* = 5.8 Hz, 1H), 4.92 (d, *J* = 16.3 Hz, 1H), 3.46 – 3.18 (m, 2H), 2.85 – 2.74 (m, 1H), 2.75 – 2.58 (m, 1H), 2.46 – 2.33 (m, 2H), 2.28 – 2.17 (m, 2H), 2.13 – 2.03 (m, 2H), 1.92 (t, *J* = 2.5 Hz, 1H), 1.87 – 1.80 (m, 2H), 1.76 – 1.69 (m, 1H), 1.69 – 1.52 (m, 1H), 1.50 – 1.29 (m, 1H); <sup>13</sup>C NMR (101 MHz, CDCl<sub>3</sub>) δ 140.2, 138.3, 129.6, 127.3, 126.8, 125.1, 84.0, 82.4, 68.7, 66.1, 48.8, 35.1, 32.5, 26.8, 25.8, 25.1, 18.1; HRMS (m/z) [M+H]<sup>+</sup> calcd. for C<sub>17</sub>H<sub>21</sub>N<sub>3</sub>, 268.1808; observed, 268.1801.

**((3aR,10bR)-3-(4-fluorobenzyl)-3a,4,5,10b-tetrahydro-3H-benzo[2,3]oxepino[4,5-d][1,2,3]triazole) (3l)**



The general procedure **A** was followed using 1-(azidomethyl)-4-fluorobenzene (45.5 mg, 0.30 mmol), 2,3-dihydrobenzo[b]oxepine (131.5 mg, 0.90 mmol), **Cat. 3** (3.0 mg, 1.2 mol%) and DMF/water = 4:1 (1.5 mL) to afford **3l** in 45% yield (40.0 mg, 0.134 mmol) as an off white solid with rr = 13.3:1 (crude rr = 3.2:1). The substrate was purified by column chromatography on basic alumina (EtOAc/hexanes = 10:90). <sup>1</sup>H NMR (400 MHz, CDCl<sub>3</sub>) δ 7.72 (d, *J* = 7.3 Hz, 1H), 7.26 – 7.17 (m, 2H), 7.16 – 7.10 (m, 1H), 7.06 (m, 1H), 7.00 – 6.85 (m, 3H), 4.97 (d, *J* = 16.6 Hz, 1H), 4.69 (d, *J* = 15.1 Hz, 1H), 4.64 (d, *J* = 15.1 Hz, 1H), 4.34 (dt, *J* = 12.5, 3.1 Hz, 1H), 3.48 – 3.25 (m, 1H), 2.63 – 2.43 (m, 1H), 2.02 – 1.81 (m, 2H); <sup>13</sup>C NMR (101 MHz, CDCl<sub>3</sub>) δ 162.5 (d, *J* = 246.6 Hz), 158.2, 131.4 (d, *J* = 3.2 Hz), 131.2, 130.3 (d, *J* = 8.1 Hz), 128.8, 126.2, 124.6, 121.7, 115.7 (d, *J* = 21.5 Hz), 81.5, 69.9, 64.4, 53.6, 32.5.

**(benzyl (S)-2-((tert-butoxycarbonyl)amino)-4-((3aR,10bR)-9-(5-((3aS,4S,6aR)-2-oxohexahydro-1H-thieno[3,4-d]imidazol-4-yl)pentanamido)-4,5,6,10b-tetrahydrobenzo[3,4]cyclohepta[1,2-d][1,2,3]triazol-3(3aH)-yl)butanoate) (3m)**

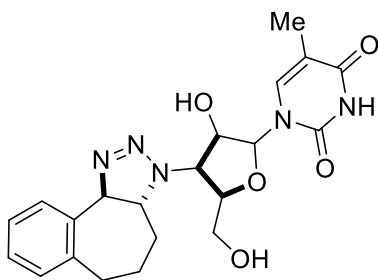


The general procedure **A** was followed using benzyl (S)-4-azido-2-((tert-butoxycarbonyl)amino)butanoate (40.0 mg, 0.12 mmol), N-(6,7-dihydro-5H-benzo[7]annulen-2-yl)-5-((3aS,4S,6aR)-2-oxohexahydro-1H-thieno[3,4-d]imidazol-4-yl)pentanamide (46.2 mg, 0.12 mmol), **Cat. 3** (1.2 mg, 1.2 mol%) and DMF (0.6 mL) to afford **3m** in 58% yield (50.1 mg, 0.07 mmol) as a white powder with an isomeric ratio (rr+dr) = 5.1:4.1:1.9:1 (determined by HPLC). The substrate was purified by column chromatography on basic alumina (MeOH/CH<sub>2</sub>Cl<sub>2</sub> = 2:98).

Since it was not possible to separate the mixture of regioisomers and diastereomers, the NMR data is reported for the mixture and all peaks have been picked.

$^1\text{H}$  NMR (400 MHz,  $\text{CDCl}_3$ )  $\delta$  8.63 (d,  $J = 37.6$  Hz, 2H), 7.58 (s, 1H), 7.34 (s, 5H), 7.04 (d,  $J = 8.1$  Hz, 2H), 6.22 (s, 1H), 5.35 – 5.05 (m, 3H), 4.80 (s, 1H), 4.53 – 4.28 (m, 3H), 3.50 – 3.19 (m, 2H), 3.12 (s, 1H), 2.86 (d,  $J = 14.6$  Hz, 1H), 2.81 – 2.51 (m, 4H), 2.42 – 2.18 (m, 4H), 1.70 (dd,  $J = 38.0$ , 21.0 Hz, 7H), 1.43 (s, 9H);  $^{13}\text{C}$  NMR (151 MHz,  $\text{CDCl}_3$ )  $\delta$  172.2, 172.1, 172.1, 172.0, 164.5, 137.8, 137.6, 137.6, 137.4, 135.2, 135.1, 135.0, 130.2, 128.6, 128.6, 128.4, 128.3, 128.2, 118.8, 118.5, 116.4, 82.1, 82.1, 80.0, 67.2, 67.1, 66.8, 66.7, 62.0, 61.8, 60.2, 60.2, 56.3, 56.1, 53.38, 51.7, 51.6, 45.6, 40.6, 40.6, 36.8, 36.8, 34.3, 32.0, 31.9, 30.8, 30.7, 29.63, 28.9, 28.5, 28.3, 28.2, 28.0, 27.9, 25.7, 25.1; HRMS ( $m/z$ ):  $[\text{M}+\text{K}]^+$  calcd. for  $\text{C}_{37}\text{H}_{49}\text{N}_7\text{O}_6\text{S}$ , 742.3357, observed; 742.3346.

**(1-((3R,4S,5R)-3-hydroxy-5-(hydroxymethyl)-4-((3aR,10bR)-4,5,6,10b-tetrahydrobenzo[3,4]cyclohepta[1,2-d][1,2,3]triazol-3(3aH)-yl)tetrahydrofuran-2-yl)-5-methylpyrimidine-2,4(1H,3H)-dione) (3n)**



The general procedure **A** was followed using 1-((3R,4S,5R)-4-azido-3-hydroxy-5-(hydroxymethyl)tetrahydrofuran-2-yl)-5-methylpyrimidine-2,4(1H,3H)-dione (70.0 mg, 0.24 mmol), alkene **S2** (103.8 mg, 0.72 mmol), **Cat. 3** (2.4 mg, 1.2 mol%) and DMF (3.6 mL) to afford **3n** in 60% yield (61.6 mg, 0.144

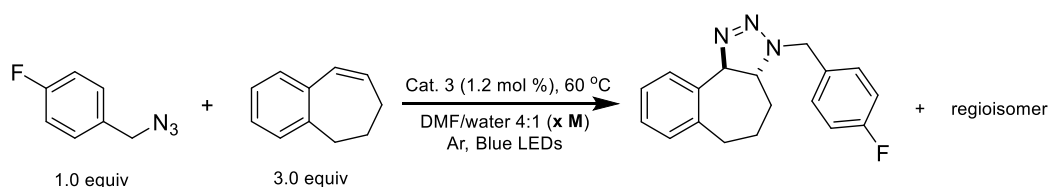
mmol) as a white powder with an isomeric ratio (rr+dr) = 2.3:1.2:1.2:1 (determined by HPLC). The substrate was purified by column chromatography on basic alumina ( $\text{MeOH}/\text{CH}_2\text{Cl}_2 = 5:95$ ).

Since it was not possible to separate the mixture of regioisomers and diastereomers, the NMR data is reported for the mixture and all peaks have been picked.

$^1\text{H}$  NMR (599 MHz,  $\text{CDCl}_3$ )  $\delta$  7.69 (d,  $J = 7.4$  Hz, 1H), 7.66 (d,  $J = 7.4$  Hz, 1H), 7.38 (d,  $J = 28.0$  Hz, 2H), 7.17 (d,  $J = 5.9$  Hz, 2H), 7.12 (t,  $J = 7.0$  Hz, 2H), 7.06 (d,  $J = 6.5$  Hz, 3H), 6.17 (t,  $J = 6.5$

Hz, 1H), 6.02 (t,  $J = 6.2$  Hz, 1H), 4.94 – 4.83 (m, 2H), 4.68 – 4.57 (m, 1H), 4.13 (dd,  $J = 36.8, 5.4$  Hz, 2H), 4.07 – 3.96 (m, 2H), 3.87 – 3.79 (m, 1H), 3.79 – 3.72 (m, 1H), 3.63 – 3.47 (m, 1H), 2.98 – 2.82 (m, 1H), 2.82 – 2.63 (m, 8H), 2.63 – 2.56 (m, 2H), 2.43 – 2.32 (m, 2H), 2.32 – 2.18 (m, 2H), 2.15 – 1.98 (m, 3H), 1.79 (s, 3H), 1.78 (s, 3H), 1.73 – 1.56 (m, 2H), 1.41 – 1.29 (m, 2H);  $^{13}\text{C}$  NMR (151 MHz,  $\text{CDCl}_3$ )  $\delta$  164.2, 150.6, 150.4, 140.1, 139.9, 133.9, 129.7, 129.7, 128.7, 127.6, 127.1, 126.8, 126.5, 124.8, 110.8, 110.7, 88.71, 87.9, 83.9, 83.1, 82.5, 82.4, 65.7, 65.6, 63.2, 61.4, 57.6, 56.6, 53.4, 39.1, 37.0, 35.0, 34.9, 34.3, 32.1, 31.9, 29.6, 24.9, 24.8, 23.2, 12.4, 12.3; HRMS ( $m/z$ ):  $[\text{M}+\text{H}-\text{N}_2]^+$  calcd. for  $\text{C}_{21}\text{H}_{25}\text{N}_5\text{O}_5$ , 400.1867; observed, 400.1855.

### 3.69. Kinetics Study: Determination of rate constant



The kinetics of the reaction were studied at three different concentrations (**0.2 M**, **0.1 M**, and **0.05 M**) with respect to 4-fluorobenzyl azide. The reaction progress was monitored by  $^{19}\text{F}$  NMR. The conversion was monitored by both disappearance of the starting material and appearance of the new regioisomeric products. No other products were detected by  $^{19}\text{F}$  NMR. All reactions were performed in triplicate. The graph between  $\ln([\text{Azide}]/[\text{Azide}]_0)$  vs. time was plotted (Figure 14). The slope of the plot determined the first order rate constant ( $k$ ) which was found to be  $2.4 \pm 0.9 \times 10^{-3} \text{ s}^{-1}$ . The half-life of the first order reaction was calculated using the formula  $t_{1/2} = 0.693/k$ . The half-life of the reaction was determined to be 4.8 min.

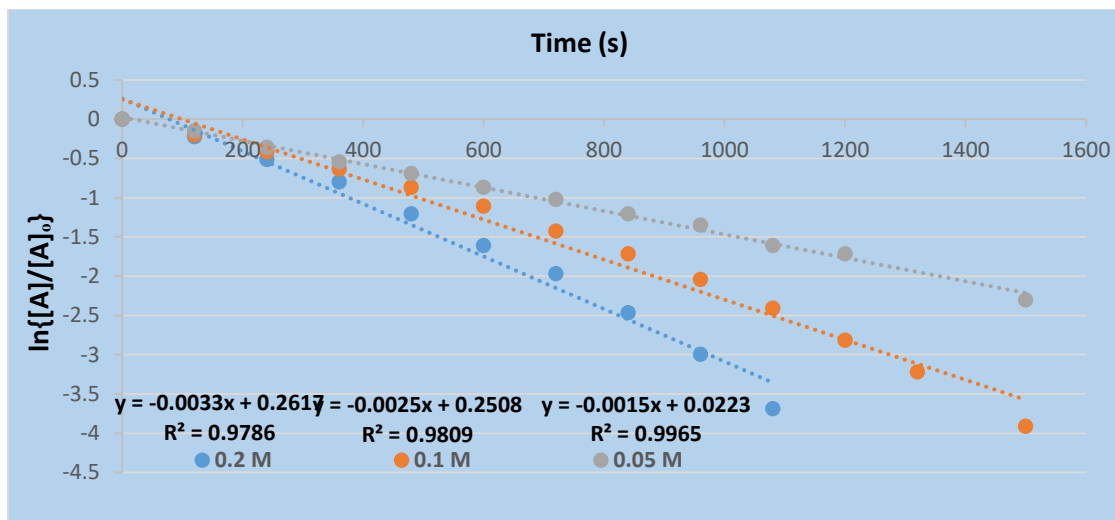
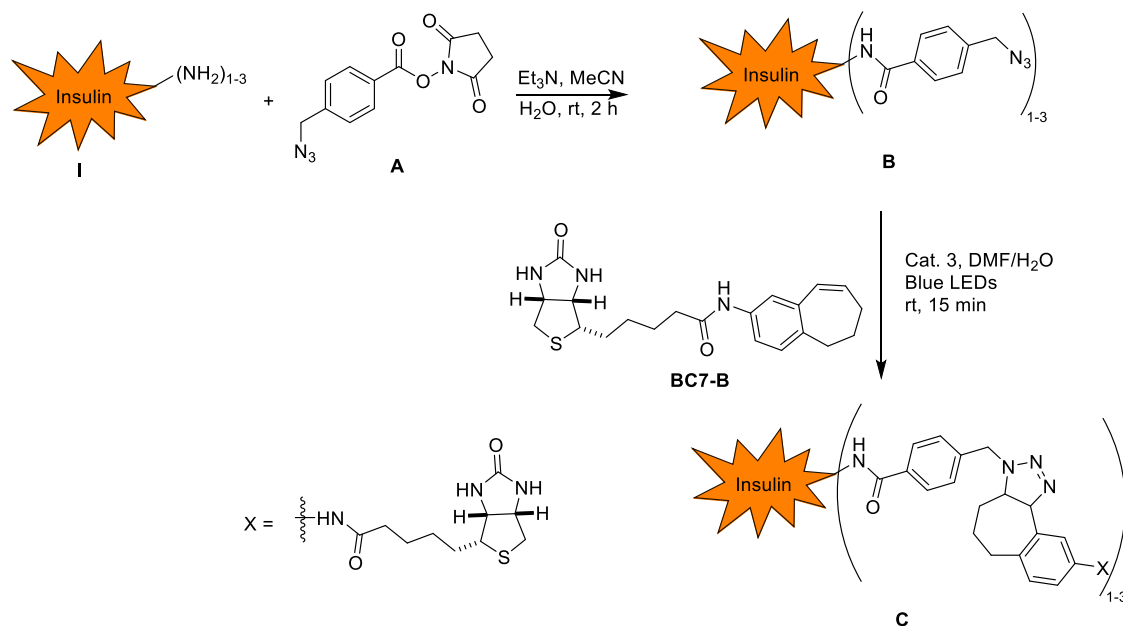


Figure 14. First order graph between  $\ln([Azide]/[Azide]_0)$  and time

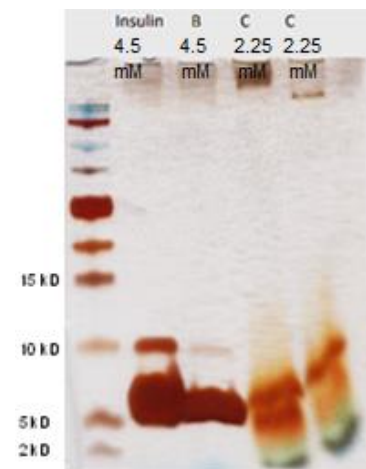
### 3.7. Insulin ligation experiment



A small amount (25  $\mu\text{g}$ ) of insulin (bovine) was dissolved in 200  $\mu\text{L}$  MeCN/water (4:1) (21.8  $\mu\text{M}$  concentration). To this solution was added  $\text{Et}_3\text{N}$  (10  $\mu\text{L}$ ) and **A** (0.5 mg). After 2 hours, solvent and excess  $\text{Et}_3\text{N}$  were removed via speed vacuum. To the residue, was added 100  $\mu\text{L}$  water and the mixture was extracted with EtOAc (2 x 50  $\mu\text{L}$ ) to remove all the excess ester **A** and other organic impurities. The aqueous layer was separated and analyzed by MALDI. The masses consistent with the mono-, di-, and tri-modified insulin can be seen with a very small amount of un-modified insulin still present. The sample was then concentrated *via* speed vacuum. To the azide modified insulin **B** was added 200  $\mu\text{L}$  DMF/water (4:1), alkene **BC7-B** (90  $\mu\text{g}$ ), **Cat 3** (0.1  $\mu\text{g}$ , 250:1 insulin:**Cat 3** by mass), and the reaction mixture was exposed to blue LED lights for 15 minutes. The reaction mixture was then analyzed by MALDI. Upon extensive dilution of the reaction mixture, MALDI indicated the formation of **C** with complete consumption of **B**.

### SDS-PAGE experiment

The above reaction was performed and all the three insulin entities, *i.e.*, unmodified insulin (**I**), azide modified insulin **B**, and biotin conjugated insulin **C** were subjected to SDS-PAGE and analyzed by a silver staining protocol. All three samples **I**, **B**, and **C**, were diluted with a 20  $\mu$ L of sample loading buffer with a final concentration of 4.5 mM, 4.5 mM, and 2.25 mM, respectively. The analysis of the gel after the silver staining confirms the presence of azide modified biotin conjugated insulin **C**.



Attempts to stain the gel with Coomassie blue did not give satisfactory results. The bands of the biotin modified insulin appeared very faint after staining the gel. However, this was somewhat expected since Coomassie blue interacts with basic amino acids such as lysine, arginine, histidine, and most of these residues were modified and were no longer available for interaction with Coomassie blue stain.<sup>46</sup>

### 3.71. Reaction compatibility in presence of thiols

In general, thiols have the potential to create problems in conjugation reactions and have been known to isomerize strained alkenes.<sup>47</sup> Consequently, we performed a compatibility experiment in the presence of various thiols and the outcomes of the reactions are tabulated below. In the reactions listed below, some competitive side reactions were observed when thiol was included (Table 6, Entry 1 vs 2-5), though not surprisingly **BC7** was stable to thiols (Entry 6). The side reactions likely stemmed from electron transfer processes initiated by the excited Ir-catalyst. Alternatively, the thiols reacted with the *t*-**BC7**. The former notion was supported by the observation that a less oxidizing photocatalyst **Cat. 4** (compared to **Ir(ppy)<sub>3</sub>**), less side product was observed (Entry 4 vs. Entry 5)  $E_{1/2}(\text{Ir}^*/\text{Ir}^-) = 0.55 \text{ V}$  for **Ir(ppy)<sub>3</sub>** and  $E_{1/2}(\text{Ir}^*/\text{Ir}^-) = 0.39 \text{ V}$  for **Cat. 4** vs  $\text{Ag}/\text{AgCl}$ .<sup>8</sup> If true, then it is conceivable that the side reactions could be minimized or even

shut down by the judicious design of the Ir-catalyst, as the emissive energy and the redox potentials are independently tunable. When *c*-**BC7** was incubated with  $\beta$ -mercaptoethanol at rt in absence of Ir-catalyst (Entry 6), no reaction was observed. The alkene *c*-**BC7** and  $\beta$ -mercaptoethanol were recovered unchanged after 19 hours.

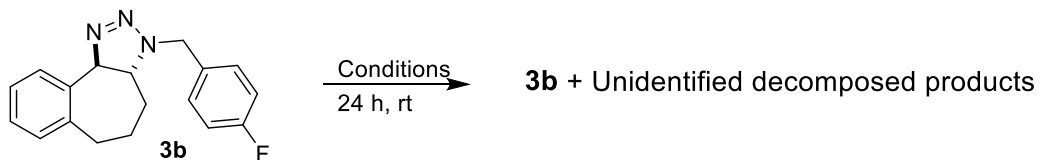
Entry	Thiol	P1 <sup>a</sup>	Ir catalyst and conditions
1.	No thiol	100%	Ir(ppy) <sub>3</sub>
2.	HS-CH <sub>2</sub> -CH <sub>2</sub> -OH	30% <sup>b</sup>	Ir(ppy) <sub>3</sub>
3.	PhSH	0% <sup>b</sup>	Ir(ppy) <sub>3</sub>
4.	CH <sub>3</sub> (CH <sub>2</sub> ) <sub>7</sub> SH	30% <sup>b</sup>	Ir(ppy) <sub>3</sub> (1.2 mol% in DMF at 45 °C)
5.	CH <sub>3</sub> (CH <sub>2</sub> ) <sub>8</sub> SH	44% <sup>b</sup>	Cat. 4 (1.2 mol% in DMF at 45 °C)
6.	No azide and no Ir Cat	- <sup>c</sup>	-

<sup>a</sup>NMR conversion. <sup>b</sup>All alkene consumed. <sup>c</sup>Alkene remains unchanged.

Table 6. Reaction outcome in presence of thiols

### 3.72. Stability studies in various buffers.

The triazoline **3b** was incubated in different acidic and basic conditions and the results are tabulated below. The decomposition of the triazoline **3b** was monitored by <sup>19</sup>F NMR.



Conditions	Outcome
5.0 eq LiOH.H <sub>2</sub> O/MeCN (1:1)	No decomposition observed
5.0 eq mercaptoethanol (0.28 M in MeCN)	63% of <b>3b</b> was still intact
PBS buffer (pH =7.4)/MeCN (1:1)	54% of <b>3b</b> was still intact
PBS buffer (pH =5.5)/MeCN (1:1)	23% of <b>3b</b> was still intact

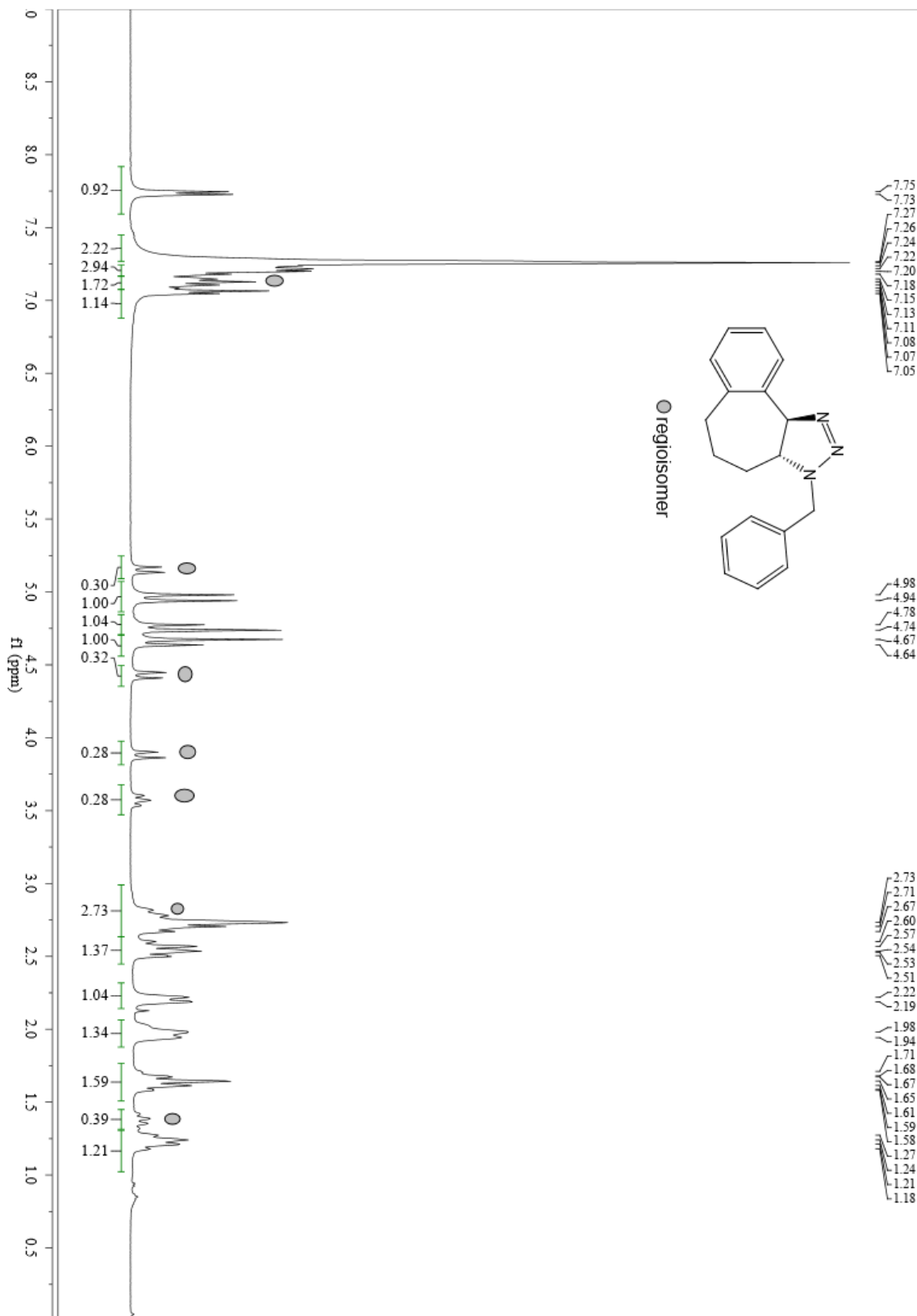
Table 7. Stability studies of Traizoline **3b**

### 3.8 References

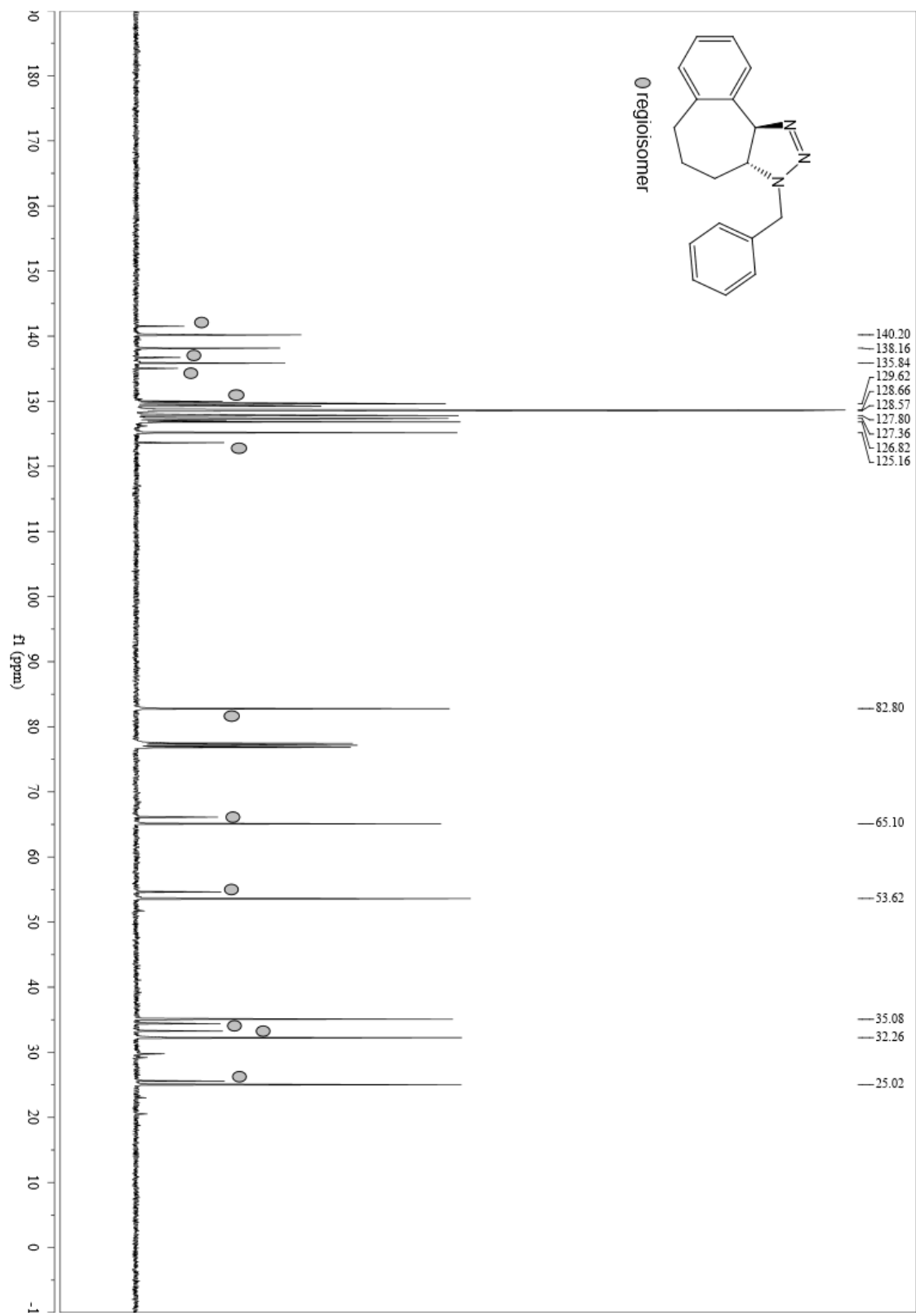
1. Tasdelen, M. A.; Yagci, Y., *Angew. Chem. Int. Ed.* **2013**, *52*, 5930.
2. Tyson, E. L.; Niemeyer, Z. L.; Yoon, T. P., *J. Org. Chem.* **2014**, *79*, 1427.
3. Wenjiao, S.; Yizhong, W.; Jun, Q.; M., M. M.; Qing, L., *Angew. Chem.* **2008**, *120*, 2874.
4. Wang, J.; Zhang, W.; Song, W.; Wang, Y.; Yu, Z.; Li, J.; Wu, M.; Wang, L.; Zang, J.; Lin, Q., *J. Am. Chem. Soc.* **2010**, *132*, 14812.
5. Yu, Z.; Ohulchansky, T. Y.; An, P.; Prasad, P. N.; Lin, Q., *J. Am. Chem. Soc.* **2013**, *135*, 16766.
6. Wang, Y.; Song, W.; Hu, W. J.; Lin, Q., *Angew. Chem. Int. Ed.* **2009**, *48*, 5330.
7. Mueller, J. O.; Schmidt, F. G.; Blinco, J. P.; Christopher, B. K., *Ang. Chem. Int. Ed.* **2015**, *54*, 10284.
8. Lim, R. K. V.; Lin, Q., *Chem. Commun.* **2010**, *46*, 7993.
9. Poloukhine, A. A.; Mbua, N. E.; Wolfert, M. A.; Boons, G.-J.; Popik, V. V., *J. Am. Chem. Soc.* **2009**, *131*, 15769.
10. Blackman, M. L.; Royzen, M.; Fox, J. M., *J. Am. Chem. Soc.* **2008**, *130*, 13518.
11. Selvaraj, R.; Fox, J. M., *Curr Opin Chem Biol* **2013**, *17*, 753.
12. Karver, M. R.; Weissleder, R.; Hilderbrand, S. A., *Bioconjugate Chem.* **2011**, *22*, 2263.
13. Zhang, H.; Trout, W. S.; Liu, S.; Andrade, G. A.; Hudson, D. A.; Scinto, S. L.; Dicker, K. T.; Li, Y.; Lazouski, N.; Rosenthal, J.; Thorpe, C.; Jia, X.; Fox, J. M., *J. Am. Chem. Soc.* **2016**, *138*, 5978.
14. Vebrel, J.; Carrié, R., *Tetrahedron* **1983**, *39*, 4163.
15. van Berkel, S. S.; Dirks, J. A.; Meeuwissen, S. A.; Pingen, D. L. L.; Boerman, O. C.; Laverman, P.; van Delft, F. L.; Cornelissen, J. J. L. M.; Rutjes, F. P. J. T., *ChemBioChem* **2008**, *9*, 1805.
16. Shea, K. J.; Kim, J. S., *J. Am. Chem. Soc.* **1992**, *114*, 4846.
17. Schoenebeck, F.; Ess, D. H.; Jones, G. O.; Houk, K. N., *J. Am. Chem. Soc.* **2009**, *131*, 8121.
18. Bach, R. D., *J. Am. Chem. Soc.* **2009**, *131*, 5233.
19. Fujita, S.; Hayashi, Y.; Nômi, T.; Nozaki, H., *Tetrahedron* **1971**, *27*, 1607.
20. Hoffmann, R.; Inoue, Y., *J. Am. Chem. Soc.* **1999**, *121*, 10702.
21. Dorr, H.; Rawal, V. H., *J. Am. Chem. Soc.* **1999**, *121*, 10229.
22. Moran, J.; Cebrowski, P. H.; Beauchemin, A. M., *J. Org. Chem.* **2008**, *73*, 1004.
23. Strickland, A. D.; Caldwell, R. A., *J. Phys. Chem.* **1993**, *97*, 13394.
24. Gritsan, N.; Platz, M., Photochemistry of Azides: The Azide/Nitrene Interface. In *Organic Azides*, John Wiley & Sons, Ltd: 2010; pp 311-372.
25. Lu, Z.; Yoon, T. P., *Angew. Chem. Int. Ed.* **2012**, *51*, 10329.
26. Du, J.; Skubi, K. L.; Schultz, D. M.; Yoon, T. P., *Science* **2014**, *344*, 392.
27. Prier, C. K.; Rankic, D. A.; MacMillan, D. W. C., *Chem. Rev.* **2013**, *113*, 5322.
28. Dai, C.; Narayanam, J. M. R.; Stephenson, C. R. J., *Nat. Chem.* **2011**, *3*, 140.
29. Ricci, A.; Chretien, M. N.; Marette, L.; Scaiano, J. C., *Photochem. Photobiol. Sci.* **2003**, *2*, 487.
30. Hein, J. E.; Fokin, V. V., *Chem. Soc. Rev.* **2010**, *39*, 1302.
31. Otto, S.; Engberts, J. B. F. N., *Org. Biomol. Chem.* **2003**, *1*, 2809.
32. Breslow, R., *Acc. Chem. Res.* **1991**, *24*, 159.
33. Sletten, E. M.; Bertozzi, C. R., *Angew. Chem. Int. Ed.* **2009**, *48*, 6974.
34. Troyer, T. L.; Muchalski, H.; Hong, K. B.; Johnston, J. N., *Org. Lett.* **2011**, *13*, 179.
35. Matikonda, S. S.; Orsi, D. L.; Staudacher, V.; Jenkins, I. A.; Fiedler, F.; Chen, J.; Gamble, A. B., *Chem. Sci.* **2015**, *6*, 1212.

36. Bhattacharya, S.; Mandal, A. N.; Ray Chaudhuri, S. R.; Chatterjee, A., *Tetrahedron Lett.* **1984**, *25*, 3007.
37. The weak signal is a result of the extensive dilution that was necessary to avoid nonionizing aggregates.
38. Metternich, J. B.; Gilmour, R., *J. Am. Chem. Soc.* **2015**, *137*, 11254.
39. Singh, A.; Teegardin, K.; Kelly, M.; Prasad, K. S.; Krishnan, S.; Weaver, J. D., *J. Organomet. Chem.* **2015**, *776*, 51.
40. Hay, M. P.; Hicks, K. O.; Pchalek, K.; Lee, H. H.; Blaser, A.; Pruijn, F. B.; Anderson, R. F.; Shinde, S. S.; Wilson, W. R.; Denny, W. A., *J. Med. Chem.* **2008**, *51*, 6853.
41. Cowan, J. A., *Tetrahedron Lett.* **1986**, *27*, 1205.
42. Roth, S.; Drewe, W. C.; Thomas, N. R., *Nat. Protoc.* **2010**, *5*, 1967.
43. Watt, D. S., Liu, C., Sviripa, V., and Zhang, W. Stilbene analogs and methods of treating cancer. Patent US2012/0196874, August 2, 2012.
44. Saito, Y.; Matsumoto, K.; Bag, S. S.; Ogasawara, S.; Fujimoto, K.; Hanawa, K.; Saito, I., *Tetrahedron* **2008**, *64*, 3578.
45. Arichi, N.; Yamada, K.-i.; Yamaoka, Y.; Takasu, K., *J. Am. Chem. Soc.* **2015**, *137*, 9579.
46. de Moreno, M. R.; Smith, J. F.; Smith, R. V., *J. Pharm. Sci.* **1986**, *75*, 907.
47. Taylor, M. T.; Blackman, M. L.; Dmitrenko, O.; Fox, J. M., *J. Am. Chem. Soc.* **2011**, *133*, 9646.

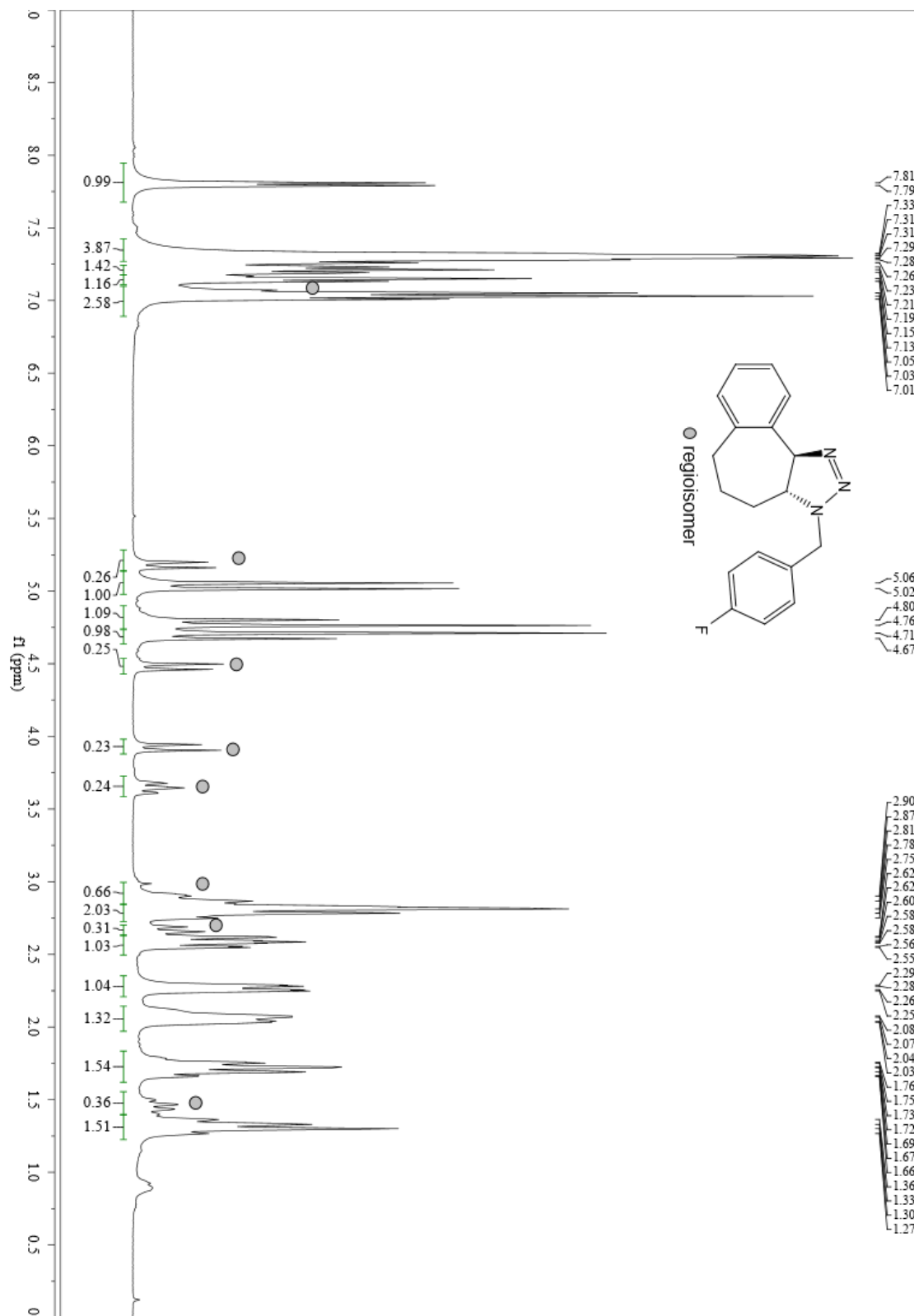
**3a (3aR,10bR)-3-benzyl-3,3a,4,5,6,10b-hexahydrobenzo[3,4]cyclohepta[1,2-d][1,2,3]triazole**



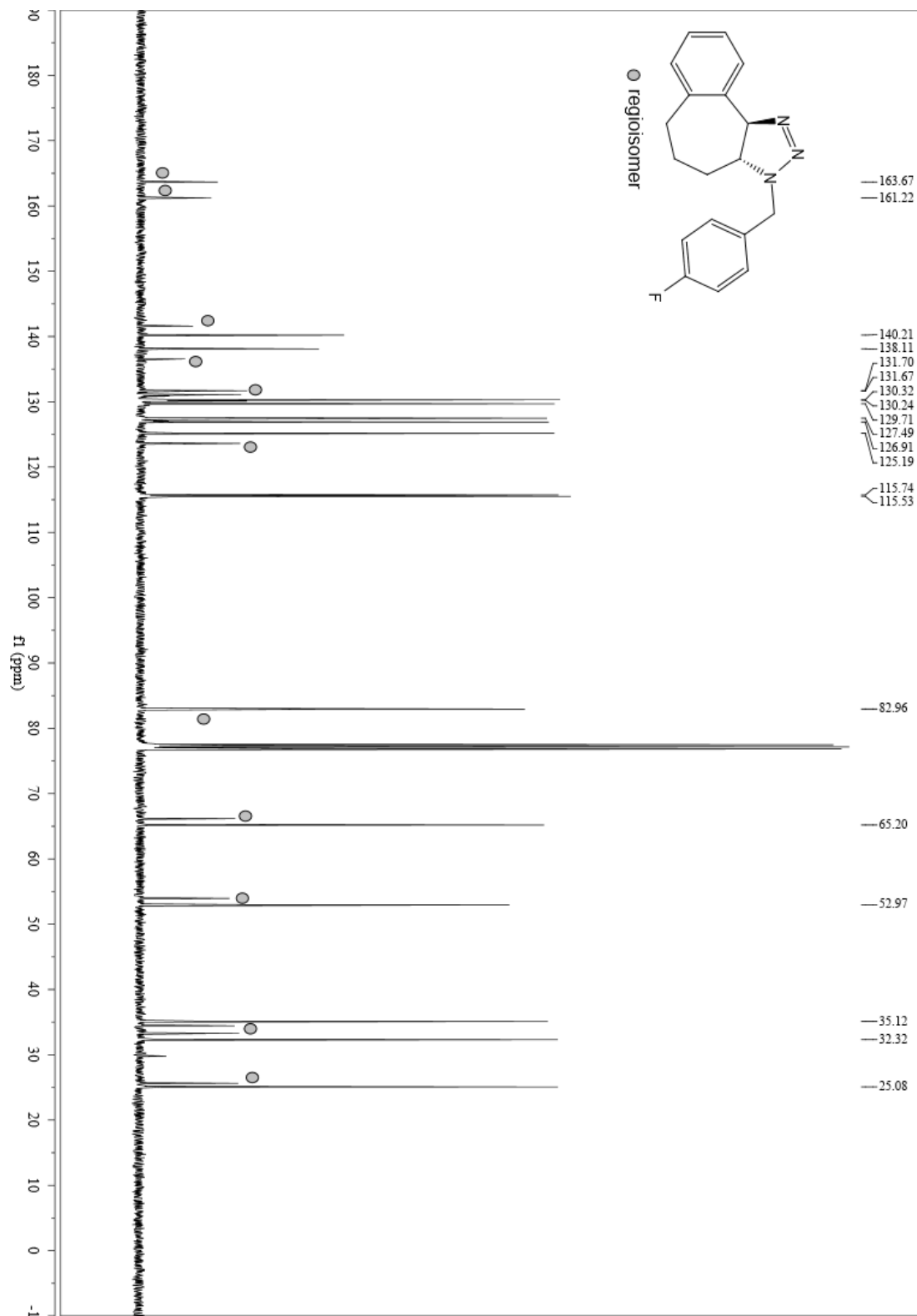
**3a (3aR,10bR)-3-benzyl-3,3a,4,5,6,10b-hexahydrobenzo[3,4]cyclohepta[1,2-d][1,2,3]triazole**



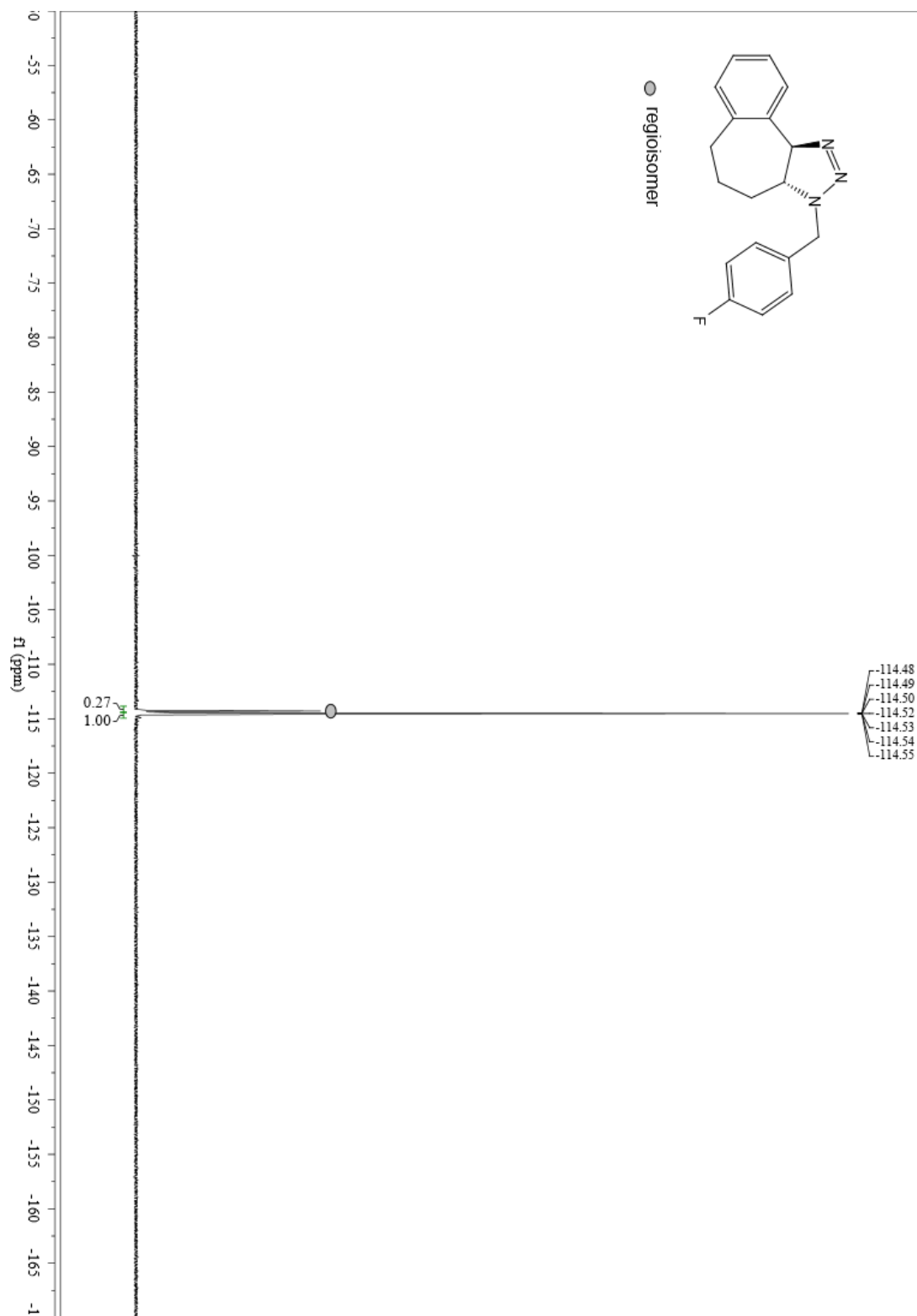
**3b (3aR,10bR)-3-(4-fluorobenzyl)-3,3a,4,5,6,10b-hexahydrobenzo[3,4]cyclohepta[1,2-d][1,2,3]triazole**



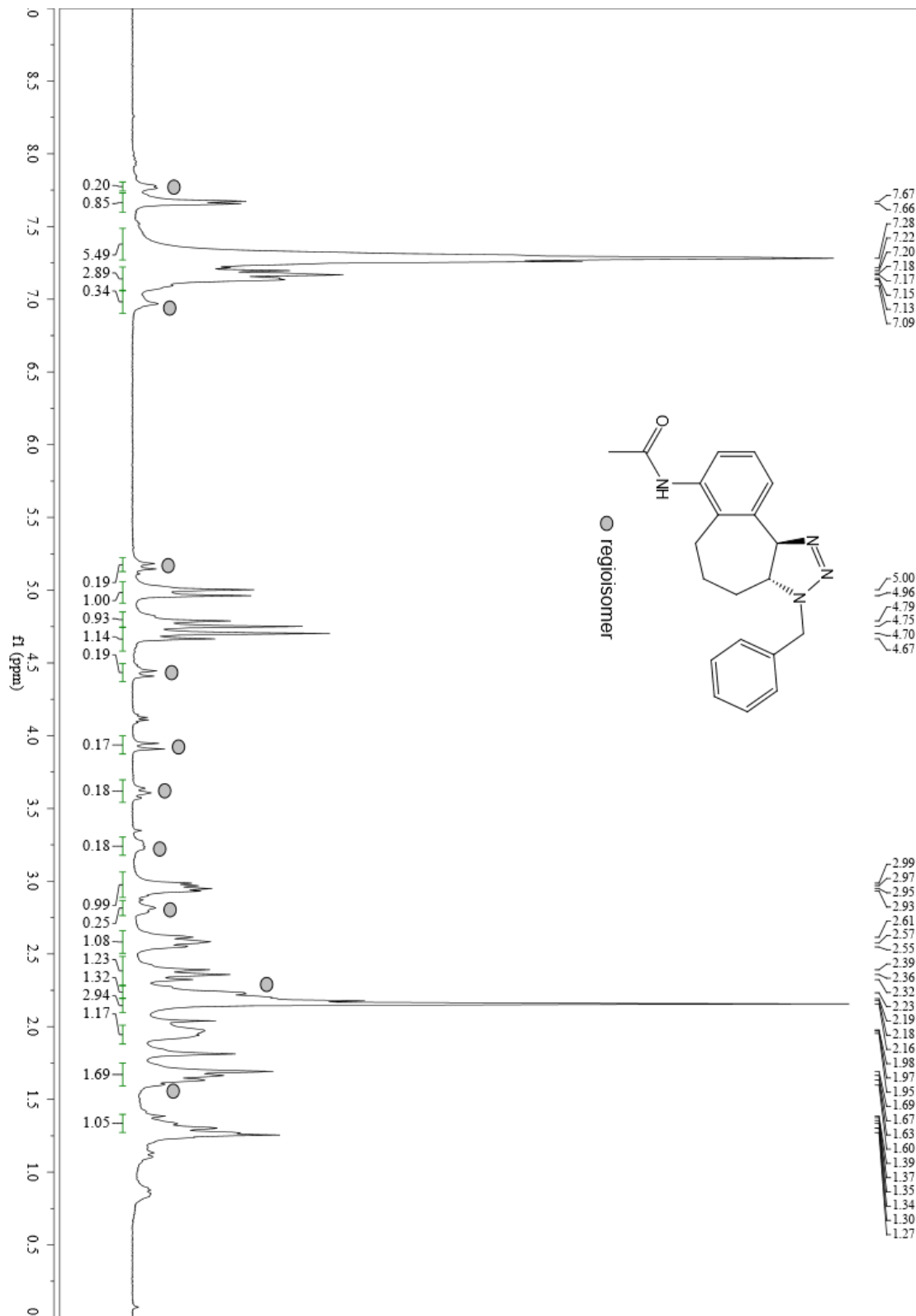
**3b (3aR,10bR)-3-(4-fluorobenzyl)-3,3a,4,5,6,10b-hexahydrobenzo[3,4]cyclohepta[1,2-d][1,2,3]triazole**



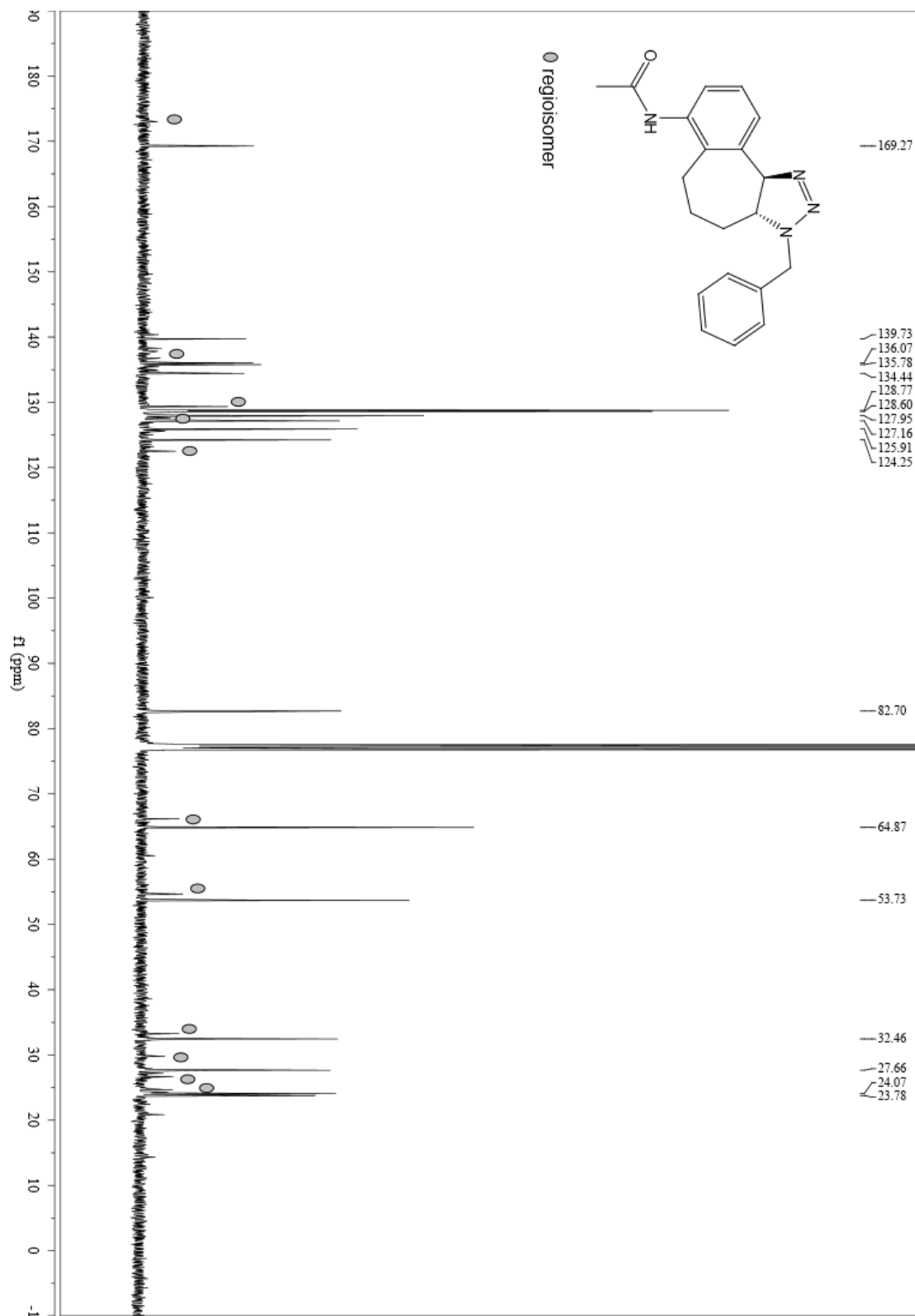
**3b (3aR,10bR)-3-(4-fluorobenzyl)-3,3a,4,5,6,10b-hexahydrobenzo[3,4]cyclohepta[1,2-d][1,2,3]triazole**



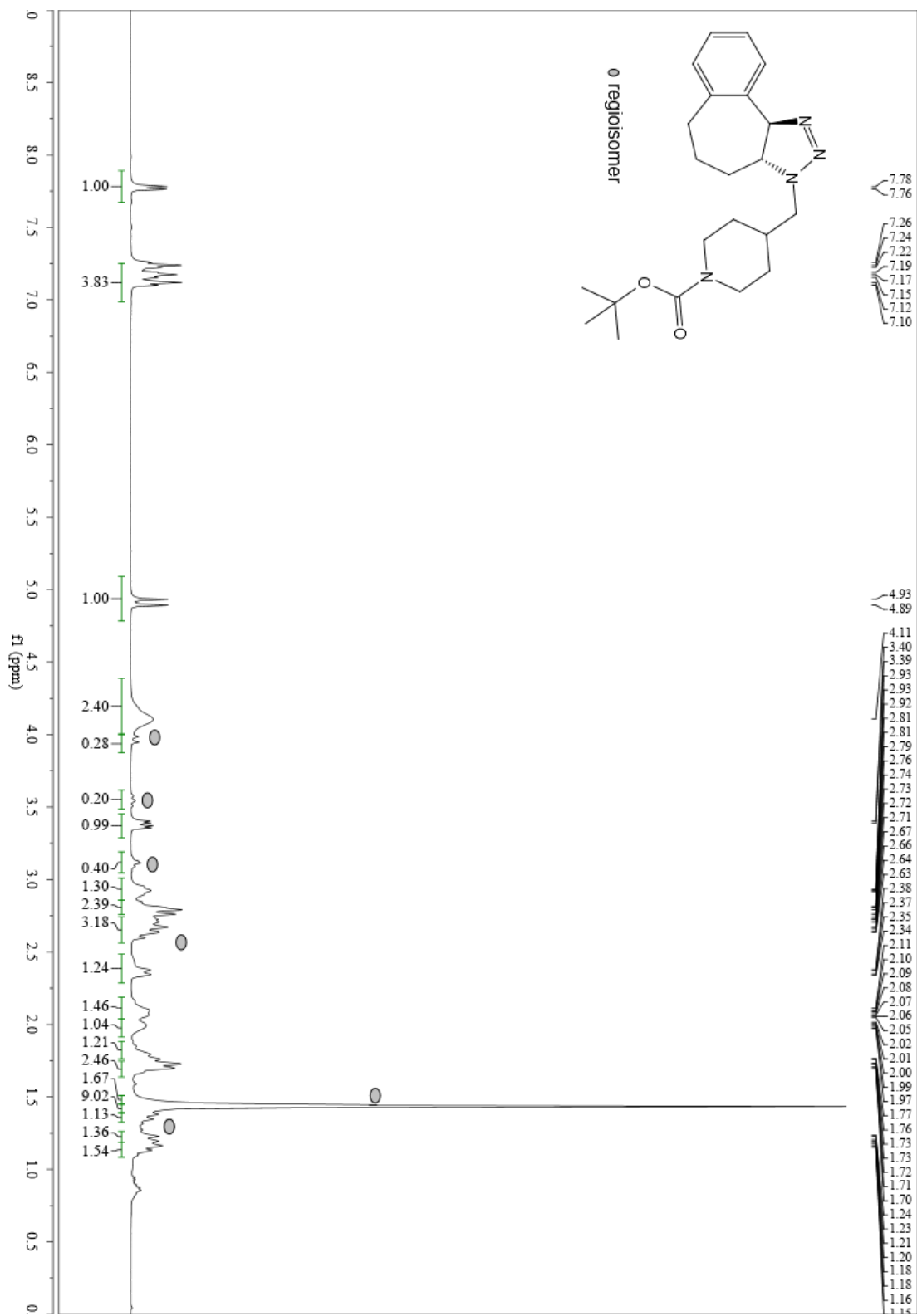
**3c N-((3aR,10bR)-3-benzyl-3,3a,4,5,6,10b-hexahydrobenzo[3,4]cyclohepta[1,2-d][1,2,3]triazol-7-yl)acetamide**



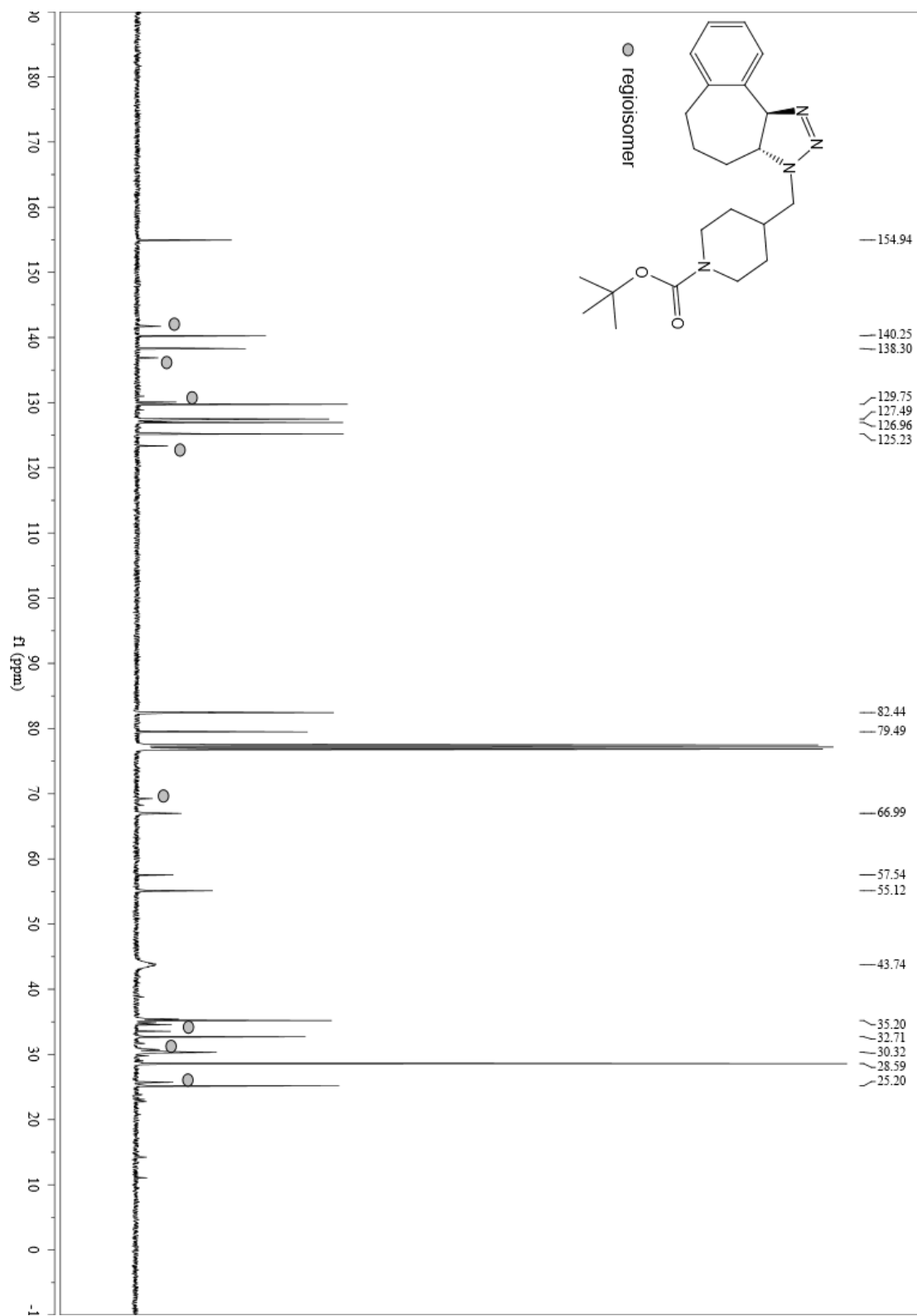
**3c N-((3aR,10bR)-3-benzyl-3,3a,4,5,6,10b-hexahydrobenzo[3,4]cyclohepta[1,2-d][1,2,3]triazol-7-yl)acetamide**



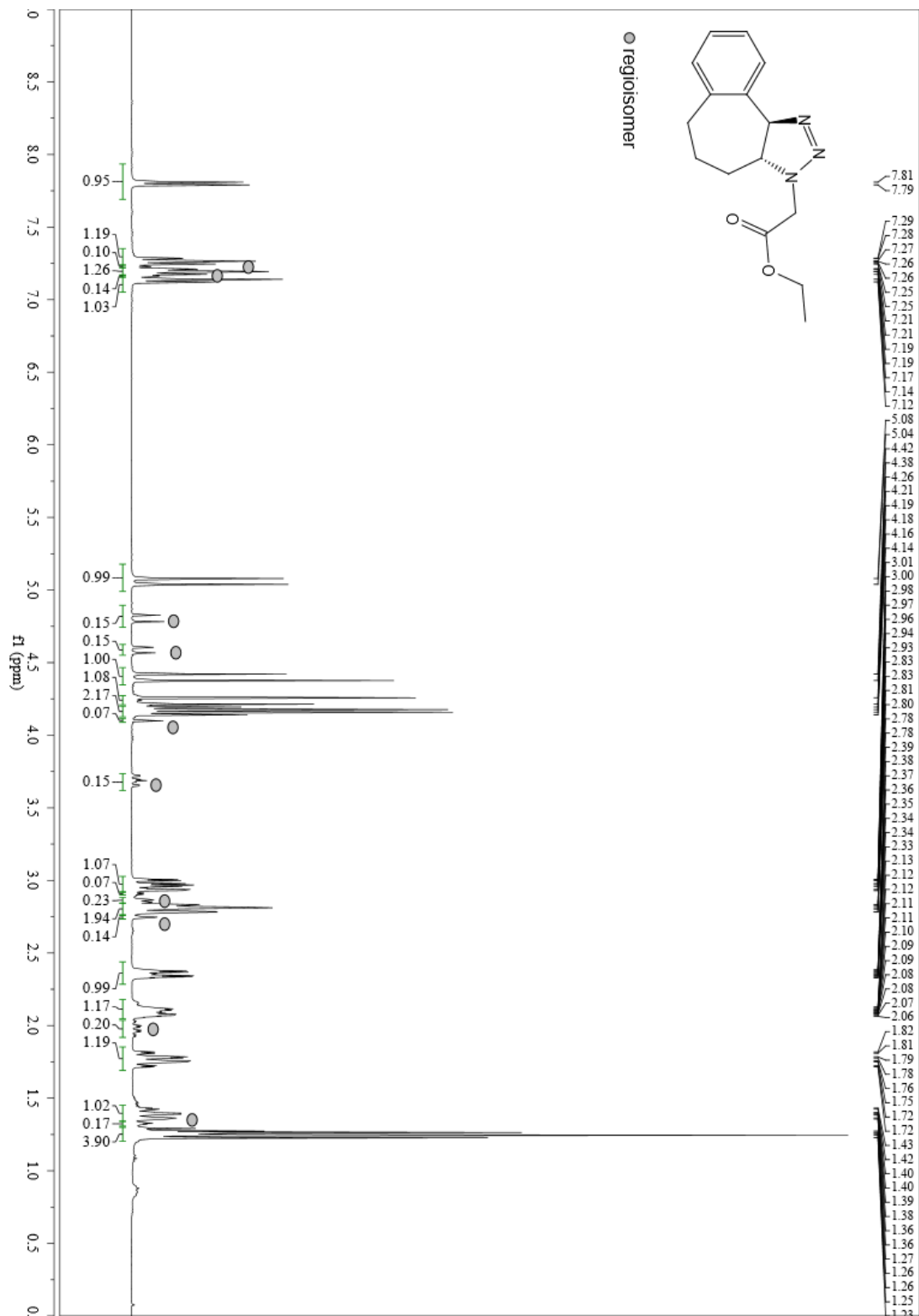
**3d** *tert*-butyl 4-(((3*aR*,10*bR*)-4,5,6,10*b*-tetrahydrobenzo[3,4]cyclohepta[1,2-*d*][1,2,3]triazol-3(3*aH*)-yl)methyl)piperidine-1-carboxylate



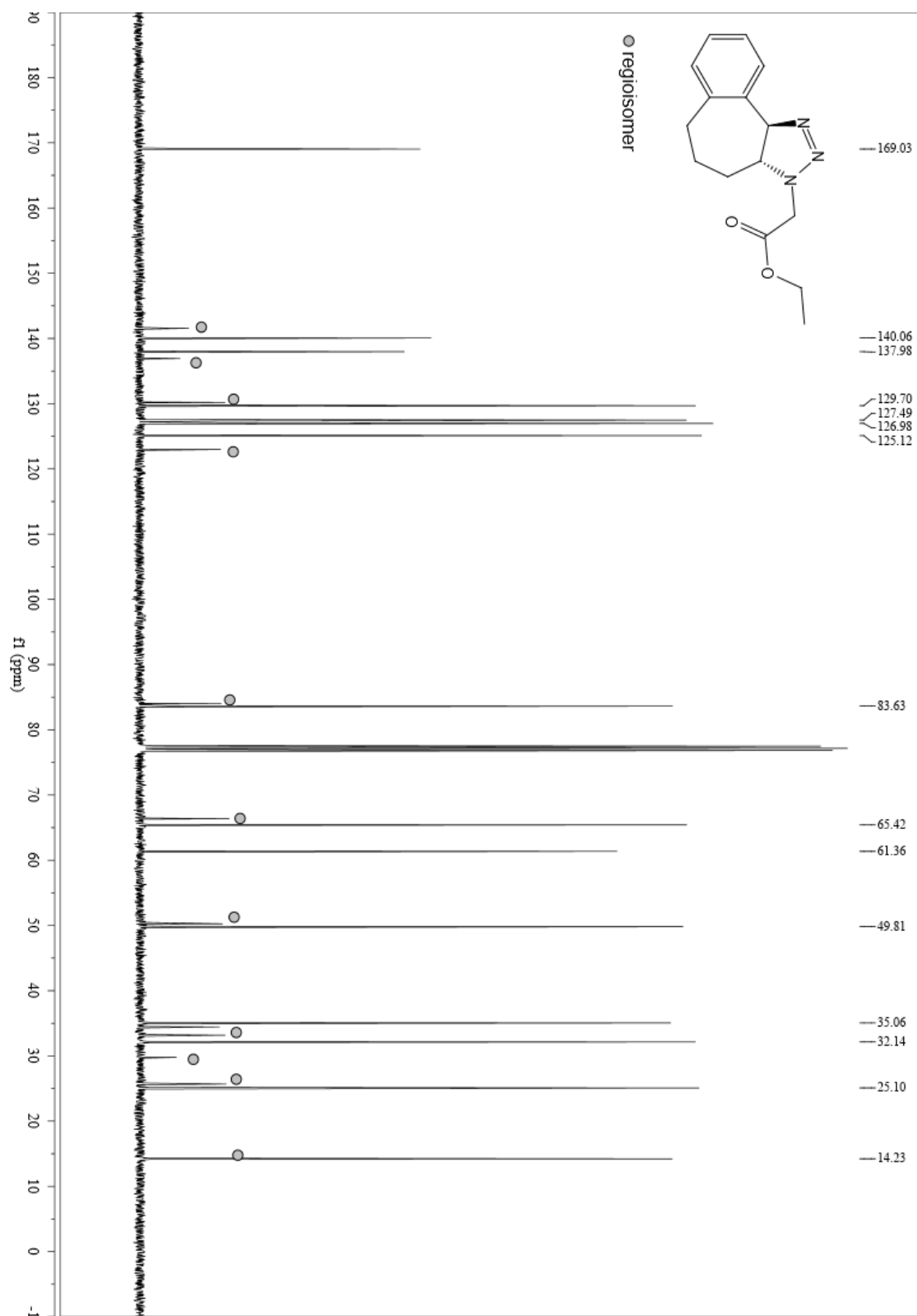
**3d** *tert*-butyl 4-(((3*aR*,10*bR*)-4,5,6,10*b*-tetrahydrobenzo[3,4]cyclohepta[1,2-*d*][1,2,3]triazol-3(3*aH*)-yl)methyl)piperidine-1-carboxylate



**3e Ethyl 2-((3aR,10bR)-4,5,6,10b-tetrahydrobenzo[3,4]cyclohepta[1,2-d][1,2,3]triazol-3(3aH)-yl)acetate**

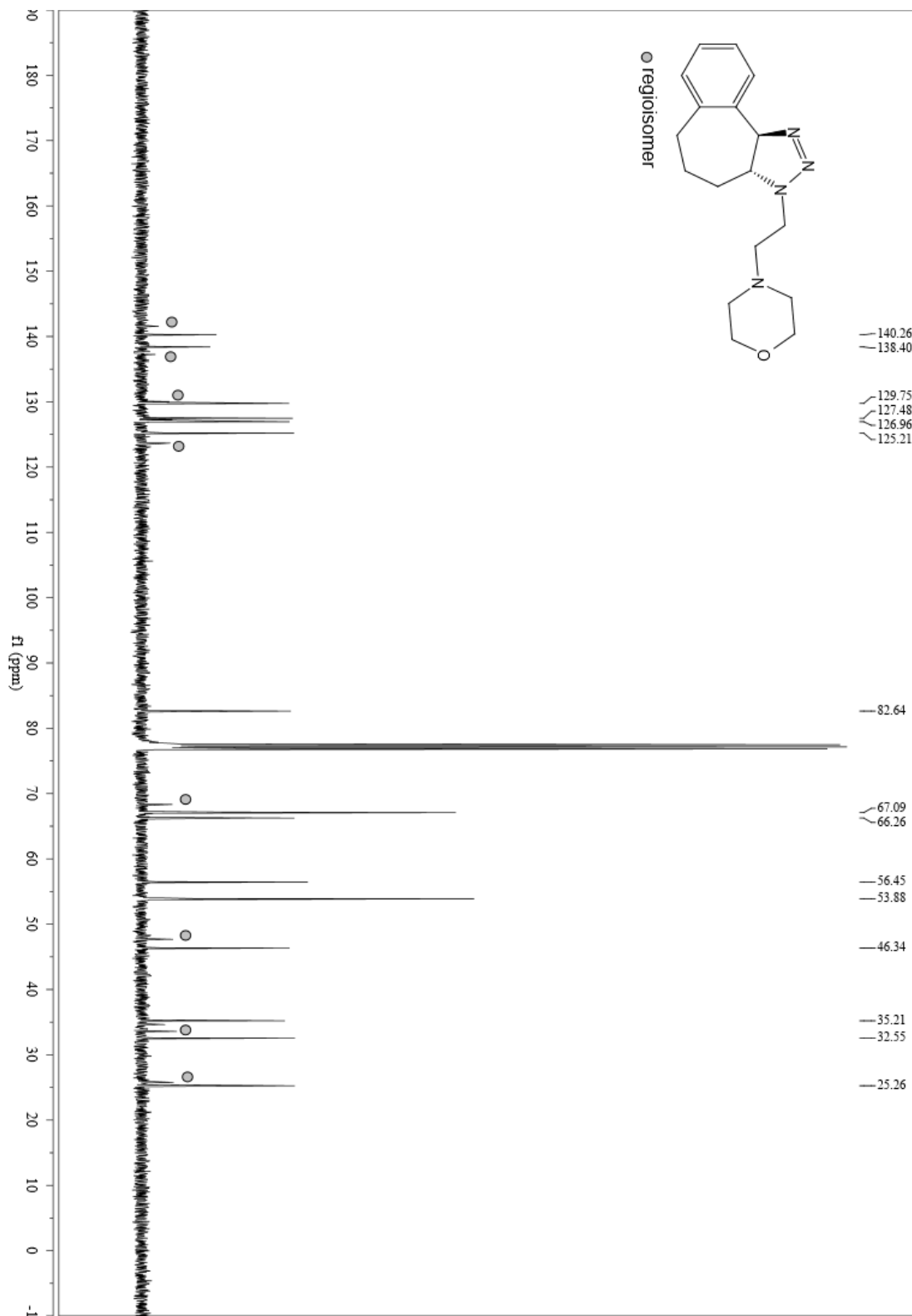


**3e Ethyl 2-((3aR,10bR)-4,5,6,10b-tetrahydrobenzo[3,4]cyclohepta[1,2-d][1,2,3]triazol-3(3aH)-yl)acetate**

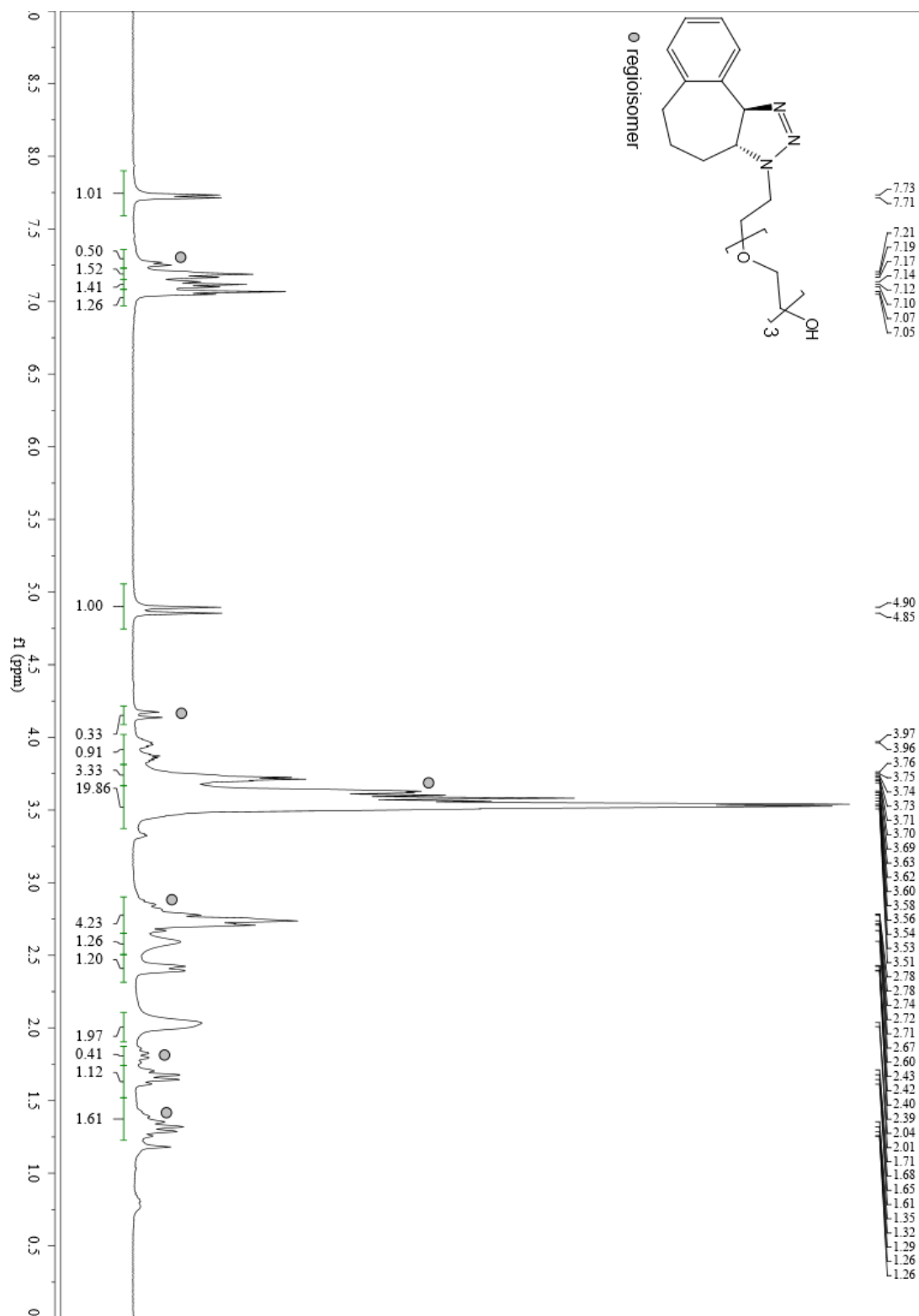




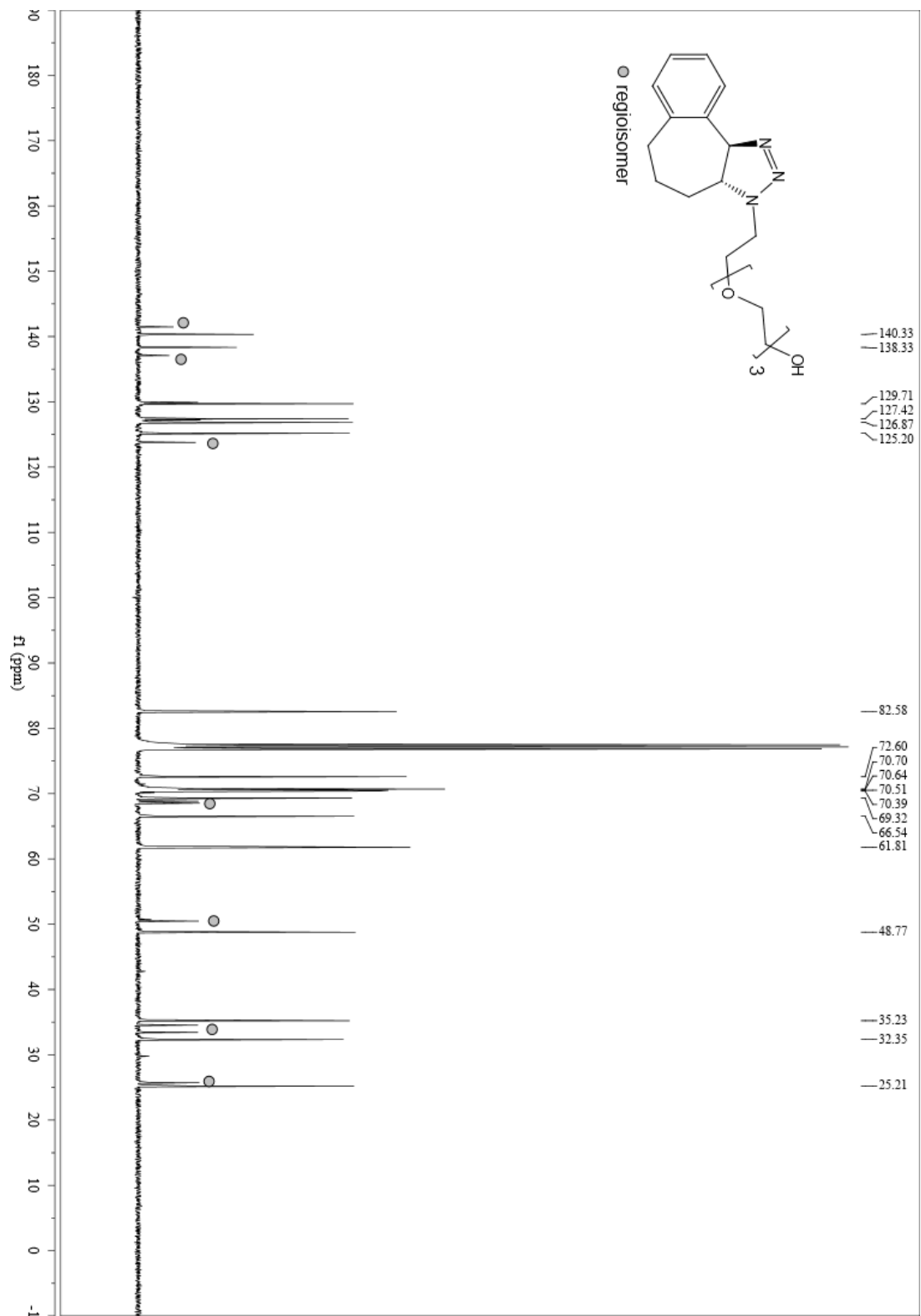
**3f 4-(2-((3aR,10bR)-4,5,6,10b-tetrahydrobenzo[3,4]cyclohepta[1,2-d][1,2,3]triazol-3(3aH)-yl)ethyl)morpholine**



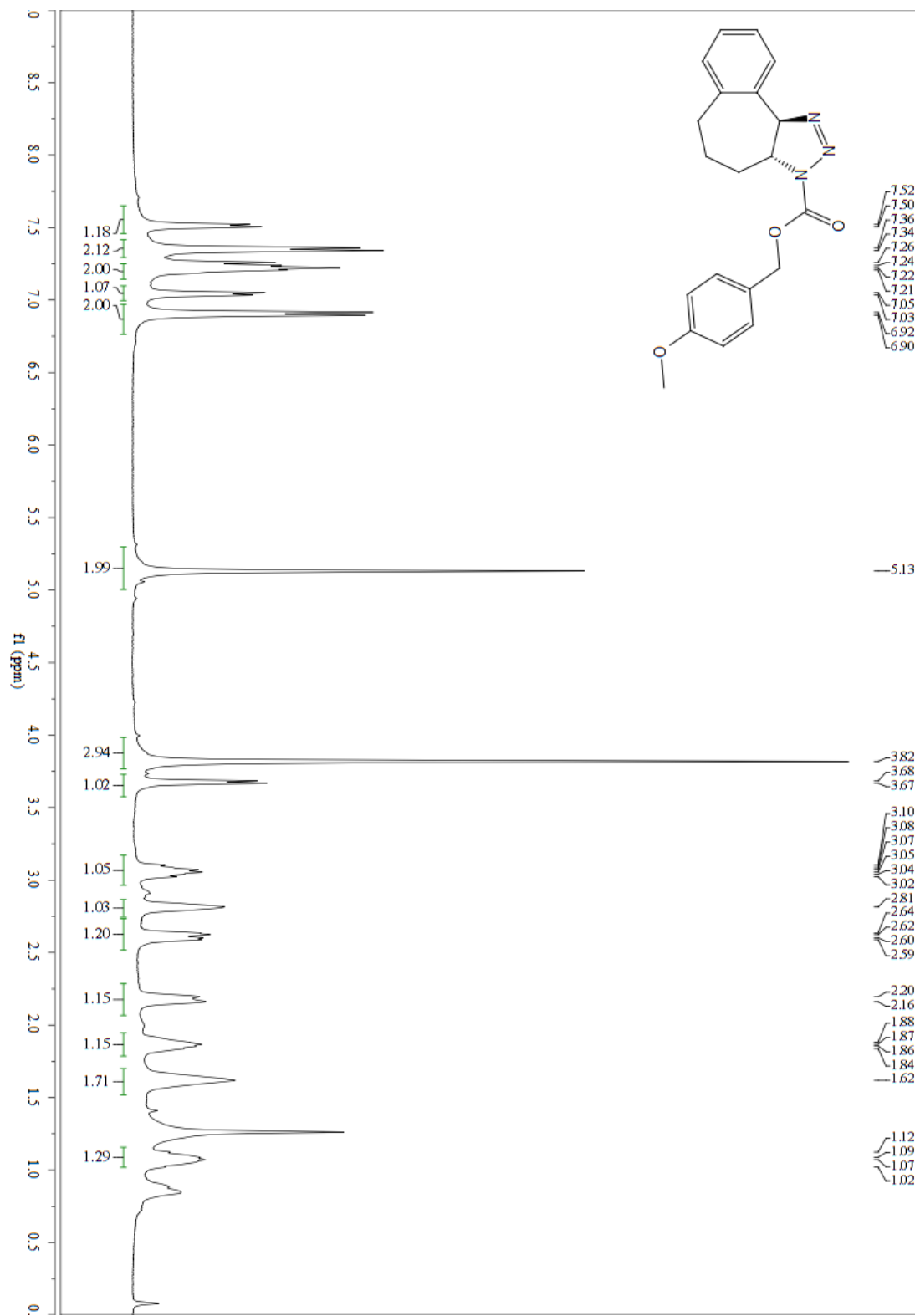
**3g 2-(2-(2-(2-((3aR,10bR)-4,5,6,10b-tetrahydrobenzo[3,4]cyclohepta[1,2-d][1,2,3]triazol-3(3aH)-yl)ethoxy)ethoxy)ethoxy)ethan-1-ol**



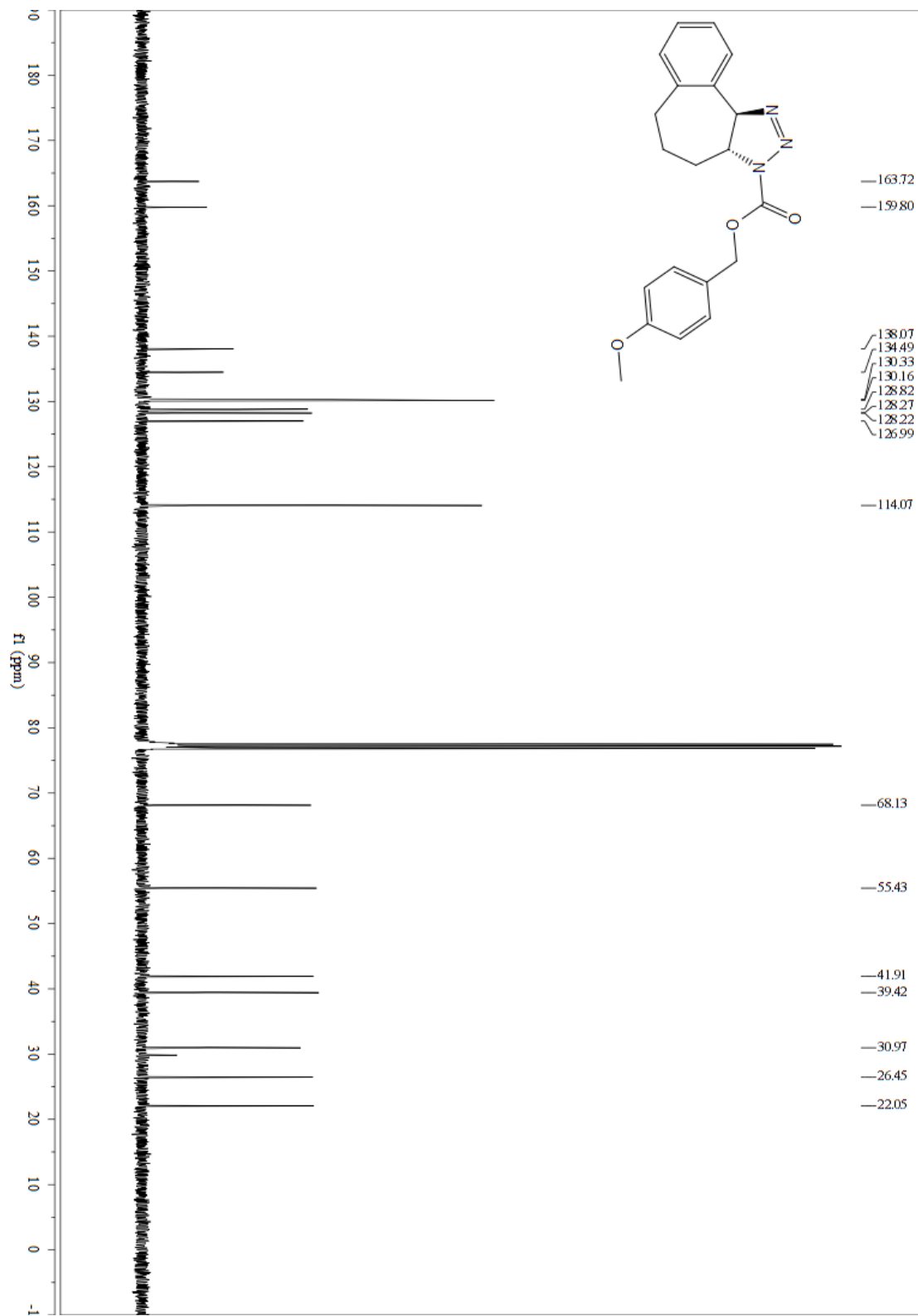
**3g 2-(2-(2-(2-((3aR,10bR)-4,5,6,10b-tetrahydrobenzo[3,4]cyclohepta[1,2-d][1,2,3]triazol-3(3aH)-yl)ethoxy)ethoxy)ethoxy)ethan-1-ol**



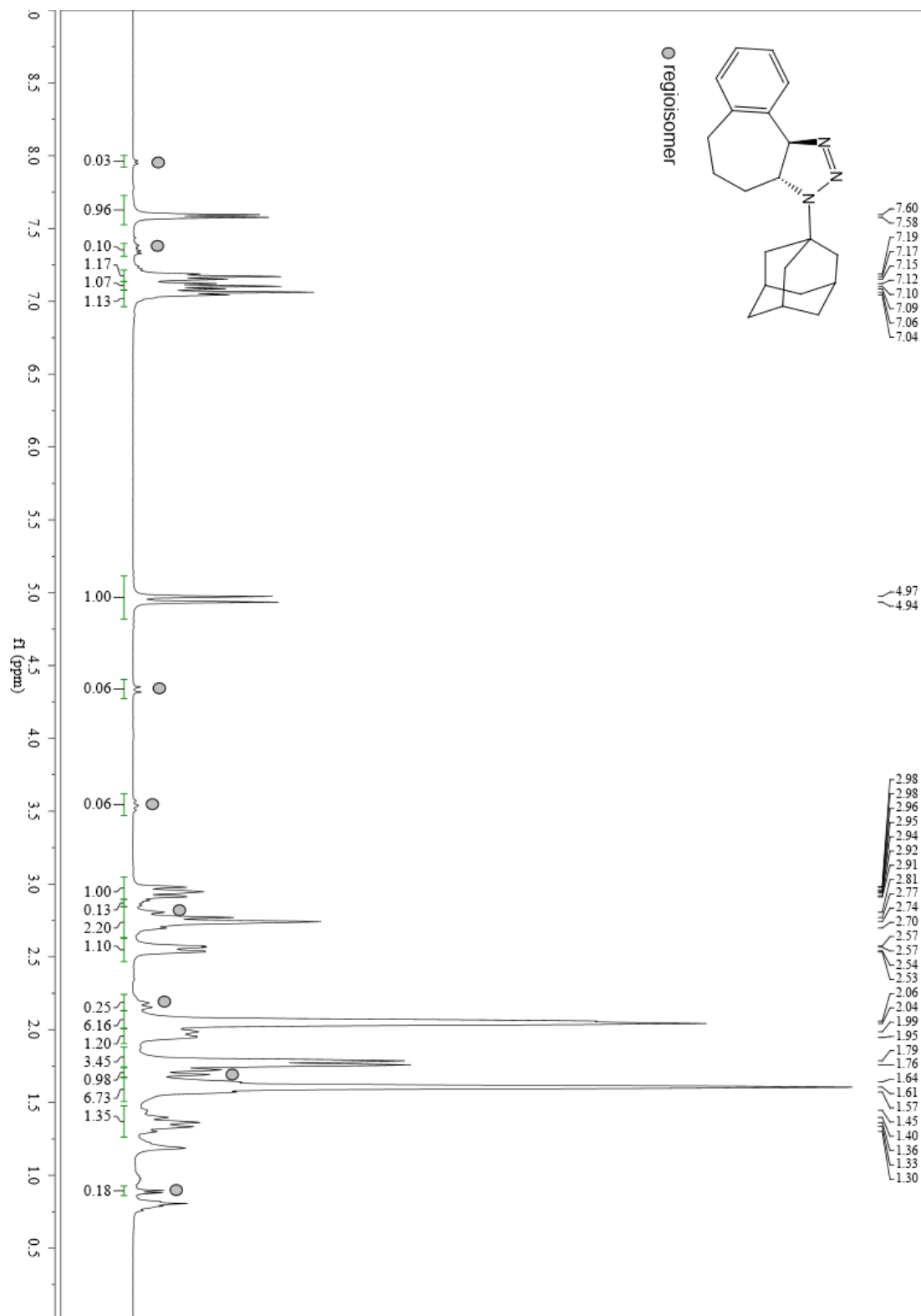
**3h 4-methoxybenzyl (3aR,10bR)-4,5,6,10b-tetrahydrobenzo[3,4]cyclohepta[1,2-d][1,2,3]triazole-3(3aH)-carboxylate**



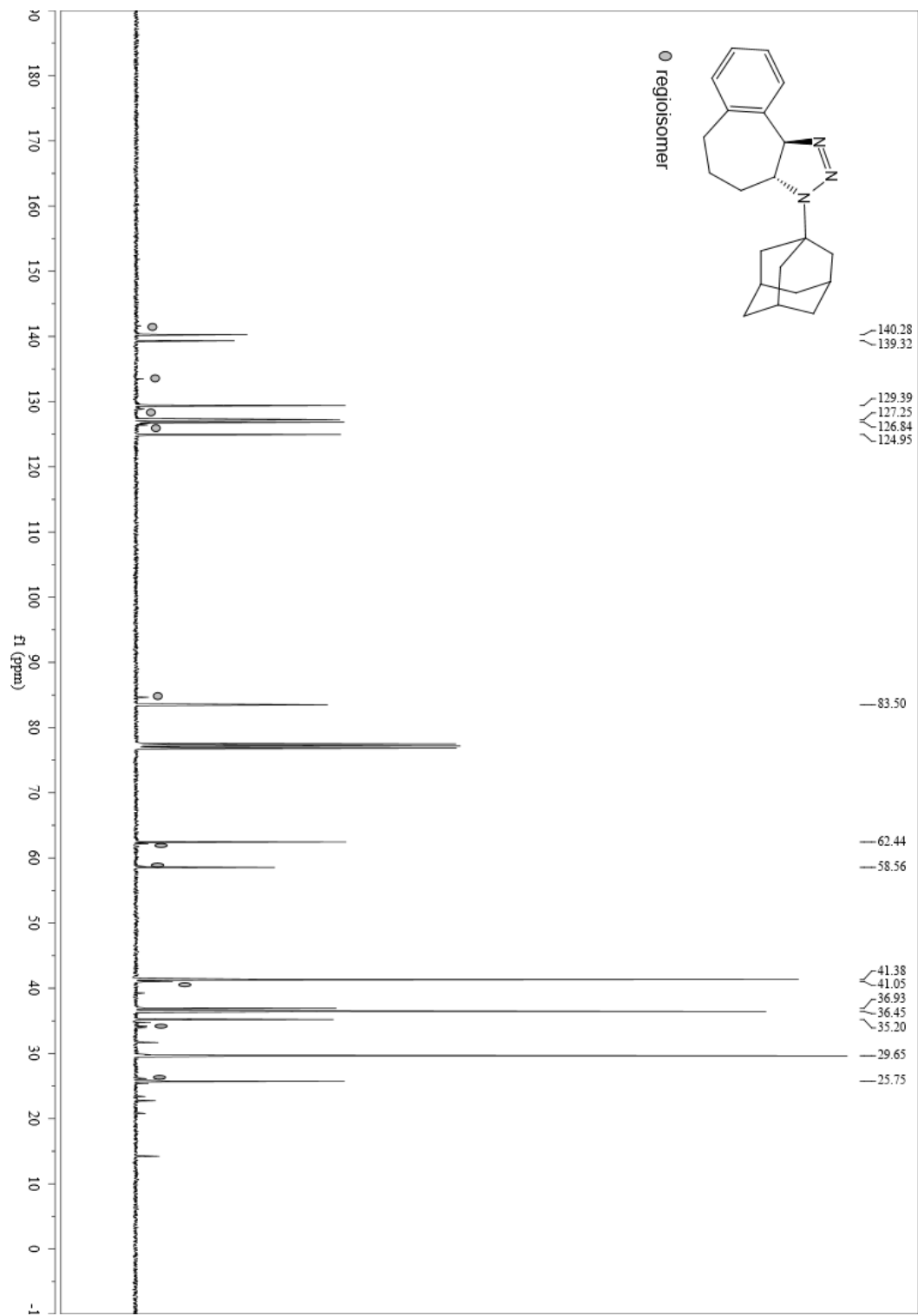
**3h 4-methoxybenzyl (3aR,10bR)-4,5,6,10b-tetrahydrobenzo[3,4]cyclohepta[1,2-d][1,2,3]triazole-3(3aH)-carboxylate**



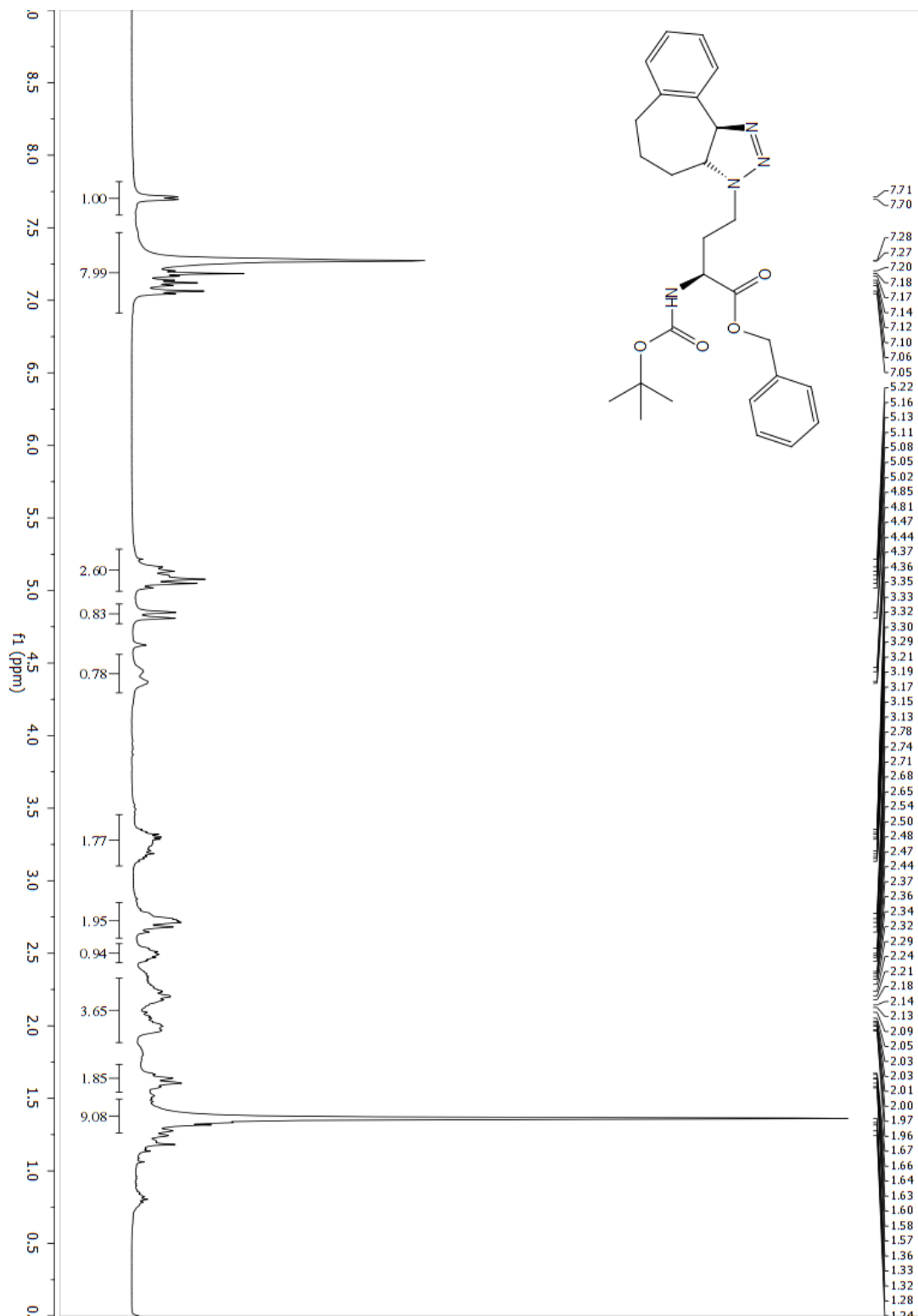
**3i (3aR,10bR)-3-((3S,5S,7S)-adamantan-1-yl)-3,3a,4,5,6,10b-hexahydrobenzo[3,4]cyclohepta[1,2-d][1,2,3]triazole**



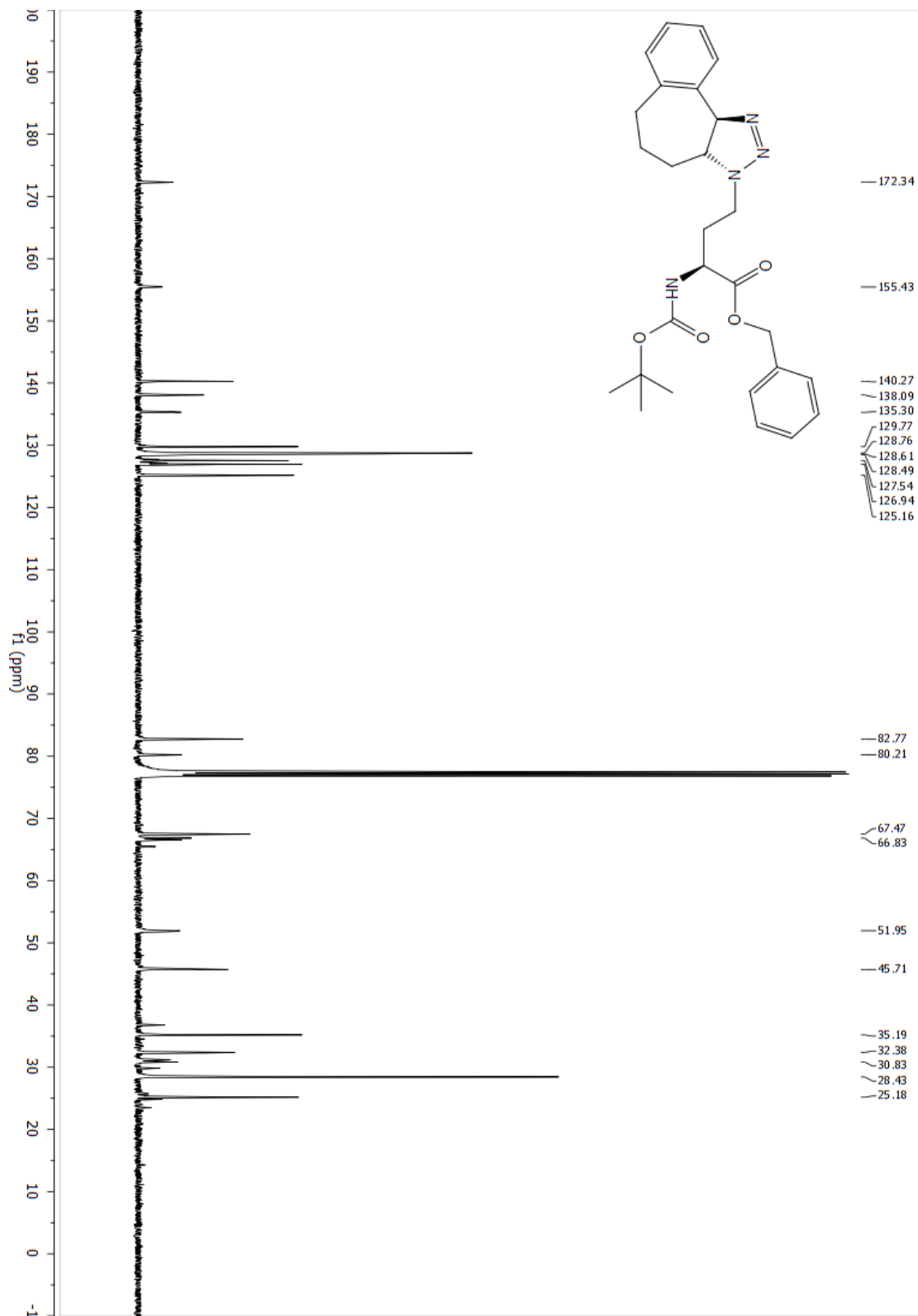
**3i (3aR,10bR)-3-((3S,5S,7S)-adamantan-1-yl)-3,3a,4,5,6,10b-hexahydrobenzo[3,4]cyclohepta[1,2-d][1,2,3]triazole**



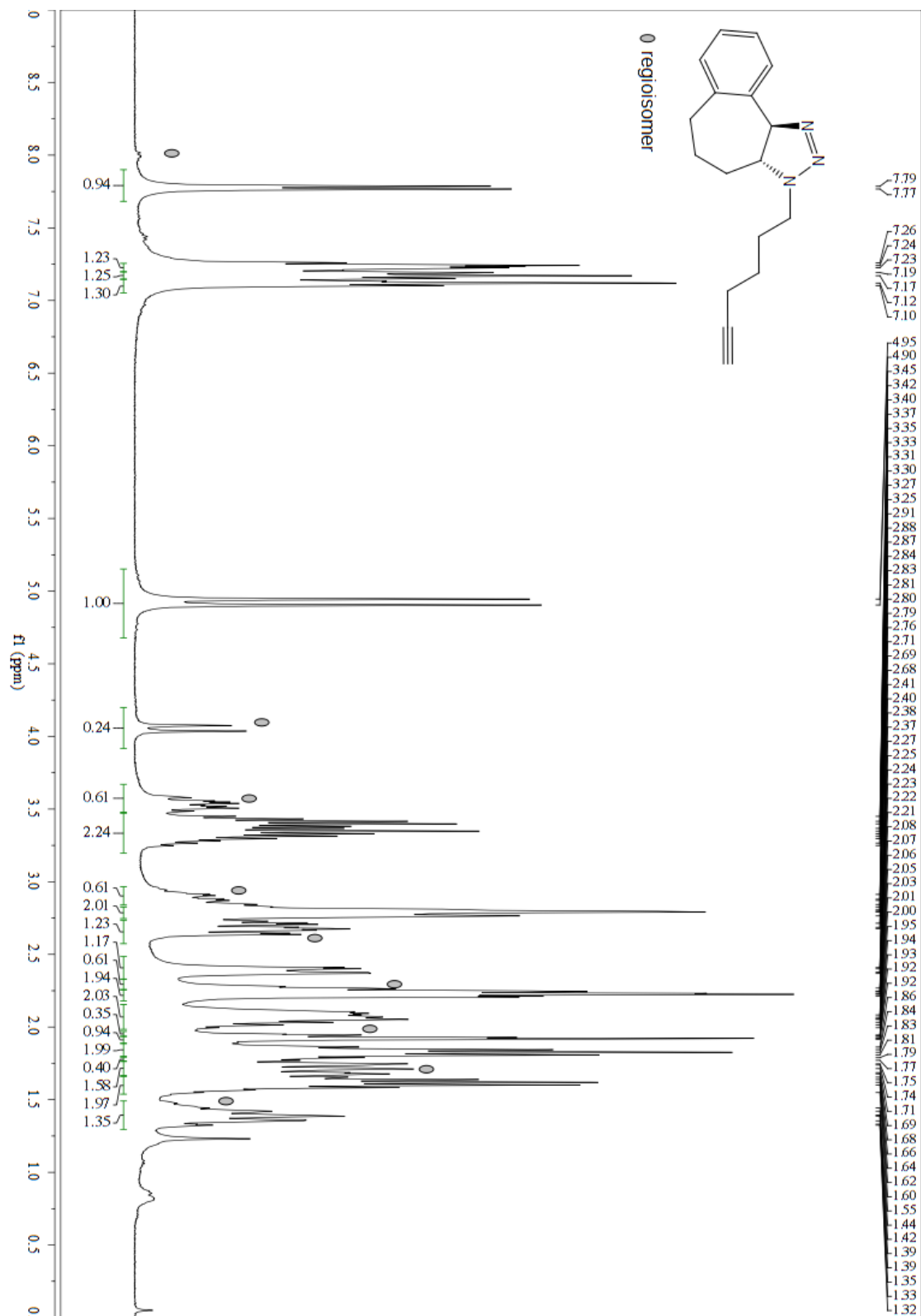
**3j Benzyl (S)-2-((tert-butoxycarbonyl)amino)-4-((3aR,10bR)-4,5,6,10b-tetrahydrobenzo[3,4]cyclohepta[1,2-d][1,2,3]triazol-3(3aH)-yl)butanoate**



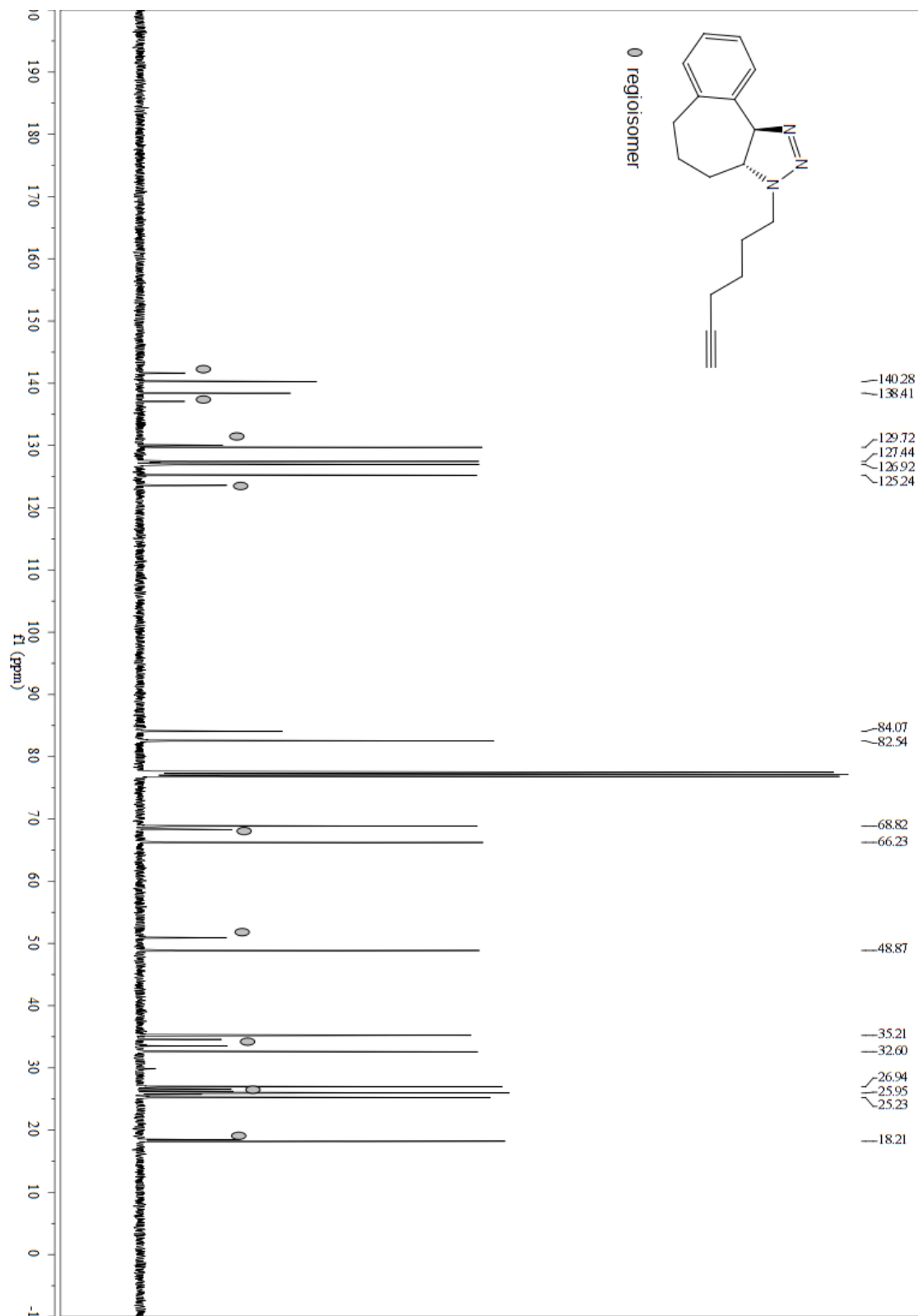
**3j Benzyl (S)-2-((tert-butoxycarbonyl)amino)-4-((3aR,10bR)-4,5,6,10b-tetrahydrobenzo[3,4]cyclohepta[1,2-d][1,2,3]triazol-3(3aH)-yl)butanoate**



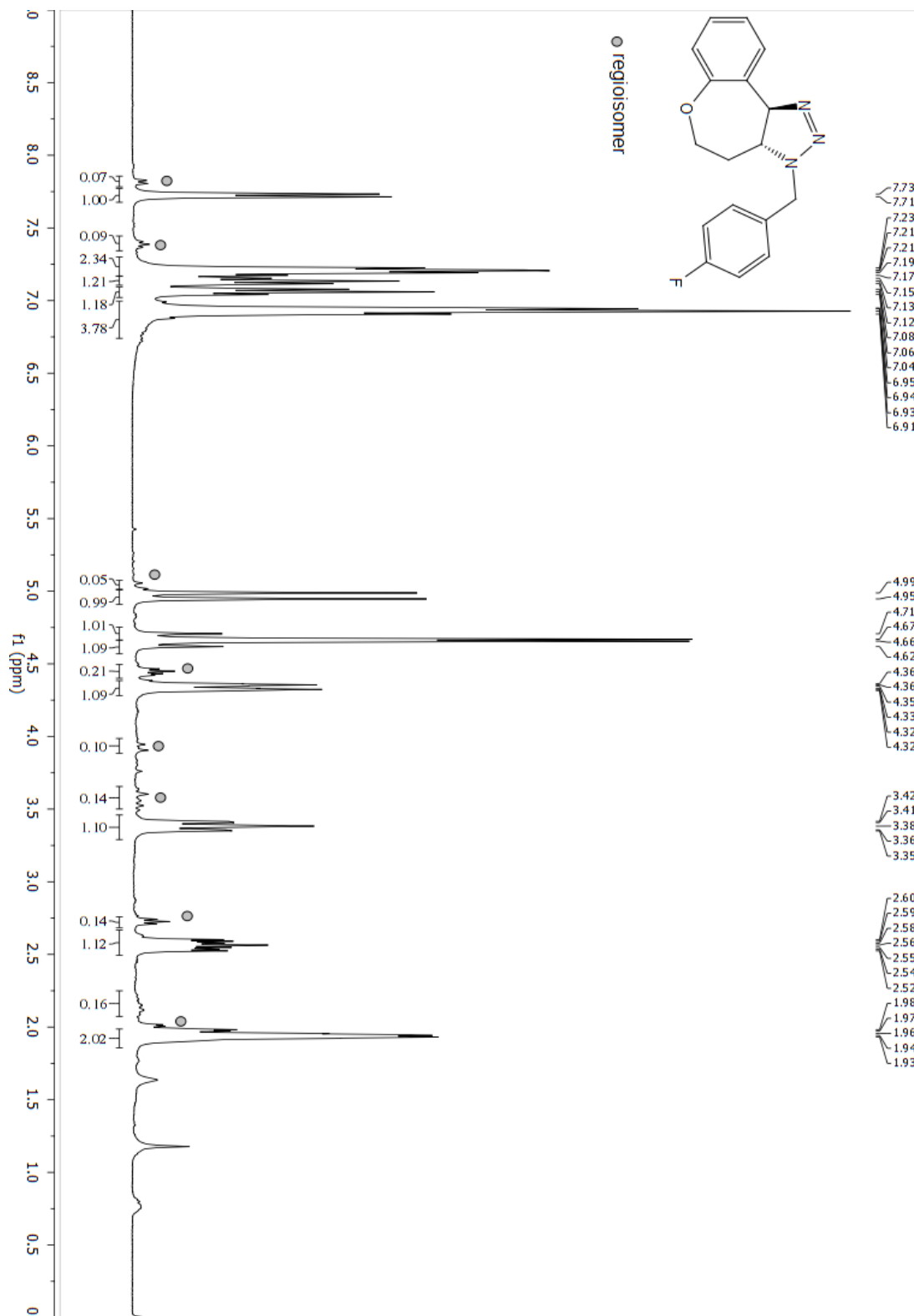
**3k (3aR,10bR)-3-(hex-5-yn-1-yl)-3,3a,4,5,6,10b-hexahydrobenzo[3,4]cyclohepta[1,2-d][1,2,3]triazole**



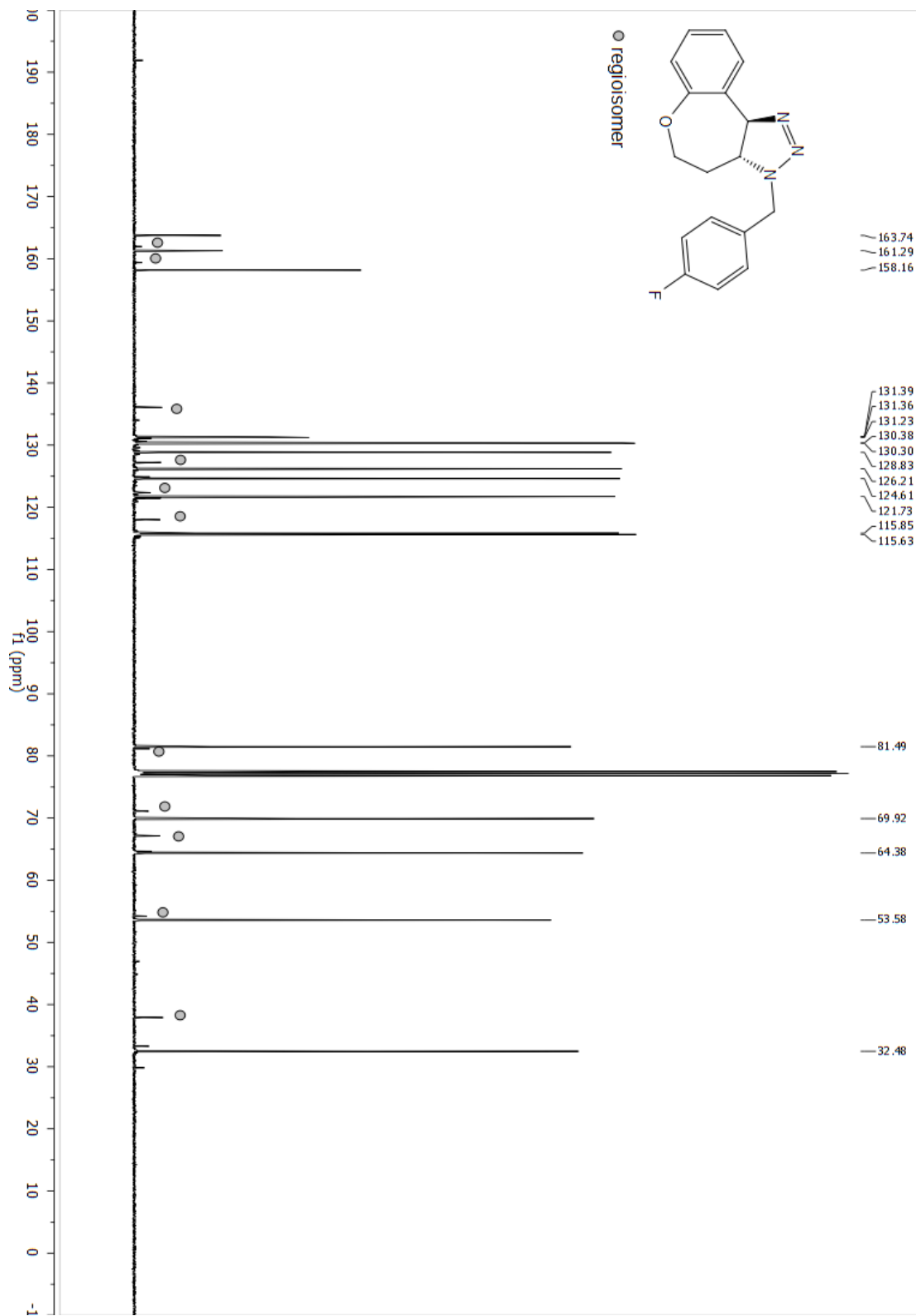
**3k (3aR,10bR)-3-(hex-5-yn-1-yl)-3,3a,4,5,6,10b-hexahydrobenzo[3,4]cyclohepta[1,2-d][1,2,3]triazole**



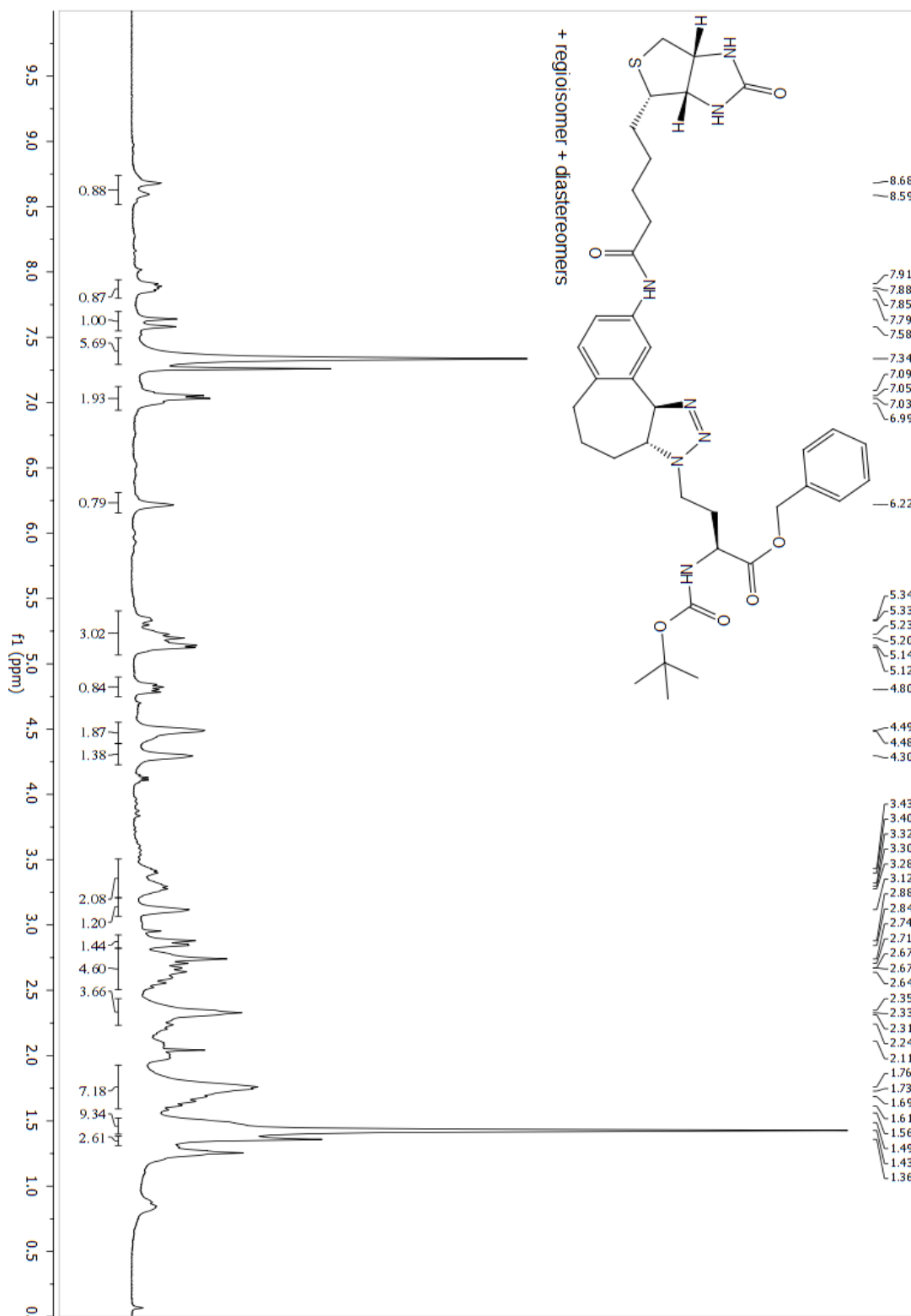
**3l (3aR,10bR)-3-(4-fluorobenzyl)-3a,4,5,10b-tetrahydro-3H-benzo[2,3]oxepino[4,5-d][1,2,3]triazole**



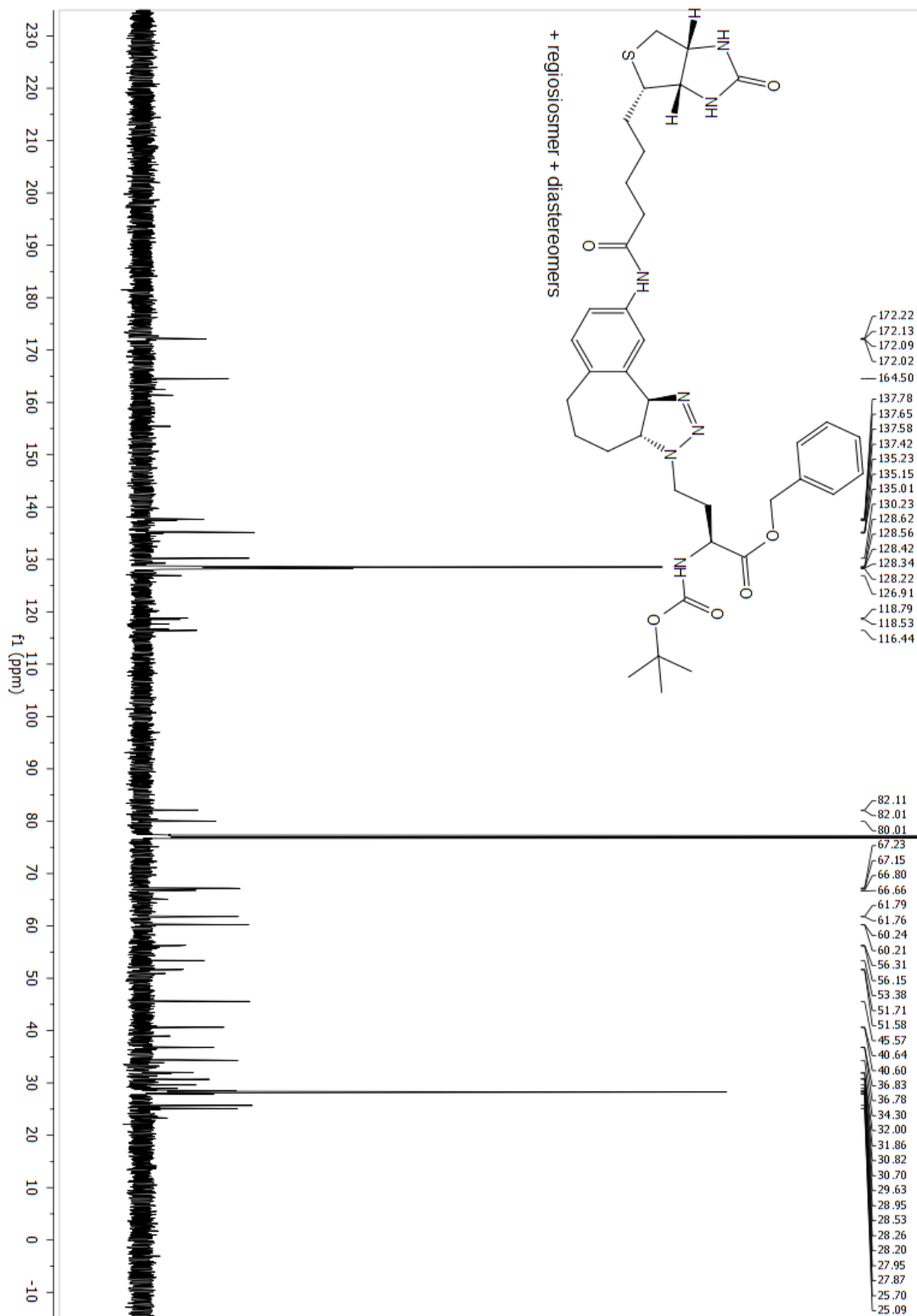
**3l (3aR,10bR)-3-(4-fluorobenzyl)-3a,4,5,10b-tetrahydro-3H-benzo[2,3]oxepino[4,5-d][1,2,3]triazole**



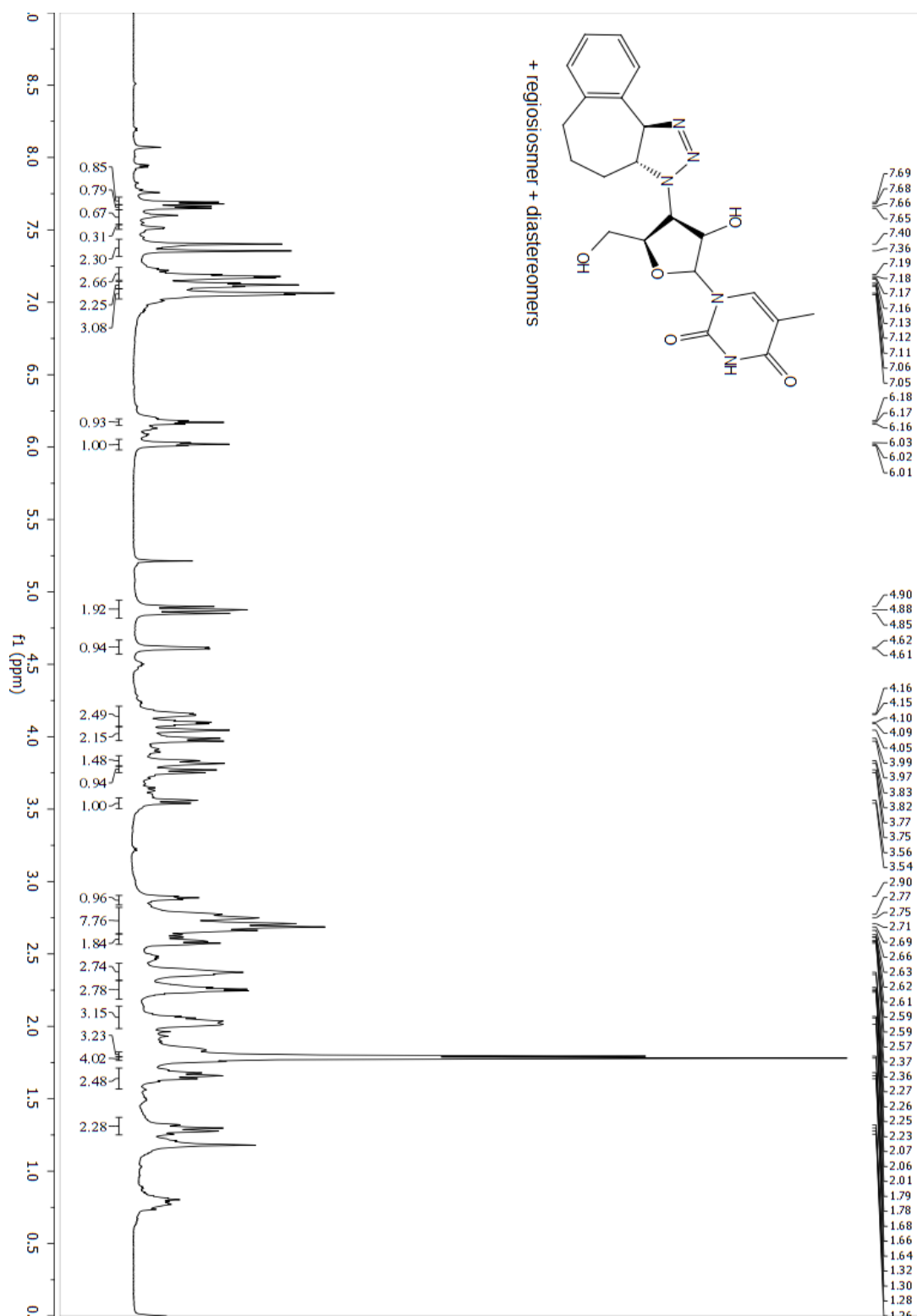
**3m benzyl (S)-2-((tert-butoxycarbonyl)amino)-4-((3aR,10bR)-9-(5-((3aS,4S,6aR)-2-oxohexahydro-1H-thieno[3,4-d]imidazol-4-yl)pentanamido)-4,5,6,10b-tetrahydrobenzo[3,4]cyclohepta[1,2-d][1,2,3]triazol-3(3aH)-yl)butanoate**



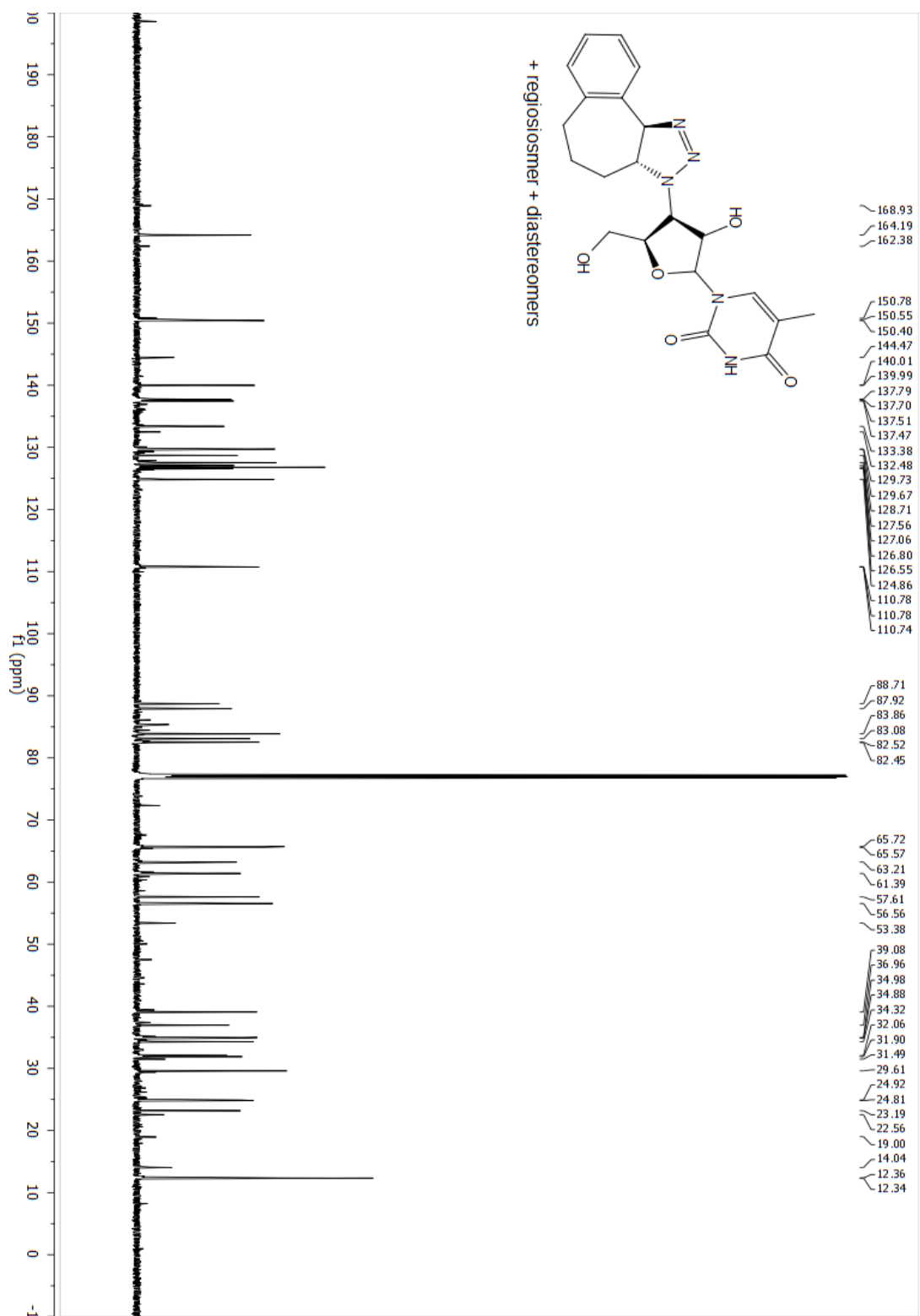
**3m benzyl (S)-2-((tert-butoxycarbonyl)amino)-4-((3aR,10bR)-9-(5-((3aS,4S,6aR)-2-oxohexahydro-1H-thieno[3,4-d]imidazol-4-yl)pentanamido)-4,5,6,10b-tetrahydrobenzo[3,4]cyclohepta[1,2-d][1,2,3]triazol-3(3aH)-yl)butanoate**



**3n 1-((3R,4S,5R)-3-hydroxy-5-(hydroxymethyl)-4-((3aR,10bR)-4,5,6,10b-tetrahydrobenzo[3,4]cyclohepta[1,2-d][1,2,3]triazol-3(3aH)-yl)tetrahydrofuran-2-yl)-5-methylpyrimidine-2,4(1H,3H)-dione**



**3n 1-((3R,4S,5R)-3-hydroxy-5-(hydroxymethyl)-4-((3aR,10bR)-4,5,6,10b-tetrahydrobenzo[3,4]cyclohepta[1,2-d][1,2,3]triazol-3(3aH)-yl)tetrahydrofuran-2-yl)-5-methylpyrimidine-2,4(1H,3H)-dione**



## CHAPTER IV

### A RARE THERMAL [2+2] CYCLOADDITION OF ARYL CYCLOHEPTENES

Continuing our efforts to develop methodologies to drive endergonic reactions and utilize it further in useful chemical synthesis, we sought to develop the [2+2] cycloaddition reactions of cycloheptenes. While we were designing cyclic alkenes for the bioconjugation reaction with azides, we came across phenyl cycloheptene (**PC7**) which did undergo [3+2] cycloaddition with azide under visible light mediated photocatalyzed conditions but did not produce azide conjugated adduct as the major product. Instead, a [2+2] cycloadduct of **PC7** was observed as the major product and when the coupling partner azide was left out from the reaction mixture, complete [2+2] dimerization of **PC7** was observed with no other byproduct forming. We became interested in developing this methodology as close scrutiny of the reaction revealed that we might be performing a thermal [2+2] cycloaddition reaction between the highly strained ground state *trans*-PC7 and *cis*-PC7. This itself becomes interesting since the thermal [2+2] cycloaddition reactions are generally considered “forbidden” because the suprafacial approach of  $\pi$ -orbitals of the alkenes does not give the necessary overlap. Despite that [2+2] cycloadditions are often energetically favorable ( $\Delta G^\circ = -18.0$  kcal/mol for dimerization of ethene),<sup>1-2</sup> they are generally kinetically much less feasible because of steric inhibition, the orbital symmetry requirements can be met via an antara- / suprafacial approach of the alkenes.<sup>3</sup> The common exception is the  $[\pi 2_s + \pi 2_a]$  of ketenes with alkenes, which is made possible because of the minimal steric hindrance of the ketene partner. Transition metal catalysis offers alternative pathways to promote [2+2] cycloaddition reactions,<sup>4-6</sup> with Ti, Mn, Fe, and Ni having been employed.<sup>7-8</sup> The presence of d-orbitals in the transition metals allows

the [2+2] reaction between alkenes by virtue of low energy pathways to metallacycle intermediates. Another way to overcome the orbital symmetry constraint is to proceed through the photochemical [2+2], in which a higher energy orbital is utilized and allows the more facile suprafacial approach of both alkenes in the cycloaddition.<sup>9</sup> Unfortunately, the direct irradiation of cycloalkenes with a high energy UV light source often produces a mixture of rearranged products.

One alternative to direct irradiation is sensitization. However, again the sensitization of the cycloalkenes, when UV light is used, generally produces a mixture of various cyclobutane stereoisomers as well as other sensitizer-alkene adducts. These are formed from different mechanisms originating on the excited state alkene surface. Another strategy which has been investigated is the formation and subsequent trapping of the ground state *trans*-cycloheptene, which can result upon relaxation from the excited state.<sup>10-11</sup> Corey and Eaton<sup>12</sup> have demonstrated the ability to generate *trans*-cycloheptenones via direct UV irradiation, and Bunce<sup>13</sup> and Margaretha<sup>14</sup> have studied their dimerization to cyclobutanes. Consequently, despite promising results, essentially not much scope was demonstrated.<sup>15</sup> This strategy becomes much more attractive if visible light can be used for excitation, because of the lower energy irradiation.<sup>16</sup>

A conceptually different approach to synthesizing cyclobutanes is to initially capture the energy in the form of ring strain. Owing to the immense ring strain (*ca.* 27-36 kcal/mol for *trans*-cycloheptene),<sup>10, 17-19</sup> subsequent energy barriers are expected to be relatively diminished. The decreased relative energy barriers of the transition states might make it possible for otherwise difficult thermal [ $\pi 2_s + \pi 2_a$ ] cycloadditions to take place for ground state alkenes. For cyclic alkenes, isomerization leads to *trans*-cycloalkenes, which are known to increase in strain energy with decreasing ring size.<sup>20</sup> The key to success, would be controlling the concentration of both the excited alkene, and the strained *trans*-cycloalkene. Based on our previous work,<sup>17, 21-22</sup> we anticipated that the use of visible light photocatalysis would allow us to carefully control the concentration of transient, highly strained, *trans*-phenylcycloheptene, which we anticipated would

either undergo the desired thermal  $[\pi 2_s + \pi 2_a]$  reaction with the more abundant *cis*-phenylcycloheptene, or alternatively simply revert back to the relaxed isomer with the evolution of heat. Moving out of the UV and into the visible spectrum would ensure that competitive photochemical [2+2] does not occur, and might make it possible to selectively perform a thermal  $[\pi 2_s + \pi 2_a]$  cycloaddition.

#### 4.1 Optimization of reaction conditions

Starting with similar conditions to our previous work,<sup>23</sup> we performed a reaction with Ir catalyst A (0.3 mol%) in MeCN, at 30 °C, under an atmosphere of argon, with 0.05 M concentration of **m-4a**, using blue LEDs. We were pleased to see 80% conversion to the desired product **d-4a** after 24 h of irradiation, as observed by <sup>19</sup>F NMR (entry 1, Table 8). Screening revealed that the reaction progressed in a number of solvents, which is consistent with a reaction that does not generate polar intermediates. However, the solvent dimethylformamide (DMF) provided full conversion within 24 h of irradiation (entry 3). Next, we examined the role of the catalyst structure in the reaction. For these experiments, lower catalyst loadings (0.08 mol%) were used to slow the reactions, and exaggerate the differences in reactivity, making it easier to discern the effects on the rates of the reactions.

We anticipated that the catalyst structure would be important, having previously observed that the catalyst volume, in addition to its emissive energy, played a significant role in the rate of isomerization of styrene derivatives; rates slowed as the photocatalyst became larger.<sup>24</sup> Indeed, we found that **Cat A**,<sup>25</sup> which is significantly smaller<sup>26</sup> than the other catalysts, gave higher conversion in the same time period than sterically larger **Cat B**, **Cat C**, and **Cat D** (entries 6-9). The emissive energies of **Cat C** and **Cat D** are substantially higher than that of catalyst **Cat B**, confirming that the exergonicity of the sensitization is not the only important feature. Thus, we used **Cat A** for further optimization. Next, the effect of catalyst loading was evaluated. With higher catalyst loadings, greater conversion to the product **d-4a** was observed within the same time period (entries

10-12). The photocatalyst is an 18-electron complex that is coordinatively saturated with three chelating ligands, making it very robust. This is evidenced by the high catalyst turnover number (1563 in entry 10), and likely represents a minimum since this was suboptimal conditions, and that the reaction had not yet reached completion.

Reaction:  $m\text{-4a} \xrightarrow[\text{MeCN, blue LEDs}]{\text{Ir cat, 30 }^\circ\text{C, Ar}} d\text{-4a}$

Cat A  
Emission: 58.6 kcal/mol  
Radius: 4.56 Å

entry	R	solvent	temp (°C)	Ir cat	cat. loading (mol%)	%conv- -ersion <sup>a</sup>	time (h)	initial [m-4a] (M)
1	F	MeCN	30	A	0.300	80	24	0.05
2	F	CH <sub>2</sub> Cl <sub>2</sub>	30	A	0.300	72	24	0.05
3	F	DMF	30	A	0.300	100	24	0.05
4	F	THF	30	A	0.300	83	24	0.05
5	F	Et <sub>2</sub> O	30	A	0.300	47	24	0.05
6	H	DMF	30	A	<b>0.0800</b>	55	37	0.05
7	H	DMF	30	B	0.0800	48	37	0.05
8	H	DMF	30	C	0.0800	36	37	0.05
9	H	DMF	30	D	0.0800	23	37	0.05
10	H	DMF	30	A	<b>0.0320</b>	50	22	<b>0.5</b>
11	H	DMF	30	A	<b>0.0640</b>	88	22	0.5
12	H	DMF	30	A	<b>0.125</b>	95	22	0.5
13	H	DMF	<b>-30</b>	A	0.125	80	18	0.5
14	H	DMF	<b>0</b>	A	0.125	79	18	0.5
15	H	DMF	<b>15</b>	A	0.125	76	18	0.5
16	H	DMF	<b>30</b>	A	0.125	95	18	0.5
17	F	DMF	30	-	-	0	18	0.5
18 <sup>b</sup>	F	DMF	30	A	0.125	0	18	0.5

Cat B  
Emission: 54.5 kcal/mol  
Radius: 5.00 Å

Cat C  
Emission: 60.1 kcal/mol  
Radius: 5.02 Å

Cat D  
Emission: 60.4 kcal/mol  
Radius: n/a Å

<sup>a</sup> Monitored by <sup>19</sup>F NMR. <sup>b</sup> Reaction was performed in dark.

Table 8. Optimization of  $[\pi_2s+\pi_2a]$  cycloaddition reaction conditions

Given that the lifetime of the strained *trans*-cycloheptene was anticipated to decrease with increasing temperature, we evaluated the effect of temperature on the reaction outcome. To our surprise, the rate of reaction was found to be relatively impervious across a range of temperatures (-30 to 15 °C) (entries 13-16), however, upon increasing to 30 °C, an increase in the reaction rate was observed. Further increase of the temperature to 45 °C and 90 °C did not lead to further

improvement. Finally, control experiments revealed that both light and photocatalyst were necessary components for the desired  $[\pi 2_s + \pi 2_a]$  cycloaddition reaction.

#### 4.2 Stereochemical assessment of diastereomers

Having determined the optimal conditions, we next assessed the stereochemical outcome of the reaction. When allylic alcohol **m-4a** was dimerized, X-ray analysis revealed that the major diastereomer was the C2-symmetric cyclobutandiol (Fig. 14), **d-4a**. Specifically, it showed that the dimerization resulted in the formation of the head-to-head regioisomer, and that both 7-membered rings were *trans*-fused onto the cyclobutane and *trans* to the other 7-membered ring. Both rings adopted a chair conformation and displayed an interaction between the pi-system and the hydroxyl proton.

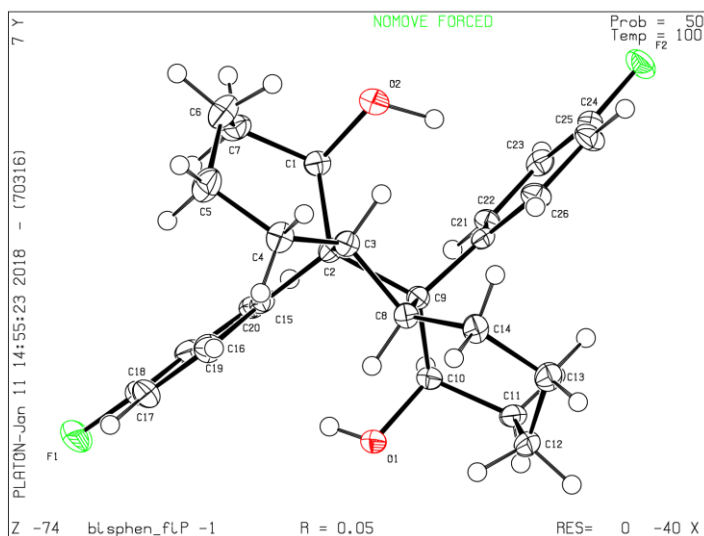


Figure 15. X-ray crystal structure of **d-4a**

This stereochemical outcome is best explained by the involvement of the ground state *trans*-cycloheptene and a *cis*-cycloheptene, operating under orbital symmetry conservation restrictions, which dictates that the olefins approach one another orthogonally.<sup>9</sup> Within this restriction, there are several potential ways in which such an orthogonal approach could occur. At the outset, the involvement of two *cis*-phenylcycloheptenes can be ruled out, because these do not dimerize on their own. Likewise, other stereochemical possibilities **A3** and **A4** (Figure 15), which are not observed, stem from the cycloaddition of two *trans*-phenyl cycloheptenes. This scenario is

both statistically unlikely, due to the short half-life of the strained cycloalkene, and furthermore, is expected to be higher in energy because of severe interactions between the phenyl rings, as well as the methylene bridges of the cycloheptene rings. A more likely scenario involves one isomerized *trans*-phenylcycloheptene and one *cis*-phenylcycloheptene,<sup>22</sup> of which there are two possible approaches (Figure 15).

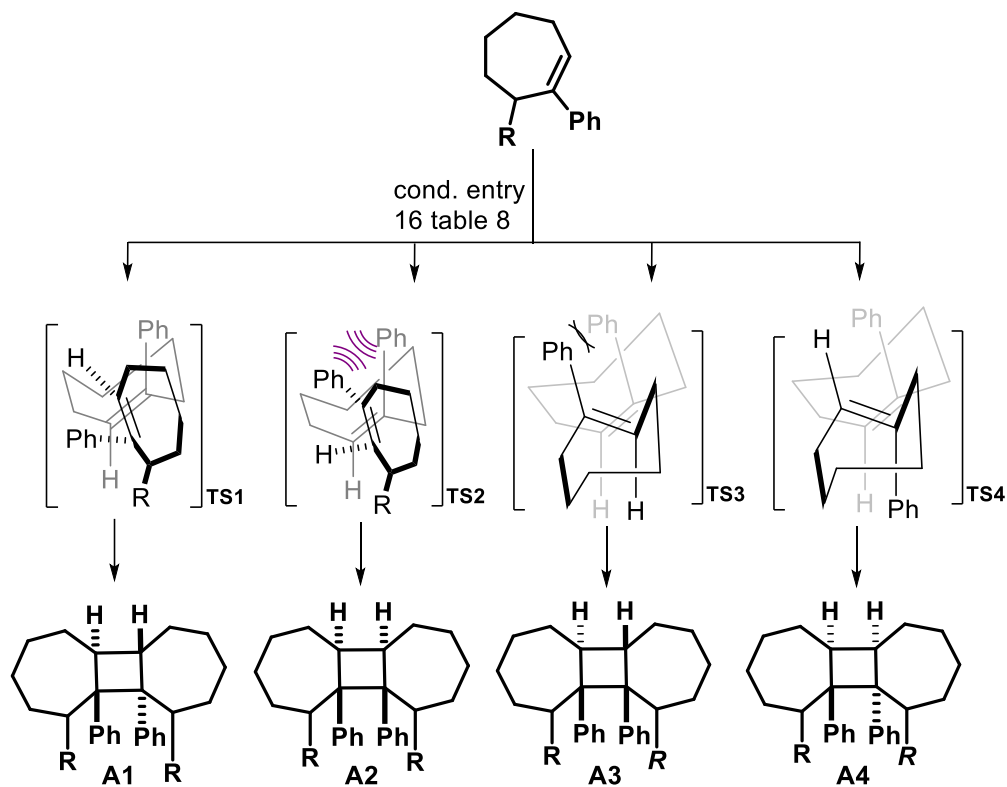


Figure 16. Rationale for the relative stereochemistry of the major observed diastereomer, **A1**, during  $[\pi 2_s + \pi 2_a]$  cycloaddition.

The major isomer, **A1** (as confirmed by X-ray analysis of **d-4a**) most probably results from the orthogonal approach of the *cis*- and *trans*-phenylcycloheptenes. This approach occurs in such a way that both the phenyl groups point away from one another (**TS1**, Figure 16) in order to minimize the steric interaction. Alternatively, if the phenyl groups approach on the same side (**TS2**), this leads to cyclobutane **A2**, in which both the phenyl groups will be *cis* to each other. It was anticipated that there would be considerable steric interaction between the phenyl groups in this transition state, which also lead to a higher energy product (*vide infra*). Thus, while up to 128

regio- and stereoisomers are possible, the reaction takes place predominantly through **TS1**, and gives primarily a cyclobutane of type **AI**.

### 4.3 Computational studies

As we were capturing a portion of the photochemical energy in the form of strain energy (*ca* 36 kcal/mol)<sup>17</sup> this raised the possibility that we could be formally performing uphill catalysis, by driving the reaction in the contra-thermodynamic direction. Thus, we became curious to learn more about the energetics of the reaction. When we searched the literature, we found that although the dimerization of ethylene to cyclobutane was exergonic in nature ( $\Delta G = -18$  kcal/mol)<sup>1-2</sup>, that the dimerization of more substituted alkenes became progressively more endergonic. In fact, Burford has calculated that the reaction is expected to be slightly endergonic with 1,2-mesityl substitution and when the methyl groups of mesitylenes were replaced with <sup>i</sup>Pr groups, the dimerization became endergonic by 5-16 kcal/mol. In general, the endergonicity of the dimerization reaction increases further with an increase in the steric bulk around the cyclobutane.<sup>27</sup> This sensitivity to the sterics is expected. First, substitution of alkenes stabilizes the starting material, ethylene being the least substituted and stable. Additionally, the cyclobutane ring dramatically exaggerates steric interactions when compared to their cyclohexane magnitudes. To probe this question, we performed the computational analysis of the thermodynamics of several [2+2] cycloadducts. Density functional theory calculations were performed (geometry/energy) on **m-4a** and **d-4a**, which indicated that this particular [ $\pi 2_s + \pi 2_a$ ] cycloaddition reaction is indeed net endothermic in nature. B3LYP/6-31 G(d) calculations of the minimized energy structures of **m-4a** and **d-4a** revealed that the [ $\pi 2_s + \pi 2_a$ ] cycloadduct **d-4a** is higher in energy as compared to **m-4a** ( $\Delta H = +5.0$  kcal/mol), highlighting the ability of photocatalysis to facilitate contra-thermodynamic catalysis.<sup>28-30</sup>

We next looked at several diastereomers of the head-to-head dimerization products of phenylcycloheptene, devoid of the OH group. The geometries of the diastereomers were minimized

using the aforementioned conditions, and the results are shown in Figure 17. In all cases, the [2+2] cycloaddition reactions were found to be endergonic in nature, but ranged from +8.4 to +28.2 kcal/mol. The major diastereomer formed in this reaction (**D1**) was found to be +12.6 kcal/mol, and closely matched the X-ray structure. This diversity of energies of the diastereomers could be in part due to the different conformations of the cycloheptane rings. Hendrickson has found that the most stable twist chair conformation is around 3 kcal/mol lower in energy than the highest energy boat conformation of cycloheptane.<sup>31</sup> Thus, with two cycloheptane rings in our structures, variation of roughly 6 kcal/mol energy difference could exist within different conformers of each diastereomer due to cycloheptane conformer. By analysis of the structures, we hoped to be able to provide some guidelines that would allow prediction of the relative stability of such tricyclic systems.

The least stable diastereomer, **D6**, which was subjected to multiple geometry optimization calculations, was found to be substantially higher in energy (+28.2 kcal/mol) than all the other structures (average **D1-D5** +10.8 kcal/mol). Chair, boat, and twist chair cycloheptane conformers were all observed. High energy **D6** displayed two chair conformers, as did the relatively more stable **D5** (+9.0 kcal/mol), indicating that cycloheptane conformer analysis is not a reliable predictor of the overall strain energy. **D6** places both phenyl groups *syn* and could cause substantial strain, but

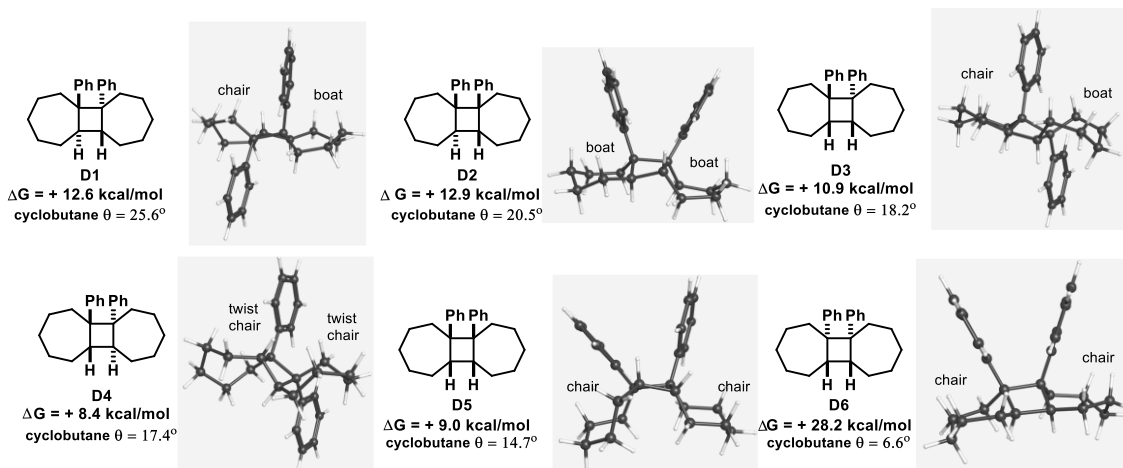


Figure 17. The energies of the various diastereomers reported are relative to the phenyl cycloheptene as calculated using B3LYP/6-31 G(d).

this is also true with **D5** and **D2** which are not as strained (+9.0 and +12.9 kcal/mol, respectively). **D6** is unique in that it is the least puckered of the cyclobutanes with a 6.6° dihedral angle,<sup>32</sup> whereas **D1-D5** range from 14.7-25.6° which likely serves to relieve the torsional strain caused by the cyclobutane substituents.

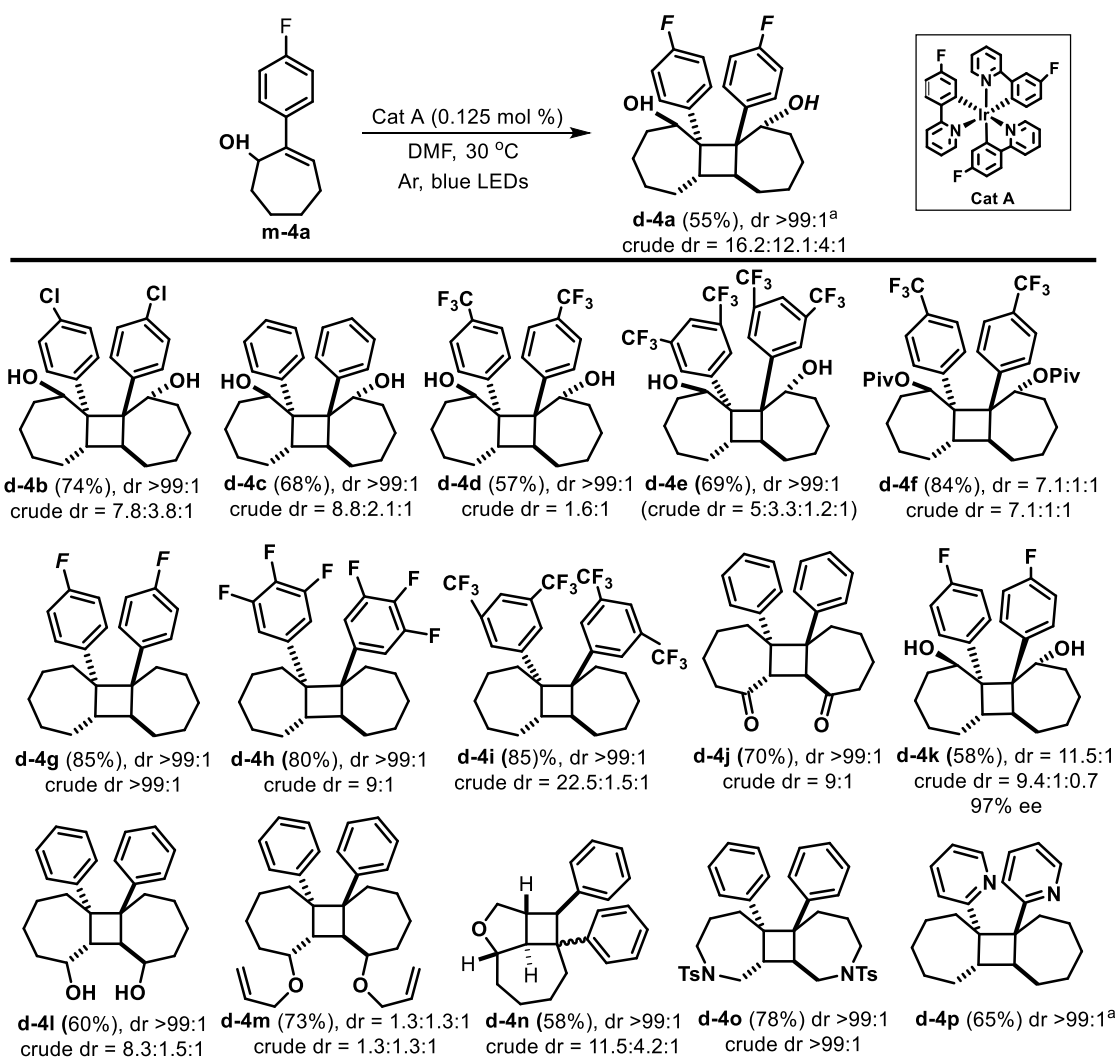
Importantly, while all of these cyclobutanes are expected to be net endergonic, they are exergonic when compared to the *trans*-cycloheptene (+36 kcal/mol)<sup>17</sup> and therefore are energetically accessible. Furthermore, while we are using highly strained molecules, the reaction exhibits a significant and synthetically useful difference in transition state energies that lead to each diastereomeric cyclobutane. Cycloheptene dimer product **d-4a**, whose calculated structure and crystal structure were well matched, was found to be of lower energy compared to the dimer **D1** (5.0 vs. 12.6 kcal/mol). This difference is likely due to an interaction between the H atoms of both the OH groups on the cycloheptane rings which point directly towards the  $\pi$ -electron cloud of the phenyl rings and is expected to have a greater stabilizing effect for **d-4a** than for **D1**.<sup>33</sup>

#### 4.4 Substrate scope of [ $\pi 2_s + \pi 2_a$ ] cycloaddition

We next explored the scope of the reaction (Table 9). A variety of functional groups were tolerated on the phenyl ring and resulted in good yields of the cyclobutane product (**d-4a**, **d-4b**, **d-4d**, **d-4f**, and **d-4h**), as well as good to excellent diastereoselectivities. In most cases, only one major diastereomer was isolated after purification. It is interesting that despite the numerous possible stereoisomers (16 in the case of R = H and 64 if R = OH) only two to four stereoisomers are ever observed in the crude reaction mixture. The [ $\pi 2_s + \pi 2_a$ ] cycloaddition appears to be the primary reaction pathway and occurs in a highly diastereoselective fashion.

When the hydroxyl group of cycloheptane in **m-4a** was substituted with a pivalyl group, **d-4a** was obtained in high yields, and good diastereoselectivity. The reaction also worked very well when there was no alcohol group present in **m-4**. It was interesting to see that the 4-

fluorophenylcycloheptene **m-4g** produced only one diastereomer **d-4g** and the reaction completed within 6 hours of irradiation. Substrates **m-4**, devoid of an OH group, were reacted in MeCN in order to take advantage of the low solubility of the product cyclobutane in MeCN. After the reaction, the cyclobutanes could be easily filtered to obtain the analytically pure product as a colorless solid, making the reaction and isolation extremely simple to carry out. The compound **m-4h** which contains three fluorine atoms on the phenyl ring was found to be highly diastereoselective, yielding the desired cyclobutane product **d-4h** in 80% yield with d.r. >99:1.



<sup>a</sup>Diastereomer confirmed by X-ray analysis.

Table 9. Substrate scope of  $[\pi_{2s}+\pi_{2a}]$  cycloaddition

Similarly, **m-4i** which contained electron withdrawing trifluoromethyl groups, also produced the desired cyclobutane product **d-4i** in 85% yield, and high diastereoselectivity (>99:1) after isolation. Cycloheptenone **m-4j** also underwent the dimerization reaction smoothly to yield the desired  $[\pi 2_s + \pi 2_a]$  adduct in 70% yield as a single diastereomer after isolation. An optically active chiral allylic alcohol **m-4k** (96% *ee*) was synthesized, and exposed to reaction conditions. **d-4k** was formed with high enantioselectivity (97% *ee*) and diastereoselectivity (11.5:1) with 58% isolated yield. Allylic alcohol (**m-4l**) with the OH group transposed to the tail carbon also produced the  $[\pi 2_s + \pi 2_a]$  cycloadduct **d-4l** in moderate yield and high d.r. (>99:1) after isolation.

In order to see whether an intramolecular cycloaddition could outcompete the intermolecular  $[\pi 2_s + \pi 2_a]$  cycloaddition, the OH group in **m-4m** was substituted with an allyl group. In this case, no intramolecular  $[\pi 2_s + \pi 2_a]$  occurred, rather only intermolecular  $[\pi 2_s + \pi 2_a]$  reaction occurred to yield **d-4m** in 73% yield, albeit with moderate d.r. of 1.3:1.3:1. The lowered d.r. suggests that the free alcohol, such as that of **m-4l**, may be important in controlling the stereochemistry of this reaction. Aside from the stereochemistry, the fact that a tethered alkene does not undergo preferential photochemical [2+2] highlights the benefits of moving to the visible region, which allows alkenyl functional groups to survive the reaction which would not likely be possible using UV irradiation.<sup>34</sup> Interestingly, replacing the allyl with a cinnamyl ether (**m-4n**) completely halts the intermolecular cycloaddition, and instead gives rise exclusively to the intramolecular cycloaddition product. After isolation, the product **d-4n** was obtained in moderate yield (58%) as an exclusive diastereomer.<sup>35</sup> It may be possible that stacking of the phenyl groups preorganizes the molecule, such that even short-lived excited state intermediates are rapidly intercepted, or because the potential for benzyl stabilization is present, a step-wise biradical could be involved. We next replaced carbon with other heteroatoms in the cycloheptene ring, which we found were also well tolerated. For instance, cycloheptene ring containing an *N-Ts* group (**m-4o**)

was synthesized and exposed to reaction conditions. The desired cycloadduct **d-4o** was obtained in good yield (78%) as a single diastereomer both before and after purification.

While the reaction requires the presence of an aryl group attached to the cycloheptene ring to make the triplet state energetically accessible, it does not necessarily have to be a phenyl derivative. A substrate containing a pyridine instead of a phenyl ring was synthesized (**m-4p**) and was exposed to reaction conditions. The desired  $[\pi 2_s + \pi 2_a]$  cyclobutane product **d-4p** was formed in 65% yield with d.r. >99:1. The relative stereochemistry was confirmed via X-ray analysis.

#### 4.5 Mechanistic investigation of reactive intermediate

The X-ray analysis of the major diastereomer **d-4a** revealed the formation of the all *trans* substituted cyclobutane ring. We believe this stereochemical outcome results from the thermal reaction of highly strained ground state *trans*-cycloheptene with the *cis*-cycloheptene. However, we recognize that the same stereochemical outcome is also possible if the reaction were to take place between the triplet biradical and the singlet ground state of *cis*-cycloheptene. Based on the arguments below, we believe that the cyclobutane formation is the result of  $[\pi 2_s + \pi 2_a]$  of *trans*-cycloheptene with the *cis*-cycloheptene and not the photochemical  $[\pi 2_s + \pi 2_s]$ .

1) We have attempted the dimerization of phenyl cyclohexene under similar conditions, but it failed to produce any cyclobutane product. Furthermore, the triplet state energy of 1-phenyl-cyclohexene is expected to be similar to 1-phenyl-cycloheptene, suggesting that excitation likely occurs in both 1-phenyl-cyclohexene and 1-phenyl-cycloheptene. In contrast, the ground state *trans*-cyclohexene, is expected to have a much shorter lifetime compared to the *trans*-cycloheptene analog. We believe if C–C bond formation were occurring through the triplet biradical, we should see similar results for these two substrates. Stated differently, the difference in their reactivity, is likely a result of the difference in populations of the *trans*-cycloalkenes.

2) Reactions that involve a triplet biradical which has been photosensitized, (such as noted in Reiser's, and Lu's work) are generally not very fast. This is likely because the triplet biradical is a reactive intermediate that can relax back to the ground state by rotating and giving off energy. The consequence, is that the reactive intermediate has a shorter lifetime which must be overcome by extensive irradiation. While it is difficult to compare different reactions quantitatively, qualitatively it is evident from the relative rates of reaction. In our case, the reaction went to completion within 6 hours of irradiation using just 0.125 mol% of the Ir catalyst. In comparison, the photodimerization of the cinnamates<sup>36</sup> was complete in 72 hours using 1 mol% of Ir catalyst. Reiser suggested that the reaction takes place from the triplet biradical intermediate. Due to the short lifetime of this intermediate, the efficiency of these reactions are significantly lower.

3) We performed radical trapping experiment using TEMPO as the radical scavenger, which showed that the reaction was unaffected by the presence of TEMPO. This also supports the idea that the triplet biradical is not the key C–C bond forming intermediate, but rather gives rise to a longer lived *trans*-cycloheptene. If the reaction is taking place from the triplet biradical intermediate, then we should see some TEMPO adduct as a byproduct and the decreased yields of the desired cyclobutane product. In fact, Lu has shown that the [2+2] cycloaddition of styrenes and 1,4-dihydropyridines is affected by the presence of radical scavengers.<sup>37</sup> They have observed decreased yields in the formation of desired cyclobutane products in the presence of TEMPO (43%) as compared to in its absence (77%). Since the reaction is occurring from a triplet biradical, the radical scavenger can intercept the triplet biradical resulting in undesired byproducts.

#### 4.51 Radical trapping experiment

In order to rule out the possibility of the triplet biradical being a C–C bond forming intermediate, a reaction was set up using **m-4g** (23.8 mg, 0.13 mmol), **Cat A** (0.125 mol%) in MeCN (0.26 mL) containing 10 mol% TEMPO as the radical scavenger. The reaction mixture was exposed to standard reaction conditions. As expected, no other product was observed and **d-4g** was

obtained as the major product (92% NMR yield). As no other radical scavenger adducts were observed, the possibility that the reaction occurs from the triplet biradical can be ruled out. This outcome supports the argument that the reaction is most probably taking place between the *trans*-cycloheptene and its *cis*-isomer.

Another reaction was set up using **m-4h** (13.6 mg, 0.06 mmol), **Cat A** (0.125 mol%) in MeCN (1.20 mL) containing TEMPO (0.07 mmol) as the radical scavenger. The reaction mixture was exposed to standard reaction conditions for 16 h. Even in presence of stoichiometric amounts of TEMPO, no other product was observed and **d-4h** was observed as the major product (100% conversion, 97% NMR yield). Interestingly, minor diastereomer was observed in very minute quantities (< 5%). This result further corroborates that reaction occurs from *trans*-cycloheptene and not from biradical intermediate.

#### 4.6 Summary

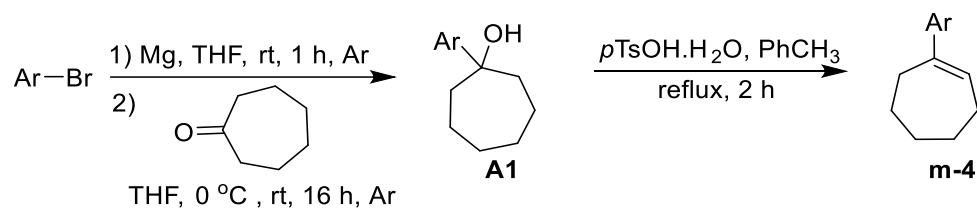
In conclusion, we have developed a method which is very mild and operationally straightforward, requires only visible light and very low concentrations of the Ir photocatalyst as well as easy to access alkenes, results in the formation of valuable cyclobutanes. The use of visible light photocatalysis makes it possible to access the highly strained *trans*-cycloheptene and avoid reaction on the excited state surface. This work demonstrates the ability to convert photochemical energy into useable forms, i.e. ring strain, which can be used to drive the synthesis of cyclobutanes and to open up a mechanistic pathway which has heretofore been energetically inaccessible. We anticipate that this reaction will spur other strategic uses of visible light energy to drive endergonic chemical synthesis.

#### 4.7 Experimental procedure

All reagents were obtained from commercial suppliers (Aldrich, VWR, TCI chemicals, Oakwood chemicals, Alfa Aesar) and used without further purification unless otherwise noted.

*N,N*-dimethylformamide (DMF) was used from a solvent purification system. Reactions were monitored by thin layer chromatography (TLC), which was obtained from Sorbent Technologies (Silica XHL TLC Plates w/UV254, glass backed 250  $\mu\text{m}$ , 20 x 20 cm), and was visualized with ultraviolet light or potassium permanganate stain. Additionally, reactions were occasionally monitored by  $^1\text{H}$ ,  $^{19}\text{F}$ -NMR (400 MHz Bruker Avance III spectrometer). Flash chromatography was carried out with Acros Organics 60  $\text{\AA}$ , mesh 50-200 micron silica gel on an automated combiflash R<sub>f</sub> version 2.1.19 equipped with UV and ELS detectors. NMR spectra were obtained on 400 MHz Bruker Avance III spectrometer, a 400 MHz Unity Inova spectrometer or a 600 MHz Unity Inova spectrometer unless otherwise noted.  $^1\text{H}$ ,  $^{19}\text{F}$  and  $^{13}\text{C}$  NMR chemical shifts are reported in ppm relative to the residual protio solvent peak ( $^1\text{H}$ ,  $^{13}\text{C}$ ). Enantiomeric excesses were determined using acDaicel Chiralpak AD-H column on HPLC instrument by Shimadzu, equipped with LC-20AD pump, SIL-20A autosampler and SPD-20AV UV detector. High resolution mass spectra (HRMS) analysis was performed on a LTQ-OrbitrapXL by Thermo Scientific Ltd.

#### 4.71. Synthesis of substrates



#### General procedure for the synthesis of cycloheptanols A1

To an oven-dried round bottomed flask was added magnesium turnings (2.0 equiv) and dry THF (1.0 M) under Ar. To this mixture was added a crystal of iodine and the reaction mixture was stirred for 10 minutes. The aryl bromide (1.0 equiv) was added and the reaction mixture was stirred for 1 h. The reaction mixture was then cooled to 0 °C and cycloheptanone (0.9 equiv) was added. The reaction mixture was allowed to warm to rt and stirred overnight under Ar. After completion, the reaction was quenched with sat.  $\text{NH}_4\text{Cl}$  extracted with EtOAc. The organic layer was separated,

dried over MgSO<sub>4</sub> and concentrated to afford the crude product that was purified by column chromatography, over silica gel using EtOAc/hexanes as eluent.

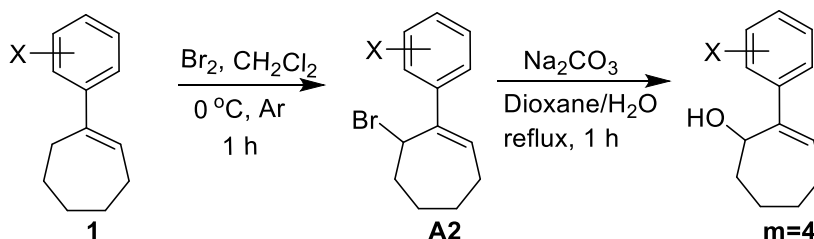
### General procedure for the synthesis of aryl cycloheptenes m-4

To the alcohol **A1** (1.0 equiv) was added toluene (0.5 M) and *p*-TsOH.H<sub>2</sub>O (10 mol%). The reaction mixture was then refluxed until the starting alcohol was consumed (TLC). The reaction mixture was then cooled to rt, and the reaction mixture was added to EtOAc and sat. NaHCO<sub>3</sub> and the layers were separated. The organic layer was separated, dried over MgSO<sub>4</sub> and concentrated to deliver the desired aryl cycloheptenes **m-4** which was used further without any purification.

The percentage yield of various aryl cycloheptenes **m-4** are tabulated below.

S. No.	Ar	% yield (over three steps)
1.	4-F phenyl ( <b>m-4g</b> )	81%
2.	3,5-bis CF <sub>3</sub> phenyl ( <b>m-4i</b> )	61%
3.	3,4,5- trifluoro phenyl ( <b>m-4h</b> )	60%

### Synthesis of phenyl cycloheptenols m-4



### General procedure for the synthesis of allylic bromo cycloheptenes A2<sup>37</sup>

To an oven-dried round bottomed flask was added **1** (1.0 equiv) and CH<sub>2</sub>Cl<sub>2</sub> (0.5 M) and the solution was cooled to 0 °C. A solution of Br<sub>2</sub> (1.0 equiv) in CH<sub>2</sub>Cl<sub>2</sub> was added dropwise under Ar and the reaction mixture stirred at 0 °C for 1 hr. The reaction mixture was then allowed to warm

to room temperature. After completion, the reaction mixture was washed with 5% NaHCO<sub>3</sub> solution. The organic layer was then dried over MgSO<sub>4</sub> and concentrated to obtain a light brown oil **A2**, which was used further without purification.

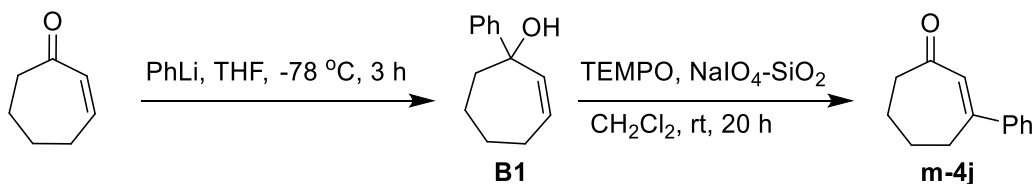
#### **General procedure for the synthesis of phenyl cycloheptenols m-4**

The allylic bromide **A2** (1.0 equiv) was dissolved in dioxane/water (1:1) (0.03 M) and then Na<sub>2</sub>CO<sub>3</sub> (2.5 equiv) was added. The resulting mixture was refluxed for 1 h. After completion, the reaction mixture was cooled to rt and the solvent was removed under reduced pressure. The residue was diluted with water and extracted with EtOAc (3 times). The combined organic layers were dried over MgSO<sub>4</sub> and concentrated to give the crude product, which was purified by column chromatography, over silica gel using EtOAc/hexanes as eluent.

The percentage yield of various substituted phenylcycloheptenols **m-4** are tabulated below.

S. No.	X	% yield (over two steps)
1.	F ( <b>m-4a</b> )	21%
2.	Cl ( <b>m-4b</b> )	51%
3.	H ( <b>m-4c</b> )	39%
4.	CF <sub>3</sub> ( <b>m-4d</b> )	52%
5.	3,5-bis CF <sub>3</sub> ( <b>m-4e</b> )	47%

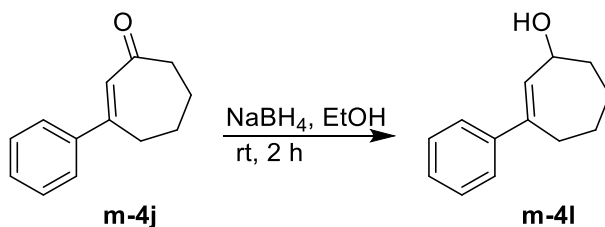
#### **Synthesis of 3-phenylcyclohept-2-en-1-one (**m-4j**)**<sup>38</sup>.



To the solution of cycloheptenone (1.0 g, 9.08 mmol) in THF (0.3 M) was added PhLi (1.8 M in butyl ether, 13.62 mmol) dropwise at -78 °C and the reaction mixture was stirred for 3 h. The reaction mixture was then quenched with sat. NH<sub>4</sub>Cl (30 mL) and extracted with EtOAc (30 mL). The organic layer was separated, dried over MgSO<sub>4</sub> and concentrated to give the crude product, which was purified by column chromatography, over silica gel using EtOAc/hexanes = 5/95 as eluent (1.0 g, 60%).

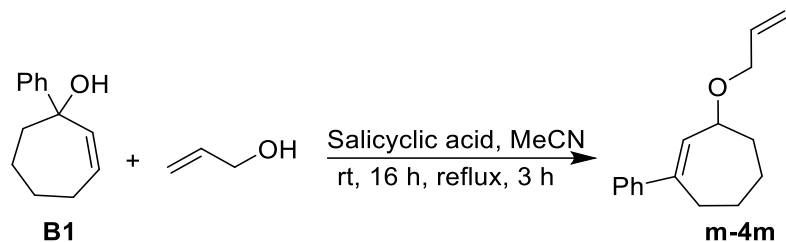
To the solution of **B1** (245.0 mg, 1.30 mmol) in CH<sub>2</sub>Cl<sub>2</sub> (0.13 M) was added TEMPO (10 mol%) and NaIO<sub>4</sub>-SiO<sub>2</sub> (4.0 g, 2.60 mmol) and the reaction mixture was stirred at rt for 20 h. The reaction mixture was filtered and the residue was washed with CH<sub>2</sub>Cl<sub>2</sub> (20 mL). The filtrate was concentrated and then purified by column chromatography, over silica gel using EtOAc/hexanes = 4/96 as eluent, to give **m-4j** (100.0 mg, 41%)

#### Synthesis of 3-phenylcyclohept-2-en-1-ol (**1l**)



To a flame dried flask was added **m-4j** (145.0 mg, 0.78 mmol) and EtOH (0.3 M) under Ar. NaBH<sub>4</sub> (59.1 mg, 1.56 mmol) was added portionwise and the reaction mixture was stirred at rt for 2 h. After completion, the reaction mixture was quenched with sat. NH<sub>4</sub>Cl and the solvent removed under reduced pressure. The residue obtained was diluted with EtOAc (20 mL) and washed with water (20 mL) and brine (20 mL). The organic layer was dried over MgSO<sub>4</sub> and concentrated to obtain the **m-4l** (144.7 mg, 99%)

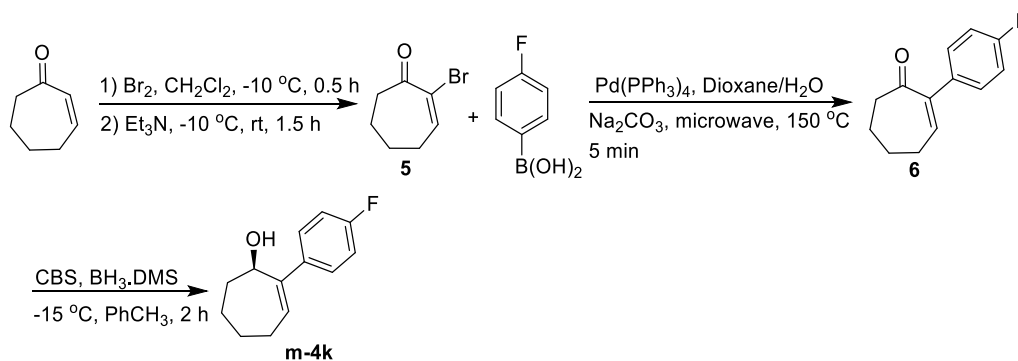
#### Synthesis of 3-(allyloxy)-1-phenylcyclohept-1-ene (**m-4m**)<sup>39</sup>



To an oven-dried flask was added **B1** (188.1 mg, 1.0 mmol) and MeCN (0.2 M). To this solution was added allylic alcohol (1.0 mL, 14.7 mmol) and salicylic acid (10 mol%) and the reaction mixture was stirred at rt for 16 h and then refluxed for 3 h. After completion, the reaction mixture was quenched with sat. NaHCO<sub>3</sub> and extracted with EtOAc. The organic layer was separated, dried over MgSO<sub>4</sub> and concentrated to obtain the crude product that was purified by column chromatography, over silica gel using EtOAc/hexanes = 5/95 as eluent, to obtain **m-4m** (120.2 mg, 53%).

Similarly, 3-(cinnamyloxy)-1-phenylcyclohept-1-ene (**m-4n**) was synthesized in 60% yield using cinnamyl alcohol instead of allyl alcohol

### Synthesis of (R)-2-(4-fluorophenyl)cyclohept-2-en-1-ol (m-4k)



### 2.6.1 Synthesis of 2-bromocyclohept-2-en-1-one (5)<sup>40</sup>

To an oven-dried round bottom flask was added **1** (500.0 mg, 4.54 mmol) and CH<sub>2</sub>Cl<sub>2</sub> (0.5 M) and the solution was cooled to -10 °C. A solution of Br<sub>2</sub> (0.26 mL, 4.99 mmol) in CH<sub>2</sub>Cl<sub>2</sub> was added dropwise under Ar and the reaction mixture stirred for 30 min at -10 °C. Then Et<sub>3</sub>N (0.89

mL, 6.35 mmol) was added and the reaction was allowed to warm to rt and stirred for 1.5 h. The reaction mixture was diluted with 1N HCl (10 ml) and extracted with CH<sub>2</sub>Cl<sub>2</sub>. The organic layer was separated, dried over MgSO<sub>4</sub> and concentrated to obtain the crude product that was purified by column chromatography, over silica gel using EtOAc/hexanes = 2/98 as eluent, to obtain **5** (500.2 mg, 60%).

#### **Synthesis of 2-(4-fluorophenyl)cyclohept-2-en-1-one (6)**

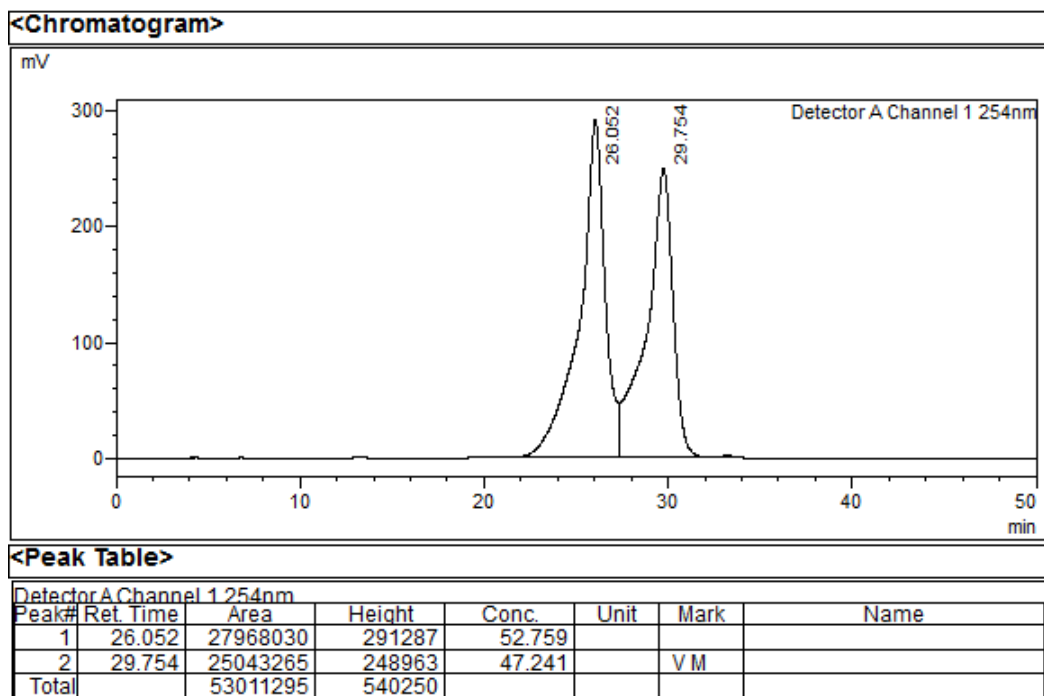
To an oven-dried microwave vial was added **5** (250 mg, 1.33 mmol), (4-fluorophenyl)boronic acid (229.9 mg, 1.60 mmol), tetrakis(triphenylphosphine)palladium(0) (4.0 mol%), Na<sub>2</sub>CO<sub>3</sub> (338.4 mg, 3.19 mmol) and dioxane/water (4:1, 0.03 M). The reaction mixture was degassed with Ar for 15 min and the reaction vial was sealed with a cap. The reaction mixture was exposed to microwave irradiations at 150 °C for 5 min. After cooling, the reaction mixture was diluted with EtOAc and water and the layers were separated. The organic layer was dried over MgSO<sub>4</sub> and concentrated to obtain the crude product that was purified by column chromatography, over silica gel using EtOAc/hexanes = 5/95 as eluent, to obtain **6** (149.2 mg, 55%).

#### **Synthesis of (R)-2-(4-fluorophenyl)cyclohept-2-en-1-ol (m-4k)<sup>41</sup>**

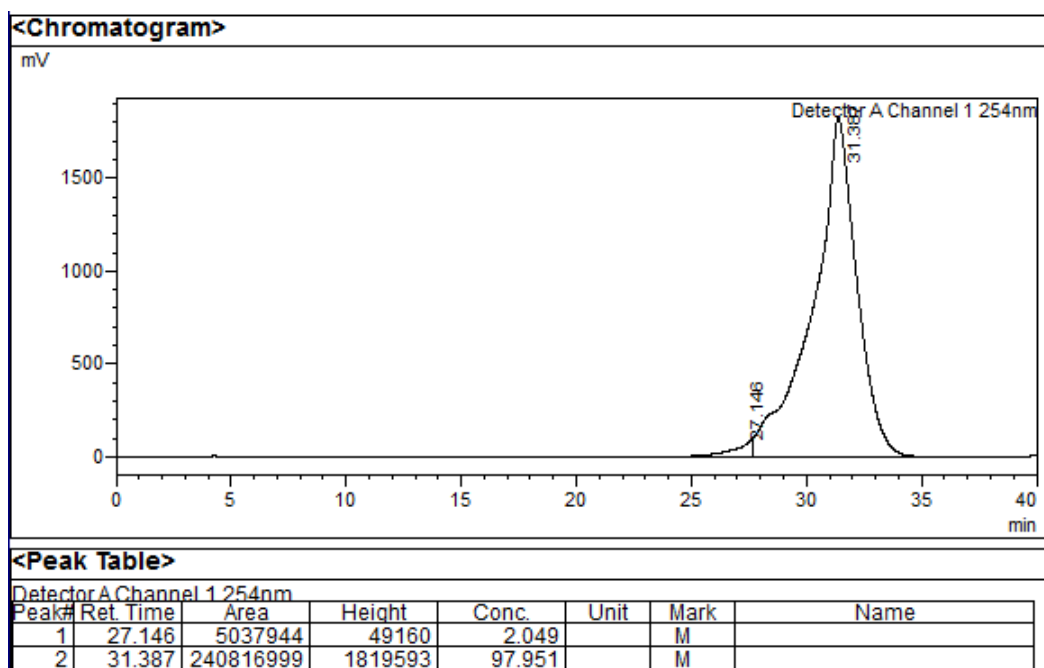
A solution of (S)-(-)-2-Methyl-CBS-oxazaborolidine (CBS) (149.6, 0.55 mmol) and borane dimethylsulfide complex (62.7 μL, 0.66 mmol) in toluene (0.03 M) was cooled to -15 °C. To this mixture was added a solution of **6** (110.2 mg, 0.55 mmol) in toluene (0.02 M) slowly over 15 min. The reaction mixture was stirred at -15 °C for 2 h and then quenched with 1 M HCl. The resulting mixture was extracted with Et<sub>2</sub>O (20 mL). The organic layer was washed once with brine and water, dried over MgSO<sub>4</sub>, and concentrated to obtain the crude product that was purified by column chromatography, over silica gel using EtOAc/hexanes = 6/94 as eluent, to obtain **m-4k** (80 mg, 72%). The enantiomeric excess (ee) was determined by HPLC. Chiralpak IC column with 0.5%

IPA in hexanes solvent system at a flow rate of 1.0 mL/min at rt was used. The *ee* of **m-4k** was found to be 96%.

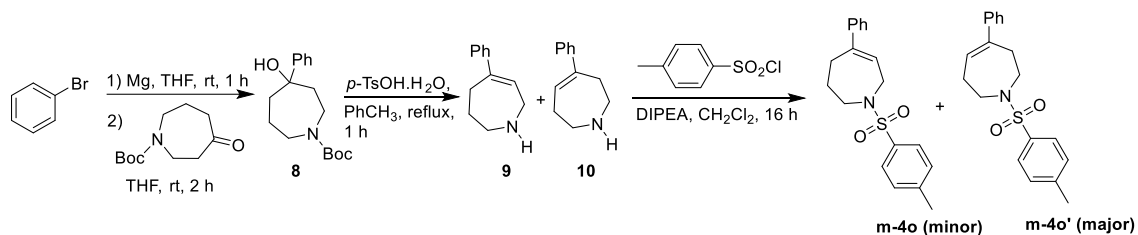
HPLC trace for rac-**m-4k**



HPLC trace for **m-4k**



**Synthesis of 5-phenyl-1-tosyl-2,3,4,7-tetrahydro-1H-azepine (m-4o)**

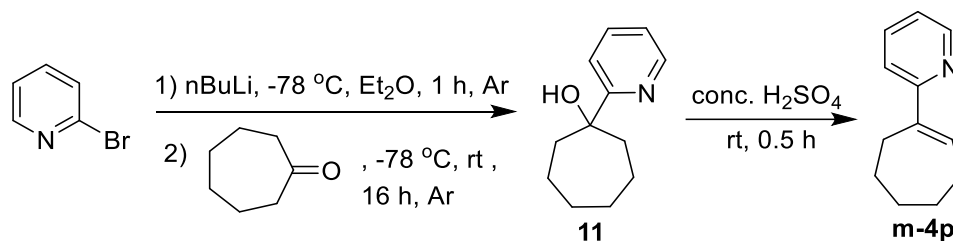


To an oven-dried round bottom flask was added magnesium turnings (285.2 mg, 11.73 mmol) and dry THF (0.5 M) under Ar. To this mixture was added a pinch of iodine and stirred for 10 minutes. Then phenyl bromide (920.1 mg, 5.86 mmol) was added and the reaction mixture was stirred for 1 h. The reaction mixture was then cooled to 0 °C and then a solution of *tert*-butyl 4-oxoazepane-1-carboxylate (1.0 g, 4.69 mmol) in THF (2.3 M) was added dropwise. The reaction mixture was then allowed to warm to rt and stirred overnight under Ar. After completion, the reaction mixture was quenched with sat. NH<sub>4</sub>Cl and the reaction mixture was extracted with EtOAc. The organic layer was separated, dried over MgSO<sub>4</sub> and concentrated to obtain the crude product (**8**) which was used further without purification.

The alcohol **8** (1.3 g, 4.65 mmol) was dissolved in toluene (0.5 M) and the *p*-TsOH.H<sub>2</sub>O (934.2 mg, 4.91 mmol) was added and the reaction mixture was refluxed for 1 h. The reaction mixture was then cooled to rt. To the reaction mixture was added EtOAc and sat. NaHCO<sub>3</sub> and the layers were separated. The organic layer was dried over MgSO<sub>4</sub>, and concentrated to obtain an inseparable mixture of regioisomeric alkenes (**9** and **10**) in a quantitative yield (rr = 1.5:1).

To the regioisomeric mixture of alkenes (800 mg, 4.62 mmol) was added 4-methylbenzenesulfonyl chloride (1.1 g, 5.55 mmol), DIPEA (1.2 mL, 6.93 mmol) and CH<sub>2</sub>Cl<sub>2</sub> (0.3 M). The reaction mixture was stirred at rt for 16 h. After completion, the reaction mixture was washed with water (10 mL) and brine (10 mL) dried over MgSO<sub>4</sub>, concentrated and then purified by column chromatography, over silica gel using EtOAc/hexanes = 8/92 as eluent, to obtain **m-4o** (270 mg, 35%) and **m-4o'** (500 mg, 65%)

#### Synthesis of 2-(cyclohept-1-en-1-yl)pyridine (**m-4p**)



To an oven-dried round bottomed flask was added 2-bromopyridine (865.2 mg, 5.48 mmol) and dry Et<sub>2</sub>O (0.2 M) under Ar. The solution was cooled to -78 °C and n-BuLi (1.6 M in hexanes, 6.02 mmol) was added dropwise and the reaction mixture was stirred for 1 h. Cycloheptanone (556.8 mg, 4.94 mmol) was added dropwise and the reaction mixture was allowed to warm to rt and stirred for 16 h. The reaction mixture was then quenched with sat. NH<sub>4</sub>Cl (30 mL) and extracted with EtOAc (30 mL). The organic layer was separated, dried over MgSO<sub>4</sub> and concentrated to obtain the crude product that was purified by column chromatography, over silica gel using EtOAc/hexanes = 5/95 as eluent, to obtain **11** (530 mg, 56% over two steps).

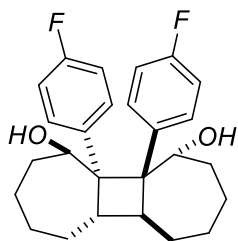
To the compound **11** (525.3 mg, 2.75 mmol) was added conc. H<sub>2</sub>SO<sub>4</sub> (5 mL) and the reaction mixture was stirred at rt for 30 min. The reaction mixture was then neutralized with sat. NaHCO<sub>3</sub> and extracted with CH<sub>2</sub>Cl<sub>2</sub> (2 x 20 ml). The organic layer was separated, dried over MgSO<sub>4</sub> and concentrated to obtain **m-4p** (310 mg, 65%) which was used further without purification.

#### **4.72 General procedure D for the visible light mediated [ $\pi 2_s + \pi 2_a$ ] cycloaddition of phenyl cycloheptenes**

To a 13 x 100 mm culture tube was added phenyl cycloheptene **m-4** (1.0 equiv), **Cat A** (0.125 mol%), and DMF or MeCN (0.5 M). The reaction mixture was sparged with Ar for 10 min. A septum was placed with a needle passing through it connected to the Ar source on other end. The reaction tube was exposed to blue LEDs at 30 °C. The progress of reaction was monitored by TLC. After complete disappearance of the starting phenyl cycloheptenes, **m-4**, the reaction mixture was diluted with EtOAc and washed with water. The organic layer was dried over MgSO<sub>4</sub> and concentrated to obtain the crude product that was purified by normal phase chromatography. Normal phase chromatography was performed with Teledyne ISCO automated chromatography system using silica as stationary phase and either EtOAc/hexanes or CH<sub>2</sub>Cl<sub>2</sub>/hexanes as mobile phase unless otherwise noted.

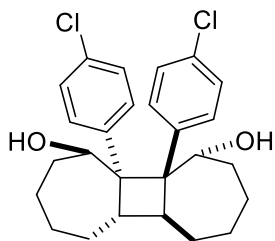
In case, where MeCN was used as solvent, the product crashes out of the solution. After completion of reaction, the white solid was filtered off and then washed with MeCN to remove the Ir catalyst. Drying under vacuum gave the desired product **d-4** which did not require any further purification.

**(1R,5aS,5bS,10R,10aS,10bS)-10a,10b-bis(4-fluorophenyl)tetradecahydrocyclobuta-  
[1,2:3,4]di[7]annulene-1,10-diol (d-4a)**



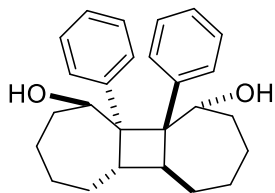
The general procedure **D** was followed using **m-4a** (100.0 mg, 0.48 mmol), **Cat A** (0.125 mol%) and DMF (1.0 mL) to afford **d-4a** in 55% yield as a white solid with dr >99:1 (crude dr = 16.2:12.1:4:1). The substrate was purified by column chromatography on silica gel (EtOAc/hexanes = 5:95). <sup>1</sup>H NMR (400 MHz, CDCl<sub>3</sub>) δ 7.98 – 7.70 (m, 1H), 7.54 – 7.35 (m, 1H), 7.22 – 7.00 (m, 2H), 4.13 – 3.99 (m, 1H), 3.60 – 3.37 (m, 1H), 2.18 – 1.93 (m, 2H), 1.91 – 1.71 (m, 1H), 1.68 – 1.56 (m, 1H), 1.48 – 1.37 (m, 2H), 1.36 – 1.20 (m, 1H), 0.26 (t, J = 2.4 Hz, 1H). <sup>13</sup>C NMR (101 MHz, CDCl<sub>3</sub>) δ 161.2 (d, J = 248.2 Hz), 140.4 (d, J = 3.8 Hz), 130.1 (d, J = 7.1 Hz), 128.5 (d, J = 7.2 Hz), 116.6 (d, J = 21.0 Hz), 115.8 (d, J = 20.5 Hz), 74.3, 61.5, 36.5, 34.5, 28.2, 26.9, 20.4. <sup>19</sup>F NMR (376 MHz, CDCl<sub>3</sub>) δ -114.47 – -115.39 (m). HRMS (ESI) (m/z): [M+Na]<sup>+</sup> calcd. for C<sub>26</sub>H<sub>30</sub>F<sub>2</sub>NaO<sub>2</sub>: 435.2106, observed: 435.2096.

**(1R,5aS,5bS,10R,10aS,10bS)-10a,10b-bis(4-chlorophenyl)tetradecahydrocyclobuta[1,2:3,4]di[7]annulene-1,10-diol (d-4b)**



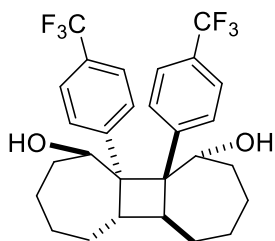
The general procedure **D** was followed using **m-4b** (100.0 mg, 0.45 mmol), **Cat A** (0.125 mol%) and DMF (0.90 mL) to afford **d-4b** in 74% yield as a white solid with dr >99:1 (crude dr = 7.8:3.8:1). The substrate was purified by column chromatography on silica gel (EtOAc/hexanes = 5:95). <sup>1</sup>H NMR (400 MHz, CDCl<sub>3</sub>) δ 7.85 – 7.66 (m, 1H), 7.50 – 7.31 (m, 3H), 4.06 (s, 1H), 3.60 – 3.29 (m, 1H), 2.08 – 1.93 (m, 2H), 1.91 – 1.73 (m, 1H), 1.67 – 1.51 (m, 1H), 1.51 – 1.36 (m, 2H), 1.36 – 1.28 (m, 1H), 0.26 (s, 1H). <sup>13</sup>C NMR (101 MHz, CDCl<sub>3</sub>) δ 143.3, 132.6, 130.1, 129.6, 129.1, 128.3, 74.0, 62.0, 36.4, 34.6, 28.1, 26.8, 20.3. HRMS (ESI) (m/z): [M+Na]<sup>+</sup> calcd. for C<sub>26</sub>H<sub>30</sub>Cl<sub>2</sub>NaO<sub>2</sub>: 467.1515, observed: 467.1513.

**(1R,5aS,5bS,10R,10aS,10bS)-10a,10b-diphenyltetradecahydrocyclobuta[1,2:3,4]di[7]annulene-1,10-diol (d-4c)**



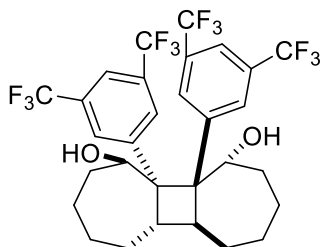
The general procedure **D** was followed using **m-4c** (100.0 mg, 0.53 mmol), **Cat A** (0.125 mol%) and DMF (1.1 mL) to afford **d-4c** in 68% yield as a white solid with dr >99:1 (crude dr = 8.8:2.1:1). The substrate was purified by column chromatography on silica gel (EtOAc/hexanes = 5:95). <sup>1</sup>H NMR (400 MHz, CDCl<sub>3</sub>) δ 7.85 (d, J = 7.9 Hz, 1H), 7.58 – 7.37 (m, 3H), 7.37 – 7.27 (m, 1H), 4.13 (appr s, 1H), 3.73 – 3.40 (m, 1H), 2.20 – 1.92 (m, 2H), 1.92 – 1.73 (m, 1H), 1.73 – 1.46 (m, 3H), 1.43 – 1.34 (m, 1H), 1.34 – 1.28 (m, 1H), 0.28 (s, 1H). <sup>13</sup>C NMR (101 MHz, CDCl<sub>3</sub>) δ 144.9, 129.5, 129.0, 128.6, 127.1, 126.6, 74.4, 62.2, 36.4, 34.5, 28.3, 26.9, 20.5. HRMS (ESI) (m/z): [M+Na]<sup>+</sup> calcd. for C<sub>26</sub>H<sub>32</sub>NaO<sub>2</sub>: 399.2295, observed: 399.2279.

**(1R,5aS,5bS,10R,10aS,10bS)-10a,10b-bis(4-(trifluoromethyl)phenyl)tetradecahydrocyclobuta[1,2:3,4]di[7]annulene-1,10-diol (d-4d)**



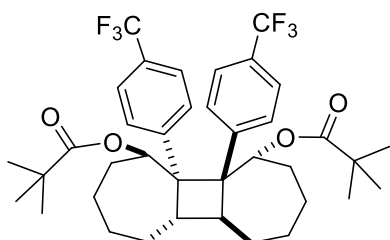
The general procedure **D** was followed using **m-4d** (150.0 mg, 0.59 mmol), **Cat A** (0.125 mol%) and DMF (1.2 mL) to afford **d-4d** in 57% yield as a white solid with dr >99:1 (crude dr = 1.6:1). The substrate was purified by column chromatography on silica gel (EtOAc/hexanes = 5:95). <sup>1</sup>H NMR (400 MHz, CDCl<sub>3</sub>) δ 7.99 (d, J = 8.0 Hz, 1H), 7.70 (t, J = 8.6 Hz, 2H), 7.59 (d, J = 8.1 Hz, 1H), 4.12 (appr s, 1H), 3.61 – 3.44 (m, 1H), 2.22 – 1.96 (m, 2H), 1.93 – 1.75 (m, 1H), 1.67 – 1.47 (m, 2H), 1.47 – 1.36 (m, 2H), 1.36 – 1.28 (m, 1H), 0.95 – 0.75 (m, 1H). <sup>13</sup>C NMR (101 MHz, CDCl<sub>3</sub>) δ 149.3, 129.2, 128.9 (q, J = 33.0 Hz), 127.2, 126.1 (q, J = 3.7 Hz), 125.9 (q, J = 3.7 Hz), 124.0 (q, J = 272.1 Hz), 73.9, 62.9, 36.6, 34.8, 28.2, 26.8, 20.3. <sup>19</sup>F NMR (376 MHz, CDCl<sub>3</sub>) δ -62.57 (s, 3F). HRMS (ESI) (m/z): [M+Na]<sup>+</sup> calcd. for C<sub>28</sub>H<sub>30</sub>F<sub>6</sub>NaO<sub>2</sub>: 535.2042, observed: 535.2053.

**(1R,5aS,5bS,10R,10aS,10bS)-10a,10b-bis(3,5-bis(trifluoromethyl)phenyl)tetradecahydrocyclobuta[1,2:3,4]di[7]annulene-1,10-diol (d-4e)**



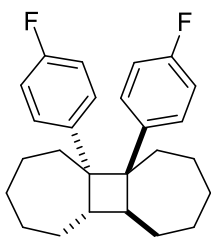
The general procedure **D** was followed using **m-4e** (100.0 mg, 0.31 mmol), **Cat A** (0.125 mol%) and DMF (0.6 mL) to afford **d-4e** in 69% yield as a white solid with dr >99:1 (crude dr = 5:3.3:1.2:1). The substrate was purified by column chromatography on silica gel (EtOAc/hexanes = 2:98). <sup>1</sup>H NMR (400 MHz, CDCl<sub>3</sub>) δ 8.25 (s, 1H), 7.77 (s, 1H), 7.75 (s, 1H), 4.06 (s, 1H), 3.63 – 3.39 (m, 1H), 2.15 – 1.97 (m, 2H), 1.94 – 1.78 (m, 1H), 1.64 – 1.46 (m, 2H), 1.44 – 1.31 (m, 2H), 1.01 – 0.86 (m, 1H), 0.06 (appr. s, 1H). <sup>13</sup>C NMR (101 MHz, CDCl<sub>3</sub>) δ 147.8, 131.8 (q, J = 33.1 Hz), 131.3 (q, J = 33.0 Hz), 129.4, 126.4, 123.2 (q, J = 272.7 Hz), 123.3 (q, J = 272.7 Hz), 120.2 – 119.7 (m) 72.8, 61.9, 36.4, 35.7, 28.0, 26.6, 20.1. <sup>19</sup>F NMR (376 MHz, CDCl<sub>3</sub>) δ -62.72 (s, 3F), -62.87 (s, 3F).

**(1R,5aS,5bS,10R,10aS,10bS)-10a,10b-bis(4-(trifluoromethyl)phenyl)tetradecahydrocyclobuta[1,2:3,4]di[7]annulene-1,10-diyl bis(2,2-dimethylpropanoate) (d-4f)**



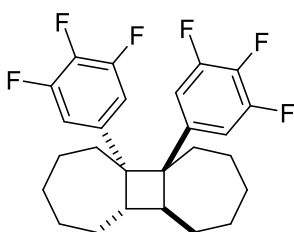
The general procedure **D** was followed using **m-4f** (60.0 mg, 0.18 mmol), **Cat A** (0.125 mol%) and DMF (0.4 mL) to afford **d-4f** in 84% yield as a white solid with dr = 7.1:1:1 (crude dr = 7.1:1:1). The substrate was purified by column chromatography on silica gel (EtOAc/hexanes = 2:98). <sup>1</sup>H NMR (400 MHz, CDCl<sub>3</sub>) δ 7.85 (d, J = 8.3 Hz, 1H), 7.62 – 7.56 (m, 3H), 5.38 – 5.22 (m, 1H), 3.55 – 3.32 (m, 1H), 2.24 – 2.08 (m, 2H), 1.95 – 1.73 (m, 1H), 1.67 – 1.47 (m, 2H), 1.34 – 1.23 (m, 2H), 0.85 (s, 9H), 0.67 – 0.55 (m, 1H). <sup>13</sup>C NMR (101 MHz, CDCl<sub>3</sub>) δ 177.0, 148.0, 129.1, 128.7, 128.1 (q, J = 33.0 Hz), 125.9 (q, J = 3.7 Hz), 125.1 (q, J = 3.8 Hz), 124.3 (q, J = 272.7 Hz), 76.3, 60.6, 40.0, 39.2, 32.0, 28.3, 27.1, 26.4, 21.2. <sup>19</sup>F NMR (376 MHz, CDCl<sub>3</sub>) δ -62.16 (s, 3F). HRMS (ESI) (m/z): [M+Na]<sup>+</sup> calcd. for C<sub>38</sub>H<sub>46</sub>F<sub>6</sub>NaO<sub>4</sub>: 703.3193, observed: 703.3187.

**(5aR,5bR,10aS,10bS)-5a,5b-bis(4-fluorophenyl)tetradecahydrocyclobuta[1,2:3,4]-di[7]annulene (d-4g)**



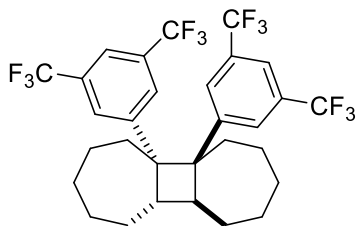
The general procedure **D** was followed using **m-4g** (114.2 mg, 0.60 mmol), **Cat A** (0.125 mol%) and MeCN (1.2 mL) to afford **d-4g** in 85% yield as a white solid with dr >99:1 (crude dr >11.5:1). The substrate was purified by column chromatography on silica gel (hexanes). <sup>1</sup>H NMR (400 MHz, CDCl<sub>3</sub>) δ 7.86 – 7.58 (m, 1H), 7.22 – 7.10 (m, 1H), 7.09 – 6.92 (m, 2H), 2.98 – 2.69 (m, 1H), 2.05 – 1.93 (m, 1H), 1.93 – 1.80 (m, 1H), 1.79 – 1.63 (m, 2H), 1.62 – 1.49 (m, 1H), 1.49 – 1.37 (m, 1H), 1.33 – 1.09 (m, 2H), 0.95 – 0.71 (m, 1H), 0.41 (dt, J = 13.4, 3.7 Hz, 1H). <sup>13</sup>C NMR (101 MHz, CDCl<sub>3</sub>) δ 160.8 (d, J = 244.2 Hz), 140.4 (d, J = 3.4 Hz), 129.9 (d, J = 7.4 Hz), 129.3 (d, J = 7.2 Hz), 115.2 (d, J = 20.7 Hz), 114.3 (d, J = 20.3 Hz), 55.8, 47.6, 42.0, 28.1, 27.9, 27.0, 26.7. <sup>19</sup>F NMR (376 MHz, CDCl<sub>3</sub>) δ -115.34 – -121.61 (m, 1F).

**(5aR,5bR,10aS,10bS)-5a,5b-bis(3,4,5-trifluorophenyl)tetradecahydrocyclobuta[1,2:3,4]di[7]annulene (d-4h)**



The general procedure **D** was followed using **m-4h** (150.0 mg, 0.66 mmol), **Cat A** (0.125 mol%) and MeCN (3.3 mL) to afford **d-4h** in 80% yield as a white solid with dr >99:1 (crude dr = 9:1). The substrate was purified by filtering the solid and then washing the solid with MeCN (1 mL). <sup>1</sup>H NMR (400 MHz, CDCl<sub>3</sub>) δ 7.52 – 7.31 (m, 1H), 6.98 – 6.53 (m, 1H), 2.98 – 2.66 (m, 1H), 1.98 – 1.84 (m, 2H), 1.84 – 1.68 (m, 1H), 1.68 – 1.58 (m, 2H), 1.54 – 1.45 (m, 1H), 1.29 – 1.08 (m, 2H), 0.95 – 0.67 (m, 1H), 0.47 (td, J = 13.4, 3.4 Hz, 1H). <sup>13</sup>C NMR (101 MHz, CDCl<sub>3</sub>) δ 152.4 (ddd, J = 65.6, 9.5, 4.5 Hz), 149.9 (ddd, J = 64.8, 9.6, 4.4 Hz), 140.7 (td, J = 6.5, 4.8 Hz), 137.7 (dt, J = 250.7, 15.5 Hz), 112.4 (dd, J = 17.3, 4.3 Hz), 112.2 – 111.8 (m), 56.3, 47.5, 41.4, 28.0, 27.4, 26.8, 26.4. <sup>19</sup>F NMR (376 MHz, CDCl<sub>3</sub>) δ -131.93 – -137.50 (m), -163.74 (tt, J = 21.0, 6.6 Hz).

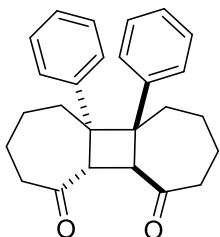
**(5aR,5bR,10aS,10bS)-5a,5b-bis(3,5-bis(trifluoromethyl)phenyl)tetradecahydrocyclobuta[1,2:3,4]di[7]annulene (d-4i)**



The general procedure **D** was followed using **m-4i** (200.0 mg, 0.65 mmol), **Cat A** (0.125 mol%) and MeCN (1.3 mL) to afford **d-4i** in 85% yield as a white solid with dr >99:1 (crude dr = 22.5:1.5:1).

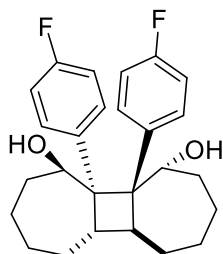
The substrate was purified by filtering the solid and then washing the solid with MeCN (1 mL). <sup>1</sup>H NMR (400 MHz, CDCl<sub>3</sub>) δ 8.23 (s, 1H), 7.80 (s, 1H), 7.60 (s, 1H), 3.08 – 2.74 (m, 1H), 2.11 – 1.95 (m, 2H), 1.92 – 1.77 (m, 1H), 1.79 – 1.70 (m, 1H), 1.69 – 1.44 (m, 2H), 1.34 – 1.03 (m, 2H), 0.79 – 0.63 (m, 1H), 0.39 (td, J = 13.4, 3.4 Hz, 1H). <sup>13</sup>C NMR (101 MHz, CDCl<sub>3</sub>) δ 146.9, 131.9 (q, J= 33.0 Hz), 131.5 (q, J= 32.8 Hz), 128.3, 128.1, 123.6 (q, J= 272.8 Hz), 123.5 (q, J= 272.6 Hz), 120.3 – 119.7 (m), 56.8, 48.1, 42.1, 27.9, 27.6, 26.7, 26.4. <sup>19</sup>F NMR (376 MHz, CDCl<sub>3</sub>) δ -62.81 (s, 3F), -62.86 (s, 3F).

**(5aR,5bR,10aS,10bS)-5a,5b-diphenyldodecahydrocyclobuta[1,2:3,4]di[7]annulene-1,10-dione (d-4j)**



The general procedure **D** was followed using **m-4j** (95.2 mg, 0.50 mmol), **Cat A** (0.125 mol%) and MeCN (1.0 mL) to afford **d-4j** in 70% yield as a white solid with dr >99:1 (crude dr = 9:1). The substrate was purified by filtering the solid and then washing the solid with MeCN (1 mL). <sup>1</sup>H NMR (400 MHz, CDCl<sub>3</sub>) δ 7.47 – 7.39 (m, 1H), 7.39 – 7.27 (m, 4H), 3.86 (s, 3H), 2.57 (dd, J = 19.2, 4.5 Hz, 1H), 2.20 – 1.90 (m, 3H), 1.78 – 1.48 (m, 14H), 1.09 (t, J = 12.6 Hz, 1H), 0.72 (td, J = 13.4, 2.5 Hz, 1H). <sup>13</sup>C NMR (101 MHz, CDCl<sub>3</sub>) δ 214.3, 141.1, 129.1, 128.8, 127.8, 126.8, 126.3, 57.1, 54.1, 43.8, 40.6, 26.7, 24.1. HRMS (ESI) (m/z): [M+Na]<sup>+</sup> calcd. for C<sub>26</sub>H<sub>28</sub>NaO<sub>2</sub>: 395.1982, observed: 395.1991.

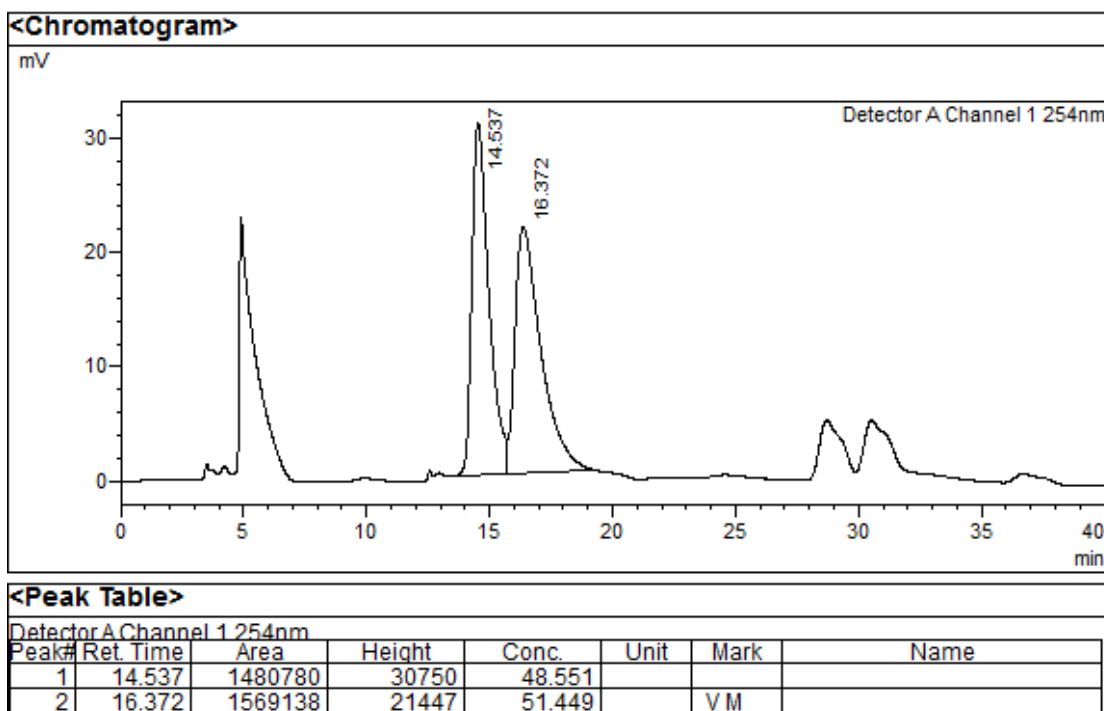
**(1R,5aS,5bS,10R,10aS,10bS)-10a,10b-bis(4-fluorophenyl)tetradecahydrocyclobuta[1,2:3,4]di[7]annulene-1,10-diol (d-4k)**



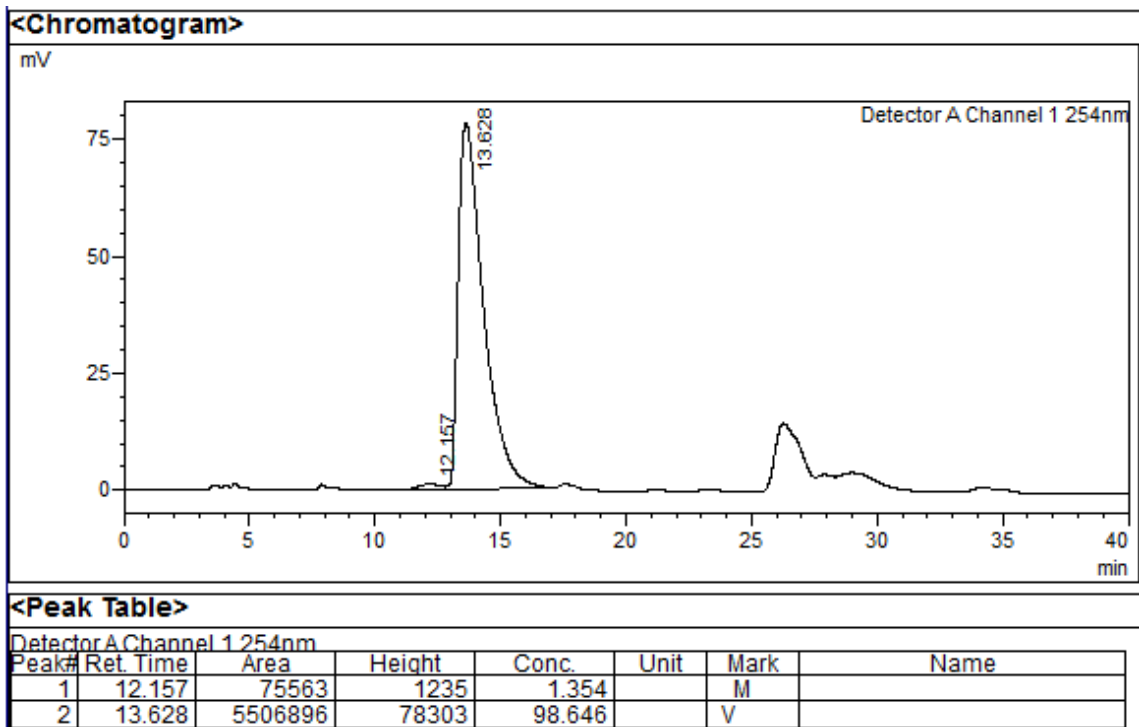
The general procedure **D** was followed using **m-4k** (38.1 mg, 0.18 mmol, 96% *ee*), **Cat A** (0.125 mol%) and DMF (0.36 mL) to afford **d-4k** in 58% yield (97% *ee*) as a white solid with dr = 11.5:1 (crude dr = 9.4:1:0.7). The substrate was purified by column chromatography on silica gel (EtOAc/hexanes = 5:95). <sup>1</sup>H NMR (400 MHz, CDCl<sub>3</sub>) δ 7.86 – 7.76 (m, 1H), 7.47 – 7.34 (m, 1H), 7.20 – 7.01 (m, 2H), 4.07 (s, 1H), 3.66 – 3.37 (m, 1H), 2.17 – 1.95 (m, 2H), 1.90 – 1.71 (m, 1H), 1.67 – 1.52 (m, 2H), 1.42 (dd, J = 22.0, 10.9 Hz, 1H), 1.30 (dt, J = 14.9, 7.2 Hz, 1H), 0.87 (t, J = 13.1 Hz, 1H), 0.27 (s, 1H). <sup>13</sup>C NMR (101 MHz, CDCl<sub>3</sub>) δ 161.2 (d, J = 248.3 Hz), 140.5 (d, J = 3.7 Hz), 130.1 (d, J = 7.2 Hz), 128.5 (d, J = 7.3 Hz), 116.6 (d, J = 21.0 Hz), 115.8 (d, J = 20.4 Hz), 74.3, 61.5, 36.5, 34.5, 28.2, 26.9, 20.4. <sup>19</sup>F NMR (376 MHz, CDCl<sub>3</sub>) δ -113.79 – -115.53 (m, 1F).

The *ee* of the product was determined by HPLC using Chiralpak IC column and 0.5% IPA in hexanes as the mobile phase at a flow rate of 1.0 mL/min at rt. The *ee* of **d-4k** was found to be 97%.

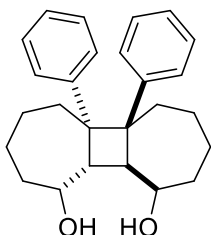
HPLC trace of crude *rac-d-4a*



HPLC trace of **d-4k**

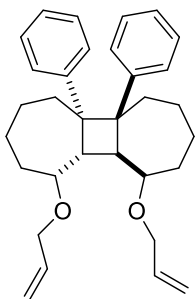


(1R,5aR,5bR,10R,10aS,10bS)-5a,5b-diphenyltetradecahydrocyclobuta[1,2:3,4]di[7]-annulene-1,10-diol (**d-4l**)



The general procedure **D** was followed using **m-4l** (100.0 mg, 0.53 mmol), **Cat A** (0.125 mol%) and MeCN (1.1 mL) to afford **d-4l** in 60% yield as a white solid with dr >99:1 (crude dr = 8.3:1.5:1). The substrate was purified by column chromatography on silica gel (EtOAc/hexanes = 10:90). <sup>1</sup>H NMR (400 MHz, CDCl<sub>3</sub>) δ 7.52 (d, J = 7.8 Hz, 1H), 7.34 – 7.22 (m, 2H), 7.21 – 7.05 (m, 2H), 4.68 (d, J = 7.4 Hz, 1H), 2.94 (s, 1H), 2.84 – 2.60 (m, 1H), 1.83 – 1.65 (m, 2H), 1.65 – 1.53 (m, 1H), 1.51 – 1.26 (m, 3H), 0.77 (q, J = 11.8, 11.4 Hz, 1H), 0.64 – 0.41 (m, 1H). <sup>13</sup>C NMR (101 MHz, CDCl<sub>3</sub>) δ 143.0, 128.6, 128.2, 128.2, 128.0, 125.9, 71.7, 57.0, 53.9, 41.5, 36.6, 27.5, 22.4. HRMS (ESI) (m/z): [M+Na]<sup>+</sup> calcd. for C<sub>26</sub>H<sub>32</sub>NaO<sub>2</sub>: 399.2295, observed: 399.2287.

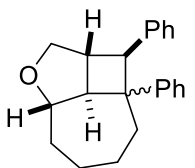
**(1R,5aR,5bR,10R,10aS,10bS)-1,10-bis(allyloxy)-5a,5b-diphenyltetradecahydrocyclo-butane [1,2:3,4]di[7]annulene (d-4m)**



The general procedure **D** was followed using **m-4m** (110.0 mg, 0.48 mmol), **Cat A** (0.125 mol%) and MeCN (0.24 mL) to afford **d-4m** in 73% yield as a white solid with dr = 2.6:1 (crude dr = 2.6:1). The substrate was purified by column chromatography on silica gel (EtOAc/hexanes = 5:95). <sup>1</sup>H NMR (400 MHz, CDCl<sub>3</sub>) δ 8.89 (d, *J* = 7.8 Hz, 1H), 7.48 (d, *J* = 8.1 Hz, 1H), 7.39 – 7.27 (m, 6H), 7.25 – 7.14 (m, 6H), 6.16 – 5.88 (m, 2H), 5.45 – 5.24 (m, 2H), 5.24 – 5.10 (m, 2H), 4.33 – 3.95 (m, 6H), 3.93 – 3.72 (m, 1H), 3.22 – 3.06 (m, 2H), 2.10 (m, 1H), 1.95 – 1.68 (m, 4H), 1.52 (m, 3H), 1.46 – 1.22 (m, 7H), 1.13 – 0.75 (m, 5H), 0.54 (td, *J* = 13.6, 13.6, 3.7 Hz, 1H), 0.40 (td, *J* = 14.5, 14.0, 3.3 Hz, 1H). <sup>13</sup>C NMR (101 MHz, CDCl<sub>3</sub>) δ 144.0, 142.9, 136.7, 136.3, 131.4, 128.6, 128.4, 128.3, 127.8, 127.7, 127.6, 127.5, 125.5, 125.3, 116.5, 115.4, 79.4, 78.2, 71.0, 69.8, 58.1, 57.1, 52.1, 49.4, 42.0, 41.3, 33.4, 31.2, 27.9, 27.3, 24.0, 22.3. HRMS (ESI) (*m/z*): [M+Na]<sup>+</sup> calcd. for C<sub>32</sub>H<sub>40</sub>NaO<sub>2</sub>: 479.2921, observed: 479.2908.

Given the low dr, it was relatively difficult to identify the distinguished product signals from the diastereomers, so all peaks were picked.

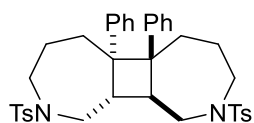
**(1S,1aR,1a1S,3aS)-1,7a-diphenyldecahydro-3-oxacyclobuta[cd]azulene (d-4n)**



The general procedure **D** was followed using **m-4n** (120.0 mg, 0.40 mmol), **Cat A** (0.125 mol%) and MeCN (0.20 mL) to afford **d-4n** in 58% yield as a white solid with dr >99:1 (crude dr = 11.5:4.2:1). The substrate was purified by column chromatography on silica gel (CH<sub>2</sub>Cl<sub>2</sub>/hexanes = 50:50). <sup>1</sup>H NMR (400 MHz, CDCl<sub>3</sub>) δ 7.20 – 7.03 (m, 6H), 6.98 (d, *J* = 6.9 Hz, 2H), 6.79 – 6.61 (m, 2H), 4.41 – 4.11 (m, 2H), 3.96 – 3.66 (m, 2H), 3.21 – 3.04 (m, 1H), 2.99 (t, *J* = 8.7 Hz, 1H), 2.55 – 2.30 (m, 2H), 2.09 (dd, *J* = 13.9, 10.7 Hz, 1H), 2.01 – 1.86 (m, 1H), 1.86 – 1.66 (m, 1H), 1.66 – 1.46 (m, 2H), 1.05 (q, *J* = 12.6, 11.6 Hz, 1H). <sup>13</sup>C

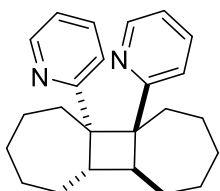
NMR (101 MHz, CDCl<sub>3</sub>) δ 143.1, 140.1, 128.4, 128.2, 127.7, 127.5, 126.3, 125.7, 83.3, 74.6, 61.4, 50.5, 48.3, 43.2, 40.3, 33.4, 27.6, 23.7. HRMS (ESI) (m/z): [M+Na]<sup>+</sup> calcd. for C<sub>22</sub>H<sub>24</sub>NaO: 327.1719, observed: 327.1708. The tentative diastereomeric relationship shown is based on magnitude of the coupling constants and NOE experiments. However, the entire structure has not been unambiguously assigned.

**(5aR,5bR,10aS,10bS)-5a,5b-diphenyl-2,9-ditosyltetradecahydrocyclobuta[1,2-c:4,3-c']bis(azepine) (d-4o)**



The general procedure **D** was followed using **m-4o** (60.0 mg, 0.18 mmol), **Cat A** (0.125 mol%) and DMF (0.90 mL) to afford **d-4o** in 71% yield as a white solid with dr >99:1 (crude dr >99:1). The substrate was purified by column chromatography on silica gel (EtOAc/hexanes = 20:80). <sup>1</sup>H NMR (400 MHz, CDCl<sub>3</sub>) δ 7.68 (d, J = 7.6 Hz, 1H), 7.54 (d, J = 8.0 Hz, 2H), 7.42 – 7.30 (m, 2H), 7.27 – 7.15 (m, 4H), 4.29 – 3.99 (m, 1H), 3.67 – 3.40 (m, 1H), 3.08 – 2.87 (m, 2H), 2.54 – 2.44 (m, 1H), 2.42 (s, 3H), 1.99 – 1.76 (m, 1H), 1.46 – 1.34 (m, 1H), 1.34 – 1.15 (m, 1H), 0.50 (dt, J = 13.4, 3.5 Hz, 1H). <sup>13</sup>C NMR (101 MHz, CDCl<sub>3</sub>) δ 143.3, 141.5, 135.2, 129.7, 128.4 (s, 2C), 128.3, 128.2, 127.4, 126.1, 57.0, 47.5, 47.2, 45.3, 41.5, 28.1, 21.6. HRMS (ESI) (m/z): [M+H]<sup>+</sup> calcd. for C<sub>38</sub>H<sub>42</sub>N<sub>2</sub>O<sub>4</sub>S<sub>2</sub>: 655.2659, observed: 655.2651.

**(5aS,5bS,10aS,10bS)-5a,5b-di(pyridin-2-yl)tetradecahydrocyclobuta[1,2:3,4]di[7]an-nulene (d-4p)**



The general procedure **D** was followed using **m-4p** (100.0 mg, 0.58 mmol), **Cat A** (0.125 mol%) and DMF (1.2 mL) to afford **d-4p** in 65% yield as a white solid with dr >99:1. The substrate was purified by column chromatography on silica gel (EtOAc/hexanes = 4:96). <sup>1</sup>H NMR (400 MHz, C<sub>6</sub>D<sub>6</sub>) δ 8.59 (s, 1H), 7.32 – 7.06 (m, 2H), 6.80 – 6.49 (m, 1H), 3.66 (s, 1H), 3.04 (s, 1H), 2.15 – 1.64 (m, 2H), 1.60 –

1.42 (m, 2H), 1.41 – 1.06 (m, 3H), 1.06 – 0.82 (m, 1H), 0.63 (s, 1H).  $^{13}\text{C}$  NMR (101 MHz,  $\text{CDCl}_3$ )  $\delta$  164.7, 148.0, 135.2, 123.0, 120.3, 56.9, 47.8, 39.2, 28.5, 27.3, 26.6, 26.3. HRMS (ESI) (m/z):  $[\text{M}+\text{H}]^+$  calcd. for  $\text{C}_{24}\text{H}_{30}\text{N}_2$ : 347.2482, observed: 347.2472.

#### 4.8 $[\pi 2_s + \pi 2_a]$ cycloaddition of other substrates.

Apart from allylic alcohols, various other functional groups, such as, azide, nitro, sulfone, aniline, thioether, at the allylic position were also tested under the optimized reaction conditions (**3a-3g**, Table 10). Although desired product was formed in all of these cases, other undesired products were also observed, which made the isolation of the desired dimer product difficult. Also other substrates, containing a furan and benzothiazole ring in place of phenyl ring, were tested under the reaction conditions. In these cases, messy reactions were observed.

Some other substrates that did not show any reactivity are outlined in Table 10. Compounds **4a**, **4b**, and **4c** did not undergo any reaction and were recovered unchanged after 18 h of irradiation.

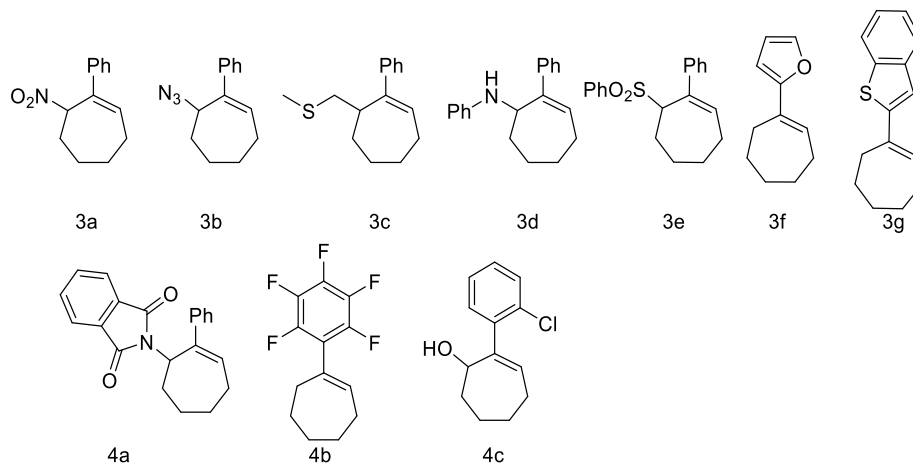


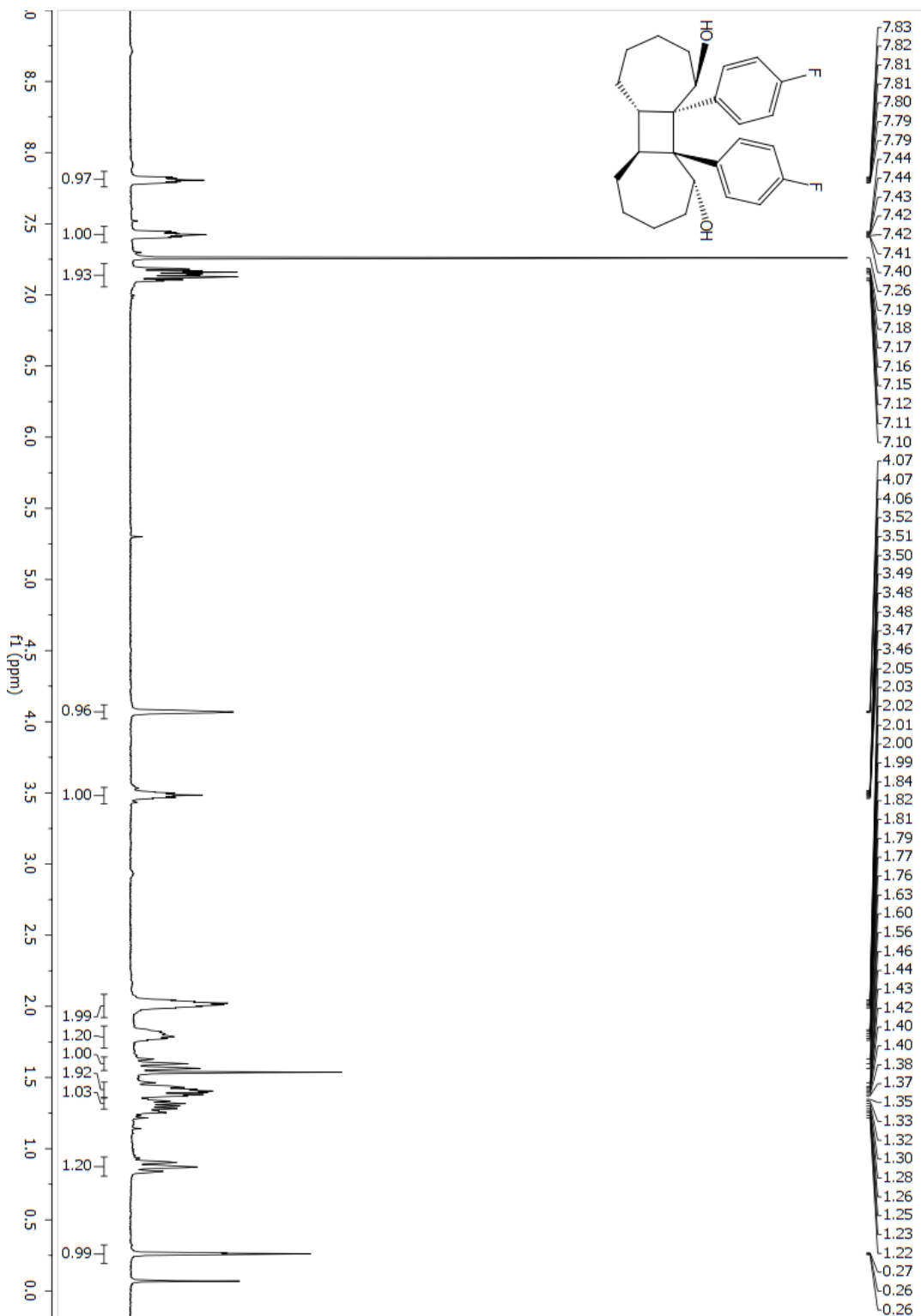
Table 10. Substrates producing undesired products/ no product

## 4.9 References

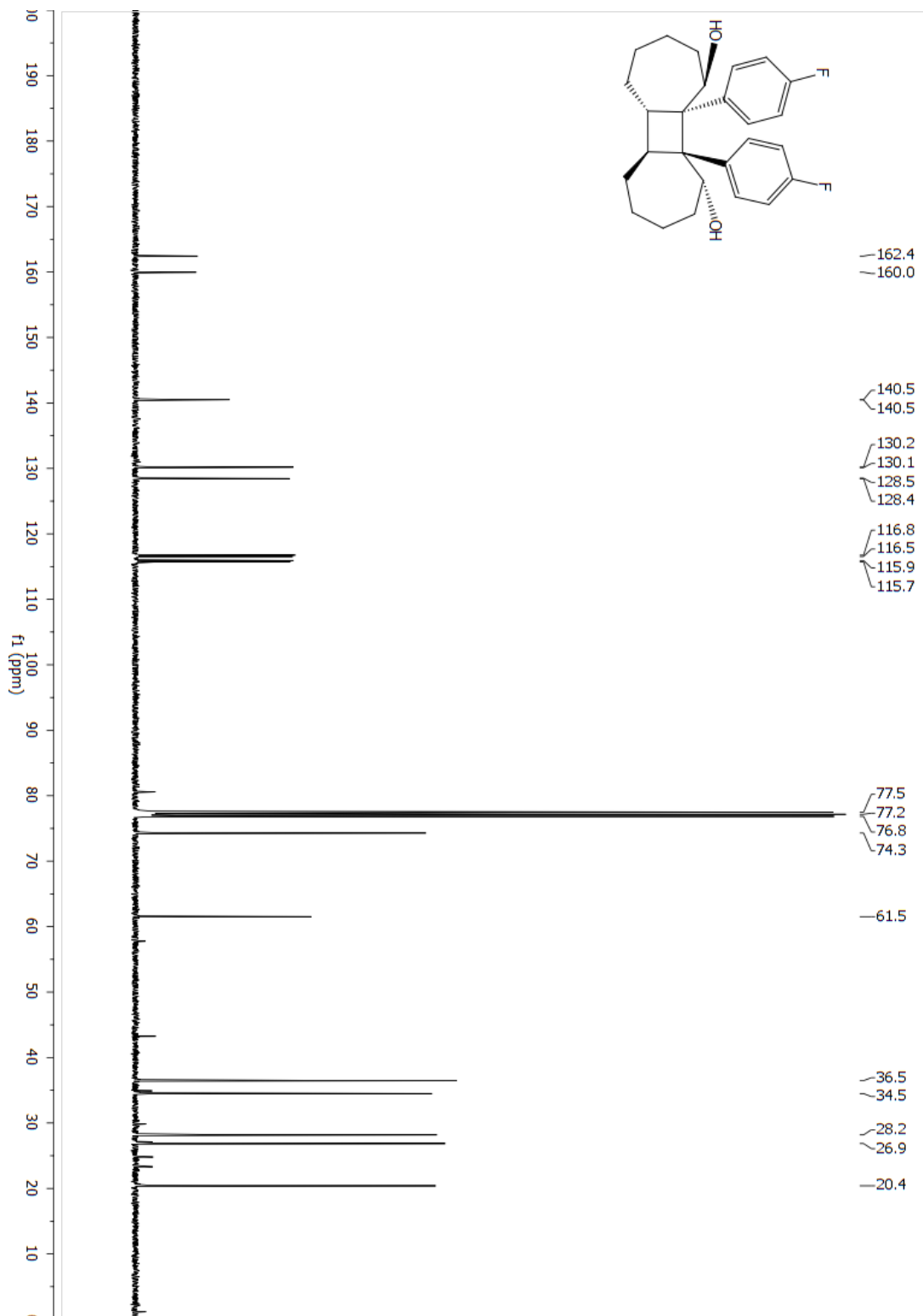
1. Jug, K.; Krüger, H.-W., *Theor Chim Acta* **1979**, *52*, 19.
2. Wiberg, K. B., *Angew. Chem. Int. Ed. Engl.* **1986**, *25*, 312.
3. Woodward, R. B.; Hoffmann, R., *Angew. Chem. Int. Ed.* **1969**, *8*, 781.
4. Nishimura, A.; Ohashi, M.; Ogoshi, S., *J. Am. Chem. Soc.* **2012**, *134*, 15692.
5. Sakai, K.; Kochi, T.; Kakiuchi, F., *Org. Lett.* **2013**, *15*, 1024.
6. Rasik, C. M.; Brown, M. K., *Angew. Chem. Int. Ed.* **2014**, *53*, 14522.
7. Heimbach, P., *Angew. Chem. Int. Ed. Engl.* **1973**, *12*, 975.
8. Hoyt, J. M.; Schmidt, V. A.; Tondreau, A. M.; Chirik, P. J., *Science* **2015**, *349*, 960.
9. Hart, H.; Dunkelblum, E., *J. Org. Chem.* **1979**, *44*, 4752.
10. Inoue, Y.; Ueoka, T.; Kuroda, T.; Hakushi, T., *J. Chem. Soc., Perkin Trans. 2* **1983**, 983.
11. Hoffmann, R.; Inoue, Y., *J. Am. Chem. Soc.* **1999**, *121*, 10702.
12. Eaton, P. E.; Lin, K., *J. Am. Chem. Soc.* **1965**, *87*, 2052.
13. Bunce, R. A.; Taylor, V. L.; Holt, E. M., *J. Photochem. Photobiol. A: Chem.* **1991**, *57*, 317.
14. Vallée, M. R. J.; Inhülsen, I.; Margaretha, P., *Helv. Chim. Acta* **2010**, *93*, 17.
15. In 1980, Evers and Mackor observed the trimerization of cycloheptene via direct irradiation in the presence of CuOTf, occurring from the thermal reaction of trans cycloheptene
16. Esser, P.; Pohlmann, B.; Scharf, H.-D., *Angew. Chem. Int. Ed. Engl.* **1994**, *33*, 2009.
17. Singh, K.; Fennell, C. J.; Coutsias, E. A.; Latifi, R.; Hartson, S.; Weaver, J. D., *Chem* **2018**, *4*, 124.
18. Allinger, N. L.; Sprague, J. T., *J. Am. Chem. Soc.* **1972**, *94*, 5734.
19. Squillacote, M. E.; DeFellipis, J.; Shu, Q., *J. Am. Chem. Soc.* **2005**, *127*, 15983.
20. Strickland, A. D.; Caldwell, R. A., *J. Phys. Chem.* **1993**, *97*, 13394.
21. Singh, K.; Staig, S. J.; Weaver, J. D., *J. Am. Chem. Soc.* **2014**, *136*, 5275.
22. Singh, A.; Fennell, C. J.; Weaver, J. D., *Chem. Sci.* **2016**, *7*, 6796.
23. Singh, A.; Kubik, J. J.; Weaver, J. D., *Chem. Sci.* **2015**, *6*, 7206.
24. Singh, A.; Teegardin, K.; Kelly, M.; Prasad, K. S.; Krishnan, S.; Weaver, J. D., *J. Organomet. Chem.* **2015**, *776*, 51.
25. The volume of the catalyst is the electrons per Å<sup>3</sup> electron density isosurface. These volumes were converted to effective radius and assuming a spherical shape for simplicity.
26. Burford, N.; Clyburne, J. A. C.; Chan, M. S. W., *Inorg. Chem.* **1997**, *36*, 3204.
27. Metternich, J. B.; Gilmour, R., *J. Am. Chem. Soc.* **2015**, *137*, 11254.
28. Metternich, J. B.; Gilmour, R., *Synlett* **2016**, *27*, 2541.
29. Molloy, J. J.; Metternich, J. B.; Daniliuc, C. G.; Watson, A. J. B.; Gilmour, R., *Angew. Chem. Int. Ed.* **2018**, *57*, 3168.
30. Hendrickson, J. B., *J. Am. Chem. Soc.* **1961**, *83*, 4537.
31. Spee, T.; Evers, J. T. M.; Mackor, A., *Tetrahedron* **1982**, *38*, 1311.
32. Bloom, J. W. G.; Raju, R. K.; Wheeler, S. E., *J. Chem. Theory Comput.* **2012**, *8*, 3167.
33. Tamura, Y.; Kita, Y.; Ishibashi, H.; Ikeda, M., *J. Chem. Soc. D* **1971**, 1167.
34. Since the crystals could not be grown, the relative stereochemistry between the two phenyl rings is unassigned.
35. Pagire, S. K.; Hossain, A.; Traub, L.; Kerres, S.; Reiser, O., *Chem. Commun.* **2017**, *53*, 12072.
36. Wang, C.; Lu, Z., *Org. Lett.* **2017**, *19*, 5888.
37. Lee, G.-A.; Lee, H.-Y.; Wang, W.-C.; Cherng, C.-H., *Tetrahedron* **2014**, *70*, 2956.

38. Shibuya, M.; Tomizawa, M.; Iwabuchi, Y., *Org. Lett.* **2008**, *10*, 4715.
39. McCubbin, J. A.; Voth, S.; Krokhin, O. V., *J. Org. Chem.* **2011**, *76*, 8537.
40. Kobayashi, Y.; Feng, C.; Ikoma, A.; Ogawa, N.; Hirotsu, T., *Org. Lett.* **2014**, *16*, 760.
41. Sundén, H.; Ma, J.-N.; Hansen, L. K.; Gustavsson, A.-L.; Burstein, E. S.; Olsson, R., *ChemMedChem* **2013**, *8*, 1283.

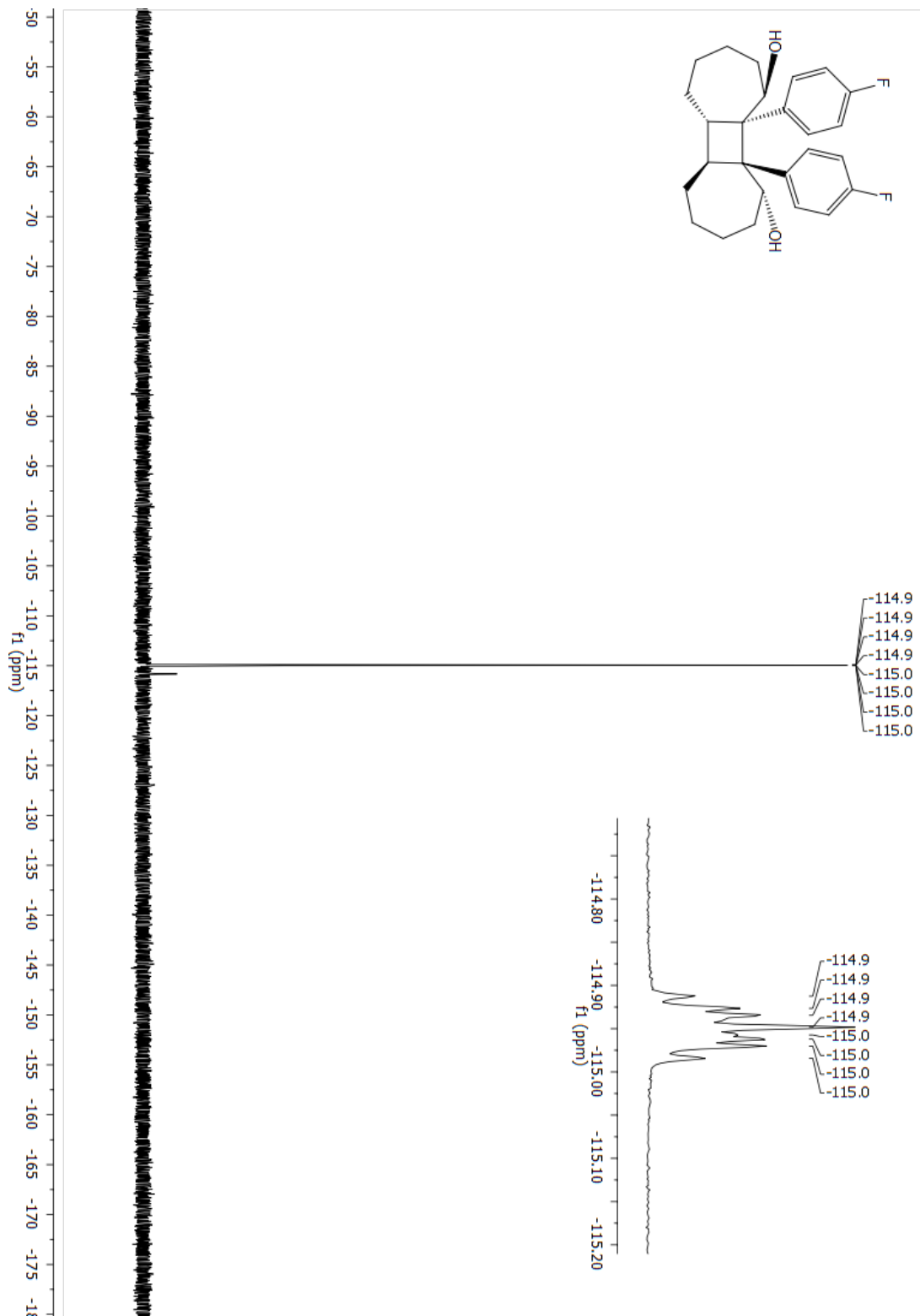
**d-4a (1R,5aS,5bS,10R,10aS,10bS)-10a,10b-bis(4-fluorophenyl)tetradecahydrocyclobuta-[1,2:3,4]di[7]annulene-1,10-diol**



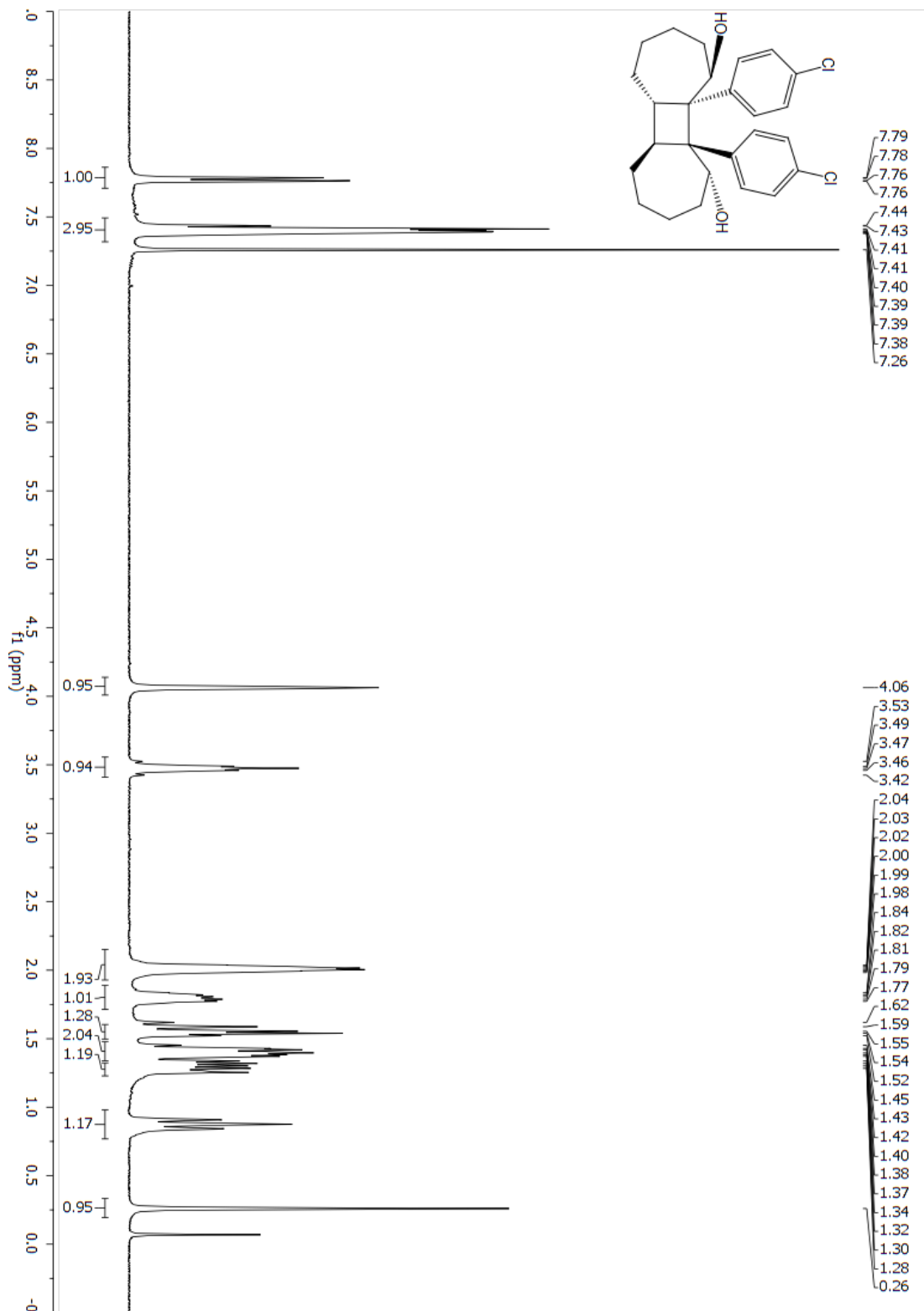
**d-4a (1R,5aS,5bS,10R,10aS,10bS)-10a,10b-bis(4-fluorophenyl)tetradecahydrocyclobuta-[1,2:3,4]di[7]annulene-1,10-diol**



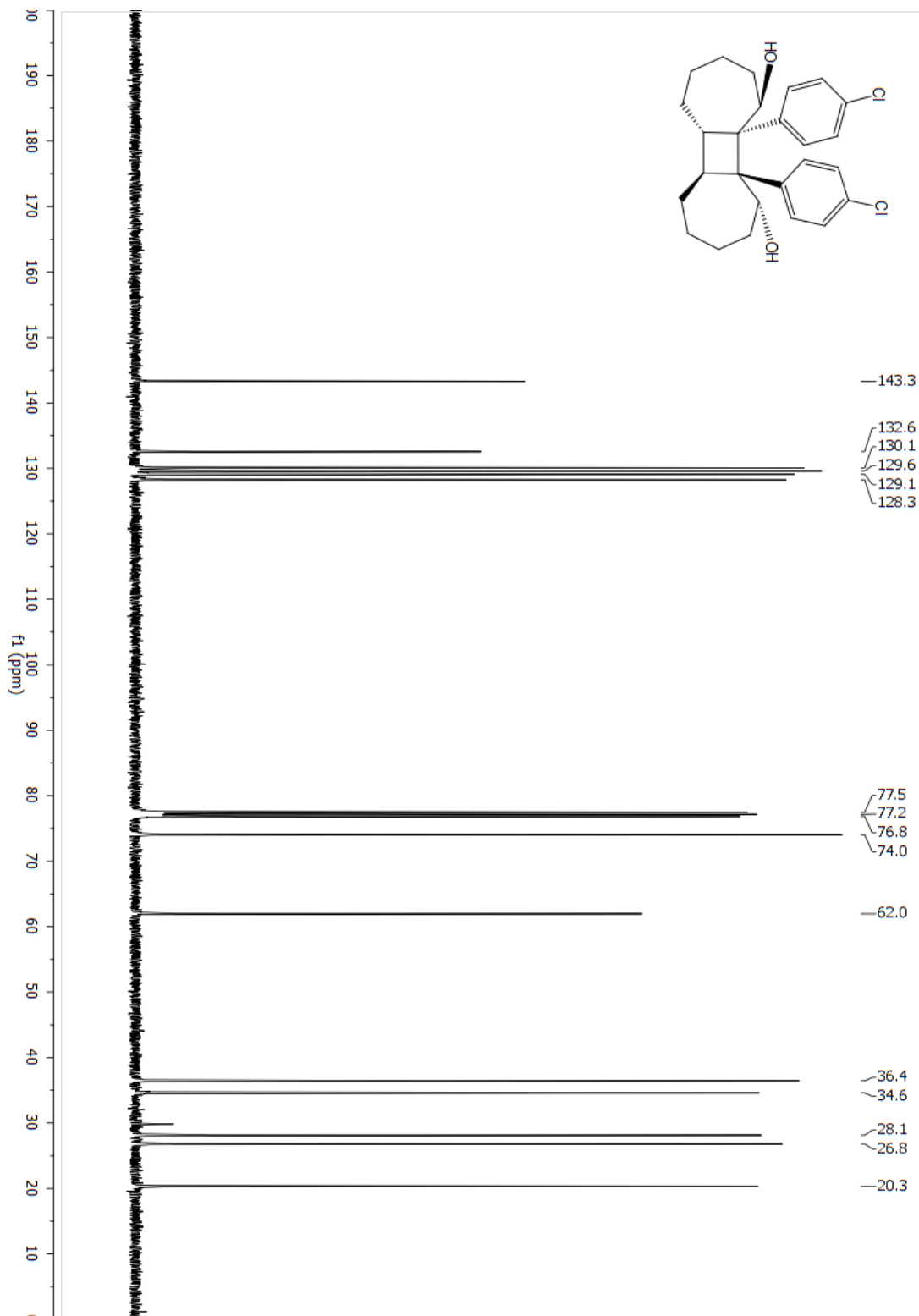
**d-4a (1R,5aS,5bS,10R,10aS,10bS)-10a,10b-bis(4-fluorophenyl)tetradecahydrocyclobuta-[1,2:3,4]di[7]annulene-1,10-diol**



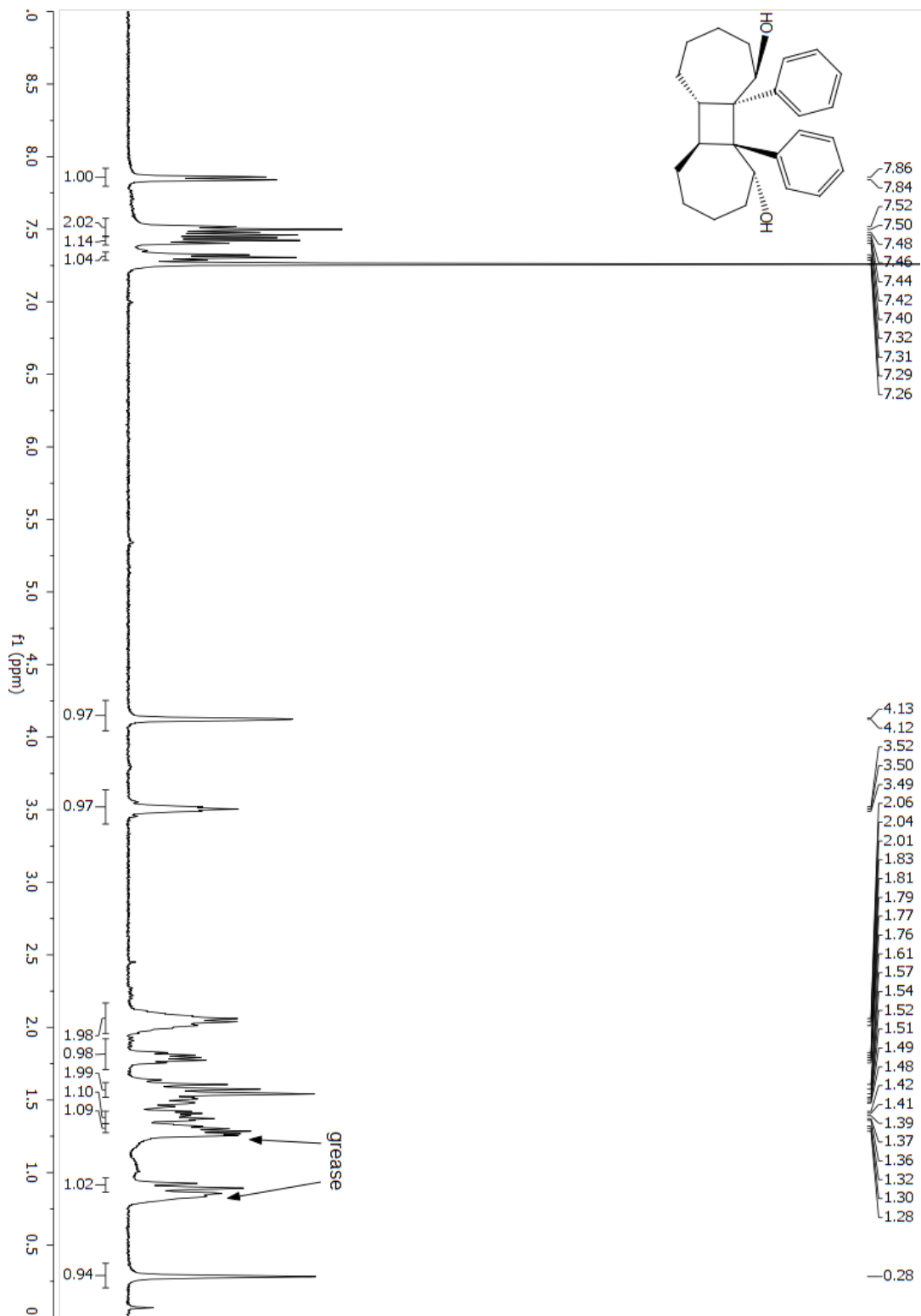
**d-4b (1R,5aS,5bS,10R,10aS,10bS)-10a,10b-bis(4-chlorophenyl)tetradecahydrocyclobuta-[1,2:3,4]di[7]annulene-1,10-diol**



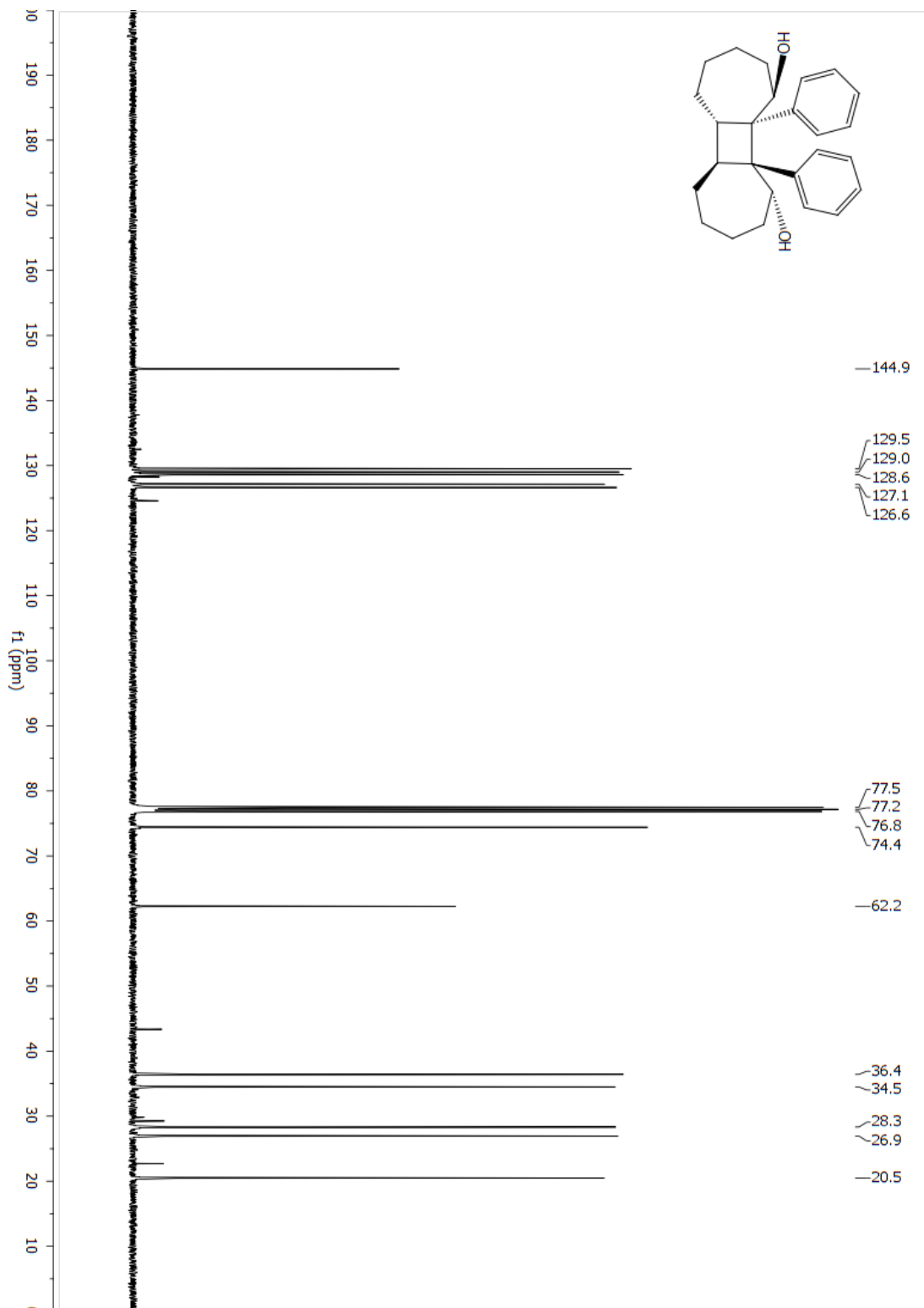
**d-4b (1R,5aS,5bS,10R,10aS,10bS)-10a,10b-bis(4-chlorophenyl)tetradecahydrocyclobuta-[1,2:3,4]di[7]annulene-1,10-diol**



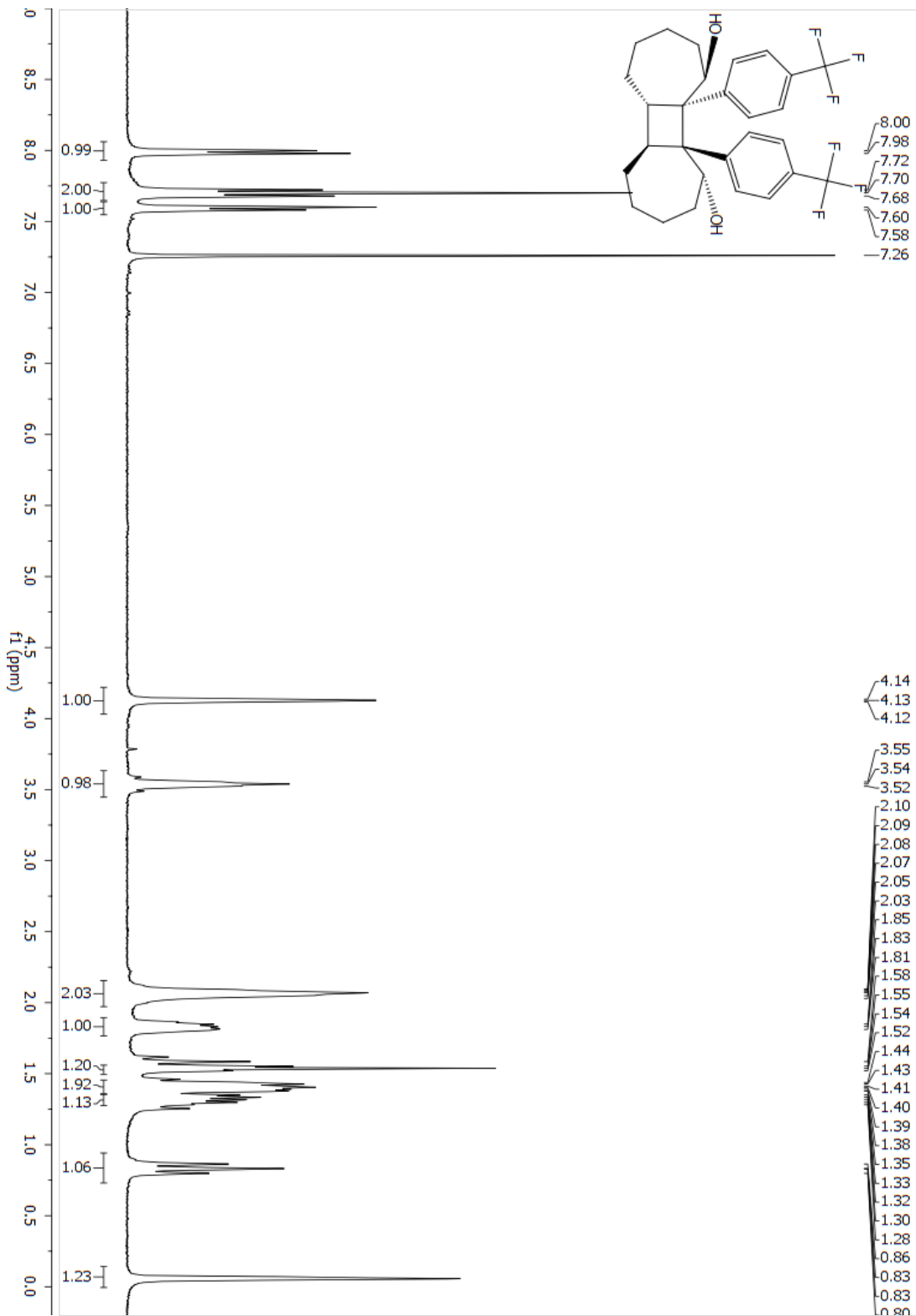
**d-4c (1R,5aS,5bS,10R,10aS,10bS)-10a,10b-diphenyltetradecahydrocyclobuta[1,2:3,4]di[7]annulene-1,10-diol**



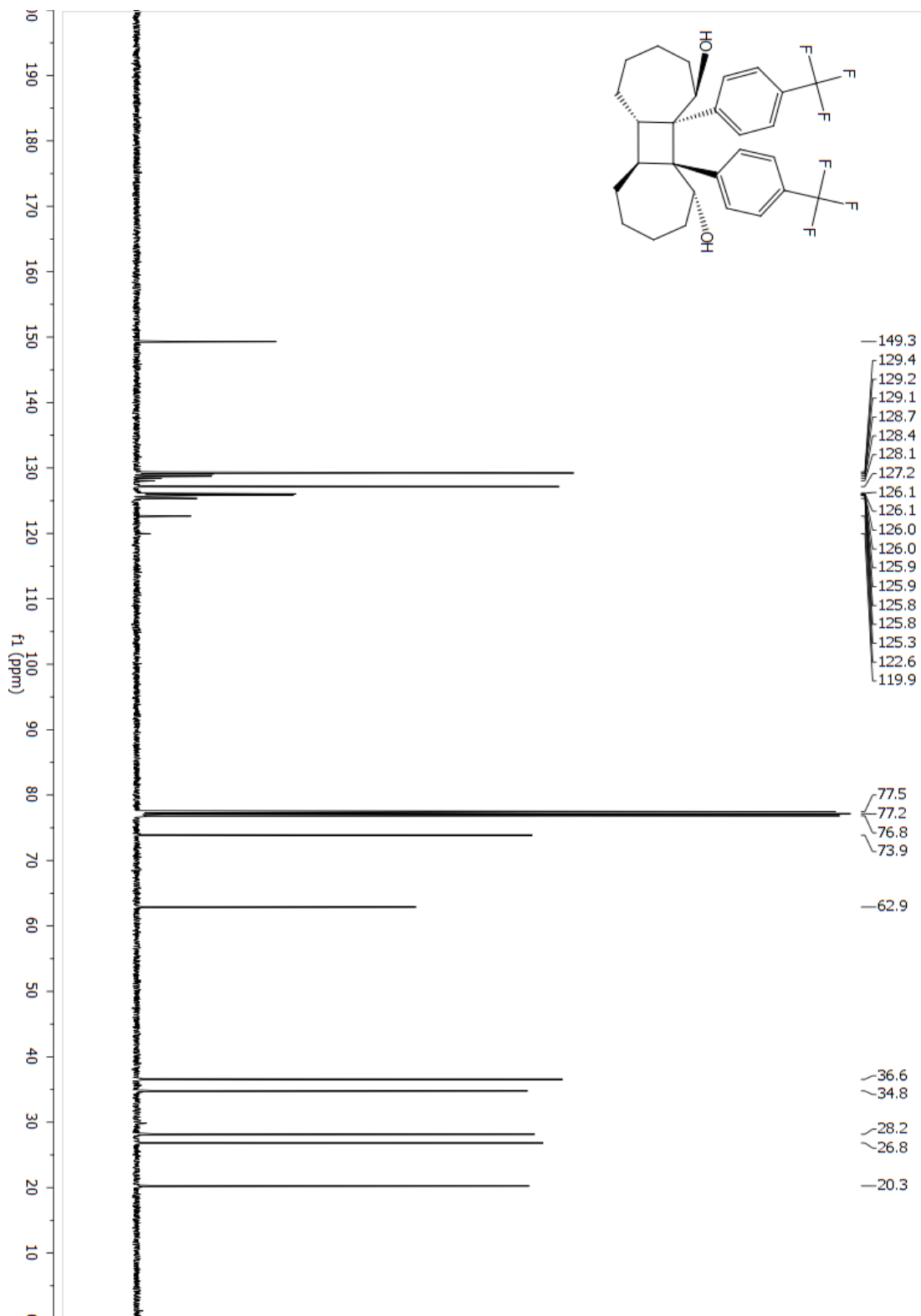
**d-4c (1R,5aS,5bS,10R,10aS,10bS)-10a,10b-diphenyltetradecahydrocyclobuta[1,2:3,4]di[7]annulene-1,10-diol**



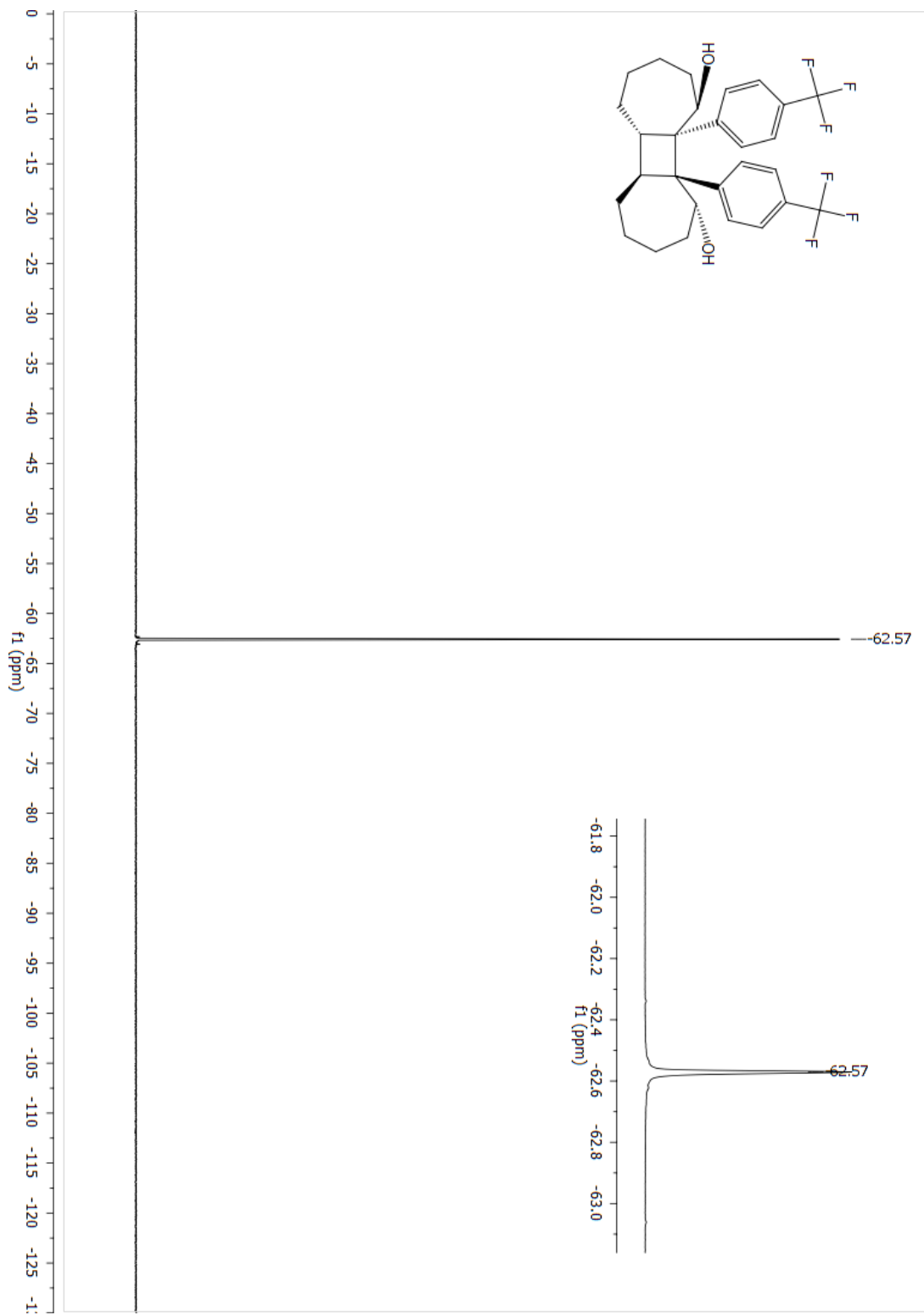
**d-4d (1R,5aS,5bS,10R,10aS,10bS)-10a,10b-bis(4-(trifluoromethyl)phenyl)tetradecahydrocyclobuta[1,2:3,4]di[7]annulene-1,10-diol**



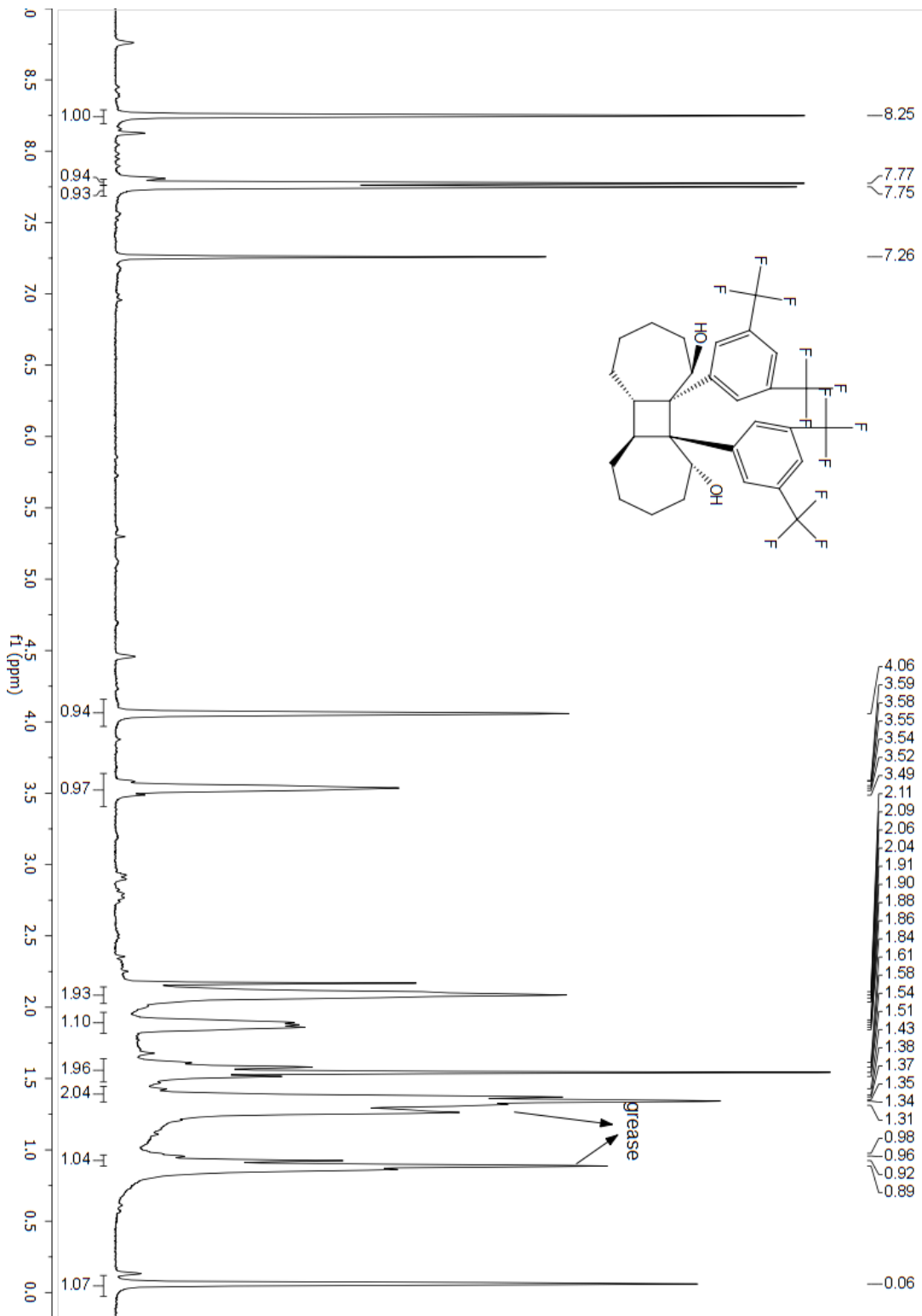
**d-4d (1R,5aS,5bS,10R,10aS,10bS)-10a,10b-bis(4-(trifluoromethyl)phenyl)tetradecahydrocyclobuta[1,2:3,4]di[7]annulene-1,10-diol**



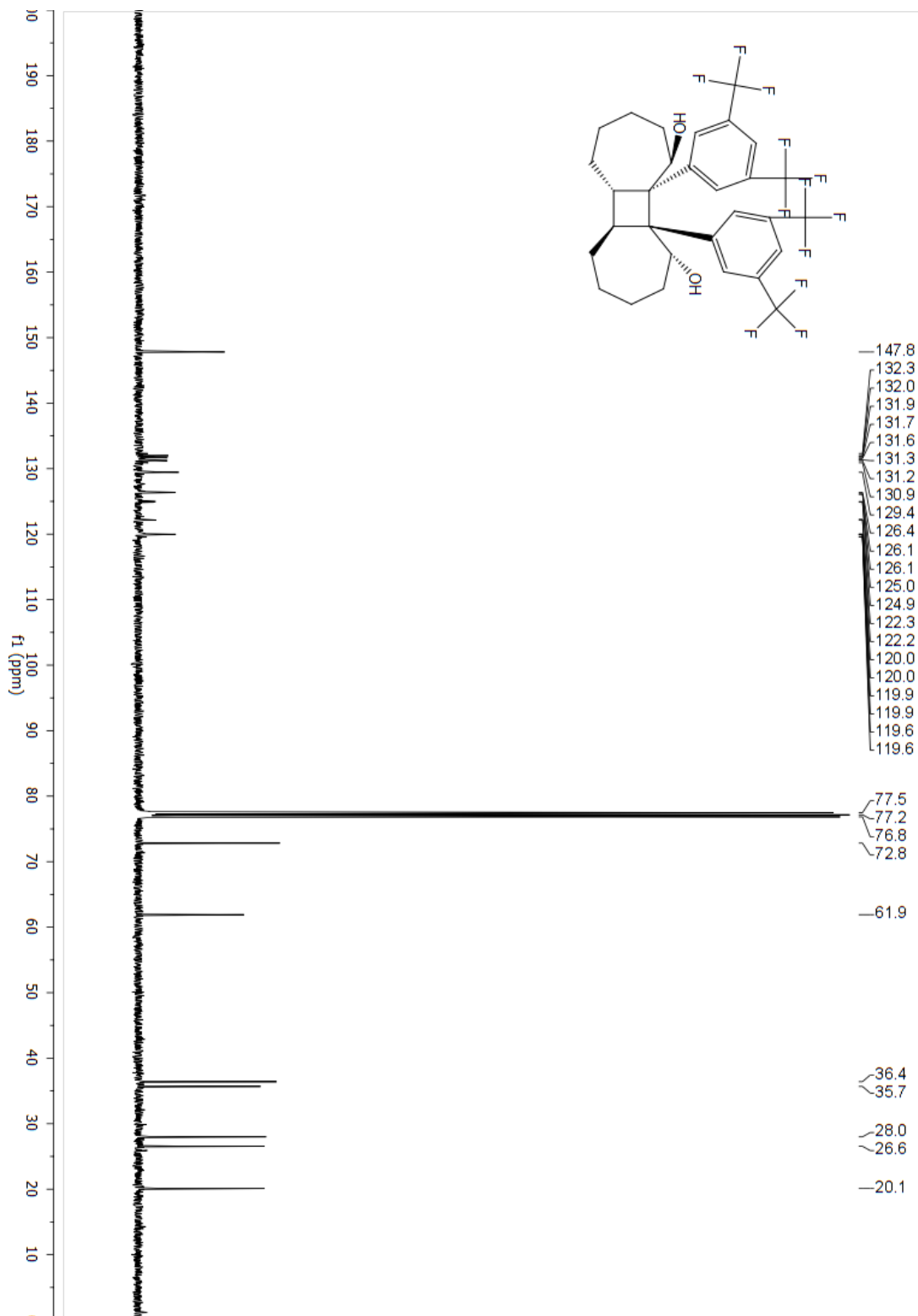
**d-4d (1R,5aS,5bS,10R,10aS,10bS)-10a,10b-bis(4-(trifluoromethyl)phenyl)tetradecahydrocyclobuta[1,2:3,4]di[7]annulene-1,10-diol**



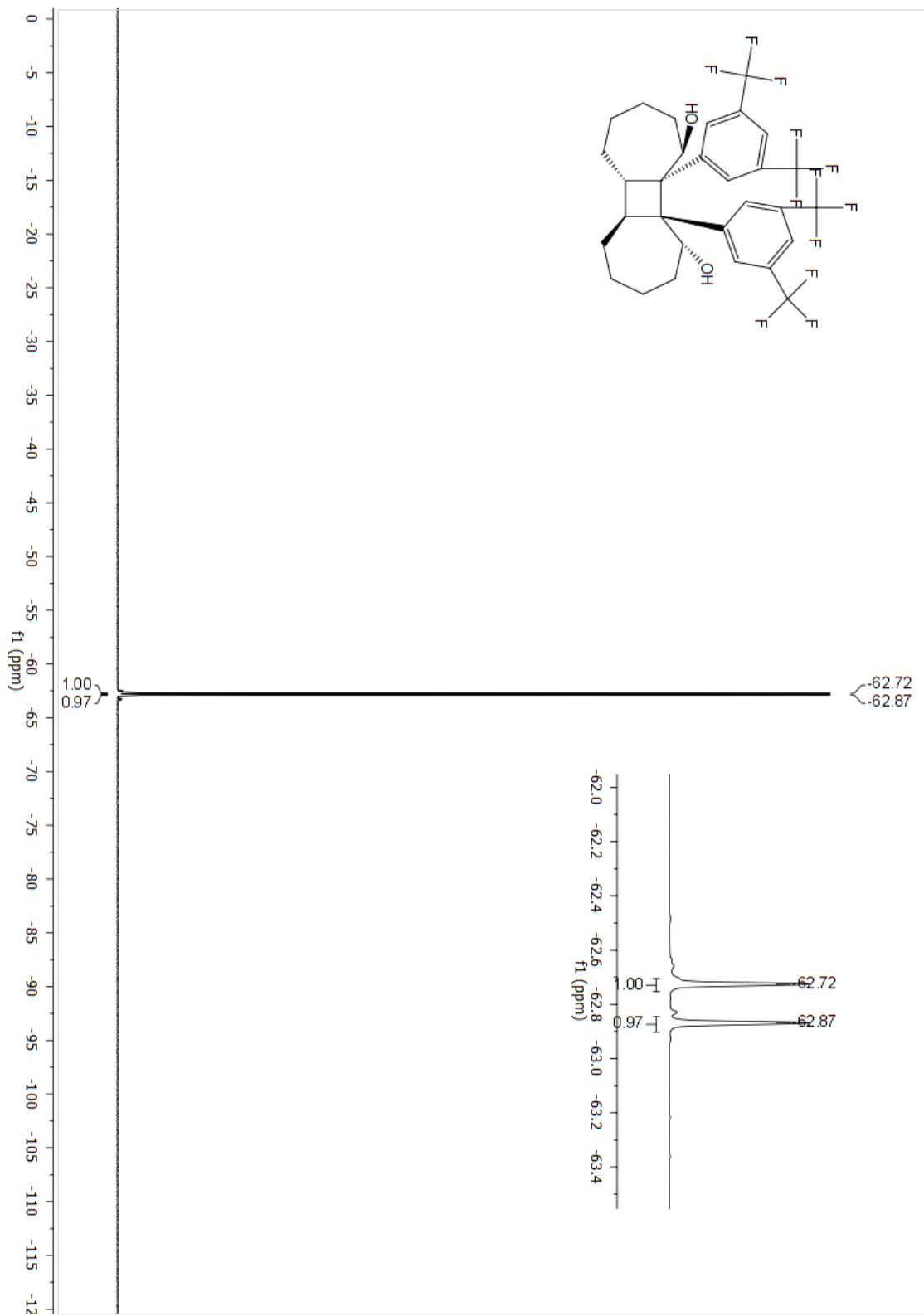
**d-4e (1R,5aS,5bS,10R,10aS,10bS)-10a,10b-bis(3,5-bis(trifluoromethyl)phenyl)tetradecahydrocyclobuta[1,2:3,4]di[7]annulene-1,10-diol**



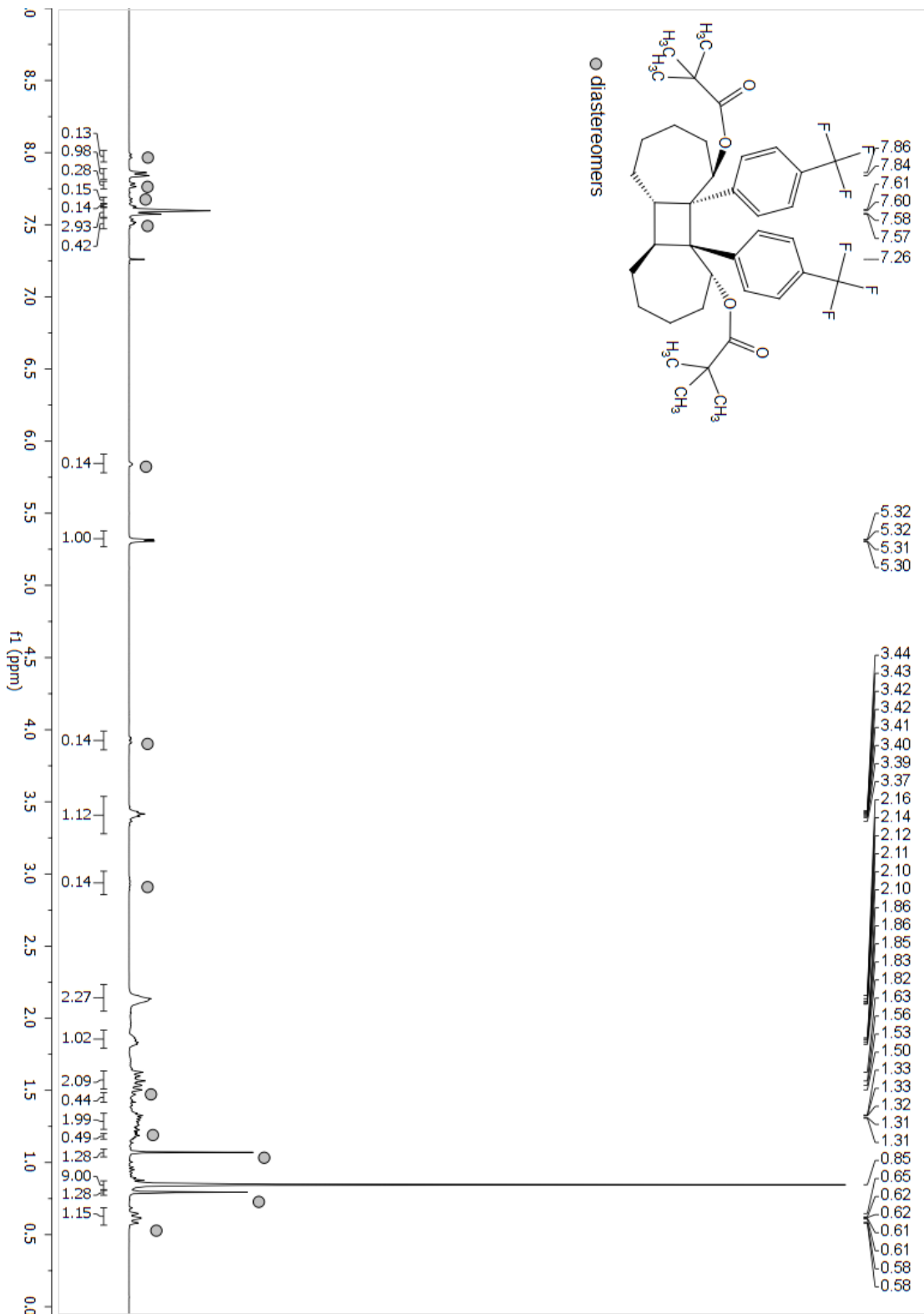
**d-4e (1R,5aS,5bS,10R,10aS,10bS)-10a,10b-bis(3,5-bis(trifluoromethyl)phenyl)tetradecahydrocyclobuta[1,2:3,4]di[7]annulene-1,10-diol**



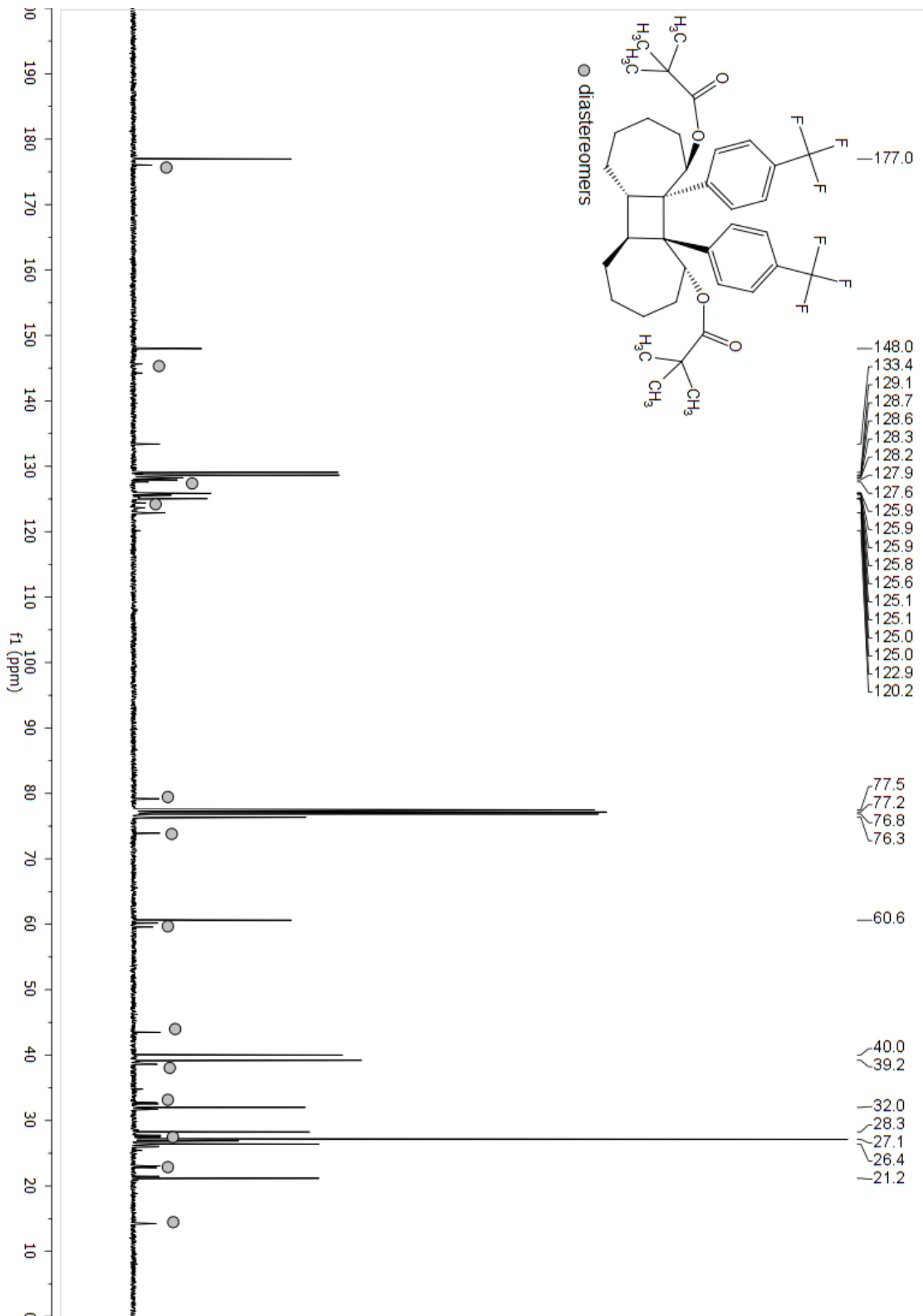
**d-4e (1R,5aS,5bS,10R,10aS,10bS)-10a,10b-bis(3,5-bis(trifluoromethyl)phenyl)tetradecahydrocyclobuta[1,2:3,4]di[7]annulene-1,10-diol**



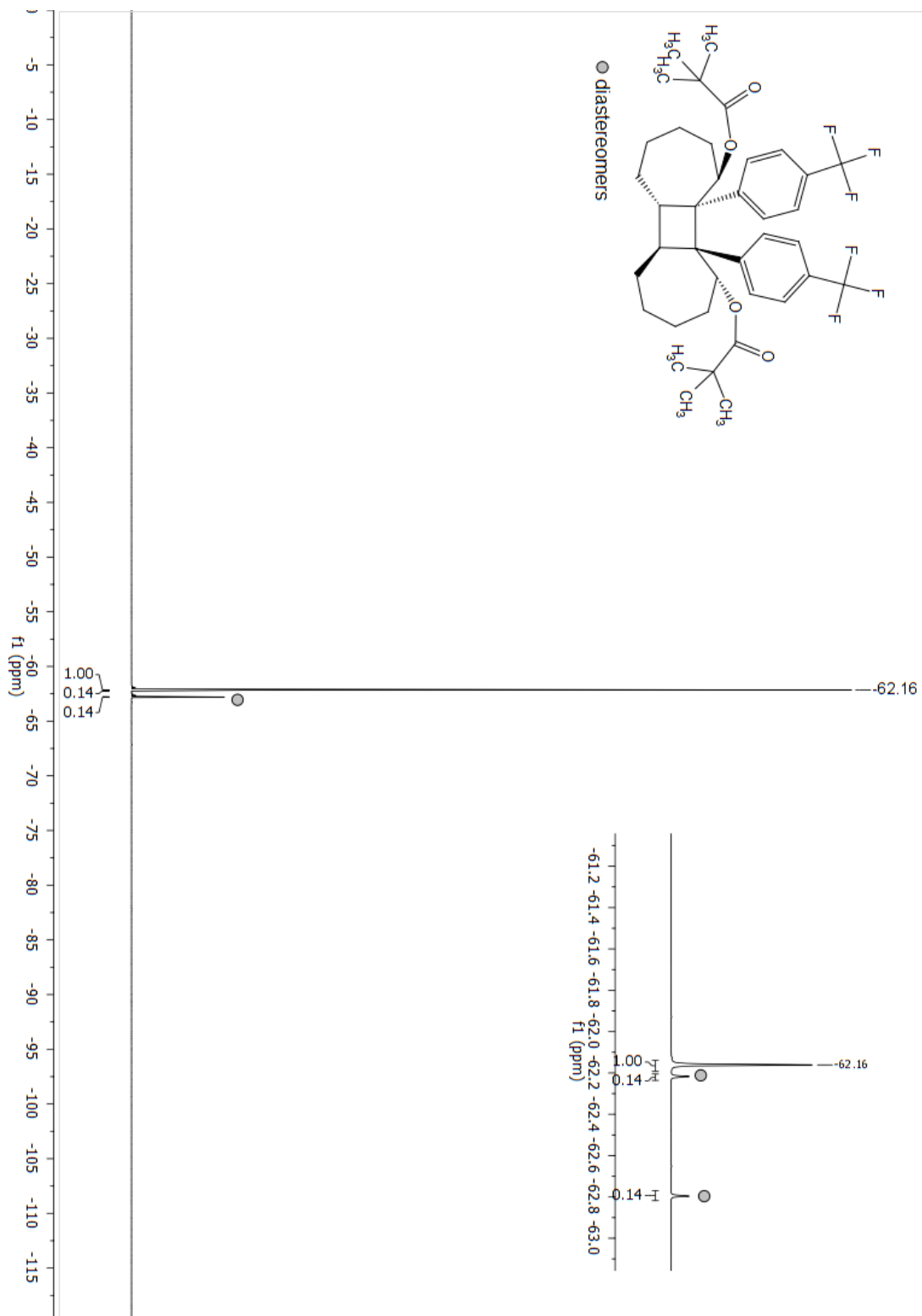
**d-4f (1R,5aS,5bS,10R,10aS,10bS)-10a,10b-bis(4-(trifluoromethyl)phenyl)tetradecahydrocyclobuta[1,2:3,4]di[7]annulene-1,10-diyl bis(2,2-dimethylpropanoate)**



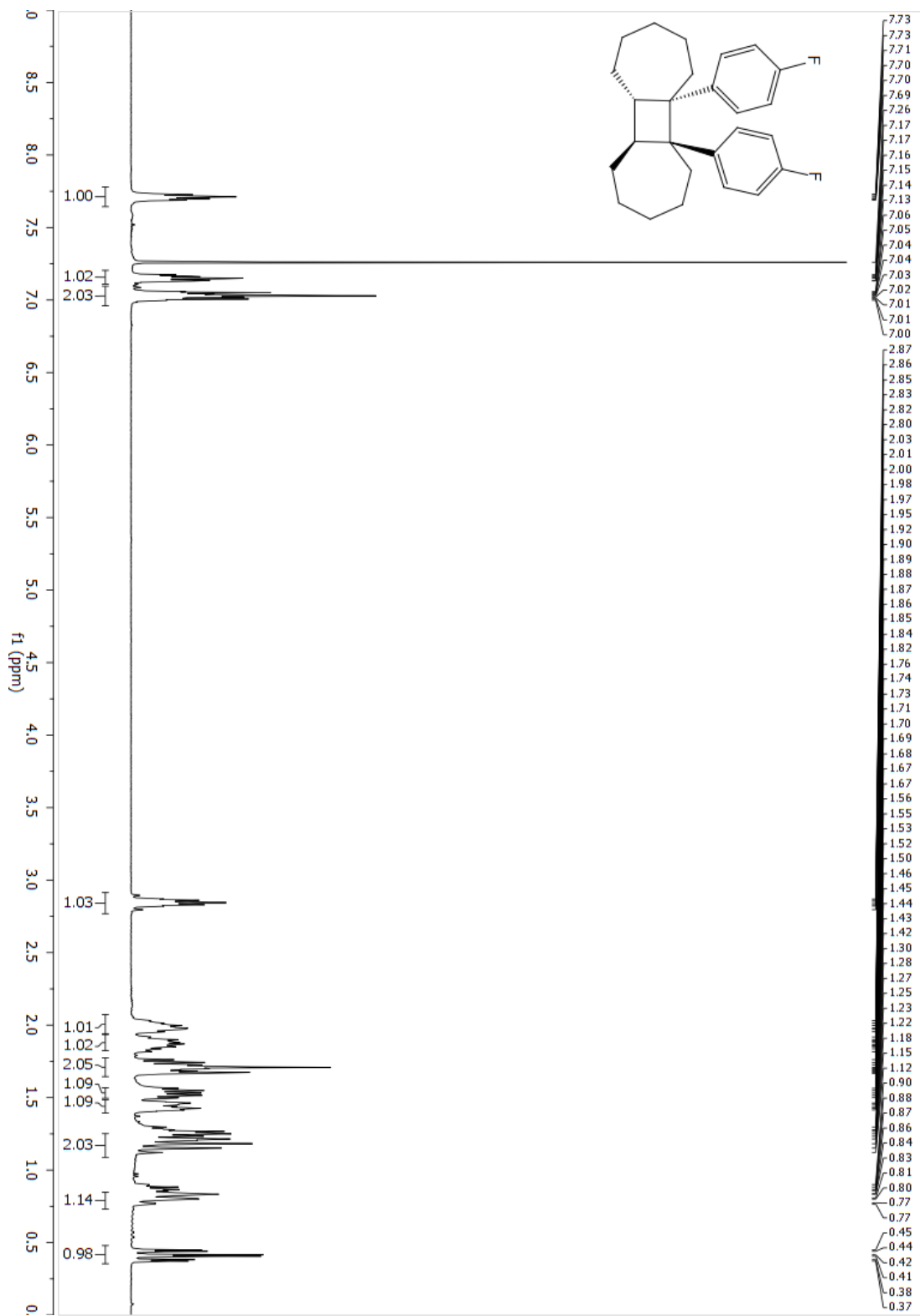
**d-4f (1R,5aS,5bS,10R,10aS,10bS)-10a,10b-bis(4-(trifluoromethyl)phenyl)tetradecahydrocyclobuta[1,2:3,4]di[7]annulene-1,10-diyl bis(2,2-dimethylpropanoate)**



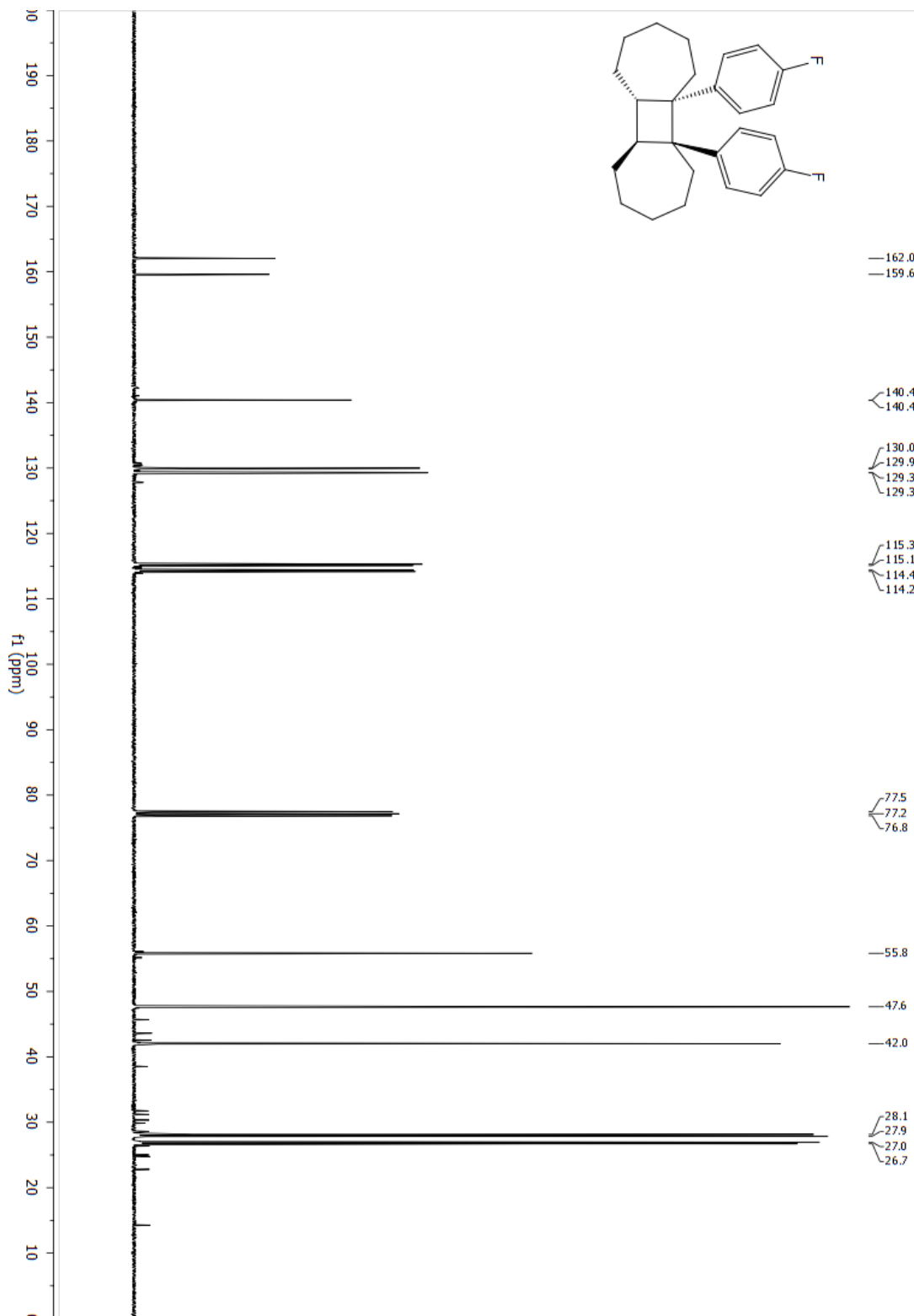
**d-4f (1R,5aS,5bS,10R,10aS,10bS)-10a,10b-bis(4-(trifluoromethyl)phenyl)tetradecahydrocyclobuta[1,2:3,4]di[7]annulene-1,10-diyl bis(2,2-dimethylpropanoate)**



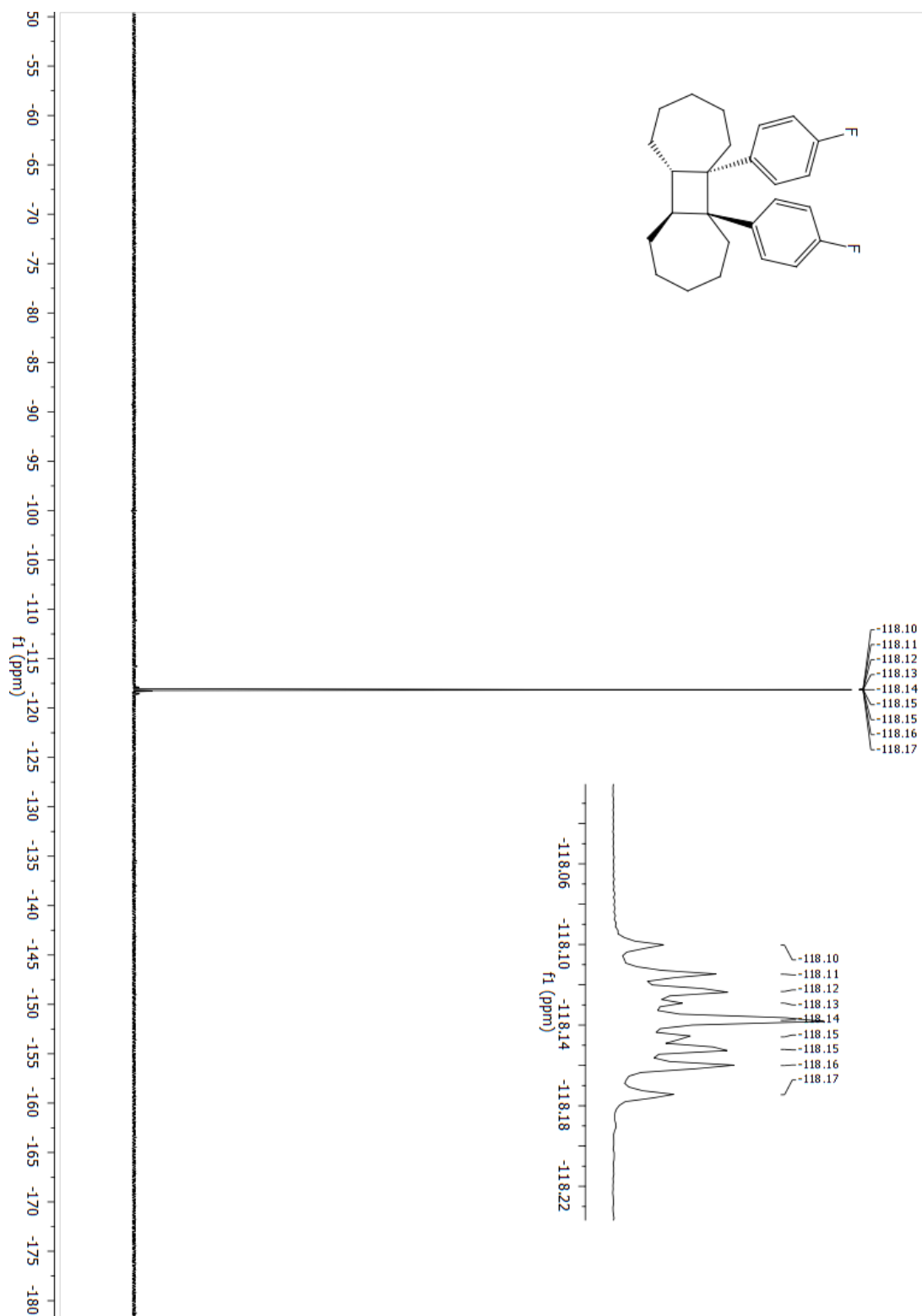
**d-4g (5aR,5bR,10aS,10bS)-5a,5b-bis(4-fluorophenyl)tetradecahydrocyclobuta[1,2:3,4]-di[7]annulene**



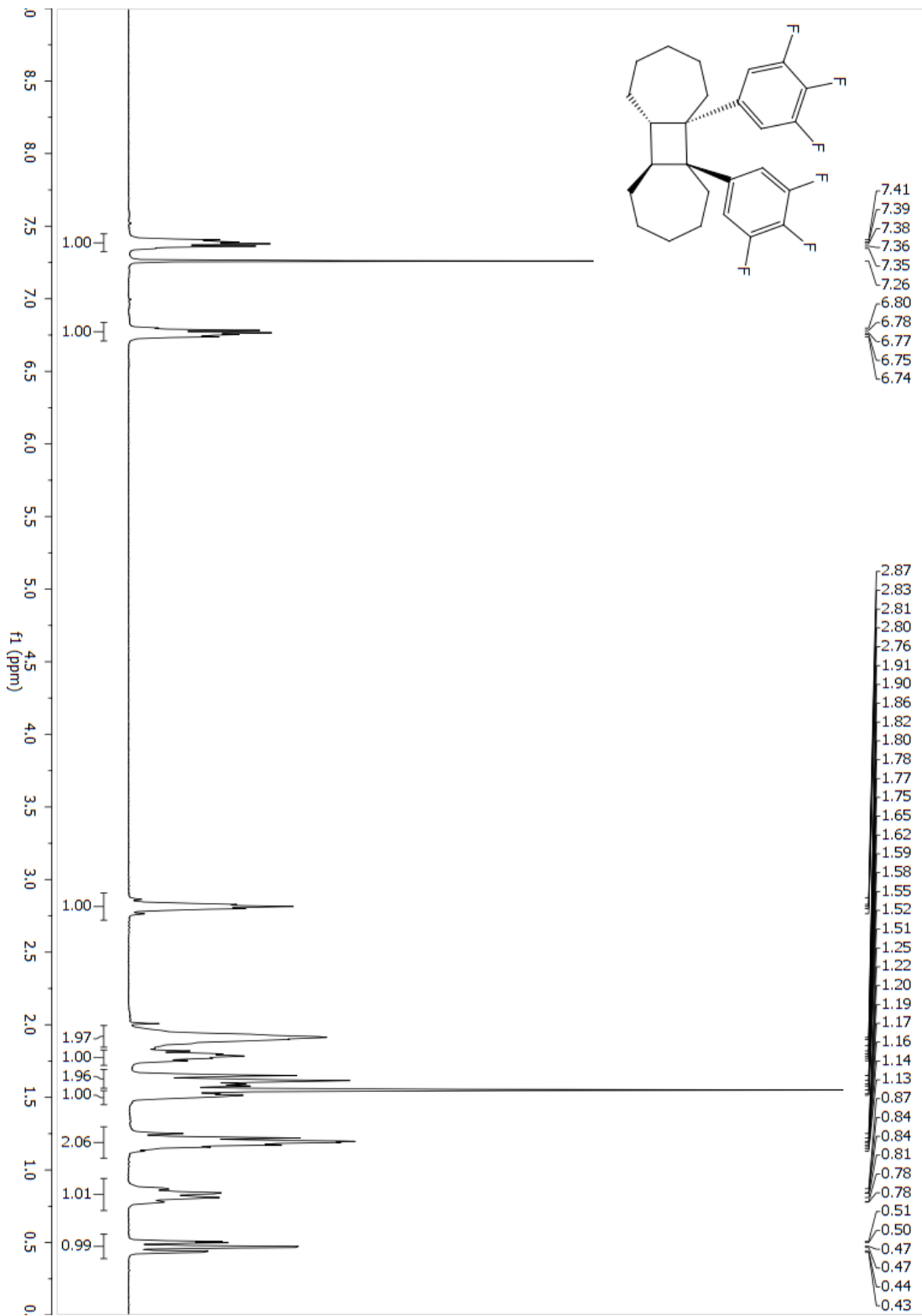
**d-4g (5aR,5bR,10aS,10bS)-5a,5b-bis(4-fluorophenyl)tetradecahydrocyclobuta[1,2:3,4]-di[7]annulene**



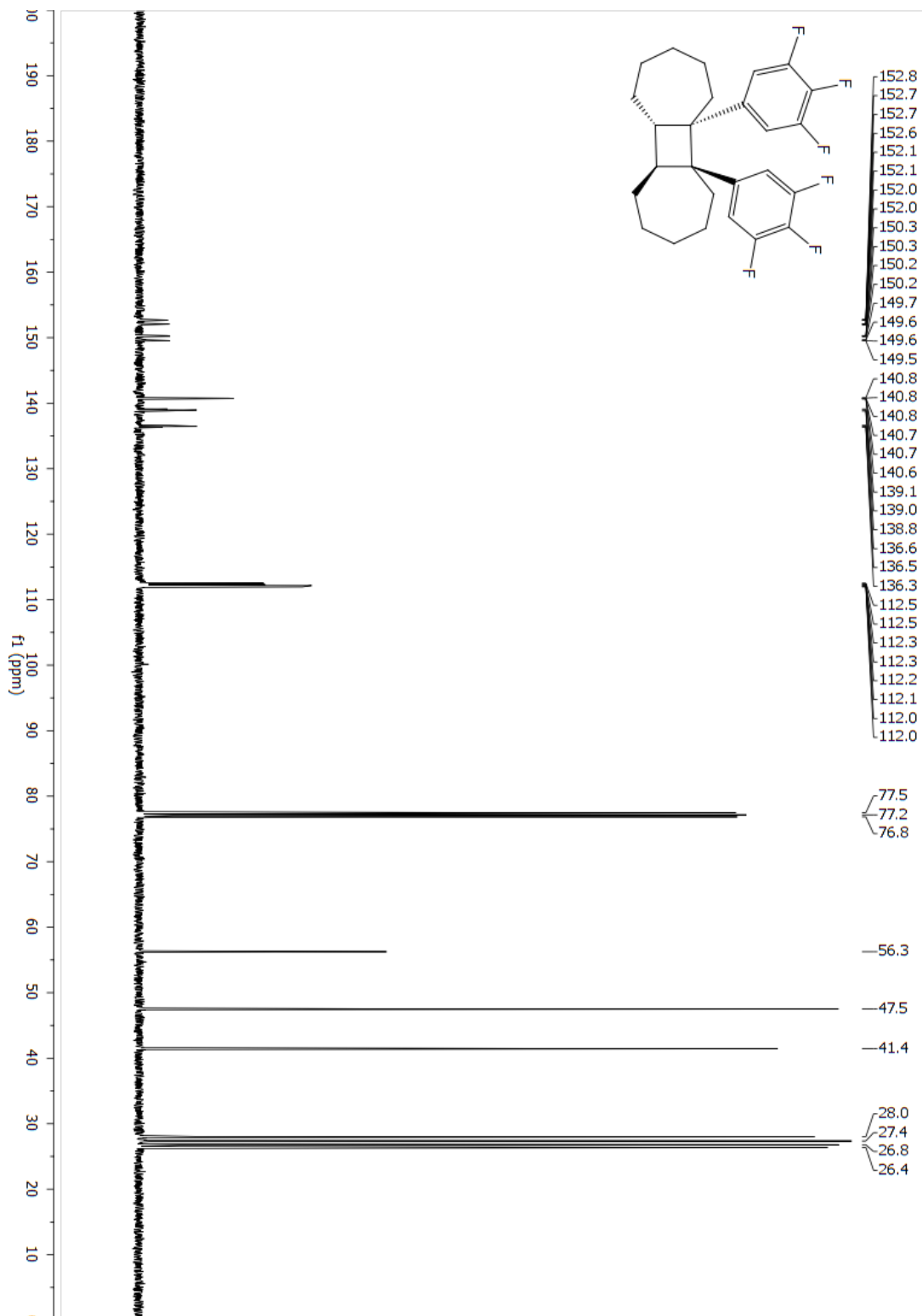
**d-4g (5aR,5bR,10aS,10bS)-5a,5b-bis(4-fluorophenyl)tetradecahydrocyclobuta[1,2:3,4]-di[7]annulene**



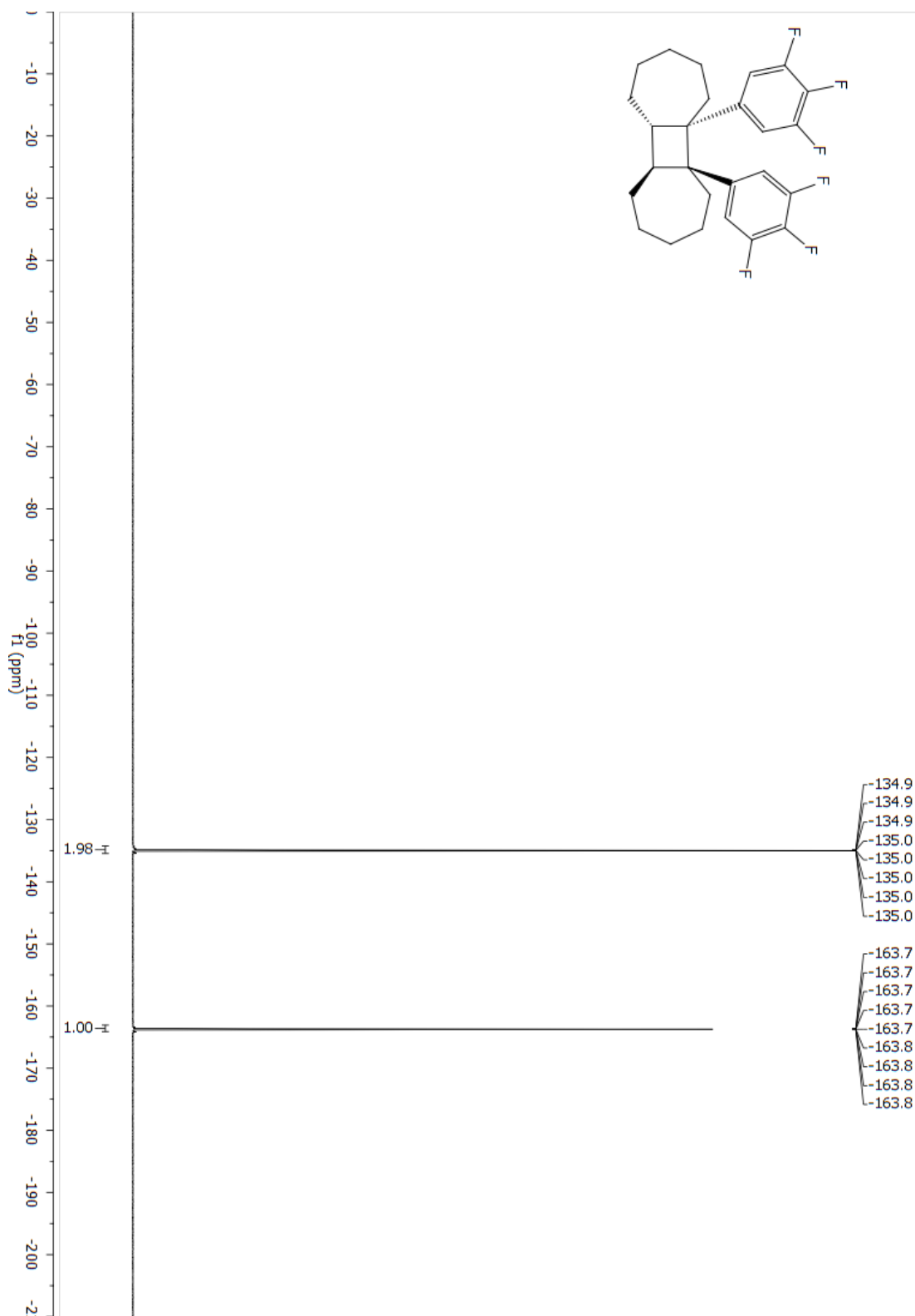
**d-4h (5aR,5bR,10aS,10bS)-5a,5b-bis(3,4,5-trifluorophenyl)tetradecahydrocyclobuta-[1,2:3,4]di[7]annulene**



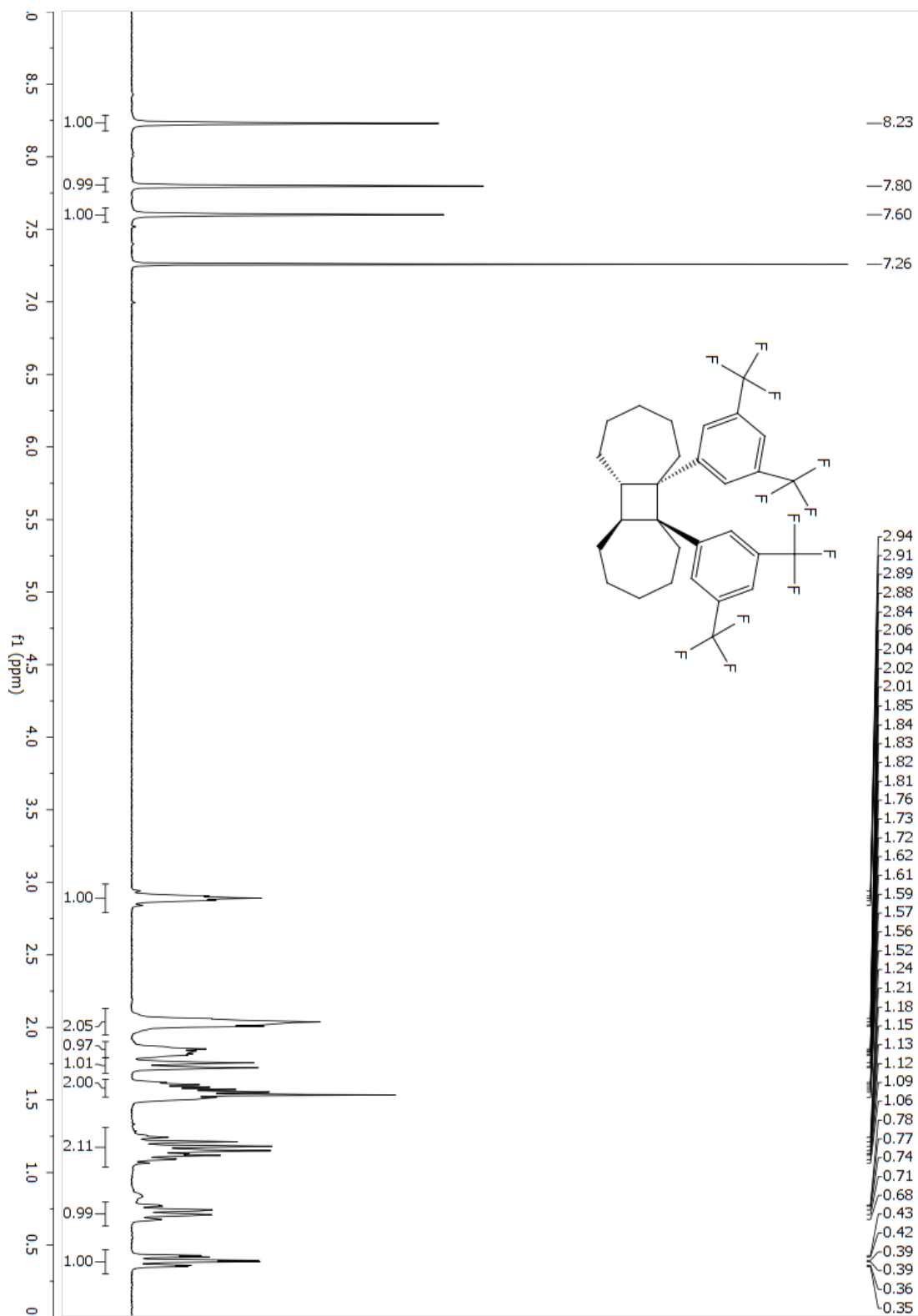
**d-4h (5aR,5bR,10aS,10bS)-5a,5b-bis(3,4,5-trifluorophenyl)tetradecahydrocyclobuta-[1,2:3,4]di[7]annulene**



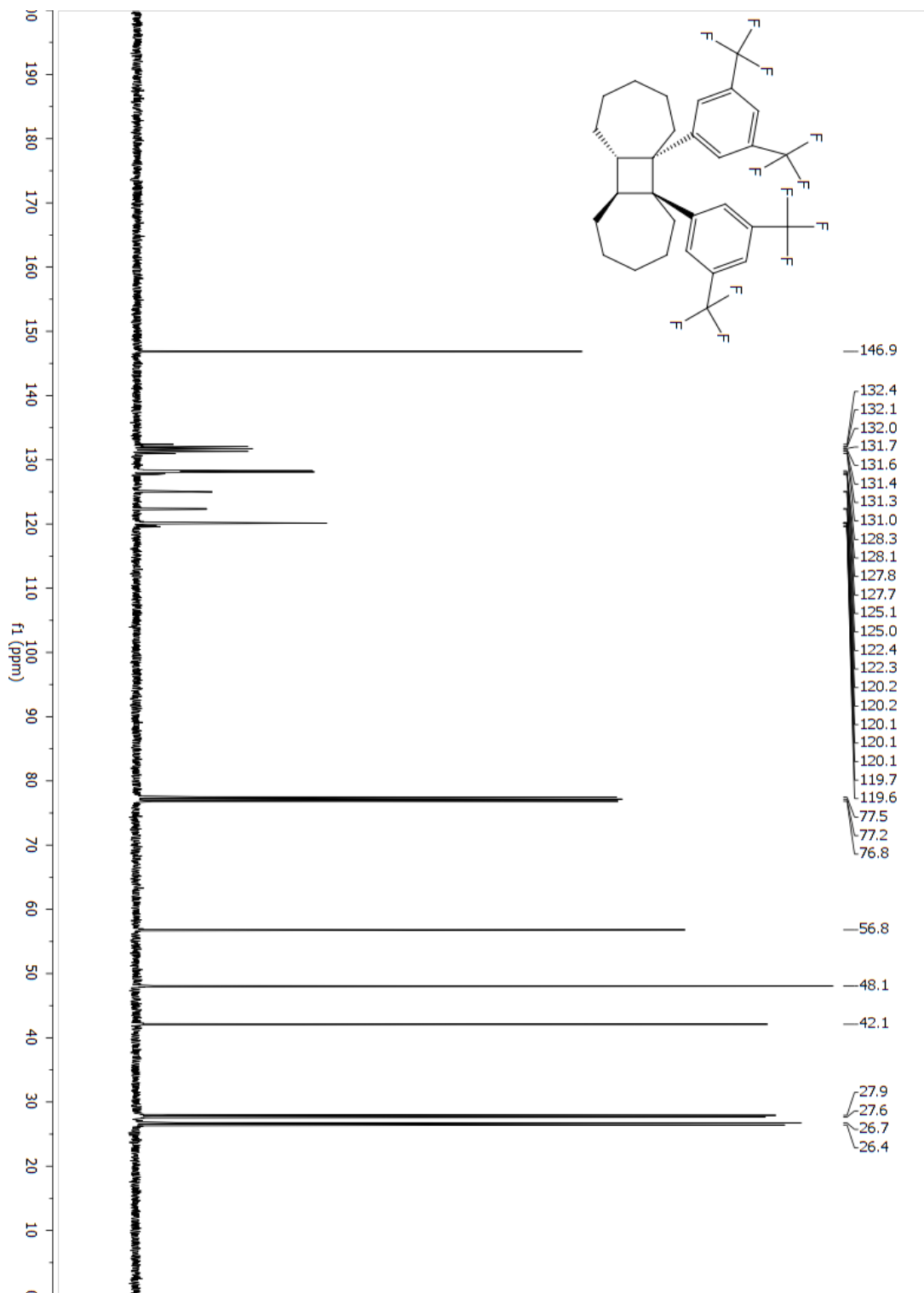
**d-4h (5aR,5bR,10aS,10bS)-5a,5b-bis(3,4,5-trifluorophenyl)tetradecahydrocyclobuta[1,2:3,4]di[7]annulene**



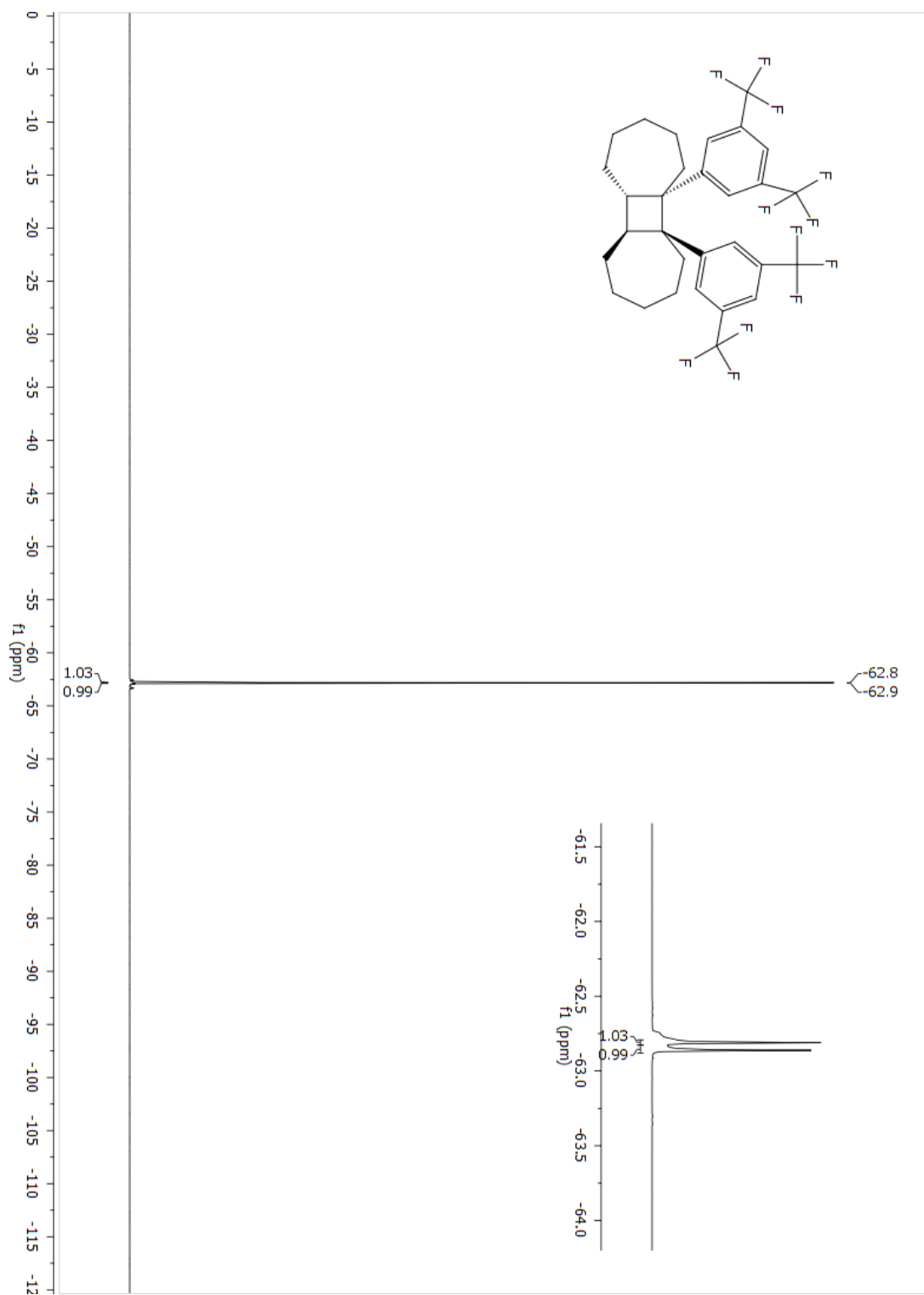
**d-4i (5aR,5bR,10aS,10bS)-5a,5b-bis(3,5-bis(trifluoromethyl)phenyl)tetradecahydrocyclobuta[1,2:3,4]di[7]annulene**



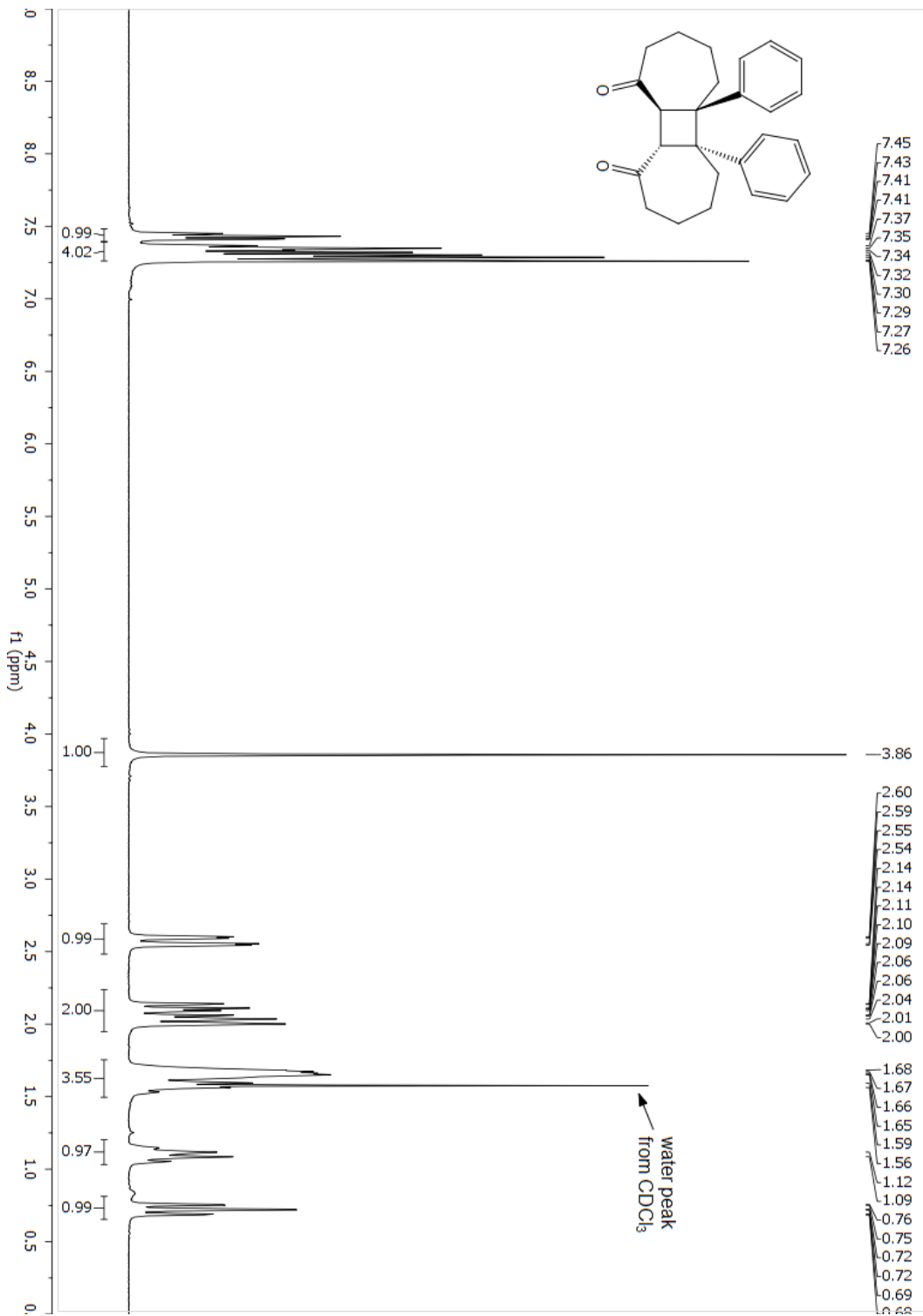
**d-4i (5aR,5bR,10aS,10bS)-5a,5b-bis(3,5-bis(trifluoromethyl)phenyl)tetradecahydrocyclobuta[1,2:3,4]di[7]annulene**



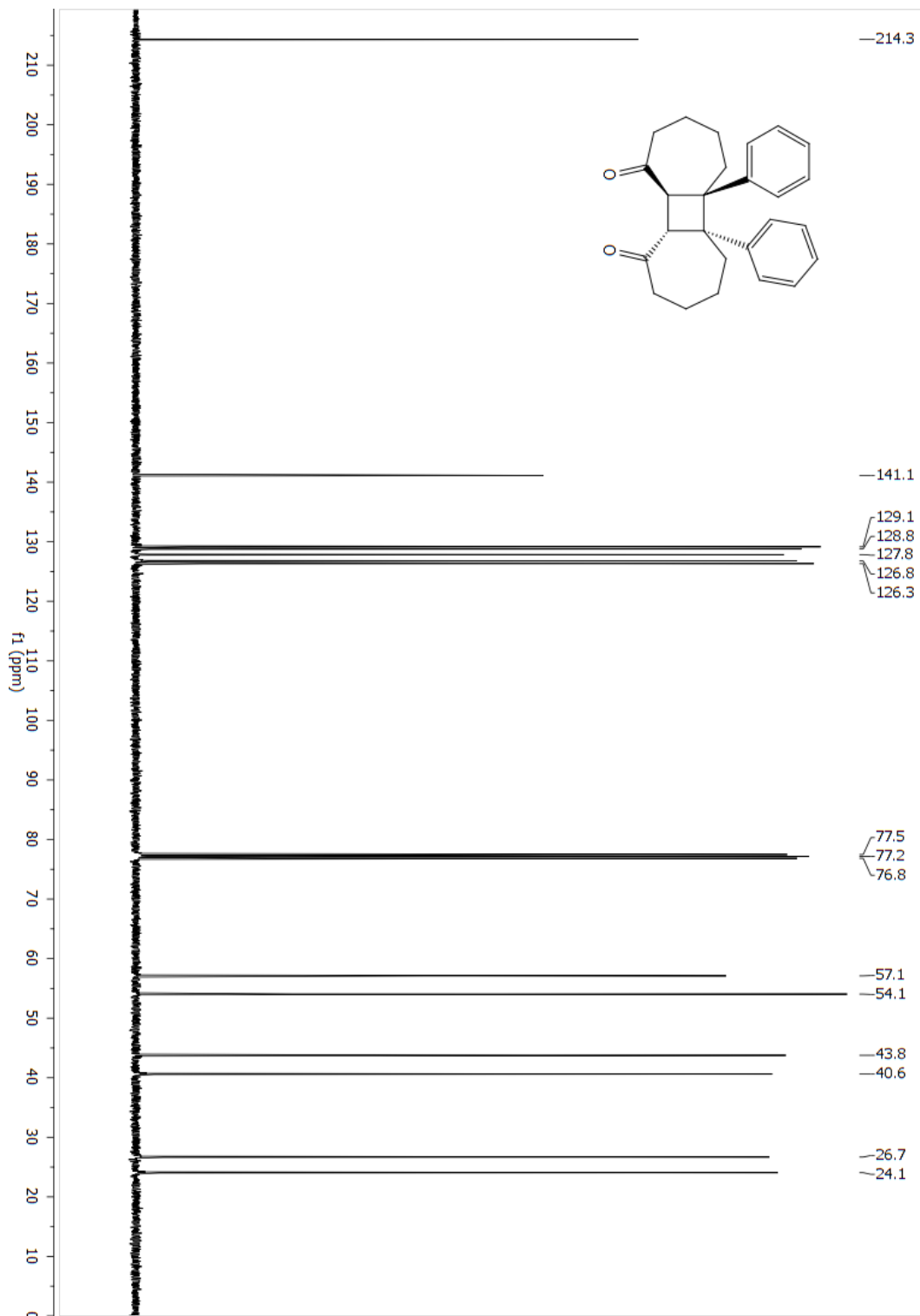
**d-4i (5aR,5bR,10aS,10bS)-5a,5b-bis(3,5-bis(trifluoromethyl)phenyl)tetradecahydrocyclobuta[1,2:3,4]di[7]annulene**



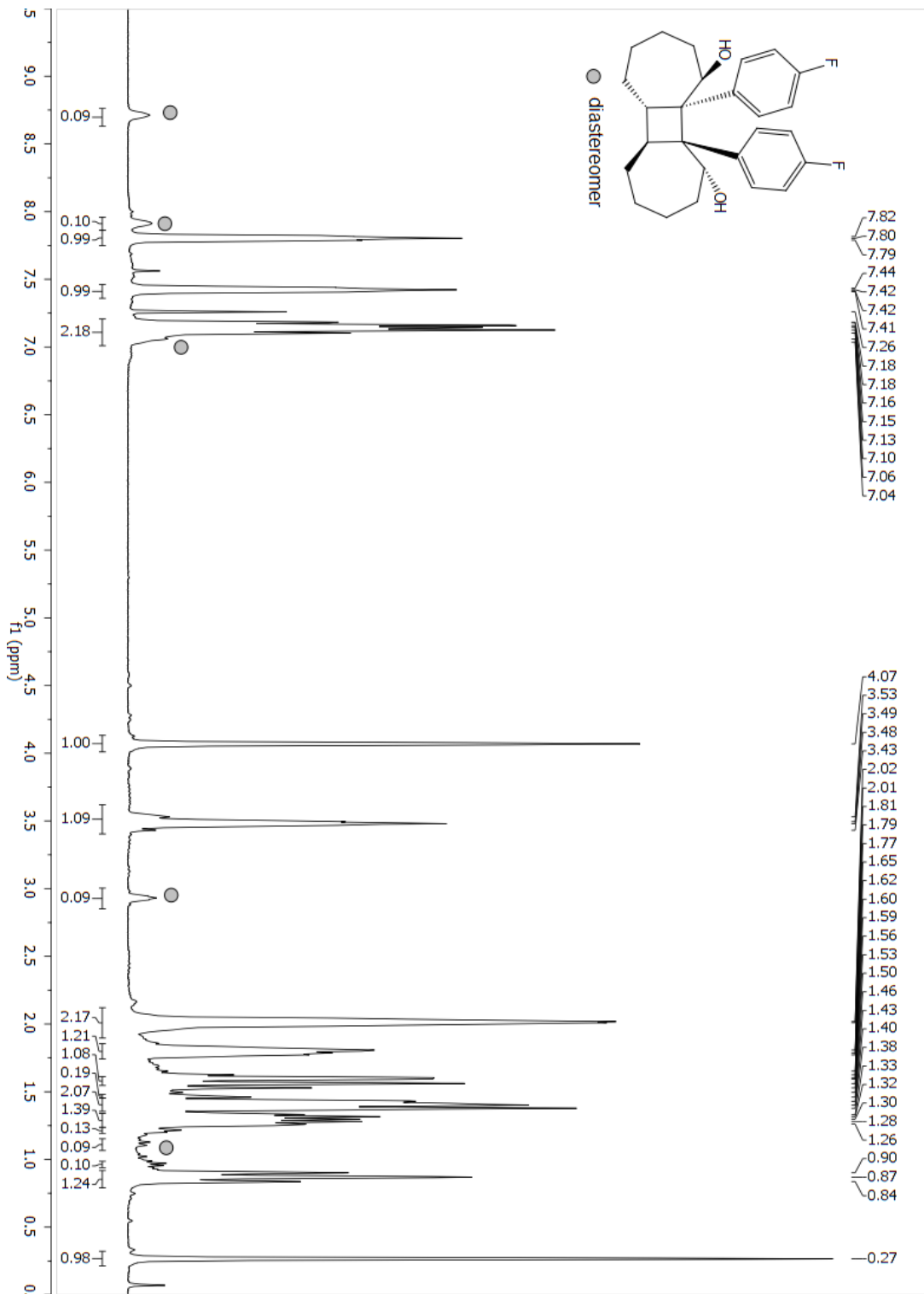
**d-4j (5aR,5bR,10aS,10bS)-5a,5b-diphenyldodecahydrocyclobuta[1,2:3,4]di[7]annulene-1,10-dione**



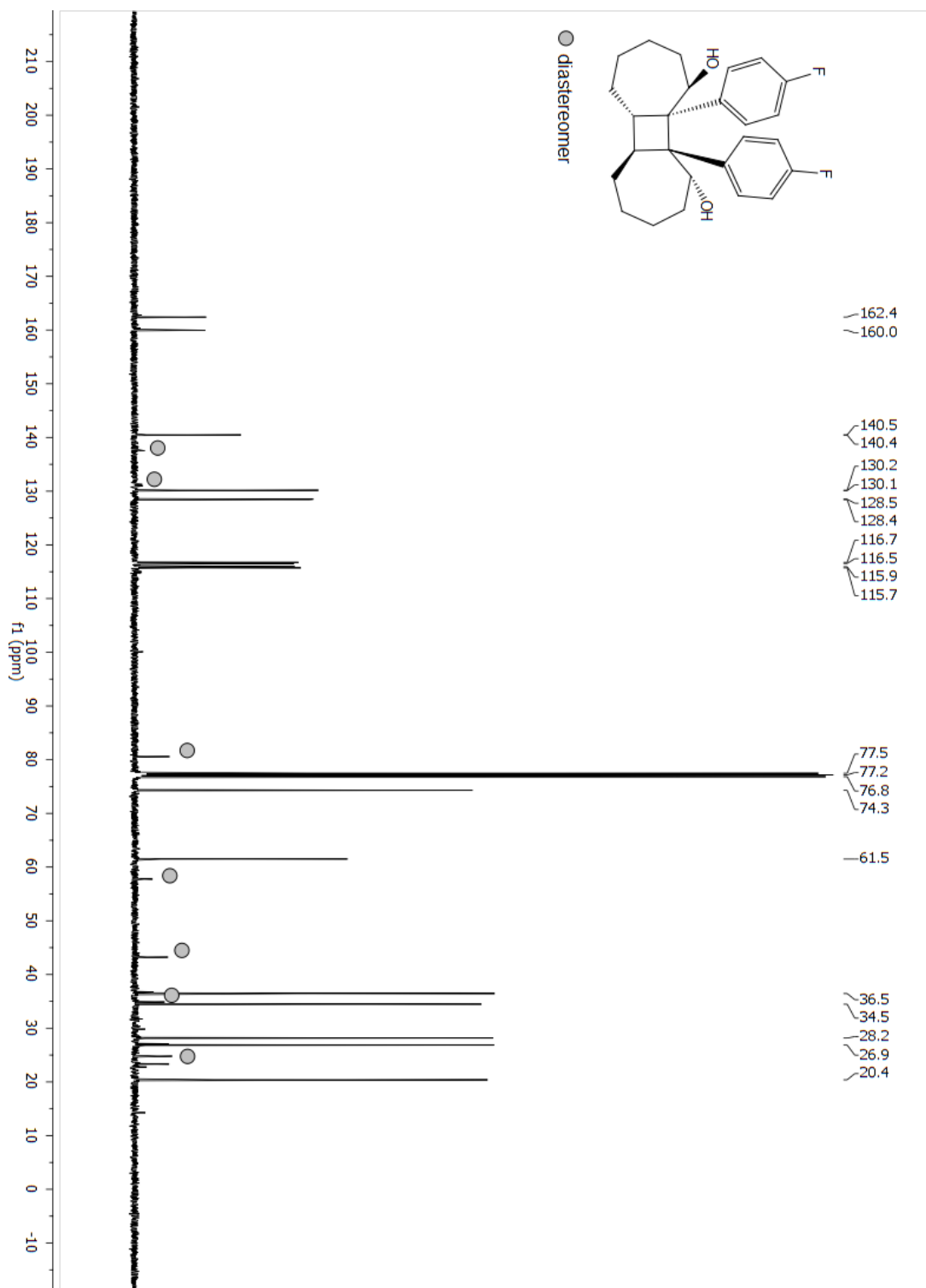
**d-4j (5aR,5bR,10aS,10bS)-5a,5b-diphenyldodecahydrocyclobuta[1,2:3,4]di[7]annulene-1,10-dione**



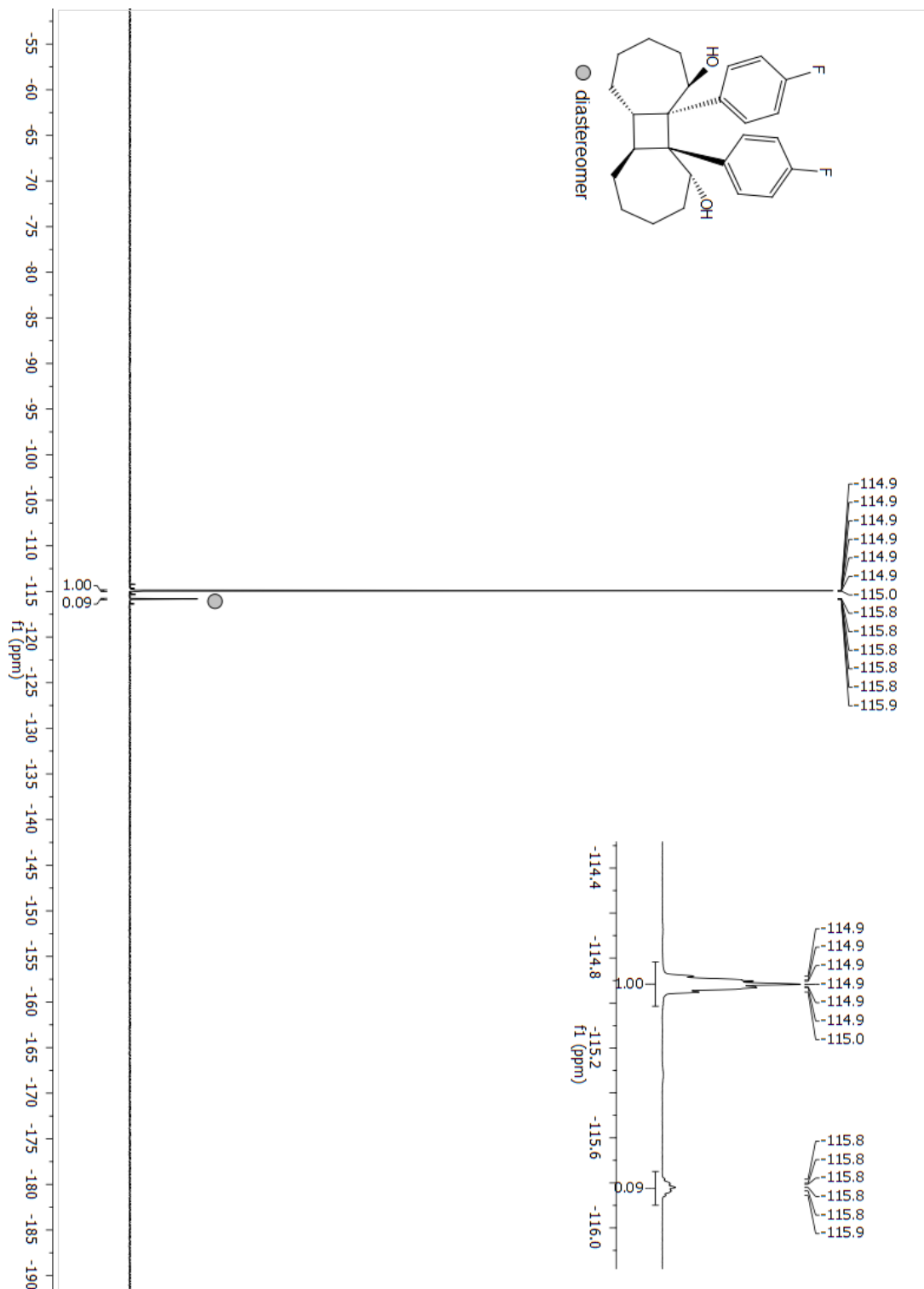
**d-4k (1R,5aS,5bS,10R,10aS,10bS)-10a,10b-bis(4-fluorophenyl)tetradecahydrocyclobuta[1,2:3,4]di[7]annulene-1,10-diol**



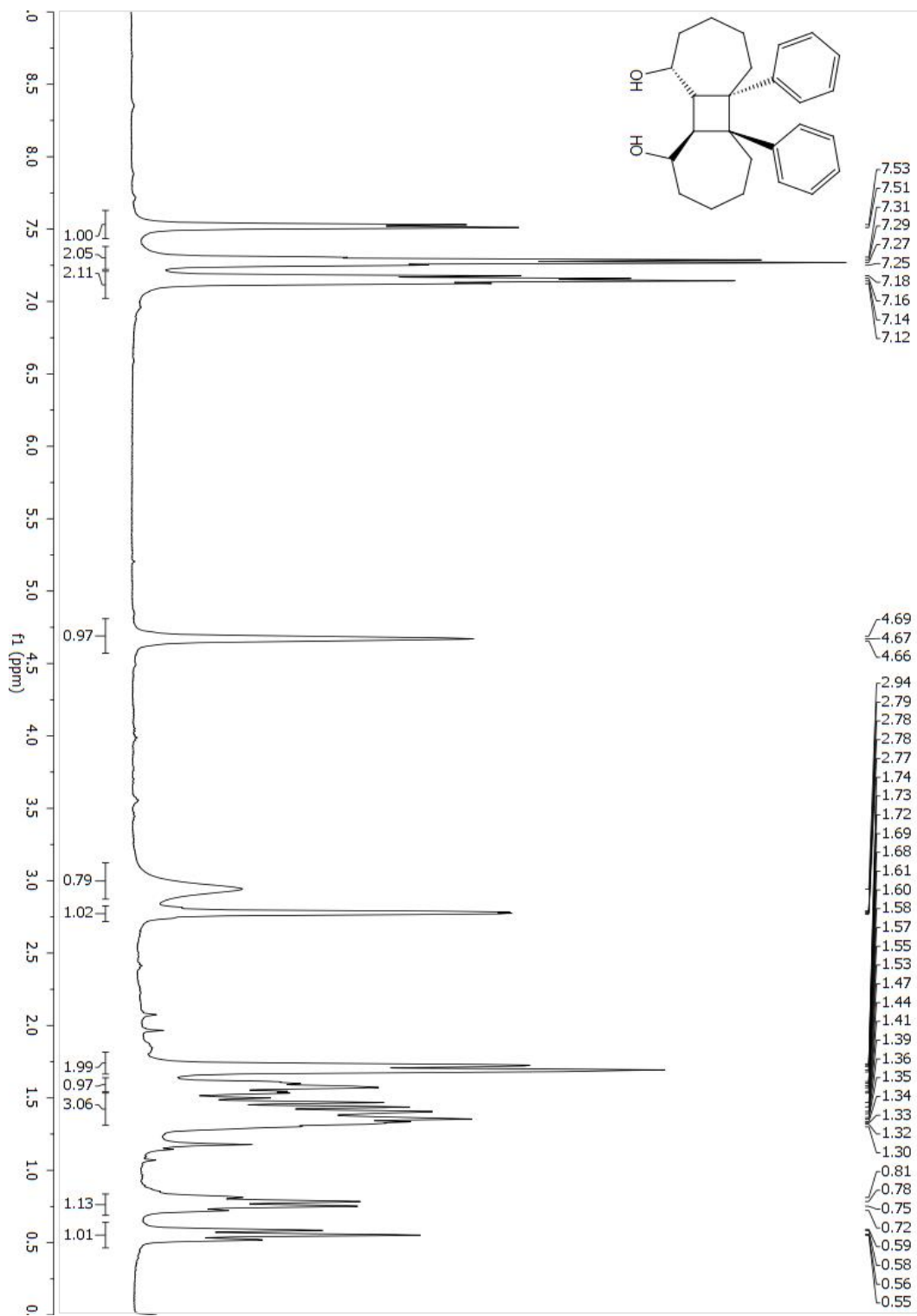
**d-4k (1R,5aS,5bS,10R,10aS,10bS)-10a,10b-bis(4-fluorophenyl)tetradecahydrocyclobuta-[1,2:3,4]di[7]annulene-1,10-diol**



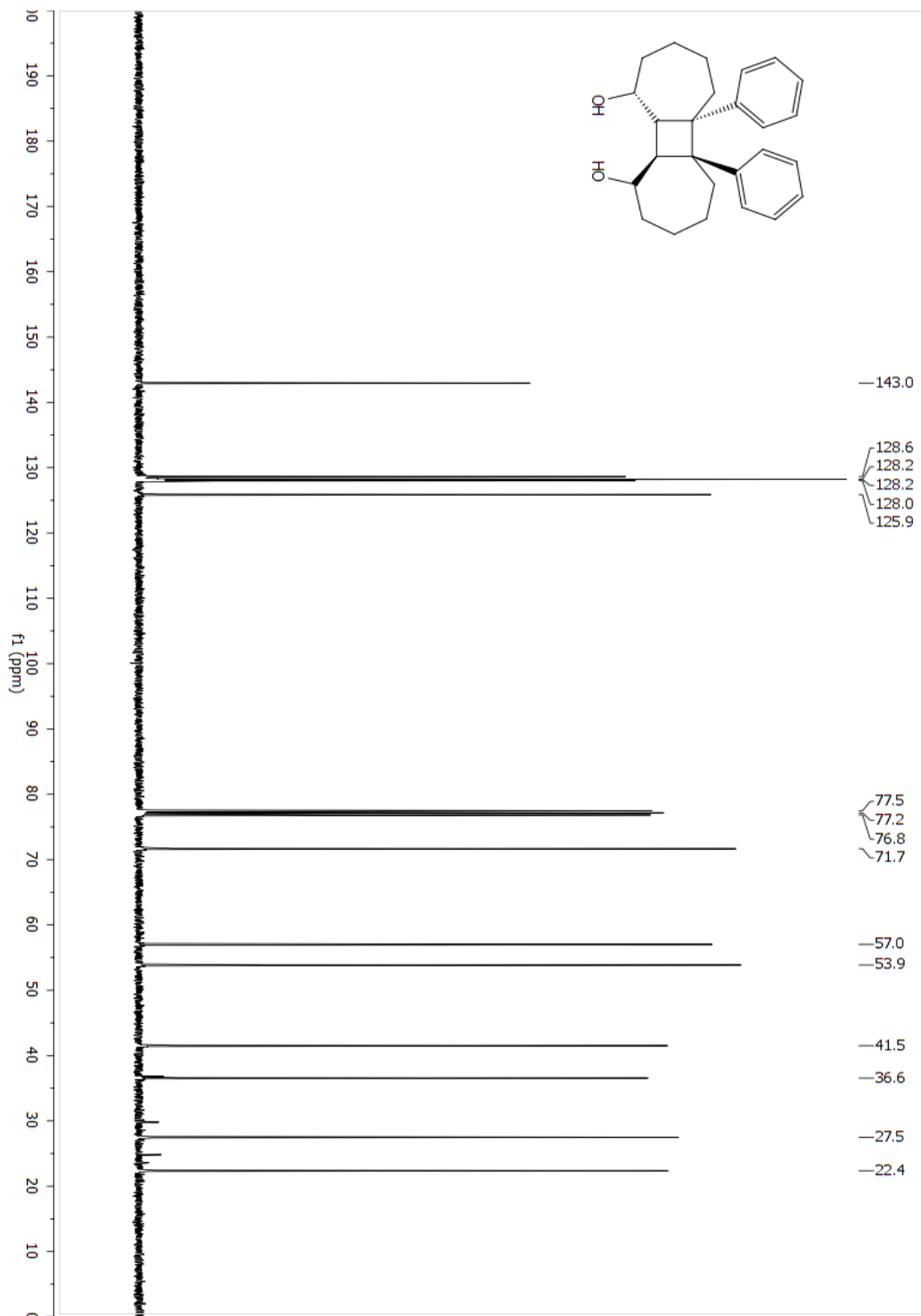
**d-4k (1R,5aS,5bS,10R,10aS,10bS)-10a,10b-bis(4-fluorophenyl)tetradecahydrocyclobuta-[1,2:3,4]di[7]annulene-1,10-diol**



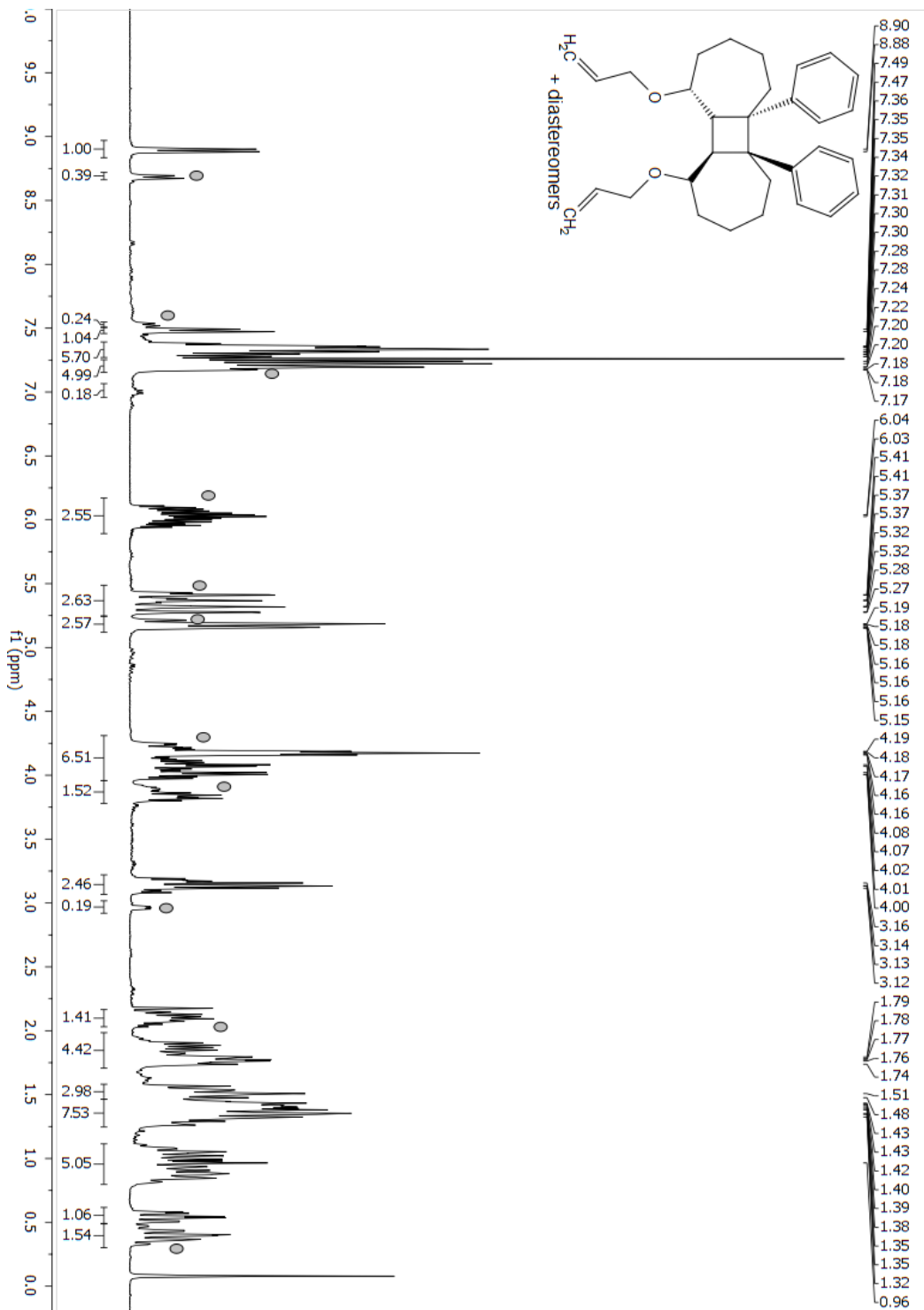
**d-4I (1R,5aR,5bR,10R,10aS,10bS)-5a,5b-diphenyltetradecahydrocyclobuta[1,2:3,4]di[7]-annulene-1,10-diol**



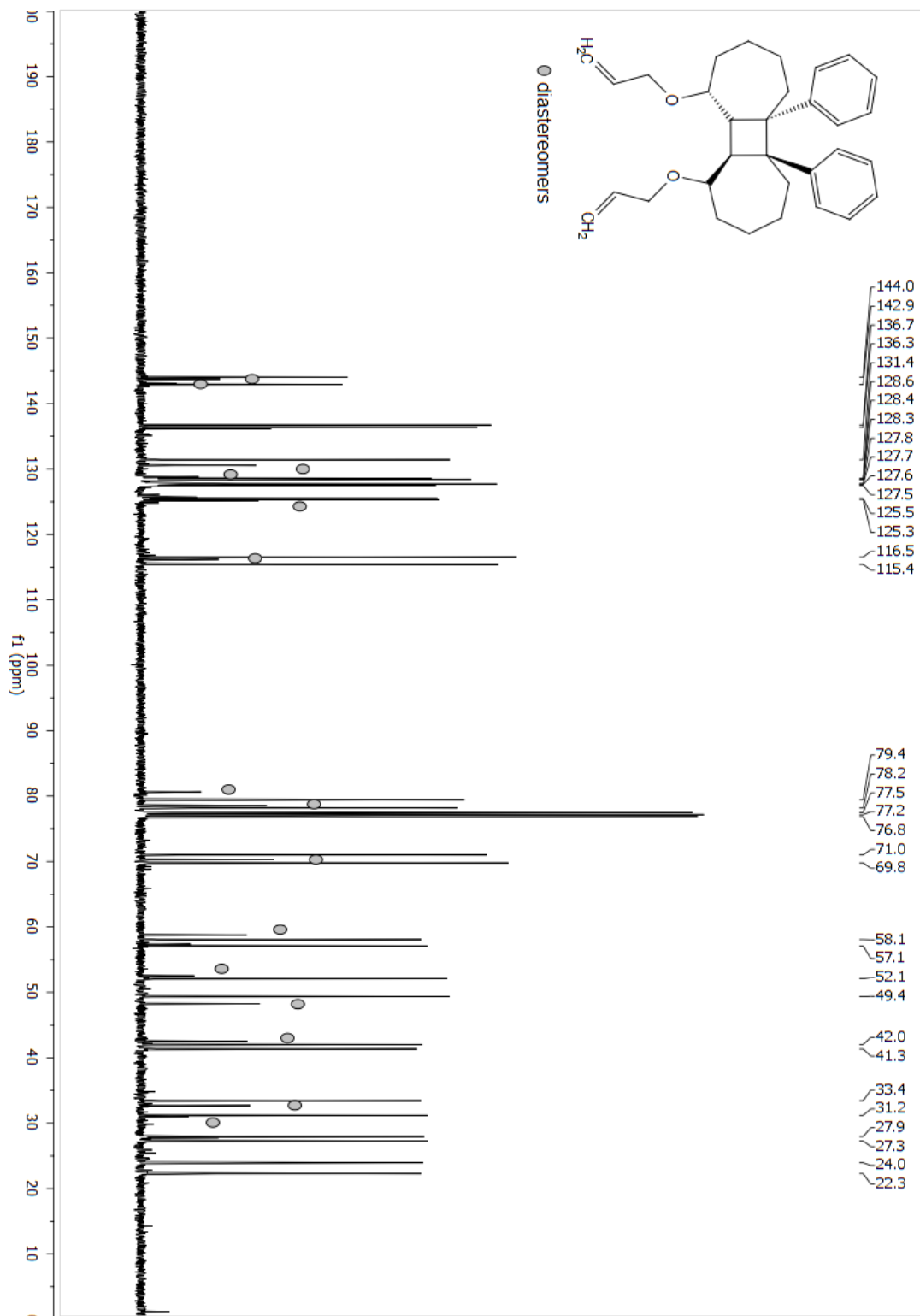
**d-4I (1R,5aR,5bR,10R,10aS,10bS)-5a,5b-diphenyltetradecahydrocyclobuta[1,2:3,4]di[7]-annulene-1,10-diol**



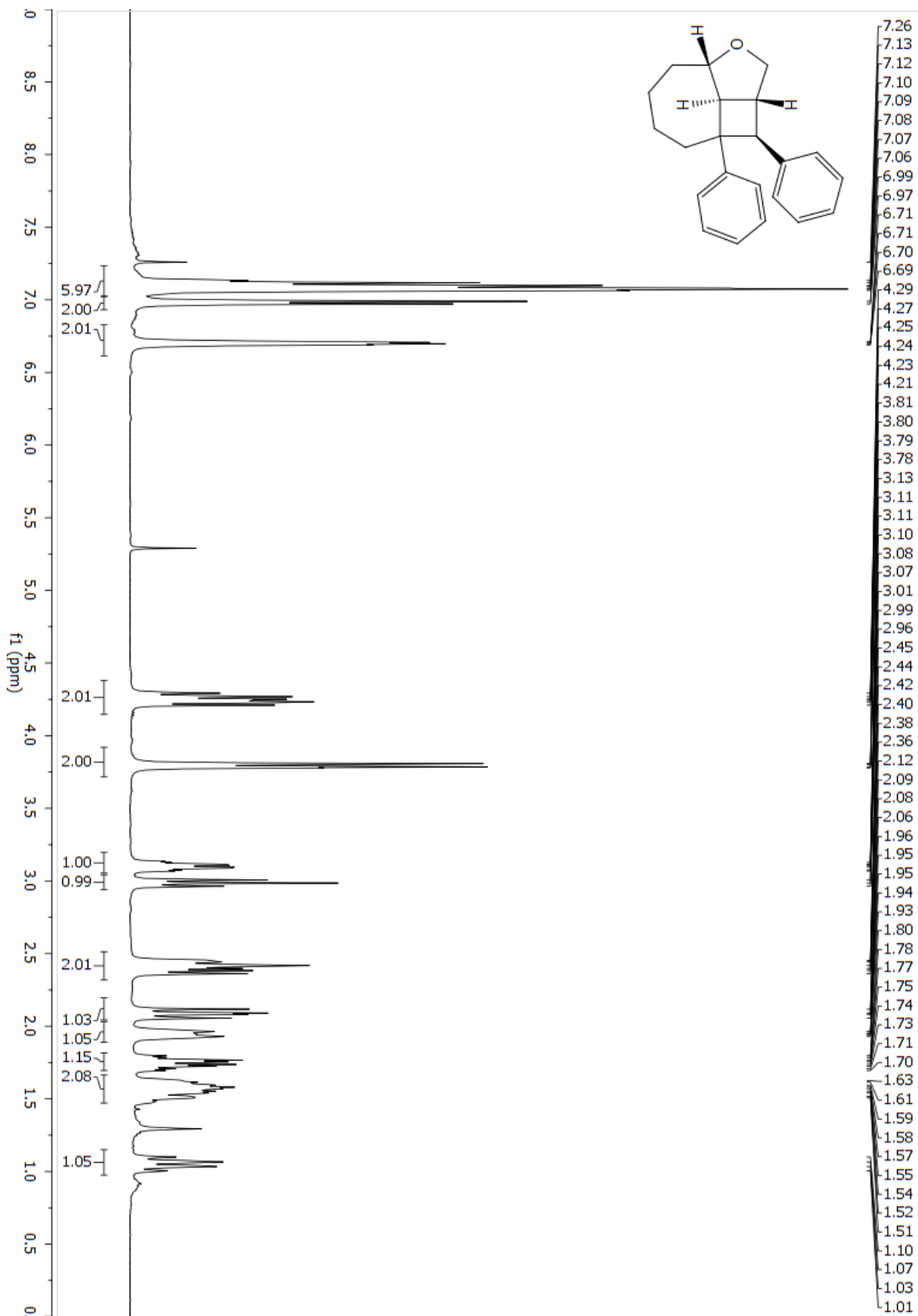
**d-4m (1R,5aR,5bR,10R,10aS,10bS)-1,10-bis(allyloxy)-5a,5b-diphenyltetradecahydrocyclo-buta [1,2:3,4]di[7]annulene**



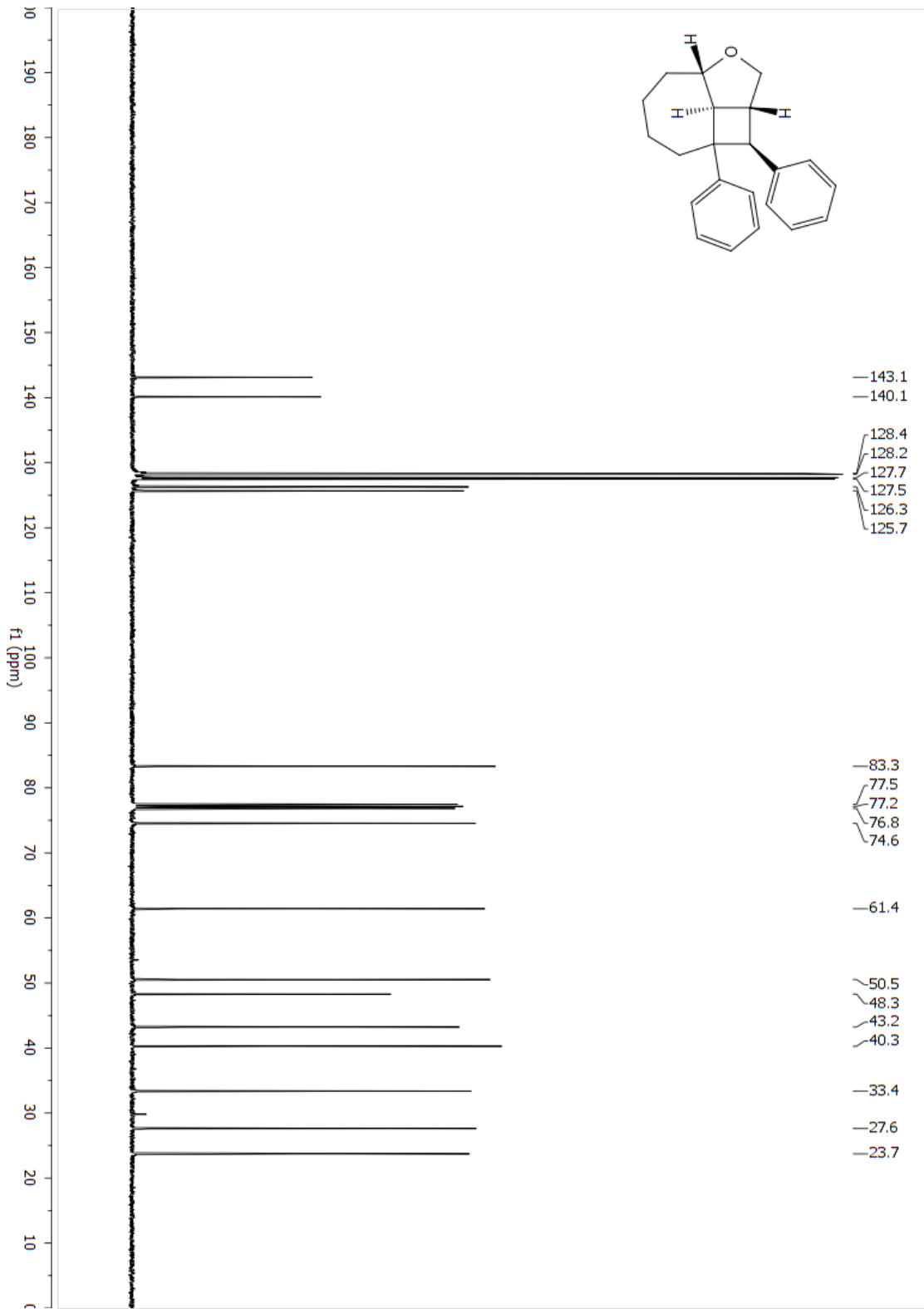
**d-4m (1R,5aR,5bR,10R,10aS,10bS)-1,10-bis(allyloxy)-5a,5b-diphenyltetradecahydrocyclo-butane [1,2:3,4]di[7]annulene**



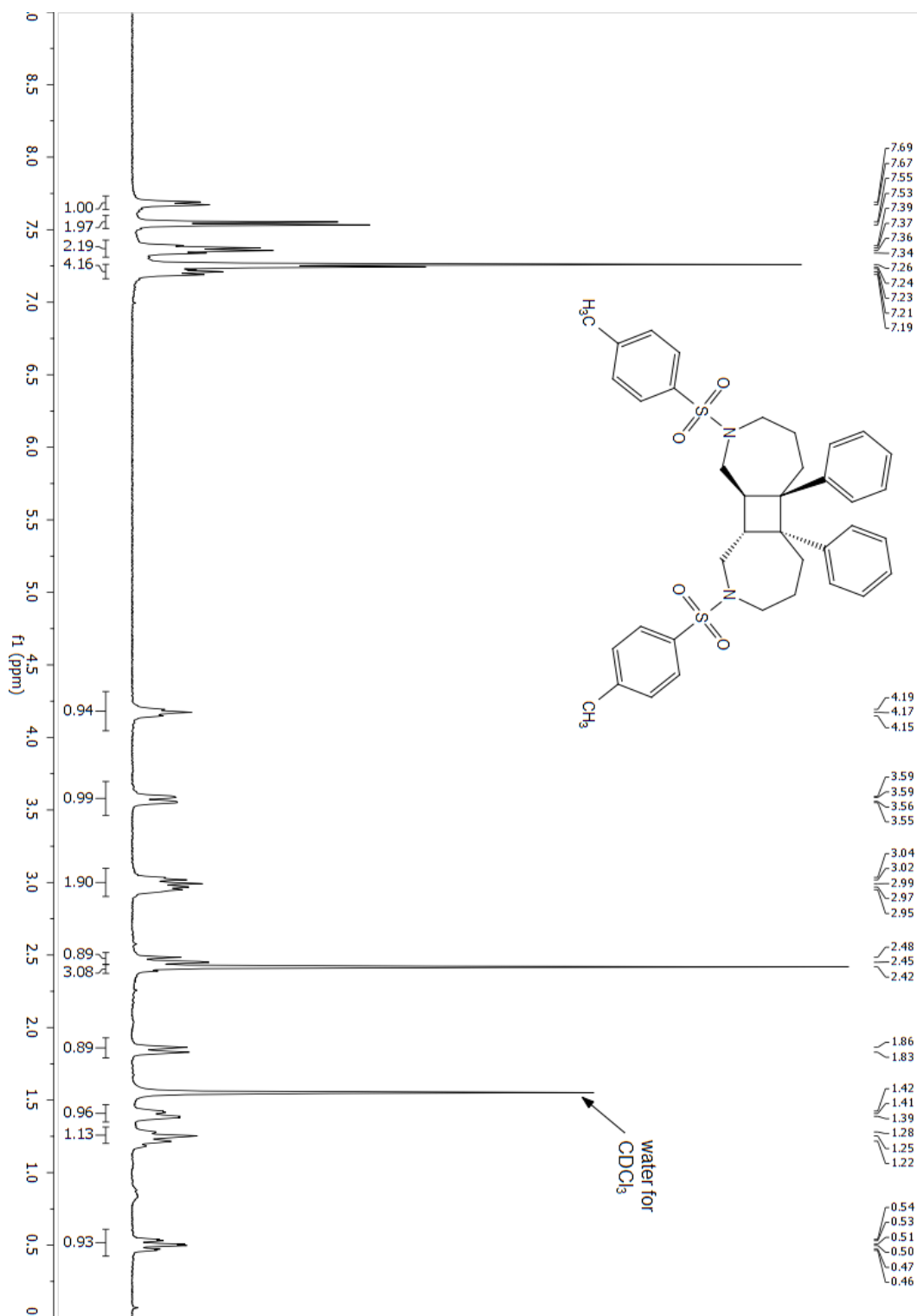
**d-4n (1S,1aR,1a1S,3aS)-1,7a-diphenyldecahydro-3-oxacyclobuta[cd]azulene**



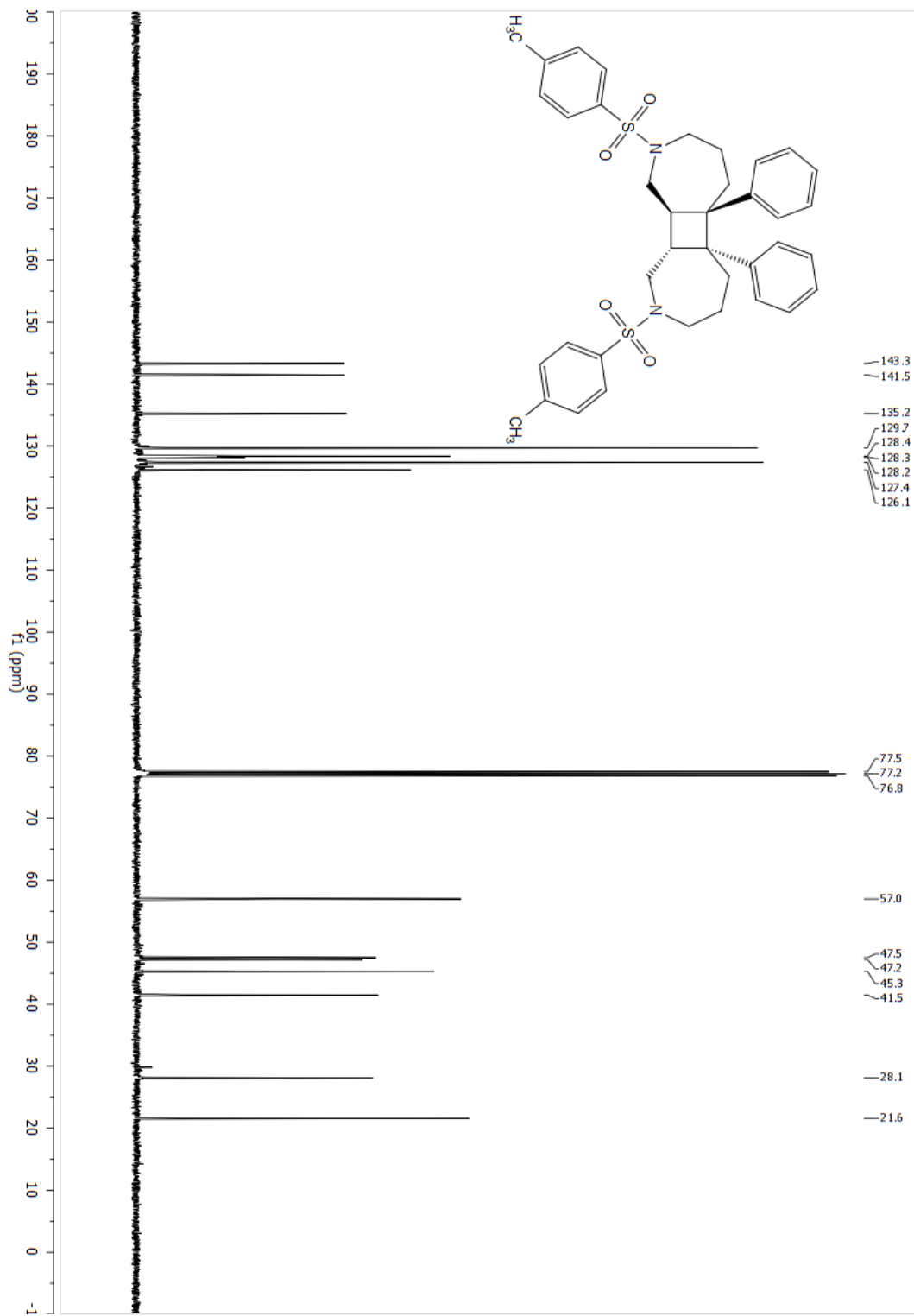
**d-4n (1S,1aR,1a1S,3aS)-1,7a-diphenyldecahydro-3-oxacyclobuta[cd]azulene**



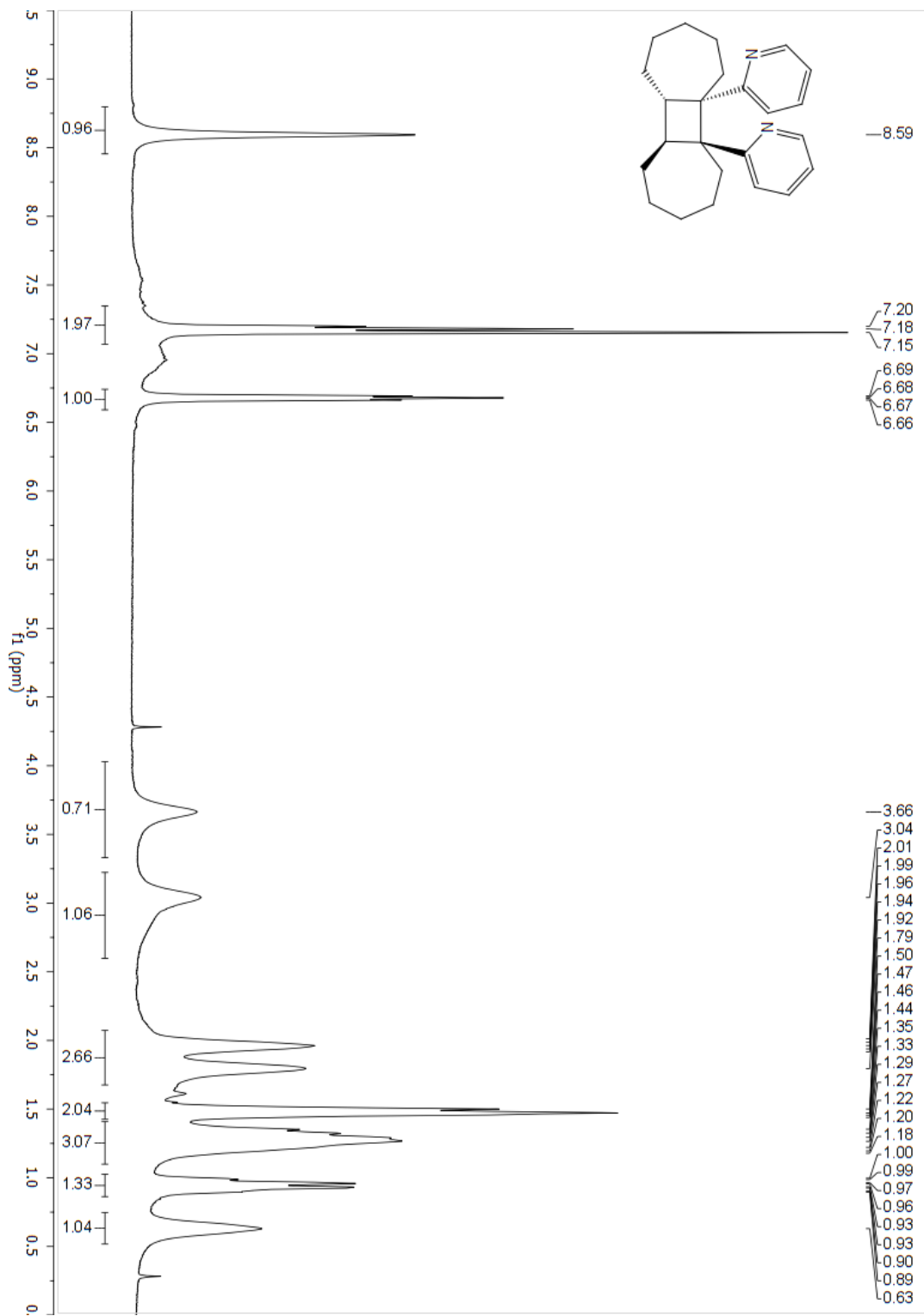
**d-4o (5aR,5bR,10aS,10bS)-5a,5b-diphenyl-2,9-ditosyltetradecahydrocyclobuta[1,2-c:4,3-c']bis(azepine)**



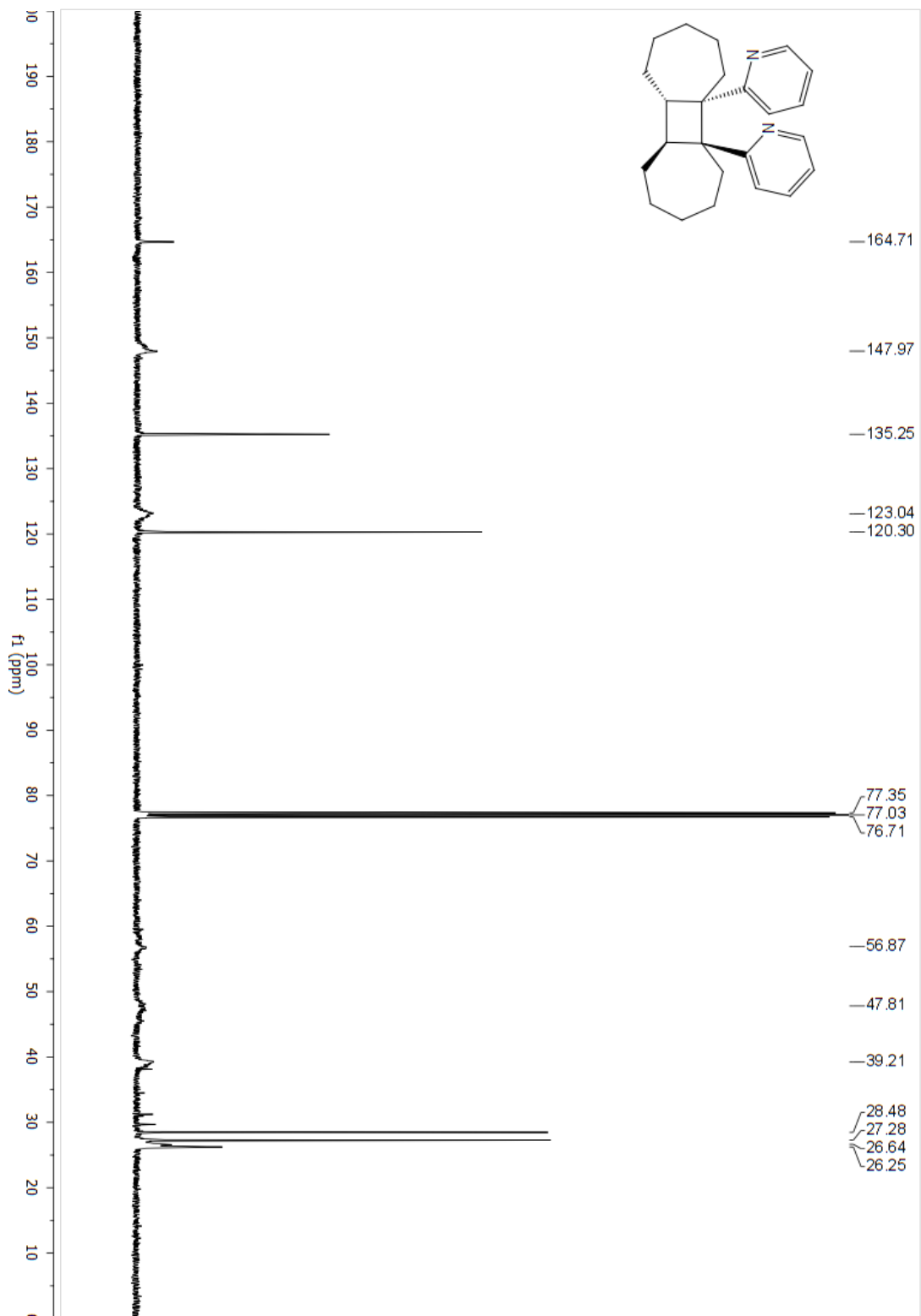
**d-4o (5aR,5bR,10aS,10bS)-5a,5b-diphenyl-2,9-ditosyltetradecahydrocyclobuta[1,2-c:4,3-c']bis(azepine)**



**d-4p (5a*S*,5b*S*,10a*S*,10b*S*)-5a,5b-di(pyridin-2-yl)tetradecahydrocyclobuta[1,2:3,4]di[7]annulene**



**d-4p (5aS,5bS,10aS,10bS)-5a,5b-di(pyridin-2-yl)tetradecahydrocyclobuta[1,2:3,4]di[7]annulene**



## CHAPTER V

### GENERATION AND UTILIZATION OF *trans*-ARYLCYCLOHEXENES IN SYNTHESIS

Expanding further on the idea of developing endergonic reactions, we sought to utilize phenylcyclohexenes. Since phenylcyclohexenes did not undergo thermal [2+2] cycloaddition like phenylcycloheptenes, we became curious to study phenylcyclohexenes under photocatalyzed conditions to see whether or not we could generate *trans*-phenylcyclohexenes. While larger *trans*-cycloalkenes have been deployed in synthesis,<sup>1-2</sup> the application of *trans*-cyclohexene in synthesis is still almost non-existent, with the exception of the recent report from the Larionov group<sup>3</sup> of an elegant exploitation of UV light mediated carboborative ring contraction. This sparsity is likely due, in part, to the use of UV light and historically strongly acidic conditions (i.e. H<sub>2</sub>SO<sub>4</sub>),<sup>4</sup> which limit the functional group tolerance. Larger, less strained *trans*-cycloalkenes can be generated by UV photolysis, and are isolable,<sup>5-7</sup> or at least readily observable.<sup>8-9</sup> Evidence for *trans*-cyclohexene was less forthcoming, however, presumably due to its high strain (*ca.* 52 kcal/mole), and correspondingly short lifetime. During pulsed photolysis experiments Dauben<sup>10-11</sup> reported having observed a transient species with a 9  $\mu$ s lifetime at room temperature and a *ca.* 7.5 kcal/mole barrier to isomerization back to the starting material. While irradiation with UV light led to multiple products, it has also been shown that if excited in acidic methanol, the *trans*-phenylcyclohexene underwent methanolysis of the olefin.<sup>4, 9, 12</sup> Importantly, this demonstrated the differential reactivity between the *cis*- and *trans*-cyclohexenes, and the potential for productive syntheses. A more challenging aspect in performing synthesis, however, is contending with the small energetic barrier to isomerization (*ca.* 7.5 kcal/mole). In order to accomplish this, we

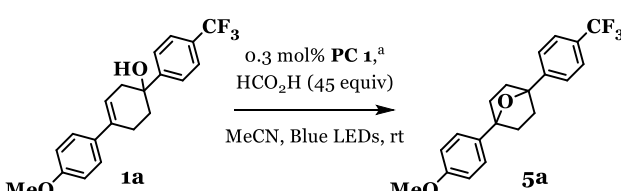
reasoned that pre-coordination of the reactive partner would be the key to overcoming the difficulties of the short lifetime of the *trans*-alkene, because it would allow the entropic penalty to be paid before the transition state, thus bringing down the energy barrier.

## 5.1 Optimization studies

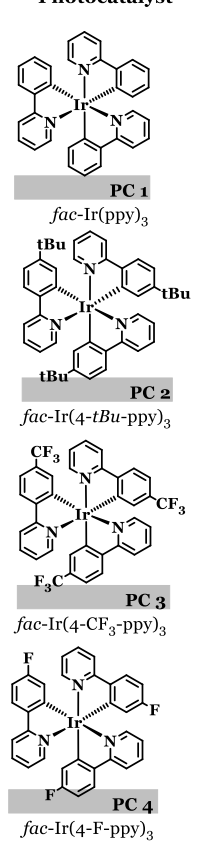
To begin our investigation, we subjected cyclohexenol **1a** to catalytic amounts of **PC1** ( $\text{Ir}(\text{ppy})_3$ ), formic acid which we anticipated would not induce elimination, due to its weak acidity, and blue LEDs (Table 11, entry 1). We were pleased to observe the formation of the desired bicyclic ether in good conversion (78%). Control reactions established the necessity of all three components (entry 2). Attempts to use a stronger Brønsted acid, such as HCl, simply led to elimination of water (entry 3).

Next, we evaluated the effect of the photocatalyst on the reaction (entries 4-6). We found, as previously demonstrated,<sup>13</sup> that both the steric volume and the emissive energy of the catalyst affected the rate of the reaction. Sterically larger photocatalysts such as **PC 2** with its much larger molecular radius effectively suppressed reactivity (entry 4 vs. 5), despite very similar emissive energy to **PC 1** (54.5 vs. 55.2 kcal/mole), indicating the likelihood of an energy transfer pathway. The most effective catalysts were relatively smaller (entries 5 and 6). The optimal catalyst was found to be **PC 4**, whose emissive energy is 58.6 kcal/mole, but is only slightly larger than standard **PC 1**. **PC 4** was used for further optimization. Evaluation of several carboxylic acids (entries 7-10), revealed that a 90% solution of formic acid was optimal, where both weaker and stronger acids were detrimental to the reaction.

Analysis of the optimal temperature revealed that the maximal reaction rate occur at 45 °C (entry 15). Curiously, examination at early time points revealed a bifurcation of the rate constant, which increased with temperatures both higher and lower than 0 °C (entries 11-16). This unusual result is



Reaction scheme showing the conversion of **1a** to **5a** using **PC 1** and formic acid in MeCN under blue LEDs at room temperature.



Chemical structures of the photocatalysts used in the study: **PC 1** (*fac*-Ir(ppy)<sub>3</sub>), **PC 2** (*fac*-Ir(4-*t*Bu-ppy)<sub>3</sub>), **PC 3** (*fac*-Ir(4-CF<sub>3</sub>-ppy)<sub>3</sub>), and **PC 4** (*fac*-Ir(4-F-ppy)<sub>3</sub>).

radius: (Å)	E <sub>emission</sub> (kcal/mol)
4.5	55.2
5.0	54.5
4.8	56.4
4.57	58.6

Entry	Modification of conditions	Conversion to <b>5a</b> <sup>b</sup>	Time
1	None	19 / 78%	3.3 h / 24 h
2	No acid, no photocatalyst, or no light	0%	24 h
3	HCl instead of <b>PC 1</b> and formic acid <sup>c</sup>	0%	24 h
4	<b>PC 2</b> instead of <b>PC 1</b>	3%	3.3 h
5	<b>PC 3</b> instead of <b>PC 1</b>	56%	3.3 h
6	<b>PC 4</b> instead of <b>PC 1</b>	91%	3.3 h
7	<b>PC 4</b> and 20 equiv of formic acid	98%	8 h
8	<b>PC 4</b> and 20 equiv of acetic acid	60%	8 h
9	<b>PC 4</b> and 20 equiv of trichloroacetic acid	7%	8 h
10	<b>PC 4</b> and 20 equiv of trifluoroacetic acid	0%	8 h
11	<b>PC 4</b> at -20 °C	41%	2 h
12	<b>PC 4</b> at -10 °C	48%	2 h
13	<b>PC 4</b> at 0 °C	17%	2 h
14	<b>PC 4</b> at 30 °C	29%	2 h
15	<b>PC 4</b> at 45 °C	61%	2 h
16	<b>PC 4</b> at 60 °C	59%	2 h

<sup>a</sup>A stock solution of catalyst was used. The concentration of **1a** was 0.05 M. <sup>b</sup>Determined by <sup>19</sup>F NMR. <sup>c</sup>The dehydrated product was detected by GCMS.

Table 11. Optimization of reaction conditions.

consistent with a highly reactive intermediate, in which lower temperatures extend the lifetime of the reactive species by reducing the free energy available for thermal reversion to the *cis*-cyclohexene species. Conversely, we expected that increased temperatures would increase the rate either by increasing the probability of the *cis*-cyclohexene encountering an excited photocatalyst to generate the reactive *trans*-cyclohexene, or alternatively, by populating higher energy conformations, which would be more capable of energy transfer.

## 5.2 Substrate scope

We initiated our exploration of the scope of the reaction by varying the substituent attached at the carbinol carbon. The reaction was remarkably tolerant to various substitutions at this position, giving the cyclized product in very good yields for electron poor arenes (**5a-5d**), electron neutral arenes (**5e** and **5f**), alkynyl (**5g**), and alkyl substituents (**5h**). The propensity of some of the carbinols

to ionize under acidic conditions (i.e. tertiary benzylic<sup>14</sup> or propargylic alcohols<sup>15</sup>), highlights the importance of using a weak acid, and demonstrates the enhanced basicity of *trans*-cyclohexene. We next explored the vinyl arene substituent (**5a** vs. **5i-5n**). The arene is an essential component of the substrate as it makes the triplet state of the alkene energetically accessible through visible light photocatalysis.<sup>16</sup>

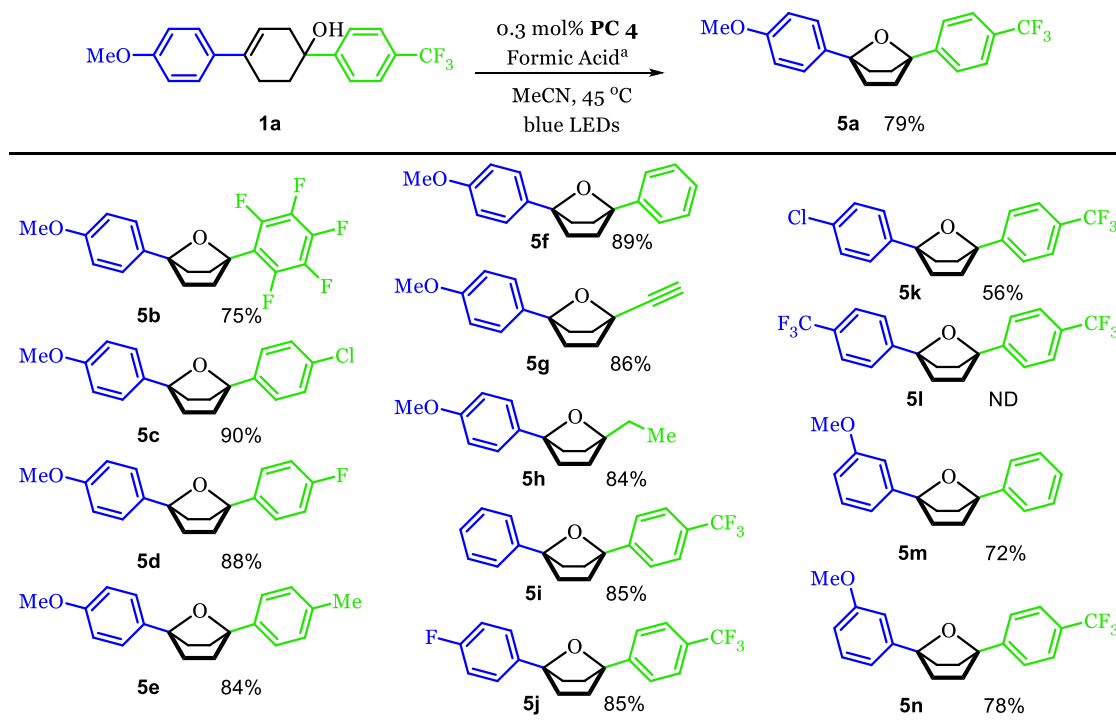


Table 12. Scope of the photocatalytic cyclization.

Because the conjugation is an important facet to triplet stabilization,<sup>17</sup> it is unlikely that the reaction would proceed with *ortho* substituents which dramatically disrupt the conjugation both in the ground state and the vertically excited triplet. Within this limitation, the arene was quite amenable to substitution with electron rich (**5a**), neutral (**5i**), and moderately electron poor (**5j** and **5k**) arenes. However, strongly electron deficient arenes (**5l**) failed to give any cyclized product. This failure may result from very sluggish protonation of the *trans*-alkene, which instead undergoes

thermal reversion to the relaxed *cis*- starting material, although electronic modulation of the HOMO–LUMO gap is possible as well, and may prevent excitation by the photocatalyst.

At this point in the investigation, several key assumptions about the reaction had been made. It was assumed that, as established previously in related transformations,<sup>13, 16, 18-20</sup> photochemical energy from a photon in the visible light region is absorbed by a photosensitizer, which after photoexcitation to a singlet, ultimately leads to a long-lived triplet excited state.<sup>21</sup> Because the catalyst is in a triplet state, and a photocatalyst radii dependency is observed (Table 11, entry 4), then the energy transfer most likely occurs *via* a Dexter<sup>22</sup> mechanism, exciting the substrate to a triplet biradical. This triplet biradical is capable of bond rotation about the former double bond. The triplet biradical rotates to an orthogonal position because not only do the former  $\pi$  electrons repel each other, but rotation also serves to relieve 1,2-eclipsing interactions. Upon returning to the ground state from the triplet landscape via a non-radiative intersystem crossing event (ISC; conical intersection) at, or very near the transition state for rotation about the double bond, the former alkene can then further rotate and relax to form either the *trans*-cyclohexene which can engage in subsequent reactivity, or unproductively reform the *cis*-alkene, evolving its energy as heat.

There were, however, several mechanistic quandaries, such as what purpose does the acid serve? Does the acid serve only as a proton source, or does it actually precoordinate as we have supposed? These questions ultimately culminate in the penultimate question: what does the transition state look like? We therefore sought to probe these questions, beginning by investigating the geometry of the transient reactive species.

### 5.3 Computational studies

To gain further insight to the reaction, and determine if the geometries we were envisioning were feasible, we set out to perform conformational analyses computationally. Since triplet state

energies would be of interest here, we settled on using Møller-Plesset (MP2)<sup>23</sup> theory, ultimately with large, correlation consistent basis sets.<sup>24-25</sup> First, we minimized the starting alcohol and

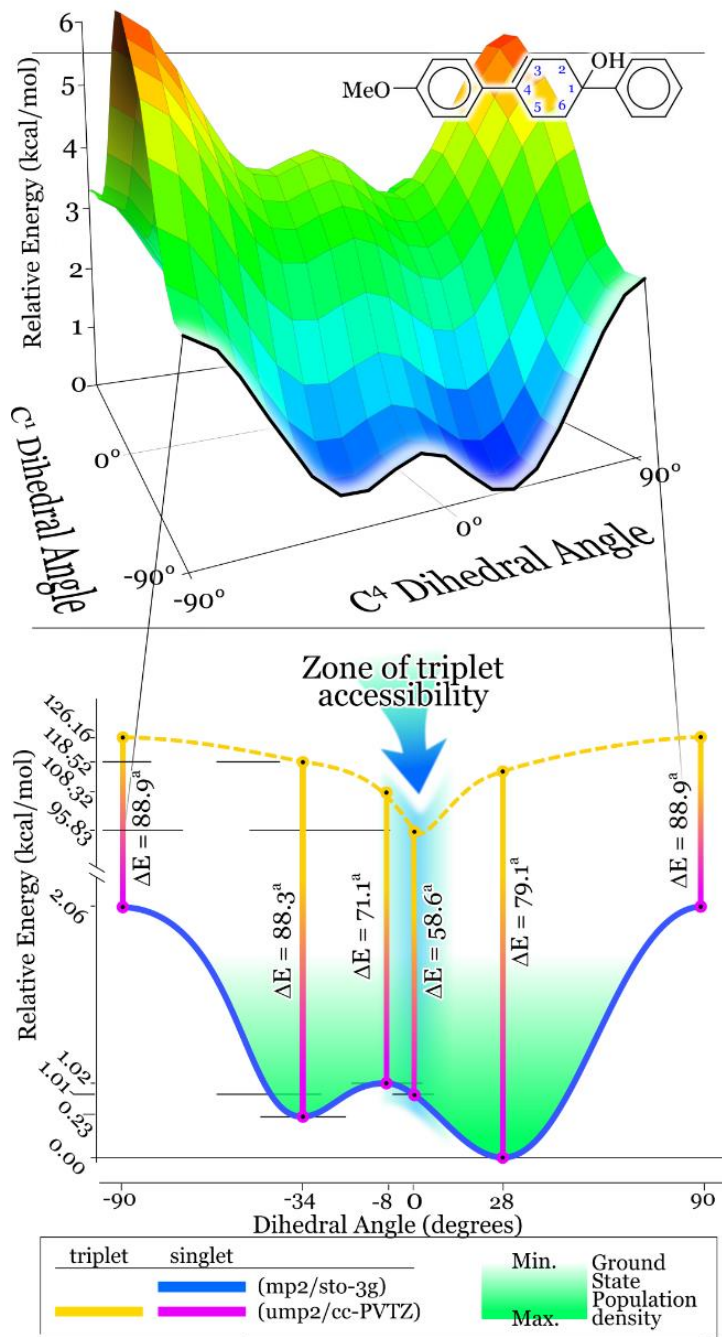


Figure 18. Conformational analyses A) Accessibility of biradical as a function of alkene conjugation. B) Singlet state energies and vertical excitations to triplet state energies. Excitation values scaled to the experimentally determined value for excitation at 0° – 58.6 kcal/mol, the emission energy of photocatalyst; other triplet state energies relative to this. Energies along

ordinate axis are relative to the lowest energy point in the singlet landscape. Singlet curve developed at MP2/STO3G; energies scaled to values determined at MP2/cc-PVTZ

performed two dihedral drivers at the freely rotatable C–C bonds connecting the three rings (Figure 18A). The carbinol phenyl (C<sup>1</sup>) preferred to rotate 90° from the adjacent ring, presumably to avoid allylic strain. Looking at the styrenyl phenyl revealed a more complex landscape, in which the lowest energy conformer has the two rings 28° out of coplanarity. We subjected the 90° cross section to an increased number of scan points for rotational angles (Figure 18B). Next, we subjected select structures to a higher level of computational theory, in order to provide insight into the relationship between the thermal and the excited state landscapes. Beginning from the minimized geometry with the methoxyphenyl ring canted 28° from planarity with the *cis*-cyclohexene ring, a vertical excitation from the singlet to the triplet state was calculated using the cc-PVTZ basis set.<sup>25</sup> The energy difference for this excitation was found to be in excess of the emissive energy of the photocatalyst. This is because the minimized geometry favors deconjugation of the methoxyphenyl dihedral angle at C<sup>4</sup> of the *cis*-cyclohexene, and therefore puts the singlet to triplet excitation energy out of reach of the photocatalyst. At *ca.* 1 kcal/mole higher energy, rotation of the methoxyphenyl ring into planarity with the *cis*-cyclohexene double bond is easily thermally accessible at a reaction temperature of 45 °C. Based on a Boltzmann distribution population analysis, increasing the reaction temperature from 0 °C to 45 °C increases the frequency of observing a molecule in the fully conjugated conformer by *ca.* 30%, based on the relative energies of these conformers. This provides some insight to support our prior supposition as to the bifurcation of reaction rate in relation to reaction temperature (Table 11, entries 13-16).

Vertical excitations from the singlet to the triplet state were calculated at minima and maxima of this landscape, as well as 0°. In lieu of performing an exhaustive and correspondingly computationally expensive ring conformer search on the cyclohexene ring, dihedral angles for rotation about the C<sup>4</sup>–methoxyphenyl ring were frozen, and a simple geometry optimization was

performed on the ground state singlet, in the gas phase. While absolute energy differences for singlet to triplet excitation are greater than expected, the trend of the gap demonstrates the importance of conjugation. Conjugation of the alkene with the methoxyphenyl  $\pi$  cloud brings the calculated excitation energy to a minimum, which is known experimentally to be within the range of the emission energy of the photocatalyst (58.6 kcal/mole).<sup>26</sup>

Next, we considered the strained *trans*-cyclohexene species. Importantly, upon ISC, the formation of the *trans*-cyclohexene generated four potential diastereomers, of which only two could lead to ring closure (axial-OH). We have termed these the *syn*-boat and the *anti*-chair (Figure 19). Calculations of the ground state energies of these species indicated that the *anti*-chair would be lower in energy by *ca.* 5.5 kcal/mole, which is consistent with the work of Johnson.<sup>27</sup> This energy difference cannot be used to anticipate the reactive conformer, however, since both are lower than the triplet state energy and thus accessible therefrom. In order to discern the reaction pathway, we would need stereochemical evidence. Since the upper limit for the energy to excite the *cis*-cyclohexane is the emission energy of the photocatalyst, then the maximum height conical intersection on the singlet state landscape must also be bounded by this restriction. It is of note that the difference between the ground state energy of the *anti*-chair *trans*-cyclohexene and the  $\lambda_{\max}$  emissive energy of the photocatalyst is approximately the same as not only the value that Dauben

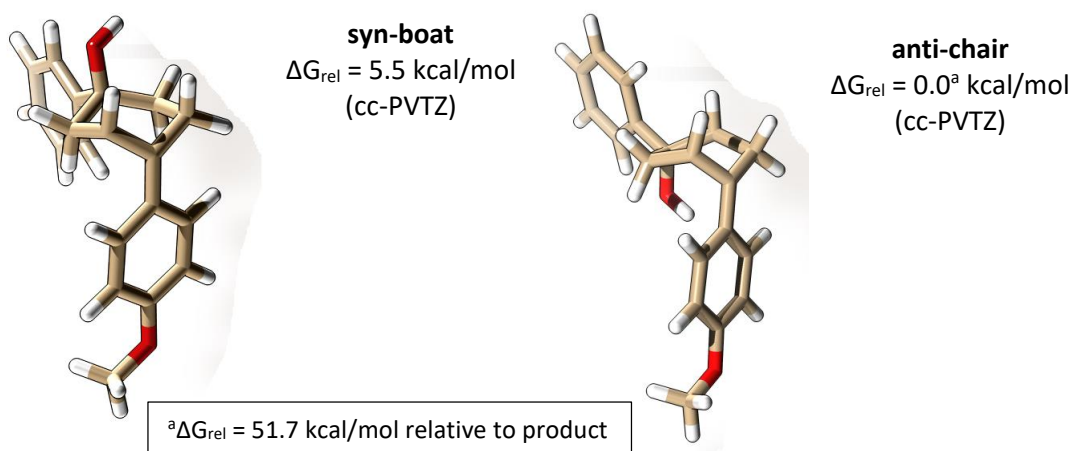


Figure 19. Potential diastereomers that leads to ring closure

found for reversion of *trans*-phenylcyclohexene to the *cis*- starting material, but also the computationally determined value determined by Johnson for simple cyclohexene.

It was envisioned that a deuterium label could provide stereochemical evidence of the geometry of the bond which undergoes hydro-alkoxylation, as the face of incorporation and the number of sites deuterated would provide mechanistic insight with regard to the reversibility of the protonation step. Submitting **1a** to reaction conditions in which a large excess of D<sub>2</sub>O was added resulted in deuterium incorporation only on the face of the cyclohexene ring opposite that of the forming ether, so that the deuterated product shows signal attenuation equivalent to the incorporation of 1 hydrogen only in the axial position of the product (Figure 20A). This was affirmed by correlation with computational NMR simulation (Figure 20B).<sup>28</sup>

### A. Experimental Spectrum (excess D<sub>2</sub>O)



### B. Simulated Spectrum

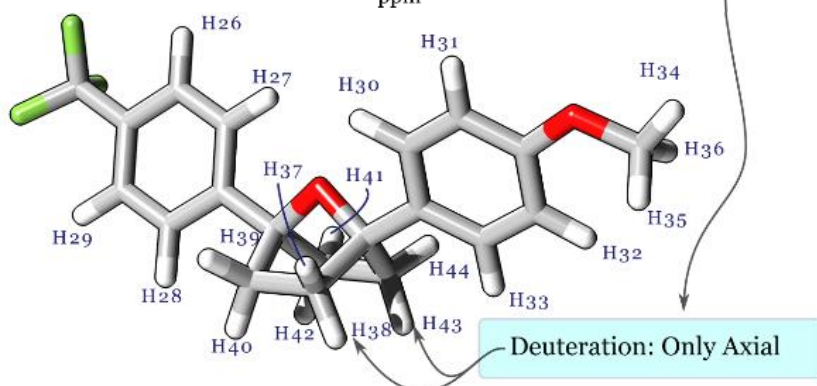
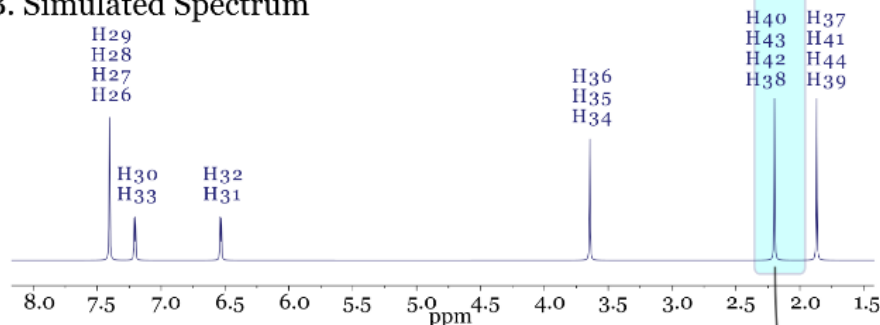


Figure 20. Deuterium incorporation with **1a** and computational identification of axial and equatorial protons of product **5a**

The presence of isotopic scrambling only on the formerly vinyl carbon indicated that the protonation/deuteration was essentially irreversible, and could have occurred in two ways. *Exo* protonation of the *syn*-boat can be ruled out, since it would lead to incorporation of the deuterium on the same side of the ring as the forming ether, not the experimentally observed product. Similarly, *endo* protonation of the *anti*-chair conformer should be ruled out because it too leads to the incorrect deuterated regioisomer. It is possible that the protonation/deuteration could have occurred from the *endo* face of the *syn*-boat *trans*-cyclohexene ring. However, because the *endo* face is the more sterically congested, it seemed unlikely to be the face of protonation. Conceivably,

the C<sup>1</sup> hydroxyl could have been serving to protonate the *endo* face of the *syn*-boat conformer. Assessment of this scenario reveals that the proton or deuteron would subsequently have to travel through the van der Waals cloud of the cyclohexane ring, likely requiring a tunneling event to arrive at the proper orbital to generate the experimentally observed product. If this did occur, one could expect a very large kinetic isotope effect (KIE), ( $k_H/k_D > 40$ ),<sup>29</sup> but it was not observed (*vide infra*). The simplest explanation is that the deuteration event happens from the *exo* face of the *anti*-chair. Although the *exo* protonation of the *anti*-chair conformer seemed the most likely, the question still to be answered was how that *exo* protonation occurred.

#### 5.4 Mechanistic investigation

In order to probe this, we next began investigating the kinetics of the reaction. Initial rate experiments indicate that the reaction is first order with respect to catalyst. With the substrate, the reaction appeared to have zero order kinetics. With formic acid at low loadings, there was a linear response to concentration, while at higher loadings it fell out of the rate expression. This led us to suspect that the acid may be undergoing a pre-rate determining step equilibrium, *i.e.* a precoordination event. Further support for the latter idea was observed in <sup>1</sup>H NMR *via* titration of the tertiary alcohol starting material (**1f**) with formic acid under anhydrous conditions, which resulted in a significant deshielding of the hydroxyl signal (Figure 21). This is consistent with hydrogen bonding of the proton with an H-bond acceptor, such as an oxygen in formic acid.<sup>30</sup>

This precoordination of the substrate and acid serve to reduce the entropy of the transition state. Importantly, we anticipate such precoordination provides a proximal proton to the *trans*-alkene upon its genesis, and that this is essential to harnessing the strain energy. Similarly, while not discussed in Larionov's<sup>3</sup> recent carboborative ring contraction, we suspect that the absence of dimerization products or products of other reaction pathways is due to the pre-coordination of a Lewis acidic trialkyl borane with the alkene, which serves a similar role to immediate protonation. We conducted tandem rate experiments with phenylcyclohexene, which is devoid of a hydroxyl

group, and **1f** under the standard reaction conditions in order to investigate the relative effect of the precoordination. These experiments revealed much faster reactivity with the substrate capable of precoordination (**1f**) than the phenylcyclohexene could achieve without a hydrogen bond to the formic acid, supportive of the assumption that the precoordination aids the reactivity.

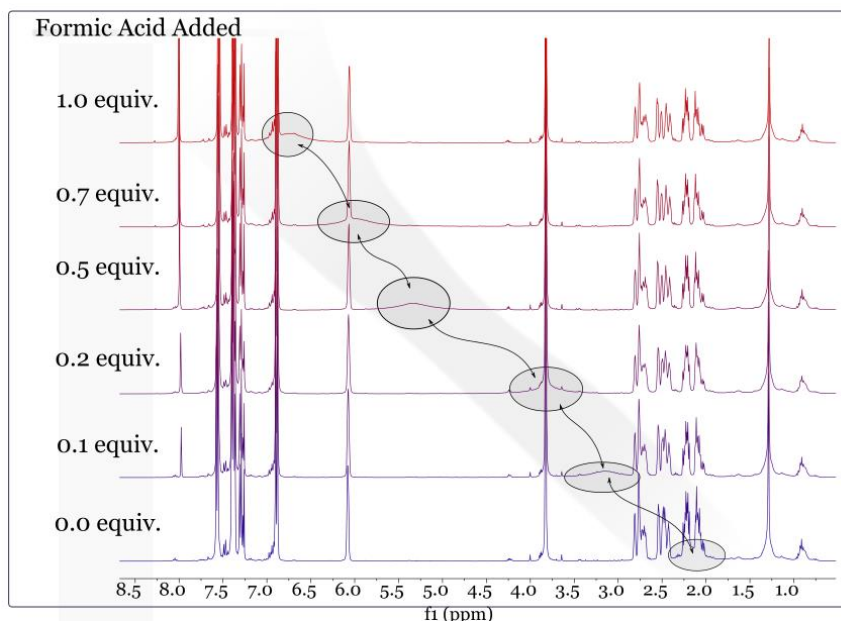


Figure 21. Titration of **1f** with formic acid

When the aqueous environment of the reaction was replaced with D<sub>2</sub>O, we observed a solvent KIE  $k_H/k_D$  of 1.5. This is unusual because it is outside the range expected for either a primary (greater than 2) or a secondary normal KIE (1 to 1.4).<sup>29</sup> Furthermore, in the case of rehybridization from an sp<sup>2</sup> to sp<sup>3</sup> carbon in the rate determining step, one would expect to observe an inverse KIE (0.8 to 1). Further obfuscating the interpretation of the observed KIE is that there are multiple sites for deuterium exchange, not only at the site observed in the final product, but also in the hydroxyl, and in formic acid itself. Additionally, if the proton/deuteron being transferred is from a formic acid coordinated to the hydroxyl group, then a nonlinear transition state is expected, and thus a diminished KIE would be expected as well. What could be said at this point was that it further suggests that the protonation of the alkene is not occurring from the endo face of the *syn*-boat

conformer. If it was, it would have to travel through the van der Waals cloud of the cyclohexene ring and would therefore likely have tunneling characteristics.<sup>29</sup>

We then sought to combine the evidence of hydrogen bonding between the hydroxyl proton and formic acid with our conformational analysis of the *trans*-cyclohexene. Since *exo* protonation of the *anti*-chair *trans*-cyclohexene is most likely, we sought to model a hydrogen bonded formic acid molecule with the *anti*-chair geometry to see if a potential transition state would be geometrically feasible. Optimization of the aforementioned geometries with a transition state minimization at low basis set and theory level (HF/3-21G) resulted in the geometry in Figure 22. This model clearly demonstrates the possibility of such a transition state, in which a formic acid bridges the gap and allows the *exo*-protonation. While we are hesitant to assign the identity of the transition state due to the inherent difficulties therein,<sup>31-32</sup> this geometry explains a nonlinear transition state and a corresponding smaller KIE

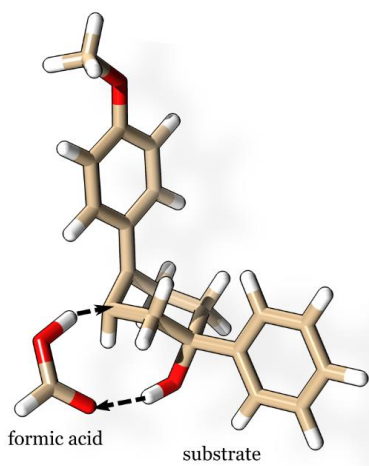
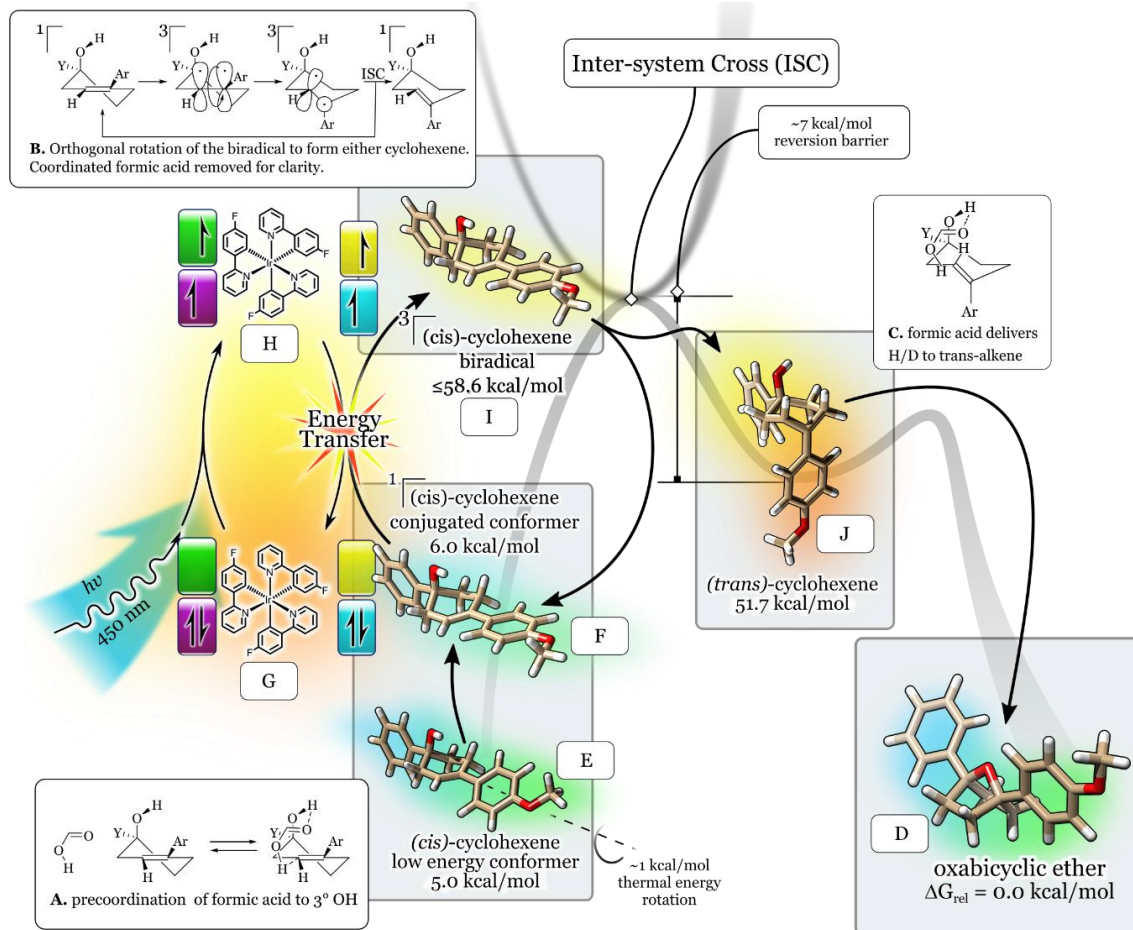


Figure 22. Presumptive transition state geometry identified by HF/3-21G. Proton transfer pathways indicated by dashed lines

Combining all of these ideas into a cohesive, tentative mechanistic proposal (Scheme 21), we believe key features include the precoordination of a formic acid with the hydroxyl proton (Scheme 21A). Upon excitation from the ground state photocatalyst (G) an excited triplet state photocatalyst (H) intercepts a *cis*-cyclohexene substrate, which is in the proper conjugated

conformer with an accessible triplet state energy (F). The triplet state photocatalyst and the singlet ground state substrate undergo Dexter energy transfer to produce the excited triplet state *cis*-cyclohexene biradical (I) and regenerate the ground state singlet photocatalyst (G). The excited triplet state substrate biradical (I) is then no longer bonding and undergoes rotation about the remaining C–C  $\sigma$  bond so that the singly occupied orbitals rotate orthogonal to each other (structures in Scheme 21B). The substrate biradical is then close in both geometry and energy to the thermal transition state for rotation, and undergoes an intersystem crossing event. Upon crossing from the triplet back into the singlet energy landscape, it can either relax to the *cis*-cyclohexene starting material (F) or continue to rotate to the *trans*-cyclohexene *anti*-chair conformer (J), which is still coordinated with the formic acid through a strong hydrogen bond (C). The protonation of the alkene through an apparent *exo*-protonation of the *anti*-chair diastereomer of the *trans*-cyclohexene likely transfers more than one hydrogen in the rate-determining step *via* a nonlinear transition state, which has substantial inverse character (Figure 22). Protonation of the alkene generates a carbenium ion, which is rapidly attacked by the alcohol oxygen to produce the oxabicyclic ether (D).



Scheme 21. Proposed mechanism of intramolecular hydroalkoxylation.

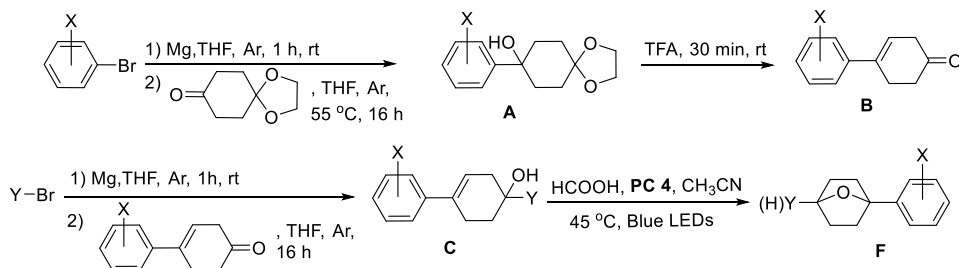
## 5.5 Summary

In conclusion, we have exploited the ability of strain energy associated with *trans*-cyclohexene to dynamically capture energy from visible light, and we have developed a strategy to exploit this energy to synthesize new organic molecules. We have highlighted some of the intricacies that should be considered when thinking about energy transfer photocatalysis, such as appropriate choice of photocatalyst not only energetically, but also geometrically, and in addition have highlighted the importance of the accessibility of the triplet state as a function of conformer conjugation. A key hydrogen bonded precoordination event makes possible the singular reactivity, and results in a product that is not otherwise accessible. Its short lifetime is a general and persistent issue that for many years has resulted in *trans*-cyclohexene's recalcitrance with regard to synthesis. We have demonstrated how precoordination with the reactive partner (an acid) can be used to

overcome this obstinacy without resorting to the use of UV light, and provided a methodology that will hopefully make synthesis involving *trans*-cyclohexene more tractable.

## 5.6 Experimental procedures

### Synthesis of substrates



### General Procedure A1 for the synthesis of A.

To an oven-dried round bottomed flask equipped with magnetic stir bar was added magnesium metal (56.1 mmol, 2.5 equiv), a crystal of I<sub>2</sub>, THF (0.5 M) then 1-bromo-4-methoxybenzene (44.9 mmol, 2.0 equiv) was added portion-wise. The mixture was stirred at room temperature for 1 hour. After the complete consumption of 1-bromo-4-methoxybenzene, the reaction mixture was cooled to 0 °C, and 1,4 cyclohexanedione monoethylene acetal (22.5 mmol, 1 equiv) in THF was added drop-wise to the reaction mixture. The reaction mixture was heated at 55 °C until completion (16-24 h). After completion, the reaction mixture was quenched by saturated NH<sub>4</sub>Cl (50 mL) and extracted with EtOAc (3 x 50 mL). The combined organic layers were washed with 0.1M NaOH (40 mL). The organic layer was separated, dried over MgSO<sub>4</sub>, and concentrated to obtain the crude product that was purified by normal phase chromatography. Normal phase chromatography was performed with a Teledyne ISCO automated chromatography system using hexane:ethyl acetate (80:20) over 0-70 column volumes using flow rate from 35-80 mL/min on a Redisep column with product detection at 254 and 288 nm.

**Table 13: Summary of various substrates A with their yields.**

S.No.	X	% yield (over two steps)
1a-h	4-Methoxy	46

1i	Hydrogen	41
1j	4-Fluorine	33
1k	4-Chlorine	40
1l	4-Trifluoromethyl	30
1m,n	3-Methoxy	84

**General Procedure B1 for the synthesis of B.**

To an oven-dried round bottomed flask equipped with a magnetic stir bar was added **A** (1 equiv) and TFA (1 M). The mixture was stirred at room temperature for 30 min. After the completion, the mixture was neutralized by the addition of saturated NaHCO<sub>3</sub>, and extracted with CH<sub>2</sub>Cl<sub>2</sub> (2 x 30 mL). The combined organic layers were washed with distilled water (10 mL). The organic layer was separated, dried over MgSO<sub>4</sub>, and concentrated to obtain the crude product that was purified by normal phase chromatography. Normal phase chromatography was performed with a Teledyne ISCO automated chromatography system using hexane:ethyl acetate (80:20) over 0-70 column volumes using flow rated from 35-80 mL/min on a 40-80 g Redisep column with product detection at 254 and 288 nm.

Table 14: Summary of various substrates **B** with their yields.

S.No	X	% yield
1a-h	Methoxy	62
1i	Hydrogen	92
1j	Fluorine	45
1k	Chlorine	96
1l	Trifluoromethyl	35
1m,n	3-Methoxy	90

General procedure **A** was followed to synthesize **C**.

**Table 15: Summary of various substrates C with their yields.**

S.No	X	Y	% yield (over two steps)
1a	4-Methoxy	4-Trifluoromethylphenyl	12
1c	4-Methoxy	4-Chlorophenyl	13
1d	4-Methoxy	4-Fluorophenyl	35
1b	4-Methoxy	Pentafluorophenyl	5
1e	4-Methoxy	4-Methylphenyl	35
1f	4-Methoxy	Phenyl	42
1g	4-Methoxy	Ethyne	45
1h	4-Methoxy	Ethyl	25
1i	Hydrogen	4-Trifluoromethylphenyl	42
1k	4-Chlorine	4-Trifluoromethylphenyl	18
1j	4-Fluorine	4-Trifluoromethylphenyl	14
1l	4-Trifluoromethylphenyl	4-Trifluoromethylphenyl	4
1m	3-Methoxy	Phenyl	35
1n	3-Methoxy	4-Trifluoromethylphenyl	48

### III. General procedure F (Photocatalytic reactions and characterization)

A 20 mL disposable scintillation vial was charged with cyclohexene substrate (1.0 equiv), catalyst **PC4** (0.3 mol%) in MeCN. The mixture was divided in equal amount into NMR tubes. The sealed glass capillary containing C<sub>6</sub>D<sub>6</sub> was put into each NMR tube to aid in the locking process. The NMR tubes were capped with rubber septa and the reaction mixture was degassed with argon bubbling for 10 minutes, and then placed in the light bath such that the lower portion of the tube was submerged under water. The reaction was monitored periodically by <sup>1</sup>H NMR. After the complete consumption of the starting material, the reaction mixture was neutralized with saturated

sodium bicarbonate solution and the layers were separated. The organic layer was washed with brine, dried over MgSO<sub>4</sub> and concentrated to obtain the crude product that was purified by normal phase chromatography using silica gel as the stationary phase and ethyl acetate/hexanes as mobile phase unless otherwise noted.

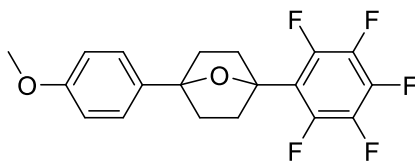
**(1-(4-methoxyphenyl)-4-(4-(trifluoromethyl)phenyl)-7-oxabicyclo[2.2.1]heptane) (5a)**



The general procedure A was followed using 4'-methoxy-4-(trifluoromethyl)-3',6'-dihydro-[1,1':4,1''-terphenyl]-1'(2'H)-ol (100.0 mg, 0.28 mmol), catalyst **PC4** (0.6 mg, 0.3 mol%), and formic acid

(580 mg, 12.6 mmol) was used to afford **5a** in 79% yield (79 mg, 0.22 mmol) as a white solid. The crude material was purified by flash chromatography using hexanes:ethyl acetate with product eluting at 5%. <sup>1</sup>H NMR (400 MHz, CDCl<sub>3</sub>) δ 7.62 (s, 4H), 7.45 (d, *J* = 8.7 Hz, 2H), 6.92 (d, *J* = 8.7 Hz, 2H), 3.83 (s, 3H), 2.30 – 2.17 (m, 4H), 2.09 – 1.92 (m, 4H). <sup>13</sup>C NMR (101 MHz, CDCl<sub>3</sub>) δ 158.8, 147.1, 134.6, 129.1 (q, *J* = 32.3 Hz), 126.5, 125.5, 125.1 (q, *J* = 3.6 Hz), 124.3 (q, *J* = 271.9 Hz), 113.6, 87.4, 86.9, 55.3, 38.7, 38.6. <sup>19</sup>F NMR (376 MHz, CDCl<sub>3</sub>) δ -62.4 (s, 3F). FT-IR cm<sup>-1</sup> 2955, 1514, 1333, 1106. GC/MS (*m/z*, relative intensity) 348 (M<sup>+</sup>, 15), 160 (30), 135 (100), 77 (38). Melting point 99-101 °C.

**(1-(4-methoxyphenyl)-4-(perfluorophenyl)-7-oxabicyclo[2.2.1]heptanes) (5b)**

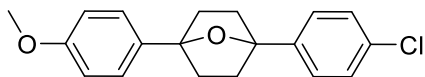


The general procedure F was followed using 2,3,4,5,6-pentafluoro-4'-methoxy-3',6'-dihydro-[1,1':4,1''-terphenyl]-1'(2'H)-ol (60.0 mg, 0.16 mmol, 1.0 equiv), catalyst **PC4** (0.3

mg, 0.3 mol%), and formic acid (171.4 mg, 3.73 mmol) was used to afford **5b** in 75% yield (45 mg, 0.12 mmol) as a white solid. The crude material was purified by flash chromatography using hexanes:ethyl acetate with product eluting at 5%. <sup>1</sup>H NMR (400 MHz, CDCl<sub>3</sub>) δ 7.42 (d, *J* = 8.8 Hz, 2H), 6.91 (d, *J* = 8.7 Hz, 2H), 3.86 – 3.78 (m, 3H), 2.37 (dq, *J* = 11.2, 5.0, 3.3, 2.4 Hz, 2H), 2.24 – 2.07 (m, 4H), 2.04 – 1.92 (m, 2H). <sup>13</sup>C NMR (101 MHz, CDCl<sub>3</sub>) δ 158.8, 144.7 (d, *J* = 255.9 Hz), 140.2 (d, *J* = 233.5 Hz), 137.7 (d, *J* = 231.8 Hz), 134.1, 126.4, 116.1 – 115.5 (m), 113.7, 87.1,

83.8, 55.3, 38.0 (t,  $J = 2.8$  Hz), 37.6.  $^{19}\text{F}$  NMR (376 MHz,  $\text{CDCl}_3$ )  $\delta$  -138.30 (dd,  $J = 22.5, 7.2$  Hz, 2F), -156.24 (tt,  $J = 21.3, 4.2$  Hz, 1F), -162.31 – -162.63 (m, 2F). FT-IR  $\text{cm}^{-1}$  2920, 1488, 1248, 1179. GC/MS ( $m/z$ , relative intensity) 370 ( $\text{M}^+$ , 20), 342 (80), 135 (50), 77 (20). Melting point 133-134 °C.

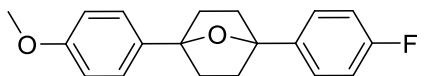
**(1-(4-chlorophenyl)-4-(4-methoxyphenyl)-7-oxabicyclo[2.2.1]heptane) (5c)**



The general procedure F was followed using 4-chloro-4'-methoxy-3',6'-dihydro-[1,1':4',1''-terphenyl]-1'(2H)-ol

(100.0 mg, 0.32 mmol), 5.4 mL of stock solution of PC4 (2.0 mg, 0.0028 mmol, 20 mL  $\text{CH}_3\text{CN}$ ), and formic acid (98.6 mg, 2.14 mmol) was used to afford **5c** in 90% yield (90 mg, 0.29 mmol) as a white solid. The crude material was purified by flash chromatography using hexanes:ethyl acetate with product eluting at 10%.  $^1\text{H}$  NMR (400 MHz,  $\text{CDCl}_3$ )  $\delta$  7.51 – 7.44 (m, 4H), 7.36 (d,  $J = 8.4$  Hz, 2H), 6.94 (d,  $J = 8.6$  Hz, 2H), 3.85 (s, 3H), 2.22 (d,  $J = 7.4$  Hz, 4H), 2.11 – 1.93 (m, 4H).  $^{13}\text{C}$  NMR (101 MHz,  $\text{CDCl}_3$ )  $\delta$  158.7 141.5, 134.8, 132.7, 128.3, 126.7, 126.5, 113.6, 87.3, 86.8, 55.3, 38.7, 38.6. FT-IR  $\text{cm}^{-1}$  2953, 1515, 1254, 1088. GC/MS ( $m/z$ , relative intensity) 314 ( $\text{M}^+$ , 20), 279 (10), 135 (100), 77 (45). Melting point 98-99 °C.

**(1-(4-fluorophenyl)-4-(4-methoxyphenyl)-7-oxabicyclo[2.2.1]heptanes) (5d)**

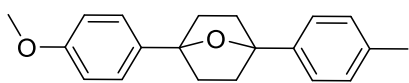


The general procedure F was followed using 4-fluoro-4'-methoxy-3',6'-dihydro-[1,1':4',1''-terphenyl]-1'(2H)-ol

(100.0 mg, 0.34 mmol, 1.0 equiv), catalyst **PC4** (0.7 mg, 0.3 mol%), and formic acid (148.2 mg, 2.14 mmol) was used to afford **5d** in 88% yield (90 mg, 0.30 mmol) as a white solid. The crude material was purified by flash chromatography using hexanes:ethyl acetate with product eluting at 5%.  $^1\text{H}$  NMR (400 MHz,  $\text{CDCl}_3$ )  $\delta$  7.64 – 7.42 (m, 4H), 7.16 – 7.02 (m, 2H), 7.02 – 6.87 (m, 2H), 3.84 (s, 3H), 2.41 – 2.15 (m, 4H), 2.15 – 1.86 (m, 4H).  $^{13}\text{C}$  NMR (101 MHz  $\text{CDCl}_3$ )  $\delta$  162.3 (d,  $J = 244.7$  Hz), 159.1, 139.2, 135.3, 127.4 (d,  $J = 7.9$  Hz), 126.9, 115.4 (d,  $J = 21.3$  Hz), 114.1, 87.6, 87.3, 55.7, 39.2, 39.1.  $^{19}\text{F}$  NMR (376 MHz,  $\text{CDCl}_3$ )  $\delta$  -115.87 (m, 1F) (FT-IR  $\text{cm}^{-1}$  2952, 1511,

1247, 1172. GC/MS ( $m/z$ , relative intensity) 298 ( $M^+$ , 100), 270 (30), 135 (100), 77 (50). Melting point 99-100 °C.

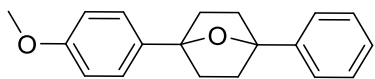
**(1-(4-methoxyphenyl)-4-(p-tolyl)-7-oxabicyclo[2.2.1]heptane) (5e)**



The general procedure F was followed using 4''-methoxy-4-methyl-3',6'-dihydro-[1,1':4',1''-terphenyl]-1'(2'H)-ol (100.0

mg, 0.34 mmol, 1.0 equiv), catalyst **PC4** (0.7 mg, 0.3 mol%),  $CH_3CN$  (7.1 mL), and formic acid (243.9 mg, 5.3 mmol) was used to afford **5e** in 84% yield (84 mg, 0.29 mmol) as a white solid. The crude material was purified by flash chromatography using hexanes:ethyl acetate with product eluting at 5%.  $^1H$  NMR (400 MHz,  $CDCl_3$ )  $\delta$  7.50 – 7.43 (m, 2H), 7.43 – 7.38 (m, 2H), 7.18 (d,  $J$  = 7.9 Hz, 2H), 6.96 – 6.87 (m, 2H), 3.82 (s, 3H), 2.35 (s, 3H), 2.19 (d,  $J$  = 8.3 Hz, 4H), 2.00 (d,  $J$  = 6.7 Hz, 4H).  $^{13}C$  NMR (101 MHz,  $CDCl_3$ )  $\delta$  158.7, 140.0, 136.6, 135.2, 128.9, 126.58, 125.2, 113.6, 87.2, 87.1, 55.3, 38.8, 38.7, 21.2. FT-IR  $cm^{-1}$  2956, 1514, 1247, 1174. GC/MS ( $m/z$ , relative intensity) 294 ( $M^+$ , 30), 150 (40), 135(100), 91 (45). Melting point 101-102 °C.

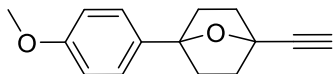
**(1-(4-methoxyphenyl)-4-phenyl-7-oxabicyclo[2.2.1]heptane) (5f)**



The general procedure F was followed using 4''-methoxy-3',6'-dihydro-[1,1':4',1''-terphenyl]-1'(2'H)-ol (100.0 mg, 0.36 mmol,

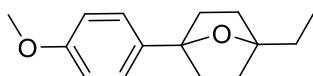
1.0 equiv), catalyst **PC4** (0.8 mg, 0.3 mol%),  $CH_3CN$  (7.5 mL), and formic acid (135.5 mg, 2.944 mmol) was used to afford **5f** in 89% yield (89 mg, 0.32 mmol) as a white solid. The crude material was purified by flash chromatography using hexanes:ethyl acetate with product eluting at 10%.  $^1H$  NMR (400 MHz,  $CDCl_3$ )  $\delta$  7.63 – 7.50 (m, 2H), 7.50 – 7.43 (m, 2H), 7.37 (d,  $J$  = 7.6 Hz, 2H), 7.33 – 7.27 (m, 1H), 7.03 – 6.85 (m, 2H), 3.82 (s, 3H), 2.32 – 2.12 (m, 4H), 2.12 – 1.92 (m, 4H).  $^{13}C$  NMR (101 MHz,  $CDCl_3$ )  $\delta$  158.7, 143.1, 135.1, 128.3, 127.0, 126.6, 125.3, 113.7, 87.3, 87.13, 55.3, 38.8, 38.7. FT-IR  $cm^{-1}$  2950, 1515, 1248, 1174. GC/MS ( $m/z$ , relative intensity) 280 ( $M^+$ , 20), 150 (40), 135 (100), 77 (100). Melting point 58-60 °C.

**(1-ethynyl-4-(4-methoxyphenyl)-7-oxabicyclo[2.2.1]heptane) (5g)**



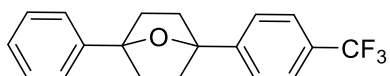
The general procedure F was followed using 4'-methoxy-3',6'-dihydro-[1,1':4',1''-terphenyl]-1'(2'H)-ol (100.0 mg, 0.44 mmol, 1.0 equiv), catalyst **PC4** (0.9 mg, 0.3 mol%), and formic acid (907 mg, 19.7 mmol) was used to afford **5g** in 86% yield (86 mg, 0.38 mmol) as a white solid. The crude material was purified by flash chromatography using hexanes:ethyl acetate with product eluting at 5%. <sup>1</sup>H NMR (400 MHz, CDCl<sub>3</sub>) δ 7.36 (d, *J* = 8.8 Hz, 2H), 6.87 (d, *J* = 8.8 Hz, 2H), 3.80 (s, 3H), 2.64 (s, 1H), 2.20 – 2.11 (m, 2H), 2.11 – 2.01 (m, 4H), 2.00 – 1.87 (m, 2H). <sup>13</sup>C NMR (101 MHz, CDCl<sub>3</sub>) δ 158.8, 133.8, 126.5, 113.6, 87.7, 82.7, 77.2, 74.4, 55.3, 38.5, 37.8. FT-IR cm<sup>-1</sup> 3238, 2922, 1513, 1255. GC/MS (*m/z*, relative intensity) 228 (M<sup>+</sup>, 15), 135 (100), 77 (70), 39 (65). Melting point 130-131 °C

**(1-ethyl-4-(4-methoxyphenyl)-7-oxabicyclo[2.2.1]heptane) (5h)**



The general procedure F was followed using 4-ethyl-4'-methoxy-2,3,4,5-tetrahydro-[1,1'-biphenyl]-4-ol (90.0 mg, 0.39 mmol), catalyst **PC4** (0.8 mg, 0.3 mol%), and formic acid (561.4 mg, 12.2 mmol) was used to afford **5h** in 84% yield (75.6 mg, 0.33 mmol) as a clear oil. The crude material was purified by flash chromatography using hexanes:ethyl acetate with product eluting at 5%. <sup>1</sup>H NMR (400 MHz, CDCl<sub>3</sub>) δ 7.37 (d, *J* = 8.7 Hz, 2H), 6.88 (d, *J* = 8.7 Hz, 2H), 3.80 (s, 3H), 2.10 – 2.01 (m, 2H), 1.96 – 1.82 (m, 4H), 1.82 – 1.64 (m, 4H), 1.04 (t, *J* = 7.6 Hz, 3H). <sup>13</sup>C NMR (101 MHz, CDCl<sub>3</sub>) δ 158.9, 135.8, 126.9, 113.9, 87.7, 86.9, 55.7, 38.8, 35.7, 28.9, 9.9. FT-IR cm<sup>-1</sup> 2964, 1515, 1245, 1175. GC/MS (*m/z*, relative intensity) 232 (M<sup>+</sup>, 20), 189 (20), 150 (30), 135 (100).

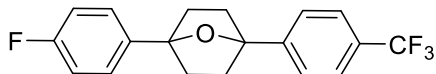
**(1-phenyl-4-(4-(trifluoromethyl)phenyl)-7-oxabicyclo[2.2.1]heptane) (5i)**



The general procedure F was followed using 4-(trifluoromethyl)-3',6'-dihydro-[1,1':4',1''-terphenyl]-1'(2'H)-ol (100.0 mg, 0.31 mmol), catalyst **PC4** (0.7 mg, 0.3 mol%), and formic acid (639.7 mg, 13.9 mmol) was used to afford **5i** in 85% yield (85 mg, 0.27 mmol) as a white solid. The crude material was purified by flash chromatography using hexanes:ethyl acetate with product eluting at 5%. <sup>1</sup>H NMR (400 MHz, CDCl<sub>3</sub>) δ 7.56 (s, 4H), 7.46 (d, 2H), 7.31 (t, *J* = 7.5 Hz, 2H), 7.23 (d, *J* = 7.3 Hz,

1H), 2.28 – 2.07 (m, 4H), 2.04 – 1.85 (m, 4H). <sup>13</sup>C NMR (101 MHz, CDCl<sub>3</sub>) δ 147.0, 142.5, 129.2 (q, *J* = 32.2 Hz), 128.3, 127.2, 125.5, 125.2, 125.2, 124.3 (q, *J*=32.2 Hz), 87.6, 86.9, 38.7, 38.6. <sup>19</sup>F NMR (376 MHz, CDCl<sub>3</sub>) δ -62.39 (s, 3F). FT-IR cm<sup>-1</sup> 2953, 1323, 1154, 1109. GC/MS (*m/z*, relative intensity) 318 (M<sup>+</sup>, 20), 145 (50), 105 (100), 77 (80). Melting point 72- 74 °C.

**(1-(4-fluorophenyl)-4-(4-(trifluoromethyl)phenyl)-7-oxabicyclo[2.2.1]heptane) (5j)**



The general procedure F was followed using 4''-fluoro-4-(trifluoromethyl)-3',6'-dihydro-[1,1':4',1''-terphenyl]-

1'(2H)-ol (100.0 mg, 0.30 mmol), catalyst **PC4** (0.6 mg, 0.3 mol%), and formic acid (616.2 mg, 13.39 mmol) was used to afford **5j** in 85% yield (85 mg, 0.25 mmol) as a white solid. The crude material was purified by flash chromatography using hexanes:ethyl acetate with product eluting at 5%. <sup>1</sup>H NMR (400 MHz, CDCl<sub>3</sub>) δ 7.54 (s, 4H), 7.37 (d, *J* = 8.0 Hz, 2H), 7.26 (d, *J* = 8.2 Hz, 2H), 2.28 – 2.06 (m, 4H), 1.90 (d, *J* = 7.5 Hz, 4H). <sup>13</sup>C NMR (101 MHz, CDCl<sub>3</sub>) δ 161.8 (d, *J* = 245.2 Hz), 146.6, 138.1 (d, *J* = 3.1 Hz), 129.1 (q, *J* = 32.3 Hz), 126.7 (d, *J* = 8.0 Hz), 125.3, 125.0 (q, *J* = 3.7 Hz), 124.1 (q, *J* = 271.9 Hz), 114.9 (d, *J* = 21.3 Hz), 87.0, 86.9, 38.5, 38.5. <sup>19</sup>F NMR (376 MHz, CDCl<sub>3</sub>) δ -62.38 (s, 3F), -115.50 – -115.66 (m, 1F). FT-IR cm<sup>-1</sup> 2949, 1510, 1324, 1119. GC/MS (*m/z*, relative intensity) 336 (M<sup>+</sup>, 20) 173 (20), 123 (100), 95 (50). Melting point 65-68 °C.

**(1-(4-chlorophenyl)-4-(4-(trifluoromethyl)phenyl)-7-oxabicyclo[2.2.1]heptane) (5k)**



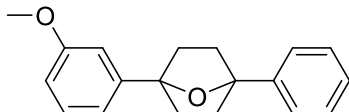
The general procedure F was followed using 4''-chloro-4-(trifluoromethyl)-3',6'-dihydro-[1,1':4',1''-terphenyl]-

1'(2H)-ol (100.0 mg, 0.28 mmol), catalyst **PC4** (0.6 mg, 0.3 mol%), CH<sub>3</sub>CN (5.9 mL) and formic acid (588.1 mg, 12.78 mmol) was used to afford **5k** in 57% yield (57 mg, 0.16 mmol) as a white solid. The crude material was purified by flash chromatography using hexanes:ethyl acetate with product eluting at 5%. <sup>1</sup>H NMR (400 MHz, CDCl<sub>3</sub>) δ 7.63 (s, 4H), 7.50 – 7.43 (m, 2H), 7.39 – 7.33 (m, 2H), 2.33 – 2.16 (m, 4H), 2.05 – 1.94 (m, 4H). <sup>13</sup>C NMR (101 MHz, CDCl<sub>3</sub>) δ 146.7 (d, *J* = 1.5 Hz), 141.1, 132.9, 129.3 (q, *J* = 32.4 Hz), 128.4, 126.6, 125.5, 125.2 (q, *J* = 3.8 Hz), 124.2 (q, *J* = 271.9 Hz), 87.1, 87.1, 38.6, 38.8. <sup>19</sup>F NMR (376 MHz, CDCl<sub>3</sub>) δ -62.40 (s, 3F). FT-IR cm<sup>-1</sup> 2922,

1321, 1124, 1067. GC/MS (*m/z*, relative intensity) 352 ( $M^+$ , 20), 173 (30), 139 (100), 115 (60).

Melting point 102-104 °C.

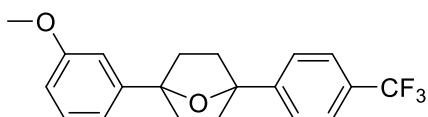
**(1-(3-methoxyphenyl)-4-phenyl-7-oxabicyclo[2.2.1]heptane) (5m)**



The general procedure F was followed using 3''-methoxy-3',6'-dihydro-[1,1':4',1''-terphenyl]-1'(2H)-ol (50.0 mg, 0.18 mmol),

catalyst **PC4** (0.4 mg, 0.3 mol%), and formic acid (152.3 mg, 3.31 mmol) was used to afford **5m** in 72% yield (36.4 mg, 0.13 mmol) as a colorless oil. The crude material was purified by flash chromatography using hexanes:ethyl acetate with product eluting at 5%.  $^1\text{H}$  NMR (400 MHz,  $\text{CDCl}_3$ )  $\delta$  7.55 (d,  $J = 7.8$  Hz, 2H), 7.40 (t,  $J = 7.5$  Hz, 2H), 7.35 – 7.27 (m, 2H), 7.21 – 7.04 (m, 2H), 6.85 (dd,  $J = 8.2, 2.5$  Hz, 1H), 3.86 (s, 3H), 2.24 (d,  $J = 6.7$  Hz, 4H), 2.03 (d,  $J = 5.8$  Hz, 4H).  $^{13}\text{C}$  NMR (101 MHz,  $\text{CDCl}_3$ )  $\delta$  159.6, 144.7, 143.0, 129.4, 128.3, 127.1, 125.3, 117.7, 112.5, 111.0, 87.45, 87.38, 55.4, 38.80, 38.75.

**(1-(3-methoxyphenyl)-4-(4-(trifluoromethyl)phenyl)-7-oxabicyclo[2.2.1]heptane) (5n)**



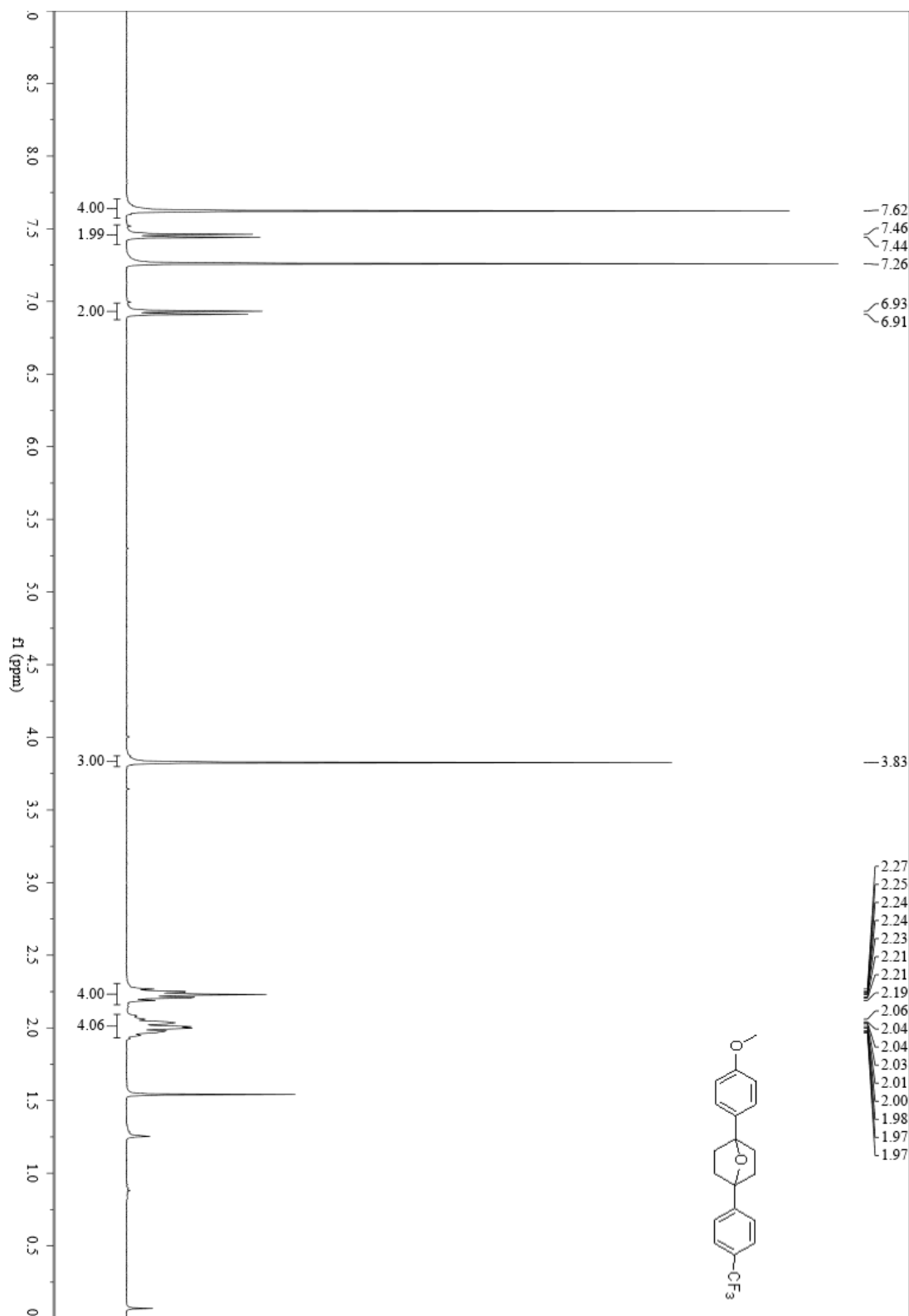
The general procedure F was followed using 3''-methoxy-4-(trifluoromethyl)-3',6'-dihydro-[1,1':4',1''-terphenyl]-

1'(2H)-ol (90.0 mg, 0.26 mmol), catalyst **PC4** (0.4 mg, 0.3 mol%), and formic acid (239.3 mg, 5.20 mmol) was used to afford **5n** in 78% yield (70.0 mg, 0.20 mmol) as a white solid. The crude material was purified by flash chromatography using hexanes:ethyl acetate with product eluting at 8%.  $^1\text{H}$  NMR (400 MHz,  $\text{CDCl}_3$ )  $\delta$  7.65 (s, 4H), 7.32 (t,  $J = 7.9$  Hz, 1H), 7.19 – 7.07 (m, 2H), 6.93 – 6.81 (m, 1H), 3.86 (s, 3H), 2.33 – 2.19 (m, 4H), 2.12 – 1.92 (m, 4H).  $^{13}\text{C}$  NMR (101 MHz,  $\text{CDCl}_3$ )  $\delta$  159.7, 147.1, 144.3, 129.5 (2C), 129.4 (q,  $J = 120.0$  Hz), 125.6 (2C), 125.3 (q,  $J = 3.8$  Hz), 117.7, 112.5, 111.1, 87.7, 87.0, 55.4, 38.7 (4C).  $^{19}\text{F}$  NMR (376 MHz,  $\text{CDCl}_3$ )  $\delta$  -62.37 (s, 3F).

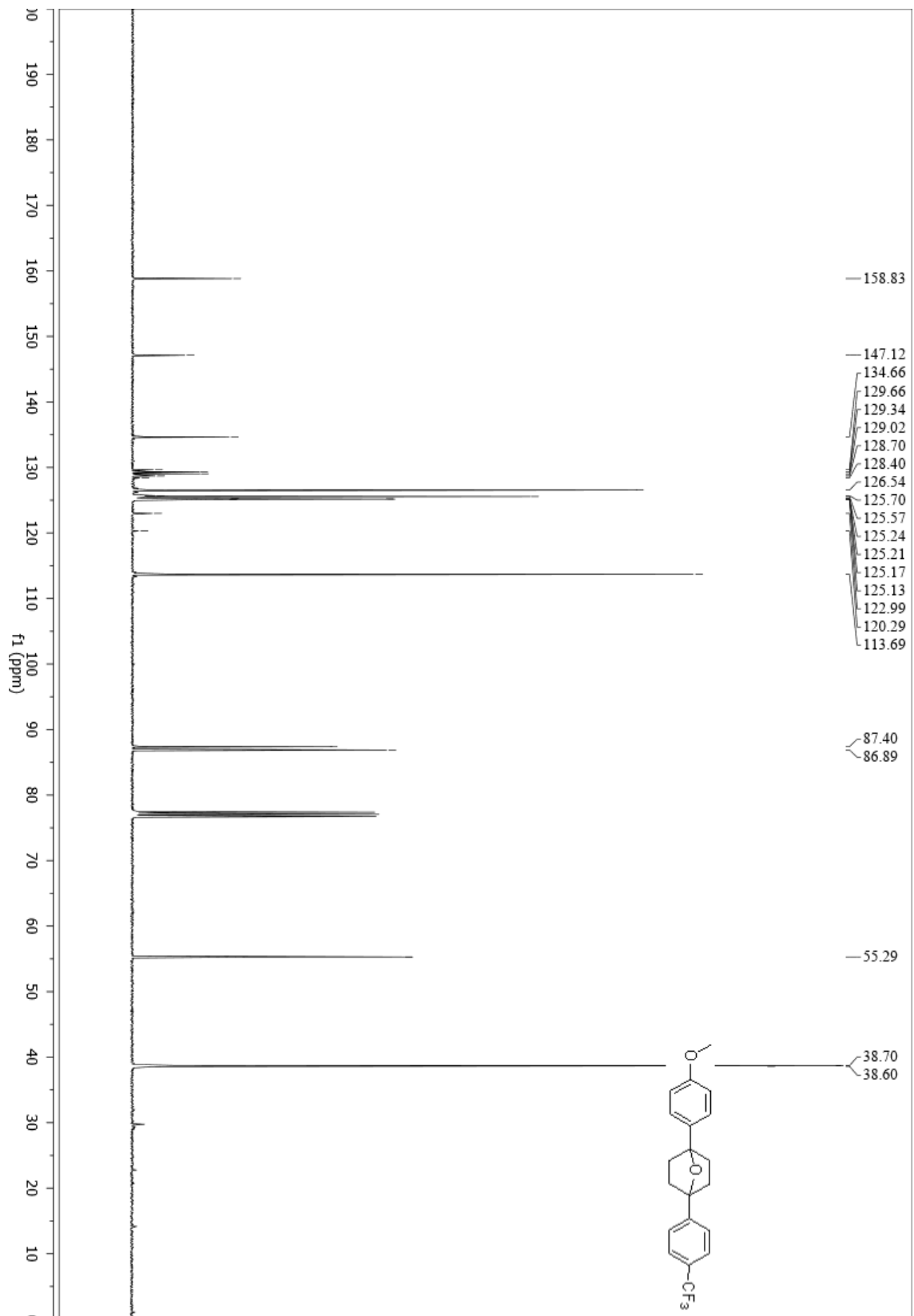
## 5.7 References

1. Dorr, H.; Rawal, V. H., *J. Am. Chem. Soc.* **1999**, *121*, 10229.
2. Nikolai, J.; Loe, Ø.; Dominiak, P. M.; Gerlitz, O. O.; Autschbach, J.; Davies, H. M. L., *J Am Chem Soc* **2007**, *129*, 10763.
3. Jin, S.; Nguyen, V. T.; Dang, H. T.; Nguyen, D. P.; Arman, H. D.; Larionov, O. V., *J. Am. Chem. Soc.* **2017**, *139*, 11365.
4. Rosenberg, H. M.; Serve, M. P., *J. Org. Chem.* **1972**, *37*, 141.
5. Stoll, M.; Hulstkamp, J.; Rouvé, A., *Helv. Chim. Acta* **1948**, *31*, 543.
6. Marshall, J. A., *Acc. Chem. Res.* **1980**, *13*, 213.
7. Cope, A. C.; Pike, R. A.; Spencer, C. F., *J. Am. Chem. Soc.* **1953**, *75*, 3212.
8. Wallraff, G. M.; Michl, J., *J. Org. Chem.* **1986**, *51*, 1794.
9. Inoue, Y.; Ueoka, T.; Kuroda, T.; Hakushi, T., *J. Chem. Soc., Perkin Trans. 2* **1983**, 983-988.
10. Dauben, W. G.; Van Riel, H. C. H. A.; Robbins, J. D.; Wagner, G. J., *J. Am. Chem. Soc.* **1979**, p 6383.
11. Bonneau, R.; Jousot-Dubien, J.; Salem, L.; Yarwood, A. J., *J. Am. Chem. Soc.* **1976**, *98*, 4329.
12. Kropp, P. J., *J. Am. Chem. Soc.* **1969**, *91*, 5783.
13. Singh, A.; Fennell, C. J.; Weaver, J. D., *Chem. Sci.* **2016**, *7*, 6796.
14. Rono, L. J.; Yayla, H. G.; Wang, D. Y.; Armstrong, M. F.; Knowles, R. R., *J. Am. Chem. Soc.* **2013**, *135*, 17735.
15. Lian, J.-J.; Chen, P.-C.; Lin, Y.-P.; Ting, H.-C.; Liu, R.-S., *J. Am. Chem. Soc.* **2006**, *128*, 11372.
16. Rackl, D.; Kreitmeier, P.; Reiser, O., *Green Chem.* **2016**, *18*, 214.
17. Monkman, A. P.; Burrows, H. D.; Hamblett, I.; Navarathnam, S.; Svensson, M.; Andersson, M. R., *J. Chem. Phys.* **2001**, *115*, 9046.
18. Singh, K.; Fennell, C. J.; Coutias, E. A.; Latifi, R.; Hartson, S.; Weaver, J. D., *Chem* **2018**, *4*, 124-137.
19. Singh, K.; Staig, S. J.; Weaver, J. D., *J. Am. Chem. Soc.* **2014**, *136*, 5275-5278.
20. Fabry, D. C.; Ronge, M. A.; Rueping, M., *Chem. Eur. J.* **2015**, *21*, 5350.
21. Flamigni, L.; Barbieri, A.; Sabatini, C.; Ventura, B.; Barigelletti, F., Photochemistry and Photophysics of Coordination Compounds: Iridium. In *Photochemistry and Photophysics of Coordination Compounds II*, Balzani, V.; Campagna, S., Eds. Springer Berlin Heidelberg: Berlin, Heidelberg, 2007; pp 143-203.
22. Dexter, D. L., *J. Chem. Phys.* **1953**, *21*, 836.
23. Head-Gordon, M.; Pople, J. A.; Frisch, M. J., *Chem. Phys. Lett.* **1988**, *153*, 503.
24. Cramer, C., *Essentials of Computational Chemistry: Theories and Models*. II ed.; John Wiley & Sons: 2004; p 216.
25. Dunning, T. H., *J. Chem. Phys.* **1989**, *90*, 1007.
26. Teegardin, K.; Day, J. I.; Chan, J.; Weaver, J., *Org. Process Res. Dev.* **2016**, *20*, 1156.
27. Johnson, R. P.; DiRico, K. J., *J. Org. Chem.* **1995**, *60*, 1074.
28. Bally, T.; Rablen, P. R., *J. Org. Chem.* **2011**, *76*, 4818.
29. Anslyn, E.; Dougherty, D., Isotope Effects. In *Modern Physical Organic Chemistry*, University Science Books: 2006; pp 429-430.
30. Günther, H., Chemical Shifts Through Hydrogen Bonding. In *NMR Spectroscopy*, John Wiley & Sons: 1995; pp 97-99.
31. Plata, R. E.; Singleton, D. A., *J. Am. Chem. Soc.* **2015**, *137*, 3811.
32. Winter, A., Making a bad calculation. *Nature Chem.* **2015**, *7*, 473.

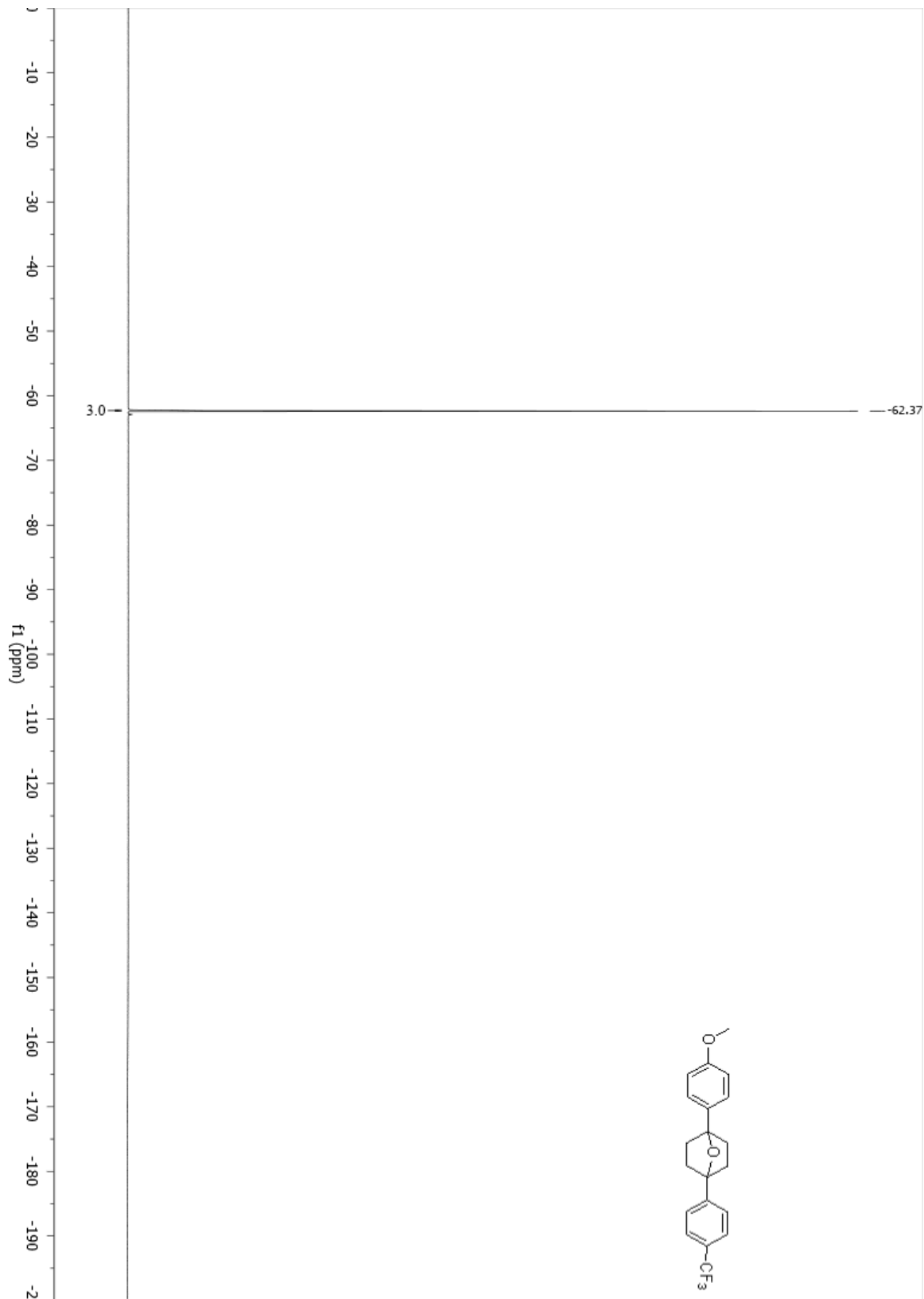
**5a (1-(4-methoxyphenyl)-4-(4-(trifluoromethyl)phenyl)-7-oxabicyclo[2.2.1]heptane)**



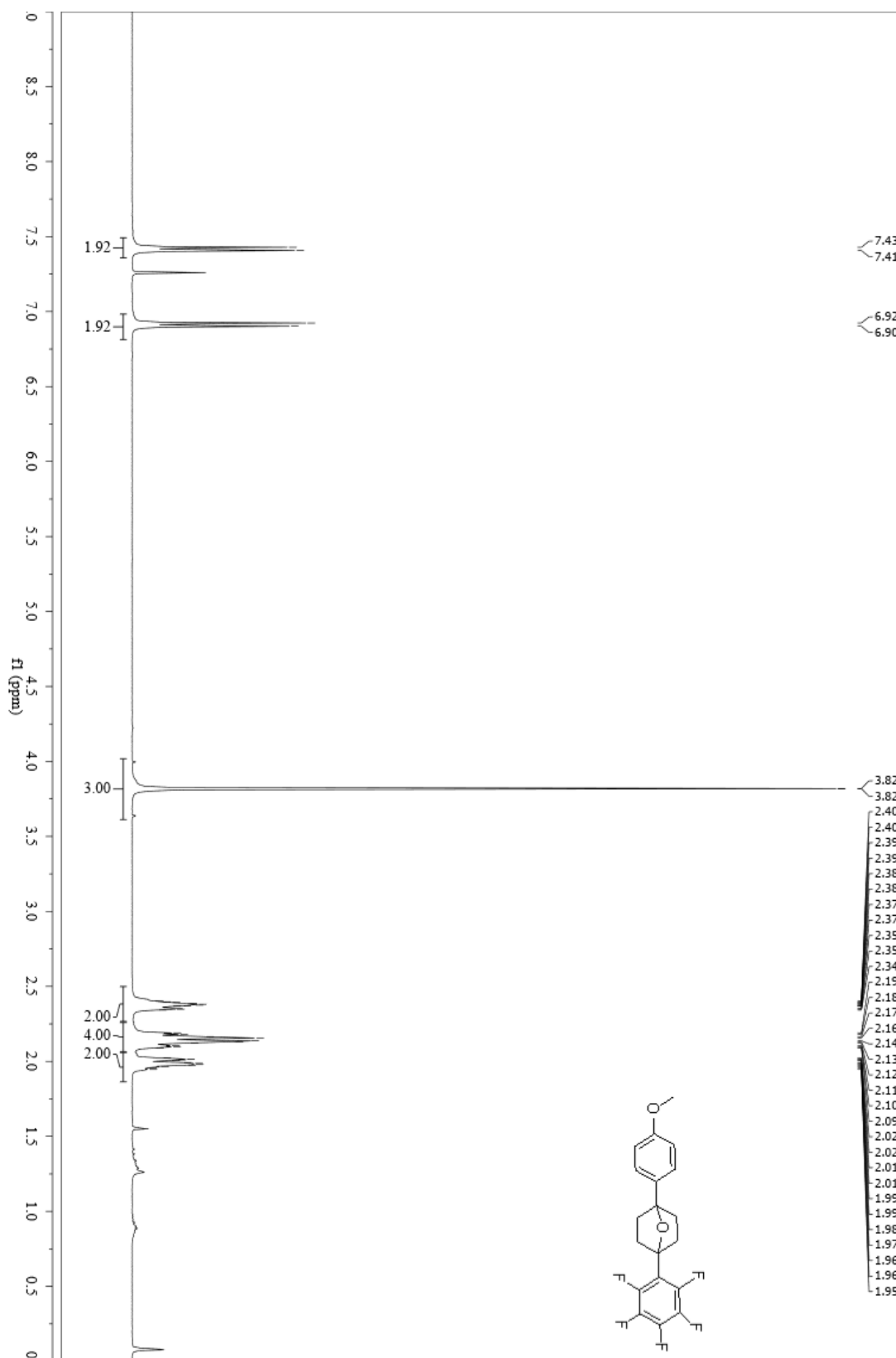
**5a (1-(4-methoxyphenyl)-4-(4-(trifluoromethyl)phenyl)-7-oxabicyclo[2.2.1]heptane)**



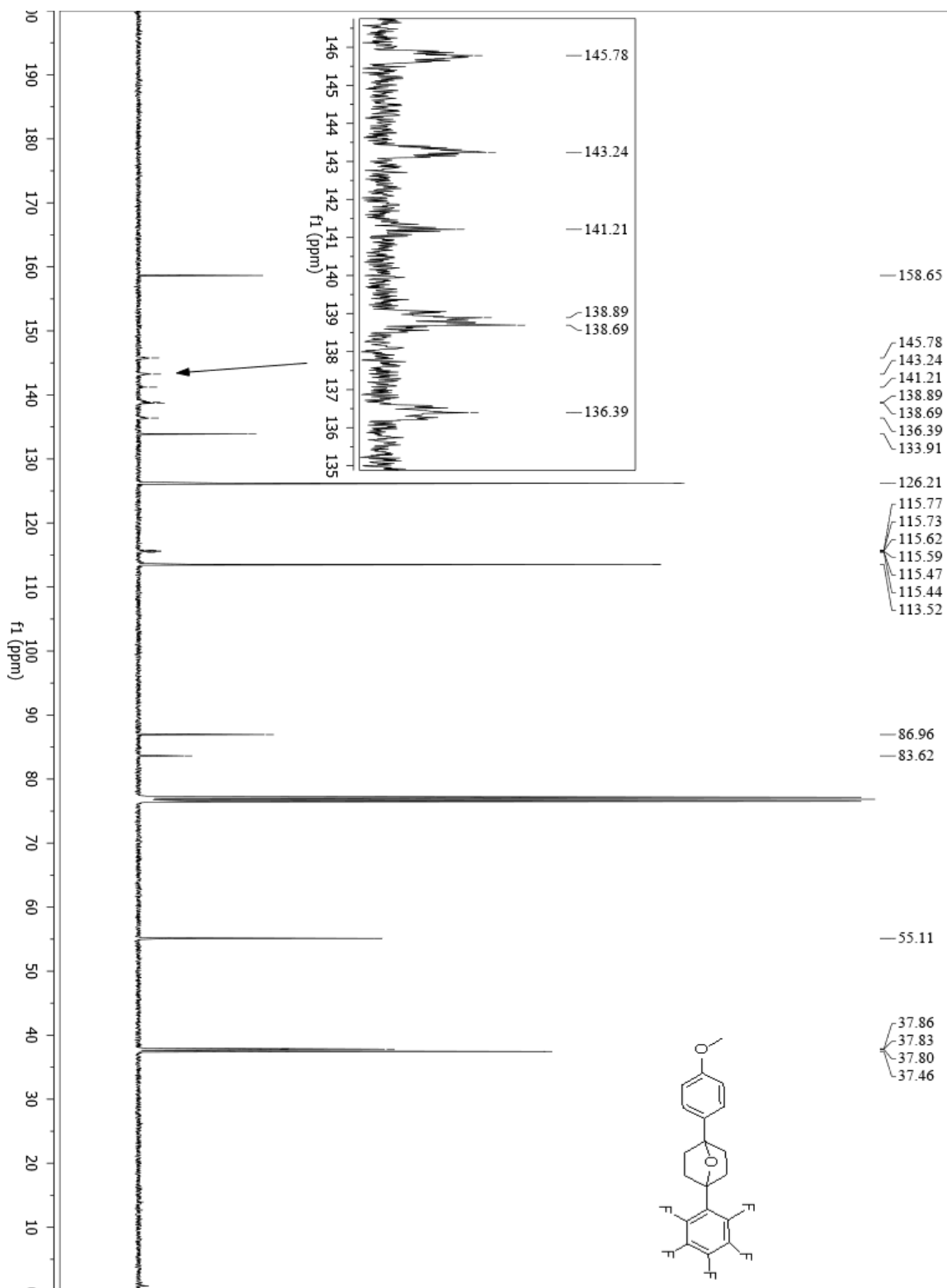
**5a (1-(4-methoxyphenyl)-4-(4-(trifluoromethyl)phenyl)-7-oxabicyclo[2.2.1]heptane)**



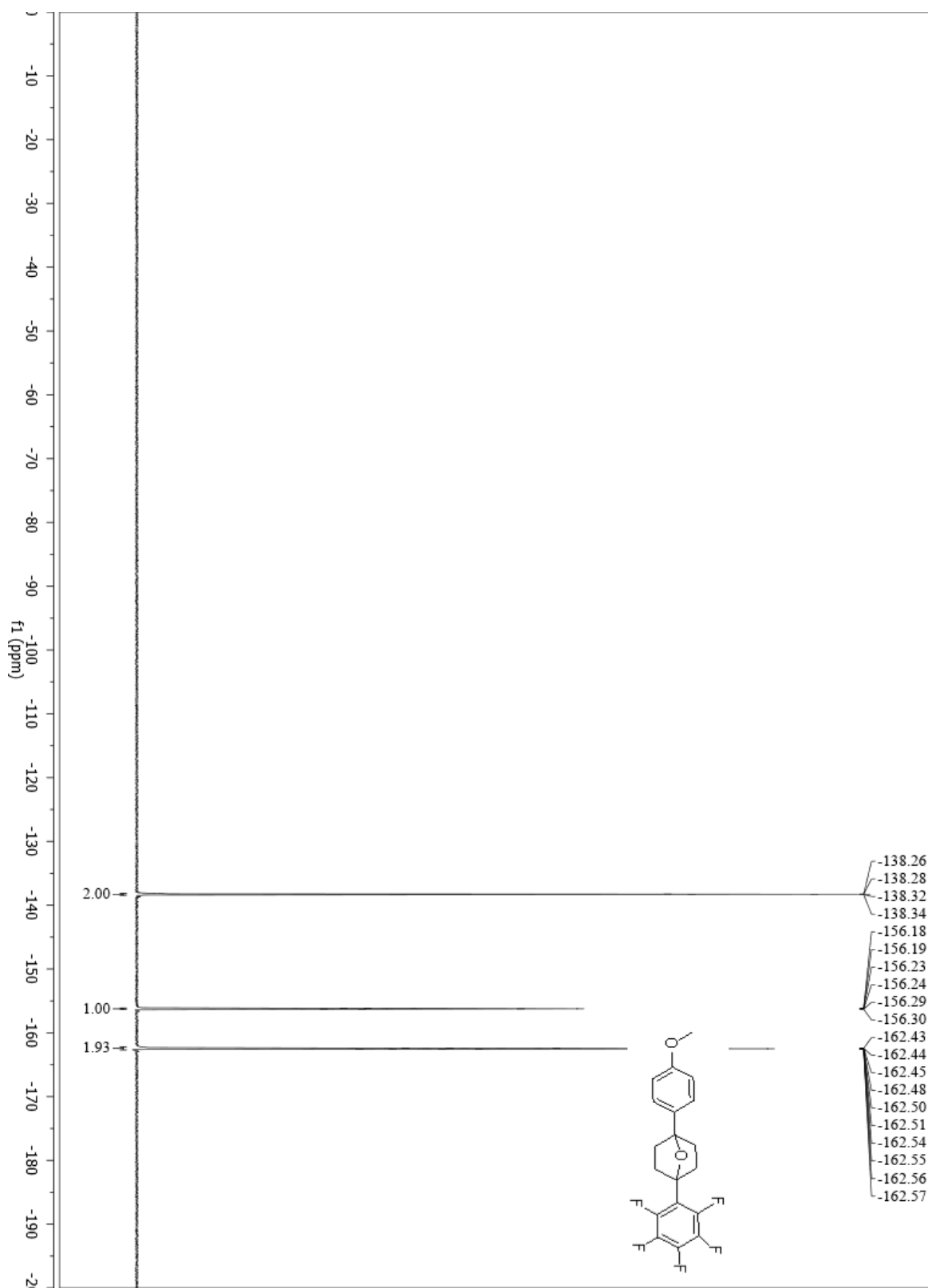
**5b (1-(4-methoxyphenyl)-4-(perfluorophenyl)-7-oxabicyclo[2.2.1]heptanes)**



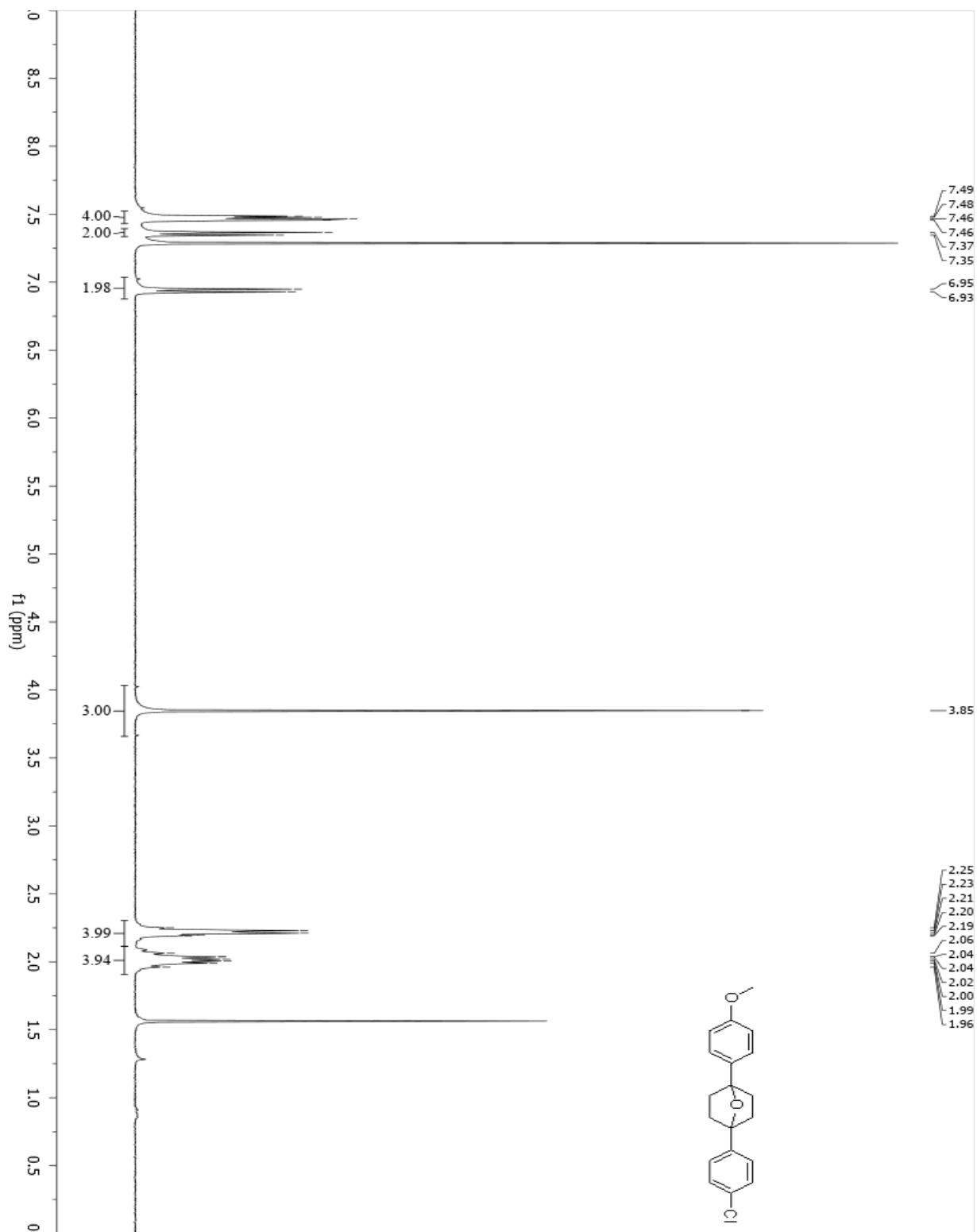
**5b (1-(4-methoxyphenyl)-4-(perfluorophenyl)-7-oxabicyclo[2.2.1]heptanes)-**



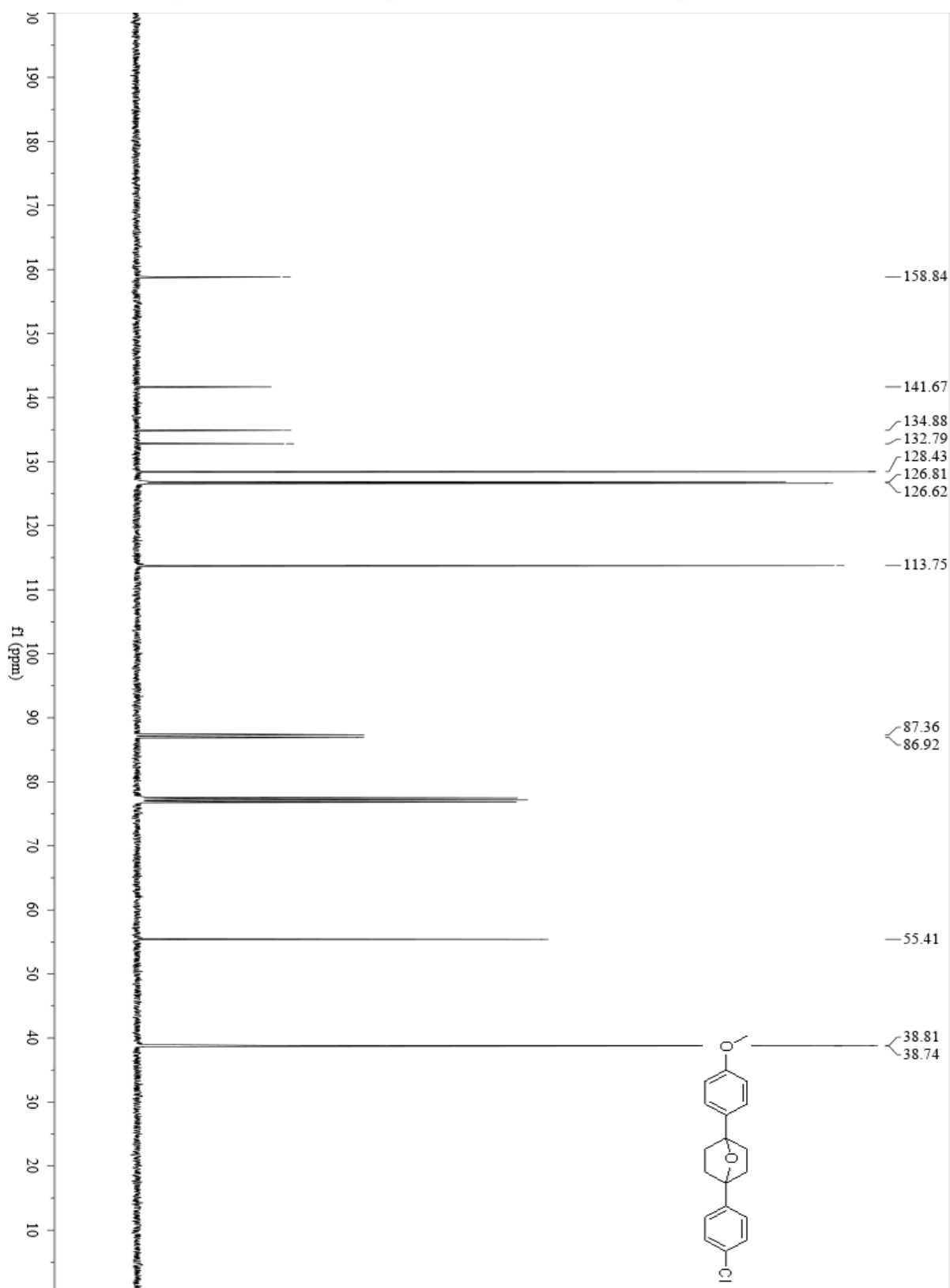
**5b (1-(4-methoxyphenyl)-4-(perfluorophenyl)-7-oxabicyclo[2.2.1]heptanes)**



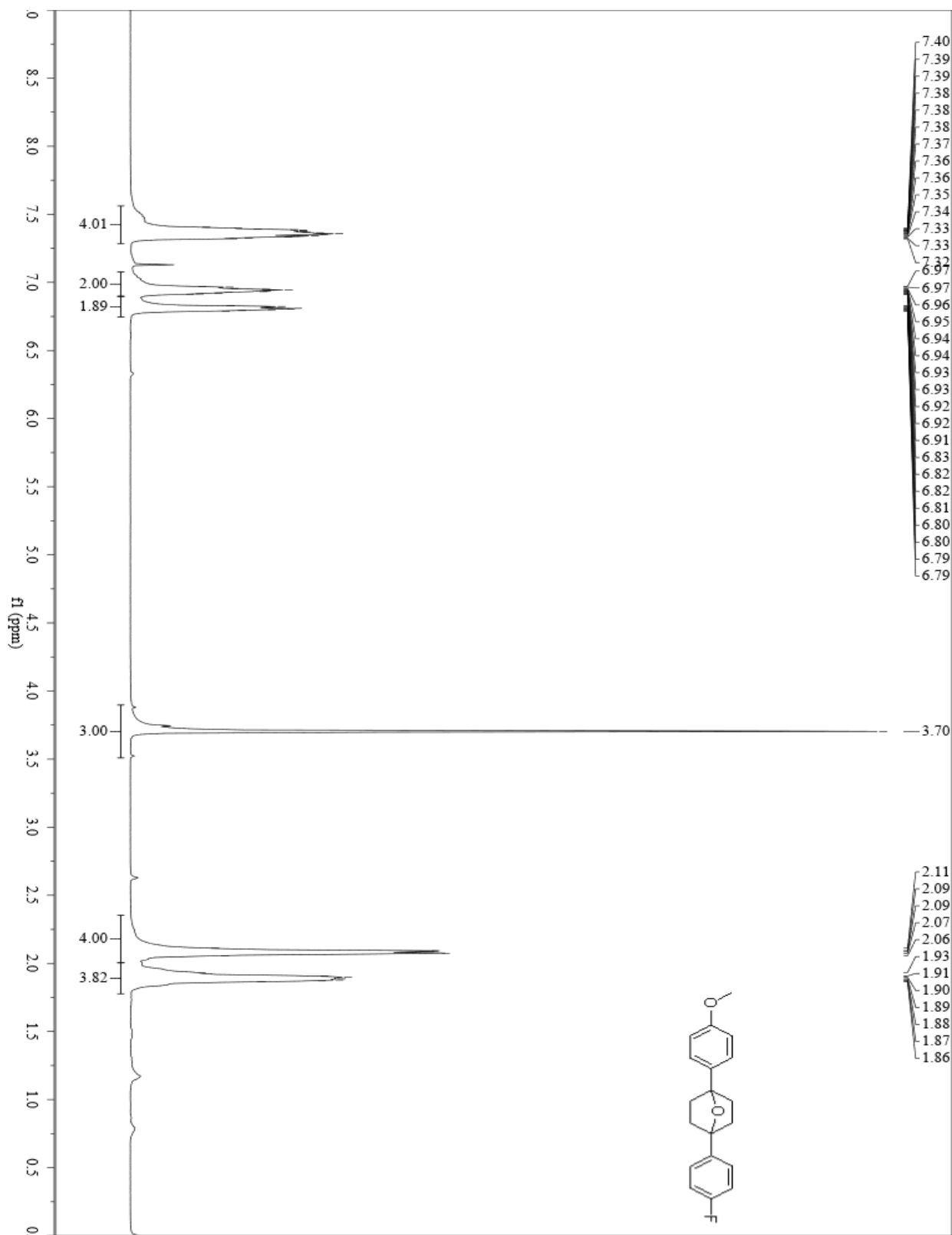
**5c (1-(4-chlorophenyl)-4-(4-methoxyphenyl)-7-oxabicyclo[2.2.1]heptane)**



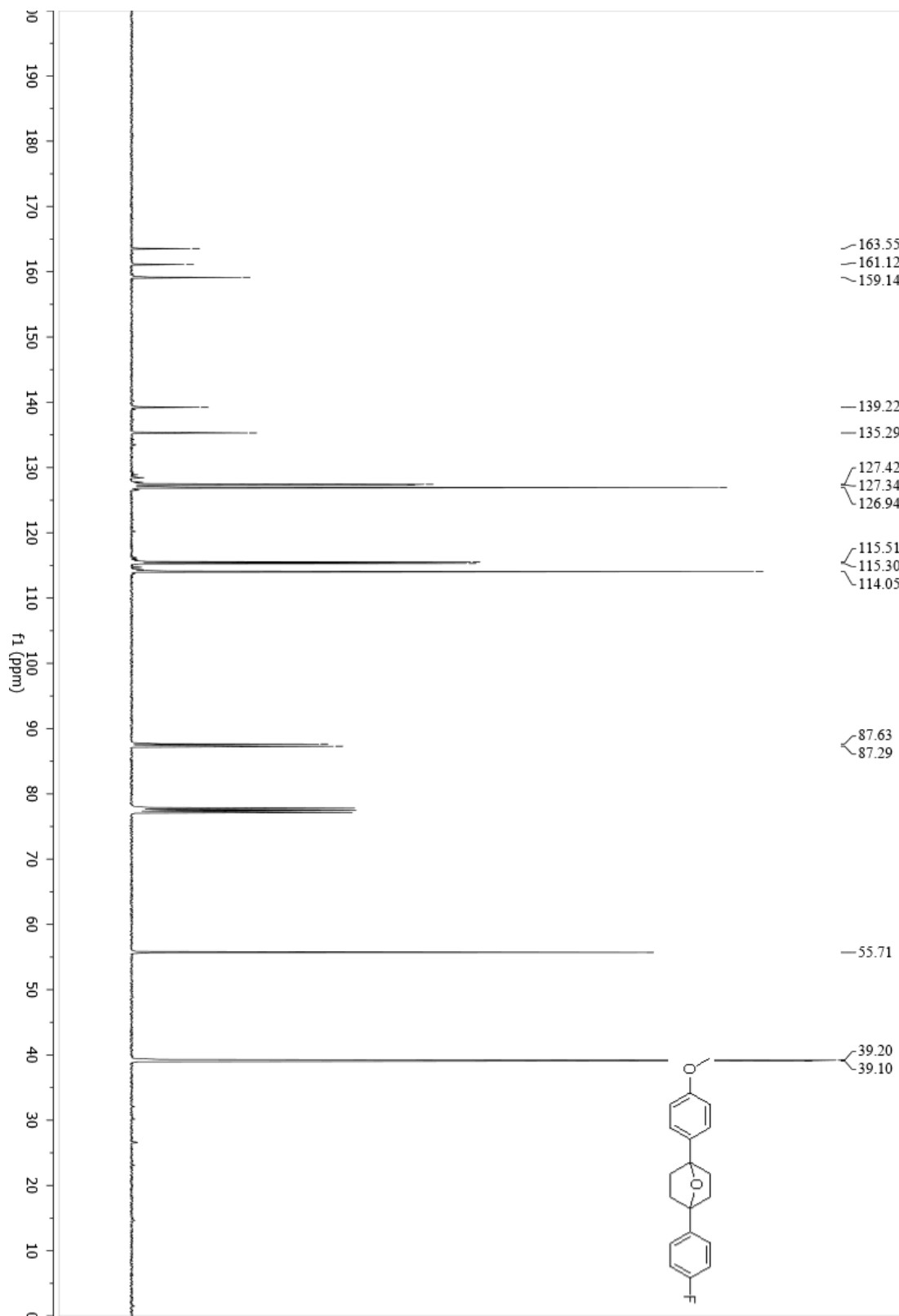
**5c (1-(4-chlorophenyl)-4-(4-methoxyphenyl)-7-oxabicyclo[2.2.1]heptane)**



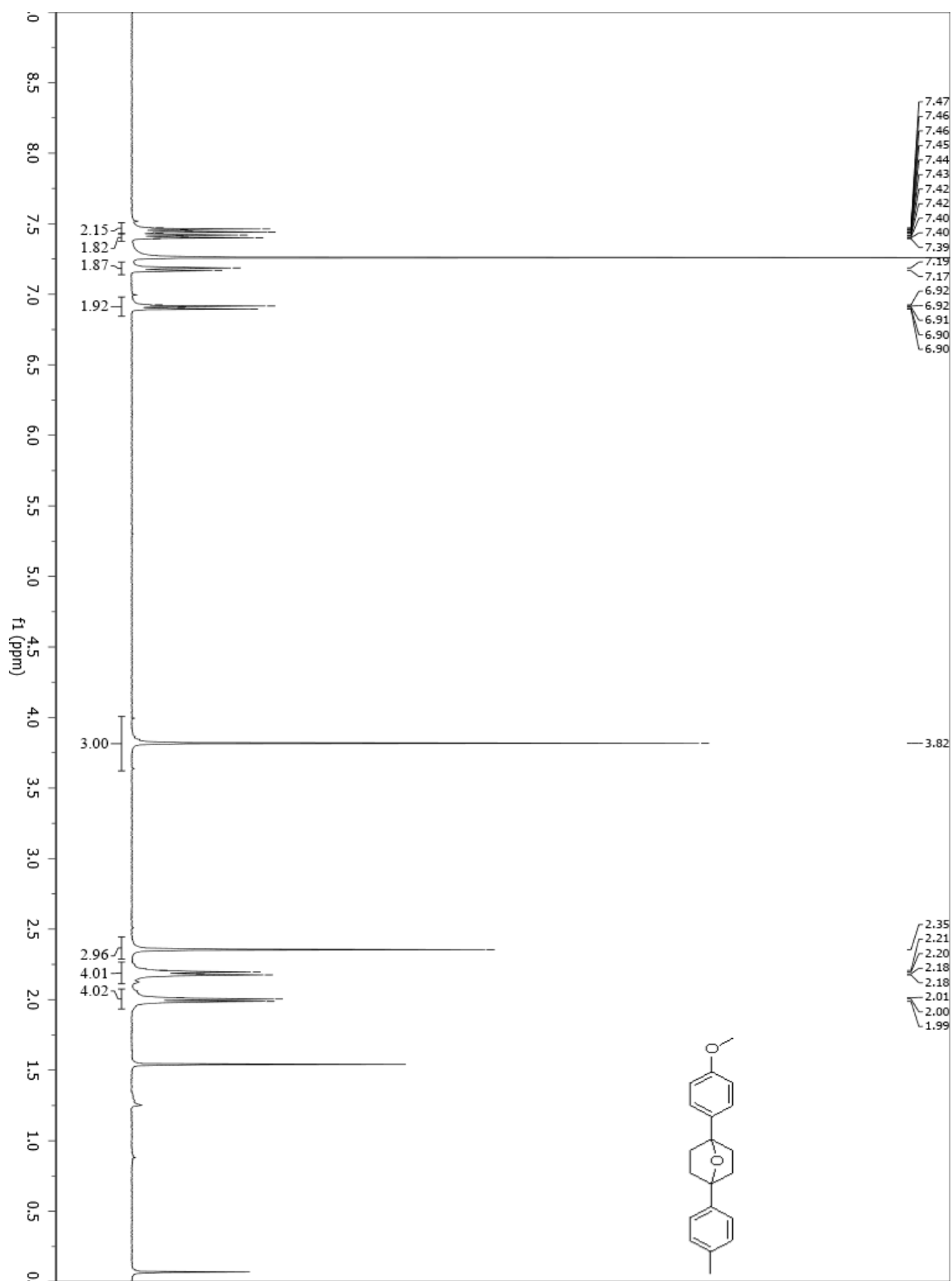
**5d (1-(4-fluorophenyl)-4-(4-methoxyphenyl)-7-oxabicyclo[2.2.1]heptanes)**



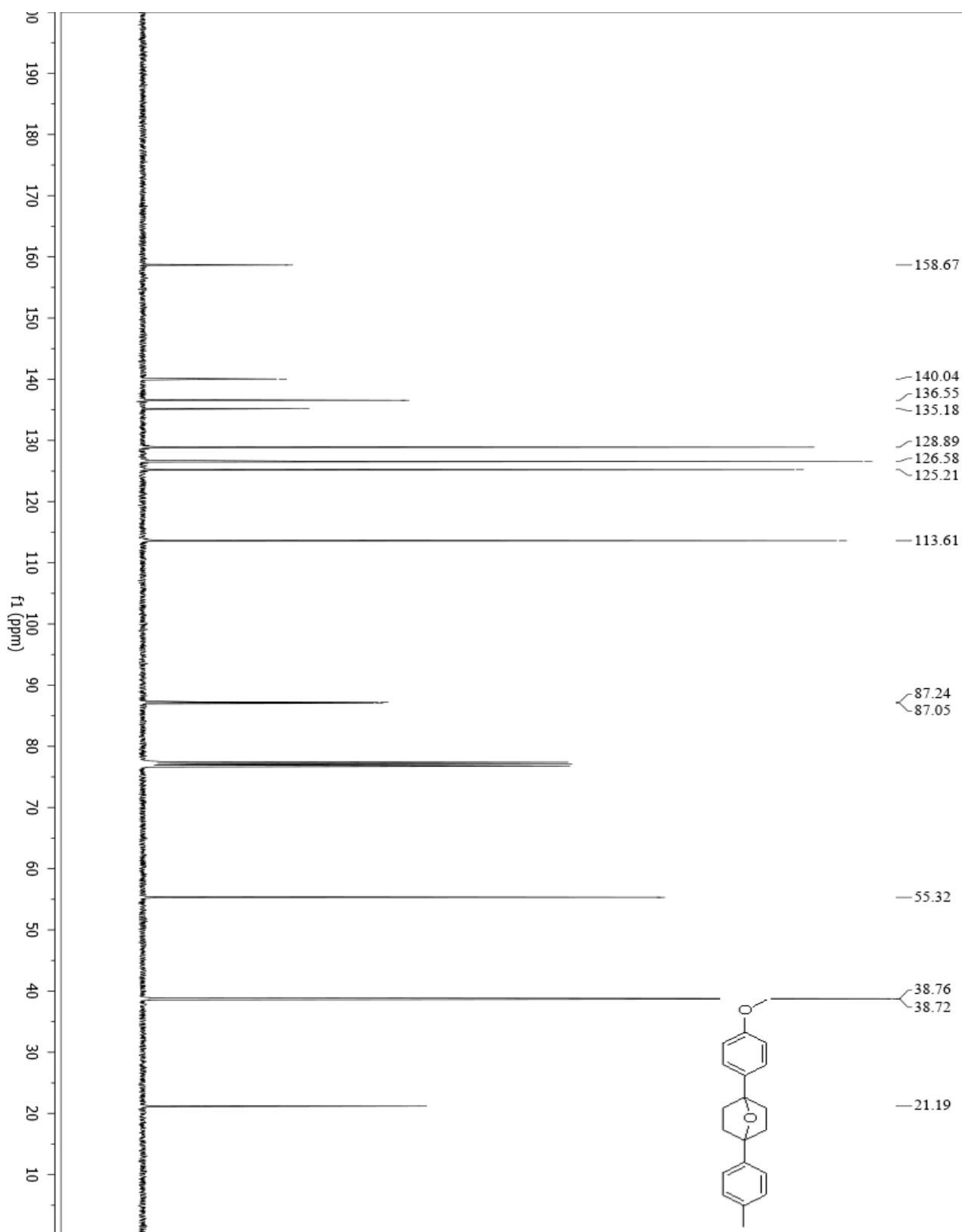
**5d (1-(4-fluorophenyl)-4-(4-methoxyphenyl)-7-oxabicyclo[2.2.1]heptanes)**



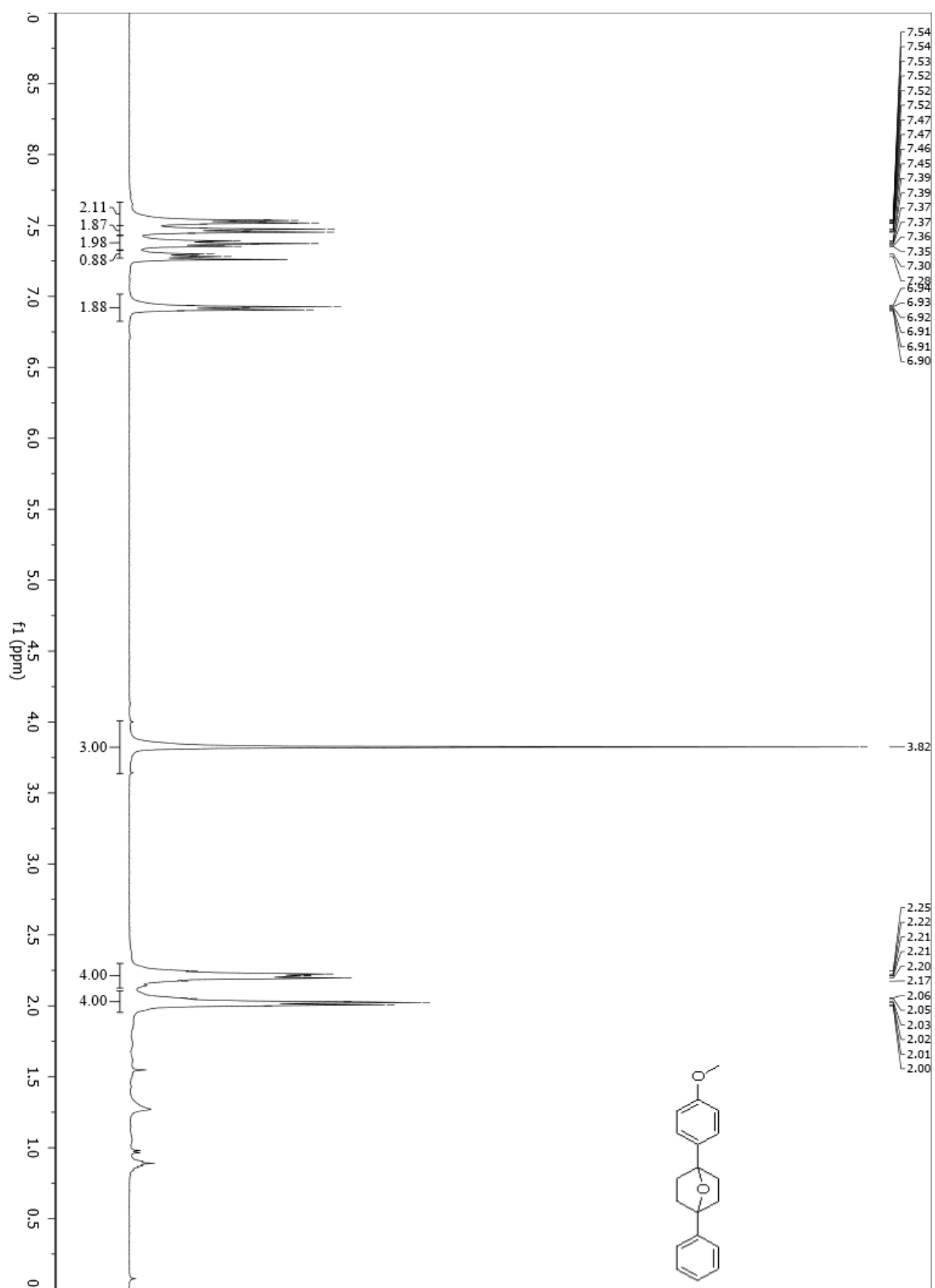
**5e (1-(4-methoxyphenyl)-4-(p-tolyl)-7-oxabicyclo[2.2.1]heptane)**



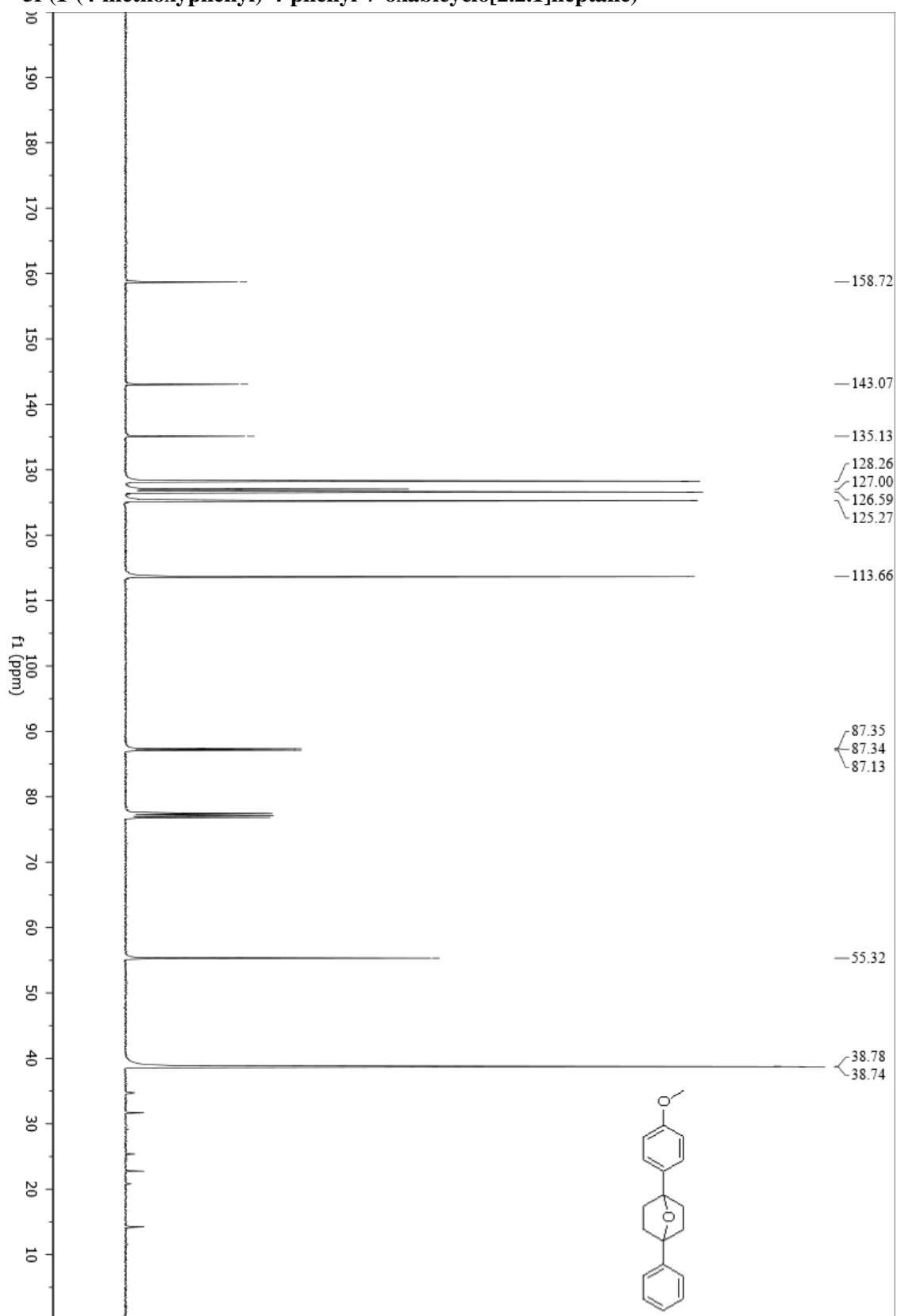
5e (1-(4-methoxyphenyl)-4-(p-tolyl)-7-oxabicyclo[2.2.1]heptane)



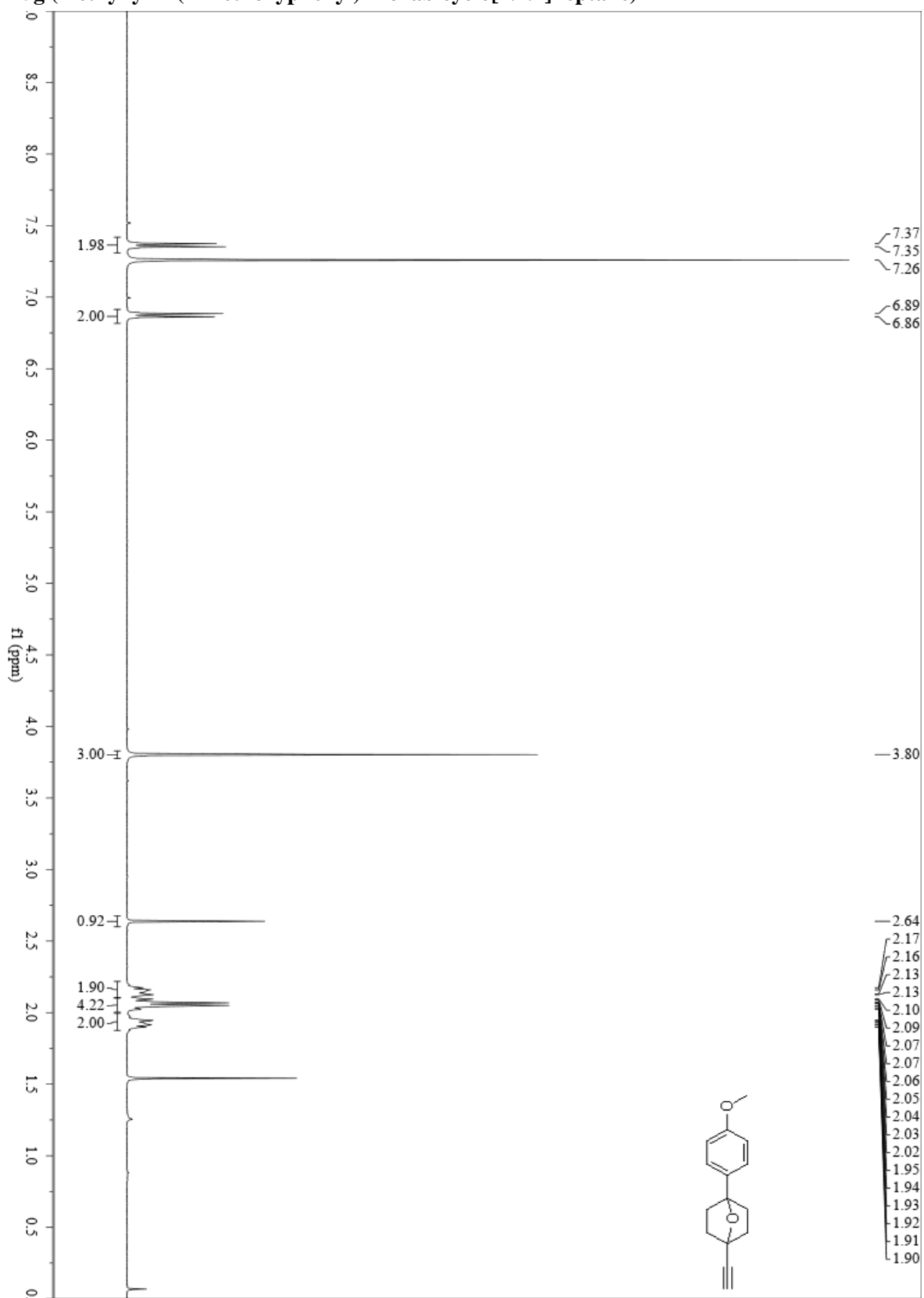
**5f (1-(4-methoxyphenyl)-4-phenyl-7-oxabicyclo[2.2.1]heptane)**



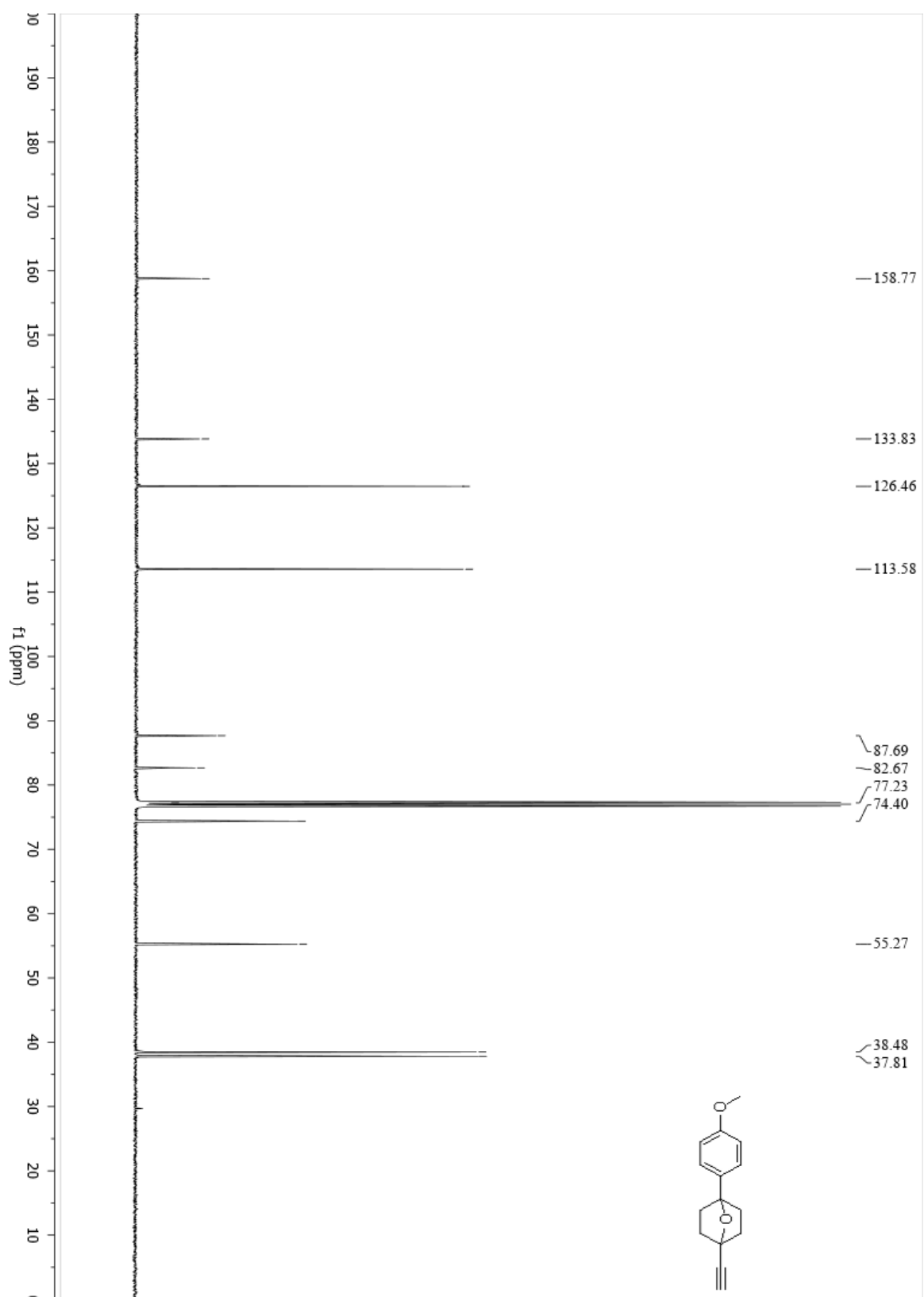
**5f (1-(4-methoxyphenyl)-4-phenyl-7-oxabicyclo[2.2.1]heptane)**



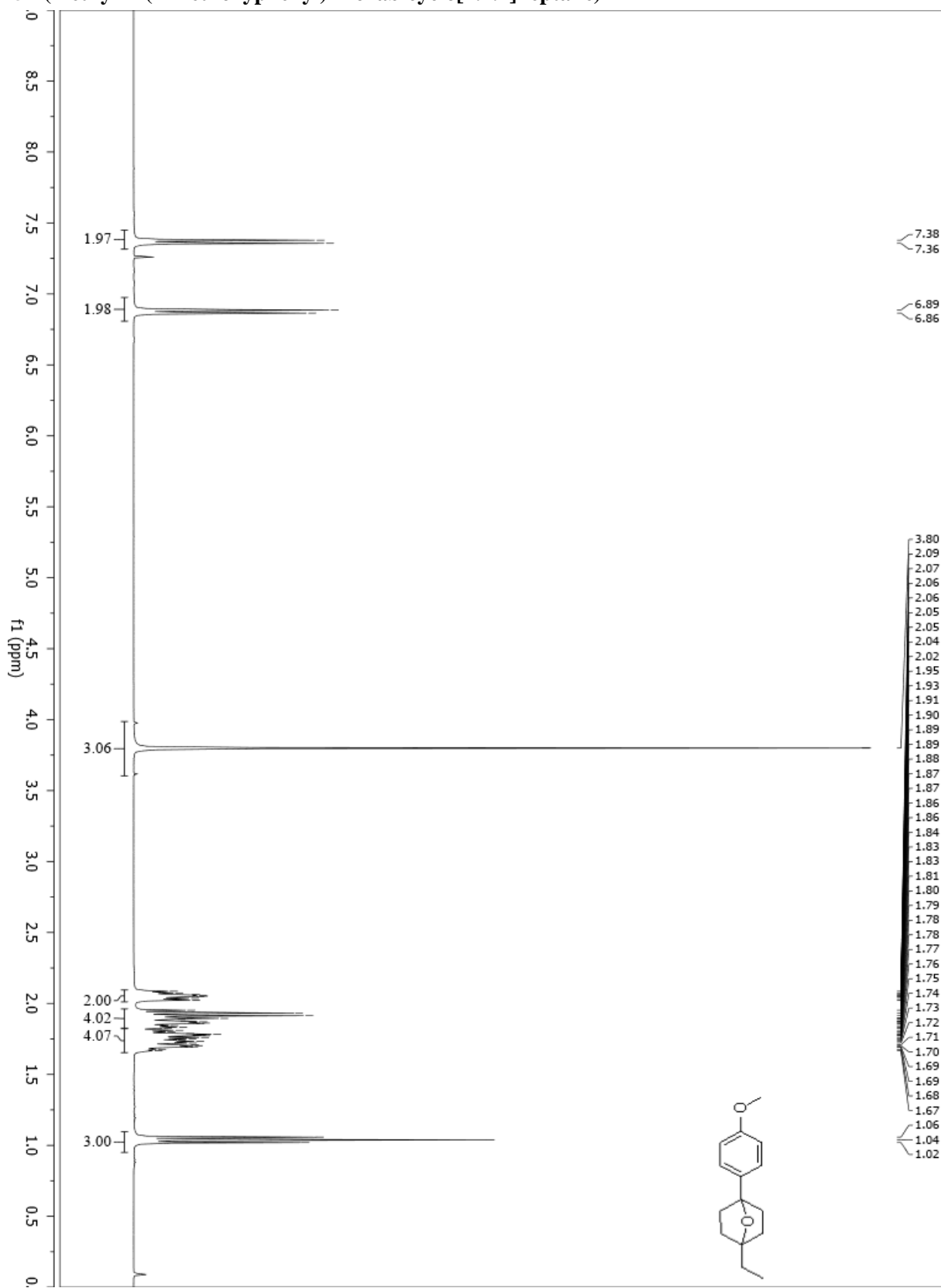
**5g (1-ethynyl-4-(4-methoxyphenyl)-7-oxabicyclo[2.2.1]heptane)**



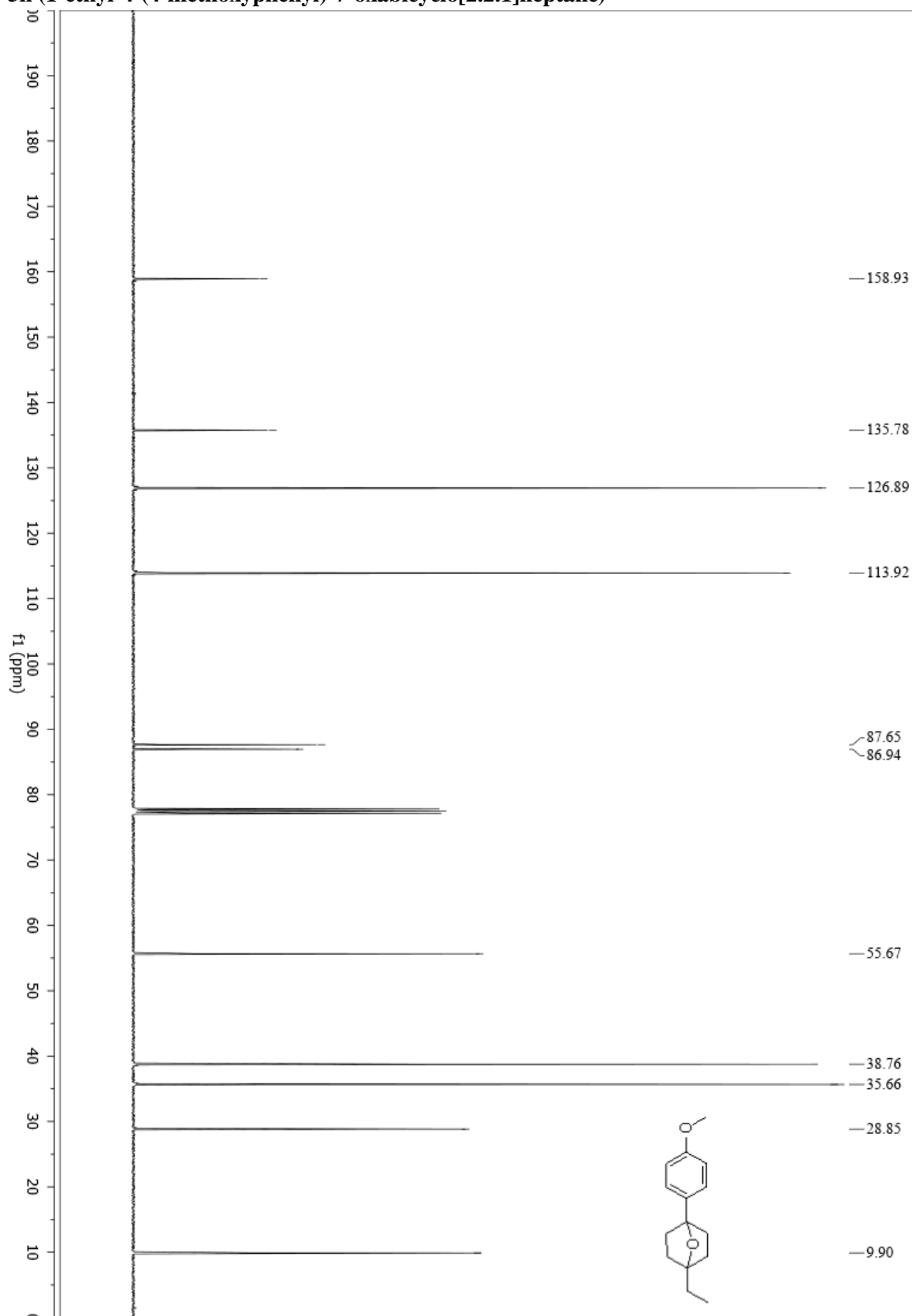
**5g (1-ethynyl-4-(4-methoxyphenyl)-7-oxabicyclo[2.2.1]heptane)**



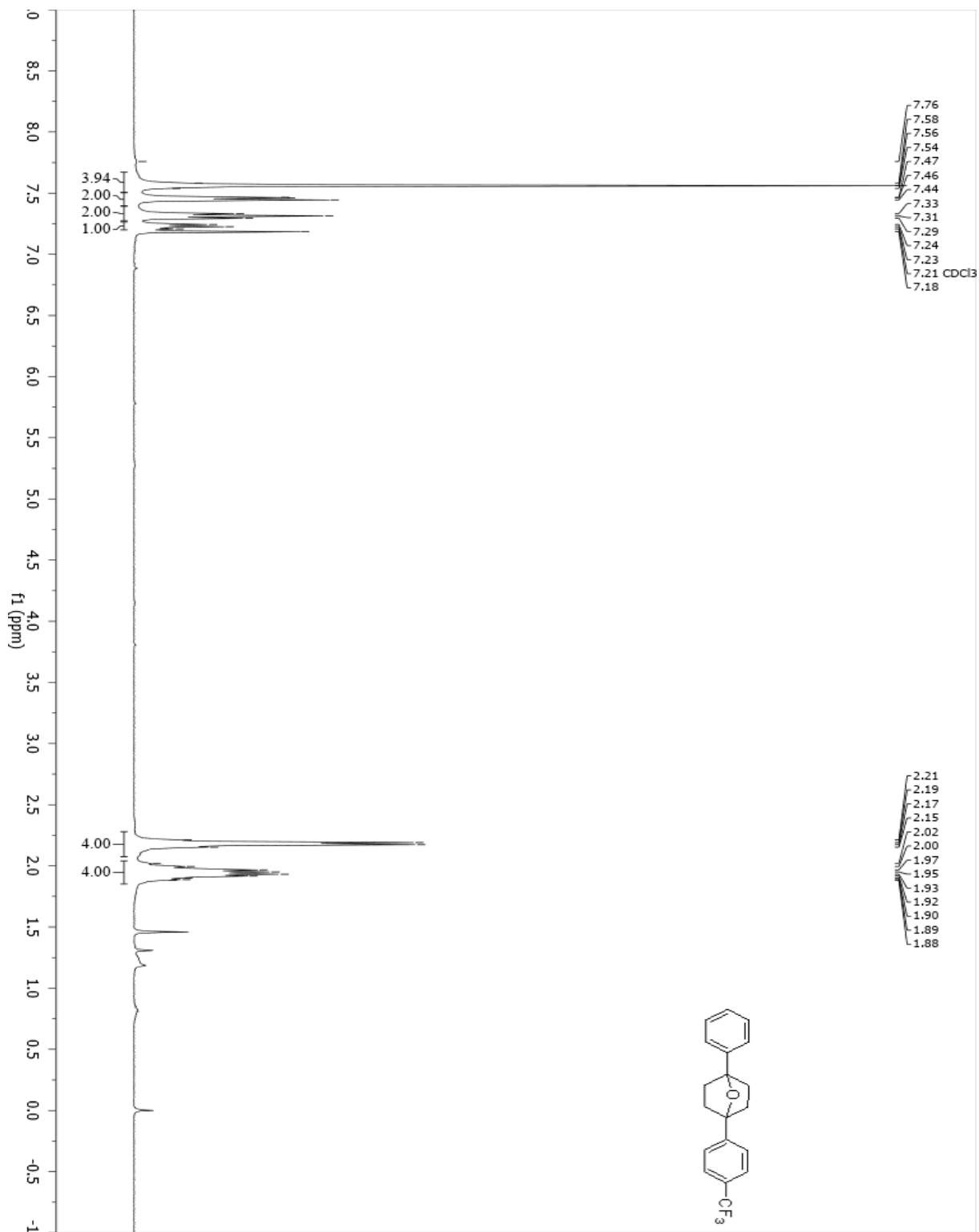
**5h (1-ethyl-4-(4-methoxyphenyl)-7-oxabicyclo[2.2.1]heptane)**



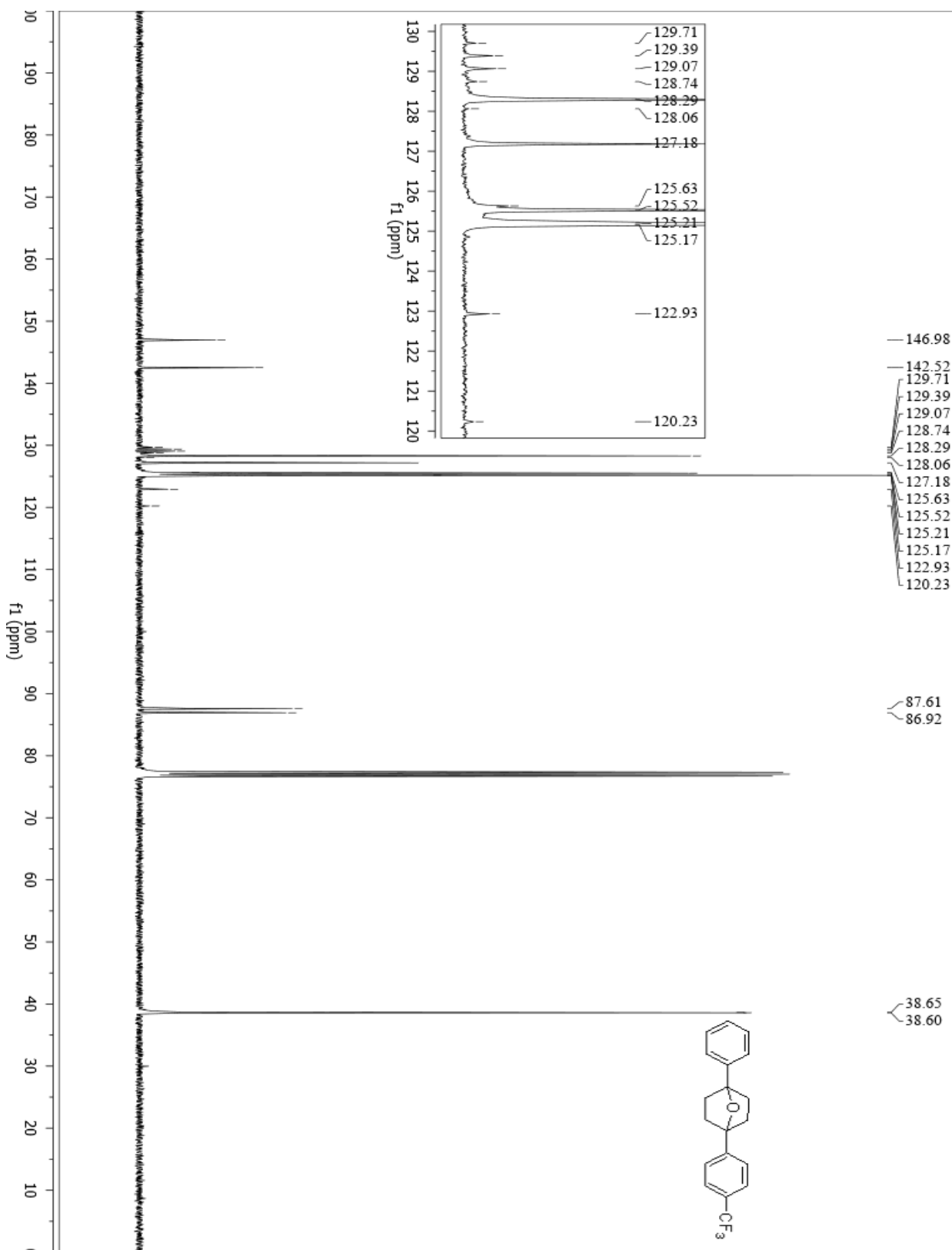
**5h (1-ethyl-4-(4-methoxyphenyl)-7-oxabicyclo[2.2.1]heptane)**



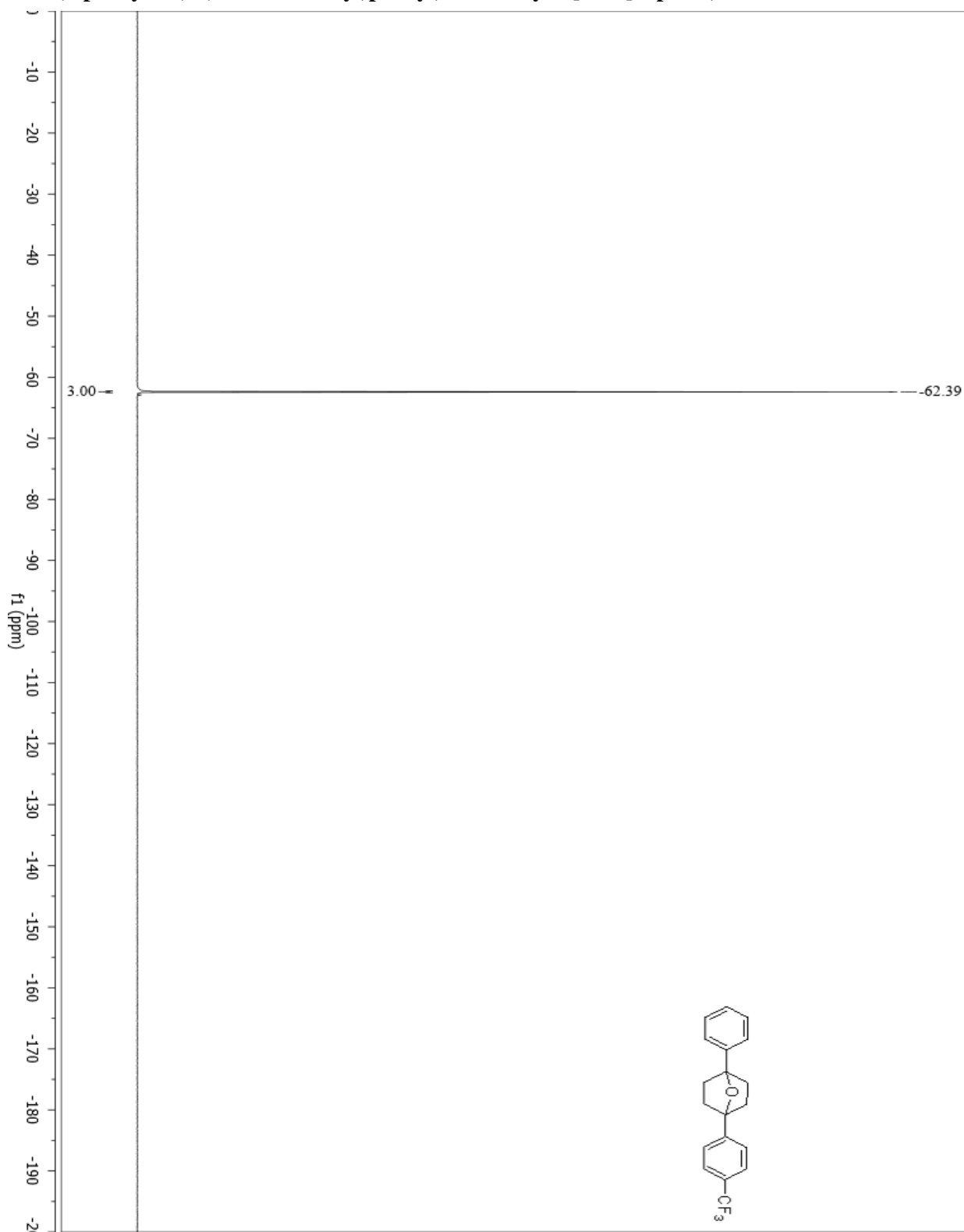
**5i (1-phenyl-4-(4-(trifluoromethyl)phenyl)-7-oxabicyclo[2.2.1]heptane)**



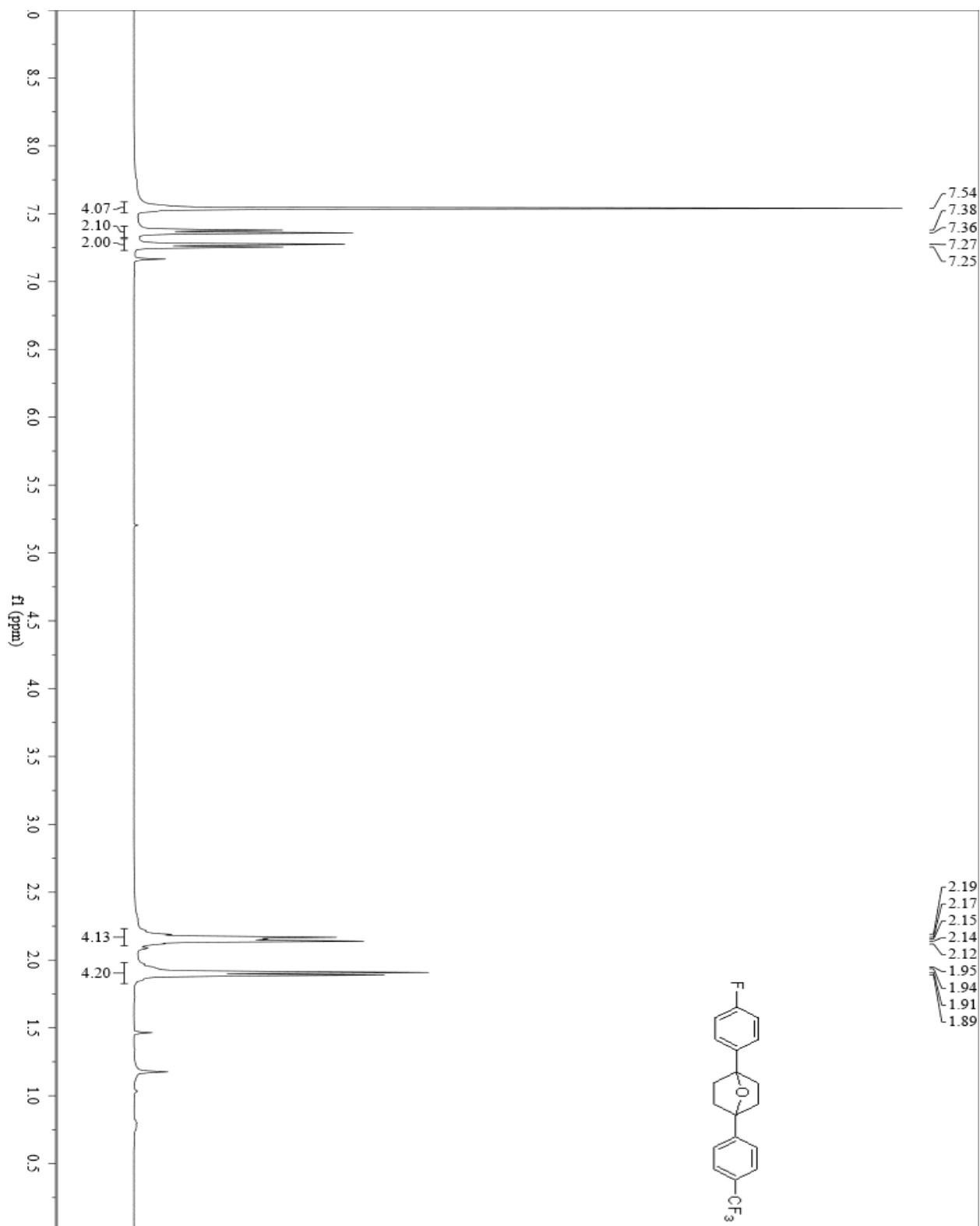
5i (1-phenyl-4-(4-(trifluoromethyl)phenyl)-7-oxabicyclo[2.2.1]heptane)



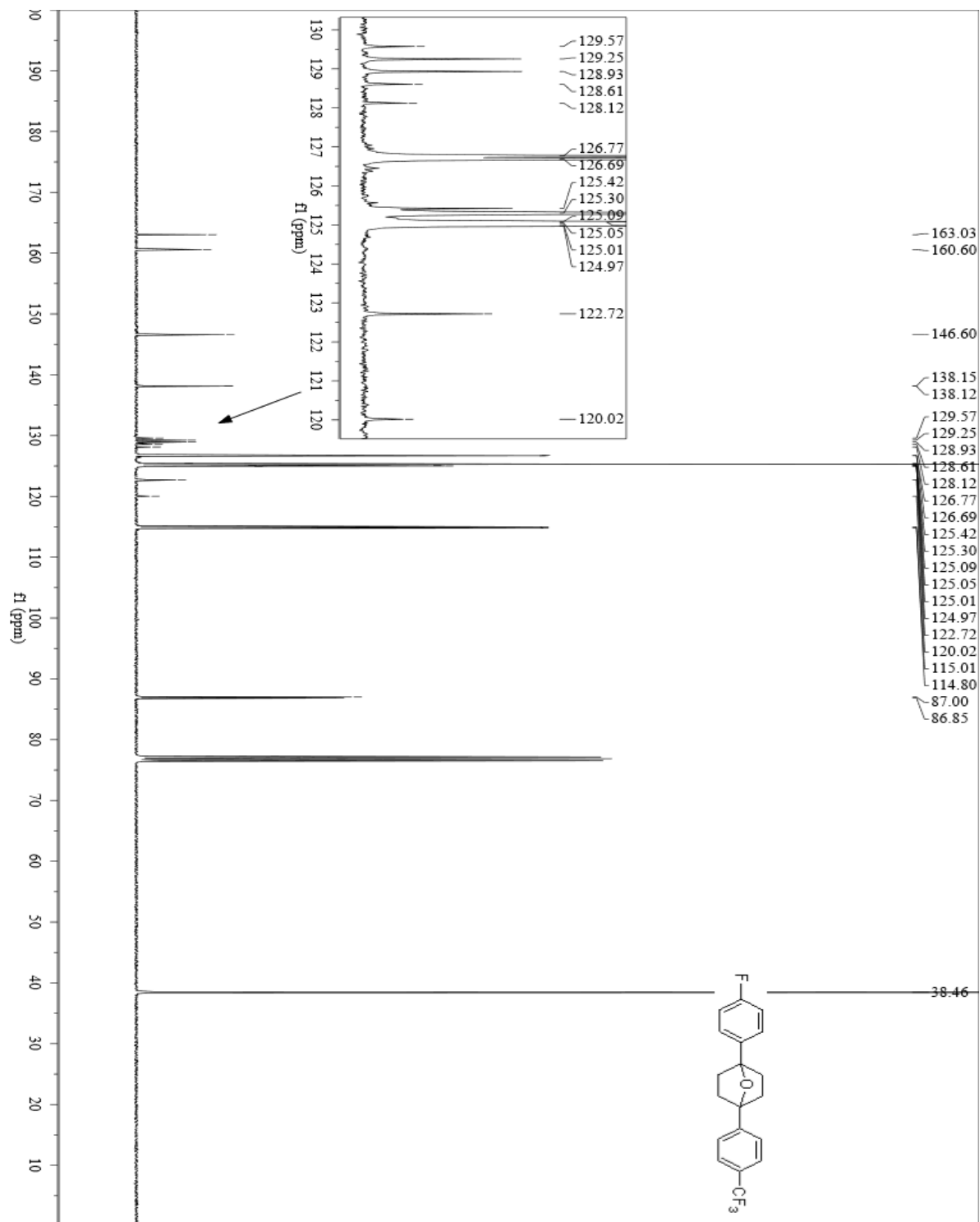
**5i (1-phenyl-4-(4-(trifluoromethyl)phenyl)-7-oxabicyclo[2.2.1]heptane)**



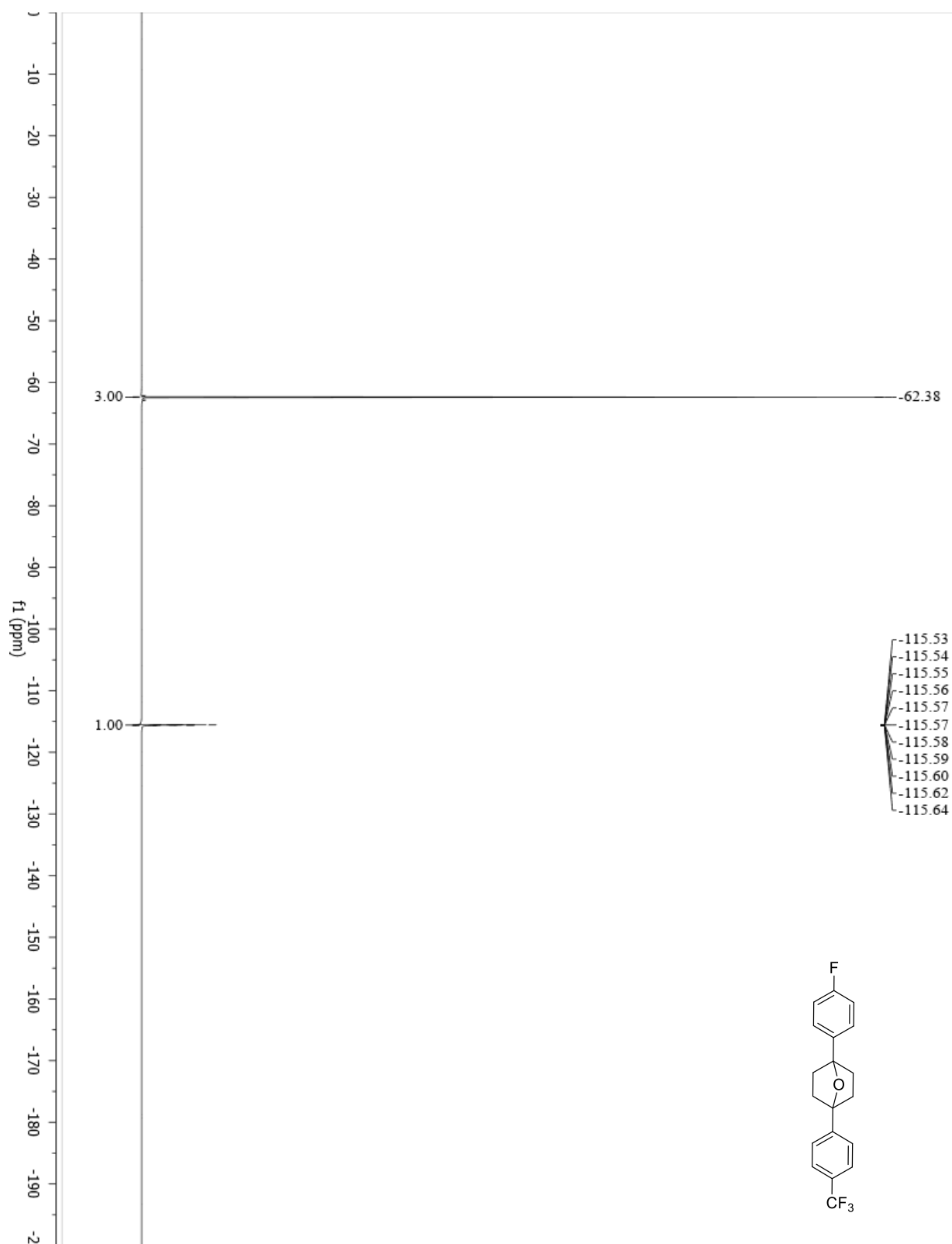
**5j (1-(4-fluorophenyl)-4-(4-(trifluoromethyl)phenyl)-7-oxabicyclo[2.2.1]heptane)**



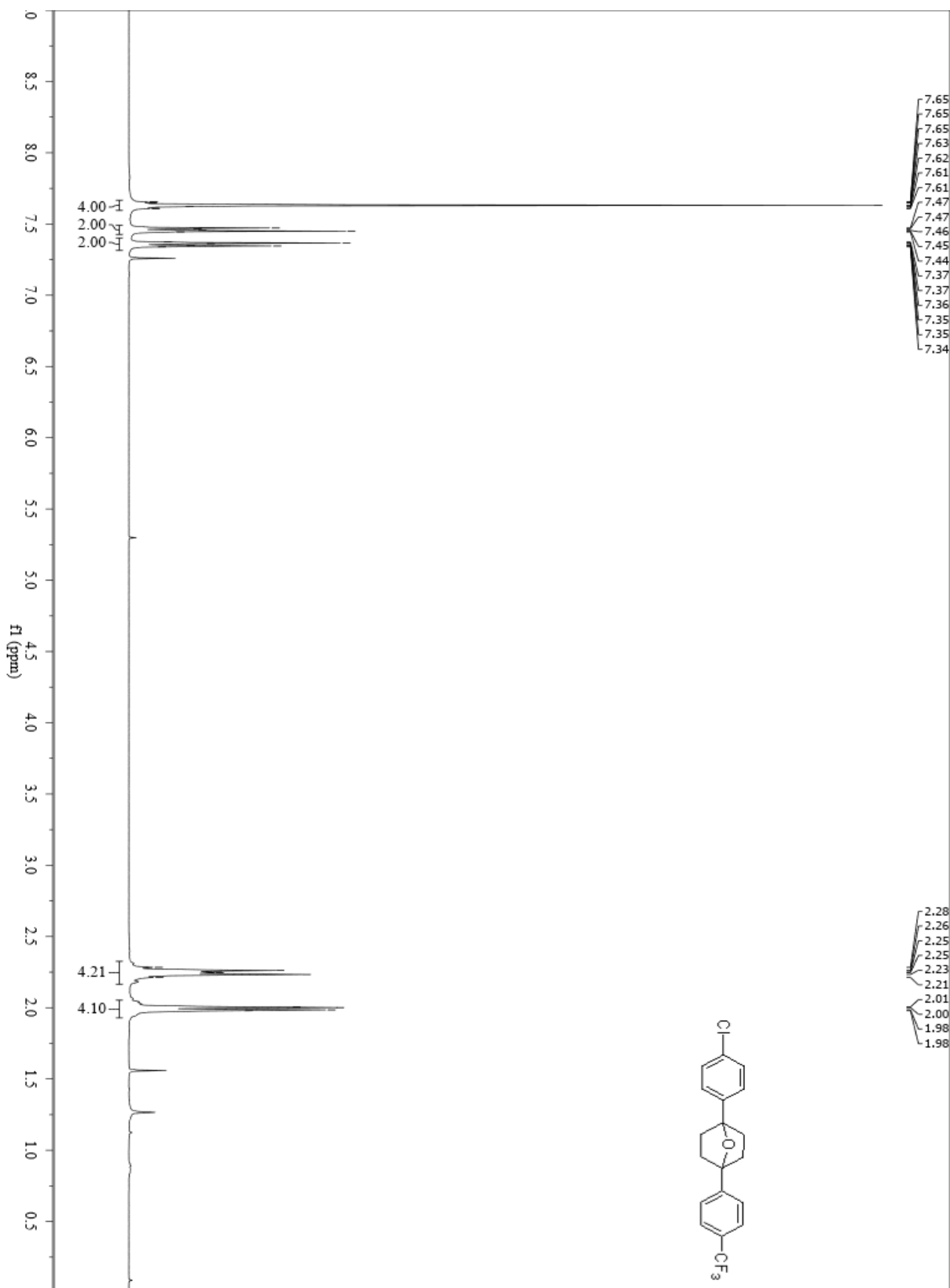
**5j (1-(4-fluorophenyl)-4-(4-(trifluoromethyl)phenyl)-7-oxabicyclo[2.2.1]heptane)**



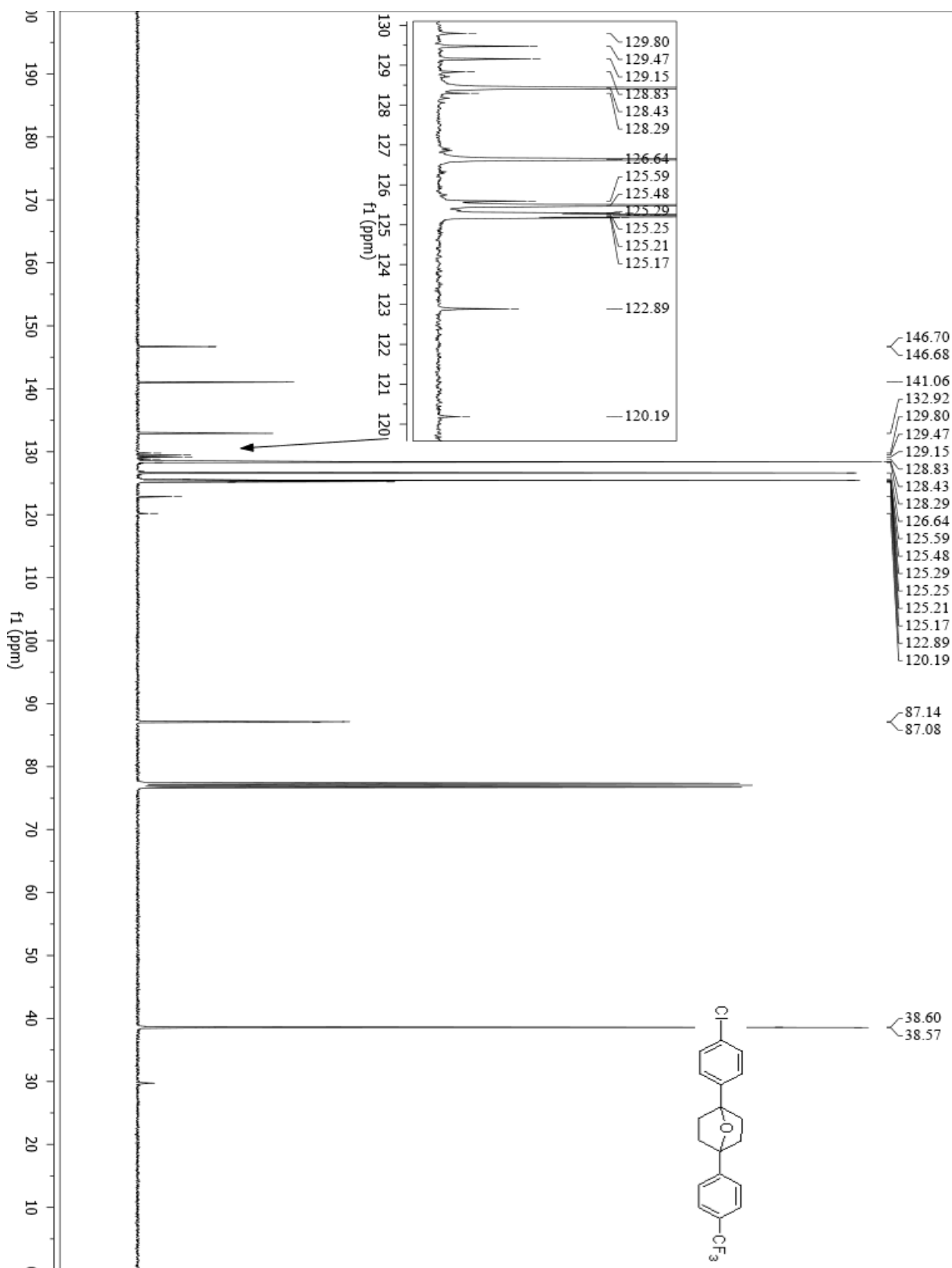
**5j (1-(4-fluorophenyl)-4-(4-(trifluoromethyl)phenyl)-7-oxabicyclo[2.2.1]heptane)**



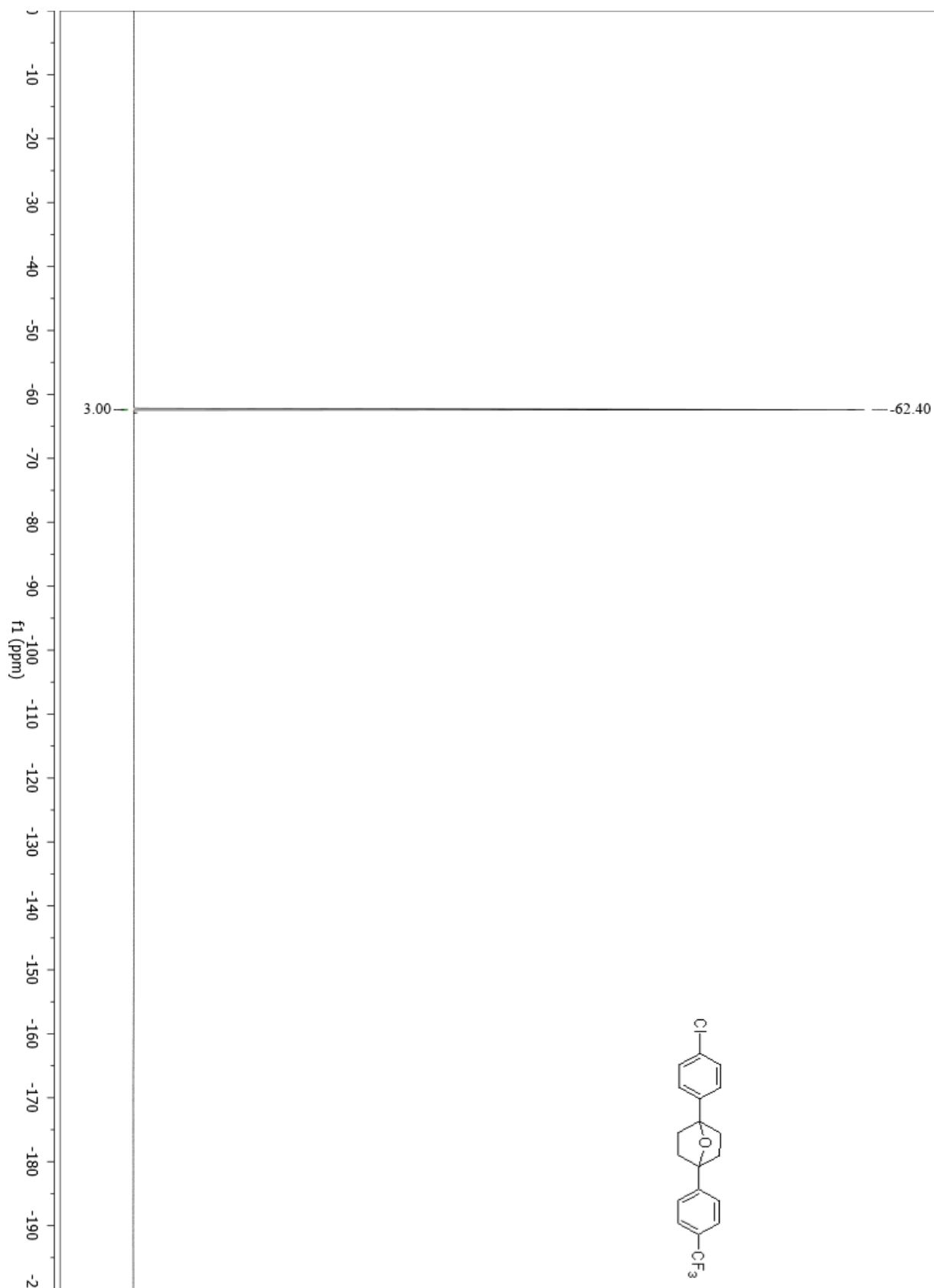
**5k (1-(4-chlorophenyl)-4-(4-(trifluoromethyl)phenyl)-7-oxabicyclo[2.2.1]heptane)**



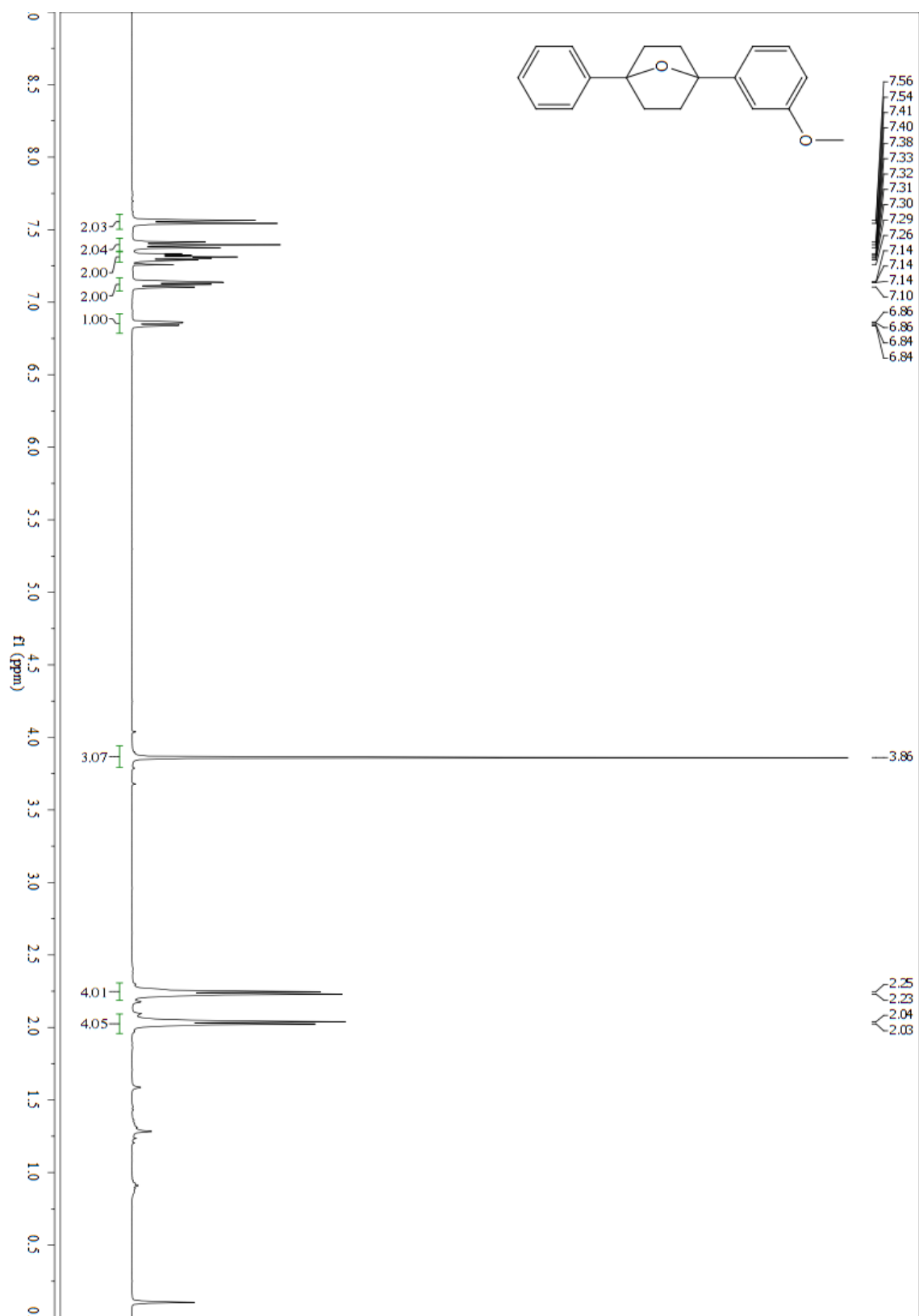
5k (1-(4-chlorophenyl)-4-(4-(trifluoromethyl)phenyl)-7-oxabicyclo[2.2.1]heptane)



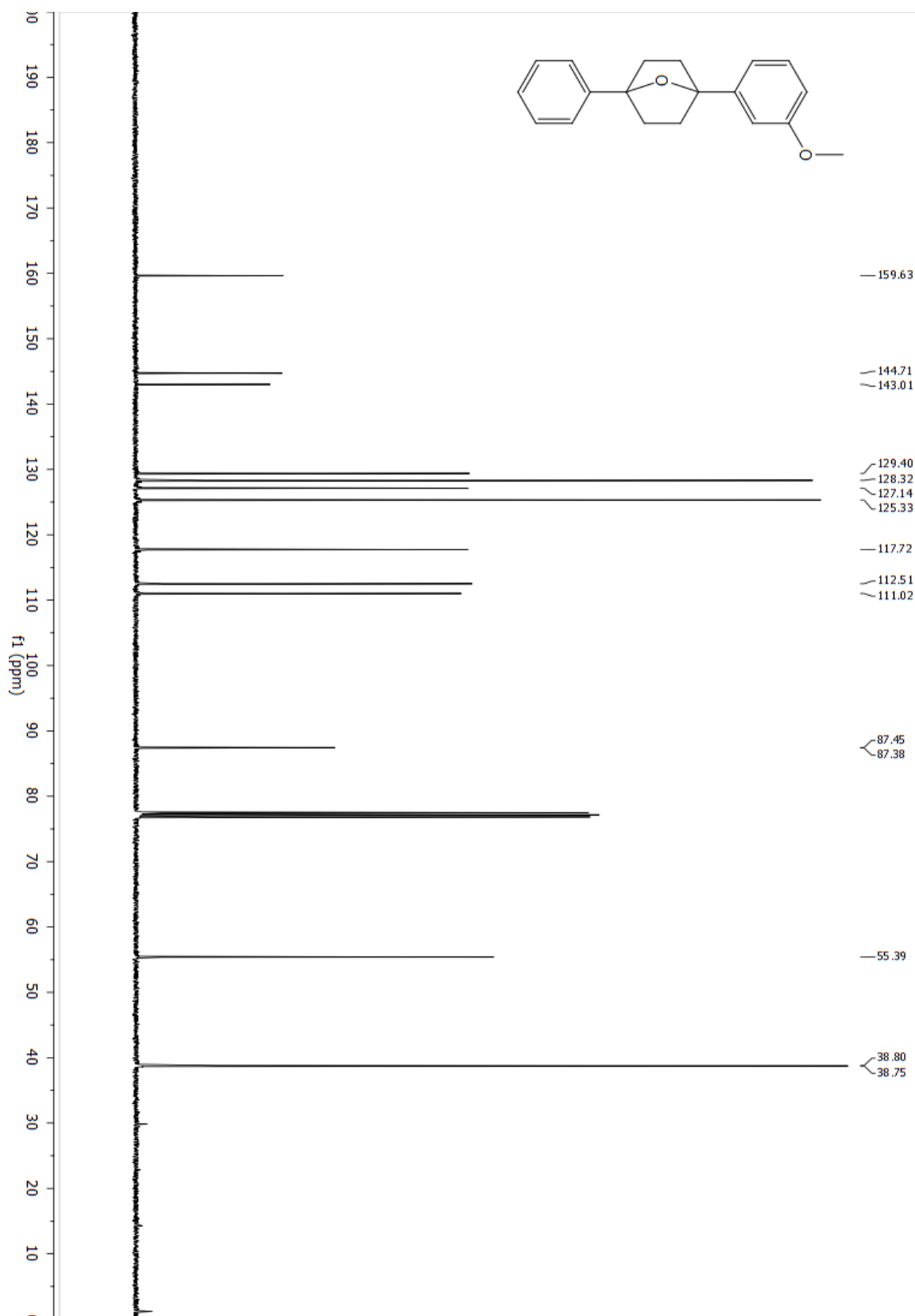
**5k (1-(4-chlorophenyl)-4-(4-(trifluoromethyl)phenyl)-7-oxabicyclo[2.2.1]heptane)**



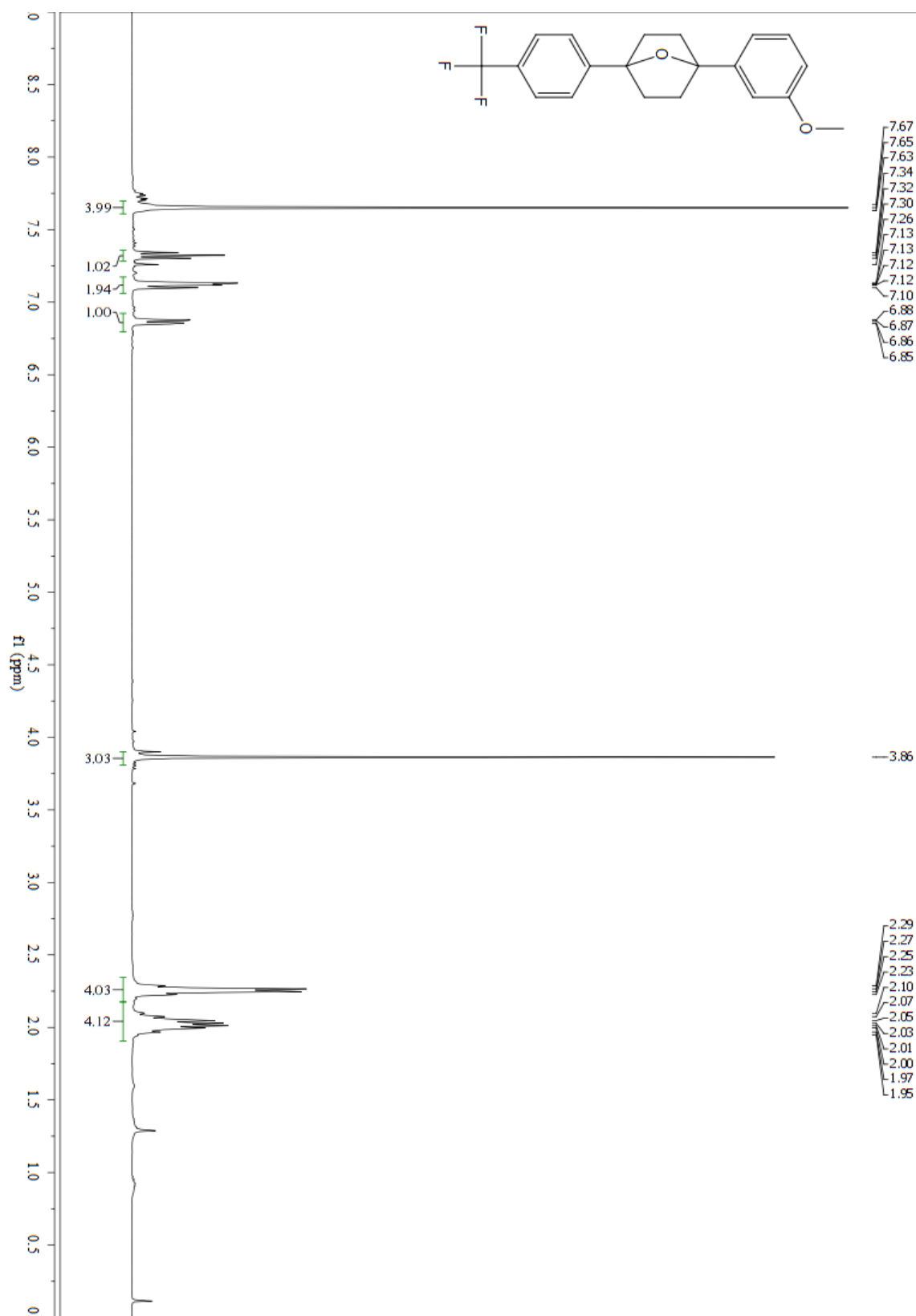
**2m (1-(3-methoxyphenyl)-4-phenyl-7-oxabicyclo[2.2.1]heptane)**



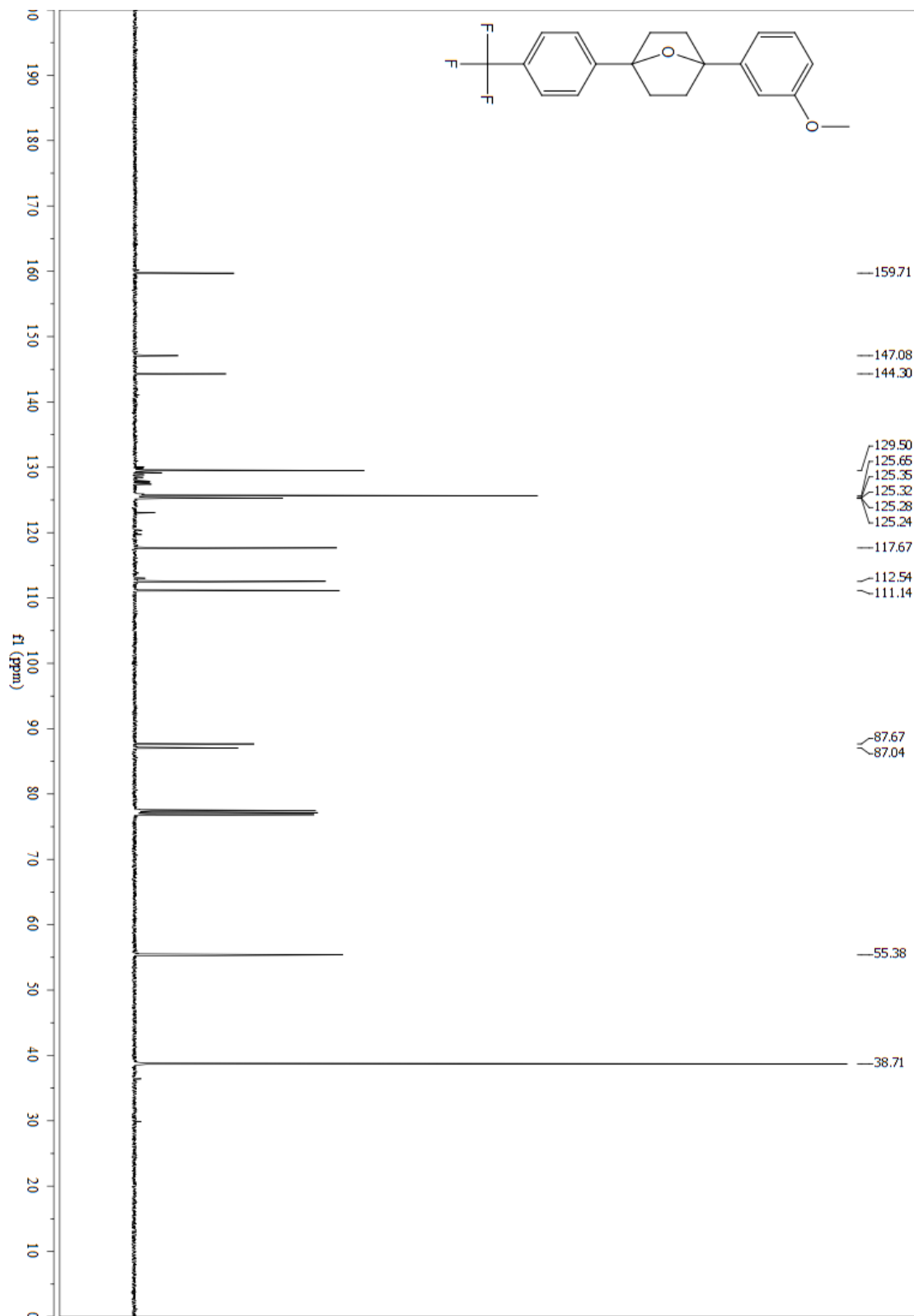
**2m (1-(3-methoxyphenyl)-4-phenyl-7-oxabicyclo[2.2.1]heptane)**



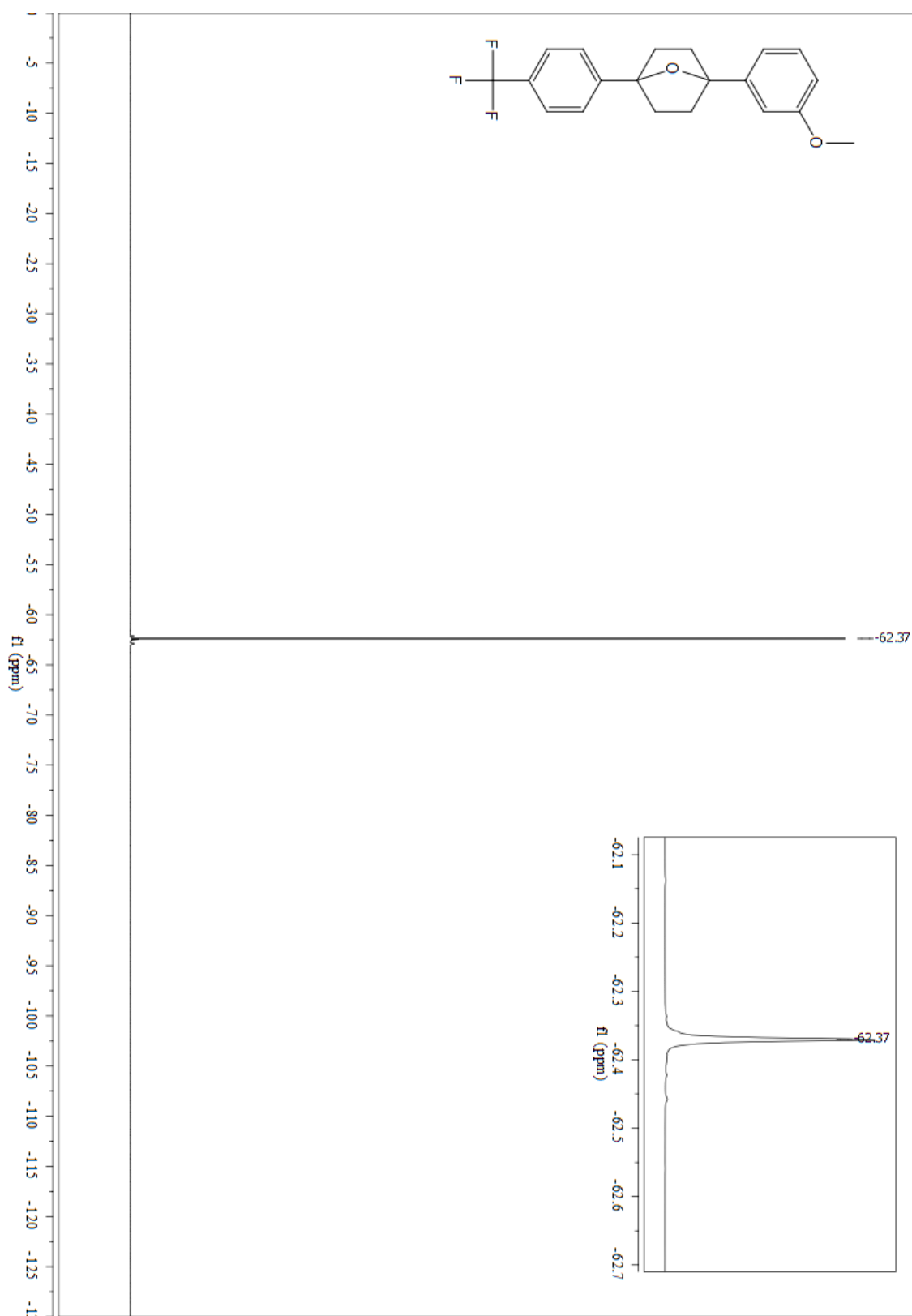
**2n (1-(3-methoxyphenyl)-4-(4-(trifluoromethyl)phenyl)-7-oxabicyclo[2.2.1]heptane)**



**2n (1-(3-methoxyphenyl)-4-(4-(trifluoromethyl)phenyl)-7-oxabicyclo[2.2.1]heptane)**



**2n (1-(3-methoxyphenyl)-4-(4-(trifluoromethyl)phenyl)-7-oxabicyclo[2.2.1]heptane)**



## APPENDIX

Intersystem crossing (ISC).

Metal Ligand Charge Transfer (MLCT)

Single Electron Transfer (SET)

Regioisomeric ratio (rr)

Diastereoisomeric ratio (dr)

Enantiomeric excess (*ee*)

Trimethylamine (TEA, Et<sub>3</sub>N)

Di-isopropylethylamine (DIPEA)

Dichloromethane (DCM)

Acetonitrile (MeCN)

Hydrogen atom transfer (HAT)

Methanol (MeOH)

*N,N*-Dimethylformamide (DMF)

Tetrahydrofuran (THF)

Thin layer chromatography (TLC)

Phenyl (Ph)

Benzyl (Bn)

Trimethylsilyl (TMS)

*tert*-Butyloxycarbonyl (Boc)

Methyl (Me)

Starting material (SM)

Bovine Serum Albumin (BSA)

VITA

Kamaljeet Singh

Candidate for the Degree of

Doctor of Philosophy

Thesis: UPHILL CATALYSIS: GENERATION OF HIGHER ENERGETIC GEOMETRICAL ISOMERS OF (CYCLO)ALKENES USING VISIBLE LIGHT PHOTOCATALYSIS AND THEIR UTILIZATION IN CHEMICAL SYNTHESSES

Major Field: Chemistry

Biographical:

Education:

Completed the requirements for the Doctor of Philosophy in Organic Chemistry at Oklahoma State University, Stillwater, Oklahoma in July, 2018.

Completed the requirements for the Master of Science/Arts in Applied Chemistry (Pharmaceuticals) at Guru Nanak Dev University, Amritsar, India in May 2009.

Completed the requirements for the Bachelor of Science in Non-Medical Science at Punjabi University, Patiala, India in April 2007.

Experience: Two years in pharmaceutical industry and five years in research.

Professional Memberships:

Phi Kappa Phi	Since 2015
American Chemical Society	Since 2015
American Chemical Society Division of Organic Chemistry	Since 2015